

The Synthesis and Biological Testing of Nucleoside Derivatives

Jenny-Lee Panayides

A thesis submitted to the Faculty of Science, University of the
Witwatersrand, Johannesburg, in fulfilment of the
requirements for the degree of Doctor of Philosophy.

Johannesburg, February 2012

The Synthesis and Biological Testing of Nucleoside Derivatives

Jenny-Lee Panayides

A thesis submitted to the Faculty of Science, University of the
Witwatersrand, Johannesburg, in fulfilment of the
requirements for the degree of Doctor of Philosophy.

Johannesburg, February 2012

Declaration

I declare this thesis is my own, unaided work (unless otherwise stipulated in the course of the text). It is being submitted for the Degree of Doctor of Philosophy in the University of the Witwatersrand, Johannesburg. It has not been submitted before for any degree or examination in any other University.

Jenny-Lee Panayides

___ day of _____ 2012

Abstract

As a first generation of compounds, the nucleosides adenosine **8**, cytidine **11**, guanosine **9**, inosine **116** and uridine **12**, as well as the sugar β -(-)-ribose **100**, were transformed into the corresponding 5'-*O*-(*tert*-butyldiphenylsilyl)- and 5'-*O*-(4,4'-dimethoxytrityl)-derivatives. These were subsequently protected as acetyl, benzoyl and allyl derivatives at various positions on the molecules, to give a range of twenty five unique compounds for biological testing.

The nucleoside and corresponding β -(-)-ribose derivatives were evaluated for their antibacterial activity against two Gram-positive (*Staphylococcus aureus* ATCC 25923 and *Bacillus cereus* DL5) and two Gram-negative bacteria (*Pseudomonas aeruginosa* ATCC 27853 and *Escherichia coli* ATCC 25922), for their anti-HIV activity against strain HLTV_{III}B as well as for their anticancer properties, by evaluating inhibition of cell proliferation in two adherent (HT-29 and Caco-2) and three suspension (HL-60, Jurkat and K-562) cell lines. From these screens, and based on the 2,3,5-triphenyltetrazolium chloride (TTC) assay, it was found that 5'-*O*-(*tert*-butyldiphenylsilyl)uridine **107**, 5'-*O*-(*tert*-butyldiphenylsilyl)-1'-*O*-methoxy- β -(-)-ribose **102** and *tert*-butyldiphenylsilyl alcohol **145** exhibited antimicrobial activity towards only the Gram-positive bacteria when compared to the ciprofloxacin **153** control. None of the compounds tested showed any antiviral activity when assayed against HIV; however, all compounds indicated some form of toxicity to the uninfected cells. Subsequent cell proliferation studies indicated pronounced activity against both the adherent and suspension cancer cell lines for 5'-*O*-(*tert*-butyldiphenylsilyl)uridine **107**, 5'-*O*-(*tert*-butyldiphenylsilyl)cytidine **134**, *tert*-butyldiphenylsilyl alcohol **145**, 5'-*O*-(4,4'-dimethoxytrityl)uridine **126** and 4,4'-dimethoxytrityl alcohol **147**. Our initial screen indicated that β -(-)-ribose derivatives do not show any significant general biological activity; whereas (*tert*-butyldiphenylsilyl)-protected nucleoside derivatives and the corresponding *tert*-butyldiphenylsilyl alcohol control are intrinsically more bio-active.

From the data reported for the anti-bacterial and the cell proliferation studies, we concluded that the nucleoside showing the most promising results was uridine **12** and our mini structure-

activity study on the uridine derivatives found that the best position for performing modifications to the nucleoside was at the 5'-OH position on the sugar ring. As such, this would become the initial focus for the synthesis of the second generation compounds. The second generation compounds included a series of ten uridine **12** and five 5-methyluridine **233** derivatives which were protected on the primary alcohol with a range of different silicon-containing protecting groups. At the same time, we used a general procedure to synthesize a series of fourteen silanols for use as control compounds.

The uridine **12**, 5-methyluridine **233** and corresponding silanol derivatives were screened for their antibacterial activity against the same two Gram-positive and two Gram-negative bacteria as above, as well as for their anticancer properties, by evaluating inhibition of cell proliferation in a series of six adherent cell lines (five human: Hs683, MCF-7, PC-3, SKMEL-28, U373, and one murine: B16F10) cell lines. The data obtained for our TTC assay showed that converting the base in 1-[(6*aR*,8*R*,9*R*,9*aS*)-9-hydroxy-2,2,4,4-tetraisopropyltetrahydro-6*H*-furo[3,2-*f*][1,3,5,-2,4]trioxadisilocin-8-yl]-pyrimidine-2,4(1*H*,-3*H*)dione **234** to the 5-methyl derivative **254** caused a corresponding loss in antibacterial activity for the compound, whereas oxidising the secondary alcohol on the 2'-position of the sugar ring to give compound **239** caused a corresponding increase in antibacterial activity. As such, we concluded that 1-[(6*aR*,8*R*,9*aR*)-2,2,4,4-tetraisopropyl-9-oxotetrahydro-6*H*-furo[3,2-*f*][1,3,5,-2,4]trioxadisilocin-8-yl]pyrimidine-2,4(1*H*,3*H*)dione **239** was the compound with the best antibacterial activity out all of the first and second generations of nucleoside derivatives assayed. The results obtained in the TTC assay, were supported by our scanning electron (SEM) and confocal scanning electron (CSLM) microscopy studies. Interestingly, the CSLM study suggests that the synthetic compound **239** is bacteriocidal and is inactivating cells, not simply inhibiting their growth. From the inhibition of cell proliferation assay performed on the fifty combined first and second generation derivatives and their corresponding controls, we found that the six most active compounds (5'-*O*-(*tert*-butyldiphenylsilyl)adenosine **142**, 5'-*O*-(*tert*-butyldiphenyl-silyl)cytidine **134**, 5'-*O*-(*tert*-butyldiphenylsilyl)uridine **107**, 2',3'-*O*-diacetyl-5'-*O*-(*tert*-butyl-diphenylsilyl)uridine **123**, 2',3'-*O*-diacetyl-5'-*O*-(4,4'-dimethoxytrityl)uridine **127** and 3-benzoyl-1-[(6*aR*,8*R*,9*R*,9*aS*)-9-hydroxy-2,2,4,4-tetraisopropyltetrahydro-6*H*-furo[3,2-*f*][1,3,-5,2,4]trioxa-disilocin-8-yl]pyrimidine-2,4(1*H*,3*H*)-dione **235**) had mean IC₅₀ values of approximately 24-28 μM.

Dedication

I dedicate this thesis to Darren Riley - you are my rock, without you I would never have had the courage to start this mammoth undertaking and without your continual encouragement and support I would never have finished. Thank you for your inspiration and guidance, you make it all worthwhile!

Acknowledgements

Many people need to be acknowledged for the contributions they have made towards the completion of this thesis:

- Ⓒ *Dr Raveen Parboosing* and *Annetta Naidoo* of the Department of Virology at UKZN for performing the anti-HIV screen on our compounds.
- Ⓒ *Dr Hajierah Davids* of the Department of Biochemistry and Microbiology at the Nelson Mandela Metropolitan University, as well as *Helen Apostolellis* and *Nurit Dahan-Farkis* of the Department of Pharmacy and Pharmacology at Wits University, for performing the initial screens for activity against cancer cell lines and toxicity to white blood cells.
- Ⓒ *Prof Robert Kiss*, *Veronique Mathieu*, *Delphine Lamoral-Theys*, *Thierry Gras* and *Laetitia Moreno YBanuls* of the Laboratory of Toxicology, at the Institute of Pharmacy which forms part of the ULB in Brussels, for the full set of cell anti-proliferation studies performed on all the first and second generation compounds synthesized.
- Ⓒ *Prof Mike Whitcomb* and *Caroline Lalkhan* of the Wits Microscopy Department, for teaching me how to use the SEM and confocal microscopes and for their help with sample preparation.
- Ⓒ *Prof Lawrence Carlton* and *Richard Mampa* of the Wits NMR Department, for the numerous specialised NMR spectra they ran for me and for allowing me so much free time on the machine for my own use.
- Ⓒ *Dr Andrew Dinsmore*, *Tommy van der Merwe*, *Martin Brits* and *Marlize Ferreira* of the Wits Mass Spectrometry Department for the many LRMS spectra they ran.
- Ⓒ The *Mass Spectrometry Department* of the Max-Planck Institute, Germany, for the numerous HRMS spectra they ran throughout the duration of the project.

I would also like to thank the following people:

- Ⓒ My chemistry supervisor, *Prof Willem van Otterlo*, for the many, many hours of work put into this project and for always encouraging me to be a better researcher. You have taught me to stand on my own and I thank you for that.
- Ⓒ My microbiology supervisor, *Prof Chrissie Rey*, you have stood by me and supported me through all the trying moments of this project and you always made me feel

welcome in the micro labs, even though at times I was a lost chemist floundering to find my way. Thank you for everything.

- ④ *Dr Denise Lindsay*, for the endless hours of time you spent teaching me the protocols and advising me on the antibacterial assays. Thank you for all the guidance you gave me, it meant the world to me.
- ④ *Caroline Lalkhan*, you went above and beyond what you needed to do and you are an exceptional teacher - it was truly an honour to have had the opportunity to spend time working with you.
- ④ I would also like to say a special word of thanks to *Prof Jo Michael* and *Prof Charles de Koning*, for their valued support and continual encouragement, and for their endless synthetic knowledge for me to call on - especially when embarking on an unfamiliar project such as this one.
- ④ The entire *Organic Research Group* for listening to me drone on about my "bugs" for hours and especially the past and present members of lab C321: Darren, Mabel, Steve, Theo, Sameshnee, Warren, Tanya, Candice, Saleem and Myron. You have made good friends and you guys ROCK!
- ④ Nathalie and Keshia of the *Food Microbiology Research Group*, for teaching me the basic aseptic techniques for the antibacterial assay and for always making the working environment such a pleasure.
- ④ The entire *Plant Biotechnology Research Group*: Nats, Imah, Maabo, Phila, Sarah, Fluffy, Rozida, Chez, Sarah Jane and Debs. You are the most fantastic people I have ever had the pleasure to work with, you made me excited to come in each day - even when it was ridiculously early! Thank you for all the laughs and smiles, I will never forget you :-)

Lastly, on a personal note:

- ④ Thanks go to my parents *Adrian* and *Vivian Panayides*, for without parents that are as supportive and encouraging as these it would not be possible to complete an undertaking as large as this one.
- ④ To my brother, *Warren Panayides*, thank you for all the laughs, smiles and good times, you always know how to make me feel better and forget about the stresses of work!

Financial Assistance

The financial assistance of the National Research Foundation of South Africa towards this research project is gratefully acknowledged. Opinions expressed in this thesis and conclusions arrived at, are those of the author, and are not necessarily to be attributed to the National Research Foundation of South Africa.

Quote

When I Get Sad - I Stop Being Sad And Be Awesome Instead. True Story.

~ Barney Stinson


Table of Contents






©	<i>Title Page</i>	<i>i</i>
©	<i>Declaration</i>	<i>ii</i>
©	<i>Abstract</i>	<i>iii</i>
©	<i>Dedication</i>	<i>v</i>
©	<i>Acknowledgements</i>	<i>vi</i>
©	<i>Financial Assistance</i>	<i>viii</i>
©	<i>Quote</i>	<i>ix</i>
©	<i>Table of Contents</i>	<i>x</i>
©	<i>Abbreviations</i>	<i>xxviii</i>
	- <i>List of General Abbreviations</i>	<i>xxviii</i>
	- <i>List of Chemical Abbreviations</i>	<i>xxxi</i>
	- <i>List of Cell Lines</i>	<i>xxxiii</i>
©	<i>Quote</i>	<i>xxxv</i>

PART 1 - FIRST GENERATION COMPOUNDS

Synthesis and Biological Testing of Various Nucleoside and α -(-)-Ribose Derivatives

Chapter 1: Introduction	2
1.1 GENERAL INTRODUCTION: BASES, NUCLEOSIDES AND NUCLEOTIDES	3
1.1.1 Base, Nucleoside and Nucleotide Structures and Nomenclature	3
1.1.2 Watson-Crick Model for Base-Pairing in DNA	9

1.2	INTRODUCTION TO BIOLOGICAL APPLICATIONS OF NUCLEOSIDES - WITH A CLOSER LOOK AT CURRENT NUCLEOSIDE BASED DRUGS	12
1.2.1	Nucleoside Derivatives Used in the Treatment of Viral Diseases	12
1.2.2	Nucleoside Derivatives Used in the Treatment of Cancer	14
1.2.3	Nucleoside Derivatives Used as Antibiotics	15
1.3	CONFORMATIONALLY RESTRICTED NUCLEOSIDE ANALOGUES	17
1.3.1	Class 1 - The Bicyclic and Tricyclic Nucleosides	17
1.3.2	Class 2 - The Cyclonucleosides	19
1.3.3	Class 3 - The Cyclic Phosphoesters	21
1.4	INTRODUCTION TO RING CLOSING METATHESIS	24
1.5	AIMS FOR PART 1	25
1.5.1	Fused Bicyclic Systems	25
1.5.2	Structure-Activity Relationships	26
Chapter 2: Results and Discussion for Synthesis		28
	Contributions to the Chapter	29
2.1	CHAPTER OVERVIEW	29
2.2	RESULTS AND DISCUSSION	29
2.2.1	Strategy Towards Fused Bicyclic Ring Systems	30
2.2.1.1	<i>The Model System: α-(-)-Ribose Derivatives</i>	30
2.2.1.2	<i>Pyrimidine-Based Nucleosides – Focusing on Uridine</i>	36
2.2.1.3	<i>Purine-Based Nucleosides – Focusing on Guanosine and Inosine</i>	41

2.2.2	Synthesis of Compounds to Conduct a Structure-Activity Study	47
2.2.2.1	<i>The Model System: α-(-)-Ribose Derivatives</i>	47
2.2.2.2	<i>Pyrimidine-Based Nucleosides – Focusing on Uridine and Cytidine</i>	53
2.2.2.3	<i>Purine-Based Nucleosides – Focusing on Guanosine, Inosine and Adenosine</i>	65
2.2.2.4	<i>Controls for Biological Assays</i>	72
2.3	CONCLUSIONS	75
	Chapter 3: Results and Discussion for Biological Testing	76
	Contributions to the Chapter	77
3.1	CHAPTER OVERVIEW	77
3.2	RESULTS AND DISCUSSION	78
3.2.1	Antibacterial Assays	78
3.2.1.1	<i>Materials and Methods</i>	78
	 <i>Bacterial Cultures</i>	78
	 <i>Synthetic Compounds</i>	80
	 <i>Evaluation of Compound Efficacy – Triphenyltetrazolium Chloride Assay</i>	84
	 <i>Statistical Analysis</i>	88
3.2.1.2	<i>Results</i>	89
3.2.1.3	<i>Discussion</i>	98
3.2.1.4	<i>Conclusions</i>	103
3.2.2	Antiviral Assays	104


3.2.2.1 <i>Materials and Methods</i>	104
Ⓢ <i>Cell Line and HIV strain</i>	104
Ⓢ <i>Compounds Used in Assay</i>	105
Ⓢ <i>Evaluation of Compound Efficacy</i>	106
Ⓢ <i>Data Analysis</i>	108
3.2.2.2 <i>Results</i>	109
3.2.2.3 <i>Discussion</i>	112
3.2.2.4 <i>Conclusions</i>	118
3.2.3 Inhibition of Cell Proliferation	118
3.2.3.1 <i>Materials and Methods</i>	119
Ⓢ <i>Cell Lines</i>	119
Ⓢ <i>Compounds Used in the Inhibition of Cell Proliferation Study</i>	120
Ⓢ <i>Evaluation of Compound Efficacy using the MTT Assay for Cell Viability Quantification</i>	124
Ⓢ <i>Other Assays Conducted</i>	125
Ⓢ <i>Data Analysis</i>	125
3.2.3.2 <i>Results of MTT Assay</i>	125
3.2.3.3 <i>Discussion for Subsequent Assays Performed</i>	138
Ⓢ <i>Annexin V Assay</i>	138
Ⓢ <i>Time Dependent Induction of Caspase 3 and Caspase 8 Activity</i>	140
Ⓢ <i>Cytochrome c Assay</i>	142
3.2.3.4 <i>Conclusions</i>	144
Summary: Work covered in Part 1	145
Ⓢ PART 1 SUMMARY – SYNTHESIS	146

©	PART 1 SUMMARY – BIOLOGICAL TESTING	148
---	--	------------

PART 2 - SECOND GENERATION COMPOUNDS

Synthesis and Biological Testing of Uridine, 5-Methyluridine and Silanol Derivatives

Chapter 4:	<i>Introduction</i>	152
4.1	GENERAL INTRODUCTION TO SILICON AND ITS CHEMISTRY	153
4.1.1	Basic Silicon Chemistry	153
4.1.2	Silicon in Protecting Group Chemistry	154
4.2	SILICON IN DRUG DISCOVERY	155
4.2.1	Bioisosteres – Sila-Substitution of Existing Drugs	155
4.2.2	General Properties of Silicon and the Impact in Medicinal Chemistry	156
	<i>4.2.2.1 Atomic Size</i>	<i>157</i>
	<i>4.2.2.2 Electronegativity</i>	<i>158</i>
	<i>4.2.2.3 Lipophilicity</i>	<i>158</i>
	<i>4.2.2.4 Novel Chemistry</i>	<i>159</i>
	<i>4.2.2.5 Limitations to Sila-Substitutions</i>	<i>159</i>
4.2.3	Examples of Drug-Like Compounds with Sila-Substitutions	160
	<i>4.2.3.1 Sila-Budipine</i>	<i>160</i>
	<i>4.2.3.2 Sila-Haloperidol</i>	<i>161</i>
	<i>4.2.3.3 Sila-Bexarotene</i>	<i>162</i>

4.3	INTRODUCTION TO SILICON IN BIOLOGICAL SYSTEMS	163
4.4	BIOLOGICAL APPLICATIONS OF SILICON CONTAINING COMPOUNDS	166
4.4.1	Synthetic Silicon Containing Compounds Showing Anti-Bacterial Activity	166
4.4.1.1	<i>The Silanols</i>	<i>166</i>
4.4.1.2	<i>The β-Ethanolamine Derivatives</i>	<i>167</i>
4.4.2	Synthetic Silicon Containing Compounds with Activity against Cancer Lines	169
4.4.2.1	<i>The (2R,3S)-Disubstituted Tetrahydropyranes</i>	<i>169</i>
4.4.2.2	<i>The Silatecans</i>	<i>171</i>
4.4.2.3	<i>The Indomethacin Derivatives</i>	<i>173</i>
4.4.2.4	<i>The Nucleoside Derivatives</i>	<i>174</i>
4.5	AIMS FOR PART 2	176
4.5.1	Synthesis of Nucleoside Derivatives	176
4.5.2	Synthesis of Silanols	178
4.5.3	Biological Testing	179
4.5.4	Summary of Aims	179
	Chapter 5: Results and Discussion for Synthesis	181
	Contributions to the Chapter	182
5.1	CHAPTER OVERVIEW	182
5.2	RESULTS AND DISCUSSION	182
5.2.1	Synthesis of Uridine Derivatives	183

5.2.1.1	<i>Uridine Derivatives Containing the 3'-O to 5'-O-Tethered Protecting Group</i>	183
5.2.1.2	<i>Uridine Derivatives with Various 5'-O-Protecting Groups</i>	189
5.2.2	Synthesis of 5-Methylridine Derivatives	192
5.2.3	Synthesis of Various Silanols	196
5.3	CONCLUSIONS	198
	Chapter 6: Results and Discussion for Bacteriology and Microscopy	200
Ⓢ	Contributions to the Chapter	201
6.1	CHAPTER OVERVIEW	201
6.2	RESULTS AND DISCUSSION	201
6.2.1	Antibacterial Assays	202
6.2.1.1	<i>Materials and Methods</i>	202
	Ⓢ <i>Bacterial Cultures</i>	202
	Ⓢ <i>Synthetic Compounds</i>	203
	Ⓢ <i>Evaluation of Compound Efficacy – Triphenyltetrazolium Chloride Assay</i>	205
	Ⓢ <i>Statistical Analysis</i>	205
6.2.1.2	<i>Results and Discussion</i>	206
6.2.1.3	<i>Conclusions</i>	214
6.2.2	Confocal Scanning Laser Microscopy (CSLM)	215
6.2.2.1	<i>Materials and Methods</i>	215
6.2.2.2	<i>Results and Discussion</i>	216
6.2.2.3	<i>Conclusions</i>	223

6.2.3 Scanning Electron Microscopy (SEM)	223
6.2.3.1 <i>Materials and Methods</i>	223
6.2.3.2 <i>Results and Discussion</i>	224
6.2.3.3 <i>Conclusions</i>	235
Chapter 7: Results and Discussion for Full Cancer Screens	237
Ⓢ Contributions to the Chapter	238
7.1 CHAPTER OVERVIEW	238
7.2 INHIBITION OF CELL PROLIFERATION STUDY	238
7.2.1 Materials and Methods	238
7.2.1.1 <i>Cell Lines and Culture Conditions</i>	238
7.2.1.2 <i>Synthetic Compounds Used in the Study</i>	241
7.2.1.3 <i>Evaluation of Compound Efficacy using the MTT Assay</i>	246
7.2.1.4 <i>Data Analysis</i>	248
7.2.2 Results and Discussion	248
7.2.3 Conclusions	264
Summary: Work covered in Part 2	266
Ⓢ PART 1 SUMMARY – SYNTHESIS	267
Ⓢ PART 1 SUMMARY – BACTERIOLOGY AND MICROSCOPY	270
Ⓢ PART 1 SUMMARY – FULL CANCER SCREEN	271

PART 3 – OVERALL CONCLUSIONS AND FUTURE WORK

Chapter 8: <i>Conclusions and Future Work</i>	273
8.1 GENERAL CONCLUSIONS	274
8.2 FUTURE WORK	282
8.2.1 Current State of the Work	282
8.2.2 The Way Forward: Part 1 – Multiple Protecting Group Additions	284
8.2.3 The Way Forward: Part 2 – Modifications to the Sugar Ring Hydroxyl Groups	285
Chapter 9: <i>References</i>	288
9.1 REFERENCES RELATING TO CHAPTER 1	289
9.2 REFERENCES RELATING TO CHAPTER 2	291
9.3 REFERENCES RELATING TO CHAPTER 3	291
9.4 REFERENCES RELATING TO CHAPTER 4	293
9.5 REFERENCES RELATING TO CHAPTER 5	295
9.6 REFERENCES RELATING TO CHAPTER 6	295
9.7 REFERENCES RELATING TO CHAPTER 7	295
9.8 REFERENCES RELATING TO CHAPTER 8	297
9.9 REFERENCES RELATING TO APPENDIX A	298
9.10 REFERENCES RELATING TO APPENDIX B	298

9.11	REFERENCES RELATING TO APPENDIX C	298
9.12	REFERENCES RELATING TO APPENDIX D	298
9.13	REFERENCES RELATING TO APPENDIX E	298
9.14	REFERENCES RELATING TO APPENDIX F	298

APPENDICES RELATING TO PART 1

Appendix A: *General Synthetic Experimental Procedures*300

A.1	Purification of Solvents	301
A.2	Experimental Techniques and Equipment Used	301
A.3	Chromatographic Separations	302
A.4	Spectroscopic and Physical Data	303
A.5	Nomenclature and Numbering of Compounds	305

Appendix B: *Experimental Procedures - Relating to Chapter 2*306

B.1	Preparation of 1'- <i>O</i> -methoxy-□-(-)-ribose [101]	307
B.2	Preparation of 5'- <i>O</i> -(<i>tert</i> -butyldiphenylsilyl)-1'- <i>O</i> -methoxy-□-(-)-ribose [102]	308
B.3	Preparation of 2',3'- <i>O</i> -diallyl-5'- <i>O</i> -(<i>tert</i> -butyldiphenylsilyl)-1'- <i>O</i> -methoxy-□-(-)-ribose [103]	309
B.4	Attempted synthesis of {[<i>(Z,6aS,7R,9R,9aS)</i> -2,5,6a,7,9,9a-hexahydro-7-methoxyfuro-[3,4- <i>b</i>][1,4]dioxocin-9-yl]methoxy}(<i>tert</i> -butyl)diphenylsilane [104]	310

B.5	Preparation of 5'- <i>O</i> -(4,4'-dimethoxytrityl)-1'- <i>O</i> -methoxy- \square -(-)-ribose [105]	313
B.6	Attempted synthesis of 2',3'- <i>O</i> -diallyl-5'- <i>O</i> -(4,4'-dimethoxytrityl)-1'- <i>O</i> -methoxy- \square -(-)-ribose [106]	314
B.7	Preparation of 5'- <i>O</i> -(<i>tert</i> -butyldiphenylsilyl)uridine [107]	315
B.8	Attempted synthesis of 2',3'- <i>O</i> -diallyl-5'- <i>O</i> -(<i>tert</i> -butyldiphenylsilyl)uridine [108]	316
B.9	Preparation of 6- <i>N</i> -(<i>N,N</i> -dimethylmethylimine)guanosine [112]	319
B.10	Preparation of 5'- <i>O</i> -(4,4'-dimethoxytrityl)-6- <i>N</i> -(<i>N,N</i> -dimethylmethylimine)guanosine [113]	320
B.11	Preparation of 2',3'- <i>O</i> -diallyl-5'- <i>O</i> -(4,4'-dimethoxytrityl)-6- <i>N</i> -(<i>N,N</i> -dimethylmethylimine)guanosine [114]	322
B.12	Attempted synthesis of (1 <i>E</i>)- <i>N</i> -{9-[(<i>Z</i> ,6 <i>aS</i> ,7 <i>R</i> ,9 <i>R</i> ,9 <i>aS</i>)-7-{[bis(4-methoxyphenyl)-(phenyl)methoxy]methyl}-2,5,6 <i>a</i> ,7,9,9 <i>a</i> -hexahydrofuro[3,4- <i>b</i>][1,4]dioxocin-9-yl]-6,9-dihydro-6-oxo-1 <i>H</i> -purin-2-yl}- <i>N,N</i> -dimethylformamidine [115]	323
B.13	Preparation of 5'- <i>O</i> -(4,4'-dimethoxytrityl)inosine [117]	324
B.14	Attempted synthesis of 2',3'- <i>O</i> -diallyl-5'- <i>O</i> -(4,4'-dimethoxytrityl)inosine [118]	325
B.15	Preparation of 2',3'- <i>O</i> -diacetyl-5'- <i>O</i> -(<i>tert</i> -butyldiphenylsilyl)-1'- <i>O</i> -methoxy- \square -(-)-ribose [119]	325
B.16	Preparation of 2',3'- <i>O</i> -diacetyl-5'- <i>O</i> -(4,4'-dimethoxytrityl)-1'- <i>O</i> -methoxy- \square -(-)-ribose [120]	327
B.17	Preparation of 2',3',5'- <i>O</i> -triacyl-1'- <i>O</i> -methoxy- \square -(-)-ribose [121]	328
B.18	Preparation of 2',3',5'- <i>O</i> -triallyl-1'- <i>O</i> -methoxy- \square -(-)-ribose [122]	329
B.19	Preparation of 2',3'- <i>O</i> -diacetyl-5'- <i>O</i> -(<i>tert</i> -butyldiphenylsilyl)uridine [123]	330
B.20	Preparation of 3- <i>N</i> -benzoyl-2',3'- <i>O</i> -diacetyl-5'- <i>O</i> -(<i>tert</i> -butyldiphenylsilyl)uridine [124]	331
B.21	Attempted synthesis of 3- <i>N</i> -benzoyl-5'- <i>O</i> -(<i>tert</i> -butyldiphenylsilyl)uridine [125]	332

B.22	Preparation of 5'- <i>O</i> -(4,4'-dimethoxytrityl)uridine [126]	334
B.23	Preparation of 2',3'- <i>O</i> -diacetyl-5'- <i>O</i> -(4,4'-dimethoxytrityl)uridine [127]	335
B.24	Preparation of 3- <i>N</i> -benzoyl-2',3'- <i>O</i> -diacetyl-5'- <i>O</i> -(4,4'-dimethoxytrityl)uridine [128]	336
B.25	Attempted synthesis of 3- <i>N</i> -benzoyl-5'- <i>O</i> -(4,4'-dimethoxytrityl)uridine [129]	337
B.26	Preparation of 2',3',5'- <i>O</i> -triacetyluridine [130]	338
B.27	Preparation of 3- <i>N</i> -benzoyl-2',3',5'- <i>O</i> -triacetyluridine [131]	339
B.28	Attempted synthesis of 3- <i>N</i> -benzoyluridine [132]	340
B.29	Preparation of 4- <i>N</i> -benzoylcytidine [133]	340
B.30	Preparation of 5'- <i>O</i> -(<i>tert</i> -butyldiphenylsilyl)cytidine [134]	342
B.31	Attempted synthesis of 4- <i>N</i> -benzoyl-5'- <i>O</i> -(<i>tert</i> -butyldiphenylsilyl)cytidine [135]	343
B.32	Attempted synthesis of 5'- <i>O</i> -(4,4'-dimethoxytrityl)cytidine [136]	344
B.33	Attempted synthesis of 4- <i>N</i> -benzoyl-5'- <i>O</i> -(4,4'-dimethoxytrityl)cytidine [137]	345
B.34	Attempted synthesis of 5'- <i>O</i> -(<i>tert</i> -butyldiphenylsilyl)guanosine [138]	346
B.35	Attempted synthesis of 5'- <i>O</i> -(4,4'-dimethoxytrityl)guanosine [139]	347
B.36	Attempted synthesis of 5'- <i>O</i> -(<i>tert</i> -butyldiphenylsilyl)-6- <i>N</i> -(<i>N,N</i> -dimethylmethyl-imine)guanosine [140]	348
B.37	Attempted synthesis of 5'- <i>O</i> -(<i>tert</i> -butyldiphenylsilyl)inosine [141]	350
B.38	Preparation of 5'- <i>O</i> -(<i>tert</i> -butyldiphenylsilyl)adenosine [142]	351
B.39	Attempted synthesis of 5'- <i>O</i> -(4,4'-dimethoxytrityl)adenosine [143]	352
B.40	Preparation of <i>tert</i> -butyldiphenylsilanol [145]	353
B.41	Preparation of 4,4'-dimethoxytrityl alcohol [147]	354
B.42	Preparation of allyl ethyl carbonate [148]	355

B.43	Preparation of bis(dibenzylideneacetone) palladium(0) [149]	356
------	---	-----

Appendix C: Experimental Procedures - Relating to Chapter 3358

C.1	Growth and Purification of Bacteria from Freezer Stocks	359
C.2	Growth and Purification of Bacteria from Freeze-Dried Swabs (as delivered by ATCC)	360
C.3	Preparation of Freezer Stocks	361
C.4	Droplet Plate Technique	362
C.5	Determination of Anti-Bacterial Activity through the use of the Triphenyl Tetrazolium Chloride (TTC) Assay	366
	<i>C.5.1 Preparation of Antibiotic/Compound Stock Solutions</i>	366
	<i>C.5.2 Preparation of Antibiotic/Compound Dilution Series</i>	367
	<i>C.5.3 Preparation of Inoculum</i>	370
	<i>C.5.4 TTC Assay</i>	371
C.6	Anti-viral Assays	374
	<i>C.6.1 Formula for Percentage of Uninfected Treated Cells</i>	375
	<i>C.6.2 Formula for the Percentage Protection</i>	375
	<i>C.6.3 Effective Concentration</i>	375
	<i>C.6.4 Cytotoxic Concentration</i>	376
	<i>C.6.5 Selectivity Index</i>	377

APPENDICES RELATING TO PART 2

Appendix D:	<i>Experimental Procedures - Relating to Chapter 5</i>	379
D.1	Preparation of 1-[(6a <i>R</i> ,8 <i>R</i> ,9 <i>R</i> ,9a <i>S</i>)-9-hydroxy-2,2,4,4-tetraisopropyltetrahydro-6 <i>H</i> -furo[3,2- <i>f</i>][1,3,5,2,4]trioxadisilocin-8-yl]pyrimidine-2,4(1 <i>H</i> ,3 <i>H</i>)-dione [234]	380
D.2	Preparation of 3-benzoyl-1-[(6a <i>R</i> ,8 <i>R</i> ,9 <i>R</i> ,9a <i>S</i>)-9-hydroxy-2,2,4,4-tetraisopropyltetrahydro-6 <i>H</i> -furo[3,2- <i>f</i>][1,3,5,2,4]trioxadisilocin-8-yl]pyrimidine-2,4(1 <i>H</i> ,3 <i>H</i>)-dione [235]	381
D.3	Preparation of 3-benzoyl-1-[(6a <i>R</i> ,8 <i>R</i> ,9 <i>R</i> ,9a <i>R</i>)-9-allyl-9-hydroxy-2,2,4,4-tetraisopropyltetrahydro-6 <i>H</i> -furo[3,2- <i>f</i>][1,3,5,2,4]trioxadisilocin-8-yl]pyrimidine-2,4(1 <i>H</i> ,3 <i>H</i>)-dione [236]	382
D.4	Attempted synthesis of 3-benzoyl-1-[(6a <i>R</i> ,8 <i>R</i> ,9 <i>R</i> ,9a <i>R</i>)-9-crotyl-9-hydroxy-2,2,4,4-tetraisopropyltetrahydro-6 <i>H</i> -furo[3,2- <i>f</i>][1,3,5,2,4]trioxadisilicon-8-yl]pyrimidine-2,4-(1 <i>H</i> ,3 <i>H</i>)-dione [237]	383
D.5	Attempted synthesis of 3-benzoyl-1-[(6a <i>R</i> ,8 <i>R</i> ,9 <i>R</i> ,9a <i>R</i>)-9-cinnamyl-9-hydroxy-2,2,4,4-tetraisopropyltetrahydro-6 <i>H</i> -furo[3,2- <i>f</i>][1,3,5,2,4]trioxadisilocin-8-yl]-pyrimidine-2,4-(1 <i>H</i> ,3 <i>H</i>)-dione [238]	384
D.6	Preparation of 1-[(6a <i>R</i> ,8 <i>R</i> ,9a <i>R</i>)-2,2,4,4-tetraisopropyl-9-oxotetrahydro-6 <i>H</i> -furo[3,2- <i>f</i>][1,3,5,2,4]trioxadisilocin-8-yl]pyrimidine-2,4(1 <i>H</i> ,3 <i>H</i>)-dione [239]	384
D.7	Attempted synthesis of 1-[(6a <i>R</i> ,8 <i>R</i> ,9a <i>R</i>)-tetrahydro-2,2,4,4-tetraisopropyl-9-methylene-6 <i>H</i> -furo[3,2- <i>f</i>][1,3,5,2,4]trioxadisilocin-8-yl]pyrimidine-2,4(1 <i>H</i> ,3 <i>H</i>)-dione [240]	385
D.8	Attempted synthesis of 1-[(6a <i>R</i> ,8 <i>R</i> ,9a <i>S</i>)-tetrahydro-9-hydroxy-2,2,4,4-tetraisopropyl-9-vinyl-6 <i>H</i> -furo[3,2- <i>f</i>][1,3,5,2,4]trioxadisilocin-8-yl]pyrimidine-2,4(1 <i>H</i> ,3 <i>H</i>)-dione [241]	386
D.9	Preparation of 1-[(6a <i>R</i> ,8 <i>R</i> ,9a <i>S</i>)-9-allyl-tetrahydro-9-hydroxy-2,2,4,4-tetraisopropyl-6 <i>H</i> -furo[3,2- <i>f</i>][1,3,5,2,4]trioxadisilocin-8-yl]pyrimidine-2,4(1 <i>H</i> ,3 <i>H</i>)-dione [242]	387

D.10	General procedure for the synthesis of 5'- <i>O</i> -silyl protected uridine derivatives	388
	<i>D.10.1 Attempted synthesis of 5'-O-(dimethylethylsilyl)uridine [243]</i>	389
	<i>D.10.2 Attempted synthesis of 5'-O-(dimethylvinylsilyl)uridine [244]</i>	389
	<i>D.10.3 Attempted synthesis of 5'-O-(allyldimethylsilyl)uridine [245]</i>	390
	<i>D.10.4 Preparation of 5'-O-(triisopropylsilyl)uridine [246]</i>	390
	<i>D.10.5 Preparation of 5'-O-(tert-butyl dimethylsilyl)uridine [229]</i>	391
	<i>D.10.6 Preparation of 5'-O-(triisobutylsilyl)uridine [247]</i>	392
	<i>D.10.7 Preparation of 5'-O-(dimethylhexylsilyl)uridine [248]</i>	393
	<i>D.10.8 Preparation of 5'-O-(trihexylsilyl)uridine [249]</i>	394
D.11	Preparation of 5'- <i>O</i> -(tripropylsilyl)-5-methyluridine [250]	395
D.12	Preparation of 5'- <i>O</i> -(tert-butyl dimethylsilyl)-5-methyluridine [251]	396
D.13	Preparation of 5'- <i>O</i> -(dimethylhexylsilyl)-5-methyluridine [252]	397
D.14	Preparation of 5'- <i>O</i> -(tert-butyl diphenylsilyl)-5-methyluridine [253]	398
D.15	Preparation of 1-[(6 <i>aR</i> ,8 <i>R</i> ,9 <i>S</i> ,9 <i>aR</i>)-tetrahydro-9-hydroxy-2,2,4,4-tetraisopropyl-6 <i>H</i> -furo[3,2- <i>f</i>][1,3,5,2,4]trioxadisilocin-8-yl](5-methylpyrimidine)-2,4(1 <i>H</i> ,3 <i>H</i>)-dione [254]	399
D.16	General procedure for the preparation of silanols	400
	<i>D.16.1 Preparation of dimethylethylsilanol [255]</i>	400
	<i>D.16.2 Preparation of triethylsilanol [176]</i>	401
	<i>D.16.3 Preparation of tripropylsilanol [256]</i>	401
	<i>D.16.4 Preparation of triisopropylsilanol [257]</i>	402
	<i>D.16.5 Preparation of butyl dimethylsilanol [258]</i>	402
	<i>D.16.6 Preparation of tributylsilanol [259]</i>	403
	<i>D.16.7 Preparation of triisobutylsilanol [260]</i>	403

D.16.8	<i>Preparation of tert-butyldimethylsilanol [261]</i>	404
D.16.9	<i>Preparation of dimethylhexylsilanol [262]</i>	404
D.16.10	<i>Preparation of trihexylsilanol [263]</i>	405
D.16.11	<i>Preparation of cyclohexyldimethylsilanol [264]</i>	405
D.16.12	<i>Preparation of benzyldimethylsilanol [265]</i>	406
D.16.13	<i>Preparation of triphenylsilanol [266]</i>	407
D.16.14	<i>Preparation of 1,3-dihydroxy-1,1,3,3-tetraisopropylidisiloxane [268]</i>	407
Appendix E: Experimental Procedures - Relating to Chapter 6		408
E.1	General Procedure for Confocal Scanning Laser Microscopy (CSLM)	409
E.1.1	Sample Preparation	409
	Ⓢ General Culture Conditions	409
	Ⓢ General Procedure for the Preparation of Bacterial Suspensions	410
	Ⓢ General Procedure for Staining of Bacteria in Suspension	411
E.1.2	Sample Analysis	411
E.2	General Procedure for Scanning Electron Microscopy (SEM)	412
E.2.1	Sample Preparation	412
	Ⓢ General Culture Conditions - Untreated Controls	412
	Ⓢ General Culture Conditions - Treatment with Synthetic Compounds and Antibiotic	412
	Ⓢ General Dehydration Procedure	413
	Ⓢ Critical Point Drying and Sample Mounting	414
E.2.2	Sample Analysis	415

Appendix F: Experimental Procedures - Relating to Chapter 8416

F.1 General Experimental Procedure for Multiple Protecting Group Additions417

SUPPORTING INFORMATION PROVIDED ON DVD

Supporting Information – Selected NMR Spectra - 1 -

- 1'-*O*-Methoxy- β -(-)-ribose [101] - 2 -
- 5'-*O*-(*tert*-Butyldiphenylsilyl)-1'-*O*-methoxy- β -(-)-ribose [102] - 3 -
- 2',3'-*O*-Diallyl-5'-*O*-(*tert*-butyldiphenylsilyl)-1'-*O*-methoxy- β -(-)-ribose [103] - 4 -
- 5'-*O*-(4,4'-Dimethoxytrityl)-1'-*O*-methoxy- β -(-)-ribose [105] - 5 -
- 5'-*O*-(*tert*-Butyldiphenylsilyl)uridine [107] - 6 -
- 3-*N*-Allyl-5'-*O*-(*tert*-butyldiphenylsilyl)uridine [109] - 7 -
- 3-*N*-Allyl-2'-*O*-allyl-5'-*O*-(*tert*-butyldiphenylsilyl)uridine [110] - 8 -
- 3-*N*-Allyl-3'-*O*-allyl-5'-*O*-(*tert*-butyldiphenylsilyl)uridine [111] - 9 -
- 6-*N*-(*N,N*-Dimethylmethylimine)guanosine [112] - 10 -
- 5'-*O*-(4,4'-Dimethoxytrityl)-6-*N*-(*N,N*-dimethylmethylimine)guanosine [113] - 11 -
- 2',3'-*O*-Diallyl-5'-*O*-(4,4'-dimethoxytrityl)-6-*N*-(*N,N*-dimethylmethylimine)guanosine [114] - 12 -
- 5'-*O*-(4,4'-Dimethoxytrityl)inosine [117] - 13 -
- 2',3'-*O*-Diacetyl-5'-*O*-(*tert*-butyldiphenylsilyl)-1'-*O*-methoxy- β -(-)-ribose [119] - 14 -
- 2',3'-*O*-Diacetyl-5'-*O*-(4,4'-dimethoxytrityl)-1'-*O*-methoxy- β -(-)-ribose [120] - 15 -
- 2',3',5'-*O*-Triacetyl-1'-*O*-methoxy- β -(-)-ribose [121] - 16 -
- 2',3',5'-*O*-Triallyl-1'-*O*-methoxy- β -(-)-ribose [122] - 17 -
- 2',3'-*O*-Diacetyl-5'-*O*-(*tert*-butyldiphenylsilyl)uridine [123] - 18 -
- 3-*N*-Benzoyl-2',3'-*O*-diacetyl-5'-*O*-(*tert*-butyldiphenylsilyl)uridine [124] - 19 -
- 2',3'-*O*-Diacetyl-5'-*O*-(4,4'-dimethoxytrityl)uridine [127] - 20 -
- 3-*N*-Benzoyl-2',3'-*O*-diacetyl-5'-*O*-(4,4'-dimethoxytrityl)uridine [128] - 21 -
- 2',3',5'-*O*-Triacetyluridine [130] - 22 -

• 3- <i>N</i> -Benzoyl-2',3',5'- <i>O</i> -triacetyluridine [131]	- 23 -
• 4- <i>N</i> -Benzoylcytidine [133]	- 24 -
• 5'- <i>O</i> -(<i>tert</i> -Butyldiphenylsilyl)cytidine [134]	- 25 -
• 5'- <i>O</i> -(<i>tert</i> -Butyldiphenylsilyl)adenosine [142]	- 26 -
• <i>tert</i> -Butyldiphenylsilanol [145]	- 27 -
• 4,4'-Dimethoxytrityl alcohol [147]	- 28 -
• Allyl ethyl carbonate [148]	- 29 -
• Bis(dibenzylideneacetone) palladium(0) [149]	- 30 -
• 2',3'- <i>O</i> -Dibenzoyl-5'- <i>O</i> -(<i>tert</i> -butyldiphenylsilyl)uridine [150]	- 31 -

Supporting Information – Selected Graphs of Biological Assay Data - 32 -

• Supporting Information from TTC Assay for Anti-Bacterial Activity – “First Generation Compounds”	- 33 -
• □(-)- <i>Ribose Derivatives</i>	- 33 -
• <i>Pyrimidine Based Nucleoside Derivatives</i>	- 38 -
• <i>Purine Based Nucleoside Derivatives</i>	- 44 -
• <i>Protecting Group Derivatives</i>	- 48 -
• Supporting Information from TTC Assay for Anti-Bacterial Activity – “Second Generation Compounds”	- 49 -
• <i>Uridine Derivatives</i>	- 49 -
• <i>5-Methyluridine Derivatives</i>	- 53 -
• <i>Silanol Derivatives</i>	- 56 -
• Supporting Information from XTT Assay for HIV Activity – “First Generation Compounds”	- 62 -

Abbreviations

List of General Abbreviations

A (base)	adenine
ADMET	acyclic cross metathesis for polymer formation
ADP	adenosine-5'-diphosphate
AIDS	Acquired Immune Deficiency Syndrome
AMP	adenosine-5'-monophosphate
ATCC	American Type Culture Collection
ATP	adenosine-5'-triphosphate
AZT	azidothymidine, also known as Zidovudine, marketed commercially as Retrovir TM
BacLight (Live/Dead)	bacterial staining kit containing two fluorescent dyes: SYTO 9 and propidium iodide
BSAC	British Society of Antimicrobial Chemotherapy
C (base)	cytosine
cAMP	3',5'-cyclic-adenosine monophosphate
CC ₅₀	50 % cytotoxic concentration
CFC	cefalotin sodium additive
cfu	colony forming units
CML	chronic myeloid leukemia
CMV	cytomegalovirus

CSLM	confocal scanning laser microscopy
dADP	2'-deoxyadenosine-5'-diphosphate
dAMP	2'-deoxyadenosine-5'-monophosphate
dATP	2'-deoxyadenosine-5'-triphosphate
DNA	deoxyribonucleic acid
EC ₅₀	50 % effective concentration
EIA	enzyme immunometric assay, also known as ELISA
ELISA	enzyme-linked immunosorbent assay
EPS	extracellular polymeric substances
FAD	flavin adenine dinucleotide, a coenzyme
FDA	United States Food and Drug Administration
FTIR	Fourier transform infrared
G (base)	guanine
ΔG^0	Gibbs Free Energy
GP	general practitioner
HBV	hepatitis B virus
HCV	hepatitis C virus
HIV	human immunodeficiency virus
HRMS	high resolution mass spectrometry
HTLV _{III} B	HIV virus strain used in XTT assay
HSV	herpes simplex virus
I (base)	inosine
IP	intellectual property

IR	infrared
LRMS	low resolution mass spectrometry/spectrum
MIC	minimum inhibitory concentration
MP	melting point
mRNA	messenger RNA - a ribonucleic acid whose sequence is complementary to that of a protein-coding gene in DNA
NAD ⁺	nicotinamide adenine dinucleotide
NADP ⁺	nicotinamide adenine dinucleotide phosphate
NHLS	National Health Laboratory Services
NMR	nuclear magnetic resonance
NSAID	non-steroidal anti-inflammatory drug
RCM	ring closing metathesis
R_f	retention factor, defined as the distance travelled by the compound divided by the distance travelled by the solvent
RNA	ribonucleic acid
ROMP	ring-opening metathesis polymerisation
RPMI	"complete medium" (tissue culture medium)
rRNA	ribosomal RNA - the RNA molecules that constitute the bulk of the ribosome, the site of polypeptide synthesis
RSV	respiratory syncytial virus
rt	room temperature
RXR	retinoid X receptor
<i>S</i> -AdoMet	<i>S</i> -adenosyl methionine
SAR	structure activity relationship

SEM	scanning electron microscopy
SI	selectivity index
T (base)	thymine
TBX	tryptone, bile salts, X-glu and agar
tlc	thin layer chromatography
tRNA	transfer RNA - small L-shaped RNAs that deliver specific amino acids to ribosomes according to the sequence of a bound mRNA
U (base)	uracil
VSV	varicella-zoster virus
WBC	white blood cells
WHO	World Health Organisation
Wits	University of the Witwatersrand

List of Chemical Abbreviations

Ac	acetyl
All	allyl
Bz	benzoyl
DMAP	4-(dimethylamino)pyridine
DMF	<i>N,N</i> -dimethylformamide
DMMI	<i>N,N</i> -dimethylmethyimine
d ₆ -DMSO	deuterated dimethylsulfoxide

DMT	4,4'-dimethoxytrityl
DMT-Cl	4,4'-dimethoxytrityl chloride
DNPH	2,4-dinitrophenylhydrazine
dppb	bis(diphenylphosphino)butane
EtOAc	ethyl acetate
FITC	fluorescein isothiocyanate
Grubbs II catalyst	Grubbs catalyst 2nd generation, benzylidene[1,3-bis(2,4,6-trimethylphenyl)-2-imidazolindinylidene]dichloro(tricyclohexylphosphine)ruthenium
Hünig's Base	<i>N,N</i> -diisopropylethylamine
Me	methyl
MTT	3-(4,5-dimethylthiazol-2-yl)-2,5-diphenyltetrazolium bromide
NaH	sodium hydride (purchased as a 60 % suspension in oil)
NP-40	synperonic NP9 (surfactant)
PBS	phosphate buffered saline
Pd(dba) ₂	bis(dibenzylideneacetone) palladium(0)
PI	propidium iodide
PMS	phenazine methosulfate
PS	phosphatidylserine
TBDPS	<i>tert</i> -butyldiphenylsilyl
TBDPS-Cl	<i>tert</i> -butyldiphenylsilyl chloride
THF	tetrahydrofuran
<i>p</i> -TsOH.H ₂ O	<i>para</i> -toluenesulfonic acid monohydrate
TTC	2,3,5-triphenyltetrazolium chloride

XTT 2,3-bis-(2-methoxy-4-nitro-5-sulfophenyl)-2*H*-tetrazolium-5-carboxyanilide

List of Cell Lines

833K (<i>solid cell line</i>)	human teratorcarcinoma cells
A2780 (<i>solid cell line</i>)	human ovarian cancer cells
B16F10 (<i>adherent cells</i>)	mouse melanoma cell line
Caco2 (<i>adherent cells</i>)	human epithelial colorectal adenocarcinoma cells
DC-3F	hamster lung cells
HeLa (<i>solid cell line</i>)	human cervix cancer cells
HL60 (<i>suspension cells</i>)	human promyelocytic leukemia cells
Hs683 (<i>adherent cells</i>)	human glioma cell line
HT-1080	human lung fibrosarcoma cells
HT29 (<i>adherent cells</i>)	human colorectal adenocarcinoma cells
Jurkat (<i>suspension cells</i>)	human T lymphocyte cells
K562 (<i>suspension cells</i>)	human myelogenous leukemia cells
MCF-7 (<i>adherent cells</i>)	human breast cancer cells
MDA-MB-435	human melanoma cell line used as a model of metastatic human breast cancer
MiaPaCa-2	human pancreatic cell line
MT-4 (<i>suspension cells</i>)	human T-cell (blood/immune cells) leukemia cell line
NiH 3T3 cells	mouse fibroblast cells

PC-3 (<i>adherent cells</i>)	human prostate cancer cell line
SKMEL-28 (<i>adherent cells</i>)	human melanoma cell line
SNB-19	human central nervous system cell line – derived from same individual as U251
SW1573 (<i>solid cell line</i>)	human non-small cell lung cancer
T-47D (<i>solid cell line</i>)	human breast cancer cells
U251	human central nervous system cell line – derived from same individual as SNB-19
U373 (<i>adherent line</i>)	human glioma cell line
WiDr (<i>solid cell line</i>)	human colon cancer cells

Quote

So, why don't you come up to the lab and see what's on the slab...

I see you shiver, with AN-TICI-PATION!!!

~ Frank 'n Furter

PART 1 - FIRST GENERATION COMPOUNDS

***Synthesis and Biological Testing of Various
Nucleoside and α -(-)-Ribose Derivatives***

Chapter 1:
Introduction

1.1 GENERAL INTRODUCTION: BASES, NUCLEOSIDES AND NUCLEOTIDES

As a class, the *bases*, sugar-coupled *nucleosides* and the phosphorylated-nucleosides, the *nucleotides*, may be considered as the most important metabolites of the cell. The nucleotides are found primarily as the monomeric units, comprising the major nucleic acids of the cell: ribonucleic acid (RNA) and deoxyribonucleic acid (DNA). However, they are also required for numerous other important functions within the cell.¹

1.1.1 Base, Nucleoside and Nucleotide Structures and Nomenclature

The nucleosides and nucleotides found in all cells are derivatives of the heterocyclic compounds, purine **1** and pyrimidine **2**.¹ These heterocyclic compounds are illustrated in **Figure 1**.

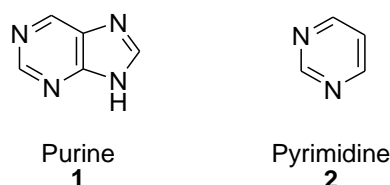


Figure 1 Structures of purine and pyrimidine heterocycles

It is the chemical basicity of the purine and pyrimidine heterocycles that has given them the common term "*bases*".¹ There are five major bases found in the DNA and RNA of cells. The derivatives of purine are known as adenine **3** and guanine **4**, and the derivatives of pyrimidine are known as thymine **5**, cytosine **6** and uracil **7**. The common abbreviations used for these five bases are: A, G, T, C and U.¹ The structures of each of the five bases are shown for clarity in **Figure 2**.

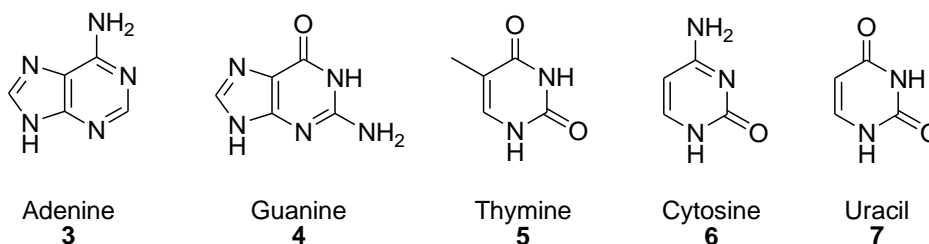


Figure 2 Structures of the five major purine and pyrimidine bases

There are also several other less common bases found in DNA and RNA, with 5-methylcytosine observed as the primary modified base. A variety of other modified bases occur in the transfer RNA strands (tRNA).¹

The purine and pyrimidine bases in the cells are linked to carbohydrates and in this form are termed *nucleosides*. The bases described in detail above are coupled to either α -ribose or 2'-deoxy- α -ribose through a β -*N*-glycosidic bond between the anomeric carbon of the ribose and the N^9 -position of a purine or the N^1 -position of a pyrimidine base.¹ The carbon atoms of the ribose ring are designated with a prime mark (') to distinguish them from the backbone numbering used in the bases.

This gives rise to the five major nucleosides:

- two purine-based nucleosides - adenosine **8** and guanosine **9**
- three pyrimidine-based nucleosides - thymidine **10**, cytidine **11** and uridine **12**

which are illustrated in **Figure 3**.

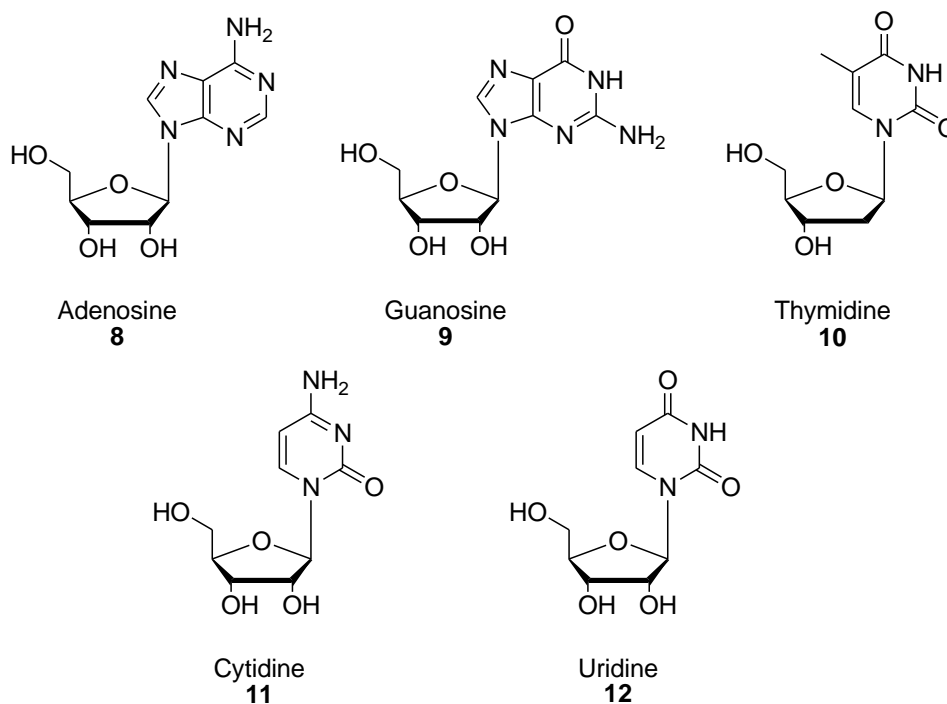


Figure 3 Structures of the five major nucleosides²

The base can exist in two distinct orientations about the *N*-glycosidic bond, which are illustrated through the use of adenosine **8** in **Figure 4** below. These conformations are identified as *syn* (*syn-8*) and *anti* (*anti-8*).¹ In naturally-occurring nucleosides, the *anti* conformation predominates, and as such will be the representation of choice used throughout this thesis.

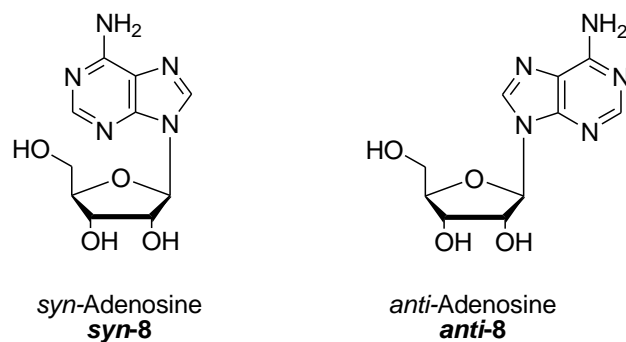


Figure 4 Possible orientations about the *N*-glycosidic bond for adenosine **8**¹

Nucleosides are found in the cell primarily in their phosphorylated form and are termed *nucleotides*. The most common site of phosphorylation of the nucleotides is on the 5'-carbon position of ribose.^{3a} Nucleotides can exist in the mono-, di- or tri-phosphorylated forms. The different levels of phosphorylation are highlighted in **Figure 5** by comparison of the various forms of adenosine, namely: adenosine **8**, adenosine-5'-monophosphate **13**, adenosine-5'-diphosphate **14** and adenosine-5'-triphosphate **15**.

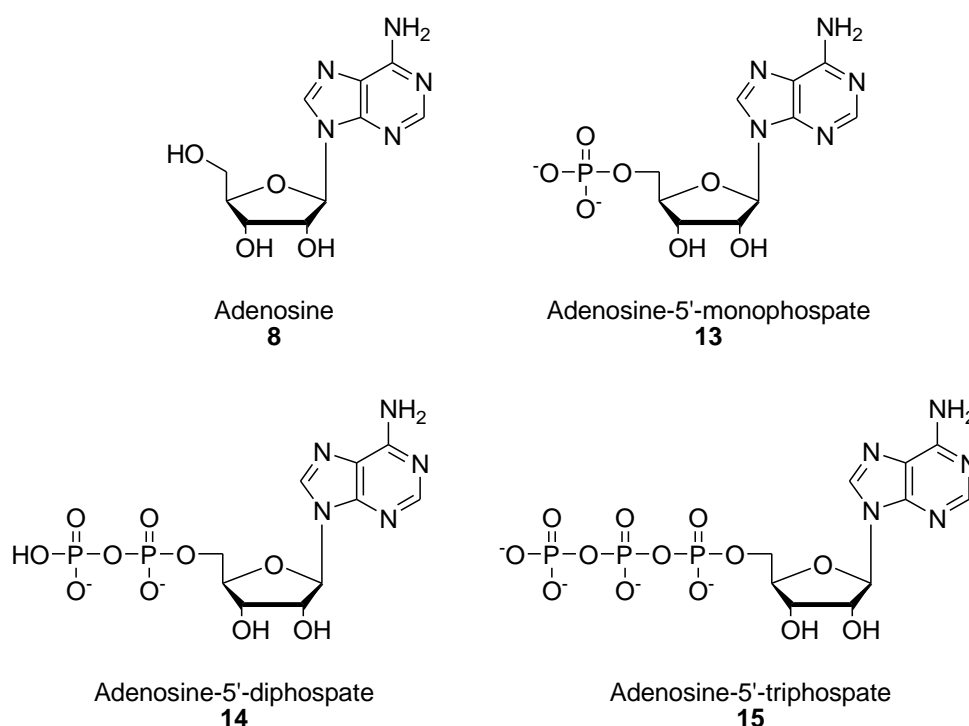


Figure 5 Various phosphorylated forms of adenosine **8**^{3a}

Nucleotides are given distinct abbreviations to allow for easy identification of their structure and state of phosphorylation. Using the example of adenosine illustrated in **Figure 5**,^{3a}

- adenosine-5'-monophosphate **13** is abbreviated as *AMP*
- adenosine-5'-diphosphate **14** is abbreviated as *ADP*
- adenosine-5'-triphosphate **15** is abbreviated as *ATP*

Note that the use of these abbreviations assumes that the nucleotide is in the 5'-phosphorylated form.

As observed in **Figure 5**, the di- and tri-phosphates of the nucleotides are linked by an acid anhydride series of bonds. The acid anhydride bonds have a high ΔG^0 (Gibbs Free Energy) for hydrolysis, giving them a high potential to transfer the phosphate group to other molecules.¹ In a nutshell, it is this property of the nucleotides that results in their involvement in group transfer reactions within the cell.

The nucleotides found in DNA are unique from those found in RNA. In DNA the ribose exists in the 2'-deoxy form and the abbreviations of the nucleotides contain a "d" designation.^{3a} The structures of the deoxyribonucleotides are illustrated in **Figure 6**.

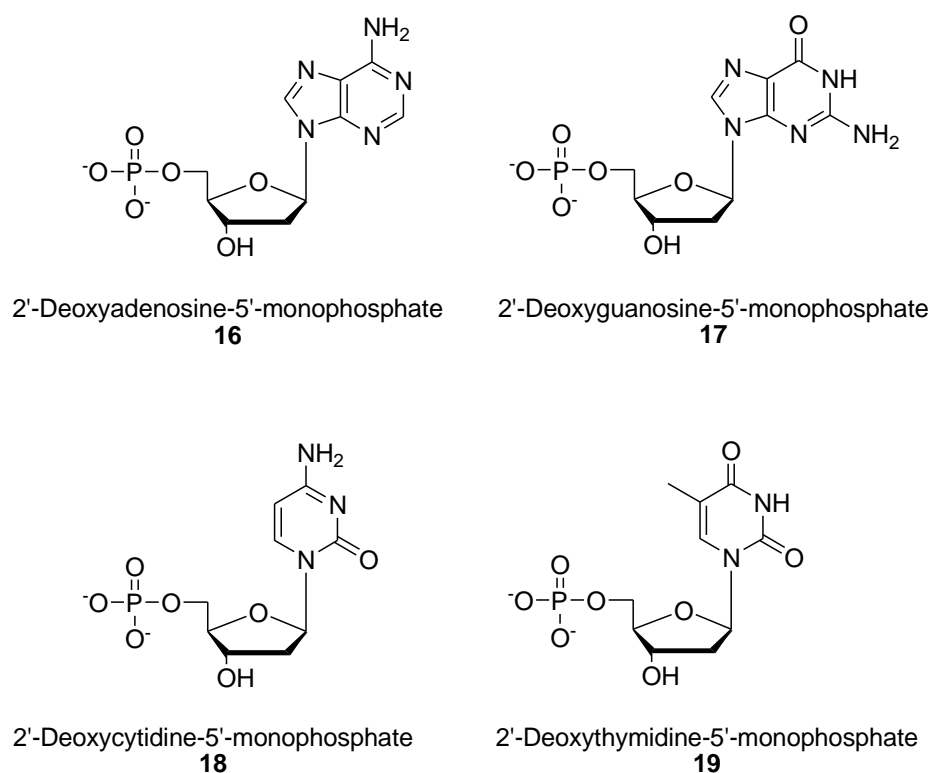


Figure 6 Structures of the deoxyribonucleotides present in DNA

The abbreviations used for DNA are given here in **Figure 7**, again using the derivatives of adenosine:

- 2'-deoxyadenosine **20** is abbreviated as *dA*
- 2'-deoxyadenosine-5'-monophosphate **16** is abbreviated as *dAMP*
- 2'-deoxyadenosine-5'-diphosphate **21** is abbreviated as *dADP*
- 2'-deoxyadenosine-5'-triphosphate **22** is abbreviated as *dATP*

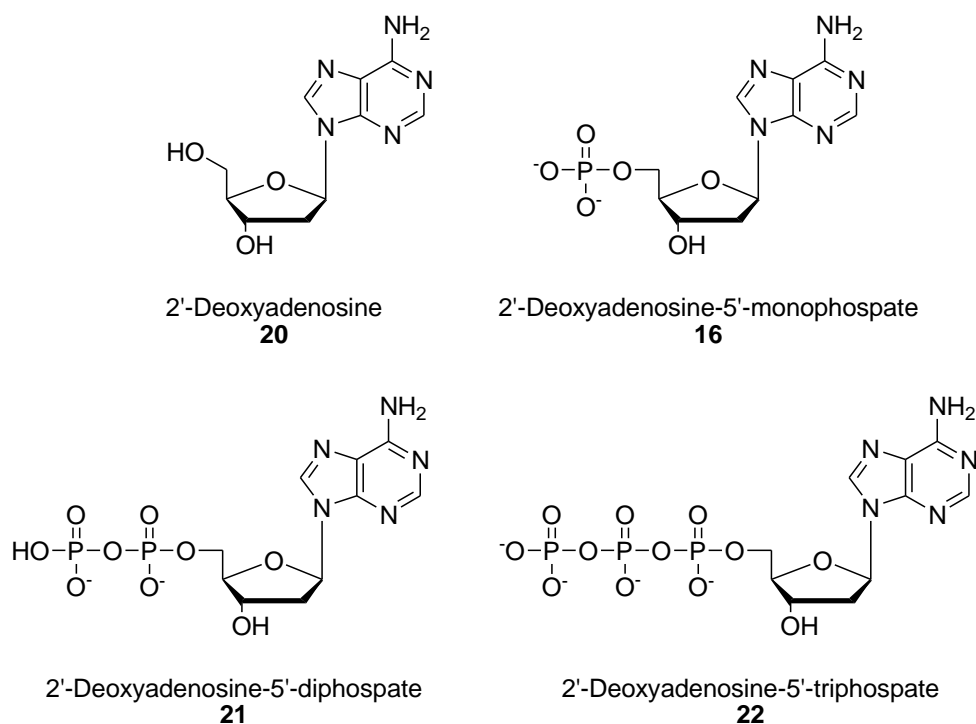


Figure 7 Various phosphorylated forms of deoxyadenosine **20**

The nucleotide uridine is never found in DNA (*ie.*: it is only present in RNA). Thymine is almost exclusively found in DNA, with thymine present in transfer RNA (tRNA) but *not* in ribosomal RNA (rRNA) or messenger RNA (mRNA).

1.1.2 Watson-Crick Model for Base-Pairing in DNA

In 1953, using X-ray diffraction data obtained from crystals of DNA, James Watson and Francis Crick proposed a model for the structure of DNA. This model was subsequently verified using additional nuclear magnetic resonance and spectroscopic data.^{3b} The model predicted that DNA would exist as a helix of two complementary anti-parallel strands, wound around each other in a rightward direction and were stabilized by hydrogen bonding (H-bonding) between the bases in the adjacent strands.

In the Watson-Crick model, the bases are in the interior of the helix aligned at a nearly 90° angle relative to the axis of the helix. Purine bases form H-bonds with pyrimidine bases, in the crucial phenomena of base-pairing (shown in **Figure 8** below). Using experimental data, they were able to show that in any given molecule of DNA, the concentration of adenine **3** equals the concentration of thymine **5**, and the concentration of cytosine **6** equals the concentration of guanine **4**. This pattern gives rise to *A-T* base-pairs containing two H-bonds and *G-C* base-pairs containing three H-bonds between the corresponding bases.^{3b} These are illustrated as the hashed bonds drawn in *red* in **Figure 8**.

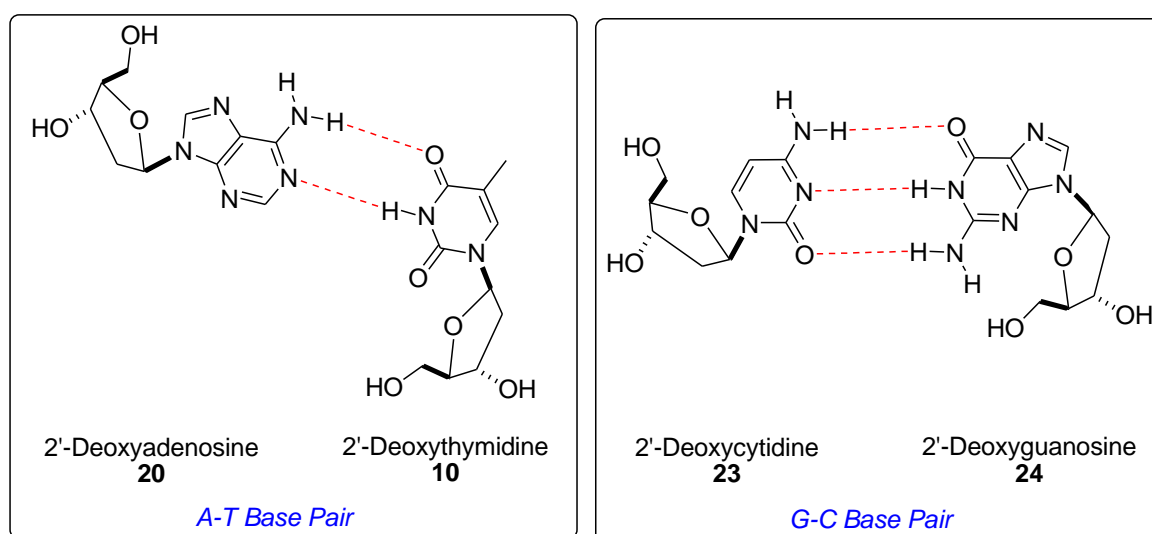


Figure 8 Chemical representation of the Watson-Crick base pairs found in DNA^{3b}

The anti-parallel nature of the helix stems from the orientation of the individual strands. From any position in the helix, one strand is orientated in the 5' -> 3' direction, and the other strand is orientated in the 3' -> 5' direction. On the exterior surface, the double helix of DNA contains two deep grooves between the ribose-phosphate chains. The grooves are of unequal size, due to the asymmetry of the deoxyribose rings as well as the structurally distinct nature of the upper surface of the base-pair relative to the lower surface. These are referred to as the major and minor grooves.^{3b} The most common of the several forms of the DNA double helix that have been shown to exist (not discussed in detail in the thesis) is illustrated in **Figure 9**.



Figure 9 Diagrammatic representation of base-pairing observed in the DNA double-helix^{3b}

Many modified nucleotides are also encountered outside of the context of DNA and RNA where they serve several other important biological functions. These functions include:

- serving as energy stores for future use in phosphate transfer reactions (which are predominantly carried out by ATP)¹
- forming a portion of several important coenzymes, such as NAD⁺, NADP⁺, FAD and coenzyme A¹
- serving as mediators of numerous important cellular processes, such as secondary messengers in signal transduction events. The predominant secondary messenger is 3',5'-cyclic-adenosine-monophosphate (cAMP), which is a cyclic derivative of AMP

formed from ATP, that is involved in passing signal transduction events from the cell surface to internal proteins (e.g.: cAMP dependent protein kinase)¹

- controlling enzymatic reactions through allosteric effects on enzyme activity¹
- having a role as endogenous ligands of G protein-coupled purinergic receptors^{1b}
- serving as activated intermediates in numerous biosynthetic reactions. These activated intermediates include *S*-adenosylmethionine (*S*-AdoMet) which is involved in methyl transfer reactions, as well as the many sugar coupled nucleotides (nucleosides) which are involved in glycogen and glycoprotein synthesis.¹

Numerous base, nucleoside and nucleotide analogues have been chemically synthesized and these have found various biological uses based on their often interesting therapeutic potential. The biological applications of the *nucleosides* are discussed in detail in **Section 1.2**, and as such, are excluded from this section.

Synthetic analogues of both the bases and the nucleotides have been utilized to inhibit specific enzymatic activities, an example of this is in the use of these analogues as anti-tumour agents. These work because they effectively interfere with the synthesis of DNA and thereby preferentially kill the rapidly dividing tumour cells.⁴ Some of the base analogues commonly used in chemotherapy are: (i) 6-mercaptopurine **25**, (ii) 5-fluorouracil **26** and (iii) 6-thioguanine **27** (structures shown in **Figure 10**).⁴ Each of the compounds **25**, **27** and **28** disrupts the normal DNA replication process by interfering with the formation of the correct Watson-Crick base-pairs.

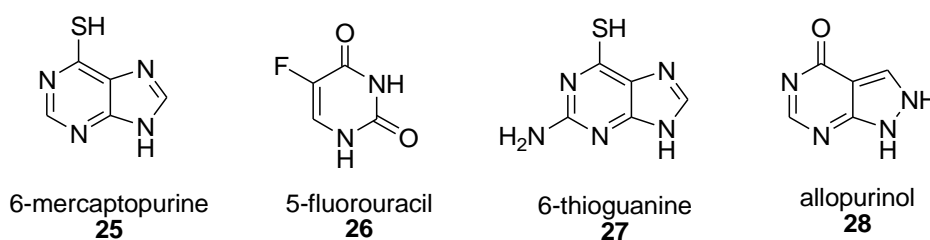


Figure 10 Synthetic base analogues used in cancer chemotherapy or the treatment of gout

Additional applications of the bases and nucleotides in current medicine include the use of several purine analogues for the treatment of gout. The most common is allopurinol **28** (**Figure 10**), which resembles hypoxanthine. Allopurinol inhibits the activity of xanthine oxidase, an enzyme involved in *de novo* purine biosynthesis.⁴ Several other nucleotide analogues are used after organ transplantation in order to suppress the immune system and reduce the likelihood of transplant rejection by the host.

1.2 INTRODUCTION TO BIOLOGICAL APPLICATIONS OF NUCLEOSIDES - WITH A CLOSER LOOK AT CURRENT NUCLEOSIDE BASED DRUGS

Nucleosides and their analogues are of enormous importance. They are an established class of clinically useful medicinal agents possessing antiviral and anticancer activity; at the same time they are one class of compounds worthy of further investigation as antibacterial agents since some derivatives have shown moderate to good activity against specific bacterial strains.⁴ This has led to our interest in the search for new nucleoside derivatives that may be screened for broad-spectrum biological activity. Please note that in the proceeding sections, we will not give a detailed discussion to the carbohydrate portions of the nucleoside molecules themselves, even though the carbohydrates are used as reference molecules for some of the biological assays conducted. The field of medicinal carbohydrate chemistry is very rich and for a more comprehensive read, please refer to the recently published "Carbohydrate-Based Drug Discovery" edited by Wong (2006, Wiley-VCH) and "Carbohydrate Drug Design" edited by Klesov, Witczak and Platt (2006, American Chemical Society Symposium Series).

1.2.1 Nucleoside Derivatives Used in the Treatment of Viral Diseases

Viral diseases remain among the greatest causes of human morbidity and economic loss for both the developed and the developing nations. The leading cause of GP/doctor's room consultations is for infectious disease problems, with the average person in the developed countries having between two and six viral infections per year.⁵

The current antiviral drug armamentarium comprises almost 40 compounds that have been officially approved for clinical use.⁶ Most of the approved drugs date from the last five years, and at least half of them are used in the treatment of human immunodeficiency virus (HIV) infections. The other antivirals that are currently available are primarily used for the treatment of hepatitis B virus (HBV), hepatitis C virus (HCV), herpes virus [herpes simplex virus (HSV), varicella-zoster virus (VSV), and cytomegalovirus (CMV)], influenza virus and respiratory syncytial virus (RSV) infections.⁶

HIV/AIDS has become the most devastating pandemic in recorded history. It has killed 40 million people in the last 20 years and the World Health Organization (WHO) estimated that at least 14 000 new infections occurred daily in 2001.⁷ According to figures from the WHO 2002 statistics, an estimated 36.1 million people worldwide are presently infected with HIV and they estimate there will be up to 100 million new infections in the next 10 years.⁸ Most HIV infections occur in the developing world, and the adverse social and economic impact of the HIV/AIDS pandemic, particularly in the developing world, is unprecedented.

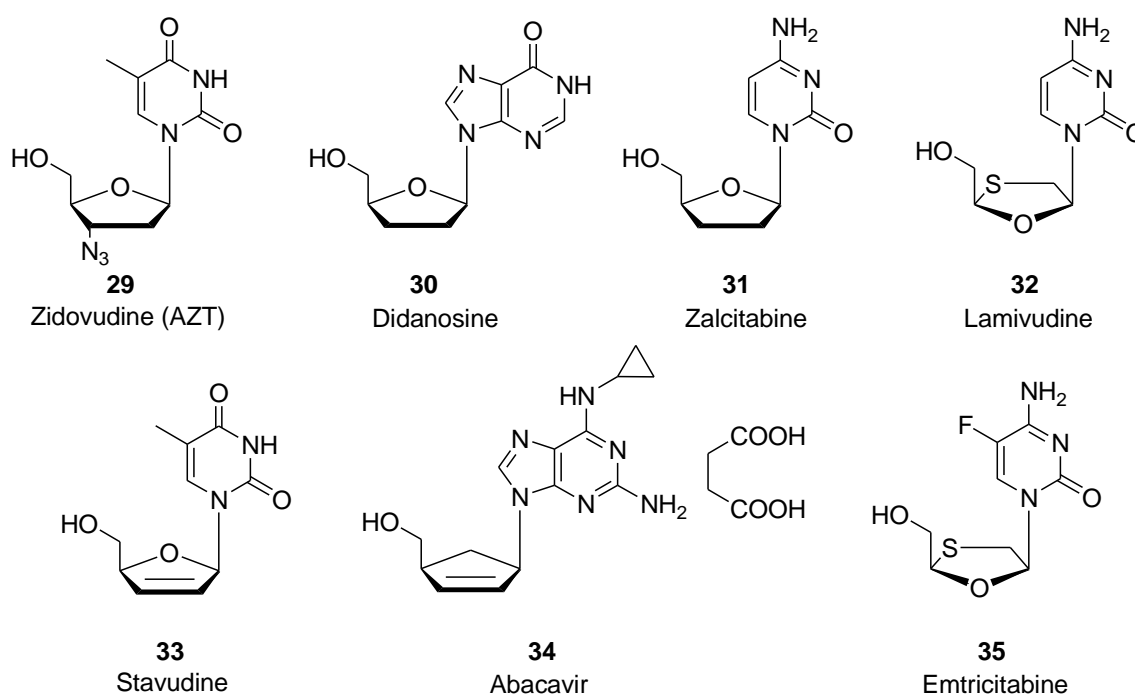


Figure 11 Selected examples of nucleoside based drugs currently used in the treatment of HIV⁸

To date, 19 drugs have been formally approved for the treatment of HIV infections. They are classified as: (i) the nucleoside reverse transcriptase inhibitors, (ii) the nucleotide reverse transcriptase inhibitors, (iii) the non-nucleoside reverse transcriptase inhibitors, (iv) the protease inhibitors and (v) the viral entry inhibitors.⁸ The large number of nucleoside-based anti-HIV drugs available has been inspirational to our synthesis and examples of the nucleoside based drugs for the treatment of HIV are shown in **Figure 11**.

1.2.2 Nucleoside Derivatives Used in the Treatment of Cancer

Approximately one in four deaths in the United States are caused by cancer, and in 2005 cancer overtook heart disease as the top killer of Americans under the age of 85.⁹ Despite dramatic advances in our understanding of the underlying biology of the disease, cancer death rates have remained constant, at roughly 200 deaths per 100 000 people, over the last thirty years - highlighting the need for new therapeutic agents.¹⁰

The biosynthesis of nucleotides is the limiting process in cell proliferation. Many of the enzymes involved in these pathways are highly active in cancer cells, but barely detectable in non-proliferating cells. Thus, nucleoside analogues that inhibit nucleotide biosynthesis are of great interest for cancer chemotherapy.

The nucleoside analogue 5-fluoro-2'-deoxyuridine **36** is an inhibitor of thymidylate synthase and has been used clinically for the treatment of leukemia and colorectal cancer for more than three decades. More recently, gemcitabine (2',2'-difluoro-2'-deoxycytidine) **37** has shown great promise for the treatment of pancreatic cancer. L-(-)-3'-Oxa-2',3'-dideoxycytidine **38** showed interesting activity against hepatocellular and prostate tumours which are generally difficult to treat, and is thus a promising new clinical candidate.¹¹

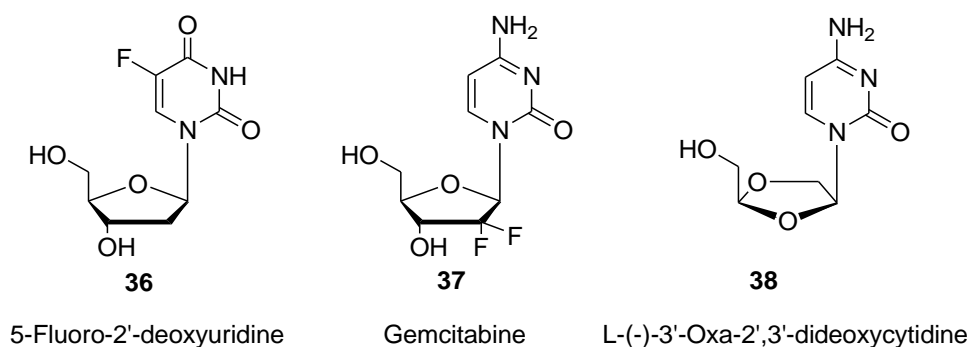


Figure 12 Examples of nucleoside analogues investigated for the treatment of cancer

1.2.3 Nucleoside Derivatives Used as Antibiotics

Since the first known use of antibiotics by the Chinese more than 2 500 years ago, a research field with immense importance for the welfare of mankind has been developed. After a decrease in interest in this topic by the end of the 20th century, the occurrence of multi-resistant strains of bacteria and the so-called “superbugs” over the past 30 years induced a revival of antibiotics research.¹² Today the most devastating of the bacterial diseases is tuberculosis, with an estimated 2 million people dying from it each year.¹²

Nucleoside antibiotics are found in a large structural variety featuring nucleosides in conjugation with other components, such as peptides, lipids, extra carbohydrate moieties and many more, sometimes unusual compositions. The structural features of nucleosides in particular indicate their potential for interacting and interfering with DNA and RNA and the related enzyme machinery.¹² Examples of nucleoside containing antibiotics are outlined in **Figure 13**.

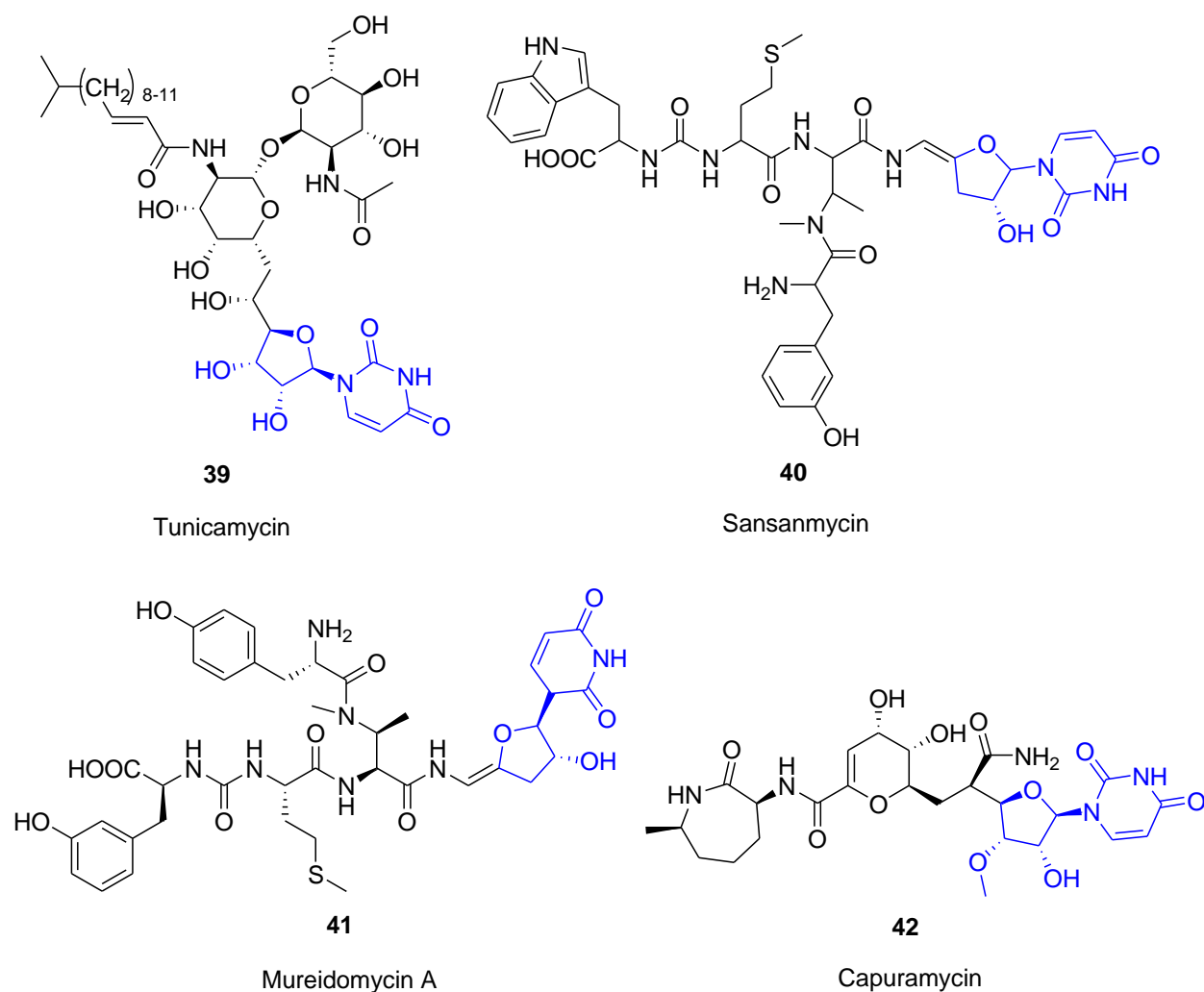


Figure 13 Nucleoside antibiotics (nucleoside core highlighted in blue)¹²

Many of these nucleoside antibiotic structures show promising activities against several bacterial strains and thus have great potential as antibacterial agents. However, they do suffer from a number of disadvantages, such as poor adsorption, complexity, chemical lability, moderate cell entry ability and most importantly, lack of selectivity and cross-activity in mammalian cells.¹² Hence, no nucleoside agent is in current clinical use for antibacterial treatment.

Clearly the ability to synthesize modified nucleosides has favourably impacted a wide range of biomedical research, including the clinical treatment of disease. They have advanced our understanding of many vital biochemical processes involving nucleotides and nucleic acids. As such, methods for the synthesis of modified nucleosides are of general interest and widespread importance.

1.3 CONFORMATIONALLY RESTRICTED NUCLEOSIDE ANALOGUES

Despite the wide number of nucleoside analogues reported, only a few effective compounds have been obtained. This inactivity may be due to either low intracellular metabolism into the corresponding nucleotide derivatives or lack of activity of such a nucleotide on the target enzyme.¹³ In the course of the search for new agents with a higher therapeutic index, the conformation equilibrium of nucleosides is considered as essential.¹³

Three different classes of conformationally restricted nucleoside analogues have been described: (i) bicyclic and tricyclic nucleosides having a bridge between two positions of the furanose ring, (ii) cyclonucleosides having a bridge between the heterocyclic base and the furanose ring, and (iii) cyclic phosphoesters having a bridge extending from the phosphorus atom of the nucleotide to either the heterocyclic base or the furanose ring.¹³

1.3.1 Class 1 - The Bicyclic and Tricyclic Nucleosides

In the case of the bicyclic nucleosides of class (i), the ring fusion to the 2',3'-positions of the glycone moiety having either *C,O*-connections such as compounds **43-52**, *O,O*-connections such as compounds **53-55** or *C,C*-connections such as compounds **56-62** have been reported. in a number of recent publications.¹³⁻¹⁷

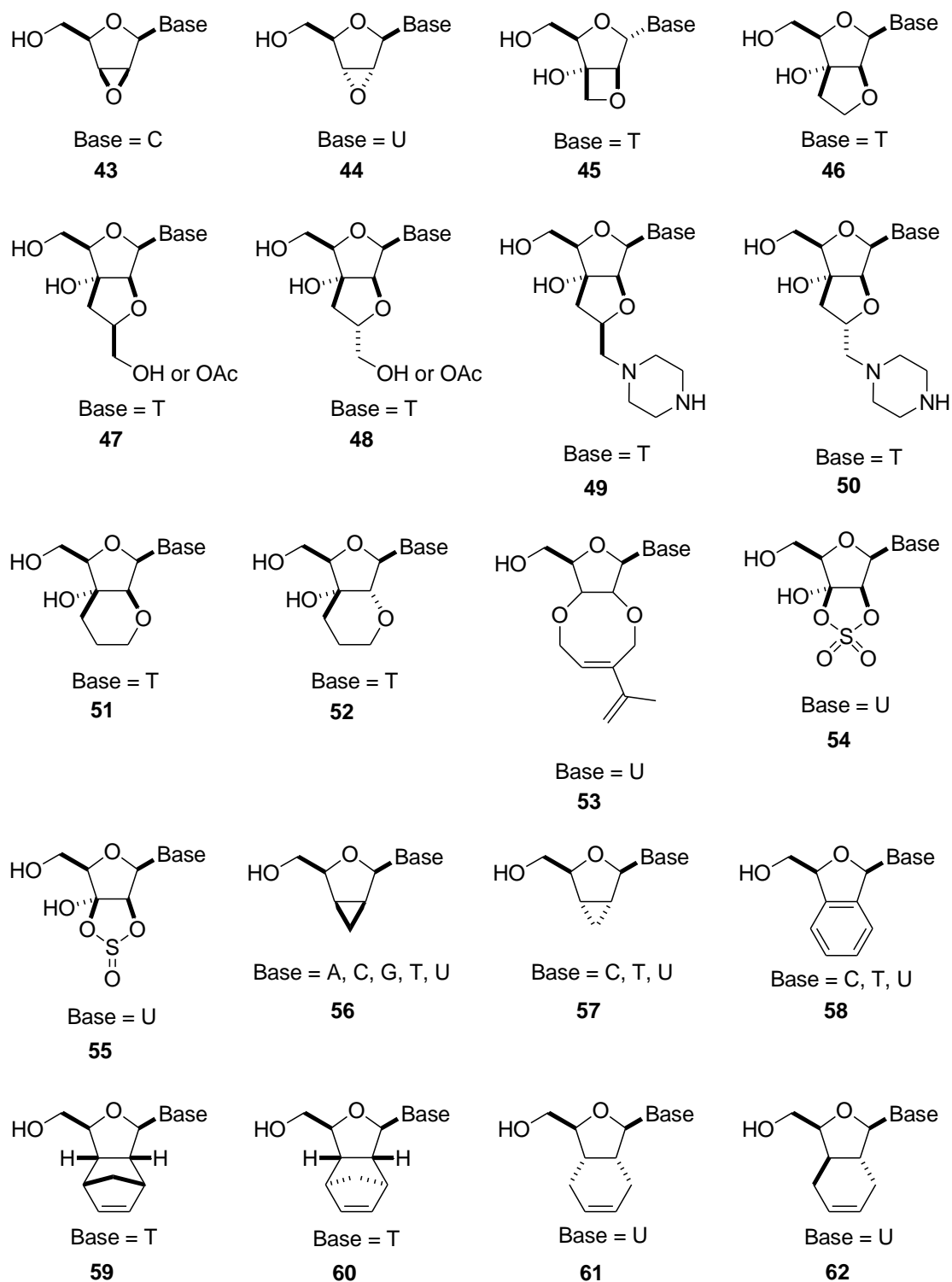


Figure 14 Examples of bicyclic nucleosides with the ring fusion at the 2',3'-positions (nucleoside: A = adenosine, C = cytidine, G = guanosine, T = thymidine and U = uridine)¹³⁻¹⁷

In the case of the bicyclic nucleosides of class (i), few examples of the ring fusion to the 3',4'-positions of the glycone moiety have been reported. One example is a *C,C*-connection, found in compound **63**, and illustrated in **Figure 15**.

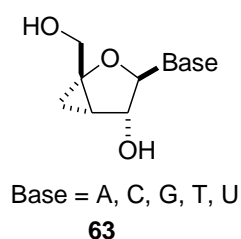


Figure 15 Example of a bicyclic nucleoside with the ring fusion at the 3',4'-positions¹⁸

Also in the case of the bicyclic nucleosides of class (i), a few examples of the ring fusion to the 2',4'-positions of the glycone moiety have been reported. Both *C,O*-connections and *C,C*-connections have been observed. Examples **64** and **65** are outlined in **Figure 16**.

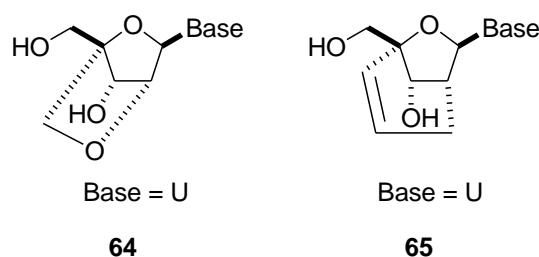


Figure 16 Examples of a bicyclic nucleoside with the ring fusion at the 2',4'-positions¹⁹⁻²⁰

1.3.2 Class 2 - The Cyclonucleosides

The second class of conformationally restricted nucleoside analogues are the cyclonucleosides. The cyclonucleosides bear additional linkages between the heterocyclic ring and the sugar moiety. Although cyclonucleosides were the target of chemists for conformational studies as early as the 1960s, the scientific literature is sparse on their

application against biological targets. However, a few of the obtained compounds have been shown to possess a wide range of antiviral or antitumour properties. The more common cyclonucleosides with known biological activities are illustrated in **Figure 17**, with the biological testing performed highlighted below each compound.²¹

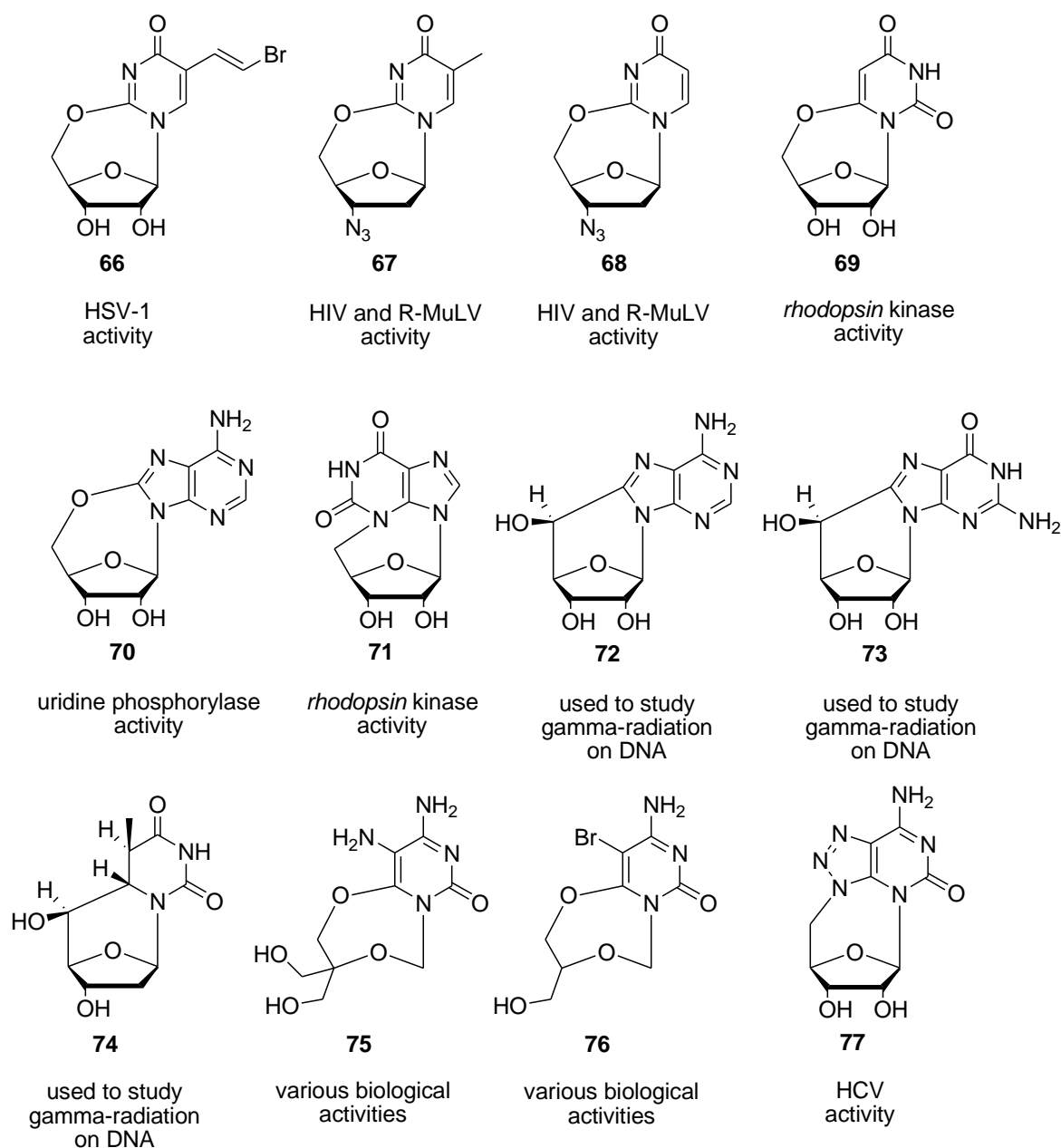


Figure 17 Structural diversity of a range of bioactive cyclonucleosides²¹

1.3.3 Class 3 - The Cyclic Phosphoesters

The third class of conformationally restricted nucleoside analogues are the cyclic phosphoesters, having a bridge extending from the phosphorus atom of the nucleotide to either the heterocyclic base or the furanose ring.

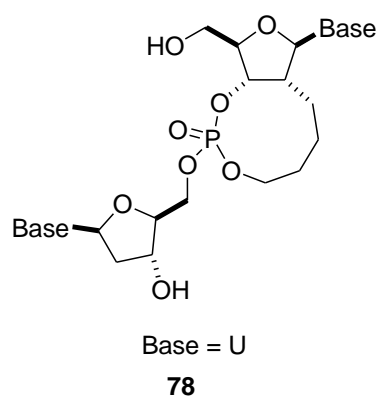


Figure 18 Representative example of a cyclic phosphoester¹⁵

Further extensions to this class include the cyclic dinucleotides, where the bridge extends from the phosphorus atom of the first nucleotide to either the base or the furanose ring of a second nucleotide. This sub-category has been extensively covered as far as synthetic preparations are concerned;²²⁻²⁷ however little or no biological testing has been undertaken to determine if the class has antibiotic, antiviral or anticancer activity.

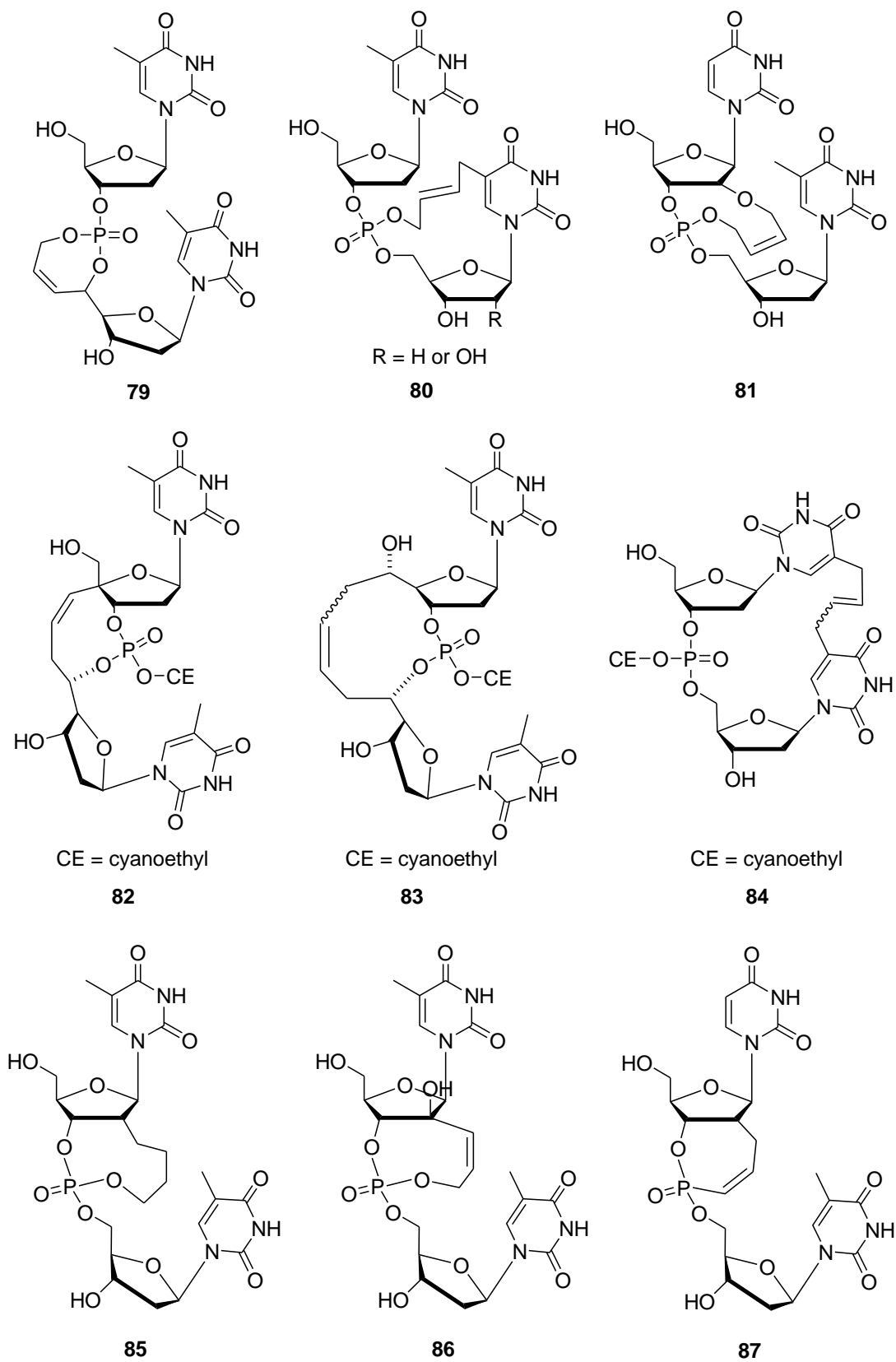


Figure 19 Examples of cyclic dinucleotides²²⁻²⁷

In general, this sub-category has been used to mimic, modulate and even stabilize secondary nucleic acid structures. Through the incorporation of the cyclic dinucleotides into oligonucleotides, an artificial bending of the standard nucleic acid structure and thereby a preorganization for the formation of secondary nucleic acid structures other than duplexes and triplexes is possible.¹⁴ For example, incorporation of these dinucleotides into oligonucleotides might result in stabilized secondary structures, like the three-way junction shown below in **Figure 20**.²⁸

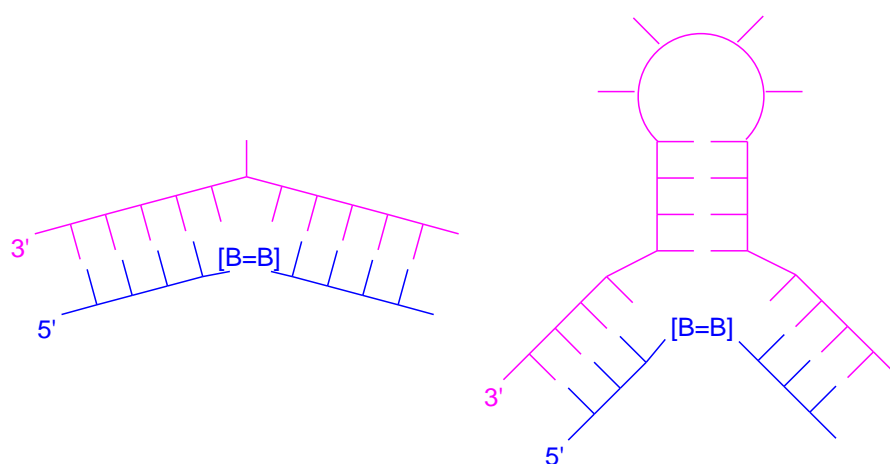


Figure 20 Schematic representations of secondary structures, like bulges (depicted on the left) and three-way junctions (depicted on the right)²⁸

In our literature search it became apparent that although there were various nucleoside derivatives that contained bicyclic and tricyclic ring systems, few of them had been further used for any biological testing. This suggested a niche area for our work as we fostered a keen interest in the possibility of testing our synthetic derivatives.

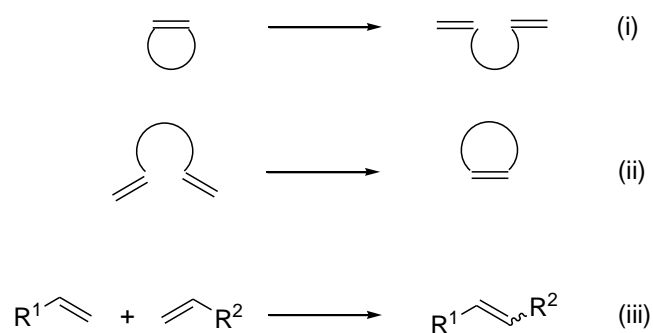
Owing to our previous experience with ring closing metathesis (RCM),²⁹⁻³³ we thought it pertinent to investigate the possibility of forming fused bicyclic systems onto the 2' and 3' positions of the sugar ring of our nucleosides utilizing this methodology. This approach will

be outlined in more detail later in this chapter, but first we felt it necessary to introduce the concept of ring closing metathesis for the non-expert reader.

1.4 INTRODUCTION TO RING CLOSING METATHESIS

Olefin metathesis is a unique carbon skeleton redistribution in which unsaturated carbon-carbon bonds are rearranged in the presence of metal carbene complexes.³⁴ With the advent of efficient catalysts, this reaction has emerged as a powerful tool for the formation of C-C bonds in chemistry. The number of applications of this reaction has dramatically increased in the past few years. Of particular significance, this type of metathesis utilizes no additional reagents beyond a catalytic amount of metal carbene and the only other product from the reaction is, in most cases, a volatile olefin such as ethylene.

Olefin metathesis can be utilized in three closely related types of reactions (**Scheme 1**): (i) ring-opening metathesis polymerization (ROMP), (ii) ring closing metathesis (RCM) and (iii) acyclic cross metathesis for polymer formation (ADMET).³⁵ Of specific interest to us is the use of RCM.



Scheme 1 Different forms of olefin metathesis³⁵

The disclosure by Grubbs that ruthenium carbene complexes of the general type **88** (**Figure 21**) are highly active single component catalysts for all types of alkene metathesis reactions denoted a real breakthrough and triggered an avalanche of interest in this transformation.³⁶ Their activity is usually lower than that of Schrock's molybdenum alkylidene **89**; however, the "late" transition metal compounds designed by Grubbs show a large tolerance towards an array of functional groups and give ease of handling, due to a reasonable stability against oxygen, water and minor impurities in solvents. This renders them exceedingly practical tools for RCM-type reactions.³⁷ The synthesis of the modified nucleosides for the PhD project will use RCM as the key step in ring formation, with the Grubbs second generation catalyst **90** being the preferred catalyst for use.

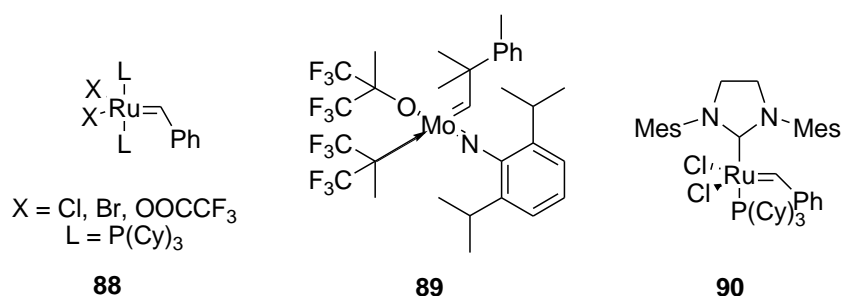
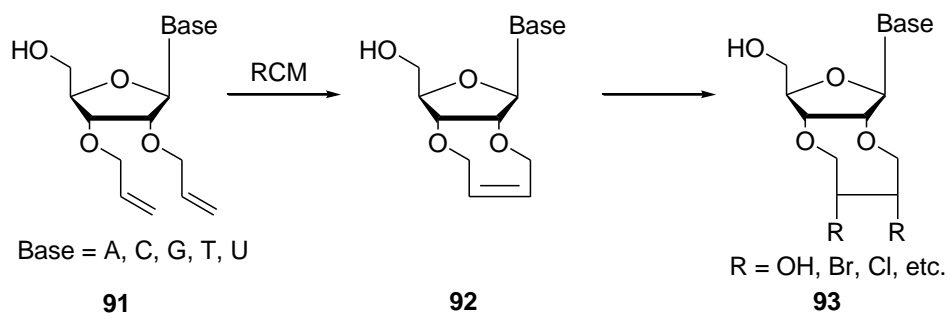


Figure 21 Known metathesis catalysts

1.5 AIMS FOR PART 1

1.5.1 Fused Bicyclic Systems

As mentioned earlier, we thought it pertinent to investigate the possibility of forming fused bicyclic systems onto the 2' and 3' positions of the sugar ring of our nucleosides utilizing the RCM methodology that we were already familiar with. The proposed synthesis in **Scheme 2** below highlights the critical RCM step and shows the bicyclic ring systems that we hoped to prepare in order to do biological activity investigations.



Scheme 2 Synthesis for 2',3'-bicyclic ring system, showing key RCM step

1.5.2 Structure-Activity Relationships

At the same time, we wished to investigate the structure activity relationships (SAR) involved when the various OH and NH positions on the nucleosides and α -(-)-ribose derivatives were protected sequentially with different protecting groups. The idea was that from this data we would be able to determine on which positions in the molecules it was essential to have free OH/NH binding sites in order to maintain the activity of the compounds.

For this study we decided to use α -(-)-ribose as the model system and to look at a range of five different nucleosides: adenosine, cytidine, guanosine, inosine and uridine. The general approach to our SAR study is outlined in **Figure 22**. Structures **94-96** outline the approach taken for the model system, α -(-)-ribose, and structures **97-99** show an example of the nucleoside approach, for uridine derivatives specifically.

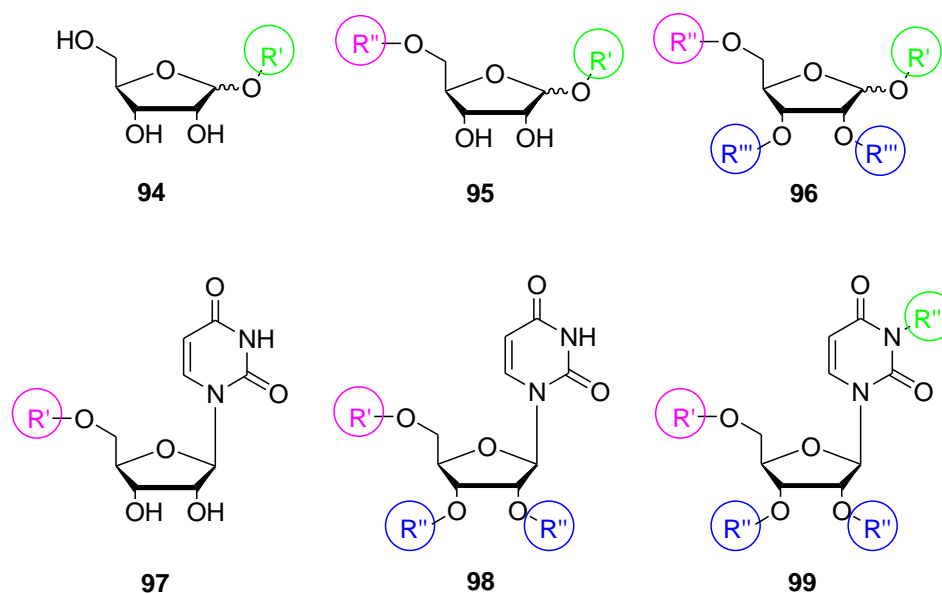


Figure 22 General overview of our intended SAR study

Full details for the synthesis of a series of 25 nucleoside derivatives (based on adenosine, cytidine, guanosine, inosine and uridine), as well as some sugar derivatives (based on α -(-)-ribose) are given in the preceding *Results and Discussion* section (**Chapter 2**). The specific experimental details are provided separately in **Appendix A** (*General Synthetic Procedures*) and **Appendix B** (*Experimental Procedures Relating to Chapter 2*), along with selected NMR spectra which are given as **Supporting Information** (*Relating to Chapter 2*), available on the attached DVD.

All information pertaining to the biological testing of this first generation of compounds is provided in the *Results and Discussion* section (**Chapter 3**). The specific experimental details and general bacteriology protocols used are provided separately in **Appendix C** (*Experimental Procedures Relating to Chapter 3*), for ease of reading. Selected graphs pertaining to the anti-bacterial, anti-HIV and cell proliferation assays, as well as selected photographs of the setups used, are provided as **Supporting Information** which is included on the attached DVD.

Chapter 2:
Results and Discussion for Synthesis

CONTRIBUTIONS TO THIS CHAPTER

All of the syntheses and compound characterization described in this chapter were performed by Ms J.-L. Panayides, while under the supervision of Prof W.A.L. van Otterlo. The work was undertaken in the School of Chemistry which forms part of the Molecular Sciences Institute at the University of the Witwatersrand.

2.1 CHAPTER OVERVIEW

This chapter describes in detail the transformation of the nucleosides adenosine, cytidine, guanosine, inosine and uridine, as well as the sugar α -(-)-ribose, into the corresponding 5'-*O*-(*tert*-butyldiphenylsilyl)- and 5'-*O*-(4,4'-dimethoxytrityl)-protected derivatives. These nucleoside derivatives were subsequently modified with the inclusion of acetyl, benzoyl and allyl functional groups at various positions on the molecules, to yield a range of 25 unique compounds for biological testing.

Full experimental details for this section, including reaction setup used and analysis of all NMR, IR, LRMS and HRMS data, as well as optical rotations, MP and R_f values can be found in **Appendix A** (*General Synthetic Procedures*) and **Appendix B** (*Experimental Procedures Relating to Chapter 2*) below. Selected NMR spectra are attached for perusal in the **Supporting Information** provided on the attached DVD.

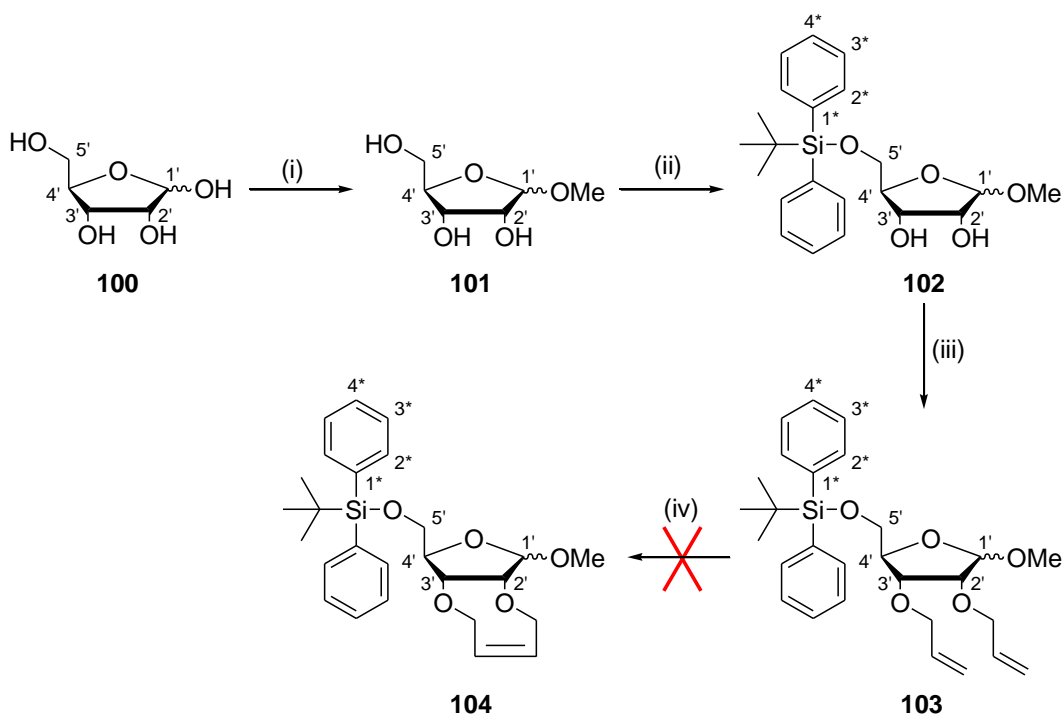
2.2 RESULTS AND DISCUSSION

As discussed in the introduction (**Chapter 1, Section 1.5**) the general synthetic aims were subdivided into two parts: (i) the use of ring closing metathesis (RCM) to form 2',3'-fused bicyclic ring systems, and (ii) the use of various protecting groups to conduct a structure-activity study.

2.2.1 Strategy Towards Fused Bicyclic Ring Systems

2.2.1.1 The Model System: α -(-)-Ribose Derivatives

In order to develop a strategy that could be utilized to form 2',3'-fused bicyclic ring systems on nucleosides, we began our work with a model study of α -(-)-ribose **100**, as the starting material was significantly cheaper than the corresponding nucleosides and the methodology developed could theoretically be used for all of the nucleosides we wished to study. An overview of the approach used is shown in **Scheme 3**.



Scheme 3 Synthetic methodology for preparation of 2',3'-fused bicyclic ring systems: (i) cat. H_2SO_4 , MeOH, 4 °C, 72 h, 100 %, (ii) 1.1 eq. TBDS-Cl, 0.1 eq. DMAP, pyridine, rt, 20 h, used as “crude”, (iii) 2.2 eq. allyl bromide, 2.2 eq. NaH, DMF, rt, 20 h, 68 % over 2 steps, (iv) various attempts, 0 %

1'-*O*-Methoxy- α -(-)-ribose **101** was prepared according to the procedure outlined in Chattopadhyaya and co-workers.³⁸ In this procedure, α -(-)-ribose **100** was methylated in the anomeric position by the reaction of a methanolic solution of the ribose with a catalytic amount of sulfuric acid at 4 °C, after which time the solution was neutralized by passage through Amberlyst A-21 resin, as shown in *Step (i)* of **Scheme 3**. Chattopadhyaya and co-workers³⁸ obtained the desired product in 98 % yield after a 24 h reaction period. Our best yield to date is 100 %, which was obtained after 72 h at 4 °C on a 33.3 mmol scale. 1'-*O*-Methoxy- α -(-)-ribose **101** was obtained as a very viscous pale yellow oil.

The spectroscopic data obtained for compound **101** correlated well with the literature values (¹H and ¹³C NMR).²⁶ The final assignments were confirmed using COSY, HSQC and DEPT-135 NMR spectra and the positions of the 2',3' and 5'-OH peaks were confirmed with a D₂O wash. The α : β ratio was determined on the ¹H NMR spectrum using the newly formed methoxy peak as the reference peak. The α : β ratio of 1:4 was based on the integrations of OMe- α (3.28 ppm) and OMe- β (3.22 ppm).

The 1'-*O*-methoxy- α -(-)-ribose **101** was then deprotonated at the more reactive 5'-OH position using pyridine as both the solvent and the base for the reaction, as shown in *Step (ii)* of **Scheme 3**. The protection of the primary alcohol with the *tert*-butyldiphenylsilyl chloride was catalysed by the addition of DMAP. After purification, the desired 5'-*O*-(*tert*-butyldiphenylsilyl)-1'-*O*-methoxy- α -(-)-ribose **102** was obtained complexed to pyridine and as such was used “crude” in subsequent reactions. Thus, no percentage yield was calculated for the yellow semi-solid foam isolated.

The formation of the compound **102** and pyridine complex was determined through spectroscopic analysis. The addition of the TBDPS group was confirmed by the presence of the *tert*-butyl peak [multiplet at 0.96-1.26 ppm, integrating for 9 H as the -C(CH₃)₃ protons] and the aromatic peaks at 7.35-7.39 ppm (2 H), 7.40-7.48 ppm (4 H) and 7.62-7.71 ppm (4 H) in the ¹H NMR spectrum. This was supported by the presence of the two peaks for the *tert*-butyl group (18.75 ppm and 16.54 ppm) as well as the new aromatic peaks (126.87-134.46 ppm) in the ¹³C NMR spectrum. The α : β ratio of 2:9 was determined using the OMe peaks as

the reference peaks in the ^1H NMR spectrum, with 3.31 ppm representing OMe- α and 3.18 ppm representing OMe- β . The peaks corresponding to the pyridine complex were also assigned in both the ^1H and ^{13}C NMR spectra and it was decided that the pyridine had complexed to the 5'-*O*-(*tert*-butyldiphenylsilyl)-1'-*O*-methoxy- β -(-)-ribose **102** and was not merely a contaminant in the spectrum, based on the lack of 2',3'-OH peaks in the ^1H NMR spectrum and our inability to remove the excess pyridine, even after prolonged periods under high vacuum with heating. HRMS confirmed the presence of the 5'-*O*-(*tert*-butyldiphenylsilyl)-1'-*O*-methoxy- β -(-)-ribose **102** fragment, as a peak corresponding to $[\text{M} + 23]^+$ was observed at 425.17547, which when the 23 for sodium was removed, corresponded well with the calculated value for $[\text{M}]^+$ 402.18625.

As outlined in *Step (iii)* of **Scheme 3**, both the 2'-OH and the 3'-OH were allylated via the deprotonation of the secondary alcohols using sodium hydride and the subsequent reaction with allyl bromide. The desired product 2',3'-*O*-diallyl-5'-*O*-(*tert*-butyldiphenylsilyl)-1'-*O*-methoxy- β -(-)-ribose **103** was obtained after purification as a bright yellow oil in 68 % yield over the two steps starting from compound **101**. The procedure used was one that was modified from the mono-allylation of nucleoside derivatives, previously performed by Lebreton and co-workers³⁹ (thymidine analogues) and Chattopadhyaya and co-workers⁴⁰ (uridine analogues).

The desired compound **103** was identified by the presence of the new peaks for the allyl chains in the NMR spectra. In the ^1H NMR spectrum two multiplets were observed corresponding to the new OCH_2 groups at 3.51-3.62 ppm and 4.03-4.17 ppm respectively. The internal alkene protons were observed as a multiplet at 5.85-5.96 ppm, while the terminal alkene protons were observed as a multiplet at 5.08-5.42 ppm. The presence of the allyl groups were mirrored in the ^{13}C NMR spectrum: 71.68 and 72.41 ppm (OCH_2 groups), 114.09 and 117.32 ppm ($\text{CH}=\text{CH}_2$) and 133.91 and 134.66 ppm ($\text{CH}=\text{CH}_2$). As before, the α : β ratio of 1:4 was determined using the OMe peaks as the reference peaks in the ^1H NMR spectrum, with 3.45 ppm representing OMe- α and 3.36 ppm representing OMe- β . The presence of the alkene protons in the allyl chain was further substantiated by the presence of the band for the C-H stretch of the $\text{CH}=\text{CH}_2$ observed at 3072 cm^{-1} in the infrared spectrum. Final

confirmation for the synthesis of the molecule came as the HRMS showed a peak at 505.23807, which corresponds to a $[M + 23]^+$ peak.

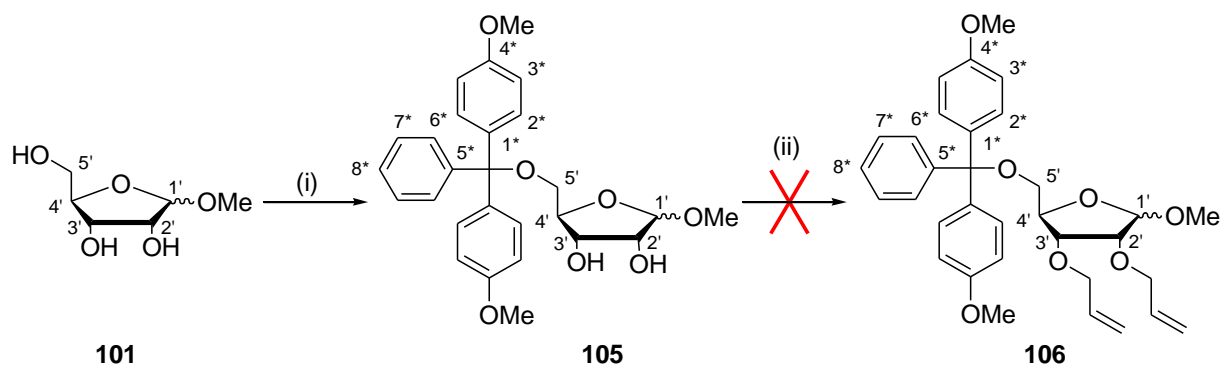
The attempted RCM reaction is shown in *Step (iv)* of **Scheme 3**. A number of different reaction conditions were used to perform the RCM reaction; however, none of them yielded any of the desired 2',3'-fused bicyclic compound **104**. The attempts are summarized in **Table 1** below.

Table 1 Reaction conditions used for the RCM on compound **104**

Catalyst	Solvent	Temperature	Time	Yield of 104
5 mol % Grubbs II 90	CH ₂ Cl ₂	rt	22 h	0 %
5 + 5 mol % Grubbs II 90	CH ₂ Cl ₂	rt + reflux	23 h + 22 h	0 %
5 + 5 mol % Grubbs II 90	toluene	60 °C	23 h + 5 h	0 %
5 + 5 mol % Grubbs II 90	toluene	80 °C + reflux	21 h + 4 h	0 %
8 + 8 mol % Grubbs II 90	toluene	microwave 50 °C	10 + 10 min	0 %
10 mol % Grubbs I	CH ₂ Cl ₂	rt	23 h	0 %

Due to the unfortunate failure of the RCM on the *tert*-butyldiphenylsilyl (TBDPS) protected derivative,* we decided to repeat the synthesis with our other protecting group 4,4'-dimethoxytrityl (DMT) in order to determine if the RCM problem was general to this class of compounds, or if it was specific to only compound **103**. The synthetic route is outlined in **Scheme 4**.

* Due to the time constraints of the project, a number of other strategies for the synthesis of the bicyclic systems that were considered were in fact not attempted. However, these approaches may provide a useful starting point for anyone repeating this work. These approaches could include the use of the "Hoveyda catalyst" as well as looking at titanium (Ti(OPrⁱ)₄) or acid-mediated chelation reactions in more detail. This would shed some light on whether or not it is in fact the other functionalities on the substrate itself which are impeding the catalytic cycle. Furthermore, alkyne methathesis-hydrogenation could possibly be attempted, however after considering this approach, we felt that it was less appropriate for small ring systems - as the strict steric strain imposed by the alkyne in the ring system would be significant in effect.



Scheme 4 Synthetic methodology for preparation of 2',3'-fused bicyclic ring systems: (i) 1 eq. DMT-Cl, 0.1 eq. DMAP, pyridine, rt, 20 h, used as “crude”, (ii) 2.2 eq. allyl bromide, 2.2 eq. NaH, DMF, rt, 20 h, 0 % or 3.2 eq. allyl ethyl carbonate **148**, 3 mol % Pd(dba)₂ **149**, 20 mol % dppb, THF, reflux, 1 h, 0 %

The preparation of compound **101** has been described previously in **Scheme 4**, *step (i)*. The 1'-*O*-methoxy-β-D-ribose **101** was then deprotonated at the more reactive 5'-OH position using pyridine as both the solvent and the base for the reaction. This is outlined in *Step (ii)* of **Scheme 3** and the protection of the primary alcohol with the 4,4'-dimethoxytrityl chloride was then catalysed by the addition of DMAP. After purification, the desired 5'-*O*-(4,4'-dimethoxytrityl)-1'-*O*-methoxy-β-D-ribose **105** was obtained complexed to pyridine and as such was used “crude” in subsequent reactions. Thus, no percentage yield was calculated for the viscous yellow oil that was isolated.

Using the same approach as before for the TBDPS-protected compound **102**, the compound **105** was identified based on its NMR spectral data. New peaks were observed in the ¹H NMR spectrum at 3.73-3.77 ppm and in the aromatic region from 6.86 to 7.46 ppm, corresponding to the two new methoxy groups and to the aromatic rings respectively. The aromatic protons were observed as a doublet of doublets at 6.86 ppm with $J = 8.85$ and 13.08 Hz and as a doublet at 7.08 ppm with $J = 8.78$ Hz. Due to the similar coupling constants for each of these peaks, they are assumed to lie directly next to each other in the molecule and can be assigned as H-3* and H-2* respectively. The remaining aromatic protons were identified as a multiplet at 7.15-7.46 ppm containing H-6*, H-7* and H-8*. The α:β ratio could not be determined for this compound as all of the peaks in the spectrum overlapped. Without one set of the

corresponding α and β peaks to measure integrations on, the ratio could unfortunately not be determined. The required peaks corresponding to the DMT protecting group were also observed in the ^{13}C NMR spectrum. The two new methoxy groups were observed as a peak at 54.99 ppm and the aromatic protons were observed as eight peaks between 108.05 and 157.79 ppm. The new quaternary carbon was distinctive and was observed at 83.58 ppm. The peaks corresponding to the pyridine complex were also assigned in both the ^1H and ^{13}C NMR spectra and it was decided that the pyridine had complexed to the 5'-*O*-(4,4'-dimethoxytrityl)-1'-*O*-methoxy- β -(-)-ribose **105** and was not merely a contaminant in the spectrum based on our inability to remove the excess pyridine even after prolonged periods under high vacuum with heating. HRMS confirmed the presence of the 5'-*O*-(4,4'-dimethoxytrityl)-1'-*O*-methoxy- β -(-)-ribose **105** fragment as a peak corresponding to $[\text{M} + 23]^+$ was observed at 489.18781, which when the 23 for sodium was removed, corresponded well with the calculated value for $[\text{M}]^+$ 466.19915.

Step (ii) of **Scheme 4** highlights the attempted allylation reaction on the “crude” 5'-*O*-(4,4'-dimethoxytrityl)-1'-*O*-methoxy- β -(-)-ribose **105**. Our initial attempts at the allylation reaction involved the use of the standard conditions employed for the preparation of the equivalent TBDPS-protected derivative. We used sodium hydride as the base to deprotonate the 2' and 3'-OH groups and then reacted them with allyl bromide at rt overnight. The desired compound **106** was not isolated, even after further purifications by distillation. It appeared as though all of the starting material had decomposed into unidentifiable compounds that did not contain the DMT group. Assuming that this method was too harsh for our system, we then attempted the far gentler palladium-catalysed allylation reaction described by Nielsen and co-workers for use on a similar system.²⁶

For the palladium-catalysed allylation reaction, the protected ribose **105** and the allyl ethyl carbonate **148** (prepared as described in the experimental **Appendix B**) were prepared as a solution in THF. To this solution was then added a pre-formed mixture of the two catalysts, bis(dibenzylideneacetone) palladium(0) **149** (prepared as described in the experimental **Appendix B**) and bis(diphenylphosphino)butane in THF. After refluxing and subsequent purification by column chromatography, unfortunately none of the desired product **106** was obtained.

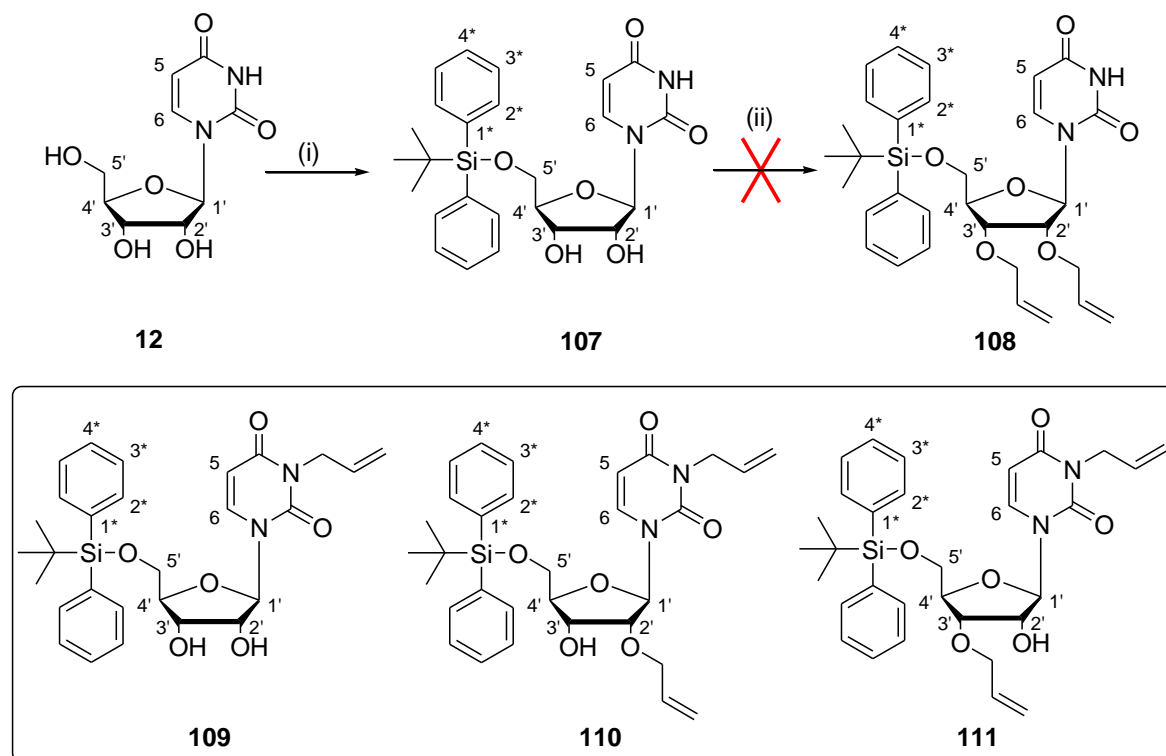
To date we have not found any references as to why this reaction would not occur. Due to the inability to form the di-allylated derivative, we were unable to attempt the RCM on this system in order to try and determine why the other RCM reaction of the 2',3'-*O*-diallyl-5'-*O*-(*tert*-butyldiphenylsilyl)-1'-*O*-methoxy- α -(-)-ribose **103** would not work.

As our model study utilizing derivatives of α -(-)-ribose **100** to devise a successful strategy for ring closing metathesis had not been entirely unambiguous, we decided to continue with the project by utilizing the strategy developed for the synthesis of nucleoside derivatives. We hoped that we would be able to use the di-allylated nucleoside derivatives to determine whether the failed RCM on the 2',3'-*O*-diallyl-5'-*O*-(*tert*-butyldiphenylsilyl)-1'-*O*-methoxy- α -(-)-ribose **103** was to be a general problem or not.

Note: A possible explanation to our observed failure when attempting the RCM reactions may be rooted in the fact that we were attempting the reactions on a *cis* di-allylated ribose derivative as opposed to a *trans* derivative. The *cis* derivative places the allyl chains in closer proximity which may make it difficult for the ruthenium insertion required for the catalytic cycle to commence. Furthermore, the product of the *cis*-methathesis reaction would most likely be more sterically strained than the *trans* product and therefore be less likely to form. Sporadic literature references to this *cis-trans* dilemma exist.^{26b-26c}

2.2.1.2 Pyrimidine-Based Nucleosides – Focusing on Uridine

The first class of nucleosides we investigated were those containing the pyrimidine ring system as the base. The representative example we began with was uridine **12** and the synthetic strategy employed is described in **Scheme 5**. For this strategy we used only the TBDPS group as our model study on α -(-)-ribose derivatives had shown that these would allylate, whereas the DMT protected α -(-)-ribose derivatives would not.



Scheme 4.5 Synthetic methodology for preparation of 2',3'-fused bicyclic ring systems: (i) 1.1 eq. TBDPS-Cl, 0.1 eq. DMAP, pyridine, rt, 22 h, 100 %, (ii) various approaches were attempted

The first step in the synthesis was to protect the most reactive alcohol, namely the primary alcohol in the 5' position of the sugar ring, as shown in *Step (i)* of **Scheme 5**. This was done by stirring the uridine **12** and the catalyst DMAP with pyridine, which serves as both the solvent and the base for the reaction. The pyridine deprotonates the alcohol and then allows for reaction with the *tert*-butyldiphenylsilyl chloride, giving HCl off as the by-product to the reaction (which was observed by the formation of a white precipitate of pyridinium hydrochloride salt). The desired product, 5'-*O*-(*tert*-butyldiphenylsilyl)uridine **107** was obtained in 100 % yield after purification, as a white foam.

This experimental procedure was obtained from the one used by Manoharan and co-workers⁴¹ to form the structurally similar 5'-*O*-(*tert*-butyldiphenylsilyl)-2,2'-anhydro-5-methyluridine. A number of previous attempts had been made to perform the protection using imidazole as

the base, along with the uridine and *tert*-butyldiphenylsilyl chloride as a solution in DMF, as outlined in Sproat and co-workers.⁴² However, we found the imidazole/DMF procedure gave little, if any of the desired product in our hands. Instead, we found that the pyridine method described above gave consistently high yields.

The formation of the 5'-*O*-(*tert*-butyldiphenylsilyl)uridine **107** was corroborated through the use of NMR spectroscopy. In the ¹H NMR spectrum a new singlet peak integrating for 9 H was observed at 1.08 ppm for the *tert*-butyl group. Several new peaks were also observed in the aromatic region of the spectrum: a multiplet at 7.37-7.44 ppm integrating for 6 H (assigned as H-3* and H-4*) and a doublet of doublets at 7.65 ppm integrating for 4 H (assigned as H-2*). Similarly, in the ¹³C NMR spectrum, new peaks were observed for the *tert*-butyl group (19.45 ppm is found to be C(CH₃)₃ and 27.20 is found to be C(CH₃)₃) and the aromatic rings (128.21 ppm is C-3*, 130.29 ppm is C-4*, 132.26 ppm is C-1* and the peak at 135.65 ppm is C-2*). The peaks were assigned with certainty through the use of COSY, HSQC and DEPT-135 spectroscopy. We found that our ¹³C NMR data correlated well to that reported by Sproat and co-workers,⁴² despite the different methodology used to obtain the desired product. Notably, in the IR spectrum, two bands were observed at 700 and 764 cm⁻¹ indicating the presence of an aromatic ring with five adjacent protons and another band was observed at 1362 cm⁻¹ corresponding to a *tert*-butyl group [-C(CH₃)₃]. HRMS confirmed the presence of the [M + 1]⁺ peak at 483.19407, which correlates to the calculated value for [M]⁺ of 482.18730.

We then attempted the allylation reaction on our newly formed 5'-*O*-(*tert*-butyldiphenylsilyl)uridine **107**, as outlined in *Step (ii)* of **Scheme 5**. The first attempt we made was using sodium hydride as the base for deprotonation of the 2' and 3' hydroxyl groups, which was followed by subsequent reaction with allyl bromide. This procedure was modified from the work done by Lebreton and co-workers³⁹ and Chattopadhyaya and co-workers⁴⁰ for performing mono-allylations on deoxy-thymidine and deoxy-uridine and derivatives. Unfortunately, none of the desired 2',3'-*O*-diallyl-5'-*O*-(*tert*-butyldiphenylsilyl)uridine **108** was isolated after purification by column chromatography. Instead a mixture of *N*- and *O*-allylated products (**110** and **111**) were obtained.

The formation of the first isomer was confirmed through the use of NMR and HRMS spectroscopy. In the ^1H NMR spectrum new peaks were observed for the allyl groups: the N- CH_2 formed part of a multiplet at 3.68-4.24 ppm, the O- CH_2 was observed as a multiplet integrating for 2 H at 4.53-4.57 ppm, the $\text{CH}=\text{CH}_2$ protons (both *N*- and *O*-allyl) formed part of a multiplet at 5.10-5.30 ppm and the $\text{CH}=\text{CH}_2$ protons (both *N*- and *O*-allyl) formed part of the multiplet at 5.73-5.93 ppm. The ^{13}C NMR spectrum also showed the presence of the new peaks for the allyl chains. The *N*-allyl was identified by the N- CH_2 peak which is characteristically found at 43.50 ppm, the $\text{CH}=\text{CH}_2$ peak was observed at 119.07 ppm and the $\text{CH}=\text{CH}_2$ peak was observed at 133.82 ppm. The *O*-allyl was identified by the O- CH_2 peak which is characteristically found at 71.72 ppm, the $\text{CH}=\text{CH}_2$ peak was observed at 118.52 ppm and the $\text{CH}=\text{CH}_2$ peak was observed at 131.90 ppm. In the HRMS the molecular ion was calculated at 562.24991 and in the spectrum was found at 562.26234.

In a similar manner, the formation of the second isomer was again confirmed through the use of NMR and HRMS spectroscopy. Characteristic peaks in the ^1H NMR spectrum include a multiplet integrating for 2 H at 3.89-3.97 ppm for N- CH_2 , a multiplet at 4.08-4.73 ppm containing the O- CH_2 protons, a multiplet at 5.12-5.48 ppm containing the $\text{CH}=\text{CH}_2$ protons for both allyl chains and a multiplet at 5.85-5.88 ppm containing the $\text{CH}=\text{CH}_2$ protons for both allyl chains. Characteristic peaks in the ^{13}C NMR spectrum for the *N*-allyl chain are: 43.08 ppm (N- CH_2) and 118.88 ppm ($\text{CH}=\text{CH}_2$), whereas characteristic peaks for the *O*-allyl chain are 71.61 ppm (O- CH_2) and 118.05 ppm ($\text{CH}=\text{CH}_2$). The peaks at 131.76 and 132.14 ppm account for the $\text{CH}=\text{CH}_2$ protons for both the *N*- and *O*-allyl chains, although assignments could not be distinguished with the data available. In the HRMS the molecular ion was calculated at 562.24991 and in the spectrum was found at 562.24544.

Unfortunately, even with the information on hand, we could not differentiate between 3-*N*-allyl-2'-*O*-allyl-5'-*O*-(*tert*-butyldiphenylsilyl)uridine **110** and 3-*N*-allyl-3'-*O*-allyl-5'-*O*-(*tert*-butyldiphenylsilyl)uridine **111**. As such, we could not assign the individual isomers with absolute certainty and we believe that this could be investigated at a later stage through the use of NOE spectroscopy.

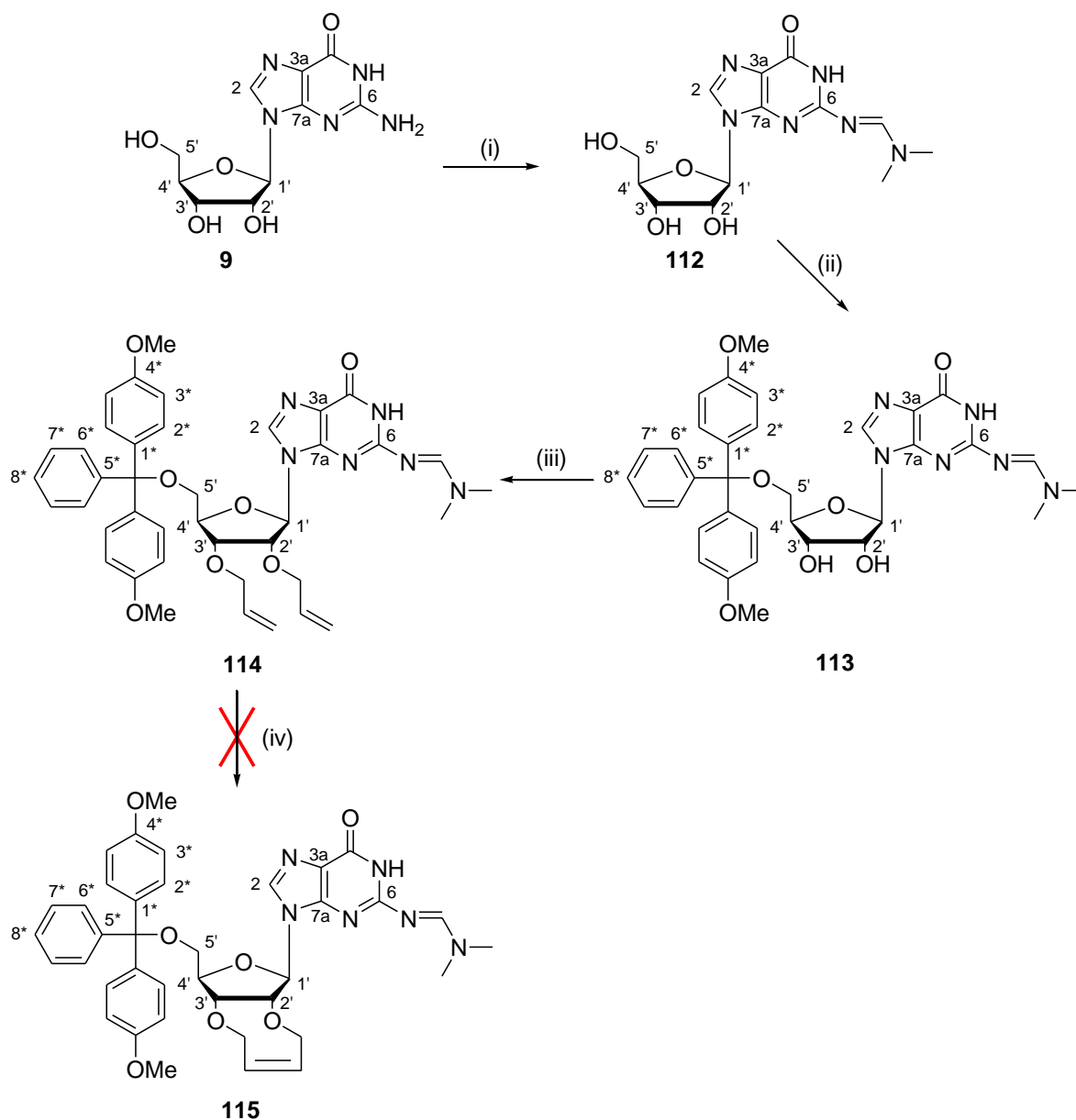
Our second attempt at the synthesis of 2',3'-*O*-diallyl-5'-*O*-(*tert*-butyldiphenylsilyl)uridine **108** involved the use of palladium catalysis, as described by Jin and co-workers⁴³ for the allylation of the 2'-OH on a similar uridine derivative and as described previously in *Section 2.2.1.1*. A solution was prepared containing 5 mol % of the 1,4-bis(diphenylphosphino)butane and 1 mol % of the bis(dibenzylideneacetone) palladium(0) **149** in THF. To this solution was then added dropwise a solution of the protected uridine **107** and the allyl ethyl carbonate **148**. After reaction at rt overnight, unreacted starting material was still observed by tlc. Thus further portions of the dppb, **148** and **149** were added and the reaction was stirred for a further 5 h. Following purification by column chromatography it was found that none of the desired compound **108** had formed, instead all that had been isolated from the reaction was the *N*-allylated byproduct **109**.

The formation of 3-*N*-allyl-5'-*O*-(*tert*-butyldiphenylsilyl)uridine **109** was confirmed by ¹H and ¹³C NMR spectroscopy. The characteristic peaks for the allyl chain were observed as follows: N-CH₂ was found as part of a multiplet at 4.16-4.55 ppm, CH=CH₂ as part of a multiplet at 5.80-5.95 ppm and CH=CH₂ was found as a multiplet integrating for 2 H at 5.18-5.29 ppm. In a similar manner, the characteristic peaks for the newly formed allyl chain were also observed in the ¹³C NMR spectrum. The N-CH₂ was observed at 43.04 ppm, the CH=CH₂ was observed at 118.18 ppm and the CH=CH₂ was found at 132.54 ppm.

The third attempt involved the same palladium catalysed methodology employed in the second method, with the only difference being the catalyst loading. We attempted to force the reaction to go to completion by using 10 mol % dppb and 5 mol % Pd(dba)₂ **149**. Unfortunately none of the desired compound **108** was isolated after column chromatography. The *N*- and *O*-allylated byproducts **109**, **110** and **111** were all isolated instead. The compounds were characterized in the same manner as described previously.

Having had no success synthesizing the 2',3'-*O*-diallyl-5'-*O*-(*tert*-butyldiphenylsilyl)uridine **108**^{42b}, we could obviously not attempt the ring closing metathesis reaction to form the 2',3'-fused bicyclic system. We then decided to proceed and prepare the 2',3'-diallyl derivatives of the purine-based nucleosides in order to test out our so-far unsuccessful RCM approach.

2.2.1.3 Purine-Based Nucleosides – Focusing on Guanosine and Inosine



Scheme 6 Synthetic methodology for preparation of 2',3'-fused bicyclic ring systems: (i) 2 eq. *N,N*-dimethylformamide dimethyl acetal, DMF, rt, 27 h, 79 %, (ii) 1 eq. DMT-Cl, 0.1 eq. DMAP, pyridine, rt, 25 h, 69 %, (iii) 3.2 eq. allyl ethyl carbonate **148**, 0.03 eq. Pd(dba)₂ **149**, 0.2 eq. dppb, THF, reflux, 75 min, 85 %, (iv) 0.05 eq. Grubbs II **90**, CH₂Cl₂, rt, 22 h, 0 % or (iv) 0.05 eq. Grubbs II **90**, CH₂Cl₂, reflux, 22 h, 0 % or (iv) 0.05 eq. Grubbs II **90**, toluene, 60 °C, 23 h, then 0.05 eq. Grubbs II **90**, toluene, reflux, 5 h, 0 %

The initial choice for a purine based nucleoside was guanosine **9** as there appeared to have been more literature data available on its synthetic reactions. We believed this would be beneficial to our synthetic strategy as we had previously had some problems handling the nucleosides. The approach taken for the synthesis of the 2',3'-diallyl derivative and the subsequent formation of the 2',3'-fused bicyclic system is outlined in **Scheme 6**.

As outlined in *Step (i)* of **Scheme 6**, the primary amine on the purine base can be protected as a *N,N*-dimethylmethyylimine through the reaction of the starting material, guanosine **9**, and *N,N*-dimethylformamide dimethyl acetal. The desired compound, 6-*N*-(*N,N*-dimethylmethyylimine)guanosine **112** was thus obtained in 79 % yield after purification. The procedure used was modified from the work done by Sproat and co-workers,⁴² wherein they performed a one-pot multiple protection of guanosine **9** to give 5'-*O*-(*tert*-butyldiphenylsilyl)-6-*N*-(*N,N*-dimethylmethyylimine)guanosine.

The synthesis of the desired compound, 6-*N*-(*N,N*-dimethylmethyylimine)guanosine **112**, was confirmed by the presence of the new peaks for the *N,N*-dimethylmethyylimine group in both the proton and carbon NMR spectra. In the ¹H NMR spectrum, the two N-CH₃ groups were observed as two new singlets, each integrating for 3 H, at 3.03 and 3.15 ppm, while the imine proton (N=CH-N) was observed as a singlet integrating for 1 H at 8.04 ppm. Similarly, the new peaks were observed in the ¹³C NMR spectrum as N-CH₃ peaks at 34.64 and 40.64 ppm and C=CH-N at 136.96 ppm. This analysis was supplemented by the presence of the new band at 1700 cm⁻¹ in the IR spectrum, which accounts for the characteristic imine (C=N) stretch. Finally, HRMS confirmed the characterization as the calculated mass for the molecular ion was 338.13387 and the [M + 1]⁺ peak was observed at 339.14123, which correlated well.

Step (ii) of **Scheme 6** shows the selective protection of the primary alcohol at the 5'-position, which is known to be more reactive than the other secondary alcohols present in the sugar ring. The primary alcohol was deprotonated using pyridine, which acted as both the base and the solvent for the reaction. This was then treated with the catalyst DMAP, before reaction with the 4,4'-dimethoxytrityl chloride at rt overnight. The desired compound, 5'-*O*-(4,4'-

dimethoxytrityl)-6-*N*-(dimethylmethyylimine)guanosine **113**, was subsequently obtained as a white powder in 69 % yield after purification. The procedure used for the reaction was adapted from that reported for the synthesis of 5'-*O*-(4,4'-dimethoxytrityl)-2'-*O*-(2-(triphenylmethylthio)ethyl)-*N*²-isobutyrylguanosine by Jin and co-workers.⁴³

The formation of the 5'-*O*-(4,4'-dimethoxytrityl)-6-*N*-(dimethylmethyylimine)guanosine **113** was confirmed by the presence of the new methoxy and aromatic protons in the ¹H NMR spectrum, as well as by the disappearance of the triplet integrating for 1 H at 5.80 ppm assigned as OH-5' in the previous compound. The characteristic methoxy groups were observed as a singlet integrating for 6 H at 3.72 ppm, while the new aromatic protons were observed as a doublet of doublets integrating for 4 H at 6.83 ppm (H-3*), as well as a multiplet integrating for 7 H at 7.20-7.26 ppm (H-2*, H-6* and H-8*) and a multiplet integrating for 2 H at 7.28-7.31 ppm (H-7*). Similarly, in the ¹³C NMR spectrum, the characteristic methoxy groups were observed at 55.06 ppm and the new aromatic carbons were observed at 113.19 ppm (C-3*), over the range of 126.74-135.58 (C-1*, C-2*, C-5*, C-6*, C-7* and C-8*) and at 144.90 (C-4*). Supporting evidence was obtained from the aromatic bands observed in the IR spectrum at 699 and 760 cm⁻¹ indicating five adjacent aromatic protons, at 826 cm⁻¹ indicating two adjacent aromatic protons and at 3090 cm⁻¹ indicating the presence of an aromatic ring system. Final confirmation of the structure came from the peak at 641.27182 ([M + 1]⁺) in the HRMS spectrum which corresponds well to the calculated value of 640.26455 for the molecular ion.

Outlined in *Step (iii)* of **Scheme 6** is the allylation reaction performed on the two secondary alcohols on the sugar ring. In initial attempts at the reaction using standard conditions, the alcohols in the 2' and 3'-positions on the ring were deprotonated using sodium hydride as the base, and were then reacted with excess allyl bromide. Unfortunately, the reactions were unsuccessful and we often isolated decomposition products. Thus, the reaction was then carried out using the previously described palladium-catalysed conditions.⁴³ Under these conditions the guanosine derivative **113** and allyl ethyl carbonate **148** (synthesis described in the experimental, **Appendix B**) were dissolved in THF and to this solution was then added a second solution containing 20 mol % of the 1,4-bis(diphenylphosphino)butane and 3 mol % of the Pd(dba)₂ catalyst **149** (preparation described in **Appendix B**). After refluxing and

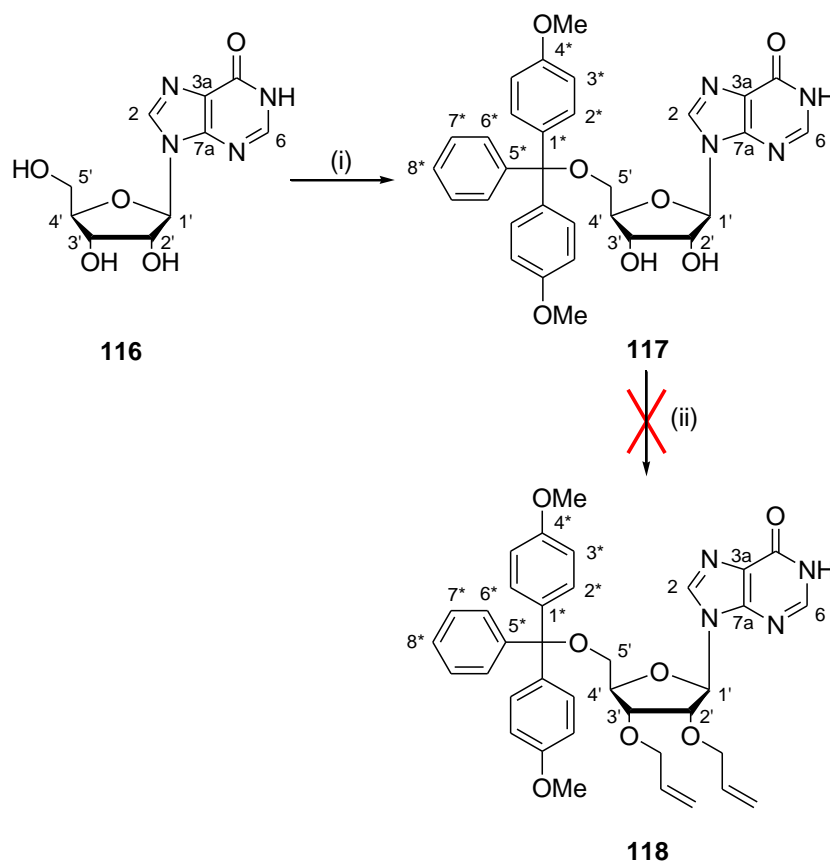
subsequent purification by column chromatography, the desired compound, 2',3'-*O*-diallyl-5'-*O*-(4,4'-dimethoxytrityl)-6-*N*-(*N,N*-dimethylmethylimine)-guanosine **114**, was obtained as a yellow foam in 85 % yield.

The formation of 2',3'-*O*-diallyl-5'-*O*-(4,4'-dimethoxytrityl)-6-*N*-(*N,N*-dimethylmethylimine)guanosine **114** was confirmed by the disappearance of the peaks for the OH-2' (broad singlet at 5.58 ppm) and OH-3' (broad singlet at 5.26 ppm) present in the ¹H NMR spectrum for compound **113**, and the appearance of the characteristic peaks for the allyl chains. The new peaks were observed as two doublets at 4.44 and 4.96 ppm respectively, each integrating for 2 H and each assigned as an OCH₂ group. Also observed was a multiplet at 5.08-5.23 ppm integrating for 4 H and identified as the two CH=CH₂ groups and a multiplet at 5.79-5.97 ppm integrating for 2 H and identified as the two CH=CH₂ groups. Similarly, in the ¹³C NMR spectrum, new peaks appeared at 86.78 and 87.94 ppm for the OCH₂ groups, at 116.92 and 119.12 ppm for the CH=CH₂ groups and at 130.17 and 130.29 ppm for the CH=CH₂ groups.

Having the di-allylated compound, 2',3'-*O*-diallyl-5'-*O*-(4,4'-dimethoxytrityl)-6-*N*-(*N,N*-dimethylmethylimine)guanosine **114** in hand, we could finally attempt the ring closing metathesis reaction as outlined in *Step (iv)* of **Scheme 6**. The first method employed for the reaction was to prepare a solution of the diene **114** in dichloromethane and then to react this with 5 mol % Grubbs II catalyst **90** at rt for 22 h, however, after this time NMR spectroscopy on a sample of crude product confirmed the presence of only unreacted starting material, so a further 5 mol % of Grubbs II catalyst **90** was added and the reaction mixture was refluxed overnight. Unfortunately, after purification, none of the desired ring-closed product **115** was obtained.

A second attempt was made at the RCM, this time the diene (2',3'-*O*-diallyl-5'-*O*-(4,4'-dimethoxytrityl)-6-*N*-(*N,N*-dimethylmethylimine)guanosine **114**) was heated to 60 °C in toluene before the addition of 5 mol % of Grubbs II catalyst **90**. After stirring overnight, NMR spectroscopy on the crude product again confirmed the presence of unreacted starting material, so a further 5 mol % of Grubbs II catalyst **90** was added and the reaction was refluxed for 5 hours. Unfortunately, none of the desired ring-closed product **115** was obtained.

Due to a lack of material and time constraints, we decided not to continue with attempts at RCM on the 2',3'-*O*-diallyl-5'-*O*-(4,4'-dimethoxytrityl)-6-*N*-(*N,N*-dimethylmethylimine)-guanosine **114** system,[†] but to instead focus on the synthesis on the similar, but structurally simpler, inosine (**116**) derivatives. The approach taken for the synthesis of the diene required for RCM is outlined in **Scheme 7**.



Scheme 7 Synthetic methodology for preparing 2',3'-fused bicyclic ring systems: (i) 1 eq. DMT-Cl, 0.1 eq. DMAP, pyridine, rt, 21 h, 78 %, (ii) 2.2 eq. allyl bromide, 2.2 eq. NaH, DMF, rt, 21 h, 0 %

In *Step (i)* of **Scheme 7**, one can see the protection of the primary alcohol in the 5'-position of the sugar ring. We employed the same methodology as used previously in the preparation of the □-(-)-ribose **100** and guanosine **9** derivatives, whereby the primary alcohol was

[†] For further information on possible RCM reactions, please refer to footnote on page 33.

deprotonated using pyridine as both the base and solvent, and the reaction was then carried out under catalytic DMAP conditions with 4,4'-dimethoxytrityl chloride. The desired compound, 5'-*O*-(4,4'-dimethoxytrityl)inosine **117**, was obtained in 78 % yield after purification by recrystallisation.

The formation of 5'-*O*-(4,4'-dimethoxytrityl)inosine **117** was identified through the use of NMR, IR and HRMS spectroscopy. In the ¹H NMR spectrum, characteristic new peaks were observed for the two methoxy groups, as a singlet integrating for 6 protons at 3.69 ppm, and for the aromatic rings, as a dd integrating for 4 protons at 6.83 ppm (H-3*), as a multiplet integrating for 7 protons at 7.12-7.14 ppm (H-2*, H-6* and H-8*) and as a multiplet integrating for 2 protons at 7.35-7.39 ppm (H-7*). Similarly, in the ¹³C NMR spectrum, characteristic new peaks were observed for the two methoxy groups (55.04 ppm) and for the aromatic rings (113.16, 126.70, 127.81, 127.83, 129.73, 144.86, 145.80 and 158.08 ppm - for assignments please refer to the experimental in **Appendix B** below). The new quaternary carbon situated between the three aromatic rings of the DMT protecting group was observed at 85.53 ppm. The band for the new methoxy group was observed at 2836 cm⁻¹ and the bands for the aromatic rings were found at 702 and 755 cm⁻¹ (5 adjacent aromatic protons), 827 cm⁻¹ (2 adjacent aromatic protons) and 3033 cm⁻¹ (aromatic protons). Final evidence for the formation of the desired compound **117** was given by the HRMS spectrum, in which a peak was observed at 593.1995 which, when 23 is removed for the sodium additive, correlated well to the calculated value for the molecular ion of 571.21823.

Outlined in *Step (ii)* of **Scheme 7** is the allylation reaction attempted on the two secondary alcohols on the sugar ring. The allylation reaction was only attempted once and for this attempt we chose to use the more rigorous reaction conditions described below in favour of the gentle palladium-catalysed method described above, in order to try and force the reaction to occur in good yield so that we had sufficient material to attempt the RCM reactions. For the allylation reaction, we took the protected inosine derivative **117** (as a solution in DMF) and deprotonated the secondary alcohols in the 2' and 3'-positions using sodium hydride as our base. We then attempted to react the material with excess allyl bromide; unfortunately, after purification we found that none of the desired 2',3'-*O*-diallyl-5'-*O*-(4,4'-dimethoxytrityl)inosine **118** had formed. We believe that the starting material decomposed

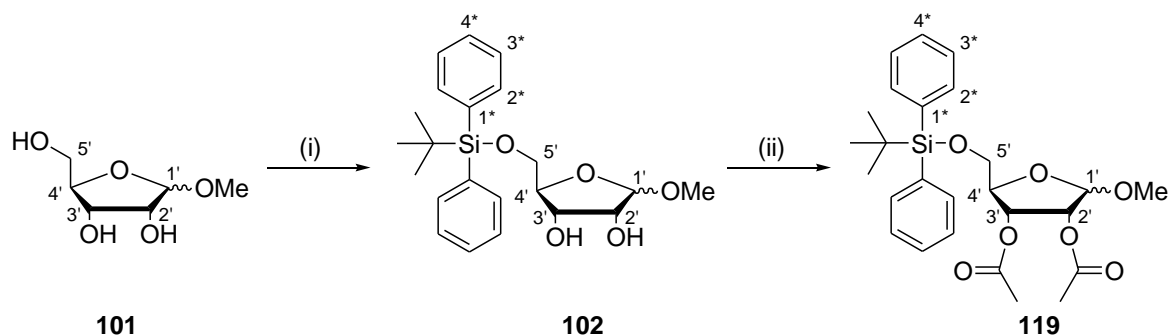
under the harsh sodium hydride conditions employed for the reaction. Due to time constraints we were unfortunately not able to repeat the reactions and attempt the RCM reaction.

As shown in **Schemes 3-7**, there were a number of difficulties associated with the synthesis of the 2',3'-*O*-diallylated α -(-)-ribose derivatives (**103** and **106**) and nucleoside derivatives (**108**, **114** and **118**). As the RCM on both the 2',3'-*O*-diallyl-5'-*O*-(*tert*-butyldiphenylsilyl)-1'-*O*-methoxy- α -(-)-ribose **103** and the 2',3'-*O*-diallyl-5'-*O*-(4,4'-dimethoxytrityl)-6-*N*-(*N,N*-dimethylmethylimine)guanosine **114** systems were unsuccessful, at this point in the project we decided to stop our investigation into the preparation of 2',3'-fused bicyclic systems and instead focus on the synthesis of derivatives for our structure-activity study. The work completed towards the fused bicyclic systems was however not in vain, as all compounds synthesized *en route* to the bicyclic systems were subsequently included in the structure-activity study.

2.2.2 Synthesis of Compounds to Conduct a Structure-Activity Study

2.2.2.1 The Model System: α -(-)-Ribose Derivatives

In order to develop a strategy that could be utilized on the nucleoside derivatives, we began our work with a model study of α -(-)-ribose **100**, as the starting material was significantly cheaper than the corresponding nucleosides. An overview of the approach used is shown in **Scheme 8**. The conversion of the α -(-)-ribose **100** into 1'-*O*-methoxy- α -(-)-ribose **101** is described in detail in *Section 2.2.1.1* above.



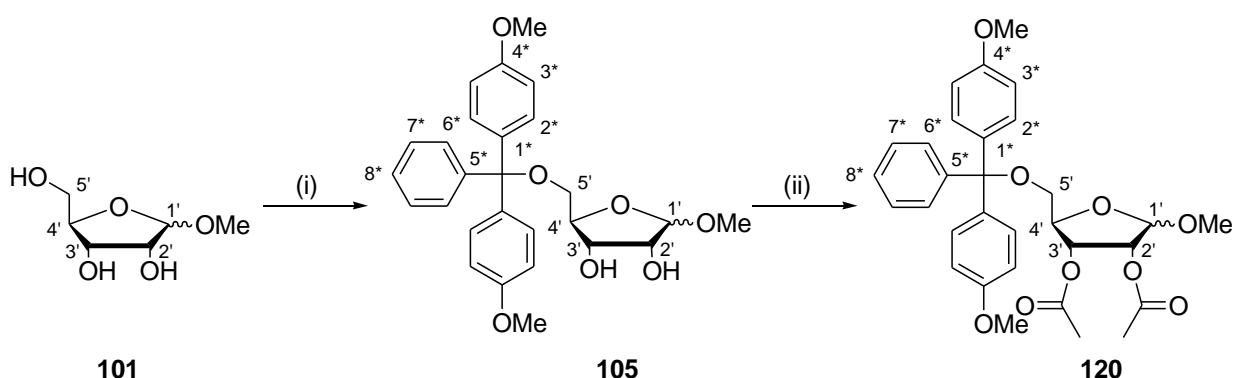
Scheme 8 Synthetic methodology for preparation of α -(-)-ribose derivatives: (i) 1.1 eq. TBDPS-Cl, 0.1 eq. DMAP, pyridine, rt, 20 h, used “crude”, (ii) 3 eq. acetic anhydride, 5 eq. pyridine, rt, 19 h, 71 % over two steps

The full description for the reaction shown in *Step (i)* of **Scheme 8** above is discussed in detail in *Section 2.2.1.1* above as the same reaction was used in *Step (ii)* of **Scheme 3**. *Step (ii)* of **Scheme 8** shows the protection of the secondary alcohols in the 2' and 3' positions on the sugar ring as acetyl groups. This reaction was carried out using pyridine as both the base and the solvent for the reaction. The desired compound, 2',3'-*O*-diacetyl-5'-*O*-(*tert*-butyldiphenylsilyl)-1'-*O*-methoxy- α -(-)-ribose **119**, was obtained as a viscous orange oil in 71 % yield over the two steps.

The formation of the desired compound **119** was induced through the use of various spectroscopic methods. In the ^1H NMR spectrum, the peaks corresponding to the OH-2' and OH-3' were replaced by new peaks for the acetyl groups. These new peaks were observed as two multiplets, each integrating for 3 H at 2.00-2.06 ppm and at 2.09-2.14 ppm, which were assigned as the two new CH_3 groups. We would have expected two singlets for the two new methyl groups, but instead observed two multiplets – we believe that this is caused by the presence of the α/β anomers in α -(-)-ribose and the fact that the peaks for the anomers are overlapping. Using the 1'-*O*-methoxy peaks, observed as a singlet at 3.34 ppm for OCH_3 (β) and as a singlet at 3.38 ppm for OCH_3 (α), we were able to determine the anomeric ratio as $\alpha:\beta = 1:3$. In a similar manner, the new groups were also observed in the ^{13}C NMR spectrum, the two new methyl groups were found at 20.88 and 22.57 ppm and the two new carbonyl

groups were found at 169.91 and 170.89 ppm respectively. Supporting data was obtained from the IR spectrum, where a new band was observed at 1747 cm^{-1} accounting for the new C=O stretch, as well as from the HRMS where a peak was observed at 509.19582, which when 23 is removed for the sodium additive, correlates well to the calculated value of 486.20738 for the desired compound 2',3'-*O*-diacetyl-5'-*O*-(*tert*-butyldiphenylsilyl)-1'-*O*-methoxy- β -(-)-ribose **119**.

In a similar manner to that described in **Scheme 8**, the second group of DMT-protected β -(-)-ribose **100** derivatives were prepared. The synthesis is shown schematically in **Scheme 9** below. The conversion of the β -(-)-ribose **100** into 1'-*O*-methoxy- β -(-)-ribose **101** is described in detail in *Section 2.2.1.1*.



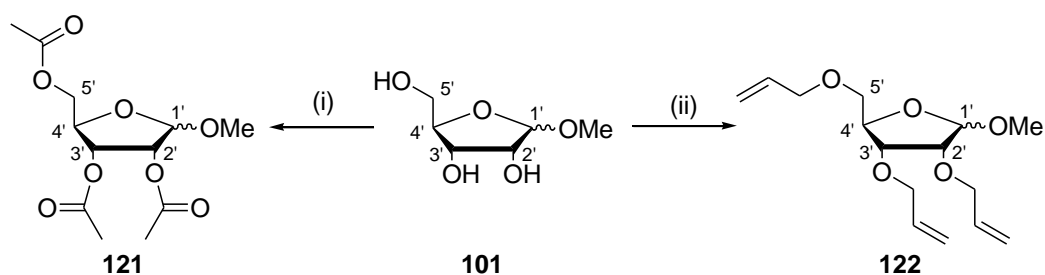
Scheme 9 Synthetic methodology for preparation of β -(-)-ribose derivatives: (i) 1 eq. DMT-Cl, 0.1 eq. DMAP, pyridine, rt, 20 h, used “crude”, (ii) 3 eq. acetic anhydride, 5 eq. pyridine, rt, 19 h, 77 % over two steps

The full description for the reaction shown in *Step (i)* of **Scheme 9** is discussed in detail in *Section 2.2.1.1* as the same reaction was used in *Step (i)* of **Scheme 4**. *Step (ii)* of **Scheme 9** highlights the protection of the secondary alcohols in the 2' and 3' positions on the sugar ring as acetyl groups. The conditions used involved the presence of pyridine to act as both the base and the solvent for the reaction and the use of acetic anhydride as the acetyl group donor. The

desired compound, 2',3'-*O*-diacetyl-5'-*O*-(4,4'-dimethoxytrityl)-1'-*O*-methoxy- α -(-)-ribose **120**, was obtained in 77 % yield over the two steps as a viscous orange oil.

The formation of 2',3'-*O*-diacetyl-5'-*O*-(4,4'-dimethoxytrityl)-1'-*O*-methoxy- α -(-)-ribose **120** was identified by the disappearance of the peaks for the 2' and 3' hydroxyl groups in the ^1H NMR spectrum at 3.80-3.95 and 4.73-5.25 ppm, and the appearance of the new multiplet integrating for 6 H at 2.01-2.14 ppm accounting for the two new methyl groups in the molecule. In the same manner, new peaks were observed at 20.80 and 20.99 ppm (two new methyl groups) and at 169.89 and 170.88 ppm (two new carbonyl groups) in the ^{13}C NMR spectrum. The α : β ratio was found to be 1:3 by correlating the integrations for the methoxy group on the sugar ring in the ^1H NMR spectrum, the peak at 3.38 ppm was for OCH_3 (β) and the peak at 3.45 ppm was for OCH_3 (α). The identification of the compound isolated from the reaction was further confirmed as **120** by the HRMS spectrum, wherein the peak observed at 573.20916 is found to be $[\text{M} + 23]^+$ and correlated well to the calculated value for the molecular ion of 550.22028.

Shown in **Scheme 10**, are the synthesis of two α -(-)-ribose **100** derivatives containing the same protecting group on all three of the hydroxyls on the sugar ring. The conversion of the α -(-)-ribose **100** into 1'-*O*-methoxy- α -(-)-ribose **101** is described in detail in *Section 2.2.1.1* above.



Scheme 10 Synthetic methodology for preparing α -(-)-ribose derivatives: (i) 4.5 eq. acetic anhydride, 7.5 eq. pyridine, rt, 22 h, 94 %, (ii) 3.3 eq. allyl bromide, 3.3 eq. sodium hydride, DMF, rt, 23 h, 100 %

Step (i) of **Scheme 10** shows the protection of the secondary alcohols, OH-2' and OH-3', as well as the protection of the primary alcohol, OH-5', with acetyl groups. This reaction was performed by deprotonating the hydroxyl groups on the sugar ring of 1'-*O*-methoxy- α -(-)-ribose **101** with pyridine and then allowing them to react with acetic anhydride overnight, to give the desired compound 2',3',5'-*O*-triacetyl-1'-*O*-methoxy- α -(-)-ribose **121** in 94 % yield as a yellow oil.

The formation of 2',3',5'-*O*-triacetyl-1'-*O*-methoxy- α -(-)-ribose **121** was confirmed based on the disappearance of the hydroxyl peaks at 4.05-4.25 ppm, 4.75-4.80 ppm and 4.93-4.99 ppm, as assigned previously in the ^1H NMR spectrum for compound **101**. The three new methyl groups, from the acetyl groups that had been added to the molecule were observed as a multiplet integrating for 9 H at 2.02-2.14 ppm. The α : β ratio was found to be 1:3 based on the integrations for 1'-*O*-methoxy group on the sugar ring – OCH₃ (β) was observed as a singlet at 3.38 ppm, while OCH₃ (α) was observed as a singlet at 3.45 ppm. In a similar manner to the ^1H NMR spectrum, new peaks were observed in the ^{13}C NMR spectrum for the three new acetyl groups: the three methyl groups were found as both the α and β anomers, grouped together at 20.67, 20.71, 20.75, 20.94 and 20.95 ppm; the three carbonyl groups were also found as both the α and β anomers, grouped together at 169.83, 169.87, 170.09, 170.64, 170.76 and 170.83 ppm. Supporting evidence for the formation of compound **121** was given by the presence of new bands in the IR spectrum, with one at 1680 cm⁻¹ assigned as C=O, one at 1738 cm⁻¹ assigned as –CO-O- and the band at 2998 cm⁻¹ assigned as –CO-CH₃. Final evidence for the formation of the desired compound **121** was given by the HRMS spectrum, in which a peak was observed at 313.08943 which, when 23 is removed for the sodium additive, correlates well to the calculated value for the molecular ion of 290.10017.

Outlined in *Step (ii)*, **Scheme 10** is allylation of all the hydroxyl groups on the sugar ring of 1'-*O*-methoxy- α -(-)-ribose **101**. The reaction occurs by the deprotonation of the primary alcohol OH-5' and the secondary alcohols OH-2' and OH-3' using sodium hydride as the base, which was followed by reaction with allyl bromide. The desired compound, 2',3',5'-*O*-triallyl-1'-*O*-methoxy- α -(-)-ribose **122** was obtained as a yellow oil in quantitative yield.

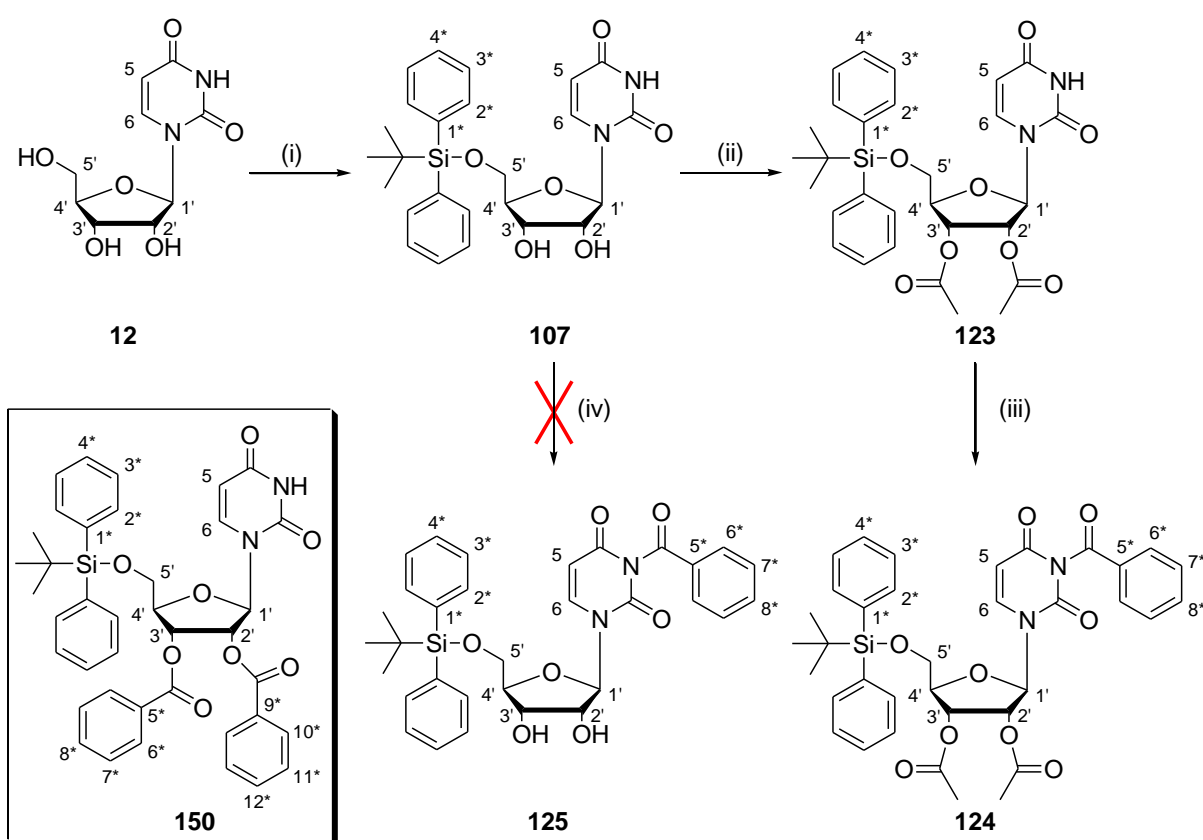
The synthesis of the desired compound, 2',3',5'-*O*-triallyl-1'-*O*-methoxy- \square -(-)-ribose **122**, was confirmed by the presence of the new peaks for the allyl chains in both the proton and carbon NMR spectra. In the ^1H NMR spectrum, the three new signals for the OCH_2 groups were observed overlapping as a multiplet from 4.01-4.17 ppm integrating for 6 H. The alkene protons were observed as a multiplet integrating for 3 H at 5.14-5.23 ppm which was assigned as the $\text{CH}=\text{CH}_2$ protons *trans* to the R group, as a multiplet integrating for 3 H at 5.24-5.36 ppm which was assigned as the $\text{CH}=\text{CH}_2$ protons *cis* to the R group and finally as a multiplet integrating for 3 H at 5.84-5.98 ppm assigned as the $\text{CH}=\text{CH}_2$ protons. Similarly, in the ^{13}C NMR spectrum the new signals for the OCH_2 groups were observed as six peaks (one for each of the three new OCH_2 carbons in the α anomer and one for each of the three new OCH_2 carbons in the β anomer) over the range 70.51-72.64 ppm. The new signals for the alkene groups were observed as three peaks for $\text{CH}=\text{CH}_2$ (β) at 116.99, 117.63 and 117.73 ppm, as three peaks for $\text{CH}=\text{CH}_2$ (α) at 117.28, 117.35 and 117.86 ppm and as five peaks at 134.61, 134.65, 134.86, 134.96 and 135.28 ppm accounting for $\text{CH}=\text{CH}_2$ (both α and β).

The α : β ratio was found to be 1:3 based on the integrations in the ^1H NMR spectrum for 1'-*O*-methoxy group on the sugar ring – OCH_3 (β) was observed as a singlet at 3.36 ppm, while OCH_3 (α) was observed as a singlet at 3.45 ppm. Substantiating evidence for the formation of compound **122** was given by the new bands in the IR spectrum: 869, 920 and 991 cm^{-1} for $\text{RCH}=\text{CH}_2$, 1647 cm^{-1} for the $\text{C}=\text{C}$ and 3080 cm^{-1} for the $\text{C}=\text{CH}_2$. The identification of the compound isolated from the reaction was further confirmed as **122** by the HRMS spectrum, wherein the peak observed at 307.15160 is found to be $[\text{M} + 23]^+$ and correlates well to the calculated value for the molecular ion of 284.16237 when the value of 23 for the sodium additive is taken into account.

Having completed the model study on \square -(-)-ribose **100** (as shown in **Scheme 8**, **Scheme 9** and **Scheme 10**) without any major problems, we were then able to move onto the preparation of the pyrimidine-based nucleoside derivatives. The nucleosides chosen for this study were uridine **12** and cytidine **11**.

2.2.2.2 Pyrimidine-Based Nucleosides – Focusing on Uridine and Cytidine

The first of the pyrimidine-based nucleosides that we chose to work on was uridine **12**. This nucleoside was chosen as we had previously worked with it on our attempted synthesis of 2',3'-fused bicyclic systems, as described in *Section 2.2.1.2*. Our approach towards the synthesis of *tert*-butyldiphenylsilyl protected derivatives is outlined in **Scheme 11**.



Scheme 11 *Synthesis of tert-butyldiphenylsilyl protected derivatives of uridine*: (i) 1.1 eq. TBBDPS-Cl, 0.1 eq. DMAP, pyridine, rt, 22 h, 100 %, (ii) 3 eq. acetic anhydride, 5 eq. pyridine, rt, 20 h, 89 %, (iii) 5 eq. benzoyl chloride, 5 eq. *N,N*-diisopropylethylamine, pyridine, rt, 2 h, 71 %, (iv) 1.3 eq. benzoyl chloride, 0.04 eq. tetra-butylammonium bromide, 8 eq. sodium carbonate, CH₂Cl₂ : H₂O, rt, 30 min, 0 %

The synthesis of 5'-*O*-(*tert*-butyldiphenylsilyl)uridine **107** was described in detail in *Section 2.2.1.2*, and was shown schematically in *Step (i)* of **Scheme 5**; as such the preparation of this compound will not be discussed further here.

In *Step (ii)* of **Scheme 11**, we see the protection of the secondary alcohols at the 2' and 3' positions on the sugar ring with acetyl groups. The experimental procedure involves the use of pyridine as both the base and the solvent for the reaction, with acetic anhydride used as the acetyl donor. The reaction was carried out at rt and yielded the desired product 2',3'-*O*-diacetyl-5'-*O*-(*tert*-butyldiphenylsilyl)uridine **123** as a cream foam in 89 % yield after purification.

The synthesis of the desired compound, 2',3'-*O*-diacetyl-5'-*O*-(*tert*-butyldiphenylsilyl)uridine **123**, was confirmed by the presence of the new peaks for the two new acetyl groups in both the proton and carbon NMR spectra. In the ^1H NMR spectrum, a new multiplet was observed at 2.11-2.14 ppm integrating for 6 H, and accounted for the two new methyl groups. The position of the acetyl groups on the sugar ring was confirmed by the disappearance of the OH-2' and OH-3' peaks, at 3.38 and 5.47 ppm, in the ^1H NMR spectrum for the starting material **107**. In the ^{13}C NMR spectrum, new peaks were observed at 20.63 and 20.85 ppm for the two new methyl groups, and new peaks were observed at 169.77 and 170.00 ppm for the two new carbonyl groups. Supporting evidence for the formation of the desired compound **123** was provided by the presence of new bands in the IR spectrum at 1113 and 1223 cm^{-1} which are characteristic of a C=O group, and are different in shift to the bands for the amide C=O groups shown at positions C-2 and C-4 in the molecule illustrated above. Final confirmation for the formation of the compound **123** came from HRMS, where peaks were observed at 567.21532 and 589.19699, accounting for $[\text{M} + 1]^+$ and $[\text{M} + 23]^+$ respectively.

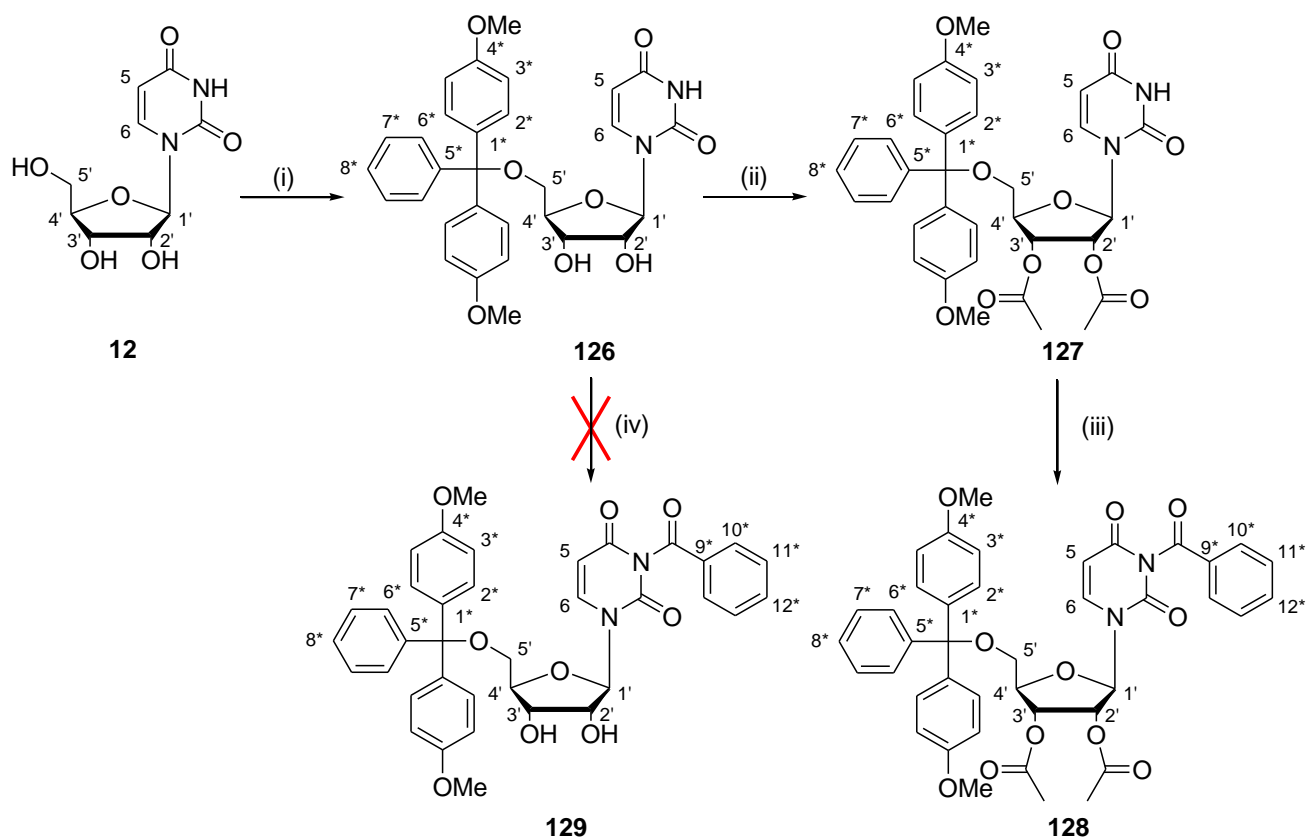
Outlined in *Step (iii)* of **Scheme 11** is the protection of the urea position on the base as a benzoyl derivative. Experimentally, the reaction occurred through the deprotonation of the amide NH using Hünig's base and the subsequent attack on the benzoyl chloride. In this instance, pyridine was used as the solvent for the reaction as the by-product for the reaction is gaseous hydrochloric acid, which is trapped by the pyridine in order to prevent decomposition

of the newly formed compound. The desired compound, 3-*N*-benzoyl-2',3'-*O*-diacetyl-5'-*O*-(*tert*-butyldiphenylsilyl)uridine **124**, was obtained as a yellow foam in 71 % yield after purification by column chromatography.

The formation of 3-*N*-benzoyl-2',3'-*O*-diacetyl-5'-*O*-(*tert*-butyldiphenylsilyl)uridine **124** was confirmed based on the disappearance of the amide NH peak in the ^1H NMR spectrum of the starting material **123**, which was originally observed as a broad singlet at 9.39 ppm. As well as by the appearance of new peaks in the ^1H NMR spectrum for the newly formed aromatic ring. These were found as part of the multiplet at 7.41-7.48 ppm (H-7*) and as part of the multiplet at 7.63-7.67 ppm (H-8*), as well as a characteristic doublet, integrating for 2 H, with $J = 7.34$ Hz, observed at 7.95 ppm (H-6*). Similarly, the new aromatic and carbonyl peaks were observed in the ^{13}C NMR spectrum as four new peaks in the range 129.32-135.54 ppm (H-5*, H-6*, H-7* and H-8*) and as one new peak at 168.62 ppm (N-C=O). Supporting evidence for the formation of the desired compound **124** was given by the presence of three new bands in the IR spectrum at 1632, 1670 and 2932 cm^{-1} , which are characteristic for the presence of a tertiary amide in the molecule. This was further substantiated by the HRMS spectrum, in which two peaks accounting for $[\text{M} + 1]^+$ and $[\text{M} + 23]^+$, were observed at 671.24173 and 693.22317 respectively, based on the calculated value for the molecular ion of 670.23466.

Step (iv) of **Scheme 11** shows the attempted synthesis of 3-*N*-benzoyl-5'-*O*-(*tert*-butyldiphenylsilyl)uridine **125** using sodium carbonate as the base for specific deprotonation of the amide NH, which is based on the procedure used by Sekine⁴⁴ for the synthesis of *N*³-benzoyl-3',5'-*O*-(1,1,3,3-tetraisopropylidisiloxane-1,3-diyl)uridine. As sodium carbonate is insoluble in most organic solvents, the reaction was carried out in a biphasic solution of $\text{CH}_2\text{Cl}_2 : \text{H}_2\text{O}$, with tetra-butylammonium bromide added as the phase transfer catalyst. This was followed by reaction with benzoyl chloride. Unfortunately, none of the desired compound, 3-*N*-benzoyl-5'-*O*-(*tert*-butyldiphenylsilyl)uridine **125**, was isolated from the reaction mixture. Instead, we were able to confirm by ^1H NMR, ^{13}C NMR and LRMS spectroscopy that we had in fact formed the unwanted 2',3'-*O*-dibenzoyl-5'-*O*-(*tert*-butyldiphenylsilyl)uridine **150** (**Scheme 11**). Full details of the ^1H NMR, ^{13}C NMR and LRMS spectroscopy are given in **Appendix B, Section B.21** and will not be discussed further.

Using a similar approach to that outlined in **Scheme 11**, we then went on to synthesise a range of DMT protected uridine derivatives. This approach is shown schematically in **Scheme 12** below.



Scheme 12 Synthesis of 4,4'-dimethoxytrityl protected derivatives of uridine: (i) 1.2 eq. DMT-Cl, 0.1 eq. DMAP, pyridine, 60 °C, 22 h, 83 %, (ii) 3 eq. acetic anhydride, 8 eq. pyridine, rt, 24 h, 90 %, (iii) 5 eq. benzoyl chloride, 5 eq. *N,N*-diisopropylethylamine, pyridine, rt, 2 h, 59 %, (iv) 1.3 eq. benzoyl chloride, 0.037 eq. tetra-butylammonium bromide, 8.3 eq. sodium carbonate, CH₂Cl₂ : H₂O, rt, 30 min, 0 %

Step (i) of **Scheme 12** shows the protection of the primary alcohol at the 5' position of the sugar ring with a DMT protecting group. Initial attempts at this synthesis involved the use of DABCO and tetra-butylammonium iodide under solvent free conditions, as described in Khalafi-Nezhad and co-workers;⁴⁵ however, under the conditions described, none of the desired compound **126** was obtained. We thus attempted the reaction using the conditions

described by Jin and co-workers⁴³ for the formation of 5'-*O*-(4,4'-dimethoxytrityl)-2'-*O*-(2-(trifluoroacetamido)-ethyl)uridine. The reaction was carried out at 60 °C, with catalytic amounts of DMAP added and using pyridine as both the base and the solvent for the reaction. The pyridine traps the HCl by-product formed during the reaction as the pyridine-hydrochloride salt, which was then removed by crystallization of the salt. The desired compound, 5'-*O*-(4,4'-dimethoxytrityl)uridine **126**, was obtained as a cream foam in 83 % yield after purification by column chromatography.

The synthesis of the desired compound, 5'-*O*-(4,4'-dimethoxytrityl)uridine **126**, was confirmed by the presence of new peaks corresponding to the methoxy groups and the aromatic rings in both the proton and IR spectra. In the ¹H NMR spectrum, a new singlet integrating for 6 H was observed at 3.78 ppm, which was identified as the peak corresponding to the two new methoxy groups. Other new peaks were observed in the aromatic region as a d integrating for 4 H, with $J = 8.70$ Hz, at 6.83 ppm and as a multiplet integrating for 9 H at 7.22-7.39 ppm, which were assigned as H-3* and overlapping peaks for H-2*, H-6*, H-7* and H-8* respectively. Similarly, new peaks were observed at 2962 cm⁻¹ which is characteristic for a OCH₃ group and at 669, 928 and 1510 cm⁻¹ which are specific for aromatic rings, with 669 cm⁻¹ accounting for 5 adjacent aromatic protons and 928 cm⁻¹ accounting for 2 adjacent aromatic protons. Final confirmation for the formation of the product was given by HRMS, in which peaks were observed at 547.20717 and 569.18944, corresponding to [M + 1]⁺ and [M + 23]⁺ respectively, based on the calculation for the molecular ion peak at 506.20022.

In *Step (ii)* of **Scheme 12**, we see the protection of the secondary alcohols at the 2' and 3' positions on the sugar ring with acetyl groups. The experimental procedure involved the use of acetic anhydride as the acetyl donor and pyridine as both the base and the solvent for the reaction. The reaction was carried out at rt and yielded the desired product 2',3'-*O*-diacetyl-5'-*O*-(4,4'-dimethoxytrityl)uridine **127** as a pale orange foam that did not require further purification by column chromatography in 90 % yield.

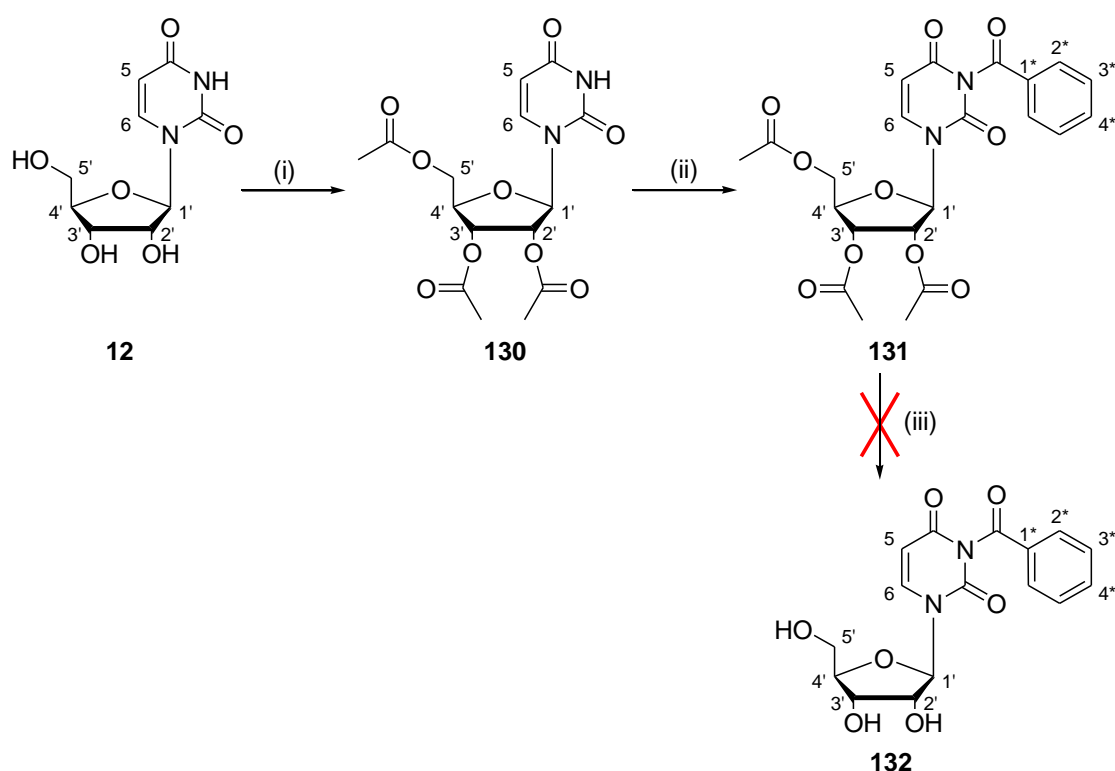
The synthesis of the desired compound, 2',3'-*O*-diacetyl-5'-*O*-(4,4'-dimethoxytrityl)uridine **127**, was confirmed by the presence of the new peaks for the two new acetyl groups in both the proton and carbon NMR spectra. In the ^1H NMR spectrum, two singlets were observed at 2.13 and 2.14 ppm, each integrating for 3 H, and were assigned to the two new methyl groups present in the molecule. Similarly, in the ^{13}C NMR spectrum, new peaks were observed at 20.65 and 20.85 ppm for the methyl groups and at 169.81 and 170.01 ppm for the carbonyl groups. Substantiating evidence was provided by the appearance of a band in the IR spectrum at 1607 cm^{-1} which is characteristic of the new C=O groups, as it appears at a different shift to those for the amide C=O groups on position C-2 and C-4 of the base. Final confirmation for the formation of compound **127** came from the HRMS, in which peaks were observed at 631.22851 for $[\text{M} + 1]^+$ and at 653.21020 for $[\text{M} + 23]^+$, based on the calculation for the molecular ion peak at 630.22135.

Outlined in *Step (iii)* of **Scheme 12** is the protection of the secondary amide position on the base as a benzoyl derivative. Hünig's base was used to deprotonate the amide and the system was then reacted with benzoyl chloride using the conditions described in detail for *Step (iii)* of **Scheme 11**. The desired compound, 3-*N*-benzoyl-2',3'-*O*-diacetyl-5'-*O*-(4,4'-dimethoxytrityl)uridine **128**, was obtained as a yellow foam in 59 % yield after purification by column chromatography.

Formation of 3-*N*-benzoyl-2',3'-*O*-diacetyl-5'-*O*-(4,4'-dimethoxytrityl)uridine **128** was confirmed by the presence of extra peaks in the aromatic region of the ^1H NMR spectrum. These were observed as part of a multiplet at 7.27-7.68 ppm integrating for 12 H (containing H-11* and H-12*) and as a doublet at 7.96 ppm ($J = 8.80\text{ Hz}$) with a characteristic shift for H-10*. As well as by the disappearance of the broad singlet at 9.34 ppm assigned as NH, in the ^1H NMR spectrum for the starting material **127**. Similarly, the new aromatic carbons were observed as peaks at 129.33 (C-10*), 130.37 (C-11*), 131.56 (C-12*) and 135.32 ppm (C-9*), and the new carbonyl group was observed as a characteristic peak at 168.68 ppm (N-C=O) in the ^{13}C NMR spectrum. Supporting data for the formation of **128** was obtained from the IR spectrum as new bands were observed at 1671 and 2934 cm^{-1} for the newly formed tertiary amide. Final characterizing data was obtained from the HRMS, wherein a peak was

observed at 757.23653, which when 23 is removed for the sodium additive, correlates well to the calculated value of 734.24756 for the molecular ion.

Step (iv) of **Scheme 12** highlights the attempted synthesis of 3-*N*-benzoyl-5'-*O*-(4,4'-dimethoxytrityl)uridine **129** using conditions similar to those used in *Step (iv)* of **Scheme 11**⁴⁴ for the preparation of the corresponding TBDPS derivative. In this case, we used sodium carbonate as the base for deprotonation of the amide NH specifically, which was followed by reaction with benzoyl chloride. As sodium carbonate is insoluble in most organic solvents, the reaction was carried out in a biphasic solution of CH₂Cl₂ : H₂O, with tetra-butylammonium bromide added as the phase transfer catalyst. Unfortunately, as happened before, none of the desired compound **129** was isolated from the reaction mixture.



Scheme 13 *Synthesis of acetyl protected derivatives of uridine:* (i) 4.5 eq. acetic anhydride, 7.5 eq. pyridine, rt, 22 h, 93 %, (ii) 5 eq. benzoyl chloride, 5 eq. *N,N*-diisopropylethylamine, pyridine, rt, 2 h, 93 %, (iii) 4.5 eq. potassium carbonate, MeOH, rt, 2 h, 0 % or 3 eq. *p*-TsOH.H₂O, CH₂Cl₂ : MeOH, rt, 24 h, 0 %

Using a modified approach to that outlined in **Scheme 11** and **Scheme 12**, we were able to synthesise a range of acetyl protected uridine derivatives. This approach is shown schematically in **Scheme 13**.

Initially, as shown in *Step (i)* of **Scheme 13**, all three of the alcohols present on the sugar ring were protected as the acetyl derivative. This reaction occurred using pyridine as both the base and the solvent for the reaction, with acetic anhydride present in excess as the acetyl donor. The desired compound, 2',3',5'-*O*-triacetyluridine **130**, was obtained as a white foam in 93 % yield after purification by column chromatography.

Formation of 2',3',5'-*O*-triacetyluridine **130** was confirmed through the presence of three new singlets in the ^1H NMR spectrum, each integrating for 3 H, and assigned as each of the newly formed methyl groups. Similarly, three new peaks were observed at 20.56, 20.65 and 20.79 ppm, which were assigned as the methyl groups, in the ^{13}C NMR spectrum. Also observed, were new peaks at 169.84 ppm for the C=O present on the C-2' and C-3' positions (originally secondary alcohols), and at 170.36 ppm for the C=O present on the C-5' position (originally the primary alcohol). Supporting data was obtained from the IR spectrum, in which peaks were observed at 1216 cm^{-1} for $-\text{CO}-\text{CH}_3$, at 1379 cm^{-1} for the CH_3 symmetrical deformation and at 1750 cm^{-1} for the new C=O groups. Other supporting data was obtained from the HRMS, in which peaks were observed at 371.10849 for $[\text{M} + 1]^+$ and at 393.09029 for $[\text{M} + 23]^+$, based on the calculation for the molecular ion peak at 370.10123.

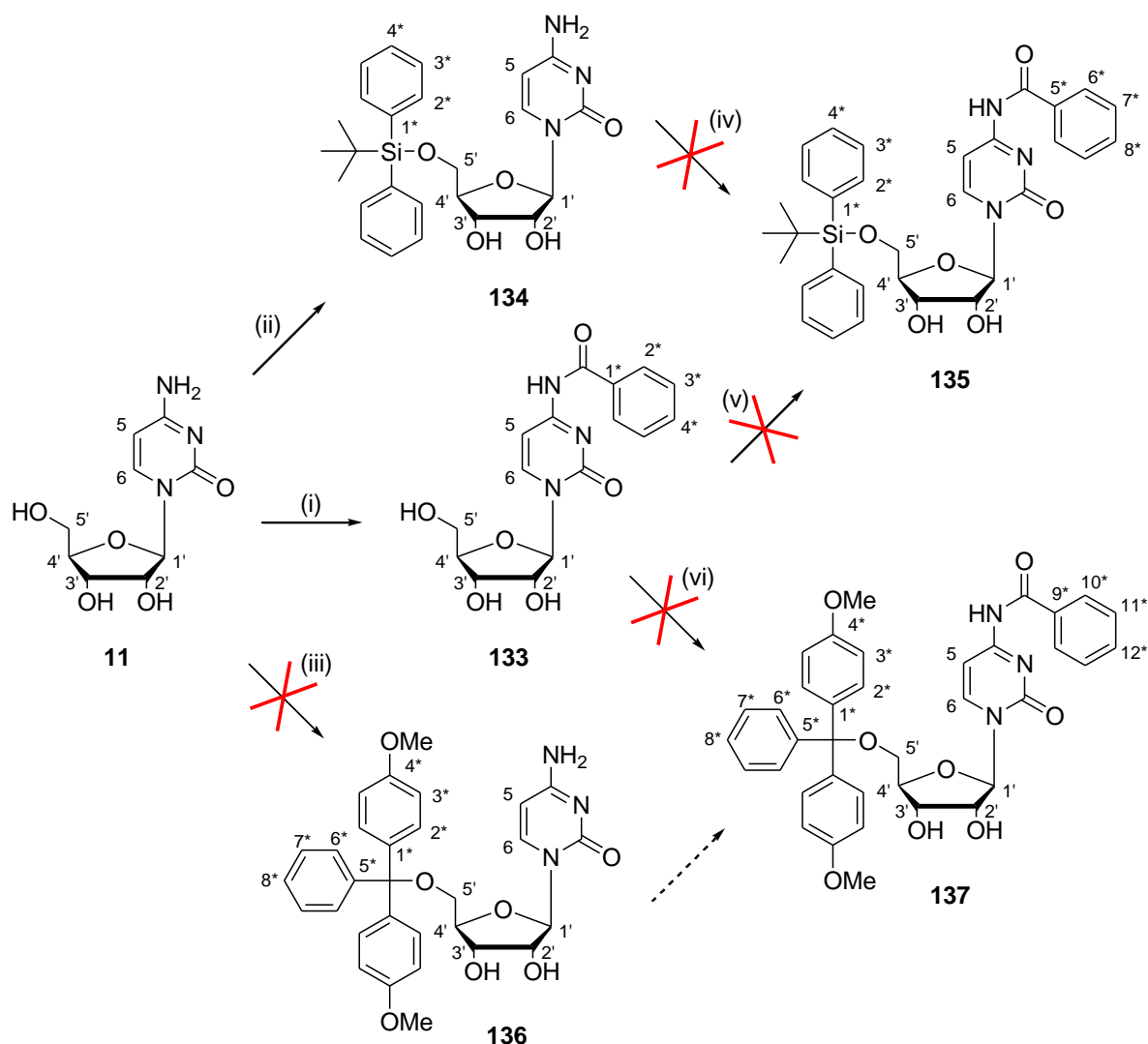
Outlined in *Step (ii)* of **Scheme 13** is the protection of the secondary amide position on the uridine base as a benzoyl derivative. The procedure used was one adapted from that reported previously by Kamimura and co-workers.⁴⁶⁻⁴⁷ The reaction occurred through the deprotonation of the amide NH using Hünig's base and the subsequent attack on the benzoyl chloride. In this instance, pyridine was used as the solvent for the reaction as the by-product for the reaction is gaseous hydrochloric acid, which was trapped by the pyridine in order to prevent decomposition of the newly formed compound. The desired compound, 3-*N*-benzoyl-2',3',5'-*O*-triacetyluridine **131**, was obtained as a bright yellow foam in 93 % yield after purification by column chromatography.

The synthesis of the desired compound, 3-*N*-benzoyl-2',3',5'-*O*-triacetyluridine **131**, was confirmed through the use of various spectroscopic techniques. The ¹H NMR spectrum shows the disappearance of the broad singlet at 9.61 ppm in the starting material (**130**) spectrum and the appearance of new peaks as part of the multiplet integrating for 3 H at 7.48-7.53 ppm (contains signal for H-3*), as a multiplet at 7.64-7.66 ppm integrating for 1 H (H-4*) and as a doublet at 7.95 ppm with $J = 7.84$ Hz integrating for 2 H (H-2*). Similarly, the ¹³C NMR shows the appearance of new peaks in the aromatic region at 129.35 (C-3*), 130.75 (C-2*), 131.47 (C-1*) and 135.37 ppm (C-4*), as well as new peaks at 169.76, 169.98 and 170.28 ppm (corresponding to the three new C=O groups). Supporting evidence for the formation of **131** was obtained from the IR spectrum as new bands were noted at 775 cm⁻¹ which is characteristic for 5 adjacent aromatic protons, and at 1540 and 1752 cm⁻¹ accounting for the presence of a tertiary amide. Final characterizing data was obtained from the HRMS, wherein a peak was observed at 497.11584, which when 23 is removed for the sodium additive, correlates well to the calculated value of 474.12744 for the molecular ion. The [M + 1]⁺ peak was also observed at 475.13429, ensuring our accurate determination of the product for the reaction as compound **131**.

Shown in *Step (iii)* of **Scheme 13** is the attempted synthesis of 3-*N*-benzoyluridine **132**. The initial attempt was to do a base catalysed deprotection on the protected uridine **131**, in order to remove all three of the acetyl groups simultaneously. The reaction was attempted using excess potassium carbonate with a methanolic solution of **131** and reacting at rt for 2 hours. After this time consumption of the starting material was noted by tlc, but none of the desired 3-*N*-benzoyluridine **132** was isolated from the reaction.

A second attempt was made at the formation of 3-*N*-benzoyluridine **132**, this time using an acid-catalysed deprotection procedure (described in Bermejo and co-workers⁴⁸ for the synthesis of similar derivatives). The reaction was conducted using excess tosic acid as a solution in CH₂Cl₂ : MeOH. Unfortunately, even after reaction at rt for 24 h, none of the desired 3-*N*-benzoyluridine **132** was isolated from the reaction mixture.

It was at this point that we ended the synthesis of uridine (**12**) derivatives and began our synthesis of the less common derivatives of cytidine (**11**). The route adopted for the synthesis of cytidine (**11**) derivatives is outlined below in **Scheme 14**.



Scheme 14 *Synthesis of derivatives of cytidine:* (i) 4 eq. benzoic anhydride, absolute EtOH, reflux, 4 h, 97 %, (ii) 1.1 eq. TBDPS-Cl, 0.1 eq. DMAP, pyridine, rt, 23 h, 100 %, (iii) 1.2 eq. DMT-Cl, 0.1 eq. DMAP, pyridine, rt, 23 h, 0 %, (iv) 4 eq. benzoic anhydride, absolute EtOH, reflux, 4 h, 0 %, (v) 1.1 eq. TBDPS-Cl, 0.1 eq. DMAP, pyridine, rt, 22 h, 0 %, (vi) 1 eq. DMT-Cl, 0.02 eq. DMAP, pyridine, rt, 20 h, 0 % or 1.2 eq. DMT-Cl, 0.1 eq. DMAP, pyridine, rt, 21 h, 0 %

Outlined in *Step (i)* of **Scheme 14** is the protection of the primary amine at the C-4 position of the base with a benzoyl group, as described by Townsend and Tipson.⁴⁹ The reaction was carried out by the stepwise additions of benzoic anhydride to a refluxing solution of cytidine **11** in absolute ethanol. After trituration with diethyl ether, the desired compound, 4-*N*-benzoylcytidine **133**, was obtained as a fluffy white powder in 97 % yield.

The formation of 4-*N*-benzoylcytidine **133** was confirmed by the presence of new aromatic peaks in the ¹H NMR spectrum, observed as a multiplet integrating for 2 H at 7.46-7.50 ppm (H-3*), another multiplet integrating for 1 H at 7.53-7.62 ppm (H-4*) and a doublet, with $J = 7.46$ Hz, integrating for 2 H at 8.00 ppm (H-2*). Similarly, new peaks were present in the ¹³C NMR spectrum, with the new aromatic carbons observed as peaks at 128.55 (C-2* and C-3*), 132.85 (C-4*) and 133.21 ppm (C-1*), along with the new peak for the amide C=O present at 167.44 ppm. Supporting evidence for the presence of the benzoyl group was given by the appearance of bands in the IR spectrum: at 670 and 741 cm⁻¹ for five adjacent aromatic protons, and at 1504 and 1601 cm⁻¹ for the new aromatic ring. Final confirmation for the formation of **133** was provided by the presence of a peak at 348.11509 ([M + 1]⁺) in the HRMS spectrum, which correlates well to the calculated value of 347.11174 for the molecular ion.

Shown in *Step (ii)* of **Scheme 14** is the protection of the primary alcohol on the 5' position of the sugar ring as a TBDPS group. The reaction was carried out using pyridine as both the base and the solvent for the reaction, with a catalytic amount of DMAP added. The deprotonated cytidine **11** was then reacted with excess *tert*-butyldiphenylsilyl chloride at rt overnight. The desired compound, 5'-*O*-(*tert*-butyldiphenylsilyl)cytidine **134**, was obtained as a white foam after purification by column chromatography in 100 % yield.

The synthesis of the desired compound, 5'-*O*-(*tert*-butyldiphenylsilyl)cytidine **134**, was confirmed through the use of various spectroscopic techniques. The ¹H NMR spectrum shows the appearance of a new singlet integrating for 9 H at 1.02 ppm for the three equivalent methyl groups, as well as the appearance of new signals in the aromatic region: as a multiplet at 7.39-7.49 ppm integrating for 6 H (H-3* and H-4*) and as a multiplet at 7.63-7.65 ppm

integrating for 4 H (H-2*). Similarly, new peaks were observed in the ^{13}C NMR spectrum at 17.79 ppm for $\text{C}(\text{CH}_3)_3$ and at 26.65 ppm for $\text{C}(\text{CH}_3)_3$ showing the presence of the new *tert*-butyl group. New peaks were also observed for the two aromatic rings at 127.96 (C-3*), 129.96 (C-4*), 132.27 (C-1*) and 134.96 ppm (C-2*) in the ^{13}C NMR spectrum. Substantiating evidence was provided by the appearance of new bands in the IR spectrum at 1109 cm^{-1} for the Si-O stretch and at 3021 cm^{-1} for the aromatic rings. HRMS gave supporting data for the formation of compound **134** as a peak was observed at 482.20978 for $[\text{M} + 1]^+$ which correlates well to the calculated value of 481.20330 for the molecular ion.

Step (iii) of **Scheme 14** shows the attempted synthesis of 5'-*O*-(4,4'-dimethoxytrityl)cytidine **136**, through the reaction of cytidine **11** with 4,4'-dimethoxytrityl chloride in the presence of catalytic DMAP and pyridine (acting as both the solvent and the base for the reaction). Unfortunately, even after numerous attempts at recrystallisation of the mixture obtained after column chromatography, none of the desired compound 5'-*O*-(4,4'-dimethoxytrityl)cytidine **136** was obtained pure. We were however able to isolate a mixture of compound **136** and a triethylamine salt, which were inseparable, as well as some of the 4,4'-dimethoxytrityl alcohol **147**.

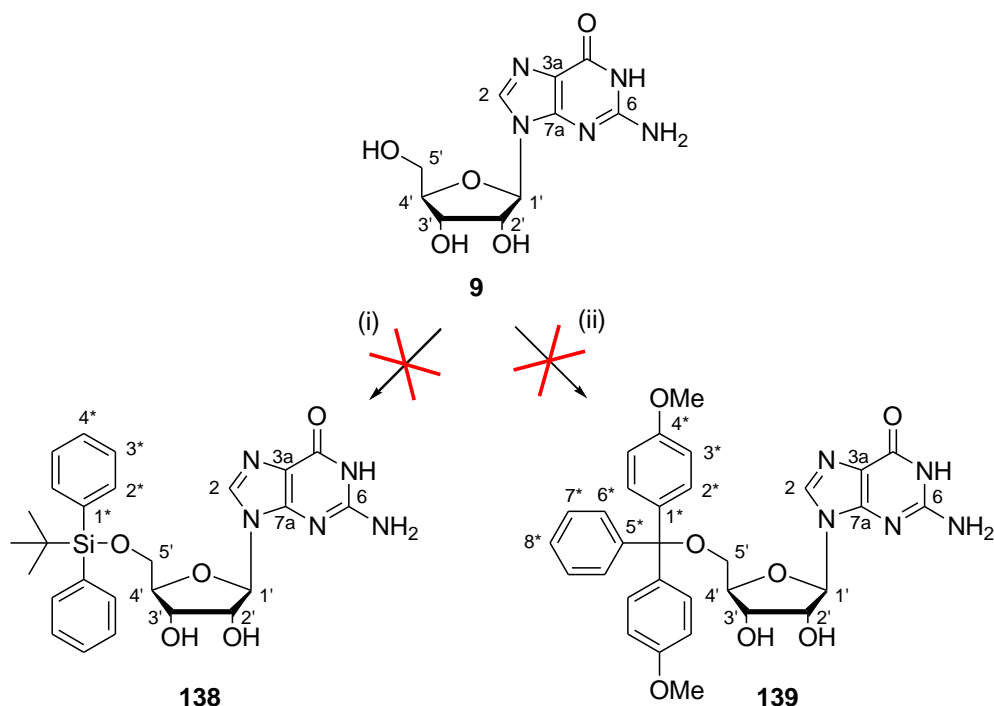
Outlined in *Step (iv)* of **Scheme 14** is the first route attempted for the synthesis of 4-*N*-benzoyl-5'-*O*-(*tert*-butyldiphenylsilyl)cytidine **135**. In this route, the compound **134** was heated to reflux in absolute ethanol before the stepwise additions of benzoic anhydride. After subsequent trituration with diethyl ether, none of the desired compound **135** was obtained. Instead, the white powder isolated from the reaction mixture was found to contain only unreacted starting material **134**. Outlined in *Step (v)* of **Scheme 14** is the second route attempted for the synthesis of 4-*N*-benzoyl-5'-*O*-(*tert*-butyldiphenylsilyl)cytidine **135**. This route shows the reaction of compound **133** with *tert*-butyldiphenylsilyl chloride in the presence of the base and solvent for the reaction, pyridine, as well as catalytic amounts of DMAP. Unfortunately, none of the desired compound 4-*N*-benzoyl-5'-*O*-(*tert*-butyldiphenylsilyl)cytidine **135** was obtained after purification by column chromatography.

Finally, shown in *Step (vi)* of **Scheme 14** is the attempted synthesis of 4-*N*-benzoyl-5'-*O*-(4,4'-dimethoxytrityl)cytidine **137**. Both methods illustrated involve the use of catalytic DMAP and have pyridine present to act as both the base and the solvent for the reaction. In both instances, the deprotonation of the primary alcohol in the 5' position of the sugar ring was immediately followed by the reaction with 4,4'-dimethoxytrityl chloride. Differences in the two methods come from the differing molar equivalents used for the DMT-Cl and DMAP, as well as in the work-up. For the first method shown, the reaction was worked up through a number of extractions with a saturated solution of NaHCO₃, CHCl₃ and brine. A recrystallisation was then attempted from EtOH/CHCl₃ and Et₂O, which was followed by purification by column chromatography. In the second method above, the reaction was quenched with the addition of EtOH and the residue obtained was recrystallised from hot MeOH. None of the desired compound 4-*N*-benzoyl-5'-*O*-(4,4'-dimethoxytrityl)cytidine **137**, was isolated from either attempt at the reaction.

Having completed the synthesis of the uridine **12** derivatives (as shown in **Scheme 11**, **Scheme 12** and **Scheme 13**), as well as having attempted the synthesis of a number of cytidine **11** derivatives (as shown in **Scheme 14**), we then decided to proceed to the preparation of the purine-based nucleoside derivatives. The nucleosides chosen for this study were guanosine **9**, inosine **116** and adenosine **8**.

2.2.2.3 Purine-Based Nucleosides – Focusing on Guanosine, Inosine and Adenosine

The first of the purine-based nucleosides that we chose to work on was guanosine **9**. This nucleoside was chosen as we had previously worked with it on our attempted synthesis of 2',3'-fused bicyclic systems, as described in *Section 2.2.1.3*. Our initial approach towards the synthesis of *tert*-butyldiphenylsilyl- and 4,4'-dimethoxytrityl-protected derivatives is outlined in **Scheme 15**.



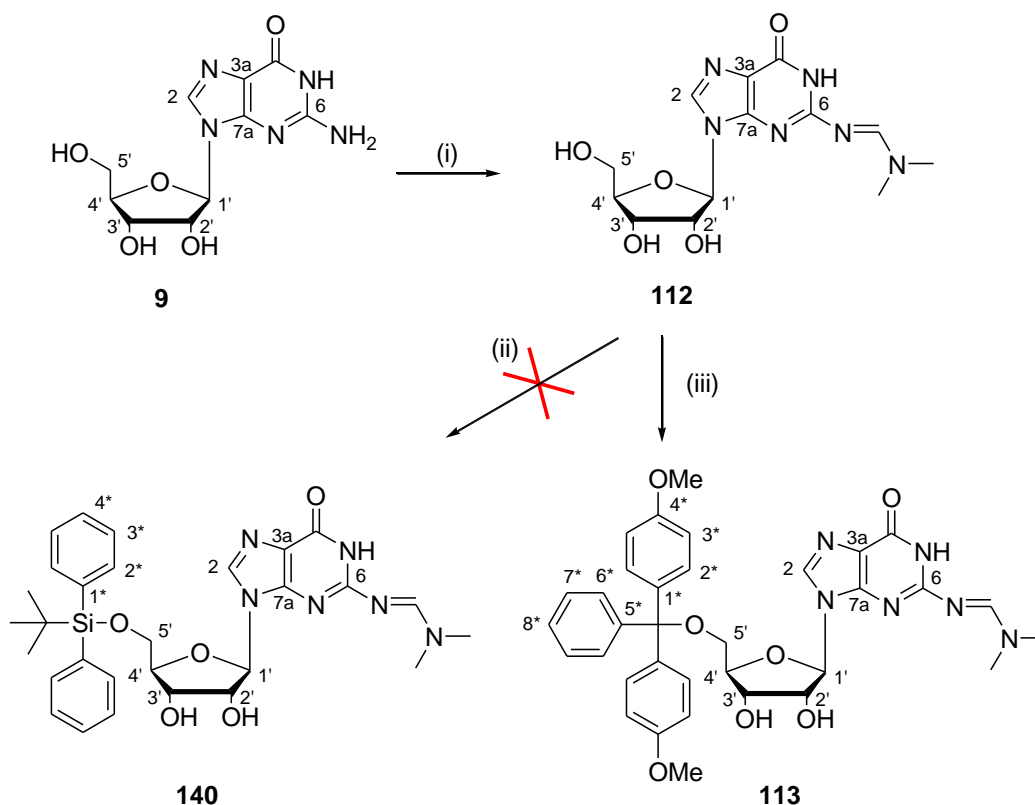
Scheme 15 Attempted synthesis of derivatives of guanosine: (i) 1.1 eq. TBDPS-Cl, 0.01 eq. DMAP, pyridine, rt, 24 h, 0 %, or 1 eq. TBDPS-Cl, 2 eq. imidazole, DMF, rt 48 h, 0 %, (ii) 1.2 eq. DMT-Cl, 0.01 eq. DMAP, pyridine, 60 °C, 20 h, 0 %

Step (i) of **Scheme 15** shows the attempted synthesis of 5'-O-(*tert*-butyldiphenylsilyl)guanosine **138**. Various attempts were made for this synthesis, the first of which involved the protection of the primary alcohol in the 5' position of the sugar ring by stirring the guanosine **9** and the catalyst DMAP with pyridine, which serves as both the solvent and the base for the reaction. The pyridine deprotonates the alcohol and then allows for reaction with the *tert*-butyldiphenylsilyl chloride, giving HCl off as the by-product to the reaction. Unfortunately, none of the desired compound **138** was isolated from the reaction (in one attempt, only unreacted guanosine **9** was isolated). Thus, a different approach was adopted, in which the guanosine **9** was prepared as a solution in distilled DMF and then imidazole was added as the base for the deprotonation, before reaction with *tert*-butyldiphenylsilyl chloride, using the procedure outlined in Sproat and co-workers.⁴² Numerous attempts at recrystallisation of the crude semi-solid failed and each time unidentifiable by-products were isolated, with none of the desired 5'-O-(*tert*-butyldiphenylsilyl)guanosine **138** being obtained.

Outlined in *Step (ii)* of **Scheme 15** is the attempted synthesis of 5'-*O*-(4,4'-dimethoxytrityl)guanosine **139**. For this reaction, guanosine **9** was dissolved in pyridine and the solution was heated to 60 °C, before the addition of excess 4,4'-dimethoxytrityl chloride and a catalytic amount of DMAP, followed by overnight reaction. Unfortunately, the only compounds isolated after column chromatography were the 4,4'-dimethoxytrityl chloride degradation products and unreacted guanosine **9**. Our belief is that if the desired compound 5'-*O*-(4,4'-dimethoxytrityl)guanosine **139** had formed, it subsequently decomposed during purification.

Having had little success protecting the primary alcohol on the 5' position of the sugar ring directly, we decided to change our approach and re-order the sequence of protection steps. We thus began our next synthesis with the protection of the primary amine of the base instead. The synthetic approach used is outlined in detail in **Scheme 16** on the following page.

Step (i) of **Scheme 16** shows the protection of the primary amine on the base using *N,N*-dimethylformamide dimethyl acetal. The detailed synthesis was described previously in *Section 2.2.1.3* as shown in *Step (i)* of **Scheme 6**.⁴² The desired compound, 6-*N*-(*N,N*-dimethylmethyylimine)guanosine **112**, was obtained in 79 % yield after purification.



Scheme 16 Synthesis of derivatives of guanosine: (i) 2 eq. *N,N*-dimethylformamide dimethyl acetal, DMF, rt, 27 h, 79 %, (ii) 1.1 eq. TBDPS-Cl, 0.1 eq. DMAP, pyridine, rt, 25 h, 0 %, or 1 eq. TBDPS-Cl, 2 eq. imidazole, DMF, rt, 20 h, 0 %, (iii) 1 eq. DMT-Cl, 0.1 eq. DMAP, pyridine, rt, 25 h, 69 %

Shown in *Step (ii)* of **Scheme 16** is the attempted synthesis of 5'-*O*-(*tert*-butyldiphenylsilyl)-6-*N*-(*N,N*-dimethylmethylimine)guanosine **140**. Two general approaches were used in these attempts, the first of which involved the use of pyridine as the base and solvent for the reaction, with catalytic amounts of DMAP added, and this was followed by reaction with excess *tert*-butyldiphenylsilyl chloride. The second approach used involved the use of imidazole as the base and DMF as the solvent, which was then followed by reaction with a molar equivalent of *tert*-butyldiphenylsilyl chloride. This approach was modified from the work done by Sproat and co-workers⁴² as discussed previously in *Section 2.2.1.3*. Neither of the approaches were successful and none of the desired 5'-*O*-(*tert*-butyldiphenylsilyl)-6-*N*-(*N,N*-dimethylmethylimine)guanosine **140** was isolated after purification by either recrystallisation or column chromatography.

Step (i) of **Scheme 17** outlines the attempted synthesis of 5'-*O*-(*tert*-butyldiphenylsilyl)inosine **141**, through protection of the primary alcohol. The reaction was attempted a number of times on various scales using pyridine as both the base and the solvent for the reaction, with catalytic amounts of DMAP added and followed by reaction with *tert*-butyldiphenylsilyl uridine. After purification by column chromatography, none of the desired compound **141** was isolated and it appeared as though it had decomposed during purification. In another attempt at the reaction, the crude residue was purified by an acid-base extraction procedure, but as before, only decomposition products were isolated. Various other attempts at the reaction were followed by purification by recrystallisation; unfortunately none of these attempts yielded any of the desired product, 5'-*O*-(*tert*-butyldiphenylsilyl)inosine **141**.

Shown in *Step (ii)* of **Scheme 17** is the protection of the primary alcohol on the 5' position of the sugar ring with a 4,4'-dimethoxytrityl group. The detailed synthesis was described previously in *Section 2.2.1.3* above, as shown in *Step (i)* of **Scheme 7**. As discussed before, the desired compound 5'-*O*-(4,4'-dimethoxytrityl)inosine **117**, was obtained in 78 % yield after purification.

It was at this point that we concluded the synthesis of inosine (**116**) derivatives and began our synthesis of the less common derivatives of adenosine (**8**). The route adopted for the synthesis of adenosine (**8**) derivatives is similar to that used for the preparation of the inosine (**116**) derivatives shown above and is outlined schematically below in **Scheme 18**. Both approaches for the synthesis of adenosine derivatives were adapted from work reported by Manoharan and co-workers⁴¹ on the protection of various modified nucleosides and oligonucleotides.

observed which correspond to the two new aromatic rings at 127.41 (C-3*), 129.39 (C-4*), 132.40 (C-1*) and 134.82 ppm (C-2*). Further evidence for the formation of compound **142** was provided by the bands observed in the IR spectrum at 626 cm⁻¹ for the Si-O stretch, at 670 and 780 cm⁻¹ for the five adjacent aromatic protons and at 1522 and 3021 cm⁻¹ for the newly formed aromatic rings. Final data on the formation of compound **142** was obtained from the HRMS, in which a peak was observed at 506.22098 which corresponds to [M + 1]⁺ when compared to the calculated value of 505.21453 for the molecular ion.

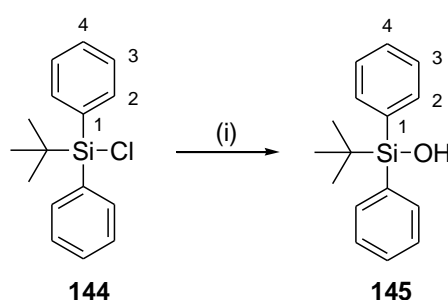
Finally, outlined in *Step (ii)* of **Scheme 18** is the attempted synthesis of 5'-O-(4,4'-dimethoxytrityl)adenosine **143**. The reaction involves the protection of the primary alcohol in the 5' position of the sugar ring, this was attempted utilizing pyridine (as both the base and the solvent for the reaction) to deprotonate the primary alcohol in the presence of a catalytic amount of DMAP. After warming to 60 °C the mixture was allowed to react with excess 4,4'-dimethoxytrityl chloride overnight. Following purification by column chromatography and numerous attempts at recrystallisation, the desired compound **143** was always isolated contaminated with a triethylamine salt. Unfortunately, no 5'-O-(4,4'-dimethoxytrityl)-adenosine **143** was obtained in sufficient purity for further biological testing.

Thus having completed the synthesis of the guanosine **9** derivatives (as shown above in **Scheme 15** and **Scheme 16**) and having attempted the synthesis of a range of inosine **116** and adenosine **8** derivatives (as shown above in **Scheme 17** and **Scheme 18**), we then continued with the synthesis of the controls required for our biological assays.

2.2.2.4 Controls for Biological Assays

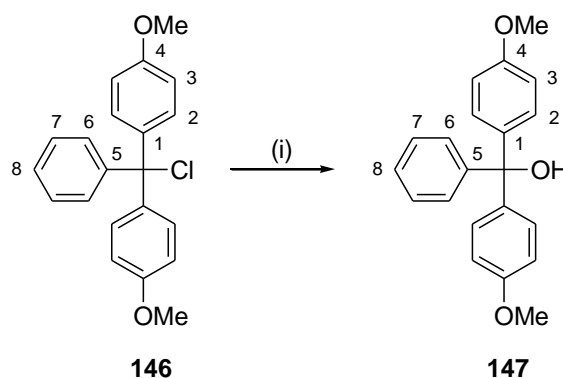
The controls required for this study were the protecting group derivatives, *tert*-butyldiphenylsilanol **145**, and 4,4'-dimethoxytrityl alcohol **147**.

The first protecting group derivative prepared as a control for the biological assays is shown in **Scheme 19**, where *Step (i)* outlines the synthesis of *tert*-butyldiphenylsilanol **145**, based on the approach previously reported by Mullen and Barany.⁵⁰ The reaction occurred by dissolving the starting material, *tert*-butyldiphenylsilyl chloride **144**, in diethyl ether and then adding to it a solution of the base potassium hydroxide in H₂O : MeOH. After reaction at rt overnight, the mixture was purified by extraction and the desired compound *tert*-butyldiphenylsilanol **145** was obtained as a opaque oil in 92 % yield.



Scheme 19 *Synthesis of the derivative of TBDPS-Cl: (i) 1.1 eq. potassium hydroxide, H₂O : MeOH, Et₂O, rt, 24 h, 92 %*

The formation of the *tert*-butyldiphenylsilanol **145** was confirmed by the presence of a broad singlet at 3.53 ppm in the ¹H NMR spectrum which disappeared when D₂O was added to the NMR sample. ¹³C NMR spectroscopy did not give any conclusive evidence for the formation of the desired product **145**, but substantiating evidence was provided by the bands in the IR spectrum at 1084 cm⁻¹ which corresponds to a C-O stretch from a C-OH group, and at 1331 cm⁻¹ which is characteristic of O-H bending. Further data supporting the formation of compound **145** was provided by the peak observed at 279 ([M + 23]⁺), with 55 % abundance in the LRMS spectrum, which correlates well to the calculated value for the molecular ion of 256, when 23 is removed for the sodium additive. HRMS data could not be determined as the compound was too volatile for detection.



Scheme 20 Synthesis of the derivative of DMT-Cl: (i) 0.5 M NaOH, THF, rt, 30 min, 87 %

The second protecting group derivative synthesized as a control for the biological assays was 4,4'-dimethoxytrityl alcohol **147**. The approach was based on that of Golding and co-workers⁵¹ and this approach is shown in **Scheme 20**. To the 4,4'-dimethoxytrityl chloride **146** was added a solution of THF and 0.5 M aqueous sodium hydroxide. The reaction was then stirred at rt for 30 min, the crude compound being obtained by extraction and then purified by column chromatography. After purification, the desired compound 4,4'-dimethoxytrityl alcohol **147** was obtained as a yellow-orange semi-solid in 87 % yield.

Formation of 4,4'-dimethoxytrityl alcohol **147** was confirmed by the presence of a broad singlet at 2.76 ppm in the ¹H NMR spectrum which exchanged with deuterium. All other peaks were observed as expected in both the ¹H and ¹³C NMR spectra. Further evidence for the formation of the alcohol group was given by the bands appearing at 1115 cm⁻¹ (C-O stretch from C-OH), 1360 cm⁻¹ (O-H bending) and 3504 cm⁻¹ (O-H stretchin) in the IR spectrum. LRMS data supported the conclusion that compound **147** had been prepared as the [M + 23]⁺ peak was observed with 7 % relative abundance in the sample.

2.3 CONCLUSIONS

Using our strategy towards fused bicyclic ring systems, we were able to synthesise the diene 2',3'-*O*-diallyl-5'-*O*-(*tert*-butyldiphenylsilyl)-1'-*O*-methoxy- β -(-)-ribose **103**, but were unable to obtain the bicyclic ring system using RCM. The inability to form the ring closed product via RCM was also observed for 2',3'-*O*-diallyl-5'-*O*-(4,4'-dimethoxytrityl)-6-*N*-(*N,N*-dimethylmethyylimine)guanosine **114**. Due to the time constraints of the project, we decided not to continue along this synthetic route and instead shifted our focus to the synthesis of a range of compounds that would be used to conduct a structure-activity study.

For these derivatives, we prepared a series of compounds that had different functional groups present on the primary hydroxyls and secondary hydroxyls on the sugar ring, as well as different groups present on the primary amines and/or amide groups of the bases. This synthesis was performed to obtain a range of sugar derivatives (β -(-)-ribose **100**) and nucleoside derivatives (adenosine **8**, cytidine **11**, guanosine **9**, inosine **116** and uridine **12**). Included in this group were the corresponding protecting group derivatives, *tert*-butyldiphenylsilyl alcohol **145** and 4,4'-dimethoxytrityl alcohol **147**.

Having the range of synthetic compounds in hand, for both the approach towards the fused bicyclic ring systems and those for the structure-activity study, we then moved on to the biological testing. For the biological testing, we assayed our range of synthetic compounds for inhibitory activity against four bacterial strains, four cancer cell lines and HIV. The results of the biological testing are discussed in detail in **Chapter 3**.

Chapter 3:
Results and Discussion for Biological Testing

CONTRIBUTIONS TO THIS CHAPTER

All of the antibacterial assays and accompanying statistical analyses were performed by Ms J.-L. Panayides, while under the supervision of both Dr D. Lindsay and Prof E.M.C. Rey. The work was performed in the School of Molecular and Cellular Biology at the University of the Witwatersrand.

*The HIV assay was performed by Ms A. Naidoo under the supervision of Dr R. Parboosing. The work was performed at the Department of Virology at the University of KwaZulu-Natal, which forms part of the National Health Laboratory Services. We would like to thank Ms A. Naidoo for the preparation of the graphs reported as **Graphs 5-11** in the proceeding text.*

*The cell proliferation studies were done by Mrs H. Apostolellis and Mrs N. Dahan-Farkas, while under the supervision of Dr H. Davids. The work was carried out at the Division of Pharmacology, which forms part of the Department of Pharmacy and Pharmacology at the University of the Witwatersrand. Dr H. Davids is currently based at the Department of Biochemistry and Microbiology at the Nelson Mandela Metropolitan University. We would like to thank Mrs N. Dahan-Farkas for the preparation of the graphs reported as **Graphs 12-15** in the proceeding text.*

3.1 CHAPTER OVERVIEW

In order to determine if the synthetic nucleoside derivatives prepared (synthesis described in **Chapter 2**) possessed general biological activity, we assayed them for antibacterial, antiviral and anticancer properties. This chapter begins with our assay of all of the synthetic compounds for broad-spectrum antibacterial activity. This is followed by an antiviral assay, wherein ten representative examples were selected from all the first generation synthetic compounds and were then tested for activity against HIV using a well known whole cell assay. Finally, we describe the assay for inhibition of cell proliferation in five cancerous cell lines. Seventeen of the first generation synthetic compounds were selected [in order to

encompass derivatives of all five nucleosides and the model α -(-)-ribose] and were then used in the assay.

3.2 RESULTS AND DISCUSSION

3.2.1 Antibacterial Assays

For this study we tested fifteen nucleoside derivatives, eight α -(-)-ribose derivatives and two synthetic controls for possible antibacterial activity. Our study involved the use of two Gram-positive and two Gram-negative bacterial strains.

3.2.1.1 Materials and Methods

Bacterial Cultures

We chose *Staphylococcus aureus* (ATCC 25923) and *Bacillus cereus* (DL5) as our representative Gram-positive bacteria. *S. aureus* strain ATCC 25923 is a clinical isolate that was deposited with the ATCC by the FDA (designation Seattle 1945) and has a biosafety level 2 ranking.⁵² *S. aureus* strain ATCC 25923 is a Gram-positive coccus, with colonies that appear very opaque, round, smooth and are golden yellow in colour. It is pathogenic and is associated with the frequent occurrence of antibiotic resistance mechanisms. It can cause a wide range of illnesses, from minor ones, such as skin infections, to life-threatening ones, such as septicemia.

B. cereus strain DL5 is an environmental isolate that was obtained from alkaline wash solutions in a South African dairy farm; as described by Lindsay and co-workers.⁵³⁻⁵⁵ *B. cereus* strain DL5 has been fully characterized and the data deposited, the accession number is

AF 363441. *B. cereus* is a Gram-positive eubacterium that forms endospores and often produces rhizoid swirling colonies. It is known to be a foodborne pathogen and a cytotoxin producer.

For the study we also used *Pseudomonas aeruginosa* (ATCC 27853) and *Escherichia coli* (ATCC 25922) as our representative Gram-negative bacteria. *P. aeruginosa* strain ATCC 27853 was isolated from blood culture and was deposited at the ATCC by A.A. Medeiros (designation Boston 41501) and has a biosafety level 2 ranking.⁵⁶ *P. aeruginosa* is often involved in hospital acquired infections, with symptoms of infection including inflammation and sepsis which can be fatal.

E. coli strain ATCC 25922 is a clinical isolate that was deposited with the ATCC by the FDA (designations FDA strain Seattle 1946, DSM1103 and NCIB 12210) and has a biosafety level 1 ranking.⁵⁷ *E. coli* strain ATCC 25922 is a Gram-negative bacterium which is rod-shaped (with motility derived from peritrichous flagella), and has colonies that are round, smooth, sharply defined and are translucent pale grey in colour. *E. coli* strains occur as part of the natural flora of the lower intestine and as such are used as indicator organisms for faecal contamination in the environment.

All of the bacterial strains were grown from either freezer stocks or freeze-dried swabs, maintained on nutrient agar plates at 4 °C and sub-cultured every 21 days. Each culture was grown in 100 cm³ nutrient broth overnight at 37 °C. A full description of the procedure used is outlined in detail in **Appendix C (Section C.1 and Section C.2)**.

The 18 hour bacterial cultures were used to determine the number of colony forming units present per millilitre of culture using the droplet plate technique, with the full procedure described in **Appendix C (Section C.3)**. From this technique we calculated the cfu/mL and log cfu/mL for each of the four bacterial strains used in the study. We found:

- *S. aureus* ATCC 25923
 - cfu/mL = 747 500 000
 - log cfu/mL = 8.87

- *B. cereus* DL5
 - cfu/mL = 1 432 500 000
 - log cfu/mL = 9.16

- *P. aeruginosa* ATCC 27853
 - cfu/mL = 1 536 666 667
 - log cfu/mL = 9.19

- *E. coli* ATCC 25922
 - cfu/mL = 3 375 000 000
 - log cfu/mL = 9.53

🌀 *Synthetic Compounds*

The compounds used in this study were prepared using standard synthetic organic chemistry techniques. A full discussion of the results obtained is given in **Chapter 2** and the detailed experimental procedures used are outlined in **Appendix B** below. For ease of reading, the compounds tested using the TTC assay are grouped according to structural similarities and are illustrated below. **Figure 23** shows the range of \square -(-)-ribose **100** derivatives.

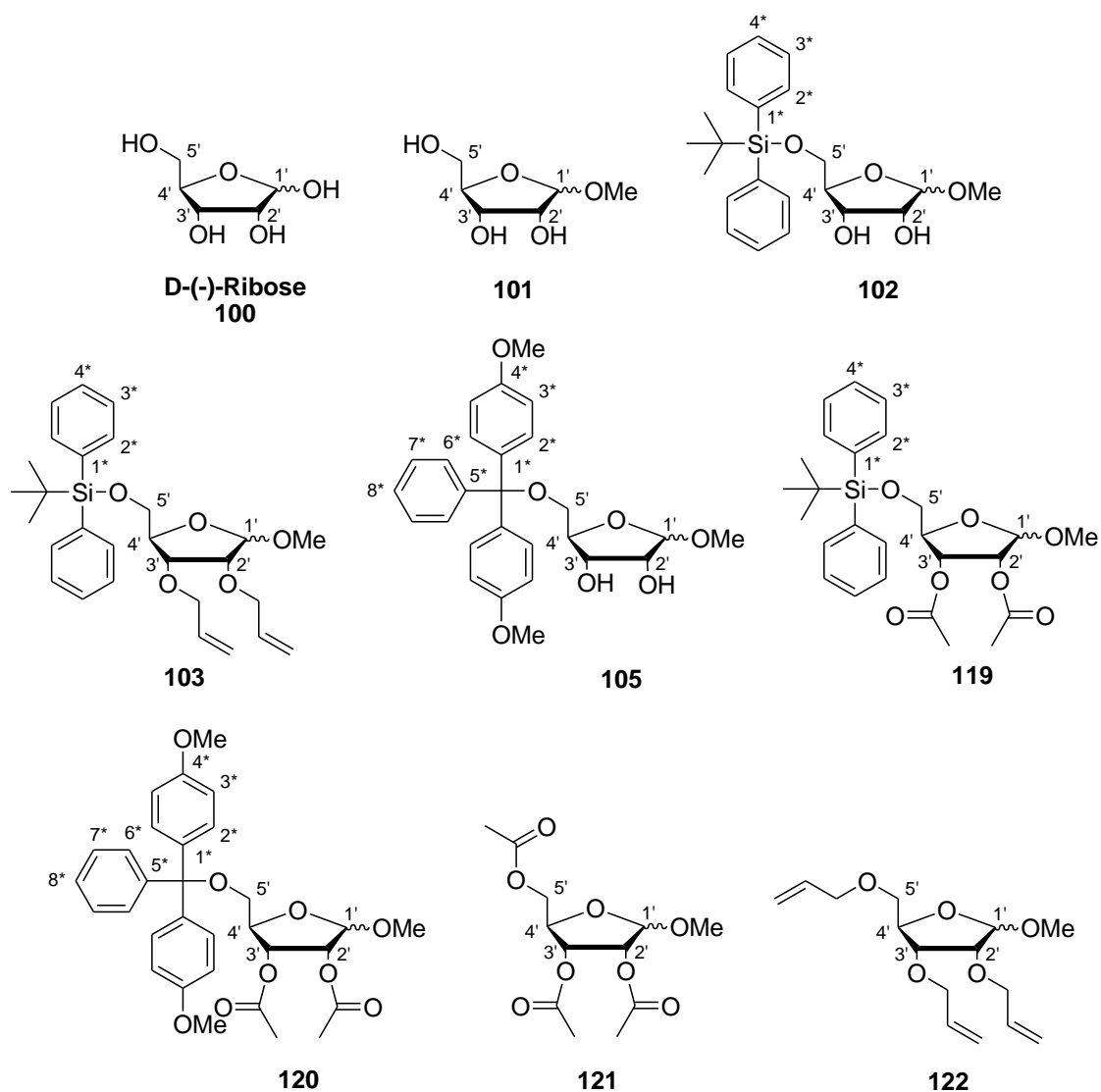


Figure 23 Synthetic compounds tested using TTC assay - □-(-)-ribose derivatives

Figure 24 highlights the pyrimidine-based nucleosides which are derivatives of uridine **12** and cytidine **11**, while **Figure 25** illustrates the purine-based nucleoside derivatives. The latter compounds are all derivatives of the nucleosides: guanosine **9**, inosine **116** and adenosine **8**.

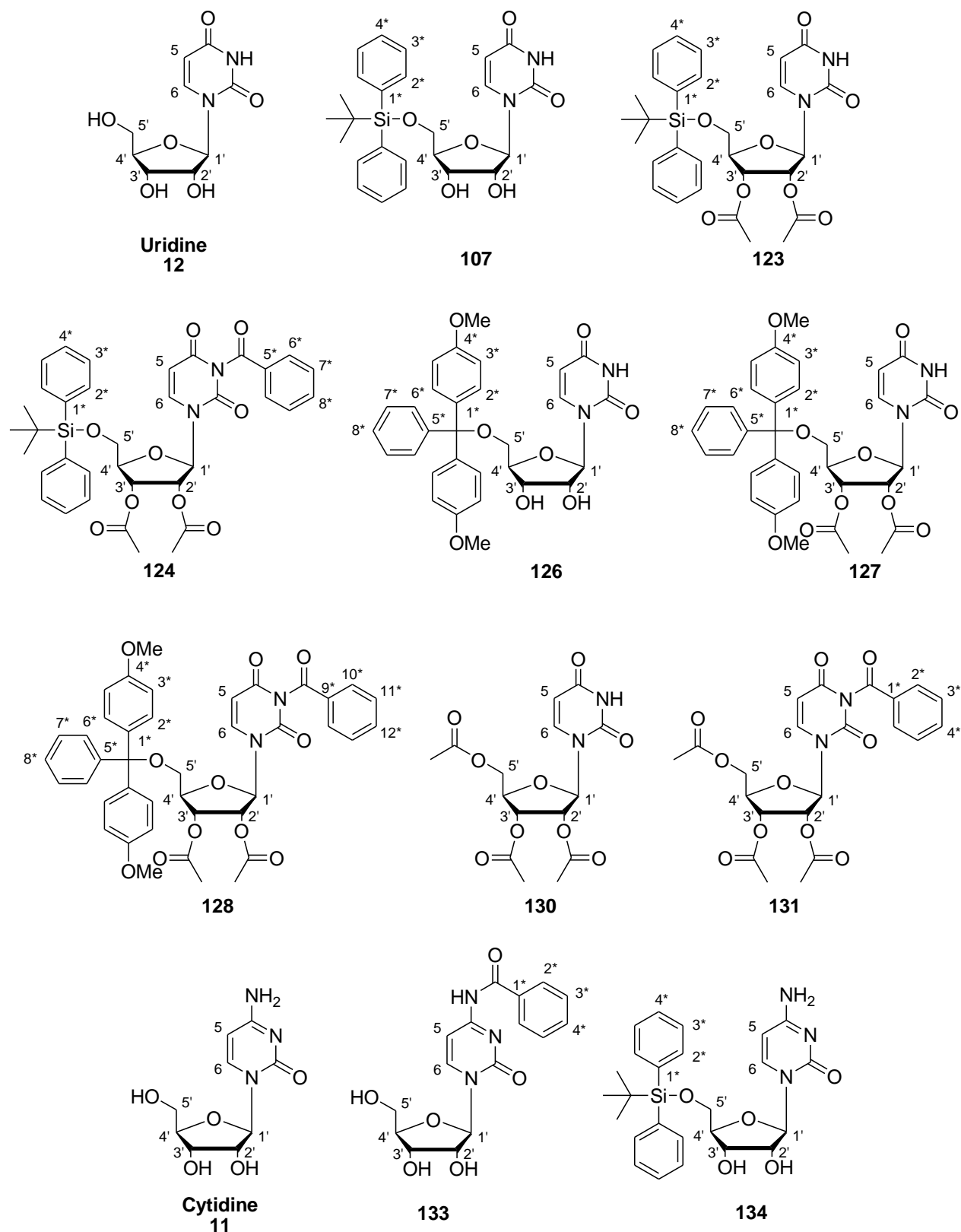


Figure 24 Synthetic compounds tested using TTC assay - pyrimidine based nucleosides

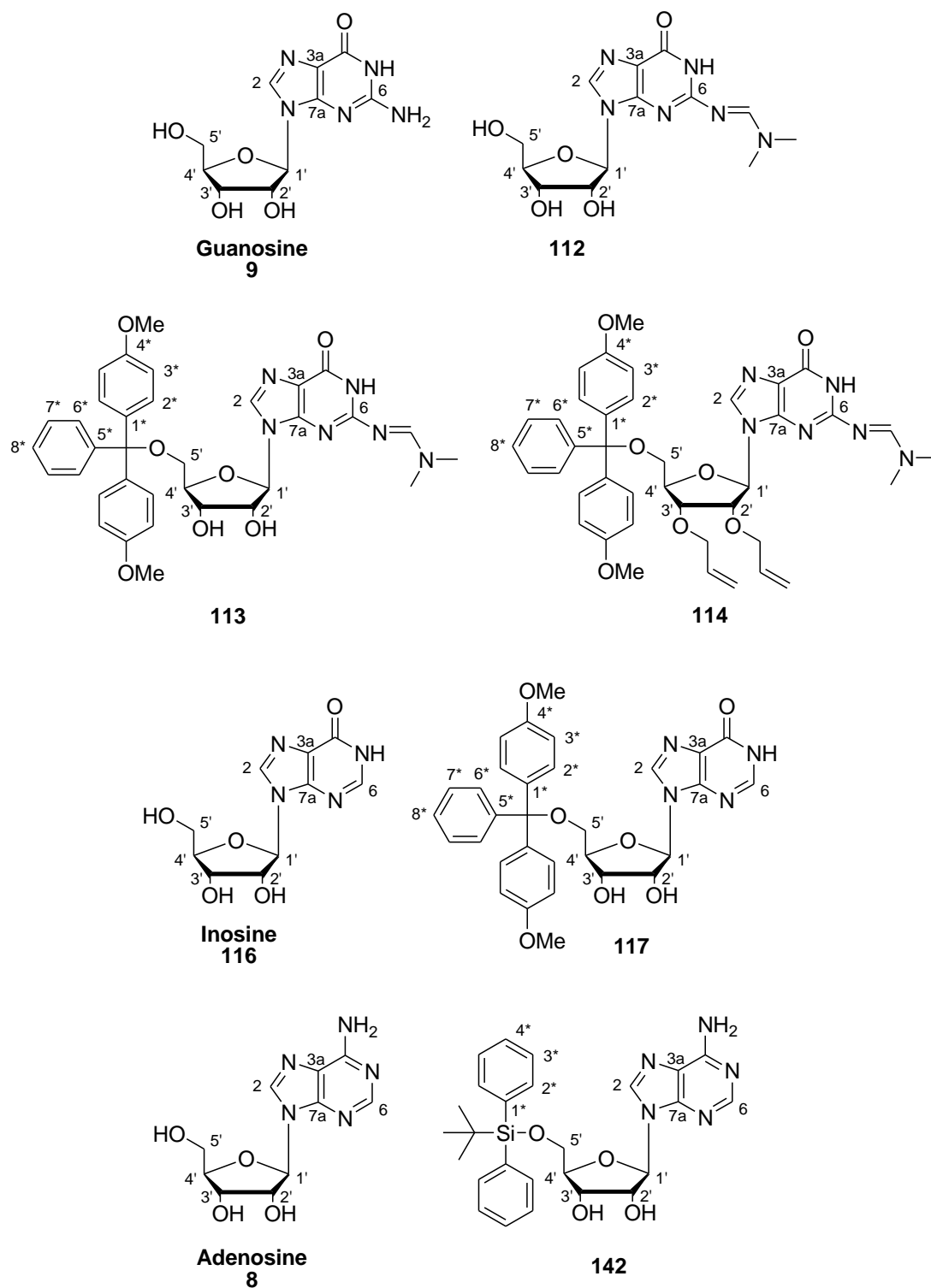


Figure 25 Synthetic compounds tested using TTC assay - purine based nucleosides

Lastly, **Figure 26** shows the two protecting group derivatives that were used as controls in the assay.

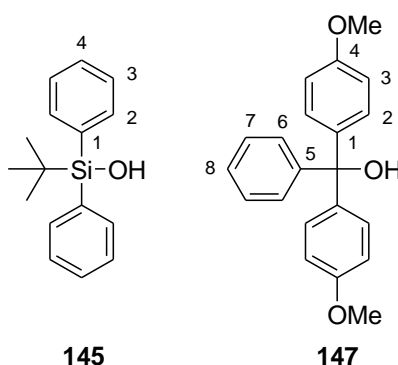


Figure 26 Synthetic compounds tested using TTC assay - protecting group derivatives

Ⓒ *Evaluation of Compound Efficacy – Triphenyltetrazolium Chloride (TTC) Assay*

The synthetic compounds, controls and the commercially available antibiotic, ciprofloxacin **153** (**Figure 27**), were used to prepare 10 000 mg/L, 1 000 mg/L, 100 mg/L, 10 mg/L and 1 mg/L stock solutions in autoclaved deionised water and molecular grade DMSO, as described in **Appendix C (Section C.5.1)**.

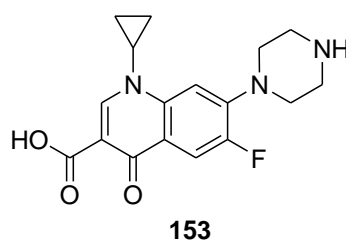


Figure 27 Ciprofloxacin

These stock solutions, for the synthetic compounds, controls and ciprofloxacin **153**, were then used immediately to prepare a series of 16 dilutions in autoclaved nutrient broth, as described

in detail in **Appendix C (Section C.5.2)**. The range of antibiotic concentrations used for determining minimum inhibitory concentrations (MICs) is universally accepted to be in doubling dilutions steps up and down from 1 mg/L as required.⁵⁸ As such, the dilution series was prepared as doubling dilutions from 256 mg/L down to 0.008 mg/L and 100 μ L of the solutions were placed in each well of the 96-well plates.

Then solutions containing 10^6 cfu/mL cells for each of the four bacteria, *S. aureus* ATCC 25923, *B. cereus* DL5, *P. aeruginosa* ATCC 27853 and *E. coli* ATCC 25922, were prepared by performing serial dilutions on the 18 hour bacterial cultures, as described in detail in **Appendix C (Section C.5.3)**. These were then added in 100 μ L portions to the wells on the 96-well plates. We were able to test one compound/antibiotic against all four bacterial strains and obtain four replicates for each compound concentration/bacterial strain combination by working across four 96-well plates at a time.

Also included on each of the plates were a series of controls: (i) the 0 % growth control, (ii) the 100 % growth control, (iii) the DMSO controls (10 mg/mL, 100 mg/mL, 250 mg/mL and 500 mg/mL concentrations) and (iv) the sterility control.

Plate1.1

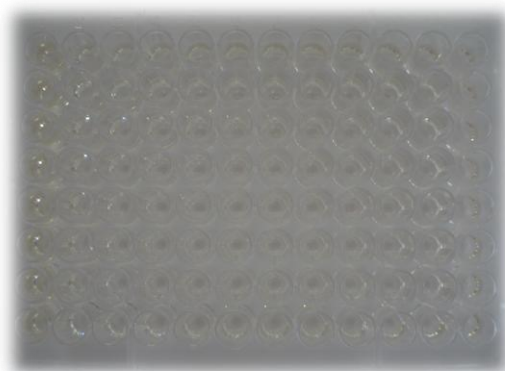


Plate 1.2

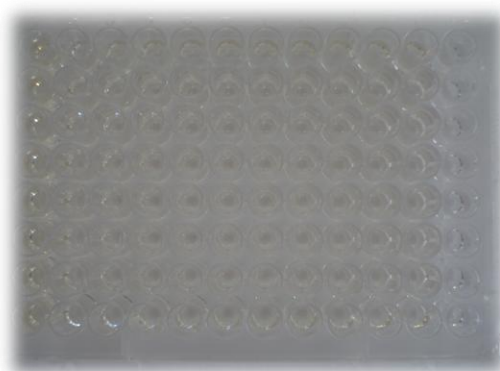


Figure 28 Photographs showing the plates before incubation with the TTC dye

Once the bacterial strains had been added to the 96-well plates, they were incubated at 37 °C for 22 hours. Following this time period, the plates were removed from the incubator. To each well of the plates was then added 10 µL of a freshly prepared solution of 5 mg/mL 2,3,5-triphenyltetrazolium chloride in phosphate buffered saline (PBS autoclaved prior to use in the solution). The plates were then incubated for a further 4 hours at 37 °C.

After this time, solubilisation of the formazan precipitate (pink) was conducted by the addition of the following reagents to each well of the 96-well plates:

- 10 µL of 3N HCl_(aq)
- 10 µL of 10 % NP-40_(aq)
- 25 µL of modified Weaver Reagent [66 % paraffin oil : 33 % CCl₄ : 1 % NP-40 (v/v)]

The plates were then incubated at 4 °C for a further 20 hours. After incubation, the plates were analyzed on an Elisa plate reader, at a wavelength of both 450 nm and 590 nm. From our pilot study, we found that the data obtained at wavelength 450 nm was in the correct absorption spectrum and gave considerably less variance than data obtained at 590 nm. Therefore, the data obtained at 450 nm was used for all subsequent assays performed. Full details for the experimental protocol used in the assay is given in **Appendix C (Section C.5.4)**.

Shown in **Figure 29** are the photographs showing what the plates of the positive control for anti-bacterial activity (we used the commercially available antibiotic ciprofloxacin **153**) looked like. One can visually see that at higher concentrations of the antibiotic, no metabolically active bacterial cells are observed. This is observed as a lack of the pink colour in the wells caused by the presence of formazan precipitate.

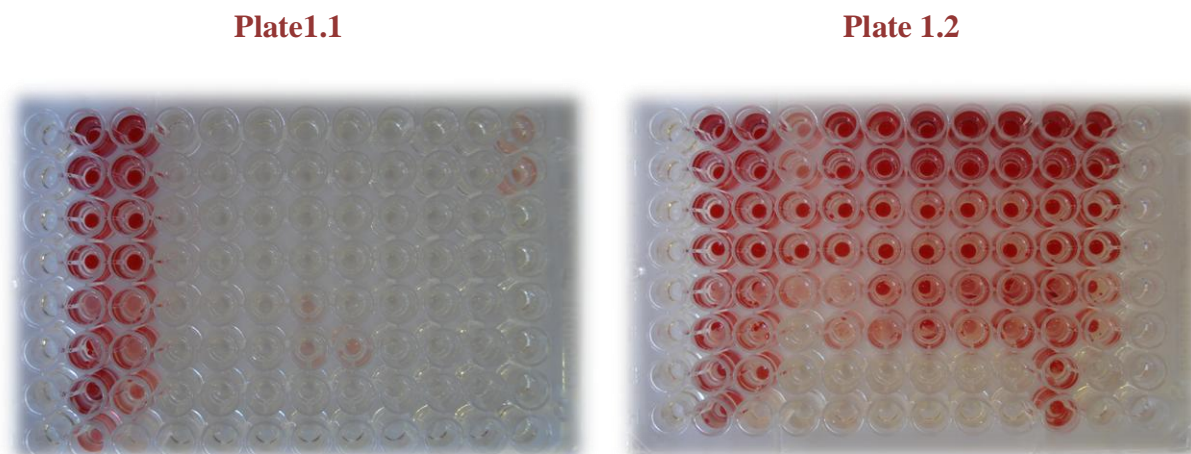


Figure 29 Photographs showing *positive controls* for antibiotic activity (plate 1.1 and 1.2 columns show: 1 = 0 % growth, 2 = 100 % growth, 3 = DMSO controls, 4-12 = doubling dilutions of test compound; plate 1.2: column 12 = sterility control).

Outlined in **Figure 30** is an example of what the corresponding plates for a negative control look like. As one can see, all of the wells containing the negative control (ie: no anti-bacterial activity) all appear as bright pink-red in colour. This is due to the fact that the clear 2,3,5-triphenyltetrazolium chloride is reduced to the pink coloured formazan precipitate in the metabolically active cells.

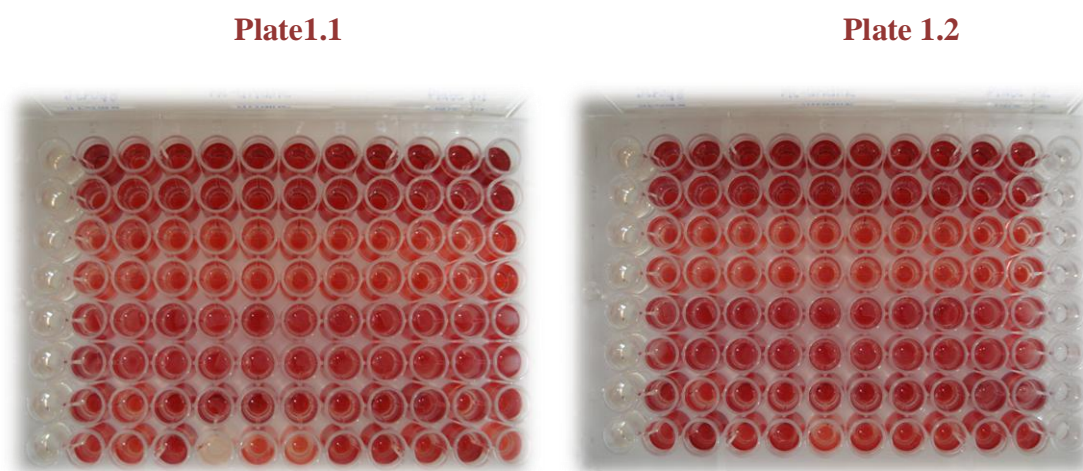


Figure 30 Photographs showing *negative controls* for antibiotic activity (plate 1.1 and 1.2 layout as described in **Figure 29**, further information given in **Figure C.10** and **Figure C.11**).

For the exact layout of the compound dilutions and internal growth and sterility controls please refer to **Appendix C (Figures C.10 and C.11)**.

Statistical Analysis

For each bacterial strain and compound/antibiotic dilution concentration combination four replicates were performed (duplicates were run on each plate and the plates were prepared in duplicate as well). Four data points were thus obtained for each combination as the absorbance for the cells. The data was corrected for the background absorptivity of the solution without bacterial growth by referencing the Elisa plate reader to column 1 (the 0 % growth control) on the plates.

For the initial determination of activity, the data was typed into Microsoft Excel and the average of the four replicates was determined. This average for the absorptions was then represented as the percentage of metabolically active cells present for each bacterial strain and compound/antibiotic dilution concentration combination, based on the value obtained for the 100 % growth control (given in column 2 on each plate).

Graphs were then plotted for the four bacterial strains, showing the percentage metabolically active cells on the y-axis against the compound/antibiotic concentration on the x-axis. From the initial graphs we determined which compounds showed antibacterial activity - any graphs displaying percentage metabolically active cells less than 10 % over a range of concentrations were classified as being positive hits.

3.2.1.2 Results

As described above, fifteen nucleoside derivatives, eight β -(-)-ribose derivatives and two synthetic controls were tested for possible antibacterial activity against two Gram-positive (*Staphylococcus aureus* strain ATCC 25923 and *Bacillus cereus* strain DL5) and two Gram-negative (*Pseudomonas aeruginosa* strain ATCC 27853 and *Escherichia coli* strain ATCC 25922) bacteria.

Each individual assay included a number of internal controls:

- (i) the 0 % growth control
- (ii) the 100 % growth control
- (iii) the DMSO controls
- (iv) the sterility control.

Included in the study were a number of control compounds, which were added to verify that the decomposition products for the synthetic compounds were not in fact the active molecules and a commercial antibiotic:

- (i) positive control for antibacterial activity (ciprofloxacin **153**)
- (ii) negative controls for each nucleoside: adenosine **8**, cytidine **11**, guanosine **9**, inosine **116**, uridine **12** and β -(-)-ribose **100**[‡]
- (iii) protecting group derivative controls (TBDPS-OH **145** and DMT-OH **147**)^{*}.

Minimum inhibitory concentrations (MICs) are considered the "gold standard" for determining the susceptibility of organisms to antimicrobials and are therefore used to judge the performance of all other methods of susceptibility testing.⁵⁸ As such, we decided to determine the MIC of our compounds based on a modified version of the standard procedure for the determination of minimum inhibitory concentrations reported by Andrews⁵⁸ (which describes an amended version of the procedure described in the BSAC Guide to Sensitivity Testing).⁵⁹

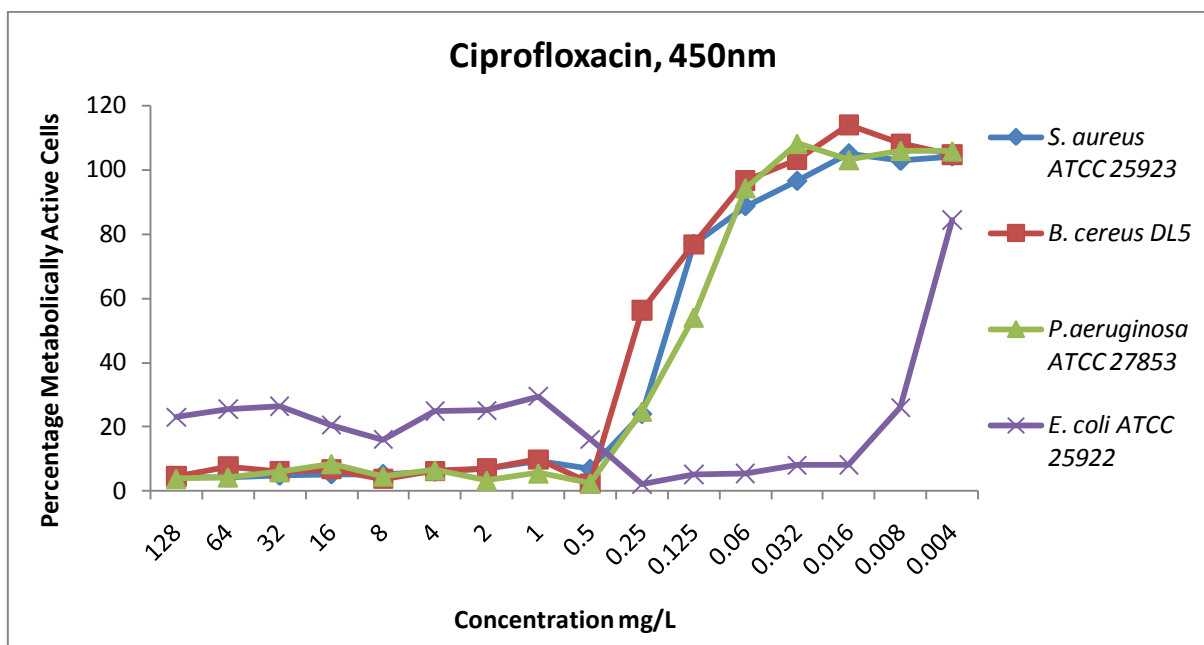
[‡] *Clarification* - the nucleosides and protecting group derivatives were included as "negative controls" in order to show the relative effects that making changes to the unprotected nucleosides/sugars would incur in the antibacterial assay. This does not imply that they would all specifically have no effect whatsoever on the bacterial systems used in this study.

The MIC is defined as the lowest concentration of a drug that will inhibit the visible growth of an organism after overnight incubation (this period is extended for organisms such as anaerobes, which require prolonged incubation time for growth).⁵⁸ For this study, we used the microdilution method described in the paper,⁵⁸ but modified the reading and interpretation section. We did not "visually" determine bacterial growth, but used the TTC assay reported by Damelin⁶⁰ to give us more accurate values for the percentage of metabolically active cells present after treatment with the synthetic compounds. As such, for this study, we have defined the MIC as the lowest concentration of synthetic compound that shows less than 10 % of the bacterial cells having metabolic activity.

The standard procedure published by Andrews⁵⁸ contained tables giving expected MIC ranges for control ATCC strains against various commercially available antibiotics. We thus chose an antibiotic, in our case ciprofloxacin **153**, and three ATCC strains from the publication for the initial assay of antibiotic activity. This was done in order to determine that our modified protocol was working correctly and allowed us to correlate our results to those obtained using the standardized procedure.

Andrews⁵⁸ suggested ranges for MIC determination with ciprofloxacin **153**, as 0.004-128 mg/L for Enterobacteriaceae, 0.015-128 mg/L for *Pseudomonas* spp. and 0.06-128 mg/L for Staphylococci. As such, we chose the range of 0.008-256 mg/L for our compound dilutions. As a dilution occurs when the bacteria are added to the compounds on the plate, this gives us a working range of 0.004-128 mg/L for the compounds, which corresponds to those recommended by Andrews.⁵⁸

Using the dilution series we then prepared a standard dilution curve for the antibiotic ciprofloxacin **153**, against each of the different bacterial strains used in the assay (*S. aureus* strain ATCC 25923, *B. cereus* strain DL5, *P. aeruginosa* strain ATCC 27853 and *E. coli* strain ATCC 25922). The curve is shown schematically in **Graph 1**.



Graph 1 Standard curve for ciprofloxacin **153**

We were then able to use the standard curve shown in **Graph 1** above to determine the minimum inhibitory concentration for the antibiotic ciprofloxacin **153**. The results obtained are reported in **Table 2**.

Table 2 MICs determined for ciprofloxacin

Compound	<i>S. aureus</i> ATCC 25923	<i>B. cereus</i> DL5	<i>P. aeruginosa</i> ATCC 27853	<i>E. coli</i> ATCC 25922
153	0.5 mg/L	0.5 mg/L	0.5 mg/L	0.016 mg/L

The MICs obtained using our modified procedure correlated well to those reported by Andrews.⁵⁸ For *S. aureus* ATCC 25923 we determined a MIC value of 0.5 mg/L using our approach - which corresponds perfectly to the MIC of 0.5 ml/L reported. In the same manner our MIC value of 0.5 mg/L, determined for *P. aeruginosa* ATCC 27853 - correlates well to the MIC of 0.25 mg/L reported. Lastly, we determined a MIC value of 0.016 mg/L for *E. coli* ATCC 25922 - which correlates well to the MIC of 0.015 mg/L reported.

Andrews⁵⁸ states that the MIC for the control used should be within one two-fold dilution of the expected MIC and all of the results we obtained fall within this range. We thus concluded that our modification to the procedure had not had a significant effect on the results obtained and we could correlate our MICs determined as the lowest concentration with less than 10 % of the cells showing metabolic activity to the data published by Andrews, wherein the MIC endpoint was determined by visible growth.

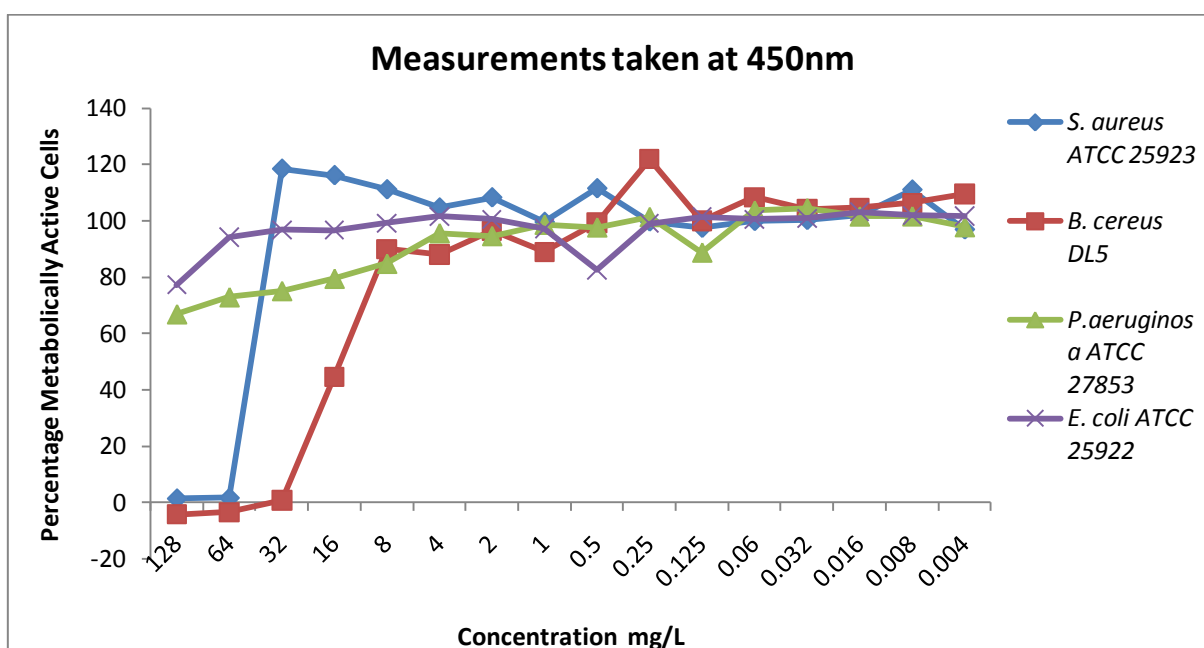
The antibacterial activity for the synthetic compounds was determined using the modified MIC determination assay, using TTC, as described above. The results obtained for α -(-)-ribose and its derivatives are shown below in **Table 3**.

Table 3 MICs determined for α -(-)-ribose and its derivatives

Compound	<i>S. aureus</i> ATCC 25923	<i>B. cereus</i> DL5	<i>P. aeruginosa</i> ATCC 27853	<i>E. coli</i> ATCC 25922
α -(-)-ribose 100	No activity	No activity	No activity	No activity
101	No activity	No activity	No activity	No activity
102	64 mg/L	32 mg/L	No activity	No activity
103	No activity	No activity	No activity	No activity
105	No activity	No activity	No activity	No activity
119	No activity	No activity	No activity	No activity
120	No activity	No activity	No activity	No activity
121	No activity	No activity	No activity	No activity
122	No activity	No activity	No activity	No activity

As expected from our negative control, no antibacterial activity was observed for α -(-)-ribose **100**. Quite surprisingly, however, we did observe activity for 5'-*O*-(*tert*-butyldiphenylsilyl)-1'-*O*-methoxy- α -(-)-ribose **102**. The compound was active against specifically the Gram-positive bacterial strains, with a MIC determined for *S. aureus* of 64 mg/L and a MIC determined for *B. cereus* of 32 mg/L. As shown in the table above, none of the other synthetic derivatives of α -(-)-ribose showed any anti-bacterial activity.

Using the dilution series we prepared a standard dilution curve for each of the different synthetic compounds, against each of the different bacterial strains used in the assay (*S. aureus* strain ATCC 25923, *B. cereus* strain DL5, *P. aeruginosa* strain ATCC 27853 and *E. coli* strain ATCC 25922), which was then used to determine the MIC values given in **Table 3** above. The curve for the active compound, 5'-*O*-(*tert*-butyldiphenylsilyl)-1'-*O*-methoxy- β -(-)-ribose **102**, is shown schematically in **Graph 2**.



Graph 2 Standard curve for 5'-*O*-(*tert*-butyldiphenylsilyl)-1'-*O*-methoxy- β -(-)-ribose **102**

These MIC values are significantly higher than those obtained for the commercially available antibiotic ciprofloxacin **153**, with MICs of 0.5 mg/L for *S. aureus* and 0.5 mg/L for *B. cereus* respectively. As such it is possible that the reduction in the number of metabolically active cells is due to toxic effects caused by the high concentration of compound in solution as opposed to the antibacterial activity of the compound itself.

The antibacterial activity for the synthetic compounds was determined using the modified MIC determination assay, using TTC, as described above. The results of the TTC assay for

the pyrimidine based nucleosides, uridine **12** and cytidine **11**, and their derivatives are shown below in **Table 4**.

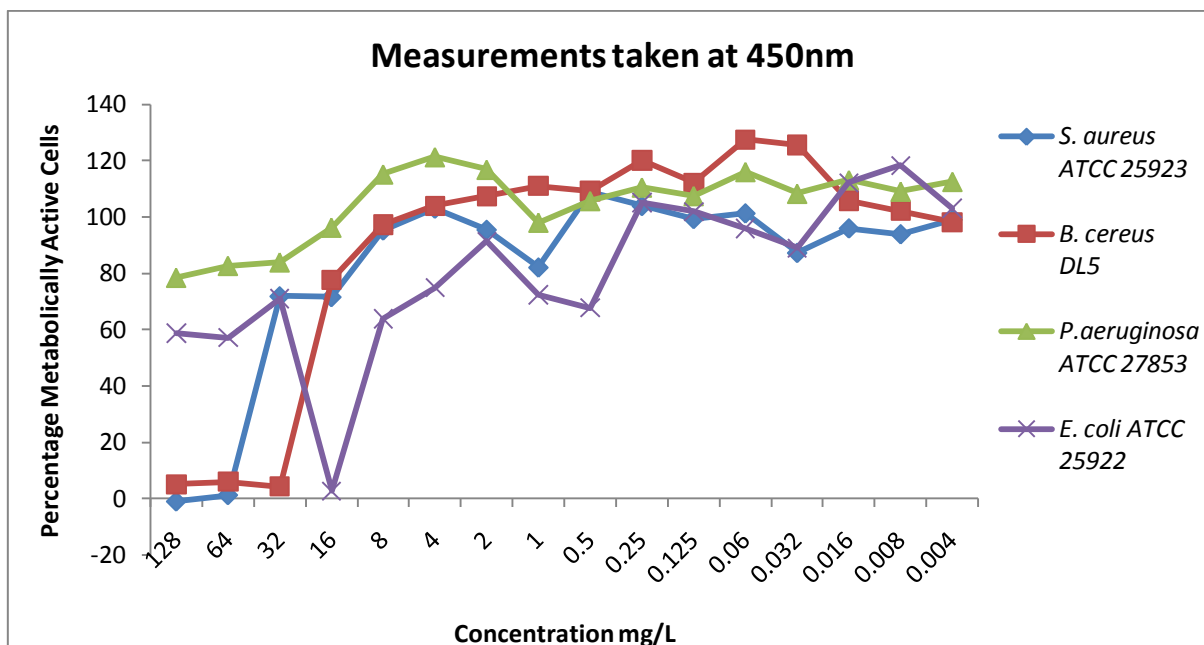
Table 4 MICs determined for the pyrimidine based nucleoside derivatives

Compound	<i>S. aureus</i>	<i>B. cereus</i>	<i>P. aeruginosa</i>	<i>E. coli</i>
	ATCC 25923	DL5	ATCC 27853	ATCC 25922
Uridine 12	No activity	No activity	No activity	No activity
107	64 mg/L	32 mg/L	No activity	No activity
123	No activity	No activity	No activity	No activity
124	No activity	No activity	No activity	No activity
126	No activity	No activity	No activity	No activity
127	No activity	No activity	No activity	No activity
128	No activity	No activity	No activity	No activity
130	No activity	No activity	No activity	No activity
131	No activity	No activity	No activity	No activity
Cytidine 11	No activity	No activity	No activity	No activity
133	No activity	No activity	No activity	No activity
134	No activity	No activity	No activity	No activity

The uridine **12** and cytidine **11** were used as negative controls for the assay as we anticipated no anti-bacterial activity to be observed by the un-modified nucleosides. As expected, no activity was recorded. From the entire range of pyrimidine based nucleoside derivatives, only one derivative showed marked anti-bacterial activity - the 5'-*O*-(*tert*-butyldiphenylsilyl)uridine **107**.

Using the dilution series we prepared a standard dilution curve for each of the different synthetic compounds, against each of the different bacterial strains used in the assay (*S. aureus* strain ATCC 25923, *B. cereus* strain DL5, *P. aeruginosa* strain ATCC 27853 and *E. coli* strain ATCC 25922), which was then used to determine the MIC values used in **Table 4**

above. The curve for the active compound, 5'-*O*-(*tert*-butyldiphenylsilyl)uridine **107**, is shown schematically in **Graph 3**.



Graph 3 Standard curve for 5'-*O*-(*tert*-butyldiphenylsilyl)uridine **107**

The 5'-*O*-(*tert*-butyldiphenylsilyl)uridine **107** was active against only the Gram-positive bacterial strains, with a MIC of 64 mg/L observed for *S. aureus* and a MIC of 32 mg/L observed for *B. cereus*. These MIC values are significantly higher than those obtained for the commercially available antibiotic ciprofloxacin **153**, with MICs of 0.5 mg/L for *S. aureus* and 0.5 mg/L for *B. cereus*, respectively.

The antibacterial activity for the synthetic purine based nucleoside compounds were determined using the modified MIC assay, described in greater detail above. The results of the TTC assay for the purine based nucleosides, guanosine **9**, inosine **116** and adenosine **8**, and their derivatives are shown below in **Table 5**.

Table 5 MICs determined for the purine based nucleoside derivatives

Compound	<i>S. aureus</i> ATCC 25923	<i>B. cereus</i> DL5	<i>P. aeruginosa</i> ATCC 27853	<i>E. coli</i> ATCC 25922
Guanosine 9	No activity	No activity	No activity	No activity
112	No activity	No activity	No activity	No activity
113	No activity	No activity	No activity	No activity
114	No activity	No activity	No activity	No activity
Inosine 116	No activity	No activity	No activity	No activity
117	No activity	No activity	No activity	No activity
Adenosine 8	No activity	No activity	No activity	No activity
142	No activity	No activity	No activity	No activity

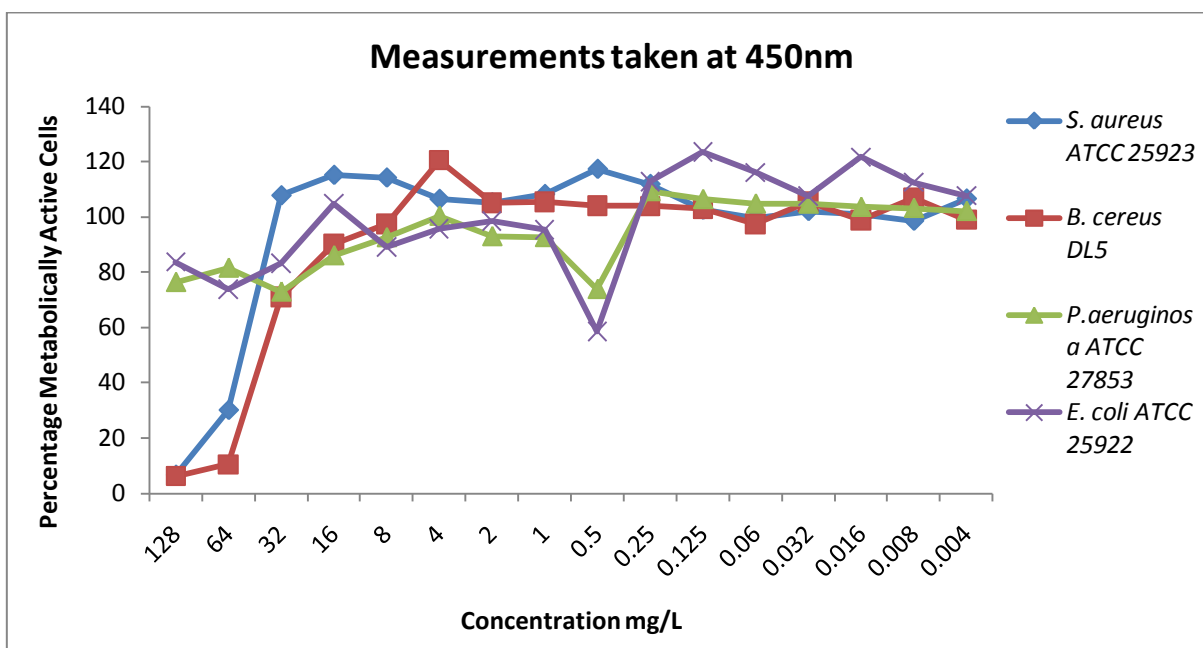
The guanosine **9**, inosine **116** and adenosine **8** were included as negative controls for the assay as we expected no anti-bacterial activity to be observed in the un-modified nucleosides. As expected, no activity was recorded for the nucleosides on their own. Unfortunately, we also found that none of the synthetic derivatives showed any activity against our Gram-positive and Gram-negative bacterial strains either.

The antibacterial activity for the synthetic protecting group derivatives were determined using the modified MIC assay described above. The results of the TTC assay for the two protecting group derivatives are shown below in **Table 6**.

Table 6 MICs determined for the protecting group derivatives

Compound	<i>S. aureus</i> ATCC 25923	<i>B. cereus</i> DL5	<i>P. aeruginosa</i> ATCC 27853	<i>E. coli</i> ATCC 25922
TBDPS-OH 145	128 mg/L	64 mg/L	No activity	No activity
DMT-OH 147	No activity	No activity	No activity	No activity

Using the dilution series we prepared a standard dilution curve for each of the different synthetic compounds, against each of the different bacterial strains used in the assay (*S. aureus* strain ATCC 25923, *B. cereus* strain DL5, *P. aeruginosa* strain ATCC 27853 and *E. coli* strain ATCC 25922), which was then used to determine the MIC values used in **Table 6** above. The curve for the active compound, *tert*-butyldiphenylsilanol **145** is given in **Graph 4**.



Graph 4 Standard curve for *tert*-butyldiphenylsilanol **145**

The *tert*-butyldiphenylsilanol **145** was active against only the Gram-positive bacterial strains, with a MIC of 128 mg/L observed for *S. aureus* and a MIC of 64 mg/L observed for *B. cereus*. These MIC values are significantly higher than those obtained for the commercially available antibiotic ciprofloxacin **153**, with MICs of 0.5 mg/L for *S. aureus* and 0.5 mg/L for *B. cereus* respectively. Unfortunately, the 4,4'-dimethoxytrityl alcohol **147** did not show any activity towards our test strains.

3.2.1.3 Discussion

For our initial antibacterial screen we were looking at three main points: (i) to investigate which group of nucleoside derivatives gave the most promising results and could be used for further studies, (ii) to perform a mini structure-activity study in order to determine which positions on the molecule were important in order to maintain activity and (iii) to determine if the presence of the nucleoside structure was intrinsic for activity

In order for us to adequately investigate which group of nucleoside derivatives gave the most promising results, we needed to compare the data obtained for each of our five different nucleoside groups. The comparison of the results obtained for the pyrimidine based nucleoside derivatives (uridine **12** and cytidine **11**) as well as for the purine based nucleoside derivatives (guanosine **9**, inosine **116** and adenosine **8**) are shown in **Table 7**.

Table 7 Comparison of data obtained from TTC assay for the five nucleoside groups

Protecting Group	Uridine	Cytidine	Guanosine	Inosine	Adenosine
TBDPS (5'-O)	Activity*	No Activity	-	-	No Activity
DMT (5'-O)	Limited Activity***	-	No Activity**	No Activity	-
Bz (4-N)	-	No Activity	-	-	-

* MIC values for *S. aureus* = 64 mg/L and *B. cereus* = 32 mg/L, ** molecule protected at the 6-N position with a *N,N*-dimethylmethyimine group. *** limited activity is the concentration with approximately 25 % metabolically active cells present, for *B. cereus* = 128 mg/L

From our initial study of the five different nucleosides, we found that the nucleoside showing the most promising results was uridine **12**. We thus concluded that it would be the nucleoside

of choice for subsequent anti-bacterial activity studies, which could not be conducted on all five nucleosides due to the time constraints of the project.

Our second goal was to perform a mini structure-activity study in order to determine which positions on the molecule were important in order to maintain any antibacterial activity. This study was conducted specifically on a range of nucleoside derivatives synthesized from one purine nucleoside (guanosine **9**) and one pyrimidine nucleoside (uridine **12**). We chose to use uridine and guanosine specifically due to their ease of handling and less complex syntheses. During the initial study described in **Table 7** above, we found that adenosine **8**, cytidine **11** and inosine **116** were in general more difficult to handle and less reactive when using our chosen protecting groups.

For the mini structure-activity study, we synthesized a range of protected derivatives by doing step-wise protection reactions. The results obtained for the anti-bacterial assay performed on these compounds are summarized in **Table 8**.

Table 8 Comparison of MIC results obtained from the structure-activity study

Nucleoside	5'-OH	2'-OH / 3'-OH	3-N(-NH) or 6-N(-NH ₂)	Results
Uridine	TBDPS			64 mg/L (<i>S. aureus</i>) 32 mg/L (<i>B. cereus</i>)
	TBDPS	Ac / Ac		Limited Activity*
	TBDPS	Ac / Ac	Bz	No Activity
	DMT			No Activity
	DMT	Ac / Ac		No Activity
	DMT	Ac / Ac	Bz	No Activity
	Ac	Ac / Ac		No Activity
	Ac	Ac / Ac	Bz	No Activity

Nucleoside	5'-OH	2'-OH / 3'-OH	3-N(-NH) or 6-N(-NH ₂)	Results
Guanosine			DMMI ^{**}	No Activity
	DMT		DMMI ^{**}	No Activity
	DMT	All / All	DMMI ^{**}	No Activity

* Limited Activity = concentration with approximately 50 % metabolically active cells present, 128 mg/L for *S. aureus* and 128 mg/L for *B. cereus*, ** DMMI = *N,N*-dimethylmethyline

For uridine, protection of the primary alcohol with the TBDPS group gives a compound **107** which exhibits Gram-positive anti-bacterial activity at high concentrations (MIC values of 64-128 mg/L). The subsequent protection of the secondary alcohols with the acetyl protecting groups yields a compound **123** that has limited anti-bacterial activity against Gram-positive bacteria (with a MIC outside the range tested, ie: >128 mg/L), but which shows approximately a 50 % reduction in the number of metabolically active cells present after treatment with the compound at a concentration of 128 mg/L. Finally, we see that when the amide nitrogen is protected with the benzoyl group to give compound **124**, no anti-bacterial activity is observed whatsoever.

This allowed us to conclude that the best position for performing changes to our nucleosides was at the 5'-OH position on the sugar ring. We also deduced that loss of either or both of the secondary alcohols (2'-OH and 3'-OH) lead to a reduction in activity of the compounds. From this we decided that the differences in the activity of the compounds, when protected at either the 2'-OH or the 3'-OH positions, would need to be further investigated at a later stage.

Protection of the free amine and amide positions on the base seemed to eliminate all activity in the synthetic molecules. Due to the small sample size, however, we felt that it was too soon to conclude that all future nucleoside derivatives needed to have free sites on the base and as such felt that it was pertinent to investigate this further.

As shown in **Table 8** above, uridine **12** again gives the more promising results for the antibacterial assay, which supports our previous conclusion that it is the nucleoside of choice for use in further assays.

For the third point, we compared the results obtained for the α -(-)-ribose derivatives with the corresponding uridine derivatives. As expected for our negative controls, α -(-)-ribose **100**, 1'-*O*-methoxyribose **101** and uridine **12**, no antibacterial activity was observed. In fact, for both α -(-)-ribose **100** and 1'-*O*-methoxyribose **101**, we observed an increase in the number of metabolically active cells for both of the Gram-positive strains when compared to our 100 % growth control. We believe that this may be due to the possibility that the bacteria are using the sugar as a food source and it is thus increasing their growth rate.

The comparison of our results obtained for the α -(-)-ribose derivatives with the corresponding uridine derivatives are outlined in **Table 9** on the following page. Where applicable, MIC values are given as the lowest concentration of synthetic compound that shows less than 10 % of the bacterial cells having metabolic activity.

As expected, the limited activity observed with 2',3'-*O*-diacetyl-5'-*O*-(*tert*-butyldiphenylsilyl)uridine **123** and 5'-*O*-(4,4'-dimethoxytrityl)uridine **126** were not mirrored in the corresponding α -(-)-ribose derivatives. This suggested that the bases on the nucleoside derivatives were necessary for molecular recognition to aid transportation within the cells.

Table 9 Comparison of data obtained from TTC assay for the \square -(-)-ribose and uridine derivatives

Starting Material	5'-OH	2'-OH / 3'-OH	Results
1'-O-Methoxyribose	TBDPS		64 mg/L (<i>S. aureus</i>) 32 mg/L (<i>B. cereus</i>)
Uridine	TBDPS		64 mg/L (<i>S. aureus</i>) 32 mg/L (<i>B. cereus</i>)
1'-O-Methoxyribose	TBDPS	Ac / Ac	No Activity
Uridine	TBDPS	Ac / Ac	Limited Activity* (128 mg/L <i>S. aureus</i>) (128 mg/L <i>B. cereus</i>)
1'-O-Methoxyribose	TBDPS	All / All	No Activity
Uridine	TBDPS	All / All	-
1'-O-Methoxyribose	DMT		No Activity
Uridine	DMT		Limited Activity** (128 mg/L <i>B. cereus</i>)
1'-O-Methoxyribose	DMT	Ac / Ac	No Activity
Uridine	DMT	Ac / Ac	No Activity
1'-O-Methoxyribose	Ac	Ac / Ac	No Activity
Uridine	Ac	Ac / Ac	No Activity

* concentration with approximately 50 % metabolically active cells present, ** concentration with approximately 25 % metabolically active cells present

Surprisingly, we found that the 5'-O-(*tert*-butyldiphenylsilyl)-1'-O-methoxy- \square -(-)-ribose **102** had the same activity against the Gram-positive bacteria as the 5'-O-(*tert*-butyldiphenylsilyl)uridine **107** at concentrations of synthetic compound between 32 and 64 mg/L. Initially we could not explain this finding, as our other research suggested that the presence of the nucleoside base was intrinsic for activity. But upon closer investigation, we

were able to conclude that the activity observed in both of these cases could be due to the hydrolysis of the compounds under biological conditions to yield the free *tert*-butyldiphenylsilanol **145**.

The protecting group derivatives were subsequently assayed to determine if they had any biological activity. As suspected, we found that *tert*-butyldiphenylsilanol **145** was active against the Gram-positive bacteria. We determined that the TBDPS-OH had a MIC value of 128 mg/L for *S. aureus* and a MIC value of 64 mg/L for *B. cereus*. We believe that these values are a factor higher than those obtained for 5'-*O*-(*tert*-butyldiphenylsilyl)-1'-*O*-methoxy- β -(-)-ribose **102** and 5'-*O*-(*tert*-butyldiphenylsilyl)uridine **107** because the sugar and nucleoside molecules are recognized by the bacterial cells and are thus transported into the cells more efficiently.

Note that all graphs derived from raw spectrophotometric data used to determine the MIC values given in this section have been included on the attached DVD, under **Supporting Information for Biological Testing (Part 1)**.

3.2.1.4 Conclusions

From the data reported above, one can conclude that the nucleoside showing the most promising results was uridine **12** and as such it would be the nucleoside of choice for our subsequent antibacterial activity studies. Our mini structure-activity study on the uridine derivatives found that the best position for performing modifications to our nucleosides was at the 5'-OH position on the sugar ring and a loss of both of the secondary alcohols (2'-OH and 3'-OH) and/or the primary amide on the base lead to a reduction in activity of the compounds. Lastly, the comparison of β -(-)-ribose derivatives to the uridine derivatives suggested that the bases on the nucleoside derivatives were necessary for molecular recognition to aid transportation within the cells.

All these conclusions were taken into account when designing the synthesis for our second generation of compounds. The synthesis of the second generation compounds are discussed in detail in **Part 2, Chapter 5** and the results obtained for the anti-bacterial assay are discussed in **Part 2, Chapter 6**. Further studies to determine a possible mode of action for our positive hits (from both the first generation and the second generation of synthetic compounds) were conducted, and include analysis of the cells by confocal microscopy and SEM. All of the results are presented together in **Chapter 6**, along with our final conclusions for the anti-bacterial assays.

3.2.2 Antiviral Assays


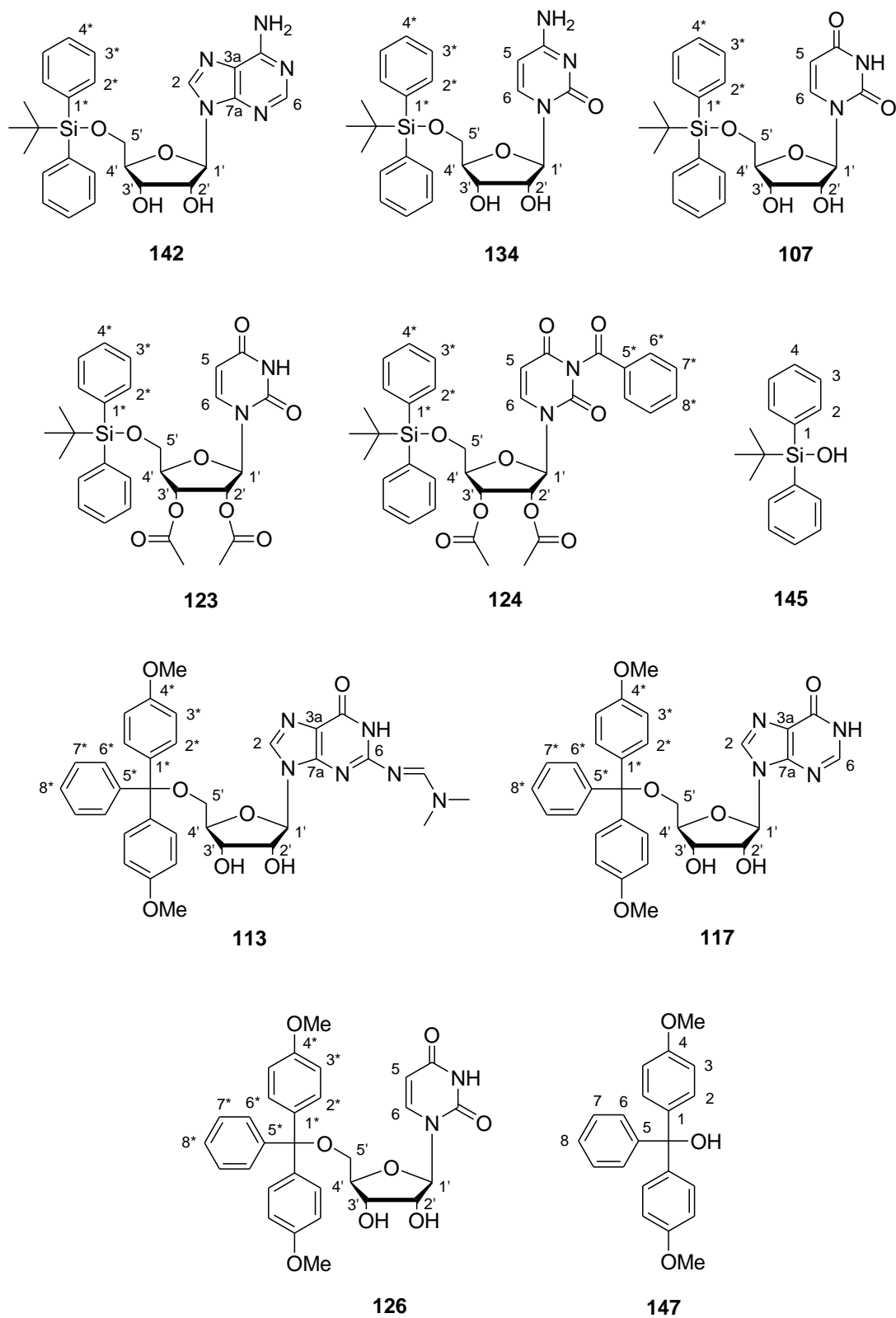
The 2,3-bis-(2-methoxy-4-nitro-5-sulfophenyl)-2*H*-tetrazolium-5-carboxyanilide (XTT) assay has been used to screen plant extracts, synthetic proteins and synthetic compounds for anti-HIV activity. The test requires cell culture conditions for the growth of an MT-4 suspension cell line and HTLV_{III}B virus. The interaction of the cells, virus and potential anti-HIV agent is measured by cell viability using the tetrazolium (XTT) salt. Spectrophotometric measurement of the yellow salt converting to an orange formazan is indicative of cell viability. The XTT assay is a modification of the original MTT assay and the protocol is reviewed by De Clerq.⁶¹

3.2.2.1 Materials and Methods

🌀 *Cell Line and HIV strain*

Cell Line: MT-4 cells (human T-cell leukemia cell line) **Virus:** HTLV_{III}B

The uninfected cells and the HTLV_{III}B infected continuous H9 cells were obtained from the National Institutes of Health AIDS Research and Reference Reagent Program (Bethesda, USA) and were used for the assay.

 *Compounds Used in Assay***Figure 31** Synthetic compounds used in the assay

The compounds used in this study were prepared using standard synthetic organic chemistry techniques. A full discussion of the synthetic results obtained is given in **Chapter 2** and the detailed experimental procedures used are outlined in **Appendix B**. For ease of reading, the compounds tested using the XTT assay are grouped according to structural similarities and are illustrated above. **Figure 31** shows the ten compounds selected for use in this assay.

Evaluation of Compound Efficacy

The XTT assay is based on the bioreduction of the XTT salt (2,3-bis-[2-methoxy-4-nitro-5-sulfophenyl]-2H-tetrazolium-5-carboxyanilide inner salt) yielding an orange formazan. Bioreduction is enhanced by the presence of an electron coupling agent such as phenazine methosulfate (PMS). Formazan production is indicative of the number of viable cells, therefore an increase or decrease in cellular viability results in a change in the amount of formazan formed, which indicates the degree of cytotoxicity caused by the test compound.

The synthetic compounds were weighed out in 50 mg portions and were then diluted with the solvent for the study, in this case DMSO, to obtain a 1000 μ L solution. Ten fold dilutions were prepared for each compound solution as: 1 / 10, 1 / 100, 1 / 1000 and 1 / 10 000 dilutions, with the tissue culture medium RPMI-1640 being used as the diluent.

Included in each assay were a number of standard controls:

- (i) AZT **29** was included as a positive control for the assay
- (ii) Lopinavir **154** was included as a positive control for the assay
- (iii) a cell suspension made up in RPMI-1640 medium was used as the untreated (negative) control for the assay
- (iii) DMSO controls were included to confirm that the solvents did not affect the results obtained from the assay

and each synthetic compound was tested in triplicate as well. The structures for the positive controls are shown in **Figure 32**.

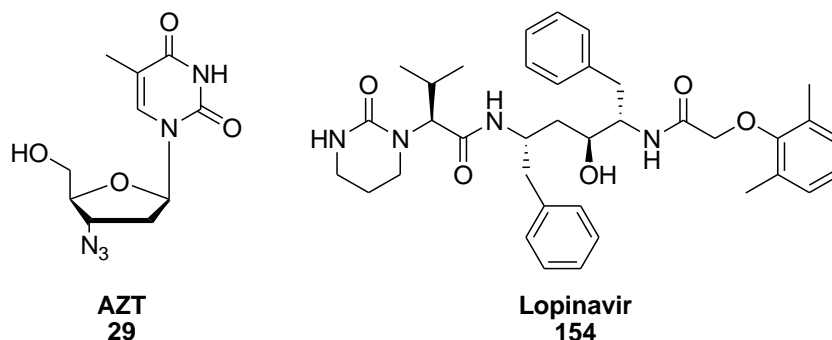


Figure 32 Compounds used as positive controls[§]

The *in vitro* XTT based Toxicology Assay Kit (Sigma-Aldrich), which contains XTT + 1 % PMS in 5 mg vials, was used for the assay. The XTT / PMS reagent mixture was prepared according to the manufacturer's instructions. The assay was performed according to the standard procedures outlined by Scudiero and co-workers⁶², Weislow and co-workers⁶³ and Cos and co-workers⁶⁴, with modifications as described herein.

Cell counts were performed and uninfected cells were prepared for use in the XTT assay as follows:

- a cell count was performed on exponentially growing MT-4 cells
- these were diluted using colourless RPMI-1640 to obtain a solution containing 6×10^5 cells/mL
- 500 μ L of the cell suspension, at the final cell concentration required, was added to each of the 1000 μ L Eppendorf tubes.
- the tubes were then centrifuged at 1000 rpm for 5 minutes

[§] The two positive controls were chosen based on their structural differences: AZT **29** is a derivative of 5-methyluridine, whereas Lopinavir **154** is structurally dissimilar as it does not contain a nucleoside or sugar motif in the structure.

- the supernatant was then discarded and 500 μL of the appropriate concentration of either the synthetic compound or positive control compound dilutions was added to the pellet
- the tubes were then vortexed gently to reconstitute the cells
- 150 μL of the cell suspension was then added to the wells of the plates
- this was all performed in triplicate.

The infected cells were prepared using a similar procedure to that described above, with the only difference being that:

- the virus was thawed and dilutions were performed with RPMI to obtain 100-300 TCID_{50}
- 50 μL of the diluted virus was added to wells containing 100 μL of the initial cell suspension, which had been diluted to 6×10^5 cells/mL

The plates containing the cells and the compound dilution series were then incubated at 37 °C with 5 % CO_2 for 5 days. The plates were read at 450 nm, with a reference wavelength of 620 nm using the Tecan Sunrise ELISA plate reader and Magellan™ software, before the addition of the XTT dye.

After the incubation time, 20 μL of the XTT / PMS reagent mixture was added to each well of the plates and the plates were further incubated at 37 °C with 5 % CO_2 for 4 hours. The plates were again read at 450 nm, with a reference wavelength of 620 nm using the Tecan Sunrise ELISA plate reader and Magellan™ software.

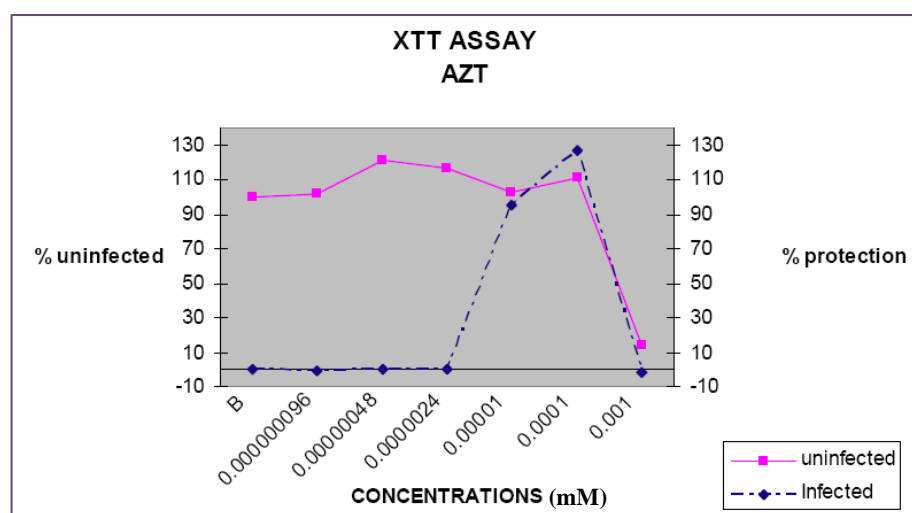
Data Analysis

The percentage protection was determined using the recorded absorbance values obtained from reading the plates on the Tecan Sunrise ELISA plate reader. The equations outlining

how the percentage protection was determined are based on those published by Cos and co-workers⁶⁴ and are described in detail in **Appendix D (Section D.6)**. The results obtained using this methodology are represented graphically in the results and discussions, *Section 3.2.2.2* and *Section 3.2.2.3*.

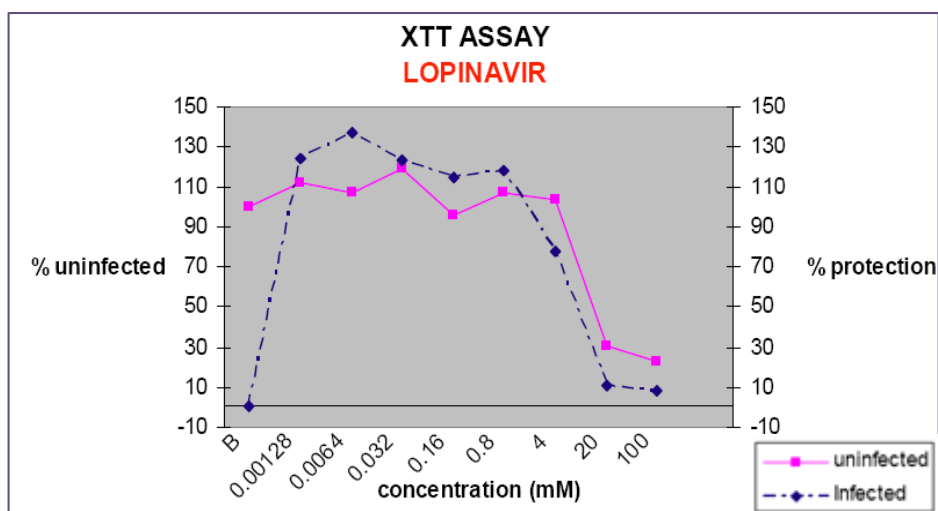
3.2.2.2 Results

The two control compounds chosen for the study were AZT **29** and Lopinavir **154** (structures are given in **Figure 32**). These known antiviral drugs were chosen in order to confirm that the protocol was working correctly and allowed us to correlate our results to those obtained using similar procedures and importantly for our study, included examples of both a nucleoside and a non-nucleoside based reverse transcriptase inhibitor. The AZT **29** tested demonstrated the expected antiviral activity when compared to data reported by Weislow and co-workers⁶³ and De Clerq and co-workers⁶⁵. The results provided to us are presented graphically in **Graph 5**.



Graph 5 Results obtained for control compound: AZT **29**

The Lopinavir **154** tested also demonstrated the expected antiviral activity and was found to correlate well to data reported by Kempf and co-workers.⁶⁶ The results we were provided with are shown graphically in **Graph 6**.



Graph 6 Results obtained for control compound: Lopinavir **154**

Shown in **Figure 31** are the ten compounds that were tested using the XTT assay. We only selected ten compounds from our range of first generation compounds for the assay due to the large costs involved in this assay. These ten compounds were chosen in such a way as to be representative of the different classes of compounds synthesized. We envisioned that we could use these ten compounds for a general screen for HIV activity, with positive results then directing us as to which groups of compounds would warrant further investigation, thus allowing us to minimize the expense of testing for HIV activity.

The results obtained for the XTT assay are summarized in **Table 10** and include a description of the compounds as demonstrating either an antiviral effect or a toxic effect towards the uninfected cells. All of the data used for determining these values are given in detail on the graphs shown in *Section 3.2.2.3* and are included on the attached DVD, under **Supporting**

Information. All of the equations used to calculate CC_{50} , EC_{50} and SI values are described in **Appendix D (Section D.6)**.

Table 10 Summary of results obtained from the XTT assay

Compound	Antiviral Effect [*]	EC_{50}	Toxic Effect	CC_{50}	SI (CC/EC)
142	No	Cannot be calculated	Yes	0.345 mM	Cannot be calculated
134	No	Cannot be calculated	Yes	3.33 mM	Cannot be calculated
107	No	Cannot be calculated	Yes	23.4 mM	Cannot be calculated
123	No	Cannot be calculated	Yes	23.1 mM	Cannot be calculated
124	No	Cannot be calculated	Yes	0.191 mM	Cannot be calculated
145	No	Cannot be calculated	Yes	1.47 mM	Cannot be calculated
113	No	Cannot be calculated	Yes	5.91 mM	Cannot be calculated
117	No	Cannot be calculated	Yes	0.0380 mM	Cannot be calculated
126	No	Cannot be calculated	Yes	1.33 mM	Cannot be calculated
147	No	Cannot be calculated	Yes	13.7 mM	Cannot be calculated

^{*} Antiviral effect is defined as $\geq 50\%$ protection, *GENERAL NOTE:* EC_{50} and SI (CC/EC) values for the table above could not be calculated as no antiviral effect was observed

Unfortunately, none of the compounds tested using the XTT assay showed any antiviral effect against HIV. As such, we decided not to invest any further time or money in the exhaustive testing of all of our first generation compounds which we had synthesized in **Chapter 2**.

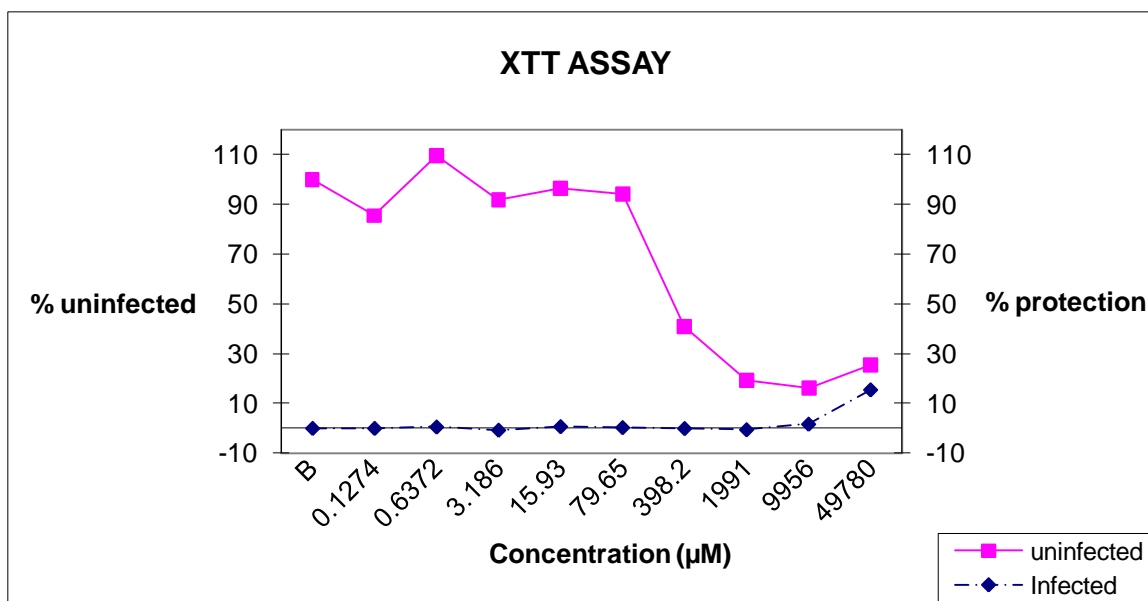
We did, however, obtain some interesting results from this study, in that a large proportion of the synthetic compounds showed toxicity towards the uninfected MT-4 cells. These interesting results obtained are discussed fully in *Section 3.2.2.3*.

3.2.2.3 Discussion

Through testing this range of ten compounds (shown in **Figure 31**) we aimed to compare:

- (i) the five different nucleosides we used for activity
- (ii) our *tert*-butyldiphenylsilyl protecting group derivatives with the 4,4'-dimethoxytrityl group derivatives
- (iii) sequentially protected derivatives as a mini structure-activity assay
- (iv) the results obtained for the nucleoside derivatives with the protecting group controls

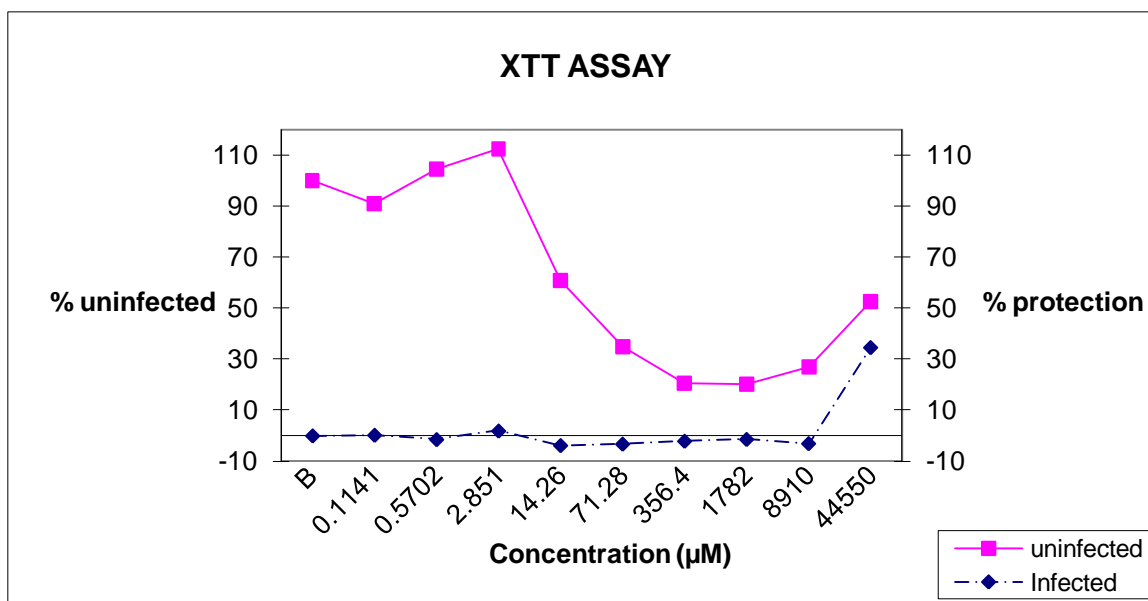
To satisfy our first two aims, we initially compared the TBDPS-protected purine nucleoside, 5'-*O*-(*tert*-butyldiphenylsilyl)adenosine **142**, with the pyrimidine nucleosides, 5'-*O*-(*tert*-butyldiphenylsilyl)cytidine **134** and 5'-*O*-(*tert*-butyldiphenylsilyl)uridine **107**. We observed that none of the TBDPS-protected compounds showed any antiviral activity at all and essentially gave 0 % protection against the virus. Interestingly, however, we did observe that 5'-*O*-(*tert*-butyldiphenylsilyl)adenosine **142** showed marked toxicity against the healthy, uninfected MT-4 cells, with a CC_{50} value of 0.345 mM (345 μ M) obtained from the study. This is shown by the gradual decrease in the percentage of uninfected cells present at concentrations of the compound above 79 μ M in **Graph 7**.



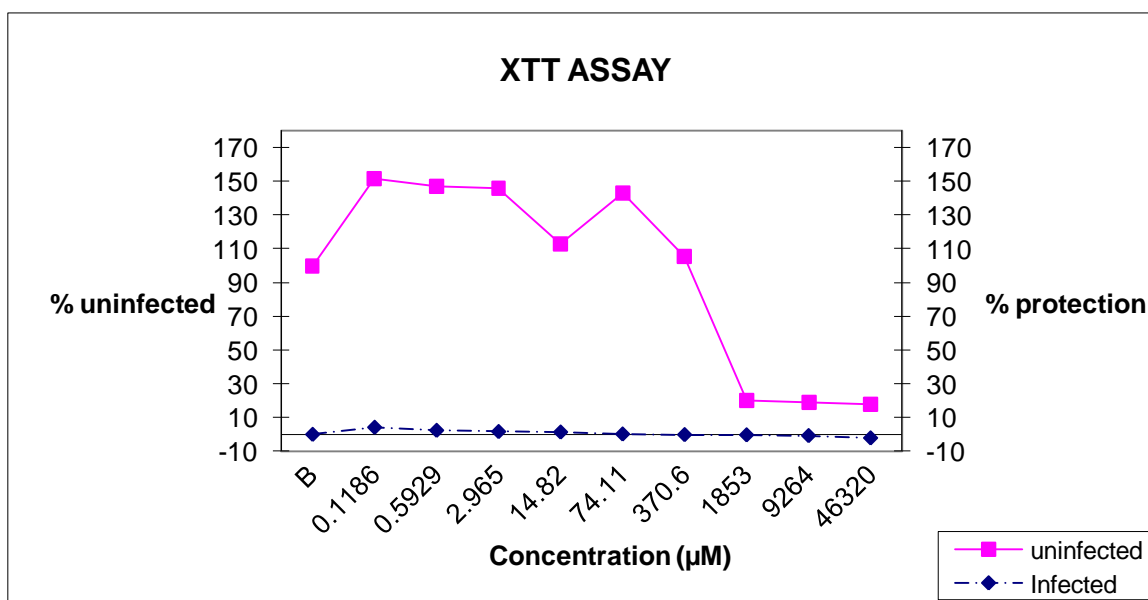
Graph 7 Results obtained from XTT assay for 5'-*O*-(*tert*-butyldiphenylsilyl)adenosine **142**, where B = blank and has none of the test compound added

After looking at the TBDPS-protected derivatives, we compared the DMT-protected purine nucleosides, 5'-*O*-(4,4'-dimethoxytrityl)-6-*N*-(*N,N*-dimethylmethylimine)guanosine **113** and 5'-*O*-(4,4'-dimethoxytrityl)inosine **117**, with the pyrimidine nucleoside, 5'-*O*-(4,4'-dimethoxytrityl)uridine **126**. We again found that none of the compounds exhibited any of the desired antiviral activity and concluded that DMT-protected nucleoside derivatives offered 0 % protection against the HIV_{IIIB} virus.

Surprisingly, we again noted that the compounds exhibited toxicity towards the uninfected MT-4 cells. As shown on **Graph 8** and **Graph 9**, we found that 5'-*O*-(4,4'-dimethoxytrityl)inosine **117** and 5'-*O*-(4,4'-dimethoxytrityl)uridine **126** gave CC₅₀ values of 0.0380 mM (38.0 µM) and 1.33 mM (1331 µM) respectively.



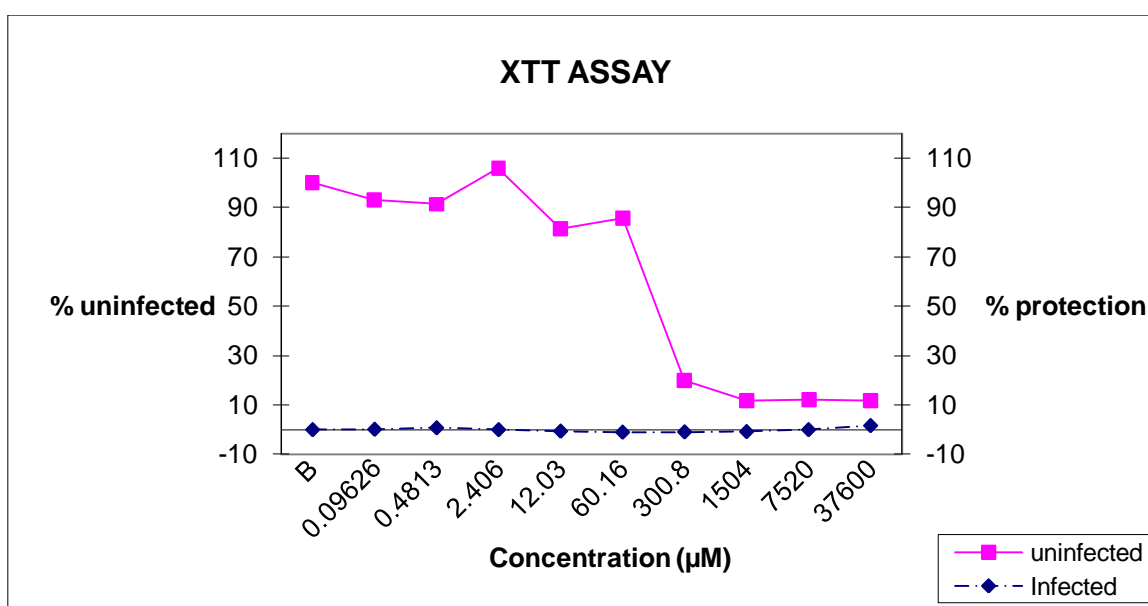
Graph 8 Results obtained from XTT assay for 5'-O-(4,4'-dimethoxytrityl)inosine **117**, where B = blank and has none of the test compound added



Graph 9 Results obtained from XTT assay for 5'-O-(4,4'-dimethoxytrityl)uridine **126**, where B = blank and has none of the test compound added

To satisfy our second aim, wherein we wanted to compare sequentially protected derivatives as a mini structure-activity assay, we tested:

- 5'-*O*-(*tert*-butyldiphenylsilyl)uridine **107**
- 2',3'-*O*-acetyl-5'-*O*-(*tert*-butyldiphenylsilyl)uridine **123**
- 3-*N*-benzoyl-2',3'-*O*-diacetyl-5'-*O*-(*tert*-butyldiphenylsilyl)uridine **124**



Graph 10 Results obtained from XTT assay for 3-*N*-benzoyl-2',3'-*O*-diacetyl-5'-*O*-(*tert*-butyldiphenylsilyl)uridine **124**, where B = blank and has none of the test compound added

Unfortunately, we found that none of the compounds exhibited the desired antiviral activity and as such we could not compare which positions on the molecule were essential for activity. But the mini-study was not in vain, as we again observed toxicity towards the uninfected MT-4 cells. In this case we observed that:

- **107**, which is protected only on the primary alcohol, has a calculated CC_{50} value of 23.4 mM
- **123**, which is protected on both the primary and secondary alcohols, has a calculated CC_{50} value of 23.1 mM

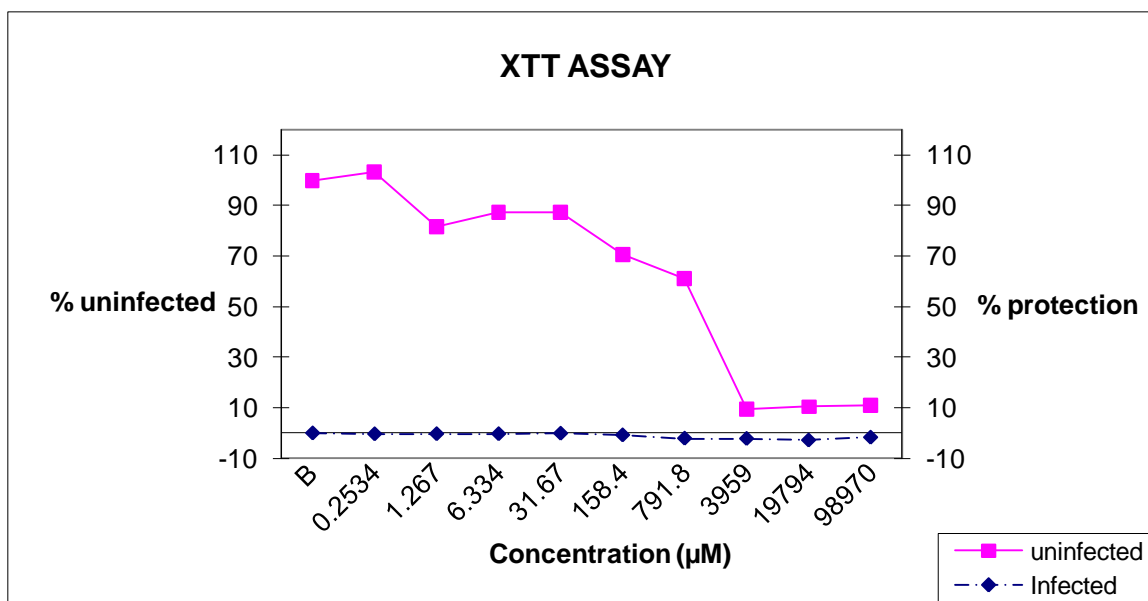
- **124**, which is fully protected on the primary and secondary alcohols as well as the secondary amide, has a calculated CC₅₀ value of 0.191 mM (shown in **Graph 10**)

These results were quite interesting – in this case compound **124**, which was the most lipophilic of the molecules studied (and would therefore have a higher probability of crossing the cellular membranes), was actually found to be the most toxic of the compounds in the series. Suggesting that high lipophilicity and toxicity are intrinsically linked for these types of nucleoside derivatives.

Our final aim was to compare the results obtained for the nucleoside derivatives with those for the protecting group derivative controls. These were included in order to determine whether the nucleoside derivatives themselves were required for activity, and, if under biological conditions the compounds were hydrolysed, i.e.: whether the protecting group derivatives themselves were active.

As expected, neither of the protecting group derivatives tested exhibited any antiviral activity. But we again noted interesting results concerning the toxicity of the molecules towards the uninfected MT-4 cells. From the data obtained, we calculated that the *tert*-butyldiphenylsilanol **145** had a CC₅₀ value of 1.47 mM and that the 4,4'-dimethoxytrityl alcohol **147** had a CC₅₀ value of 13.7 mM. **Graph 11** shows the data obtained for *tert*-butyldiphenylsilanol **145**.

The CC₅₀ value of 1.47 mM for the *tert*-butyldiphenylsilanol **145** was considerably higher than that obtained for 5'-*O*-(*tert*-butyldiphenylsilyl)adenosine **142** of 0.345 mM, but significantly less than those obtained for 5'-*O*-(*tert*-butyldiphenylsilyl)cytidine **134** (3.33 mM) and 5'-*O*-(*tert*-butyldiphenylsilyl)uridine **107** (23.4 mM). Due to the vast spread of data obtained, no specific conclusion could be deduced and we feel that this problem would need to be further investigated.



Graph 11 Results obtained from XTT assay *tert*-butyldiphenylsilanol **145** and where B = blank and has none of the test compound added

In a similar manner, the results obtained for the 4,4'-dimethoxytrityl alcohol **147** (CC_{50} of 13.7 mM) were compared to those obtained for 5'-*O*-(4,4'-dimethoxytrityl)-6-*N*-(*N,N*-dimethylmethylimine)guanosine **113** (CC_{50} of 5.91 mM), 5'-*O*-(4,4'-dimethoxytrityl)inosine **117** (CC_{50} of 0.0380 mM) and 5'-*O*-(4,4'-dimethoxytrityl)uridine **126** (CC_{50} of 1.33 mM). In this case however, the result obtained for the 4,4'-dimethoxytrityl alcohol **147** was always significantly higher than those obtained for the nucleoside derivatives. As such, we deduced that the nucleoside was necessary for the toxic activity observed and that the hydrolysis product on its own was not highly toxic towards uninfected MT-4 cells.

All graphs used to determine the CC_{50} values given in this section have been included on the attached DVD, under **Supporting Information**.

3.2.2.4 Conclusions

We found that none of the range of synthetic nucleoside and protecting group derivatives assayed showed any antiviral activity towards HIV_{III}B. However, we did observe that a large number of the compounds were toxic towards the uninfected MT-4 cells (human T-cell leukemia cell line) at millimolar levels. This was quite unexpected and we believed that it suggested that our synthetic compounds may be toxic towards specifically cancerous cells. This possibility would, however, need to be fully investigated and as such we decided to deviate from our initial aims of screening our synthetic derivatives for anti-bacterial and antiviral activity, to instead focus on the subsequent screening of all of the "first generation" compounds for possible anticancer activity. The results of this exhaustive study are discussed in the following sections.

3.2.3 Inhibition of Cell Proliferation

The MTT colorimetric assay was used to determine the cytotoxic activity of the synthetic compounds and controls after a 24 hour exposure period to the different cell lines. The MTT assay is similar to the TTC assay used to determine anti-bacterial activity and the XTT assay used to determine anti-HIV activity, as they are all based on the same principle, that tetrazolium structures are bio-reduced to formazan structures in metabolically active cells. As such, only a very broad description of the methodology used is given in *Section 3.2.3.1*.

Compounds exhibiting positive results in the MTT assay were then subjected to subsequent testing: (i) an Annexin V flow cytometry assay was used to determine whether apoptosis or cell necrosis was induced, (ii) both Caspase-3/CPP32 and Caspase-8 colorimetric assays were performed to determine caspase expression and (iii) cytochrome *c* fractions in the mitochondrial and cytoplasmic fractions were determined by the enzyme immunometric assay.

3.2.3.1 Materials and Methods

Cell Lines

For this assay, five cell lines were used, of which three were suspension lines and two were adherent lines. The suspension lines used were: HL-60, K-562 and Jurkat cells, while the adherent lines used were HT-29 and Caco-2 cells. White blood cells (WBC) were also included in the assay as a control to confirm if the compounds were inhibiting the growth of healthy, non-cancerous cells.

The HL-60 suspension cell line is a human leukemic cell line derived from a 36 year old woman with acute promyelocytic leukemia at the National Cancer Institute.⁶⁷ It has been widely used for laboratory research on how certain kinds of blood cells are formed. The HL-60 cultured cell line provides a continuous source of human cells for studying the molecular events of myeloid differentiation and the effects of physiologic, pharmacologic and virologic elements on this process.⁶⁸

The Jurkat cell line was established in the late 1970s from the peripheral blood of a 14 year old boy with T cell leukemia.⁶⁹ Jurkat cells are an immortalized line of T lymphocyte cells that are used to study acute T cell leukemia, T cell signaling and the expression of various chemokine receptors susceptible to viral entry.⁷⁰ Jurkat cells are also useful in science because of their ability to produce interleukin 2.⁷⁰ The primary use, however, is to determine the mechanism of differential susceptibility of cancers to drugs and radiation.

K-562 were the first human immortalized myelogenous leukemia line to be established.⁷¹ K-562 cells are non-adherent and of the erythroleukemia type. The line was derived from a 53 year old female chronic myeloid leukemia (CML) patient in blast crisis.⁷²

The HT-29 cell line is an adherent human colorectal adenocarcinoma cell line. HT-29 cells are human intestinal epithelial cells.

Caco-2 is an immortalized line of heterogeneous human epithelial colorectal adenocarcinoma cells, developed by the Sloan-Kettering Institute for Cancer Research.⁷³ The adherent Caco-2 cell line is widely used with *in vitro* assays to predict the absorption rate of candidate drug compounds across the intestinal epithelial cell barrier.⁷⁴ Caco-2 may also refer to a cell monolayer absorption model, where cell-based functional assays may be used as a model for assessing intestinal transport of lead compounds in drug discovery.⁷⁵

All of the cell lines used in the study were routinely maintained in Dulbecco's Modified Eagles Medium supplemented with 5 % heat-inactivated foetal bovine serum. The cell lines were maintained in 75 cm³ flasks at 37 °C in a 95 % O₂ : 5 % CO₂ humidified incubator using standard culture techniques.

Fresh human white blood cells were isolated according to the *Versagene DNA Purification Kit* standard protocol provided by the supplier.

🌀 *Compounds Used in the Inhibition of Cell Proliferation Study*

Seventeen of the range of compounds synthesized in **Chapter 2** were selected for use in this study to encompass derivatives of all five of the different nucleosides and β -(-)-ribose. Compounds used in this study have been re-drawn and grouped according to their structural similarities for ease of reading. **Figure 33** shows the pyrimidine-based nucleoside derivatives, **Figure 34** shows the purine-based nucleoside derivatives and **Figure 35** shows the derivatives of β -(-)-ribose.

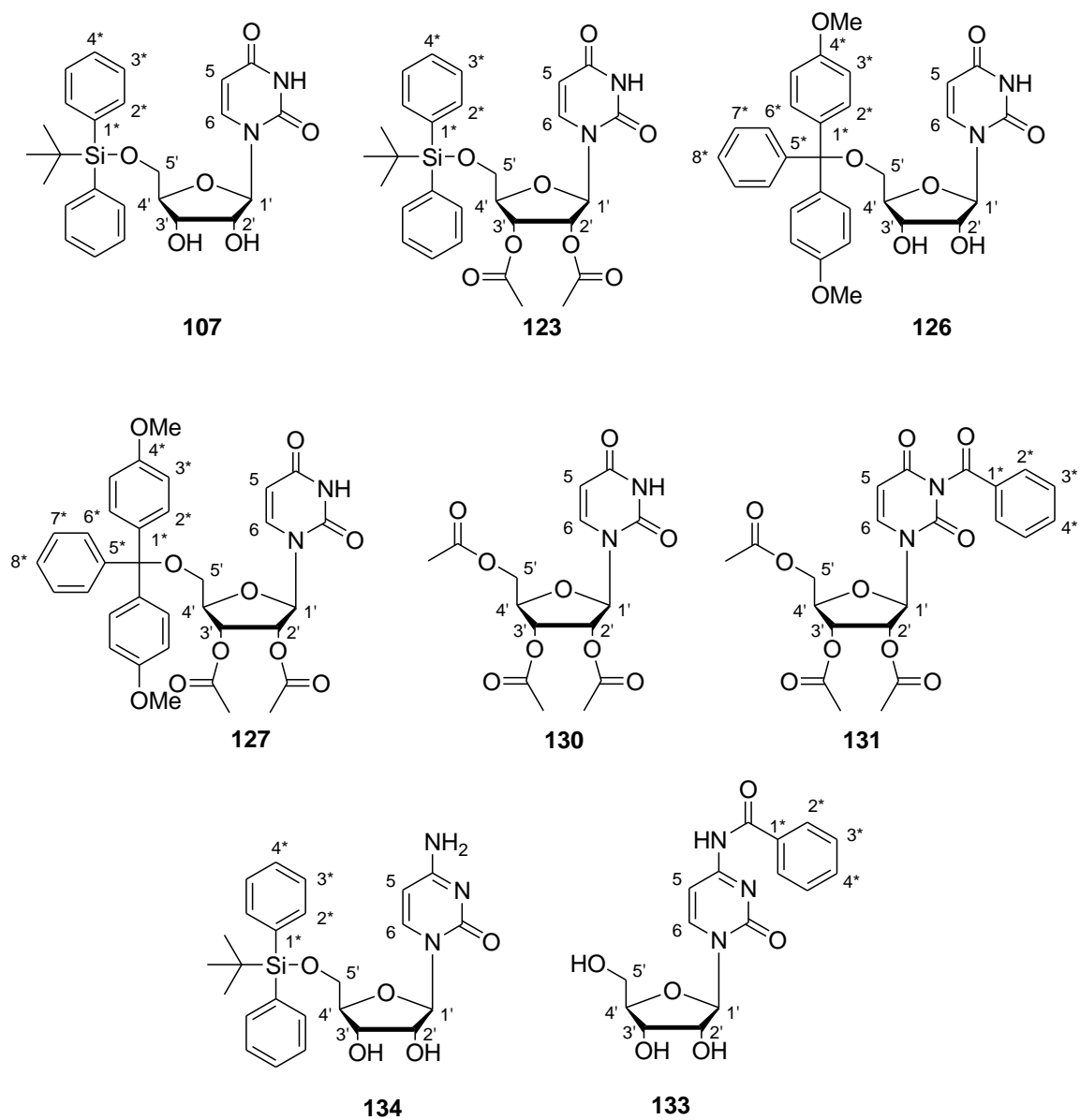


Figure 33 Pyrimidine-based nucleoside derivatives

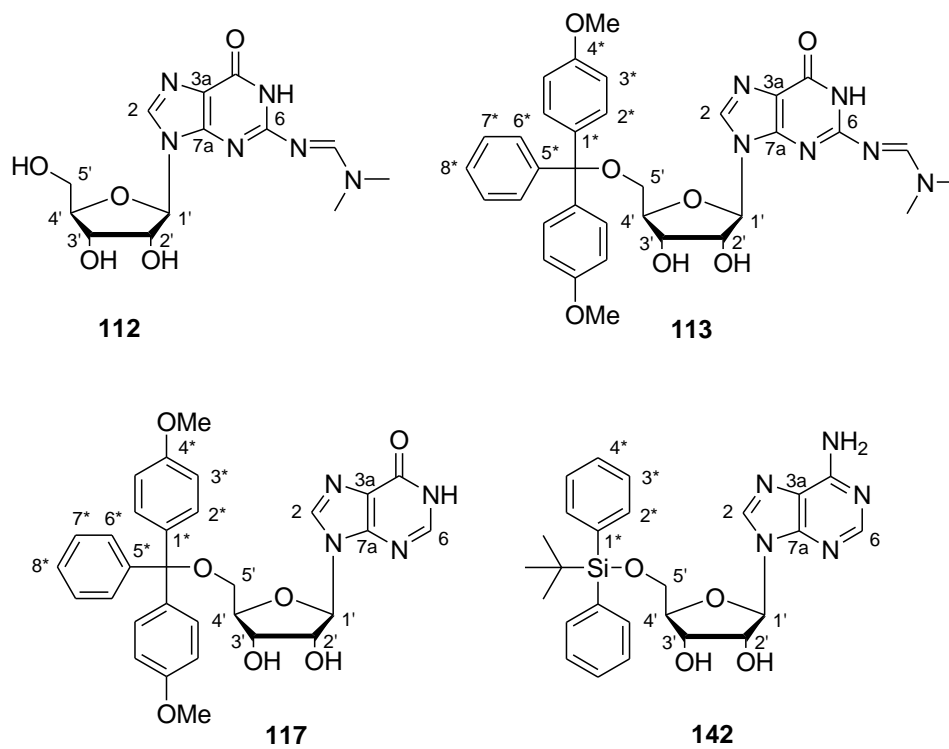


Figure 34 Purine-based nucleoside derivatives

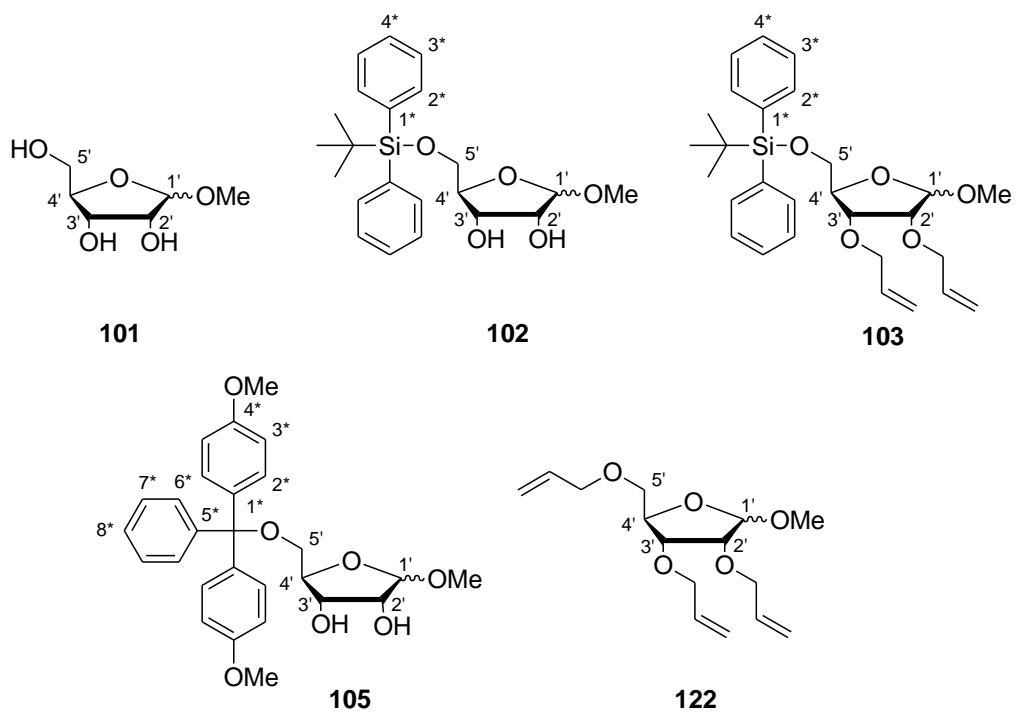


Figure 35 Derivatives of α -(-)-ribose

Also included in the study were the protecting group derivatives, to act as a control to indicate if the protecting group portion of the molecule is causing any observed activity. The unmodified nucleosides and β -(-)-ribose were included as negative controls for the study. Camptothecin **155** was included as our positive control as it is a well researched anticancer agent. The structures for the control compounds are shown in **Figure 36**.

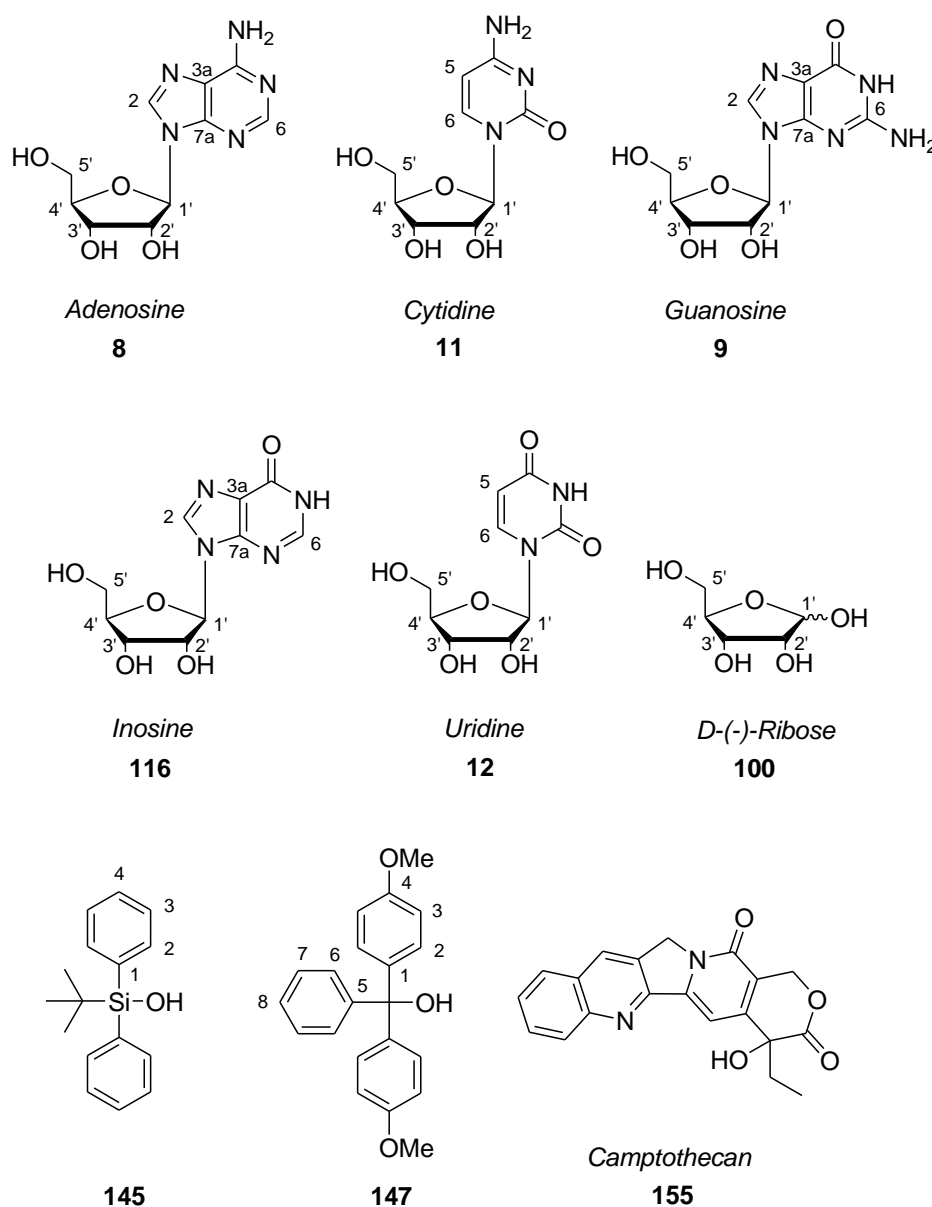


Figure 36 Control compounds

© *Evaluation of Compound Efficacy using the MTT Assay for Cell Viability Quantification*

The cells used, HL-60, K-562, HT-29, Caco-2 and white blood cells, were counted and diluted into fresh media (Dulbecco's Modified Eagles Medium supplemented with 5 % heat-inactivated foetal bovine serum) at concentrations of 30 000 cells/well. An aliquot of 180 μ L was seeded into each well of a 96-well plate. The plates were then placed in an incubator (37 °C, 5 % CO₂, volume fraction) and the cells were allowed to divide for a period of 24 h.

The cells were exposed to the different classes of synthetic compounds and controls described above, with a final concentration of 100 μ g/mL in the wells. The 96-well plates were then incubated at 37 °C for an additional 24 hours to allow the cells to interact with the synthetic compounds. After the 24 hour incubation period, the plates were removed from the incubator and an aliquot of 50 μ L of a 0.5 % 3-(4,5-dimethylthiazol-2-yl)-2,5-diphenyltetrazolium bromide (MTT) in 1 mM phosphate buffered saline (PBS) at pH 7.4, was layered onto the media. The plates were again incubated at 37 °C for another 2 hours.

After this time, the plates were then centrifuged at 3000 rpm (Afrox Sorvall T 6000D) for 5 minutes. Following centrifugation, the medium was very carefully aspirated and the formazan precipitate obtained was dissolved in 200 μ L DMSO. The absorbance was then read at 540 nm using the Absorbance Labsystems Multiskan MS, version 2.4.

The controls used in the assay consisted of:

- (i) medium alone without cells giving the 0 % growth control
- (ii) cells and medium with no test compound added, giving the 100 % growth control
- (ii) cells and medium with camptothecin **155** added

Compounds showing cytotoxicity at a concentration of 100 $\mu\text{g/mL}$ were further diluted in ten-fold dilutions to obtain the IC_{50} concentrations. All tests were performed in triplicate.

Other Assays Conducted

Only compounds exhibiting positive results in the MTT assay were subjected to subsequent testing. An Annexin V flow cytometry kit was used to determine whether apoptosis or cell necrosis was induced. Caspase-3/CPP32 and Caspase-8 colorimetric assay kits were used to determine caspase expression. Cytochrome *c* fractions in the mitochondrial and cytoplasmic fractions were determined by the Enzyme Immunometric Assay (EIA) kit. No further details will be provided on the methodology used in these assays, as all protocols were performed according to standard instructions provided by the manufacturer's of the kits.

Data Analysis

The results from the MTT assay are expressed as the concentration of synthetic compound required to give a 50 % inhibition (IC_{50}). The Enzfitter and Prism3 programs were used to determine the IC_{50} values for the test compounds.

3.2.3.2 Results of MTT Assay

The assay for inhibition of cell proliferation was broken down into two groups based on the type of cells investigated. The initial investigation involved the use of three suspension cell lines, HL-60, K-562 and Jurkat cells, with the results obtained compared to those for white blood cells (WBC), i.e.: healthy, non-cancerous cells.

The positive control used in this assay was the commercial compound camptothecin **155**. As expected, camptothecin **155** showed inhibition of proliferation for all of the suspension cell lines. Surprisingly, however, there was quite a low cell viability for the white blood cells - highlighting the toxicity of camptothecin **155** towards healthy, non-cancerous cells. The results obtained are given in **Table 11**.

Table 11 Percentage cell viability of the suspension cell lines when treated with 100 μ M camptothecin for 24 hours

Compound	HL-60	Jurkat	K-562	WBC
Camptothecin	23.359 \pm	8.889 \pm	39.623 \pm	34.622 \pm
155	0.721 %	0.694 %	0.933 %	2.028 %

The pyrimidine-based nucleosides, uridine **12** and cytidine **11**, were included as negative controls for the assay, as we did not expect them to inhibit the growth of the suspension cell lines. The results obtained for the assay of the pyrimidine-based nucleoside derivatives are given in detail in **Table 12** below.

We observed that 5'-*O*-(*tert*-butyldiphenylsilyl)uridine **107** exhibited cytotoxic activity towards the suspension cell lines, with the percentage of viable cancer cells between 5-10 % after treatment with 100 μ M of the synthetic compound for 24 hours. This shows significantly more activity than the positive control, camptothecin **155**, which had 9-40 % viable cells remaining after the corresponding treatment. Interestingly, we noted that the synthetic compound, 5'-*O*-(*tert*-butyldiphenylsilyl)uridine **107** had 61.460 \pm 4.481 % of the white blood cells viable, in comparison to the meagre 34.622 \pm 2.028 % viable after treatment with the camptothecin **155**. This suggests that 5'-*O*-(*tert*-butyldiphenylsilyl)uridine **107** shows a degree of selective toxicity against the cancer lines with minimal cytotoxicity directed against the white blood cells.

The 2',3'-*O*-diacetyl-5'-*O*-(*tert*-butyldiphenylsilyl)uridine **123** which is protected on the secondary alcohols as well as the primary alcohol, showed considerably lower activity than

that for the 5'-*O*-(*tert*-butyldiphenylsilyl)uridine **107** which is only protected on the primary alcohol. For the HL-60 cell line, the percentage of viable cells increased from 5.619 ± 0.348 % for 5'-*O*-(*tert*-butyldiphenylsilyl)uridine **107** to 11.180 ± 0.525 % for 2',3'-*O*-diacetyl-5'-*O*-(*tert*-butyldiphenylsilyl)uridine **123**. In a similar manner, the percentage viable cells increased from 6.333 ± 0.601 % to > 50 % (ie: the compound is not active) in the Jurkat cell line, and from 9.355 ± 0.108 % to 35.530 ± 2.364 % in the K-562 cell line. This suggests that increasing the number of free hydroxyls on the molecules, by protecting the secondary alcohols, decreases the activity of the synthetic compounds towards the suspension cell lines. What was startling for us, was the discovery that the 2',3'-*O*-diacetyl-5'-*O*-(*tert*-butyldiphenylsilyl)uridine **123** was able to have activity towards the cancer cell lines, and yet to allow all (100.774 ± 2.402 %) of the white blood cells to remain viable after treatment, thus showing truly selective toxicity towards the cancer cell lines.

We noted that the 5'-*O*-(*tert*-butyldiphenylsilyl)cytidine **134** exhibited cytotoxic activity towards the suspension cell lines, with the percentage of viable cells remaining after treatment between 16-36 % and the white blood cells at 101.893 ± 2.027 %. These values are considerably lower than those obtained for 5'-*O*-(*tert*-butyldiphenylsilyl)uridine **107** and suggest that uridine is the better target for the further development of lead compounds.

In a similar manner, we observed that the 5'-*O*-(4,4'-dimethoxytrityl)uridine **126** showed selective toxicity towards the cancer cell lines. With a percentage cell viability of 5-9 % observed for the suspension cell lines and 82.687 ± 2.088 % observed for the white blood cells after treatment for 24 hours with 100 μ M of the test compound. As previously noted, the activity was significantly reduced when the secondary alcohols were protected. We observed that 2',3'-*O*-diacetyl-5'-*O*-(4,4'-dimethoxytrityl)uridine **127** was not active against any of the suspension cell lines.

Interestingly, none of the synthetic compounds that were prepared without the *tert*-butyldiphenylsilyl or 4,4'-dimethoxytrityl protecting groups showed any activity towards the suspension cell lines.

Table 12 Percentage cell viability of the suspension cell lines when treated with 100 μ M of the pyrimidine nucleosides and their derivatives for 24 hours

Compound	HL-60	Jurkat	K-562	WBC
Uridine	Compound	Compound	Compound	Compound
12	Not Active	Not Active	Not Active	Not Active
107	5.619 \pm 0.348 %	6.333 \pm 0.601 %	9.355 \pm 0.108 %	61.460 \pm 4.481 %
123	11.180 \pm 0.525 %	Compound Not Active	35.530 \pm 2.364 %	100.774 \pm 2.402 %
126	6.505 \pm 0.483 %	5.222 \pm 0.977 %	8.281 \pm 0.246 %	82.687 \pm 2.088 %
127	Compound Not Active	Compound Not Active	Compound Not Active	Compound Not Active
130	Compound Not Active	Compound Not Active	Compound Not Active	Compound Not Active
131	Compound Not Active	Compound Not Active	Compound Not Active	Compound Not Active
Cytidine	Compound	Compound	Compound	Compound
11	Not Active	Not Active	Not Active	Not Active
134	25.994 \pm 0.623 %	16.000 \pm 1.323 %	35.632 \pm 0.947 %	101.893 \pm 2.027 %
133	Compound Not Active	Compound Not Active	Compound Not Active	Compound Not Active

Note: Synthetic compounds are defined as not active if the cell viability is greater than 50 %

The results obtained for the assay of the purine-based nucleoside derivatives are given in detail in **Table 13**. The purine-based nucleosides, guanosine **9**, inosine **116** and adenosine **8**, were included as our negative controls for the assay, as we did not expect them to inhibit the growth of the suspension cell lines.

Table 13 Percentage cell viability of the suspension cell lines when treated with 100 μ M of the purine nucleosides and their derivatives for 24 hours

Compound	HL-60	Jurkat	K-562	WBC
Guanosine	Compound	Compound	Compound	Compound
9	Not Active	Not Active	Not Active	Not Active
112	Compound	Compound	Compound	Compound
	Not Active	Not Active	Not Active	Not Active
113	29.316 \pm 0.450 %	8.778 \pm 0.694 %	Compound Not Active	92.788 \pm 2.688 %
Inosine	Compound	Compound	Compound	Compound
116	Not Active	Not Active	Not Active	Not Active
117	8.309 \pm 0.051 %	6.833 \pm 0.167 %	22.957 \pm 0.679 %	76.474 \pm 1.211 %
Adenosine	Compound	Compound	Compound	Compound
8	Not Active	Not Active	Not Active	Not Active
142	27.864 \pm 0.541 %	18.333 \pm 1.167 %	45.530 \pm 0.731 %	59.262 \pm 2.027 %

Note: Synthetic compounds are defined as not active if the cell viability is greater than 50 % after treatment

As suggested by the results obtained for the pyrimidine-based nucleoside derivatives, the purine-based nucleoside derivatives protected at the primary alcohol with bulky protecting groups also showed selective toxicity towards the cancer cell lines.

5'-*O*-(4,4'-Dimethoxytrityl)-6-*N*-(*N,N*-dimethylmethylimine)guanosine **113** showed percentage cell viabilities of 29.316 ± 0.450 % for HL-60, 8.778 ± 0.694 % for Jurkat and no activity for K-562; relative to the 92.788 ± 2.688 % obtained for the white blood cells. In a similar manner 5'-*O*-(4,4'-dimethoxytrityl)inosine **117** gave percentage cell viabilities of 8.309 ± 0.051 % for HL-60, 6.883 ± 0.167 % for Jurkat and 22.957 ± 0.679 % for K-562; relative to the 76.474 ± 1.211 % obtained from the white blood cells. Also, 5'-*O*-(*tert*-butyldiphenylsilyl)adenosine **142** showed percentage cell viabilities of 27.864 ± 0.541 % for HL-60, 18.333 ± 1.167 % for Jurkat and 45.530 ± 0.731 % for K-562; relative to that of 59.262 ± 2.027 % obtained for the white blood cells.

The third group of compounds assayed were those derived from β -(-)-ribose. These were prepared in order to determine if the base on the nucleosides was required for activity in the compounds, or if the corresponding sugar derivatives on their own would be sufficiently active. The results obtained for the assay of β -(-)-ribose **100** and its derivatives are given in detail in **Table 14** below as the percentage cell viability after treatment with 100 μ M of compound for 24 hours.

We observed that only one of the derivatives of β -(-)-ribose showed any activity against the cancer cell lines. The 5'-*O*-(4,4'-dimethoxytrityl)-1'-*O*-methoxyribose **105** gave a percentage cell viability of 45.976 ± 0.489 % for the HL-60 cell line and no activity towards the Jurkat and K-562 cell lines. After treatment with 5'-*O*-(4,4'-dimethoxytrityl)-1'-*O*-methoxyribose **105**, 98.213 ± 2.623 % of the white blood cells were viable. This limited activity for 5'-*O*-(4,4'-dimethoxytrityl)-1'-*O*-methoxyribose **105** and lack of activity for all of the other β -(-)-ribose derivatives suggests that the base on the nucleoside would be required in all synthetic derivatives which have potential as lead compounds for cancer therapy.

Table 14 Percentage cell viability of suspension cell lines when treated with 100 μ M α -(-)-ribose and its derivatives for 24 hours

Compound	HL-60	Jurkat	K-562	WBC
α -(-)-Ribose	Compound	Compound	Compound	Compound
100	Not Active	Not Active	Not Active	Not Active
101	Compound Not Active	Compound Not Active	Compound Not Active	Compound Not Active
102	Compound Not Active	Compound Not Active	Compound Not Active	Compound Not Active
103	Compound Not Active	Compound Not Active	Compound Not Active	Compound Not Active
105	45.976 \pm 0.489 %	Compound Not Active	Compound Not Active	98.213 \pm 2.623 %
122	Compound Not Active	Compound Not Active	Compound Not Active	Compound Not Active

Note: Synthetic compounds are defined as not active if the cell viability is greater than 50 % after treatment

The last class of compounds assayed were the protecting group derivatives, *tert*-butyldiphenylsilanol **145** and 4,4'-dimethoxytrityl alcohol **147**. These compounds were included in our assay as a control in order to determine if the possible products formed by hydrolysis within the cells were in fact the active agents. The results are summarized in **Table 15**, which indicates that neither of the protecting group derivatives exhibit any activity towards the suspension cell lines tested.

Table 15 Percentage cell viability of the suspension cell lines when treated with 100 μ M of the protecting group controls for 24 hours

Compound	HL-60	Jurkat	K-562	WBC
TBDPS-OH	Compound	Compound	Compound	Compound
145	Not Active	Not Active	Not Active	Not Active
DMT-OH	Compound	Compound	Compound	Compound
147	Not Active	Not Active	Not Active	Not Active

Note: Synthetic compounds are defined as not active if the cell viability is greater than 50 % after treatment

As discussed previously, the assay for inhibition of cell proliferation was broken down into two groups based on the type of cells investigated. The second assay involved the use of two adherent cell lines, Caco-2 and HT-29, with the results obtained again compared to those for white blood cells (WBC), ie: healthy, non-cancerous cells.

The positive control used in this assay was again the commercial drug camptothecin **155**. As expected, camptothecin **155** showed inhibition of proliferation for both of the adherent cell lines. Again, we noted that there was quite a low cell viability for the white blood cells - highlighting the toxicity of camptothecin **155** towards healthy, non-cancerous cells. The results obtained are given in **Table 16**.

Table 16 Percentage cell viability of the adherent cell lines when treated with 100 μ M of camptothecin for 24 hours

Compound	Caco-2	HT-29	WBC
Camptothecin	12.769 \pm	11.443 \pm	34.622 \pm
155	0.166 %	0.201 %	2.028 %

The results obtained for the assay of the pyrimidine-based nucleoside derivatives against two adherent cell lines are given in detail in **Table 17**. The pyrimidine-based nucleosides, uridine

12 and cytidine **11**, were included as negative controls for the assay, as we did not expect them to inhibit the growth of the suspension cell lines.

We observed that 5'-*O*-(*tert*-butyldiphenylsilyl)uridine **107** exhibited cytotoxic activity towards the adherent cell lines, with the percentage viable cells for Caco-2 at 37.443 ± 1.007 % and for HT-29 as 29.373 ± 0.556 %. When compared to the percentage cell viability of 61.460 ± 4.481 % for the white blood cells, we can conclude that the compound shows a degree of selective toxicity towards the cancer cells.

In a similar manner, the percentage cell viability of 26.070 ± 0.173 % for Caco-2 and of 27.770 ± 1.172 % for HT-29, when compared to the percentage cell viability of 82.687 ± 2.088 % for the white blood cells, suggests that 5'-*O*-(4,4'-dimethoxytrityl)uridine **126** also shows selective toxicity towards adherent cancer cells.

Both 2',3'-*O*-diacetyl-5'-*O*-(*tert*-butyldiphenylsilyl)uridine **123** and 2',3'-*O*-diacetyl-5'-*O*-(4,4'-dimethoxytrityl)uridine **127**, which are protected on all of the primary and secondary alcohols, showed no activity towards the adherent cell lines. This suggests that decreasing the number of free hydroxyls on the molecules, through the protection of the secondary alcohols, causes a loss in activity towards the adherent cell lines. This correlates to the results observed for the suspension cell lines, where the protection of the secondary alcohols also lead to a decrease in activity.

We noted that the 5'-*O*-(*tert*-butyldiphenylsilyl)cytidine **134** exhibited cytotoxic activity towards the adherent cell lines as well, with the percentage of viable cells remaining after treatment as 37.200 ± 0.384 % for Caco-2, 25.593 ± 0.697 % for HT-29 and 101.893 ± 2.027 % for the white blood cells. This again correlates to the results obtained for the suspension cell lines, as previously described.

Table 17 Percentage cell viability of the adherent cell lines when treated with 100 μ M of the pyrimidine nucleosides and their derivatives for 24 hours

Compound	Caco-2	HT-29	WBC
Uridine	Compound	Compound	Compound
12	Not Active	Not Active	Not Active
107	37.443 \pm 1.007 %	29.373 \pm 0.556%	61.460 \pm 4.481 %
123	Compound Not Active	Compound Not Active	Compound Not Active
126	26.070 \pm 0.173 %	27.770 \pm 1.172 %	82.687 \pm 2.088%
127	Compound Not Active	Compound Not Active	Compound Not Active
130	Compound Not Active	Compound Not Active	Compound Not Active
131	Compound Not Active	Compound Not Active	Compound Not Active
Cytidine	Compound	Compound	Compound
11	Not Active	Not Active	Not Active
134	37.200 \pm 0.384 %	25.593 \pm 0.697 %	101.893 \pm 2.027%
133	Compound Not Active	Compound Not Active	Compound Not Active

Note: Synthetic compounds are defined as not active if the cell viability is greater than 50 %

None of the synthetic compounds that were prepared without the *tert*-butyldiphenylsilyl or 4,4'-dimethoxytrityl protecting groups showed any activity towards the suspension cell lines.

The results obtained for the assay of the purine-based nucleoside derivatives are given in detail in **Table 18**. The nucleosides, guanosine **9**, inosine **116** and adenosine **8**, were again included as our negative controls for the assay.

Table 18 Percentage cell viability of the adherent cell lines when treated with 100 μ M of the purine nucleosides and their derivatives for 24 hours

Compound	Caco-2	HT-29	WBC
Guanosine	Compound	Compound	Compound
9	Not Active	Not Active	Not Active
112	Compound	Compound	Compound
	Not Active	Not Active	Not Active
113	Compound	Compound	Compound
	Not Active	Not Active	Not Active
Inosine	Compound	Compound	Compound
116	Not Active	Not Active	Not Active
117	Compound	Compound	Compound
	Not Active	Not Active	Not Active
Adenosine	Compound	Compound	Compound
8	Not Active	Not Active	Not Active
142	Compound	Compound	Compound
	Not Active	Not Active	Not Active

Note: Synthetic compounds are defined as not active if the cell viability is greater than 50 %

Interestingly, none of the purine-based nucleoside derivatives showed any activity towards the adherent cell lines. This result was surprising as the 5'-*O*-(4,4'-dimethoxytrityl)-6-*N,N,N*-dimethylmethylimine)guanosine **113**, 5'-*O*-(4,4'-dimethoxytrityl)inosine **117** and 5'-*O*-(*tert*-butyldiphenylsilyl)adenosine **142** showed inhibition of cell proliferation for all of the suspension cell lines used.

The next group of compounds assayed were those derived from β -(-)-ribose **100**. The results obtained for the assay of β -(-)-ribose and its derivatives are given in detail in **Table 19** as the percentage cell viability after treatment with 100 μ M of compound for 24 hours.

Table 19 Percentage cell viability of adherent cell lines when treated with 100 μ M of β -(-)-ribose and its derivatives for 24 hours

Compound	Caco-2	HT-29	WBC
β -(-)-Ribose	Compound	Compound	Compound
100	Not Active	Not Active	Not Active
101	Compound Not Active	Compound Not Active	Compound Not Active
102	Compound Not Active	Compound Not Active	Compound Not Active
103	Compound Not Active	Compound Not Active	Compound Not Active
105	Compound Not Active	Compound Not Active	Compound Not Active
122	Compound Not Active	Compound Not Active	Compound Not Active

Note: Synthetic compounds are defined as not active if the cell viability is greater than 50 %

We observed that none of the derivatives of α -(-)-ribose showed any activity against the adherent cancer cell lines. This correlates to the results obtained for the suspension cell lines, where only one of the compounds, 5'-*O*-(4,4'-dimethoxytrityl)-1'-*O*-methoxyribose **105**, showed limited activity towards only the HL-60 cell line. This lack of activity again suggests that the base on the nucleosides is intrinsic for activity against cancer cell lines.

The last class of compounds assayed were the protecting group derivatives, *tert*-butyldiphenylsilanol **145** and 4,4'-dimethoxytrityl alcohol **147**. These compounds were included in our assay as a control in order to determine if the possible products formed by hydrolysis within the cells were in fact the active agents. The results are summarized in **Table 20**.

Table 20 Percentage cell viability of the adherent cell lines when treated with 100 μ M of the protecting group derivatives for 24 hours

Compound	Caco-2	HT-29	WBC
TBDPS-OH	6.884 \pm	5.643 \pm	Compound
145	0.205 %	0.171 %	Not Active
DMT-OH	13.767 \pm	13.133 \pm	Compound
147	1.060 %	0.571 %	Not Active

Note: Synthetic compounds are defined as not active if the cell viability is greater than 50 % after treatment

The *tert*-butyldiphenylsilanol **145** shows a percentage cell viability of 6.884 \pm 0.205 % for Caco-2 and a viability of 5.643 \pm 0.171 % for HT-29. This result was quite surprising as the compound had previously not shown any activity towards the suspension cell lines. In a similar manner, the 4,4'-dimethoxytrityl alcohol **147** gave a cell viability of 13.767 \pm 1.060 % for Caco-2 and 13.133 \pm 0.571 % for HT-29, which was again unexpected as the compound had also not shown activity towards the suspension cell lines. These new results suggested that the small molecule derivatives could possibly be transported into the cells without the requirement for the nucleoside groups. However, this could not be substantiated as yet based

on the small sample size that we had used and as such would need to be further investigated. The synthesis of a "second generation" of compounds based on these findings are discussed in detail in **Chapter 5**.

3.2.3.3 Discussion for Subsequent Assays Performed

Cells are killed by either necrosis or apoptosis. When DNA is damaged in normal cells, it is either repaired or the cell undergoes apoptosis. In cancer cells, however, DNA repair does not often occur and the apoptotic levels are extremely low.⁷⁶ Only compounds exhibiting positive results in the MTT assay (discussed in detail in *Section 3.2.3.2* above) were subjected to a series of subsequent tests to try and determine the mechanism by which cell death is initiated.

As described in the *Materials and Methods, Section 3.2.3.1* above, an Annexin V flow cytometry kit was used to determine whether apoptosis or cell necrosis was induced. Caspase-3/CPP32 and Caspase-8 colorimetric assay kits were used to determine caspase expression. Cytochrome *c* fractions in the mitochondrial and cytoplasmic fractions were determined by the Enzyme Immunometric Assay (EIA) kit. As this work was performed by students in the Department of Pharmacy and Pharmacology at the University of the Witwatersrand and not by myself. A brief overview of a few representative results will thus be given here, as opposed to a detailed analysis (which will be given in the MSc dissertations for N. Dahan-Farkis⁷⁷ and H. Apostolellis⁷⁸).

Annexin V Assay

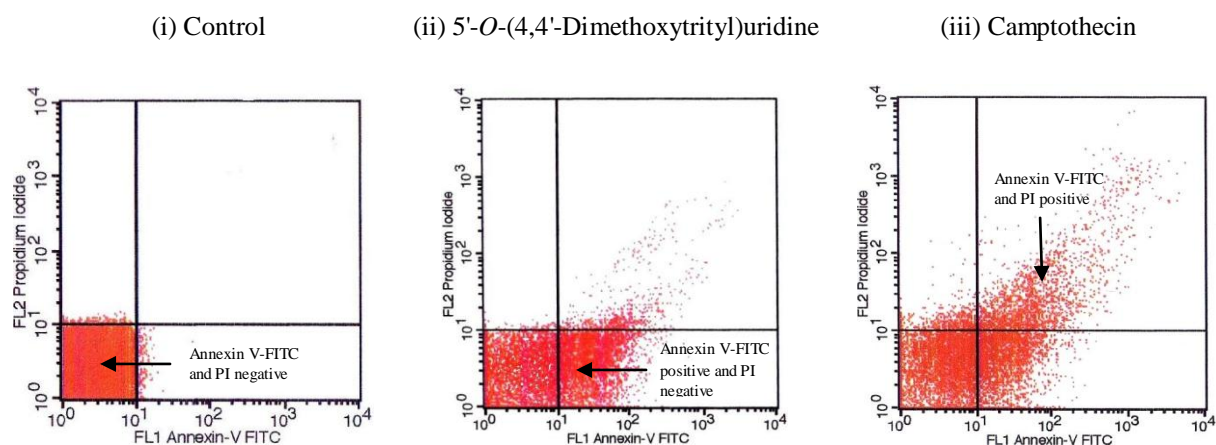
Annexin V is a useful tool for the detection of apoptotic cells as it binds preferentially to negatively charged phospholipids, such as phosphatidylserine (PS), which then leaves it exposed on the outer layer of the plasma membrane of the cell. The translocation of the PS occurs in both necrosis and apoptosis - hence, Annexin V is combined with propidium iodide (PI). In this assay, the cell staining was assessed using fluorescein isothiocyanate (FITC)

labeled Annexin V (which gave green fluorescence) as well as the dye excluded of PI (which was negative for red fluorescence). Using this approach, it was possible to detect and quantitate the apoptotic cells on a single-cell basis by flow cytometry, and they were able to identify:

- the intact cells (Annexin V-FITC = negative, PI = negative)
- early apoptotic cells (Annexin V-FITC = positive, PI = negative)
- late apoptotic or necrotic cells (Annexin V-FITC = positive, PI = positive)

The control, untreated HT-29 cells were mainly Annexin V-FITC and PI negative, indicating that they were viable and not undergoing apoptosis [as shown in **Graph 12 (ii)**]. After a 24 hour exposure to the commercial control, camptothecin **155**, there were two primary populations of cells, the first were the viable, non-apoptosing cells (Annexin V-FITC and PI negative) and the second group contained the cells undergoing apoptosis (Annexin V-FITC positive and PI negative). A small population of cells, 18.7 %, were observed as both Annexin V-FITC and PI positive, indicating that they were in end-stage apoptosis [shown in **Graph 12 (iii)**].

The example shown in **Graph 12 (ii)** is of our synthetic compound, 5'-*O*-(4,4'-dimethoxytrityl)uridine **126** incubated with HT-29 cells. After 24 hour exposure, there were two populations of cells observed: (i) viable, non-apoptosing cells (Annexin V-FITC and PI negative), and (ii) cells undergoing apoptosis (Annexin V-FITC positive and PI negative). Similar results were observed for the other active compounds and cell lines combinations used.

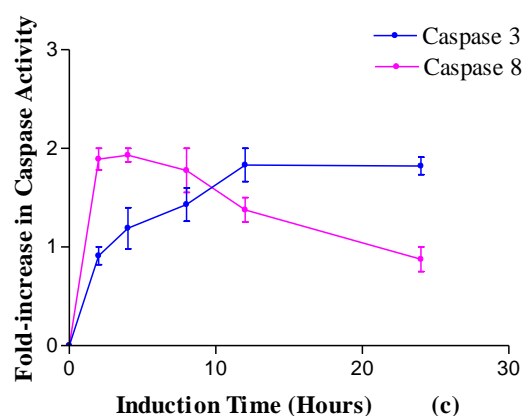
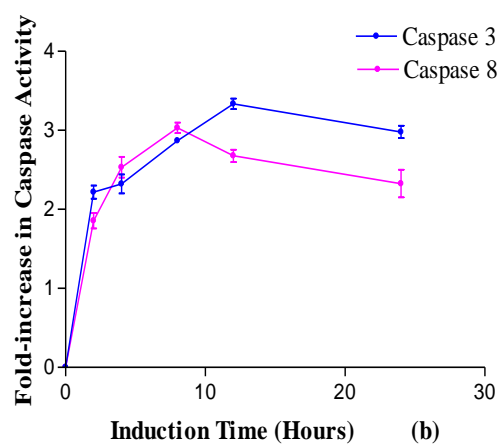
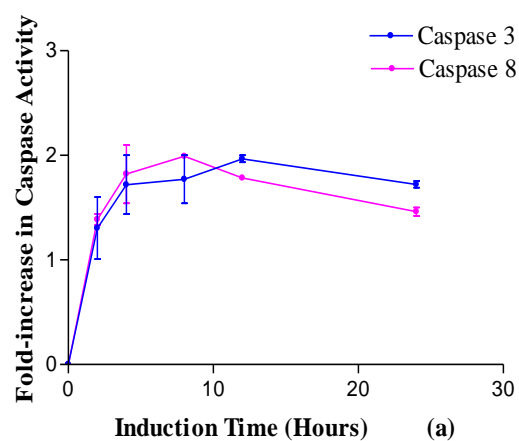


Graph 12 Annexin V-FITC staining in control and apoptotic HT-29 cells, induced by camptothecin **155** and 5'-O-(4,4'-dimethoxytrityl)uridine **126**

Ⓢ *Time Dependent Induction of Caspase-3 and Caspase-8 Activity*

A specific feature of apoptosis is protein hydrolysis, which involves the activation of caspases. First, the initiator caspase, Caspase-8, cleaves and this then activates one of the effector caspases, Caspase-3. Once activated, Caspase-3 then cleaves the polypeptides that ultimately undergo proteolysis in the apoptotic cells.

Examples of the results obtained for three of our synthetic compounds are shown in **Graph 13**, with graph (a) representing HT-29 cells treated with 5'-O-(4,4'-dimethoxytrityl)uridine **126**, graph (b) representing HT-29 cells treated with 5'-O-(*tert*-butyldiphenylsilyl)uridine **107** and graph (c) representing Caco-2 cells treated with 5'-O-(*tert*-butyldiphenylsilyl)cytidine **134**.



Graph 13 Time-dependent induction of Caspase-3 and Caspase-8 activity by: (a) HT-29 cells treated with 5'-O-(4,4'-dimethoxytrityl)uridine **126**, (b) HT-29 cells treated with 5'-O-(*tert*-

butyldiphenylsilyl)uridine **107** and (c) Caco-2 cells treated with 5'-*O*-(*tert*-butyldiphenylsilyl)cytidine **134**

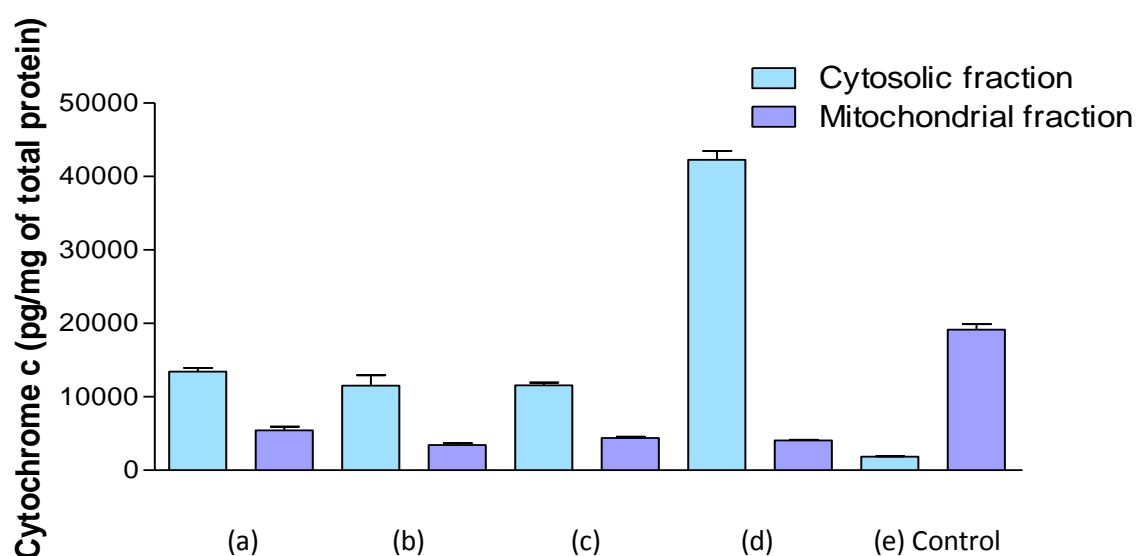
Maximal Caspase-8 expression was observed in the HT-29 and Caco-2 cells within 4-8 hours of exposure to our synthetic derivatives. After 8 hours, the activity of Caspase-8 declined in HT-29 cells treated with 5'-*O*-(4,4'-dimethoxytrityl)uridine **126** and 5'-*O*-(*tert*-butyldiphenylsilyl)uridine **107**, whereas that of Caspase-3 increased, indicating that the proteolytic phase of apoptosis was initiated. In the Caco-2 cells, Caspase-8 activity only decreased after 12 hours exposure to 5'-*O*-(*tert*-butyldiphenylsilyl)cytidine **134**.

Cytochrome c Assay

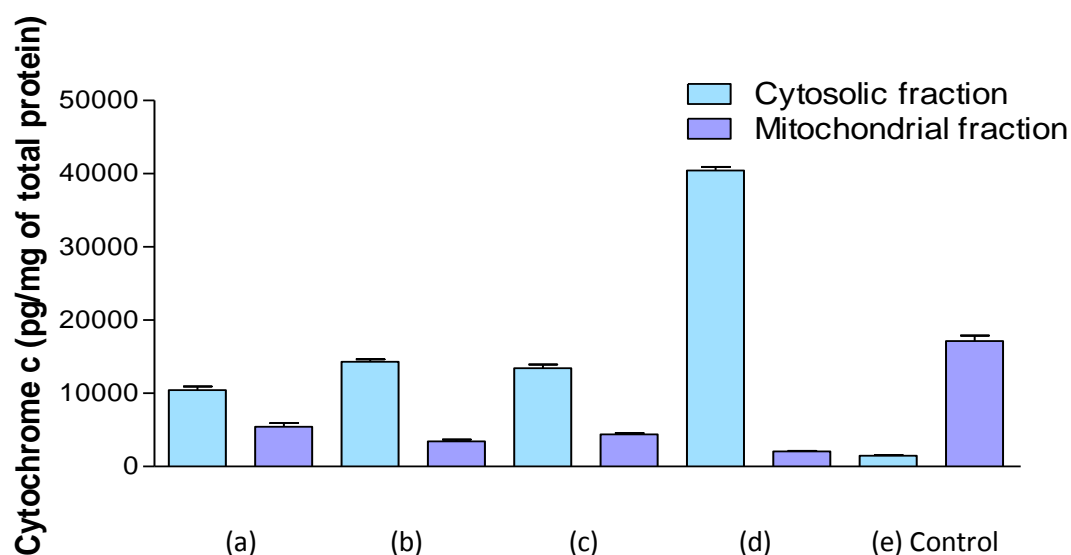
During apoptosis, cytochrome *c* has been shown to shift from the mitochondria to the cytoplasm. Cytochrome *c* measurement can therefore lead to a greater understanding of many diseases at the cellular level. For this study, the amount of cytochrome *c* in the cell lysates was quantified by a human cytochrome *c* Elisa assay.

Representative examples of the data obtained for all our synthetic compounds are shown in **Graph 14** and **Graph 15**, which show results obtained for the HT-29 and Caco-2 cells when treated with 5'-*O*-(4,4'-dimethoxytrityl)uridine **126**, 5'-*O*-(*tert*-butyldiphenylsilyl)uridine **107** and 5'-*O*-(*tert*-butyldiphenylsilyl)cytidine **134**.

Cytochrome *c* concentrations were significantly higher in the cytosolic protein fractions ($p \leq 0.05$) than in the mitochondrial protein fractions of the HT-29 cells (shown in **Graph 14**) and the Caco-2 cells (shown in **Graph 15**). The cytochrome *c* concentration in the cytosol of cells treated with camptothecin **155** was significantly higher ($p \leq 0.05$) than in the cytosol of cells treated with the other synthetic compounds.



Graph 14 Concentrations of cytochrome *c* (pg/mg) in the cytosolic and mitochondrial fractions of HT-29 cells after treatment with: (a) 5'-*O*-(4,4'-dimethoxytrityl)uridine **126**, (b) 5'-*O*-(*tert*-butyldiphenylsilyl)uridine **107**, (c) 5'-*O*-(*tert*-butyldi-phenylsilyl)cytidine **134** and (d) camptothecin **155**, for 24 hours



Graph 15 Concentrations of cytochrome *c* (pg/mg) in the cytosolic and mitochondrial fractions of Caco-2 cells after treatment with: (a) 5'-*O*-(4,4'-dimethoxytrityl)uridine **126**, (b) 5'-*O*-(*tert*-butyldiphenylsilyl)uridine **107**, (c) 5'-*O*-(*tert*-butyldi-phenylsilyl)cytidine **134** and (d) camptothecin **155**, for 24 hours

3.2.3.4 Conclusions

The following synthetic compounds:

- 5'-*O*-(*tert*-butyldiphenylsilyl)uridine **107**
- 2',3'-*O*-diacetyl-5'-*O*-(*tert*-butyldiphenylsilyl)uridine **123**
- 5'-*O*-(4,4'-dimethoxytrityl)uridine **126**
- 5'-*O*-(*tert*-butyldiphenylsilyl)cytidine **134**
- 5'-*O*-(4,4'-dimethoxytrityl)-6-*N*-(*N,N*-dimethylmethyline)guanosine **113**
- 5'-*O*-(4,4'-dimethoxytrityl)inosine **117**
- 5'-*O*-(*tert*-butyldiphenylsilyl)adenosine **142**
- *tert*-butyldiphenylsilanol **145**
- 4,4'-dimethoxytrityl alcohol **147**

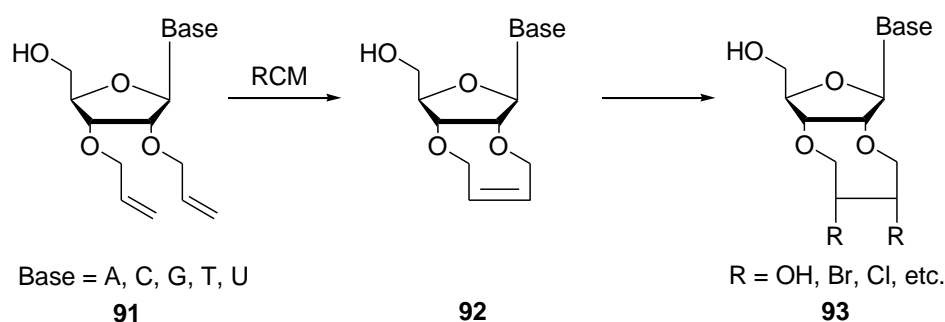
show a degree of selective cytotoxicity against the cancer cell lines tested, with minimal cytotoxicity directed against the white blood cells.

The synthetic compounds, described above, also proved to be effective in inducing apoptosis, modulating the expression of Caspase-3 and Caspase-8, as well as causing the release of cytochrome *c* from the mitochondria into the cytosol. The cytotoxic effects of these derivatives therefore suggest potential for further development in cancer therapy as promising lead compounds.

Summary:
Work Completed in Part 1

Ⓢ PART 1 SUMMARY – SYNTHESIS

As described in our aims for part 1, we thought it pertinent to investigate the possibility of forming fused bicyclic systems onto the 2' and 3' positions of the sugar ring of our nucleosides utilizing the ring closing metathesis methodology that we were already familiar with. The synthesis in **Scheme 21** below highlights the critical RCM step and shows the bicyclic ring systems that we hoped to prepare in order to do biological activity investigations.



Scheme 21 Synthesis for 2',3'-bicyclic ring system, showing key RCM step

Using our planned strategy towards fused bicyclic ring systems, we were able to synthesise the various dienes (including 2',3'-*O*-diallyl-5'-*O*-(*tert*-butyldiphenylsilyl)-1'-*O*-methoxy- β -(-)-ribose **103** and 2',3'-*O*-diallyl-5'-*O*-(4,4'-dimethoxytrityl)-6-*N*-(*N,N*-dimethylmethyl-imine)guanosine **114**), but were unable to obtain the bicyclic ring systems via our proposed ring closing metathesis route. Due to the time constraints of the project, we decided not to continue along this synthetic route and instead shifted our focus to the synthesis of a range of compounds that would be used to conduct a structure-activity study.

At the same time, we wished to investigate the structure activity relationships (SAR) involved when the various OH and NH positions on the nucleosides and β -(-)-ribose derivatives were protected sequentially with different protecting groups. The idea was that from this data we

would be able to determine on which positions in the molecules it was essential to have free OH/NH binding sites in order to maintain the activity of the compounds. Structures **94-96** outline the approach taken for the model system, α -(-)-ribose **100**, and structures **97-99** show an example of the nucleoside approach, for uridine **12** derivatives specifically.

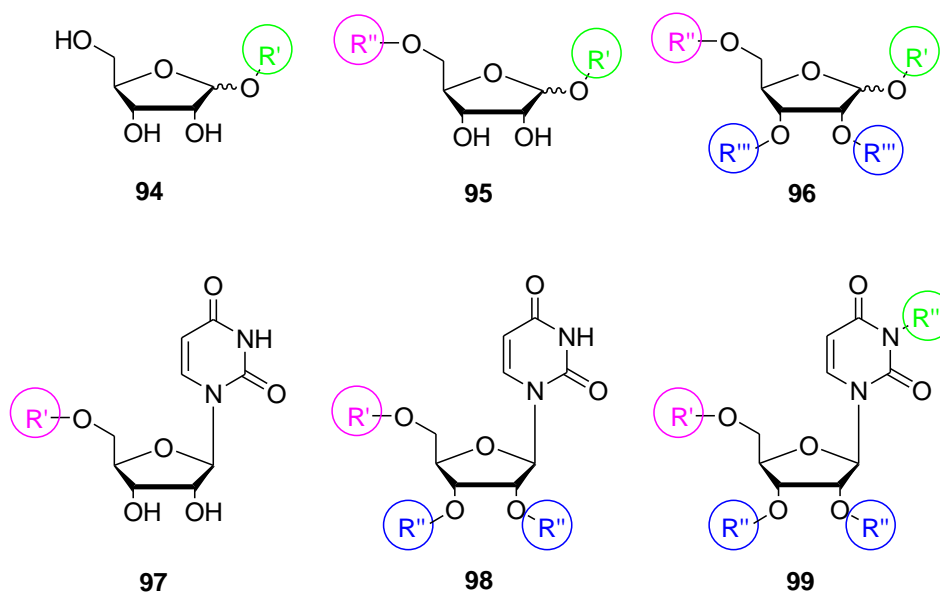


Figure 37 General overview of our intended SAR study

For these derivatives, we prepared a series of compounds that had different functional groups present on the primary hydroxyls and secondary hydroxyls on the sugar ring, as well as different groups present on the primary amines and/or amide groups of the bases. This synthesis was performed to obtain a range of sugar derivatives (α -(-)-ribose **100**) and nucleoside derivatives (adenosine **8**, cytidine **11**, guanosine **9**, inosine **116** and uridine **12**). Included in this group were the corresponding protecting group derivatives, *tert*-butyldiphenylsilyl alcohol **145** and 4,4'-dimethoxytrityl alcohol **147**.

Having the range of synthetic compounds in hand, for both the approach towards the fused bicyclic ring systems and those for the structure-activity study, we then moved on to the

biological testing. For the biological testing, we assayed our range of synthetic compounds for inhibitory activity against four bacterial strains, four cancer cell lines and HIV.

🌀 PART 1 SUMMARY – BIOLOGICAL TESTING

The nucleoside and corresponding β -(-)-ribose derivatives were evaluated for their antibacterial activity against two Gram-positive (*Staphylococcus aureus* ATCC 25923 and *Bacillus cereus* DL5) and two Gram-negative bacteria (*Pseudomonas aeruginosa* ATCC 27853 and *Escherichia coli* ATCC 25922).

The results from the TTC assay for anti-bacterial activity showed that 5'-*O*-(*tert*-butyldiphenylsilyl)uridine **107**, 5'-*O*-(*tert*-butyldiphenylsilyl)-1'-*O*-methoxy- β -(-)-ribose **102** and *tert*-butyldiphenylsilyl alcohol **145** exhibited activity towards only the Gram-positive bacteria when compared to the ciprofloxacin **153** control. From the data reported for the anti-bacterial assay, we concluded that the nucleoside showing the most promising results was uridine and as such it would be the nucleoside of choice for our subsequent anti-bacterial activity studies. Our mini structure-activity study on the uridine derivatives found that the best position for performing modifications to our nucleosides was at the 5'-OH position on the sugar ring and that a loss of either or both of the secondary alcohols (2'-OH and 3'-OH) and/or the primary amide on the base lead to a reduction in activity of the compounds. Lastly, the comparison of β -(-)-ribose derivatives to the uridine derivatives suggested that the bases on the nucleoside derivatives were necessary for molecular recognition to aid transportation within the cells.

We found that none of the range of synthetic nucleoside and protecting group derivatives assayed showed any antiviral activity towards HIV_{III}B. However, we did observe that a large number of the compounds were toxic towards the uninfected MT-4 cells (human T-cell leukemia cell line) at millimolar levels. This was quite unexpected and we believed that it suggested that our synthetic compounds may be toxic towards specifically cancerous cells.

This possibility was subsequently investigated in our cell proliferation studies, where most of the synthetic compounds were screened for their "anti-cancer" properties against two adherent (HT-29 and Caco-2) and three suspension (HL-60, Jurkat and K-562) cell lines. The results of this exhaustive study showed that 5'-*O*-(*tert*-butyldiphenylsilyl)uridine **107**, 5'-*O*-(4,4'-dimethoxytrityl)uridine **126** and 5'-*O*-(*tert*-butyldiphenylsilyl)cytidine **134** were active against both the suspension and the adherent cell lines. Whereas, *tert*-butyldiphenylsilanol **145** was active against only the adherent lines and 4,4'-dimethoxytrityl alcohol **147** was active against only the suspension cell lines.

In general, all of the active compounds show a degree of selective cytotoxicity against the cancer cell lines tested, with minimal cytotoxicity directed against the white blood cells. The synthetic compounds, described above, also proved to be effective in inducing apoptosis, modulating the expression of caspase 3 and caspase 8, as well as causing the release of cytochrome *c* from the mitochondria into the cytosol. The cytotoxic effects of these derivatives therefore suggest potential for further development in cancer therapy.

For all of the biological testing, we have found that β -(-)-ribose derivatives, in general, do not show any significant biological activity. Whereas (*tert*-butyldiphenylsilyl)-protected nucleoside derivatives and the corresponding *tert*-butyldiphenylsilyl alcohol control seem to be intrinsically bio-active. As such, we extrapolated that a second generation of synthetic compounds derived from the nucleoside uridine and containing silyl-protecting groups would be the best way to develop promising lead compounds.

We then moved on to the preparation and testing of our second generation of compounds, which follows in detail in **Part 2** of this thesis. An introduction to our ideas for our second generation of compounds is given in **Chapter 4** below, followed by the synthesis of the compounds (which is discussed in detail in **Chapter 5**). The results obtained for the subsequent anti-bacterial assay are discussed in detail in **Chapter 6**, with further studies to determine a possible mode of action for our positive hits (from both the first generation and the second generation of synthetic compounds) included, along with the analysis of the cells by confocal microscopy and SEM. The results obtained for the subsequent anti-cancer assays

on the second generation of compounds will be presented in **Chapter 7**. This is followed by an overall summary of the work performed on our second generation compounds.

PART 2 - SECOND GENERATION COMPOUNDS

***Synthesis and Biological Testing of Uridine,
5-Methyluridine and Silanol Derivatives***

Chapter 4:
Introduction

4.1 GENERAL INTRODUCTION TO SILICON AND ITS CHEMISTRY

Silicon and carbon are alike in so many ways, and yet, they are so different. This dichotomy was behind a good portion of the interest in silicon chemistry in the 20th century. Other sources of fascination with this element were the endless variety of natural silicates in minerals and clays and the remarkable properties of the synthetic silicones. In recent decades, silicon has thoroughly penetrated areas as diverse as organic synthesis and microelectronics.

Josef Michl, Editor, Chemical Reviews, 1995⁷⁹

4.1.1 Basic Silicon Chemistry

Silicon is the 14th element in the periodic table and although it does not occur naturally in free form, in its combined forms, it accounts for about 25 % of the Earth's crust.⁸⁰ So as not to confuse silicon with silicone, a brief definition of each is given below:

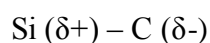
- *SILICON* – is used to refer to the elemental material
- *SILICONE* – refers to materials in which silicon is bonded to oxygen

Silicon forms stronger bonds than carbon to oxygen and the halogens, and weaker bonds to carbon and hydrogen. Much of organosilicon chemistry is driven by the formation of strong oxygen-silicon or oxygen-fluoride bonds at the expense of other weaker bonds.⁸¹ In contrast, π bonds between silicon and other elements are very weak and may be considered unimportant in the applications of silicon to organic synthesis.⁸¹

The bonds between silicon and other atoms are generally significantly longer than those between carbon and the corresponding atoms. A good example of this used in organic synthesis is found in the fact that the trimethylsilyl group is less sterically demanding than its

carbon analogue (the *tert*-butyl group). This is generally ascribed to the increased distance between the silicon atom and its point of attachment to the molecule in question.⁸¹

Silicon is considerably more electropositive than carbon; as such carbon-silicon bonds are strongly polarized.⁸¹ The direction of polarization is shown below:



4.1.2 Silicon in Protecting Group Chemistry

The use of organosilyl protecting groups has undergone great growth in the last two decades and they are now highly likely to be used in any synthesis of reasonable complexity.⁸² The first group to be used extensively was Me_3Si **156**, but recently bulkier groups such as *t*- BuMe_2Si **157**, (*t*-hexyl) Me_2Si **158** and *t*- BuPh_2Si **159** (**Figure 38**), which form more stable silylated products, have come into fairly widespread use.

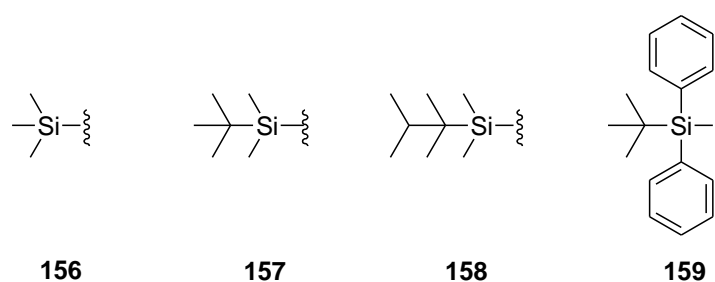


Figure 38 Various Organosilyl Protecting Groups

Deprotection of compounds containing bulky organosilyl protecting groups is usually achieved by treatment with fluoride ion (usually derived from tetra-butylammonium fluoride).

The silicon-containing product thus formed is a silanol (Si-OH) species or a silanol/silyl fluoride mixture. After isolation of the required organic material, the organosilicon by-product is usually discarded as waste, even on industrial scale.⁸² There are, however, a number of publications detailing the recovery and subsequent reconversion of these silanols to the starting chlorosilanes.⁸² This work will however not be discussed in the course of this thesis.

4.2 SILICON IN DRUG DISCOVERY

“Some of the fundamental differences between carbon and silicon can lead to marked alterations in the physiochemical and biological properties of the silicon-containing analogues...and the resulting benefits can be exploited in the drug design process.”

Graham A. Showell, Amedis Pharmaceuticals Ltd.⁸³

4.2.1 Bioisosteres – Sila-Substitution of Existing Drugs

In modern medicinal chemistry, current drug developers are often forced to look at the existing families of drugs for design inspiration. Some recent data suggests that as little as thirty-two scaffolds exist in current use and that these account for as many as half of all the compounds which have been approved as drugs by the FDA.⁸⁴ These studies have also shown that a relatively small number of functional groups account for the majority of side-chains found in drugs today.⁸⁵

This has led to the emergence of bioisosteres in drug design. This strategy is exemplified by the use of a bioisostere to improve the properties of a molecule and/or obtain new classes of compounds without prior art in the patent literature.⁸³ Well known examples of bioisosteres are shown in the **Figure 39**.

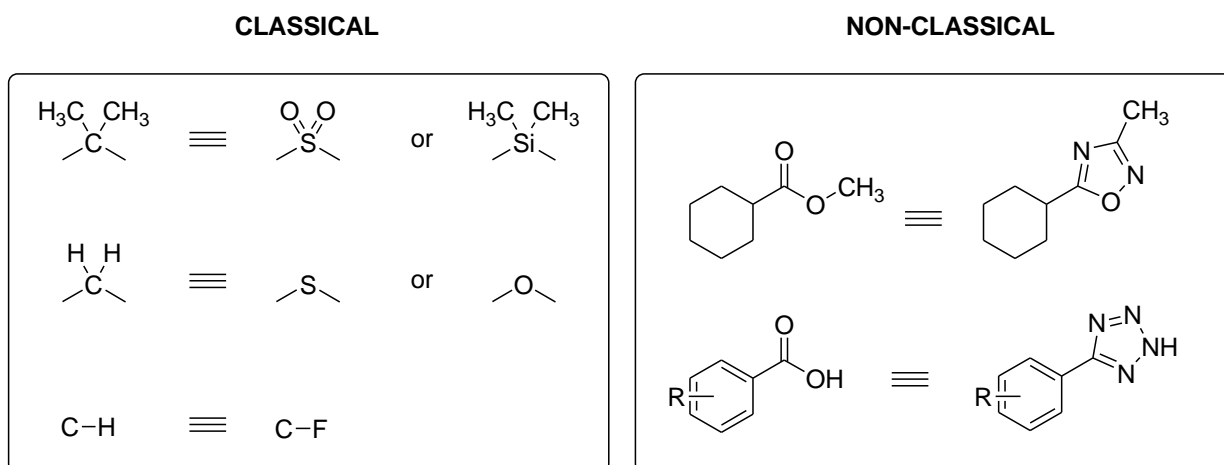


Figure 39 Examples of Classical and Non-Classical Bioisosteres⁸³

During the 1970's Reinhold Tacke pioneered the concept of a "silicon switch" or sila-substitution in which one or more carbon atoms of an existing molecule could be swapped for silicon atoms.⁸⁶ Such a "silicon switch" could be considered as a classical tetravalent bioisostere (as illustrated in **Figure 39** above).⁸³ However, the concept remained widely underutilized and it wasn't until the last decade that the properties of organosilicon agents have begun to be more fully utilized in drug discovery and development.⁸³ As an example, consider that in 2001, less than 1 % of all patent applications in the drug discovery field related to compounds containing phosphorus, silicon and the other less common elements.⁸⁷

Sila-substitution into drug-like scaffolds provides an exciting approach to search for novel drug-like candidates that have beneficial biological properties when compared with similar traditional carbon-based scaffolds, and in addition, would have a clear intellectual property position.⁸⁸

4.2.2 General Properties of Silicon and the Impact in Medicinal Chemistry

It is well known that both carbon and silicon possess four valence electrons. As such, similarities with respect to the chemistry of silicon and carbon may therefore be expected,

although it is known that in several aspects the two elements differ substantially from one another.⁸³ Some of the fundamental differences between carbon and silicon that can lead to marked alterations in the physico-chemical and biological properties of the silicon-containing analogues, which can be exploited in the drug design process, are highlighted in **Table 21**.⁸³

Table 21 The Properties and Potential Benefits of Silicon in Medicinal Chemistry⁸³

Property	Difference	Potential Benefit
Atomic Size	Altered bond lengths and bond angles	Altered <i>in vitro</i> potency Modified selectivity Altered rate of metabolism
Electronegativity	Increased H-bond strength and acidity of silanols	Improved potency in pharmacophores where H-bonding is important
Lipophilicity	Increased lipophilicity of silicon compound	Improved <i>in vivo</i> half-life Enhanced tissue distribution
Novel Chemistry	IP opportunities	Novel compounds exploiting established SAR

4.2.2.1 Atomic Size

Silicon containing bonds are always longer than the corresponding carbon analogues:

- C-C bond length is approximately 1.54 Å vs.
- C-Si bond length of approximately 1.87 Å⁸⁶

This difference leads to subtle changes in the size and shape of silicon-containing compounds when compared with carbon-containing compounds.⁸⁸ This can lead to changes in the way that the silicon analogues interact with specific proteins and/or enzymes. This can have a marked effect on the compounds pharmacological profile.^{83, 88}

4.2.2.2 Electronegativity

As carbon is more electronegative than silicon, different bond polarizations occur for carbon specific bonds relative to silicon specific bonds. An area in which this has potential benefits for the “silicon switch” approach is in hydrogen-bond strength and acidity.⁸³ In this context, the hydrogen-bond strength of the silanol is more favourable as a donor than that of the carbinol.^{88, 89} As a consequence, in molecules where the carbinol functions as a hydrogen-bond donor, the use of a silanol moiety can provide the benefit of improved potency.^{88,90}

4.2.2.3 Lipophilicity

As a general rule, silicon-containing compounds are more lipophilic than their corresponding carbon analogues. By altering the lipophilicity of a molecule, one can modify the molecules *in vivo* effects – for example, a small increase in lipophilicity can markedly increase the volume of distribution of the molecule, reflecting in increased tissue penetration.^{88,91} As a consequence, the silicon-containing molecule will be less prone to hepatic metabolism and the plasma half-life of the molecule may be improved (in situations where liver metabolism is significant in the original carbon-based compounds).⁸⁸

In addition, lipophilicity plays an important role in the ability of drug candidates to cross the blood-brain barrier.⁸⁸ It has been shown that many *in silico* models predicting blood-brain barrier permeation contain a descriptor that relates specifically to lipophilicity.⁹²

4.2.2.4 Novel Chemistry

The chemistry of single bonds heavily dominates the chemistry of silicon, as such, its use as a tetrahedral bioisostere of carbon is appropriate. The C=O double bond of a ketone is favoured over its hydrated form, whereas the formation of a Si=O double bond is disfavoured over its hydrate, the silicon diol.⁸⁸

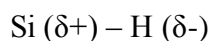
Organosilicon compounds can be synthesized where the carbon counterparts are much more difficult to obtain, or do not exist at all under normal experimental conditions. Using this approach allows for the opportunity to identify novel compounds with distinct modes of action and possibly unlicensed IP. An area where silicon has been effective in this respect is in the design of protease inhibitors.⁸⁸

4.2.2.5 Limitations to Sila-Substitutions

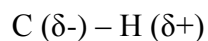
Although the incorporation of silicon represents an excellent tetrahedral isostere of carbon, it also has some important limitations. The first of which is that there are no direct sila-equivalents for the following carbon systems:



Another major limitation is that silicon cannot form physiologically stable Si-H containing compounds. The Si-H bond is not only weaker than its C-H equivalent, but also has reversed polarity as shown schematically.⁸³



vs.



As such, the Si-H bond behaves differently to the C-H bond. For example, the Si-H bond is easily cleaved by water under non-acidic conditions to yield the corresponding silanol (Si-OH), whereas the C-H bond would not be cleaved at all under the same conditions.⁸³

4.2.3 Examples of Drug-Like Compounds with Sila-Substitutions

To date, none of the examples of silicon-containing drugs under clinical review are direct sila-substitutions of known marketed drugs. However, a significant body of work has been performed in this area over the last few years. The summary below will focus on only the true silicon switches of known marketed drugs and serves as a brief introduction to the area at large. A more in-depth review of the synthetic and medicinal chemistry associated with the direct silicon switches of known drugs has been given by Pooni and Showell.⁹³

4.2.3.1 Sila-Budipine

Budipine **160** is a monoamine uptake inhibitor that has been launched for the treatment of Parkinson's disease. In the late 1980's Stasch⁹⁴ reported on the substitution of the carbon atom within the core of the 4,4-diphenyl of budipine with a silicon atom, **161**.⁹³ This substitution is shown in **Figure 40**.

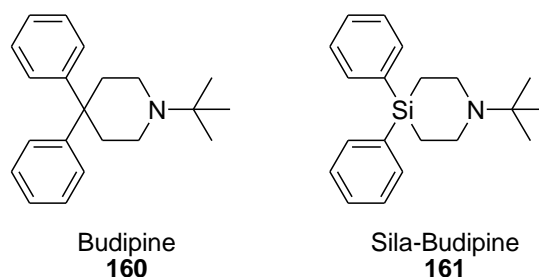


Figure 40 Structures of Budipine **160** and Sila-Budipine **161**

This sila-analogue showed an increase in lipophilicity, which is important in centrally acting drugs (such as those for the treatment of Parkinson's disease) as they can improve the molecules penetration of the blood-brain barrier.⁹³

4.2.3.2 Sila-Haloperidol

When considering the neuropsychiatric disorder schizophrenia, it is widely accepted that changes in neurotransmitter systems (such as the excessive stimulation of dopamine D₂ receptors) are involved, even though the exact pathogenesis is still unclear. Dopamine over-activity is associated with the psychotic symptoms of schizophrenia such as delusions, hallucinations and thought disorders. The antipsychotic agent haloperidol **162** acts by blocking the dopamine D₂ receptor as well as other serotonin receptors.⁹³

In 2004 Tacke and co-worker⁹⁵ reported the synthesis of sila-haloperidol **163**. After testing the binding affinities of the carbon and silicon-derivatives of haloperidol against various recombinant dopamine receptors, they were able to show that sila-substitution of haloperidol had modulated the receptor selectivity profile,⁹³ which suggested that the haloperidol **162** and sila-haloperidol **163** would differ substantially *in vivo*.

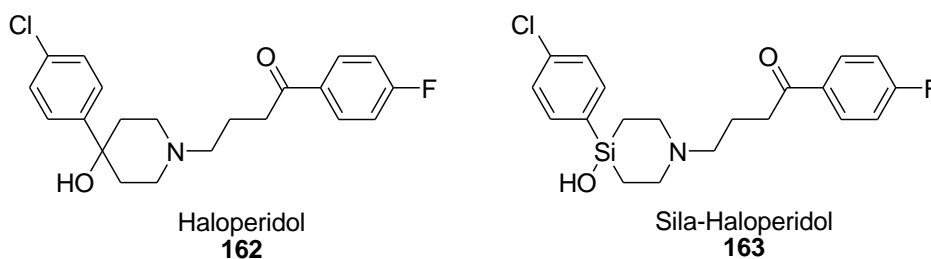


Figure 41 Structures of Haloperidol **162** and Sila-Haloperidol **163**

4.2.3.3 Sila-Bexarotene

Bexarotene **164** is a retinoid X receptor (RXR)-selective retinoid agonist that is marketed under the name TargretinTM. It is currently used in the treatment of cutaneous T-cell lymphoma and is undergoing Phase III clinical trials for the treatment of non-small cell lung cancer.⁹³

Retinoids are analogues of retinoic acid, an active metabolite of vitamin A. The retinoids bind to and thus activate retinoid X receptors – causing them to act as transcription factors that regulate the expression of genes, which control cell differentiation and proliferation.⁹³ Various synthetic retinoids have been prepared and then tested for clinical use – Bexarotene **164** is one such example.⁹⁶

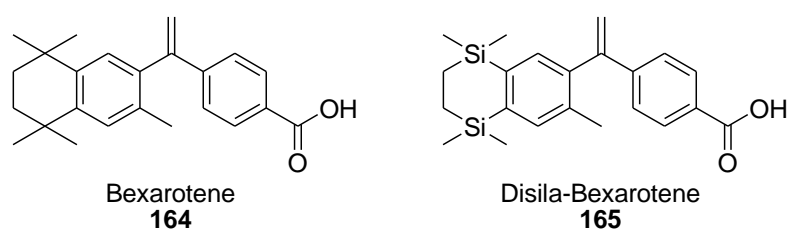


Figure 42 Structures of Bexarotene **164** and Disila-Bexarotene **165**

Daiss and co-workers⁹⁷ outlined the synthesis and agonist activity screen of a disila-substituted derivative of bexarotene **165**, wherein two of the carbon atoms had been substituted with silicon atoms. During the screening for agonist activity using a hRXR β cell-based luciferase assay, they found that disila-bexarotene **165** had a comparable response to bexarotene **164**.⁹³ As the disila-substitution of the tetrahydronaphthalene core of bexarotene gave an equally potent compound in the *in vitro* assays, this clearly shows that silicon can effectively be used as a bioisostere for carbon.⁹³

4.3 INTRODUCTION TO SILICON IN BIOLOGICAL SYSTEMS

Traditionally the use of silicon in drug discovery has been somewhat limited by the perceived toxicity of silicon itself, despite the wealth of chemical diversity and biological functionality that silicon affords to the synthetic chemist.

Concerns over the toxicity of silicon have arisen due to the fact that silicon was historically regarded as having “metallic” characteristics. When viewing the trends of the group IV elements of the periodic table, carbon is considered as strictly non-metallic, silicon as essentially non-metallic, germanium as a metalloid and both tin and lead as metallic.⁸³ As the electropositive elements are ordered, silicon is currently classified as one of the least metallic.⁸⁸

In a literature review from 1971, Garson and Kirtchner stated that: “*evidence is now available to establish that organosilicon compounds per se, are not toxic*”.^{83,98} The current toxicological data⁸³ now suggests that LD₅₀ results are generally showing similar toxicities for the silicon-containing compounds when compared to their direct carbon-containing counterparts and the review further concludes that silicon itself conveys no systematic toxic liability on chemically stable molecules.

Despite this indication to the contrary, to date no silicon-containing drugs have been licensed for use in humans by the regulatory authorities in either the United States or the European Union. However, one example of a license exists in the former Eastern Europe – for a compound silabolin **166** (**Figure 43**) which is currently used for the treatment of muscle wasting diseases.

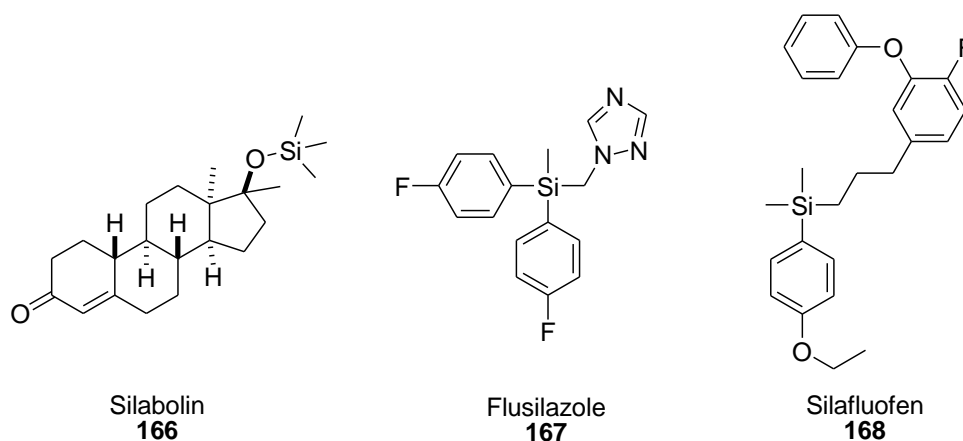


Figure 43 Silbolin **166** and the Agrochemicals Flusilazole **167** and Silafluofen **168**

In addition to silbolin **166**, six other organosilicon compounds have been used in human clinical trials (compounds **169-174** in **Figure 44**).^{83, 88} Another two, flusilazole **167** and silafluofen **168** (**Figure 43**) are marketed as agrochemicals and as such have been fully considered in terms of their potential effects on human exposure.⁸⁸ Evaluation of the available clinical and toxicological data on the compounds shown below supports the hypothesis discussed above that silicon is not inherently toxic.⁸⁸

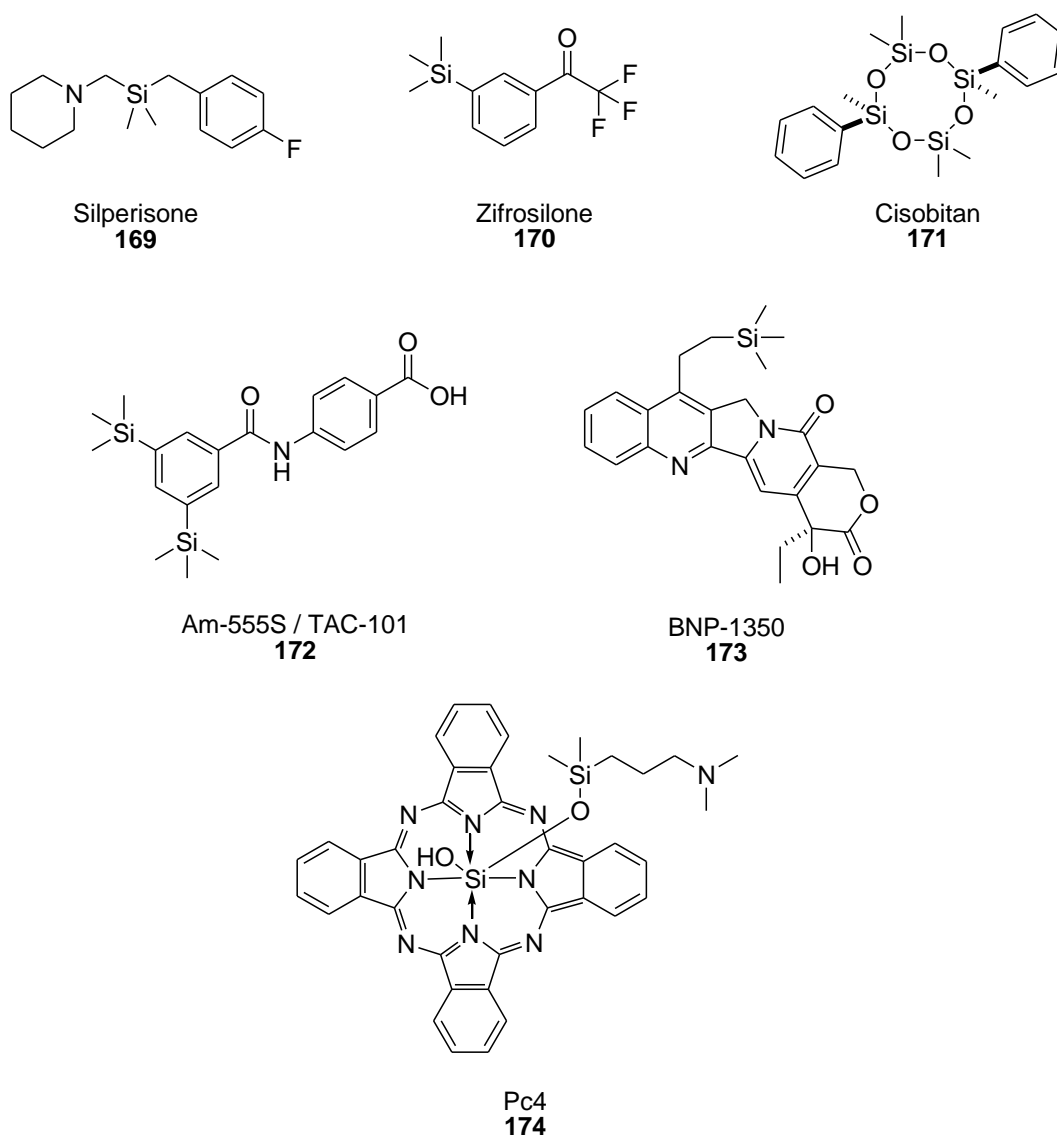


Figure 44 Silicon based compounds tested for human toxicity

Silperisone **169** is a neuromuscular antagonist for the treatment of muscle spasms.⁹⁹ Zifrosilone **170** is a neostigmine analogue which functions as an acetylcholinesterase inhibitor for the treatment of Alzheimer's disease.¹⁰⁰ Some of the phenyl-containing polysiloxanes have been shown to have oestrogenic activity – with cisobitan **171** the most potent.⁸⁸ Cisobitan **171** has hormonal agonist activity equivalent to that of oestradiol, but shows a lower acute toxicity. The compound has been patented as an anti-infertility agent and has also been examined for the treatment of human prostate cancer.¹⁰¹⁻¹⁰³

Compound Pc4 **174** is a silicon-containing phthalocyanine which is currently undergoing Phase I clinical trials for the laser photodynamic therapy of cancer.¹⁰⁴ Compound Am-555S / TAC-101 **175** is an orally active retinoic acid receptor [(RAR)- α/β] agonist, which underwent Phase II clinical trials for the treatment of liver cancer in 2004. It had previously undergone Phase I clinical trials for the treatment of lung cancer in 1999-2000.¹⁰⁵

One of the most clinically advanced drugs is a karenitacin compound BNP-1350 **173**, a fourth-generation compound derived from a novel class of camptothecin **155** analogues. BNP-1350 **173** has successfully completed a number of Phase I clinical trials and was currently in Phase II clinical trials for the treatment of recurrent malignant brain tumours and non-small cell lung cancer.¹⁰⁶

4.4 BIOLOGICAL APPLICATIONS OF SILICON CONTAINING COMPOUNDS

The section below highlights a selection of a few compounds in the recent synthetic literature that have shown either anti-bacterial activity or some activity against cancer cell lines, however, it should be noted that these types of compounds have also found to be of relevance to other medicinal areas such as the treatment of HIV.^{106b}

4.4.1 Synthetic Silicon-Containing Compounds Showing Anti-Bacterial Activity

4.4.1.1 The Silanols

Kim, Baney and co-workers published articles in 2006¹⁰⁷ and 2007,¹⁰⁸ as well as a patent in 2008,¹⁰⁹ outlining the possible use of trialkylsilanols as a novel class of antimicrobial agents. They reported the discovery of a new and unexpected class of powerful biocides based upon compounds derived through simple chemistry from silicon intermediates, the “silicon alcohols” or silanols.¹⁰⁷

Antimicrobial screens with the silanols, *tert*-butanol and siloxanes were conducted against a Gram-negative bacterium, *Escherichia coli*, and a Gram-positive bacterium, *Staphylococcus aureus*.¹⁰⁷ They found that the number of viable bacteria reduced was more than eight orders of magnitude greater than the corresponding alcohols, when the silanol treatments were used. Triethylsilanol **175** in particular, exhibited a strong antimicrobial effect at a very low concentration within ten minutes of application. Examples of the compounds tested are given in **Figure 45**.

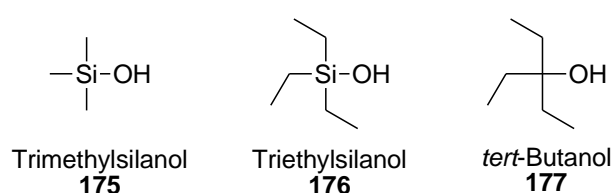


Figure 45 Compounds screened as antimicrobial agents by Kim, Baney and co-workers¹⁰⁷

These novel biocide silanols can be prepared from low cost intermediates derived from the commercial processes associated with the silicone industry. Silanols are also considered environmentally benign because of their transitory nature and ultimate conversion to CO₂, SiO₂ and H₂O.¹⁰⁷

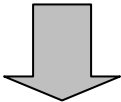
4.4.1.2 The β -Ethanolamine Derivatives

In 2006, Zablotskaya and co-workers¹¹⁰ published an article in which they investigated the structure activity relationships that existed between a wide variety of trialkylsilyl substituents at the oxygen atom of different β -ethanolamine derivatives (compounds given in **Figure 46**). The compounds were tested for antimicrobial activity using the well diffusion method, in Mueller Hinton Agar 2, at concentrations of 0.5 mg / 0.1 mL and 1 mg / 0.1 mL of the synthetic compounds. Activity was then determined by measuring the diameter (in

millimeters) of zones showing complete inhibition, to give the zone of growth inhibition for each sample. The compounds were tested for antimicrobial activity against:

- *Staphylococcus aureus* ATCC 25923 (Gram positive bacterium)
- *Bacillus cereus* ATCC 117788 (Gram positive bacterium)
- *Proteus mirabilis* NCIM2241 (Gram negative bacterium)
- *Escherichia coli* ATCC 25922 (Gram negative bacterium)
- *Candida tropicalis* ATCC 4563 (fungal strain)
- *Candida albicans* ATCC 2091 (fungal strain)

From this study, it was evident that the overall potency of the unsilylated compounds was enhanced on the introduction of the silyl group. All of the organosilicon containing β -ethanolamine methiodides were found to have some activity against at least one of the bacterial and fungal strains used. In general, the fungal and Gram-negative strains were more resistant to the synthesized compounds when compared to the Gram-positive ones.

$$[R^1R^2R^3Si OCH_2CH_2NMe_3]^+ I^-$$


COMPOUND	R ¹	R ²	R ³
178	CH ₃	CH ₃	C ₃ H ₇
179	CH ₃	CH ₃	C ₇ H ₁₅
180	CH ₃	CH ₃	C ₈ H ₁₇
181	CH ₃	CH ₃	C ₁₀ H ₂₁
182	CH ₃	CH ₃	C ₁₁ H ₂₃
183	CH ₃	CH ₃	C ₁₆ H ₃₃
184	C ₂ H ₅	C ₂ H ₅	C ₂ H ₅
185	C ₂ H ₅	C ₄ H ₉	C ₄ H ₉
186	CH ₃	C ₇ H ₁₅	C ₇ H ₁₅
187	CH ₃	C ₁₀ H ₂₁	C ₁₀ H ₂₁

Figure 46 The β -triorganyl(*N,N*-dimethylaminoethoxy)silane methiodides **178-187** screened for anti-bacterial activity by Zablotskaya and co-workers¹¹⁰

Zablotskaya and co-workers¹¹⁰ suggested that the enhancement of activity could be rationalized on the basis that their structures possessed an Si-O bond, which then increased the lipophilicity of the parent alkanolamine. This change would favour the permeation of their modified compounds far more efficiently through the lipid layer of the test microorganism, thereby destroying them more aggressively.

4.4.2 Synthetic Silicon Containing Compounds with Activity against Cancer Lines

4.4.2.1 The (2*R*,3*S*)-Disubstituted Tetrahydropyranes

In 2005 Padrón and co-workers¹¹¹ published an interesting article in which they showed that the *tert*-butyldimethylsilyl group could act as an enhancer to drug cytotoxicity against human tumour cells.

The group constructed a series of enantiomerically pure (2*R*,3*S*)-disubstituted tetrahydropyranes with diverse functionalities using known methodologies, selected examples are given in **Figure 47** (compounds **188-199**). In addition to the *tert*-butyldimethylsilyl group, other common protecting groups for the hydroxyl functionality, such as allyl, acetate and benzoate, were also used to obtain appropriate derivatives (not pictured here).

The pure compounds were then evaluated *in vitro* against HL60 human leukemia cells and MCF7 human breast cancer cells. The synthetic derivatives bearing the *tert*-butyldimethylsilyl group at position 3 of the ring considerably induced cytotoxicity in the cancer cells.¹¹¹ On the basis of the growth inhibition parameters, a structure-activity relationship was obtained. Overall the results show that the *tert*-butyldimethylsilyl group may not only be seen as a protecting group for organic synthesis, but as a plausible strategy to introduce lipophilicity in drugs, which is anticipated to aid in their cellular uptake and may thus act to modulate their cytotoxic activity.

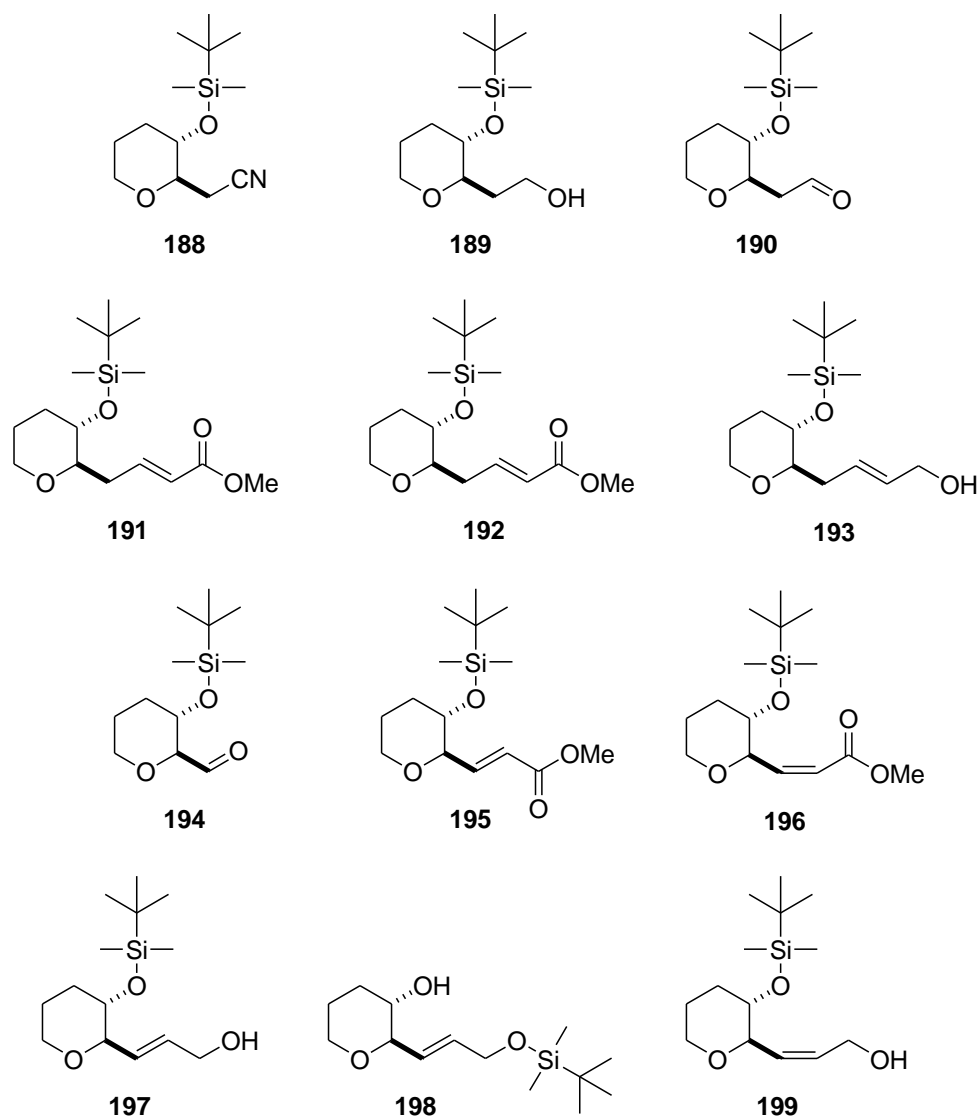


Figure 47 Compounds screened for cytotoxicity against human tumour cells by Padrón and co-workers¹¹¹

The group did further studies into the enhancement of drug cytotoxicity by silicon-containing groups, by further screening the above compounds and some more advanced derivatives against T-47D, HeLa, SW1573, WiDr and A2780 cells *in vitro*, thus obtaining representative results for a wide range of solid tumour cell lines. The results obtained were published in 2006¹¹² and supported the conclusions drawn in the paper discussed above.

4.4.2.2 The Silatecans

(2*S*)-Camptothecin (**20S**)-**155** is the parent of a family of anti-tumour agents that are currently on the front lines of cancer chemotherapy. Topotecan **200** has been approved for use in the USA and the prodrug irinotecan **201** has been approved for use in the USA, France and Japan.¹¹³ A number of other related agents have shown some promising results and are currently in various stages of clinical trials.¹¹³

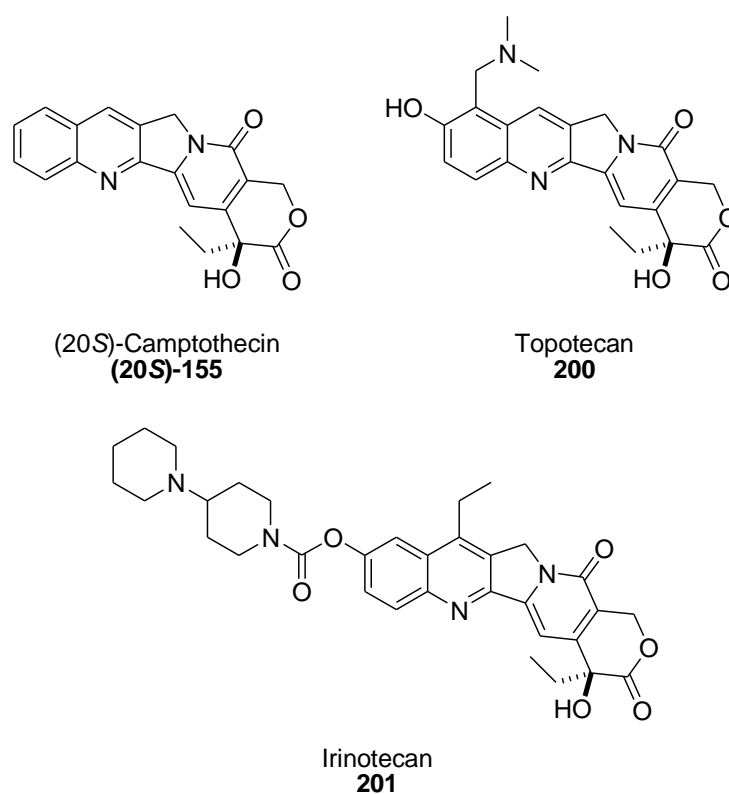


Figure 48 The camptothecin family of anti-tumour agents

Related variants of a cascade radical annulation route, developed by the Curran group¹¹³, were used to prepare a range of new substituted (2*S*)-7-silylcamptothecins (silatecans). A series of unsubstituted 7-silylcamptothecins were also prepared using the standard Friedlander methodology.¹¹³ A selection of these derivatives are outlined in **Figure 49**.

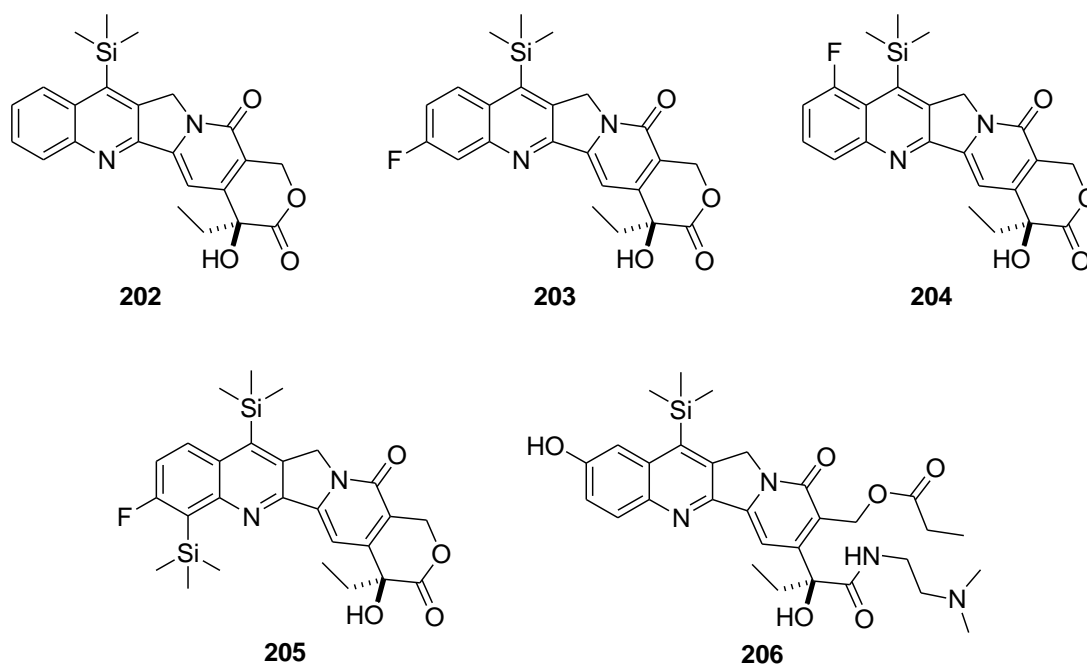


Figure 49 Selected examples of the 7-silylcamptothecins (silatecans)

The camptothecin derivatives were evaluated for their inhibition effects on the growth of HL60 (human promyelocytic leukemia), 833K (human teratocarcinoma) and DC-3F (hamster lung) cells *in vitro*.¹¹³ The authors found that all of the new compound were as potent, or more potent than camptothecin **155**. This is important because even by today's standards, camptothecin **155** is still regarded as a challenging benchmark, whose activity is not easy to surpass. The results also showed that the 7-trimethylsilyl-10-camptothecin derivative **206** is highly active.¹¹³

Compound **202** showed superior *in vivo* chemotherapeutic effects, when compared to camptothecin **155**, in tumour bearing mice. This superior activity was recorded in terms of tumour volume reduction against sarcoma-180 in B₆D₂F₁ mice at several equivalent doses.¹¹³ For Lewis lung carcinoma, compound **203** showed a comparable anti-tumour effect to camptothecin **155**, at a four-fold lower dose. This shows that there is clear promise that the *in vitro* results will be indicative of *in vivo* activity for this class of compounds.

4.4.2.3 The Indomethacin Derivatives

Indomethacin **207** is a non-steroidal anti-inflammatory drug (NSAID) which is indicated for use in rheumatoid arthritis, ankylosing spondylitis and osteoarthritis.¹¹⁴ Indomethacin **207** has also demonstrated activity in the treatment and prevention of human cancer;¹¹⁵⁻¹¹⁸ however, the adverse side-effects have limited its use in cancer patients. In a study by West and co-workers,¹¹⁴ the synthesis and biological testing of a series of sila-substituted derivatives **208-210** of indomethacin **207** was reported, which the researchers had prepared in an effort to improve the safety and biological activity of indomethacin. It was shown how an organosilicon fragment was introduced into indomethacin **207** by converting the carboxylic acid group into a sila-amide (**Figure 50**).

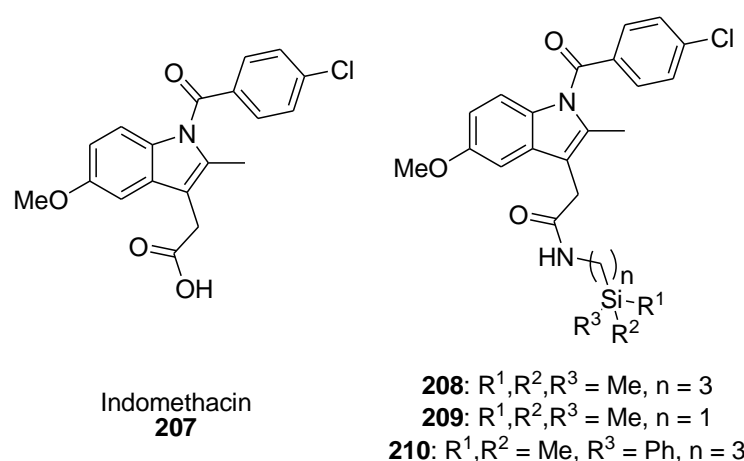


Figure 50 Structure of indomethacin **207** and the silicon-containing amide derivatives of indomethacin **208-210**¹¹⁴

The cell growth inhibitory activity for the sila-indomethacin derivatives **208-210** was determined against the human MiaPaCa-2 pancreatic cell line. The sila-derivatives demonstrated significant inhibition of cancer cell growth: indomethacin **207** itself had a IC₅₀ value of 170 μM when tested against the human MiaPaCa-2 cells, whereas West and co-workers¹¹⁴ demonstrated IC₅₀ values of 4.78 μM (**210**) to 20.0 μM (**209**) for their sila-

indomethacin derivatives. Using *in vitro* pharmacology (enzyme assays) they were also able to demonstrate that the sila-indomethacin derivatives **208** and **210** were selective COX-2 inhibitors that were superior to indomethacin **207**.

4.4.2.4 The Nucleoside Derivatives

In a paper investigating the kinetics and biological implications of the silylation-desilylation of the triorganosilyl derivatives of some biologically active heterocyclic bases (5-fluorouracil, barbituric acid and xanthine derivatives) and uridine, Lukevits and co-workers¹¹⁹ showed that in contrast to uridine, 5'-*O*-*tert*-butyldimethylsilyluridine **229** (**Figure 51**) exhibited some anti-tumour activity.

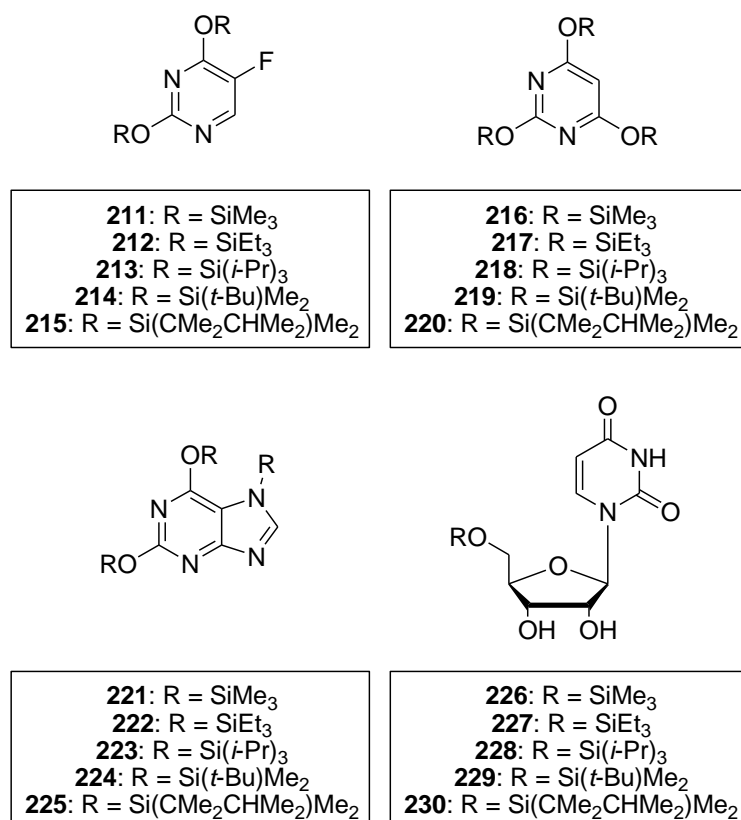


Figure 51 Trialkylsilyl derivatives of some heterocyclic bases and uridine¹¹⁹

The *tert*-butyldimethylsilyl groups appear able to temporarily block the hydrophilic functions of the molecules and do not undergo instant hydrolysis, and were chosen by the group as the *tert*-butyldimethylsilyl chloride is commercially available. The results for the biological trials were compared to data obtained for the unsilylated precursors. Lukevits and co-workers¹¹⁹ were able to show that 5'-*O-tert*-butyldimethylsilyluridine **229** suppressed the development of HT-1080 (fibrosarcoma in human lungs – 96 % inhibition at 100 µg/mL) and NiH 3T3 cells (fibroblasts in mice – 95 % inhibition at 100 µg/mL) in culture. Under the same conditions, uridine **12** showed a complete absence of any activity.

A more recent example of a nucleoside derivative exhibiting anti-cancer activity was reported by Fenlon and co-workers.¹²⁰ The paper describes the syntheses and anti-cancer screening results for 3'-*O*-silatranylthymidines (shown in **Figure 52**).

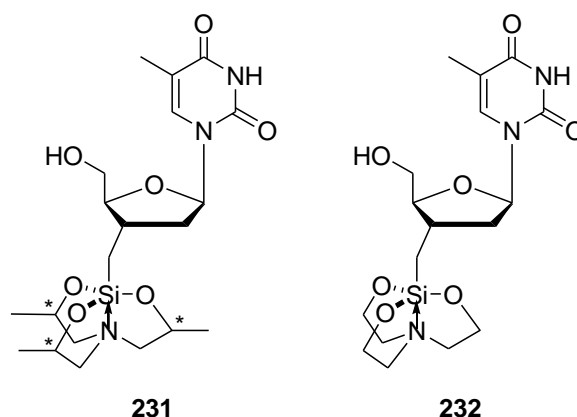


Figure 52 Examples of 3'-*O*-silatranylthymidines prepared by Fenlon and co-workers¹²⁰

The diastereomeric mixture of 3'-*O*-(trimethylsilatranyl)thymidine **231** was assayed against human breast (MDA-MB-435) and central nervous system (SNB-19 and U251) cancer cell lines at a fixed concentration (1.0×10^{-4} M) of compounds for a 48 hour period. They found that the growth percentages from cells treated with compound **231** were: (i) breast 54 % and (ii) central nervous system 83 %, when compared to untreated control cells (growth = 100 %). In the case of silatranylthymidine **232**, no activity was observed in the central nervous system

and lung cells, with 81 % growth seen in the breast cell line (which correlates to 19 % inhibition of growth).

Since **231** is a mixture of four diastereomers, it would be expected that each of the individual diastereomers would have different activity, given that it is widely accepted that stereochemistry influences pharmacological activity according to the preliminary publication.¹²⁰ Work on the synthesis and screening of each of the individual diastereomers is ongoing in the group.

4.5 AIMS FOR PART 2

4.5.1 Synthesis of Nucleoside Derivatives

The results of the biological testing of our "first generation" of compounds described in detail in **Part 1, Chapter 3**, highlighted the concept that molecules containing the silicon protecting group (*tert*-butyldiphenylsilyl, found in 5'-*O*-(*tert*-butyldiphenylsilyl)uridine **107** and 5'-*O*-(*tert*-butyldiphenylsilyl)-1'-*O*-methoxy- β -ribose **102**), were specifically active against the Gram-positive bacterial strains, *Staphylococcus aureus* ATCC 25923 and *Bacillus cereus* DL5. These findings were supported by our literature review (described in detail in **Section 4.4.1**), which highlighted the importance of silicon-containing groups in biologically active molecules.

In our cell proliferation studies, described in **Part 1**, we found that 5'-*O*-(*tert*-butyldiphenylsilyl)uridine **107** and 5'-*O*-(*tert*-butyldiphenylsilyl)cytidine **134** were active against both the suspension (HL-60, Jurkat and K-562) and adherent (HT-29 and Caco-2) cell lines assayed. The interest in the use of silicon-protecting groups to enhance the anti-cancer properties of synthetic compounds was further supported by our literature review findings (discussed in detail in **Section 4.4.2**).

Based on these findings, the decision was taken to synthesise a "second generation" of compounds that contained various other silicon protecting groups, to determine if these results suggested a general trend of activity or if they were specific to the *tert*-butyldiphenylsilyl group.

From the data reported for the anti-bacterial and the cell proliferation studies as well as literature precedent,¹²⁰ we concluded that the nucleoside showing the most promising results was uridine **12** and as such it would be the nucleoside of choice for the "second generation compounds" to be synthesised. Our mini structure-activity study on the uridine derivatives found that the best position for performing modifications to the nucleoside was at the 5'-OH position on the sugar ring and as such this would become the initial focus for the synthesis of the "second generation compounds".

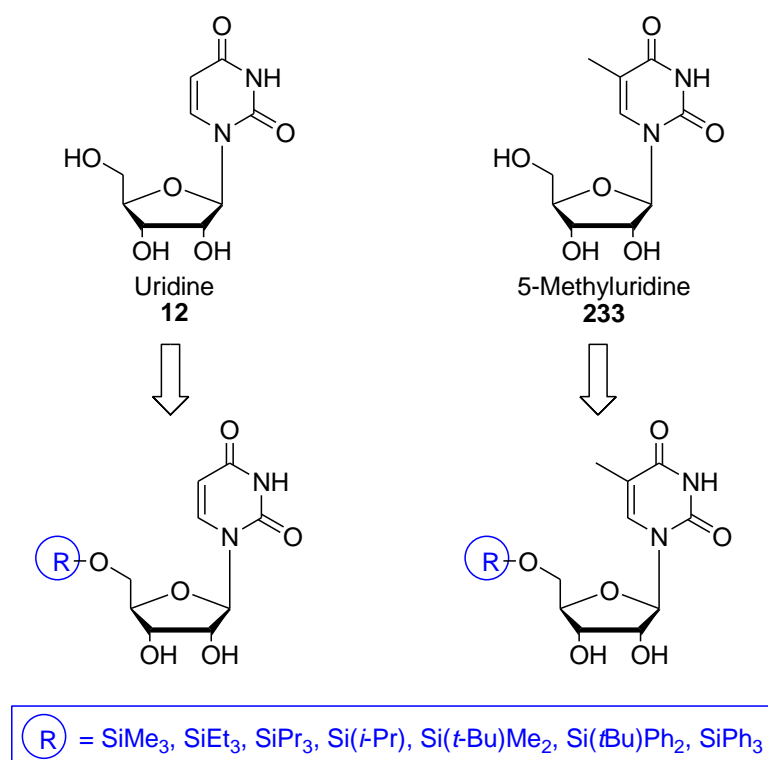


Figure 53 Proposed second generation silicon-protected uridine **12** and 5-methyluridine **233** derivatives

The proposed “second generation compounds” included a series of uridine **12** and 5-methyluridine **233** derivatives which were protected on the primary alcohol with a range of different sized silicon-containing protecting groups. We hoped that this would allow us to find the optimally sized silicon-containing protecting group that would impart good biological activity. An overview of the proposed synthetic derivatives is given in **Figure 53**.

4.5.2 Synthesis of Silanols

In **Part 1**, we were intrigued when we observed that *tert*-butyldiphenylsilyl alcohol **145** exhibited similar anti-bacterial activity against the Gram-negative strains. During our literature review, we found only one other example of this trend – where it was reported by Kim and co-workers¹⁰⁷⁻¹⁰⁹ that trimethylsilanol **175** and triethylsilanol **176** also exhibited an inhibitory effect against one each of the Gram-negative and Gram-positive bacteria.

In our cell proliferation studies, described in **Part 1**, we found that *tert*-butyldiphenylsilyl alcohol **145** exhibited activity against only the adherent (HT-29 and Caco-2) cell lines assayed. To the best of our knowledge, this is the first reported example of a silanol showing any anti-cancer activity. As a class, we believed that the silanols would warrant further investigation.

As such, we decided to include a range of silanols of varying molecular sizes for evaluation of biological activity. We envisaged that we would include a range of all of the different “molecular sizes” and also included all of the silicon-containing protecting groups we proposed to work with when preparing the nucleoside derivatives as control substances. An overview of the proposed silanols to be tested is given in **Figure 54**.

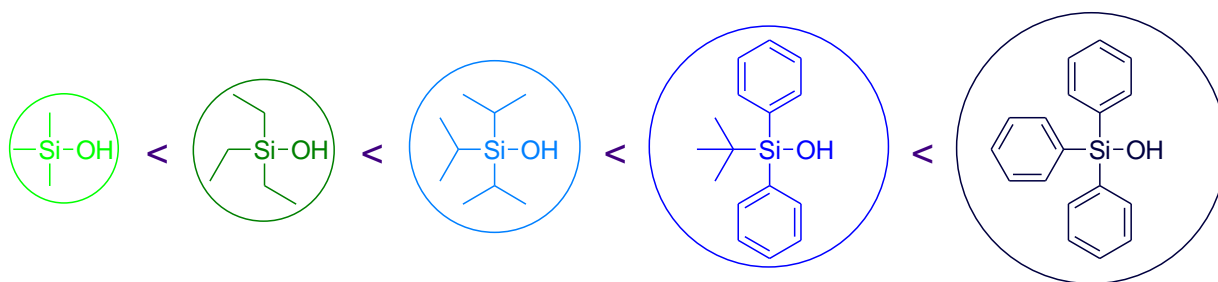


Figure 54 Proposed silanols to be included in the second generation of compounds

4.5.3 Biological Testing

We then envisaged that we would assay all of our second generation silicon-protected uridine **12** and 5-methyluridine **233** derivatives, and the corresponding silanols, for anti-bacterial activity against the same two Gram-negative bacterial strains (*Pseudomonas aeruginosa* ATCC 27853 and *Escherichia coli* ATCC 25922) and the same two Gram-positive bacterial strains (*Staphylococcus aureus* ATCC 25923 and *Bacillus cereus* DL5) that were used in **Part 1**.

As an extension to the biological testing, we planned to screen our second generation of compounds against a wider range of cancer cell lines than initially used in **Part 1** in order to more accurately determine their selective ability for the inhibition of cancerous cell proliferation.

4.5.4 Summary of Aims

To summarise, the general synthetic aims for our "second generation compounds" were subdivided into three parts:

- (i) to synthesise a range of silicon-protected uridine derivatives
- (ii) to synthesise a range of silicon-protected derivatives of 5-methyluridine and

- (iii) to synthesise the range of corresponding silanols.

This was to be followed by the biological testing of our “second generation compounds” which would be broken down into two parts:

- (i) to screen our compounds for anti-bacterial activity against two Gram-positive and two Gram-negative bacteria
- (ii) to perform cell proliferation studies against a broader range of cancer cell lines than initially used.

Chapter 5:
Results and Discussion for Synthesis

CONTRIBUTIONS TO THIS CHAPTER

All of the syntheses and compound characterization described in this chapter were performed by Ms J.-L. Panayides, while under the supervision of Prof W.A.L. van Otterlo. The work was undertaken in the School of Chemistry which forms part of the Molecular Sciences Institute at the University of the Witwatersrand.

5.1 CHAPTER OVERVIEW

This chapter outlines the synthesis of a range of uridine and 5-methyluridine derivatives. These were prepared through the addition of various silicon-containing protecting groups at either the 5'-*O*-position or tethered to both the 3'-*O*- and 5'-*O*-positions on the sugar ring, followed by subsequent modifications at either the amide position on the base (3-NH) or at the secondary alcohol on the sugar ring (2'-OH). At the same time all of the silyl-chlorides used as the silicon-containing protecting groups were converted into the corresponding silanols to be used as controls for our subsequent biological assays. In total, a range of 15 unique nucleoside derivatives and 13 silanols were prepared as a second generation of compounds for testing as possible anti-bacterial and/or anti-cancer agents.

5.2 RESULTS AND DISCUSSION

As discussed in the introduction (**Chapter 4**, *Section 4.5.4*) the general synthetic aims were sub-divided into three parts: (i) the synthesis of uridine derivatives, (ii) the synthesis of derivatives of 5-methyluridine and (iii) the synthesis of the corresponding silanols.

Full experimental details for this section, including the reaction setups used and full analysis of all NMR, infrared and mass spectral data, as well as optical rotations, melting points and R_f values are given in **Appendix D** (*Experimental Procedures – Relating to Chapter 5*). NMR

spectral data for representative examples of the various classes of compounds prepared in this chapter are provided in the **Supporting Information** provided on the attached DVD.

5.2.1 Synthesis of Uridine Derivatives

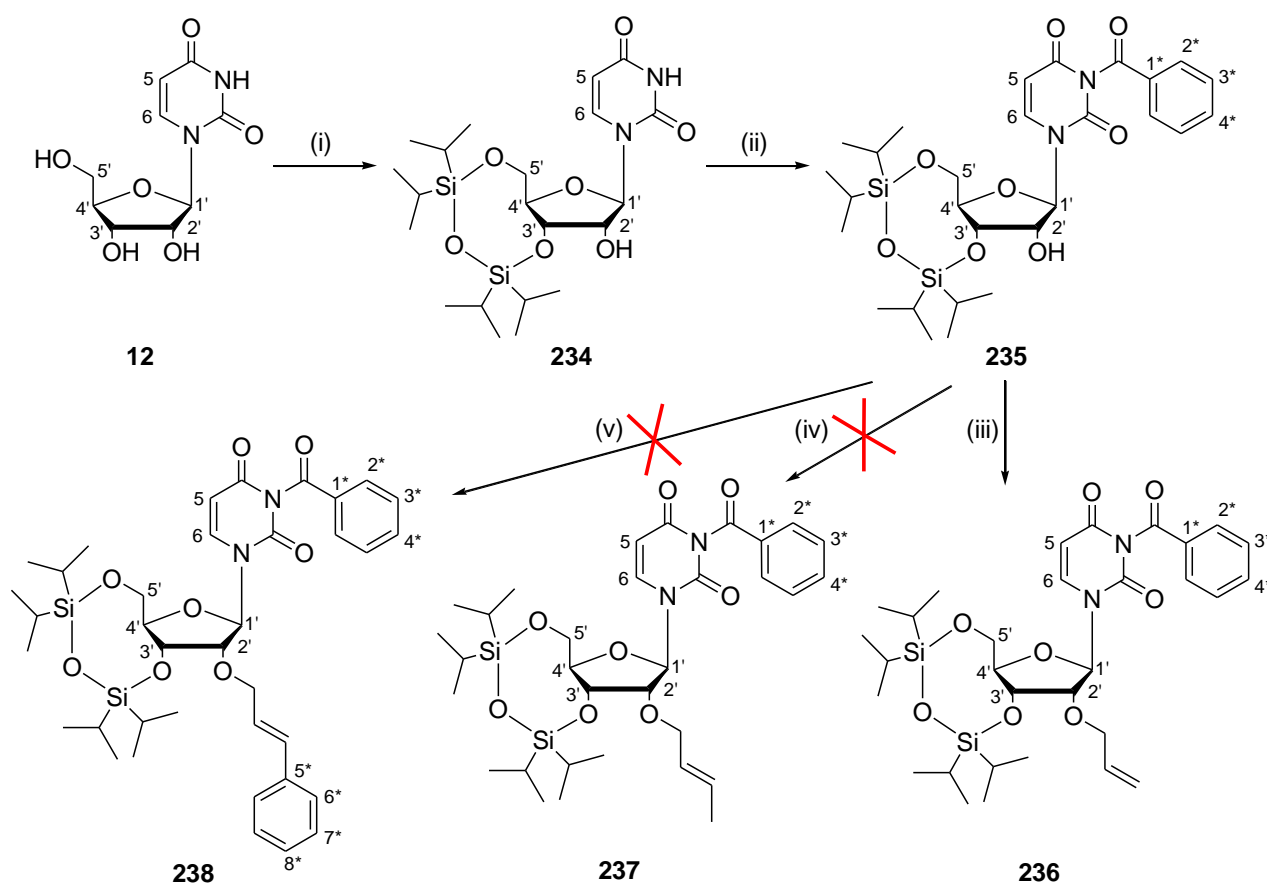
We began our synthesis of a range of uridine derivatives by first using the 1,1,3,3-tetraisopropylidisiloxane protecting group looking at various modifications to the tethered protected system. This was followed by the synthesis of a wide range of uridine derivatives, all protected at only the 5'-*O*-position on the sugar ring with various silicon-containing protecting groups - starting with the small dimethylethylsilyl chloride and moving up through the range to the very bulky trihexylsilyl chloride group. We hoped that using a range of various sized silicon-containing protecting groups would allow us to determine which size range was optimal for biological activity in the compounds.

5.2.1.1 Uridine Derivatives Containing the 3'-*O* to 5'-*O*-Tethered Protecting Group

To date, the 1,1,3,3-tetraisopropylidisiloxane protecting group has found frequent use in nucleoside chemistry and an overview of the approach used for the synthesis of the tethered 1,1,3,3-tetraisopropylidisiloxane protected uridine derivatives is shown in **Scheme 21**. The initial step, *Step (i)*, shows the protection of both the 3'-OH and 5'-OH groups on uridine **12** simultaneously using a small excess of 1,3-dichloro-1,1,3,3-tetraisopropylidisiloxane in the presence of pyridine as both the base and the solvent for the reaction. The reaction mixture obtained was evaporated, subjected to extraction procedures and then purified by column chromatography. The desired compound, 1-[(6*R*,8*R*,9*R*,9*aS*)-9-hydroxy-2,2,4,4-tetraisopropyltetrahydro-6*H*-furo[3,2-*f*][1,3,5,2,4]trioxadisilocin-8-yl]pyrimidine-2,4-(1*H*,3*H*)-dione **234** was obtained as a white foam in 85 % yield.

The spectroscopic data obtained correlated well with the literature values (both ¹H and ¹³C NMR spectra) reported previously by Matsuda and co-workers.¹²¹ The four CH(CH₃)₂ protons

and twenty four $\text{CH}(\text{CH}_3)_2$ protons were observed together as a multiplet integrating for 28 H at 1.02-1.10 ppm in the ^1H NMR spectrum. In the ^{13}C NMR spectrum, the four new SiCH carbons were observed as peaks at 12.42, 12.88, 12.93 and 13.33 ppm, while the eight new CH_3 groups were observed as peaks at 16.76, 16.88, 16.92, 16.99, 17.20, 17.25, 17.34 and 17.43 ppm respectively. Interestingly, a new Si-CH stretch was also observed in the infrared spectrum, at 1247 cm^{-1} .



Scheme 21 *Synthesis of TIPDS derivatives:* (i) 1.05 eq. 1,3-dichloro-1,1,3,3-tetraisopropylidisiloxane, pyridine, $0\text{ }^\circ\text{C}$ - rt, 21 h, 85 %, (ii) 1.3 eq. benzoyl chloride, 7.7 eq. Na_2CO_3 , 0.04 eq. tetrabutylammonium bromide, CH_2Cl_2 : H_2O (1 : 2), rt, 2 h, 99 %, (iii) 2.5 eq. allyl bromide, 2.5 eq. NaH, THF, rt, 23 h, 21 %, (iv) 2.5 eq. crotyl bromide, 2.5 eq. NaH, THF, rt, 23 h, 0 %, (v) 2.5 eq. cinnamyl bromide, 2.5 eq. NaH, THF, rt, 23 h, 0 %

Step (ii) shows the protection of the 3-*N*-amide as the corresponding benzoyl derivative. The reaction was performed by dissolving the starting material **234**, sodium carbonate and tetrabutylammonium bromide in a two-phase solution of dichloromethane and distilled water. To this mixture was then added the excess benzoyl chloride and the reaction mixture was allowed to stir very vigorously at room temperature. The reaction mixture was then purified by extraction and the residue obtained was dissolved in 1,2-dichloroethane and allowed to stand at room temperature for 66 hours. This step was performed to allow the *O*-/*N*-rearrangement to occur. After this time the residue obtained after evaporation was purified by column chromatography. The desired compound 3-benzoyl-1-[(6*aR*,8*R*,9*R*,9*aS*)-9-hydroxy-2,2,4,4-tetraisopropyltetrahydro-6*H*-furo[3,2-*f*][1,3,5,2,4]trioxadisilocin-8-yl]pyrimidine-2,4-(1*H*,3*H*)-dione **235** was obtained as a white foam in 99 % yield.

We were able to show that the desired 3-*N*-benzoyl compound had formed by the disappearance of the broad singlet integrating for one proton at 9.64 ppm in the ¹H NMR spectrum of the starting material, and the occurrence of new peaks at 7.50 (t, *J* = 7.7 Hz), 7.66 (t, *J* = 7.4 Hz) and 7.93 ppm (d, *J* = 7.2 Hz), which were assigned as H-3*, H-4* and H-2* respectively. This assignment of structure was further supported by the presence of new peaks in the ¹³C NMR spectrum at 129.11 (C-3*), 130.43 (C-2*), 131.38 (C-1*), 135.10 (C-4*) and 168.53 (Ph-C=O) ppm. We also observed the characteristic signal at 762 cm⁻¹ in the fingerprint region of the infrared spectrum for 5 adjacent aromatic protons. In addition, it was found that all assignments reported for compound **235** correlated well to those previously reported by Sekine.¹²²

Scheme 21, *Step (iii)* shows the deprotonation of the secondary alcohol at the 2'-position on the sugar ring, using sodium hydride as the base in the solvent THF. This was followed by the reaction of the O⁻ with an excess of allyl bromide, to give the desired compound **236** as a clear oil in 21 % yield after purification by extraction and column chromatography.

The formation of 3-benzoyl-1-[(6*aR*,8*R*,9*R*,9*aR*)-9-allyl-9-hydroxy-2,2,4,4-tetraisopropyltetrahydro-6*H*-furo[3,2-*f*][1,3,5,2,4]trioxadisilocin-8-yl]pyrimidine-2,4-(1*H*,3*H*)-dione **236** was indicated clearly in the ¹H NMR spectrum by the loss of the broad singlet at 2.04 ppm

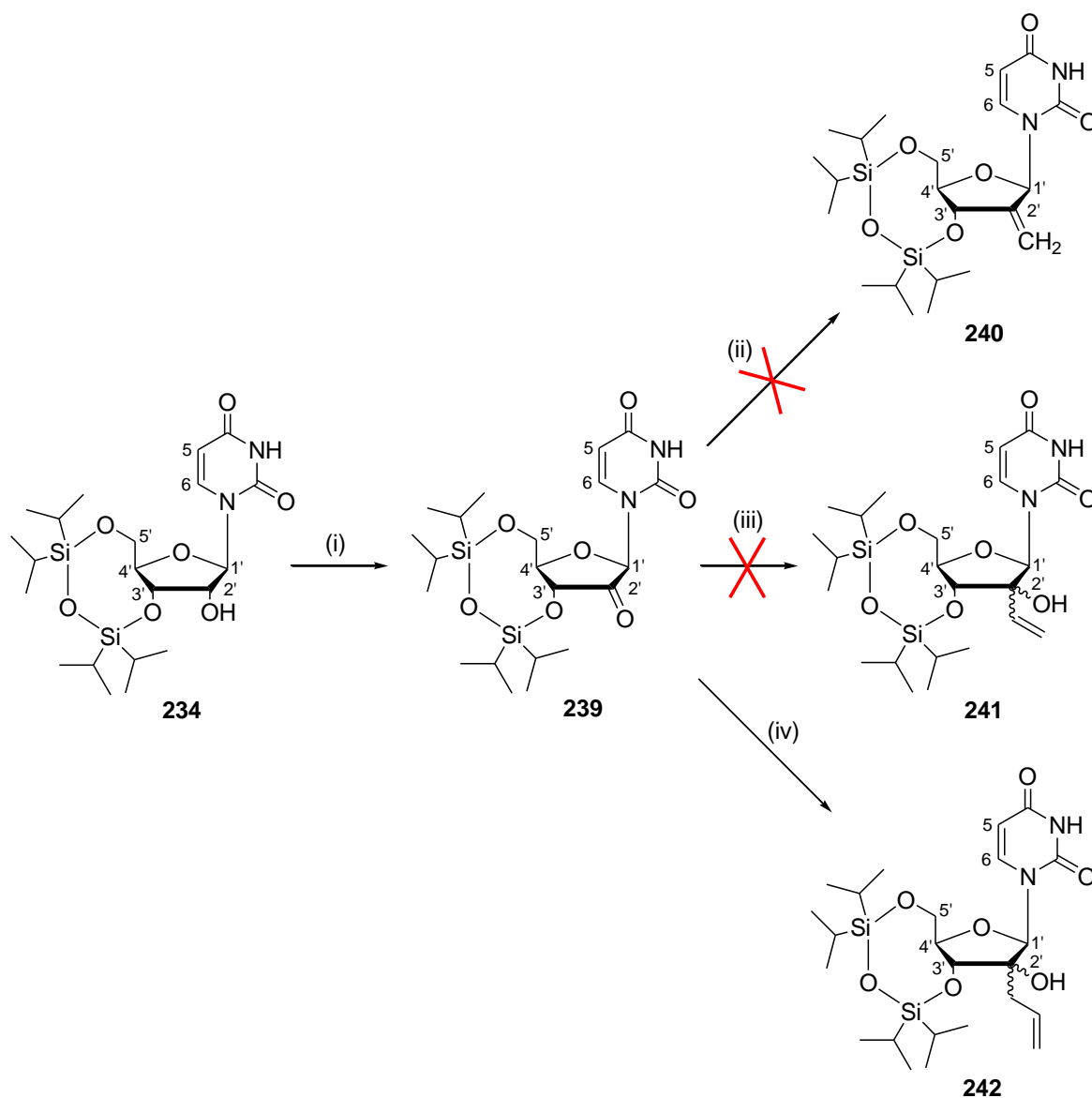
assigned as OH-2' for the starting material, and the appearance of the new doublet of doublets at 4.39 ppm integrating for 2 H and assigned as OCH₂, the two doublet of doublets at 5.21 and 5.39 ppm, each integrating for 1 H and assigned as CH=CH₂ and finally, the multiplet at 5.81-5.95 ppm integrating for 1 H and assigned as CH=CH₂. Similarly, new peaks were observed at 71.22, 117.41 and 134.27 ppm in the ¹³C NMR spectrum, correlating to OCH₂, CH=CH₂ and CH=CH₂ respectively.

As outlined in *Step (iv)* and *Step (v)* of **Scheme 21**, the deprotonated secondary alcohol on the 2'-position of the sugar ring was also reacted with crotyl- and cinnamyl bromide respectively, using the same conditions as outlined for the reaction with allyl bromide (*Step (iii)*, **Scheme 21**). Unfortunately, after work-up by extraction and purification by column chromatography, neither of these reactions yielded any of the desired compounds **237** and **238**. Due to the time constraints of the project, this approach was not investigated further.

Shown schematically in **Scheme 22** is the oxidation of the secondary alcohol, 2'-OH on the sugar ring, followed by attempts made at the derivitisation of the ketone. As stated, *Step (i)* shows the reaction of our protected uridine derivative **234** with the pre-formed oxidation complex (prepared from chromium (VI) trioxide, pyridine and acetic anhydride). After stirring at rt for two hours, the reaction mixture was added dropwise into stirring ethyl acetate and the resulting suspension was pumped through a short silica gel column to remove the chromium precipitates. The filtrate obtained was then concentrated to dryness and the residue obtained was purified by column chromatography. The desired compound 1-[(6a*R*,8*R*,9a*R*)-2,2,4,4-tetraisopropyl-9-oxotetrahydro-6*H*-furo[3,2-*f*][1,3,5,2,4]trioxadisilo-cin-8-yl]pyrimidine-2,4(1*H*,3*H*)-dione **239** was obtained pure as a white foam in 80 % yield.

NMR spectroscopic data obtained for compound **239** correlated well to that reported by Matsuda and co-workers.¹²¹ We observed the disappearance of the broad singlet present at 3.62 ppm, and assigned as OH-2', in the ¹H NMR spectrum for the starting material. Similarly, a new peak at 204.72 ppm was observed in the ¹³C NMR spectrum accounting for the formation of the new carbonyl in the 2'-position of the sugar ring. Interestingly, the characteristic new carbonyl group on the sugar ring of the molecule gave rise to a peak at

1724 cm^{-1} in the infrared spectrum and caused the optical rotation values to shift from 15.596° ($c = 1.09$ in CH_2Cl_2) for the starting material to -17.822° ($c = 1.01$ in CH_2Cl_2) for the newly formed product **239**.



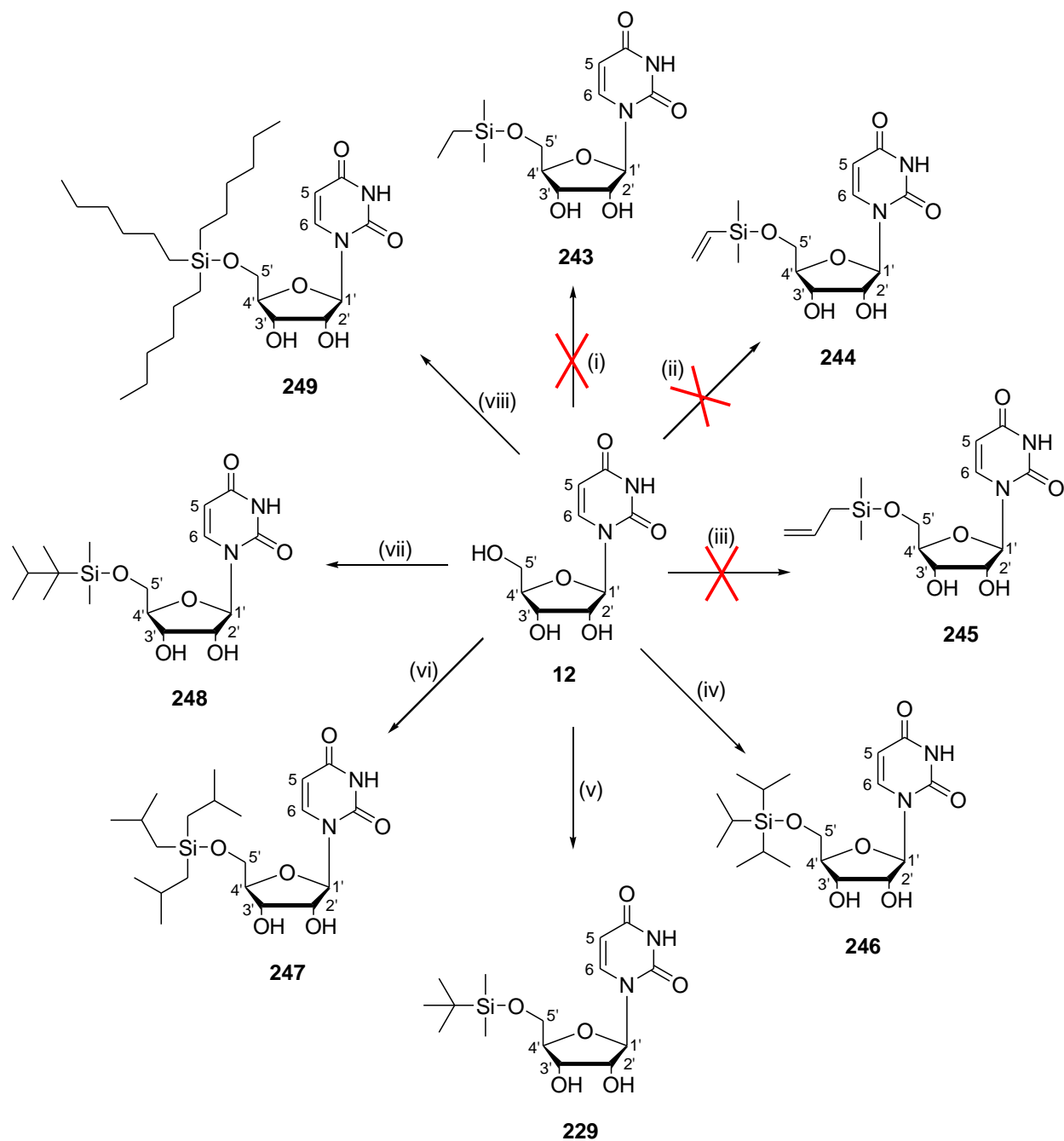
Scheme 22 *Synthesis of other TIPDS derivatives:* (i) Oxidation complex: 3 eq. chromium (VI) trioxide : 6 eq. pyridine : 3 eq. acetic anhydride, CH_2Cl_2 , rt, 2 h, 80 %, (ii) 7 eq. methyl triphenylphosphonium bromide, 7 eq. *n*-butyllithium, THF, 0°C - rt, 3 h, 0 %, (iii) 5 eq. vinyl magnesium bromide, THF, -60°C , 20 h, 0 %, (iv) 5 eq. allyl magnesium bromide, THF, -60°C , 18 h, 38 % based on recovery of unreacted starting material

Shown in *Step (ii)* of **Scheme 22** is our attempt at the Wittig reaction to convert the C=O in the 2'-position of the sugar ring to a C=CH₂. The reaction was performed by stirring the methyl triphenylphosphonium bromide in THF until a suspension had formed and then adding to this suspension the *n*-butyllithium. The reaction immediately changed colour and was allowed to stir at 0 °C until all of the suspended particles had dissolved. To the stirring solution was then added compound **239** batch-wise. After 3 hours tlc indicated consumption of the starting material, so the reaction was worked-up by extraction and purified by column chromatography. Unfortunately, none of the desired compound **240** was obtained after chromatography.^{121b}

Step (iii) of **Scheme 22** shows our first attempt at the Grignard addition to compound **239**. The solution was formed of the starting material **239** in THF and was then cooled to -60 °C, before the addition of the excess vinyl magnesium bromide. After stirring overnight, the reaction mixture was worked-up by extraction and purified by column chromatography. None of the desired compound **241**, was isolated after purification.^{121b}

As outlined in *Step (iv)* of **Scheme 22**, is the second attempt at the Grignard addition to the oxidised TIPDS-uridine derivative **239**. Again, a solution was formed of the starting material **239** in THF and this was cooled to -60 °C, before the addition of the excess allyl magnesium bromide. The reaction mixture was allowed to stir at -60 °C overnight and was then worked-up by extraction and purified by column chromatography. The desired compound **242** was obtained as a clear oil in 38 % yield based on the recovery of unreacted starting material. *rac*-1-[(6*aR*,8*R*,9*S*,9*aR*)-Tetrahydro-9-allyl-9-hydroxy-2,2,4,4-tetraiso-propyl-6*H*-furo[3,2-*f*][1,3,5,2,4]trioxadisilocin-8-yl]pyrimidine-2,4(1*H*,3*H*)-dione **242** was identified by the appearance of a broad singlet at 2.48 ppm integrating for 1 H (assigned as OH-2') and by the appearance of characteristic peaks for the allyl chain: multiplet integrating for 2 H at 2.70-2.72 ppm (OCH₂), multiplet integrating for 2 H at 5.33-5.37 ppm (CH=CH₂) and a multiplet integrating for 1 H at 6.05-6.09 ppm (CH=CH₂) in the ¹H NMR spectrum. This was further supported by the appearance of new peaks in the ¹³C NMR spectrum at 36.80 ppm for the OCH₂ group, at 121.10 ppm for the CH=CH₂ and at 130.19 ppm for the CH=CH₂. Final confirmation was given by the presence of a peak assigned as [M + H]⁺ at 527.26033 in the HRMS, with C₂₄H₄₃N₂O₇Si₂⁺ requiring a peak of 527.26033.

5.2.1.2 Uridine Derivatives with Various 5'-O-Protecting Groups



Scheme 23 Synthesis of 5'-O-protected uridine derivatives: General Procedure for Steps (i)-(viii): 1.1 eq. silyl chloride, 0.1 eq. DMAP, pyridine, rt, 18-22 h, (i) 0 %, (ii) 0 %, (iii) 0 %, (iv) 45 %, (v) 88 %, (vi) 27 %, (vii) 99 %, (viii) 31 %

The synthesis of 5'-*O*-protected uridine derivatives is shown in detail in **Scheme 23**. The general procedure used in *Steps (i) - (viii)* was to fill all glassware required for the reactions with a 5 % trimethylsilyl chloride : hexane solution and allow it to stand at room temperature overnight. After this time, the glassware was oven-dried, placed under high vacuum and allowed to cool to rt under an argon atmosphere. This was step was performed in order to “silylate” the surface of the glassware, it was found to have a significant effect and leading to improvement on the overall reaction yields.

The uridine **12** and a catalytic amount of DMAP were then stirred with distilled pyridine until a solution had formed. To this stirring solution was then added the excess silyl chloride and the reaction mixture was allowed to stir at rt overnight (18-22 h). After this time, the reactions were worked up by extraction and if required by crude NMR, purified further by column chromatography. The results obtained are summarized in **Table 21**.

Table 21 Reaction conditions and results obtained for the synthesis of 5'-*O*-protected uridine derivatives

Compound Code	Protecting Group	Further Purification	Percentage Yield
243	Chlorodimethylethylsilane	Not Required	0 %
244	Dimethylvinylchlorosilane	Not Required	0 %
245	Allyldimethylsilyl chloride	Not Required	0 %
246	Triisopropylsilyl chloride	Column Chromatography	45 %
229	<i>tert</i> -Butyldimethylsilyl chloride	Column Chromatography	88 %
247	Chlorotriisobutylsilane	Column Chromatography	27 %
248	Dimethylhexylsilyl chloride	Not Required	99 %
249	Chlorotrihexylsilane	Column Chromatography	31 %

The formation of the 5'-*O*-protected uridine derivatives was confirmed through the use of proton and carbon NMR spectroscopy, as well as low and high resolution mass spectrometry. Unfortunately, the preparations for compounds **243**, **244** and **245** were unsuccessful, with none of the desired compounds being obtained. We suspect that this may be due to the

unstable nature of the compounds themselves, but this could not be confirmed as none of the desired compounds could be isolated after column chromatography.

The preparation of 5'-*O*-(triisopropylsilyl)uridine **246** was confirmed by the presence of a new multiplet in the ^1H NMR spectrum at 1.04-1.14 ppm integrating for 21 H, accounting for the three $\text{CH}(\text{CH}_3)_2$ protons and the eighteen $\text{CH}(\text{CH}_3)_2$ protons. This was supported by the presence of two new peaks in the ^{13}C NMR spectrum at 11.90 and 17.94 ppm, assigned as the $\text{CH}(\text{CH}_3)_2$ and $\text{CH}(\text{CH}_3)_2$ carbons respectively. For the compound $\text{C}_{18}\text{H}_{33}\text{N}_2\text{O}_6\text{Si}^+$, the HRMS required a peak at 401.21024 and we observed a peak at 401.20968 which is effectively the $[\text{M} + \text{H}]^+$ peak.

The synthesis of 5'-*O*-(*tert*-butyldimethylsilyl)uridine **229** was shown by the presence of peaks at 0.12 (6 H, singlet) and 0.92 (9 H, singlet) ppm accounting for $\text{Si}(\text{CH}_3)_2$ and $\text{C}(\text{CH}_3)_2$ in the ^1H NMR spectrum. The corresponding peaks were also observed at -5.55 ($\text{Si}(\text{CH}_3)_2$), 18.40 ($\text{C}(\text{CH}_3)_2$) and 25.90 ($\text{C}(\text{CH}_3)_2$) ppm in the ^{13}C NMR spectrum. Final confirmation for the formation of the desired compound was given by the presence of a peak at 359.16336 in the HRMS which is found to be for $[\text{M} + \text{H}]^+$ ($\text{C}_{15}\text{H}_{27}\text{N}_2\text{O}_6\text{Si}^+$ requires 359.16329).

5'-*O*-(Triisobutylsilyl)uridine **247** was identified by the appearance of a doublet of doublets at 0.67 ppm integrating for 6 H (assigned as the three SiCH_2 's) as well as by the appearance of characteristic peaks in the ^1H NMR spectrum for the $\text{CH}(\text{CH}_3)_2$ at 0.96 and 1.83 ppm, which are assigned as $\text{CH}(\text{CH}_3)_2$ (18 H, doublet, $J = 6.6$ Hz) and $\text{CH}(\text{CH}_3)_2$ (3 H, septet, $J = 6.6$ Hz) respectively. The formation of **247** was further supported by the appearance of new peaks in the ^{13}C NMR spectrum at 24.20 ppm for $\text{CH}(\text{CH}_3)_2$, 24.99 ppm for SiCH_2 and 26.36/26.43 ppm for $\text{CH}(\text{CH}_3)_2$. Final confirmation was given by the presence of a peak assigned as $[\text{M} + \text{H}]^+$ at 443.25685 in the HRMS, with the M^+ peak for $\text{C}_{21}\text{H}_{39}\text{N}_2\text{O}_6\text{Si}^+$ calculated as 443.25719.

Furthermore, the preparation of 5'-*O*-(dimethylhexylsilyl)uridine **248** was confirmed by the presence of a new singlet in the ^1H NMR spectrum at 0.02 ppm integrating for 6 H, accounting for the three $\text{Si}(\text{CH}_3)_2$ protons, as well as a doublet of doublets at 0.75 ppm

integrating for 12 H as assigned as $\text{CH}(\text{CH}_3)_2$ plus $\text{C}(\text{CH}_3)_2$, and lastly, a septet at 1.50 ppm integrating for 1 H and assigned as the $\text{CH}(\text{CH}_3)_2$ peak. This was supported by the presence of five new peaks in the ^{13}C NMR spectrum at -3.49, 18.44, 20.20, 25.41 and 34.06 ppm, assigned as the $\text{Si}(\text{CH}_3)_2$, $\text{C}(\text{CH}_3)_2$, $\text{CH}(\text{CH}_3)_2$, $\text{C}(\text{CH}_3)_2$ and $\text{CH}(\text{CH}_3)_2$ carbons respectively. For the compound $\text{C}_{17}\text{H}_{31}\text{N}_2\text{O}_6\text{Si}^+$, the HRMS required a peak at 387.19459 and we observed a peak at 387.19505 which is effectively the $[\text{M} + \text{H}]^+$ peak.

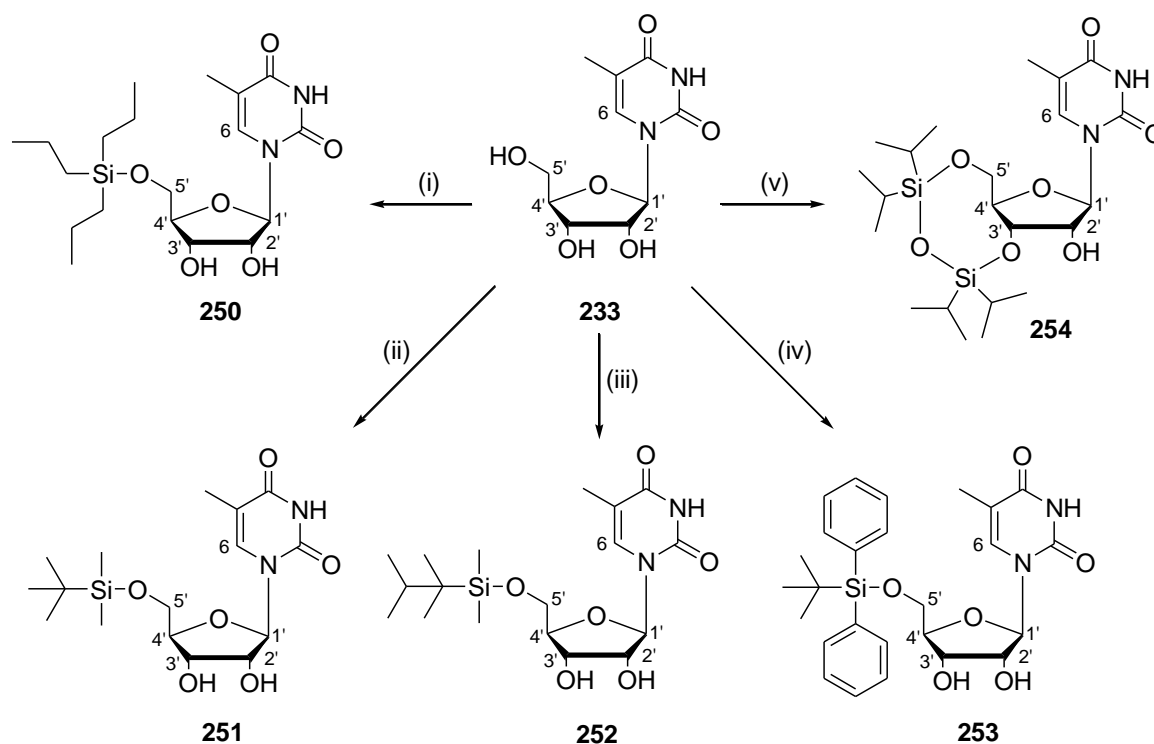
Finally, the synthesis of 5'-*O*-(trihexylsilyl)uridine **249** was shown by the presence of peaks at 0.60-0.65 (multiplet, 6 H), 0.88 (triplet, 9 H) and 1.27-1.30 (multiplet, 24 H) ppm accounting for the SiCH_2 , CH_3 and $\text{SiCH}_2\text{CH}_2\text{CH}_2\text{CH}_2\text{CH}_2\text{CH}_3$ protons respectively, in the ^1H NMR spectrum. The corresponding peaks were observed at 13.32 (SiCH_2), 14.09 (CH_3) and 22.56/23.04/31.46/33.23 ($\text{SiCH}_2\text{CH}_2\text{CH}_2\text{CH}_2\text{CH}_2\text{CH}_3$) ppm in the ^{13}C NMR spectrum. Final confirmation for the formation of the desired compound was given by the presence of a peak at 527.35042 in the HRMS which is found to be for $[\text{M} + \text{H}]^+$ ($\text{C}_{27}\text{H}_{51}\text{N}_2\text{O}_6\text{Si}^+$ requires 527.35109).

5.2.2 Synthesis of 5-Methyluridine Derivatives

In order to determine if a methyl group at the 5-position on the base would affect the activity of the compounds, we synthesized five derivatives of 5-methyluridine protected at the 5'-*O*-position on the sugar ring, which correlated to derivatives previously prepared for uridine. We then anticipated that we would be able to compare the activity of the corresponding 5-methyluridine and uridine derivatives to correlate activity. This biological testing is discussed in detail in **Chapter 6** (anti-bacterial assays) and **Chapter 7** (anti-cancer assays).

Scheme 24, *Step (i)* shows the preparation of 5'-*O*-(tripropylsilyl)-5-methyluridine **250** by the reaction of uridine **12** with excess chlorotripropylsilane in the presence of a catalytic amount of DMAP and pyridine (acting as both the base and the solvent for this reaction). After purification by column chromatography, the desired compound **250** was obtained pure as a white semi-solid in a low yield of 19 % yield.

The synthesis of 5'-*O*-(tripropylsilyl)-5-methyluridine **250** was shown by the presence of three new multiplets in the ^1H NMR spectrum, at 0.61-0.67 ppm integrating for 6 H, at 0.94-0.99 ppm integrating for 9 H and at 1.33-1.42 ppm integrating for 6 H, accounting for the SiCH_2 , CH_2CH_3 and CH_2CH_3 groups respectively. The corresponding peaks were observed at 12.48 ppm (SiCH_2), 16.73 ppm (CH_2CH_3) and 18.34 ppm (CH_2CH_3) in the ^{13}C NMR spectrum. Final confirmation for the formation of the desired compound **250** was given by the presence of a peak at 415.22569 in the HRMS which is found to be for $[\text{M} + \text{H}]^+$ ($\text{C}_{19}\text{H}_{35}\text{N}_2\text{O}_6\text{Si}^+$ requires 415.22589).



Scheme 24 Synthesis of 5-methyluridine derivatives: (i) 1.1 eq. chlorotripropylsilane, 0.1 eq. DMAP, pyridine, rt, 21 h, 19 %, (ii) 1.1 eq. *tert*-butyldimethylsilyl chloride, 0.1 eq. DMAP, pyridine, rt, 20 h, 93 %, (iii) 1.1 eq. dimethylhexylsilyl chloride, 0.1 eq. DMAP, pyridine, rt, 21 h, 80 %, (iv) 1.1 eq. *tert*-butyldiphenylsilyl chloride, 0.1 eq. DMAP, pyridine, rt, 20 h, 100 %, (v) 1.05 eq. 1,3-dichloro-1,1,3,3-tetraisopropyl disiloxane, pyridine, 0 °C - rt, 20 h, 40 %

Shown in *Step (ii)* of **Scheme 24** is the protection of the primary alcohol in the 5'-position of the sugar ring using *tert*-butyldimethylsilyl chloride as the protecting group. The reaction occurred in the presence of a catalytic amount of DMAP and used pyridine as both the base and the solvent for the reaction. The desired compound, 5'-*O*-(*tert*-butyldimethylsilyl)-5-methyluridine **251**, was obtained pure as a white powder after extraction and as such no further purification was required. The compound **251** was obtained in 93 % yield from its direct synthetic precursor, in this case 5-methyluridine **233**.

5'-*O*-(*tert*-Butyldimethylsilyl)-5-methyluridine **251** was identified by the appearance of two singlets at 0.15 and 0.16 ppm integrating for 6 H [assigned as the Si(CH₃)₂ groups] as well as by the appearance of a characteristic singlet at 0.96 ppm, integrating for 9 H, which is assigned as the C(CH₃)₃ group in the ¹H NMR spectrum. The formation of **251** was further supported by the presence of a peak assigned as [M + H]⁺ at 373.17903 in the HRMS, with C₁₆H₂₉N₂O₆Si⁺ requiring a peak at 373.17894. Interestingly, new bands were observed in the infrared spectrum, at 1362 and 1388 cm⁻¹ for the CH₃ symmetrical deformations on the newly added *tert*-butyl group, and other new bands were also observed at 831 cm⁻¹ in the fingerprint region and at 1258 cm⁻¹ for the Si-CH₃ stretching.

Outlined in *Step (iii)* of **Scheme 24** is the reaction of 5-methyluridine **233** with dimethylhexylsilyl chloride in the presence of DMAP and pyridine. After stirring at room temperature under an argon atmosphere for 21 hours, the reaction was quenched by the addition of distilled water and worked-up by extraction. The desired compound, 5'-*O*-(dimethylhexylsilyl)-5-methyluridine **252**, was obtained pure as a white solid in 80 % yield after extraction; thus further purification was not required.

The preparation of 5'-*O*-(dimethylhexylsilyl)-5-methyluridine **252** was confirmed by the presence of three new peaks in the ¹H NMR spectrum: a singlet at 1.00 ppm integrating for 6 H and assigned as Si(CH₃)₂, a doublet of doublets at 1.75 ppm integrating for 12 H and assigned as CH(CH₃)₂ plus C(CH₃)₂ and finally, a septet at 1.49 ppm integrating for 1 H and assigned as CH(CH₃)₂. For the compound C₁₈H₃₃N₂O₆Si⁺, the HRMS required a peak at 401.21024 and we observed a peak at 401.20968, which is effectively the [M + H]⁺ peak.

Step (iv) of **Scheme 24** shows the reaction of 5-methyluridine **233** with *tert*-butyldiphenylsilyl chloride. The reaction occurs in the presence of a catalytic amount of DMAP and uses pyridine as both the base and the solvent for the reaction. The desired compound, 5'-*O*-(*tert*-butyldiphenylsilyl)-5-methyluridine **253**, was obtained pure as a white foam after extraction and azeotropic distillation of the pyridine using toluene as the co-solvent, in an excellent quantitative yield.

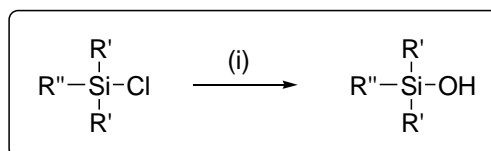
The synthesis of 5'-*O*-(*tert*-butyldiphenylsilyl)-5-methyluridine **253** was shown by the presence of a new singlet at 1.12 ppm (integrating for 9 H) and new multiplets at 7.40-7.43 (integrating for 6 H) and 7.68-7.71 ppm (integrating for 4 H), accounting for Si(CH₃)₃, H-3* plus H-4* and H-2* respectively, in the ¹H NMR spectrum. Final confirmation for the formation of the desired compound was given by the presence of a peak at 497.20971 in the HRMS which is found to be for [M + H]⁺ (C₂₆H₃₃N₂O₆Si⁺ requires 497.21024).

Scheme 24, *Step (v)* shows the preparation of 1-[(6*aR*,8*R*,9*S*,9*aR*)-tetrahydro-9-hydroxy-2,2,4,4-tetraisopropyl-6*H*-furo[3,2-*f*][1,3,5,2,4]trioxadisilocin-8-yl](5-methylpyrimidine)-2,4-(1*H*,3*H*)-dione **254**, by the reaction of 5-methyluridine **233** with excess 1,3-dichloro-1,1,3,3-tetraisopropylidisiloxane in the presence of pyridine as both the base and the solvent for the reaction. The reaction mixture was stirred at room temperature under an argon atmosphere for 20 hours, was worked-up by extraction and then purified by column chromatography. The desired compound **254**, was obtained in 40 % yield as a white foam after purification.

Compound **254** was identified by the appearance of a new multiplet at 1.04-1.10 ppm integrating for 28 H in the ¹H NMR spectrum, which was assigned to the four CH(CH₃)₂ and the four CH(CH₃)₂ groups in the molecule. The formation of **254** was further supported by the appearance of new peaks in the ¹³C NMR spectrum at 12.45, 12.57, 12.68 and 12.93 ppm for the four CH(CH₃)₂ carbons, and at 16.81, 16.94, 16.96, 17.04, 17.22, 17.23, 17.33 and 17.41 ppm for the eight CH(CH₃)₂ carbons. Final confirmation was given by the presence of a peak assigned as [M + H]⁺ at 501.24409 in the HRMS, with C₂₂H₄₁N₂O₇Si₂⁺ requiring a peak at 501.24468.

5.2.3 Synthesis of Various Silanols

Due to the interesting anti-bacterial and anti-cancer assay results obtained for the previously tested *tert*-butyldiphenylsilanol (**145**), we decided to also synthesize a group of silanols ranging in size from dimethylethylsilanol all the way up to triphenylsilanol for further testing. These compounds were also important as several of them served as controls for our other uridine and 5-methyluridine derivative assays. These silanols correspond to the by-products that could be formed by hydrolytic cleavage of the commercially available protecting groups when under biological conditions.



Scheme 6.5 General scheme for the synthesis of the silanols (i) 1 eq. silyl chloride, Et₂O, 1.1 eq. KOH in H₂O : MeOH (4 : 1), rt, 18 h

The general procedure adopted for the synthesis of the silanols was to prepare a solution of the silyl chloride in diethyl ether. To this solution was then added in a single portion, a solution of potassium hydroxide in a 4 : 1 mixture of water and methanol. In general, the solutions warmed up after the additions and a white precipitate was observed almost immediately. The reactions were then allowed to stir at room temperature overnight and were worked-up using standard extraction procedures. NMR spectra were obtained of the crude mixtures for all silanols prepared in this series and due to their purity, no column chromatography was required.

As an example of the procedure to analyze the formation of the silanols, the identification of butyldimethylsilanol **258** is discussed in detail below. The same approach was used for all the

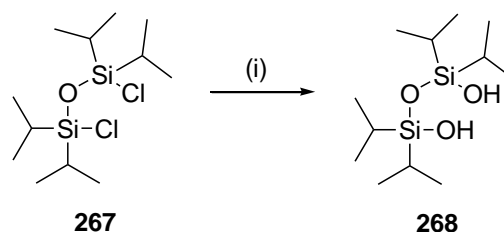
silanols prepared in this series and as such, they are not all described here – for the full analysis, please refer to **Appendix D** (*Experimental Procedures – Relating to Chapter 5*).

Table 22 Synthetic yields for the various silanols prepared

Compound Formed	R'	R''	Percentage Yield
255	<i>Methyl</i> (-CH ₃)	<i>Ethyl</i> (-CH ₂ CH ₃)	2 %
176	<i>Ethyl</i> (-CH ₂ CH ₃)	<i>Ethyl</i> (-CH ₂ CH ₃)	86 %
256	<i>Propyl</i> [-(CH ₂) ₂ CH ₃]	<i>Propyl</i> [-(CH ₂) ₂ CH ₃]	100 %
257	<i>Isopropyl</i> [-CH(CH ₃) ₂]	<i>Isopropyl</i> [-CH(CH ₃) ₂]	98 %
258	<i>Methyl</i> (-CH ₃)	<i>Butyl</i> [-(CH ₂) ₃ CH ₃]	66 %
259	<i>Butyl</i> [-(CH ₂) ₃ CH ₃]	<i>Butyl</i> [-(CH ₂) ₃ CH ₃]	98 %
260	<i>Isobutyl</i> [-CH ₂ CH(CH ₃) ₂]	<i>Isobutyl</i> [-CH ₂ CH(CH ₃) ₂]	98 %
261	<i>Methyl</i> (-CH ₃)	<i>tert-Butyl</i> [-C(CH ₃) ₃]	72 %
262	<i>Methyl</i> (-CH ₃)	<i>Thexyl</i> [-C(CH ₃) ₂ CH(CH ₃) ₂]	95 %
263	<i>Hexyl</i> [-(CH ₂) ₅ CH ₃]	<i>Hexyl</i> [-(CH ₂) ₅ CH ₃]	100 %
264	<i>Methyl</i> (-CH ₃)	<i>Cyclohexyl</i> (-C ₆ H ₁₁)	92 %
265	<i>Methyl</i> (-CH ₃)	<i>Benzyl</i> [-CH ₂ (C ₆ H ₅)]	90 %
266	<i>Phenyl</i> (-C ₆ H ₅)	<i>Phenyl</i> (-C ₆ H ₅)	93 %

Butyldimethylsilanol **258** was identified by the peaks observed as: a singlet at 0.03 ppm integrating for 6 H [$\text{Si}(\text{CH}_3)_2$], a multiplet at 1.48-1.53 ppm integrating for 2 H (SiCH_2), a triplet at 0.88 ppm integrating for 3 H (CH_2CH_3) and a multiplet at 1.25-1.36 ppm integrating for 4 H (SiCH_2CH_2 and CH_2CH_3) in the ^1H NMR spectrum. Unfortunately, the OH peak was not observed in the ^1H NMR spectrum, but the presence of the OH group was confirmed by the Si-O band at 1016 cm^{-1} , the band for O-H bending at 1412 cm^{-1} and the band for O-H stretching at 3575 cm^{-1} which was evident in the infrared spectrum for the compound. The ^{13}C NMR spectrum for the compound corresponded well to the desired compound, with peaks observed at 0.36 ($\text{Si}(\text{CH}_3)_2$), 13.83 (CH_2CH_3), 18.11 (SiCH_2), 25.52 (SiCH_2CH_2) and 26.39 (CH_2CH_3) ppm.

In a similar manner to that described for the series of silanols above, we were able to synthesize compound, 1,3-dihydroxy-1,1,3,3-tetraisopropyldisiloxane **268**, in 100 % yield (shown in **Scheme 26**).



Scheme 26 *Synthesis of the TIPDS derivative:* (i) 1 eq. silyl chloride, Et_2O , 1.1 eq. KOH in $\text{H}_2\text{O} : \text{MeOH}$ (4 : 1), rt, 18 h, 100 %

5.3 CONCLUSIONS

We made use of an approach used to synthesize a range of tethered 1,1,3,3-tetraisopropyldisiloxane protected uridine derivatives. From this group of compounds we obtained five molecules that were modified in various positions on the sugar ring as well as at

the amide position on the base. We intended to use these compounds as an extension to the mini structure-activity relationship determined using the "first generation" of compounds synthesized (the biological testing is described in detail in **Part 1, Chapter 3**).

Using our general approach for the synthesis of 5'-*O*-silyl protected uridine derivatives, we were able to synthesize a further five uridine derivatives and another five 5-methyluridine derivatives. At the same time, we derived a general procedure for the conversion of silyl chlorides to silanols, and used the procedure to synthesize a series of fourteen silanols, ranging from low to high molecular weight and spanning a wide range of chemical space. We aimed to screen these compounds for inhibitory activity against four bacterial strains and to extend this to include further cell proliferation studies. The results obtained for the bacterial assays are discussed in detail in **Chapter 6** and the results for the extended cell proliferation studies are described in **Chapter 7**.

Chapter 6:
Results and Discussion for
Bacteriology and Microscopy

CONTRIBUTIONS TO THIS CHAPTER

All of the antibacterial assays and accompanying statistical analyses were performed by Ms J.-L. Panayides, while under the supervision of both Dr D. Lindsay and Prof E.M.C. Rey. The work was performed in the School of Molecular and Cellular Biology at the University of the Witwatersrand.

6.1 CHAPTER OVERVIEW

The "second generation" of uridine, 5-methyluridine and silanol derivatives were evaluated for their antibacterial activity against two Gram-positive (*Staphylococcus aureus* ATCC 25923 and *Bacillus cereus* DL5) and two Gram-negative (*Pseudomonas aeruginosa* ATCC 27853 and *Escherichia coli* ATCC 25922) bacteria. The compounds showing the most promising results from the antibacterial assays were then used for further studies involving scanning electron and confocal microscopy. The results of both the bacterial assays and the microscopy are presented in detail in this chapter.

In order to determine if our "second generation" of synthetic uridine, 5-methyluridine and silanol derivatives possessed antibacterial properties, we assayed them for inhibitory activity against two Gram-positive and two Gram-negative bacterial strains. In total, 14 nucleoside derivatives and 12 silanols were screened as our second generation of compounds. We then analysed the results obtained for the antibacterial assays of both the "first generation" and the "second generation" of compounds and subjected those compounds demonstrating the most promising results to a further study involving scanning electron and confocal microscopy.

6.2 RESULTS AND DISCUSSION

This section is broken down into three parts, the first of which contains the results obtained for the TTC assays performed on our "second generation" compounds, the second of which

presents some of the results obtained from the confocal microscopy that was used to validate our results obtained from the TTC assay and the last of which highlights the SEM work performed in order to determine a possible site of action for the synthetic compounds.

6.2.1 Antibacterial Assays

6.2.1.1 Materials and Methods

Bacterial Cultures

As described in detail in **Chapter 3, Section 3.2.1.1**, we used *S. aureus* (ATCC 25923) and *B. cereus* (DL5) as our representative Gram-positive bacteria, and *P. aeruginosa* (ATCC 27853) and *E. coli* (ATCC 25922) as our representative Gram-negative bacteria. All of the bacterial strains were grown from either freezer stocks or freeze-dried swabs, maintained on nutrient agar plates at 4 °C and subcultured every 21 days, with each culture grown up in 100 mL nutrient broth overnight at 37 °C. A full description of the procedure used is outlined in detail in **Appendix C (Section C.1 and Section C.2)** below.

The 18 h bacterial cultures were used to determine the number of colony forming units present per millilitre of culture using the droplet plate technique (the full procedure is given in **Appendix C, Section C.3** below). From this technique, the calculated cfu/mL and log cfu/mL for the four bacterial strains were obtained:

- | | | |
|-----------------------------------|-----------------------------|-------------------|
| • <i>S. aureus</i> ATCC 25923 | cfu/mL = 7.47×10^8 | log cfu/mL = 8.87 |
| • <i>B. cereus</i> DL5 | cfu/mL = 1.43×10^9 | log cfu/mL = 9.16 |
| • <i>P. aeruginosa</i> ATCC 27853 | cfu/mL = 1.54×10^9 | log cfu/mL = 9.19 |
| • <i>E. coli</i> ATCC 25922 | cfu/mL = 3.38×10^9 | log cfu/mL = 9.53 |

 Synthetic Compounds

The compounds used in this study were prepared using standard synthetic organic chemistry techniques. A full discussion of the results obtained during the synthesis is provided in **Chapter 5** and the detailed experimental procedures used are given in **Appendix D**. For ease of reading, the compounds tested using the TTC assay are grouped according to structural similarities and are illustrated below:

- as derivatives of uridine (**Figure 55**)
- as derivatives of 5-methyluridine (**Figure 56**)
- and as silanols (**Figure 57**)

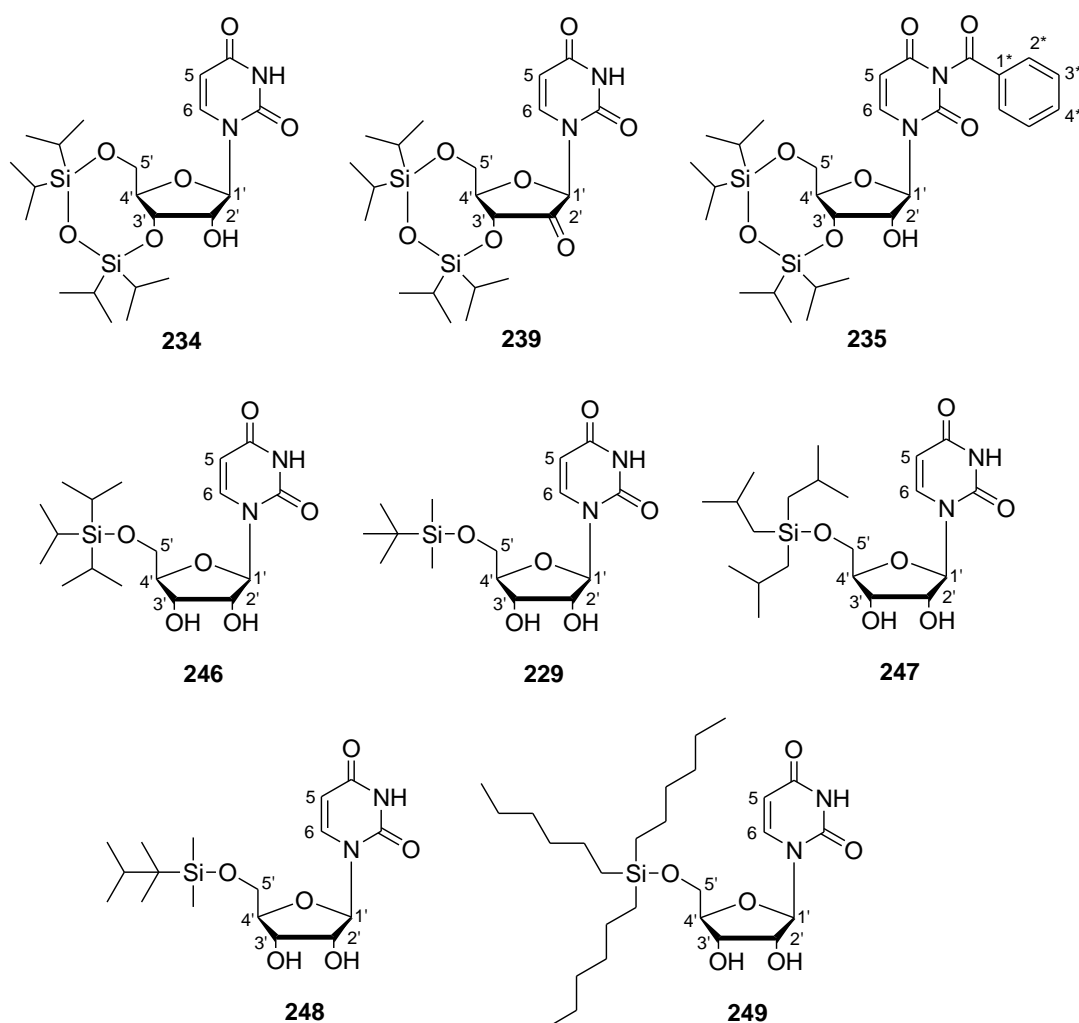


Figure 55 "Second Generation" compounds used in TTC assay - Uridine derivatives

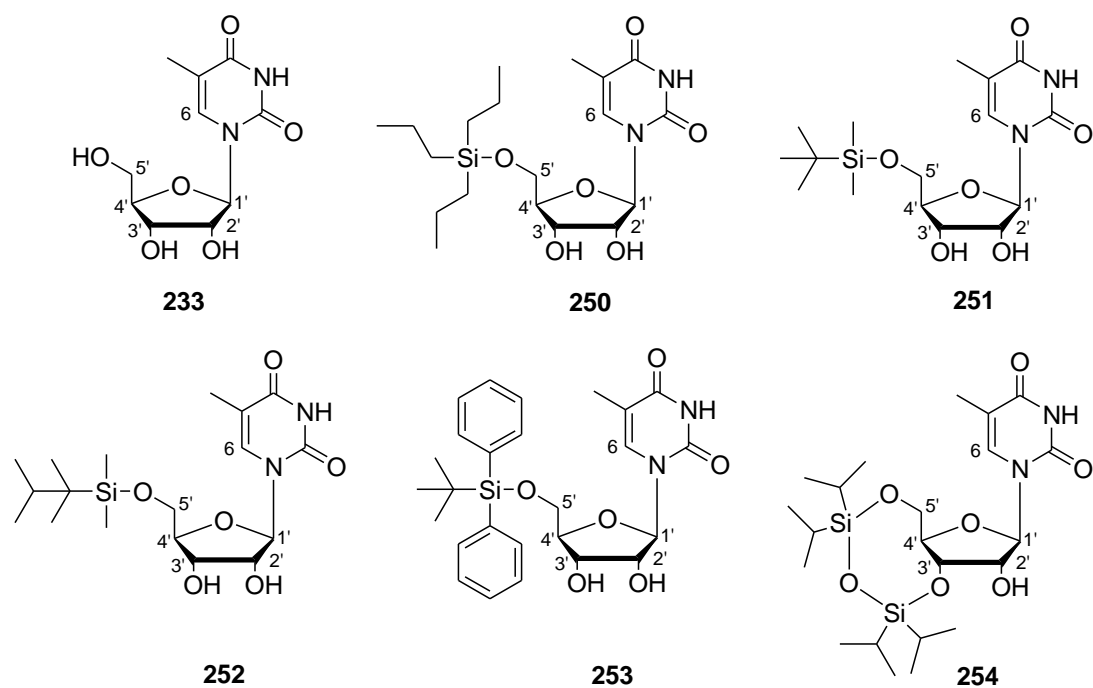


Figure 56 "Second Generation" compounds used in TTC assay - 5-Methyluridine derivatives

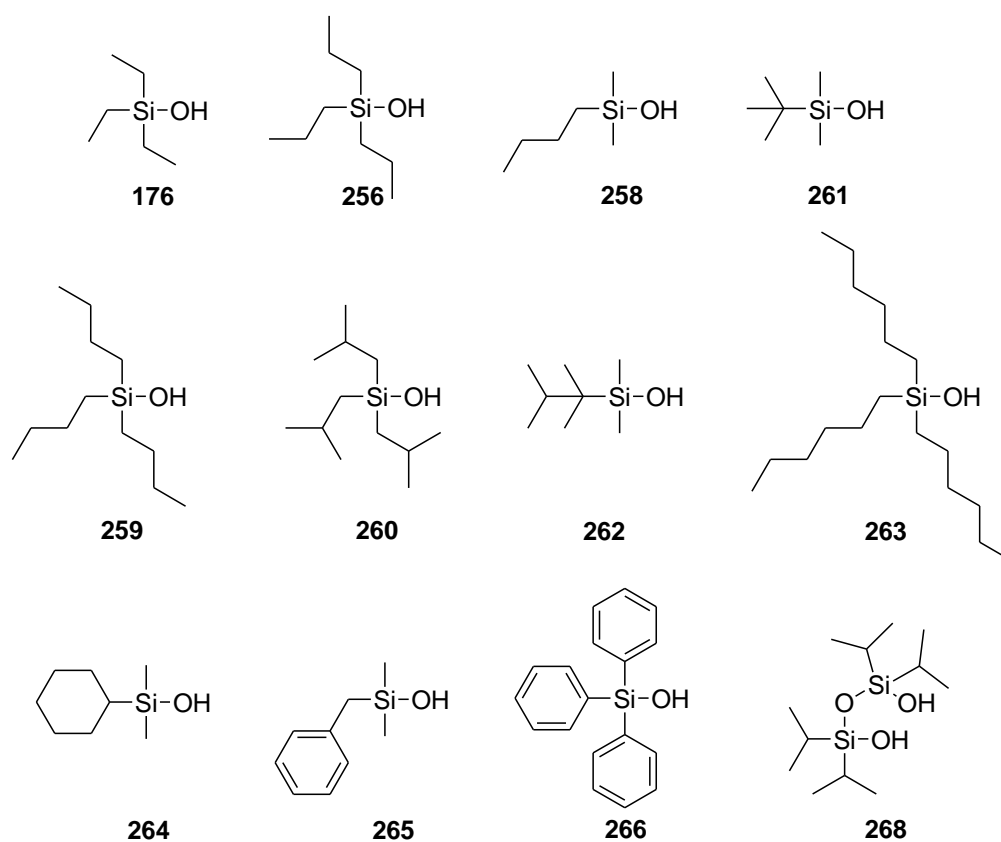


Figure 57 "Second Generation" compounds used in TTC assay - Silanol derivatives

© *Evaluation of Compound Efficacy – Triphenyltetrazolium Chloride Assay*

The synthetic compounds and the control compound, the commercially available antibiotic ciprofloxacin **153**, were used to prepare 10 000 mg/L, 1 000 mg/L, 100 mg/L, 10 mg/L and 1 mg/L stock solutions using autoclaved de-ionised water and molecular grade DMSO, as described in **Appendix C, Section C.5.1**. These stock solutions were used immediately to prepare a series of 16 standard dilutions in autoclaved nutrient broth. The standard dilutions were then used in the triphenyltetrazolium chloride assay, full details of which have already been described in **Chapter 3**, with further descriptions highlighted in **Appendix C, Section C.5.2**. As such, no further explanatory notes will be given here.

© *Statistical Analysis*

For each bacterial strain and compound/antibiotic dilution concentration combination four replicates were performed (duplicates were run on each plate and the plates were prepared in duplicate as well). Four absorbance data points were thus obtained for each combination (bacterial strain/compound/dilution). The data was corrected for the background absorbance of the solution without bacterial growth by referencing the ELISA plate reader to the 0 % growth control on the plates.

For the initial determination of activity, the data was typed into Microsoft Excel and the average of the four replicates was determined. This average for the absorbances was then represented as the percentage of metabolically active cells present for each bacterial strain and compound/antibiotic dilution concentration combination, based on the value obtained for the 100 % growth control specific to each plate.

Graphs were then plotted for the four bacterial strains, showing the percentage metabolically active cells on the y-axis against the compound/antibiotic concentration on the x-axis. From the initial graphs we determined which compounds showed antibacterial activity and any

graphs displaying percentage metabolically active cells less than 10 % over a range of concentrations were classified as being positive hits.

6.2.1.2 Results and Discussion

As described above, ten uridine derivatives, five 5-methyluridine derivatives and fourteen silanols were tested for possible antibacterial activity against the two Gram-positive and two Gram-negative bacteria. The study again used ciprofloxacin **153** as the antibiotic control and each individual assay included a number of internal controls: (i) the 0 % growth control, (ii) the 100 % growth control, (iii) the DMSO controls and (iv) a sterility control.

The *Minimum Inhibitory Concentrations* (MICs) for the synthetic compounds were again determined according to the procedure described by Andrews.⁵⁸ The standard curve obtained for the antibiotic control, ciprofloxacin **153**, was drawn in **Chapter 3**, as **Graph 1**, and was used to calculate the MICs for ciprofloxacin **153**. The results obtained were as follows:

- *S. aureus* ATCC 25923 0.5 mg/L
- *B. cereus* DL5 0.5 mg/L
- *P. aeruginosa* ATCC 27853 0.5 mg/L
- *E. coli* ATCC 25922 0.016 mg/L

The antibacterial activity for the synthetic compounds was determined using the modified MIC determination assay, using TTC, as described in detail in **Chapter 3**, *Section 3.2.1.1*. The results obtained for the "second generation" of uridine derivatives are shown in **Table 23**.

Table 23 MICs determined for the uridine derivatives

Compound	<i>S. aureus</i>	<i>B. cereus</i>	<i>P. aeruginosa</i>	<i>E. coli</i>
	ATCC 25923	DL5	ATCC 27853	ATCC 25922
Uridine 12	No activity	No activity	No activity	No activity
246	No activity	No activity [#]	No activity [#]	No activity [#]
229	No activity	No activity [#]	No activity	No activity
247	No activity	No activity	No activity	No activity
248	No activity	No activity	No activity	No activity
249	No activity	No activity	No activity	No activity
234	16 mg/L	16 mg/L	No activity	No activity
239	8 mg/L	8 mg/L	No activity	No activity
235	No activity	No activity	No activity	No activity

[#] Very high concentrations of the synthetic compound (64-128 mg/L) caused a reduction in the percentage metabolically active cells, but not below the standard cut-off value of 10 %

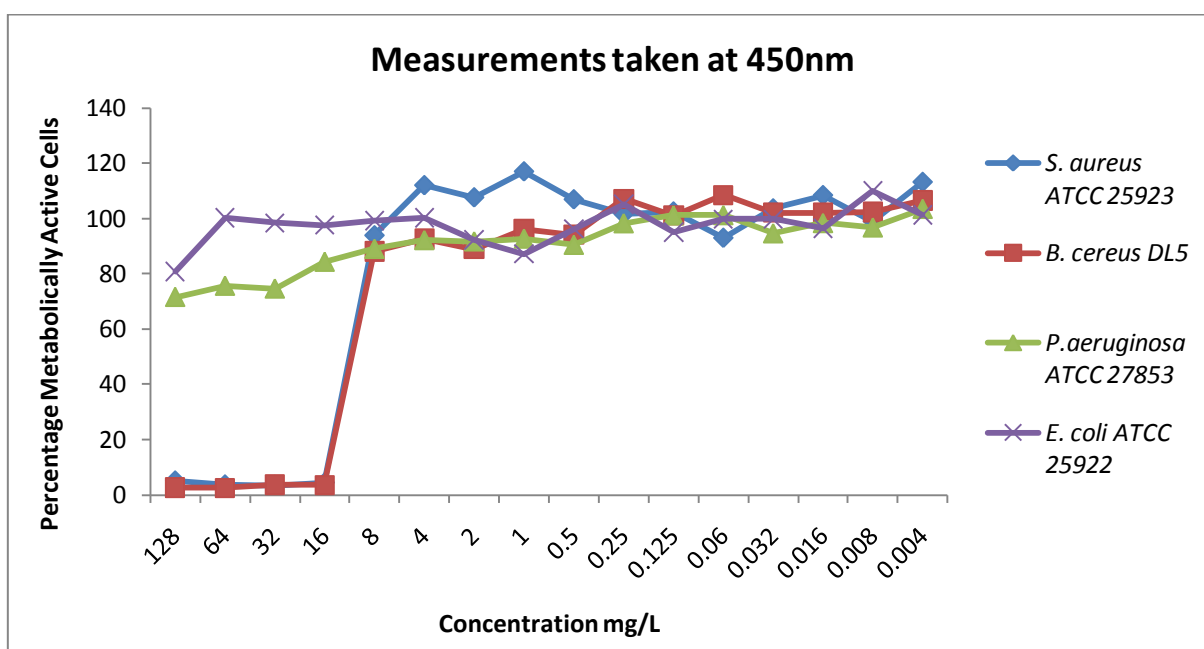
As expected for our negative control, no antibacterial activity was observed for uridine **12**. In fact, no significant activity was observed for any of the "second generation" compounds synthesized with silicon-based protecting groups present at the 5'-*O*-position on the sugar ring (compounds **246-249** and **229**). This was quite disappointing as in our initial screen we had obtained interesting results for 5'-*O*-(*tert*-butyldiphenylsilyl)uridine **107**, with MIC values obtained of 64 mg/L for *S. aureus* (ATCC 25923) and 32 mg/L for *B. cereus* (DL5).

The original data had suggested the possibility of using silicon protected uridine derivatives as the starting off point for the synthesis of our second generation of compounds, but it appears that the antibacterial activity is not widespread throughout the class of compounds and we had unwittingly picked the active species by chance in the first round of testing.

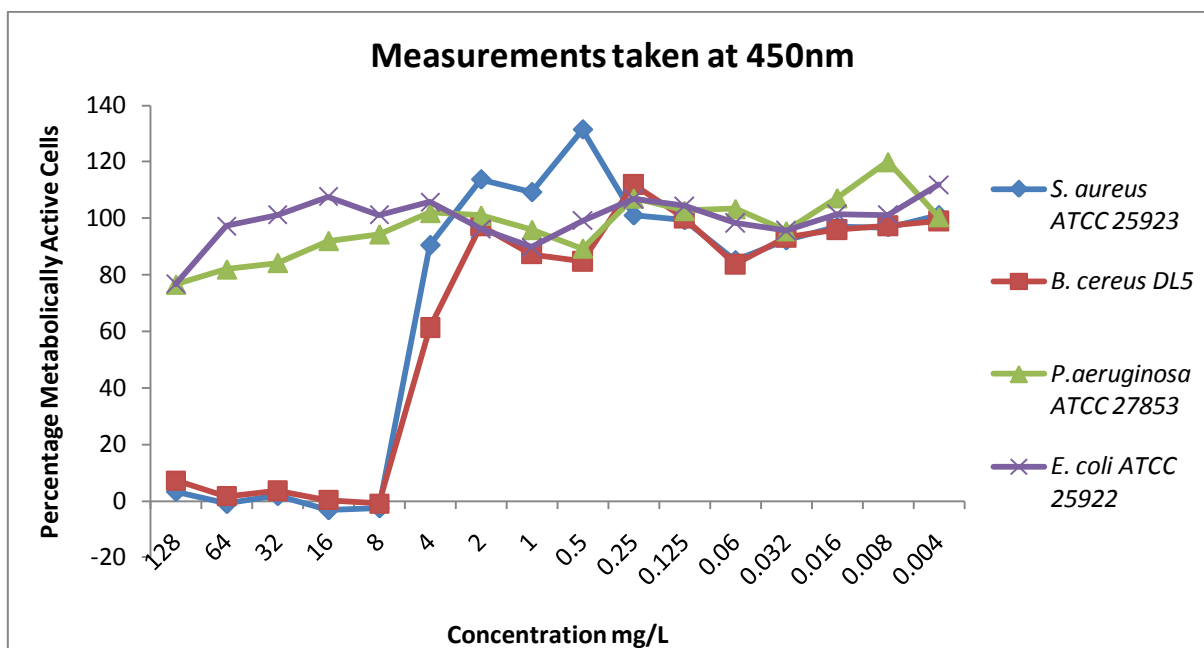
However, our other batch of protected uridine derivatives, those containing two silicon atoms in each of the tethered protecting groups (compounds **234**, **235** and **239**, **Table 23** above), yielded some very interesting results. For compounds **234** and **230**, we again found activity

only against in the Gram-positive bacteria, but this time we observed a dramatic improvement in the range of active concentrations for the synthetic compounds (when compared to the higher concentrations required for activity in the synthetic compounds containing only one silicon-protecting group).

Using the dilution series we prepared a standard curve for each of the different synthetic compounds, against each of the different bacterial strains used in the assay (*S. aureus* ATCC 25923, *B. cereus* DL5, *P. aeruginosa* ATCC 27853 and *E. coli* ATCC 25922), which was then used to determine the MIC values quoted in **Table 23**. The curves for the active compounds, 1-[(6*aR*,8*R*,9*R*,9*aS*)-9-hydroxy-2,2,4,4-tetraisopropyltetrahydro-6*H*-furo[3,2-*f*]-[1,3,5,2,4]trioxadisilocin-8-yl]pyrimidine-2,4(1*H*,3*H*)dione **234** and 1-[(6*aR*,8*R*,9*aR*)-2,2,4,4-tetraisopropyl-9-oxotetrahydro-6*H*-furo[3,2-*f*][1,3,5,2,4]trioxadisilocin-8-yl]pyrimidine-2,4-(1*H*,3*H*)dione **239**, are shown schematically in **Graph 16** and **Graph 17**.



Graph 16 Standard curve for 1-[(6*aR*,8*R*,9*R*,9*aS*)-9-hydroxy-2,2,4,4-tetraisopropyltetrahydro-6*H*-furo[3,2-*f*][1,3,5,2,4]trioxadisilocin-8-yl]pyrimidine-2,4(1*H*,3*H*)dione **234**



Graph 17 Standard curve for 1-[(6a*R*,8*R*,9a*R*)-2,2,4,4-tetraisopropyl-9-oxotetrahydro-6*H*-furo[3,2-*f*][1,3,5,2,4]trioxadisilocin-8-yl]pyrimidine-2,4(1*H*,3*H*)dione **239**

The MIC values obtained for 1-[(6a*R*,8*R*,9*R*,9a*S*)-9-hydroxy-2,2,4,4-tetraisopropyltetrahydro-6*H*-furo[3,2-*f*][1,3,5,2,4]trioxadisilocin-8-yl]pyrimidine-2,4(1*H*,3*H*)dione **234** were 16 mg/L for *S. aureus* (ATCC 25923) and 16 mg/L for *B. cereus* (DL5). These values are significantly higher than those obtained for the commercially available antibiotic ciprofloxacin **153**, with MICs of 0.5 mg/L for *S. aureus* and 0.5 mg/L for *B. cereus* respectively; however, they do show an improvement on the MICs obtained for the active compound in our "first generation" of compounds (32-64 mg/L).

Interestingly, when the 2'-*O*-position on the sugar ring was oxidised to the corresponding ketone, we found an increase in antibacterial activity by a single dilution factor. The MIC values obtained for 1-[(6a*R*,8*R*,9a*R*)-2,2,4,4-tetraisopropyl-9-oxotetrahydro-6*H*-furo[3,2-*f*][1,3,5,2,4]trioxadisilocin-8-yl]pyrimidine-2,4(1*H*,3*H*)dione **239** were 8 mg/L for *S. aureus* (ATCC 25923) and 8 mg/L for *B. cereus* (DL5). This suggests that the 2'-OH on the sugar ring is perhaps not required for recognition and transport pathways within the Gram-positive bacterial cells, as its conversion to a ketone increases the activity of the synthetic molecules.

The antibacterial activity for the synthetic 5-methyluridine derivatives was then determined using the modified TTC assay, as described above. The MIC results obtained from the assay for 5-methyluridine and its derivatives are shown in **Table 24**.

Table 24 MICs determined for the 5-methyluridine derivatives

Compound	<i>S. aureus</i>	<i>B. cereus</i>	<i>P. aeruginosa</i>	<i>E. coli</i>
	ATCC 25923	DL5	ATCC 27853	ATCC 25922
5-Methyluridine 233	No activity	No activity	No activity	No activity
250	No activity	No activity	No activity	No activity
251	No activity	128 mg/L	No activity	No activity
252	No activity	No activity [#]	No activity [#]	No activity [#]
253	No activity	No activity	No activity	No activity
254	32 mg/L	32 mg/L	No activity	No activity

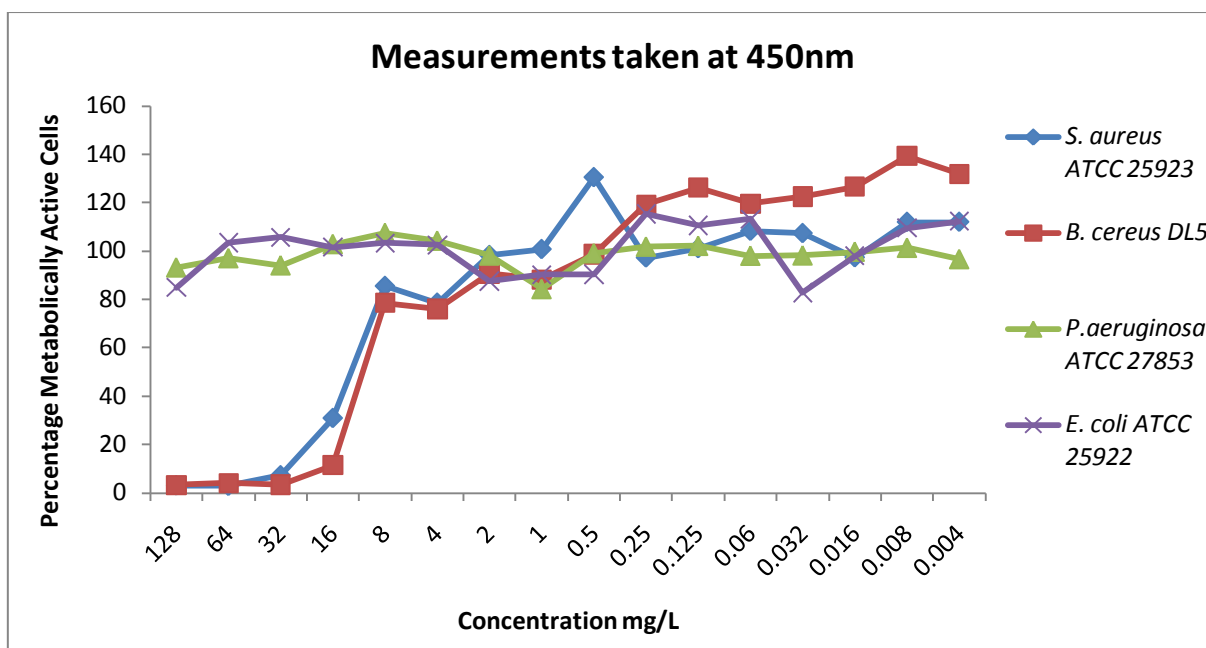
[#] Very high concentrations of the synthetic compound (64-128 mg/L) caused a reduction in the percentage metabolically active cells, but not below the standard cut-off value of 10 %

The 5-methyluridine **233** was used as a negative control for the assay as we anticipated no antibacterial activity to be observed by the un-modified nucleoside. As expected, no activity was observed for the 5-methyluridine **233** in any of the bacterial strains tested.

Using the values obtained for the various compound dilution series, we prepared standard curves for each of the different synthetic compounds, against each of the four different bacterial strains used in the assay (*S. aureus* ATCC 25923, *B. cereus* DL5, *P. aeruginosa* ATCC 27853 and *E. coli* ATCC 25922). These standard curves were then used to determine the MIC values quoted in **Table 24**.

From the entire range of 5-methyluridine derivatives synthesized and tested, only one derivative showed any antibacterial activity - this was found to be the 1-[(6aR,8R,9S,9aR)-tetrahydro-9-hydroxy-2,2,4,4-tetraisopropyl-6H-furo[3,2-f][1,3,5,2,4]trioxadisilocin-8-yl](5-methylpyrimidine)-2,4-(1H,3H)-dione **254**. This compound was active against only the Gram-

positive bacteria, with MIC values of 32 mg/L observed for both *S. aureus* (ATCC 25923) and *B. cereus* (DL5). The standard curve for the active compound **254** is shown schematically in **Graph 18**.



Graph 18 Standard curve of 1-[(6aR,8R,9S,9aR)-tetrahydro-9-hydroxy-2,2,4,4-tetraisopropyl-6H-furo[3,2-f][1,3,5,2,4]trioxadisilocin-8-yl](5-methylpyrimidine)-2,4-(1H,3H)-dione **254**

What is interesting to note from a structure-activity point of view is that the MIC values for this series are:

- | | | | |
|-------|---------------------|-----------------------------|---------|
| (i) | Compound 234 | <i>S. aureus</i> ATCC 25923 | 16 mg/L |
| | | <i>B. cereus</i> DL5 | 16 mg/L |
| (ii) | Compound 239 | <i>S. aureus</i> ATCC 25923 | 8 mg/L |
| | | <i>B. cereus</i> DL5 | 8 mg/L |
| (iii) | Compound 254 | <i>S. aureus</i> ATCC 25923 | 32 mg/L |
| | | <i>B. cereus</i> DL5 | 32 mg/L |

This suggests that converting the base in uridine to the 5-methyl derivative causes a corresponding loss in antibacterial activity for the compound, whereas oxidising the secondary alcohol on the 2'-position of the sugar ring causes a corresponding increase in antibacterial activity for the compound. As such, we can conclude that 1-[(6*aR*,8*R*,9*aR*)-2,2,4,4-tetraisopropyl-9-oxotetrahydro-6*H*-furo[3,2-*f*][1,3,5,2,4]trioxadisilocin-8-yl]pyrimidine-2,4-(1*H*,3*H*)dione **239** was the best compound out of both the "first generation" and "second generation" of nucleoside derivatives for antibacterial activity.

At this point, we then screened all of our silanols for antibacterial activity, based on the interesting results obtained for *tert*-butyldiphenylsilanol **145** in the original assays. The antibacterial activity for the synthetic compounds was determined using the modified MIC determination assay, described in greater detail in the introductory sections above. The results of the TTC assay for the various silanols are given in **Table 25**.

Table 25 MICs determined for the various silanols

Compound	<i>S. aureus</i> ATCC 25923	<i>B. cereus</i> DL5	<i>P. aeruginosa</i> ATCC 27853	<i>E. coli</i> ATCC 25922
Triethylsilanol 176	No activity	No activity	No activity	No activity
Tripropylsilanol 256	No activity	No activity	No activity	No activity
Butyldimethylsilanol 258	No activity	No activity	No activity	No activity
<i>tert</i> -butyldimethylsilanol 261	No activity	No activity	No activity	No activity
Tributylsilanol 259	No activity	No activity	No activity	No activity
Triisobutylsilanol 260	No activity	No activity	No activity	No activity
Dimethylhexylsilanol 262	No activity	No activity	No activity	No activity
Trihexylsilanol 263	No activity	No activity	No activity	No activity
Cyclohexyldimethylsilanol 264	No activity	No activity	No activity	No activity
Benzoyldimethylsilanol 265	No activity	No activity	No activity	No activity
Triphenylsilanol 266	No activity	No activity	No activity	No activity
1,3-Dihydroxy-1,1,3,3-tetraisopropylidisiloxane 268	No activity [#]	64 mg/L	No activity [#]	No activity [#]

Very high concentrations of the synthetic compound (64-128 mg/L) caused a reduction in the percentage metabolically active cells, but not below the standard cut-off value of 10 %

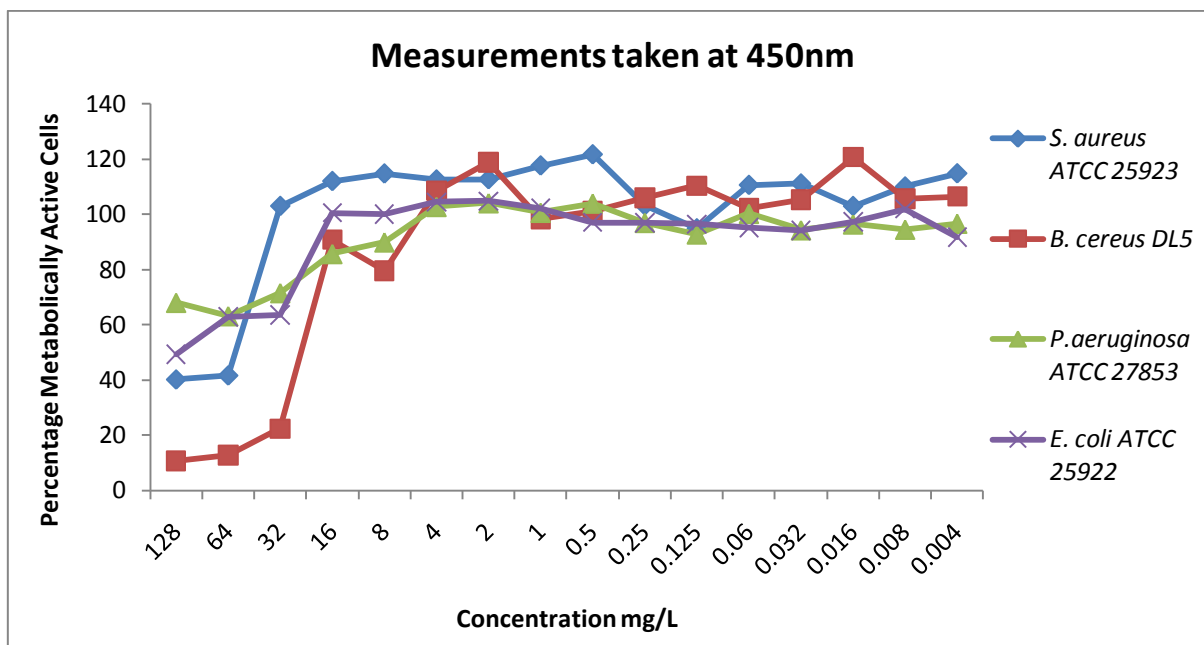
In the initial assays, we obtained MIC values for *tert*-butyldiphenylsilanol **145** of 128 mg/L for *S. aureus* (ATCC 25923) and 64 mg/L for *B. cereus* (DL5). The *tert*-butyldiphenylsilanol **145** was active against only the Gram-positive bacterial strains; however, the MIC values were significantly higher than those obtained for the commercially available antibiotic, ciprofloxacin **153** (MICs of 0.5 mg/L for both *S. aureus* and *B. cereus*). As such, we could not rule out the possibility that the reduction in the number of metabolically active cells could be due to the toxic effects caused by the high concentration of compound in solution, as opposed to the antibacterial activity of the compound itself.

Recently published papers on the use of silanols as a novel class of antimicrobial agents, by Kim and co-workers^{123,124} suggested that *tert*-butyldimethylsilanol could have antibacterial properties. Owing to these publications, we had decided to synthesize a range of silanols covering a large chemical space and subjected them to our modified TTC assay but the results were rather disappointing.

Using the dilution series results for each of these synthetic silanols, we prepared a standard dilution curve for each of the different silanols, against each of the different bacterial strains used in the assay (*S. aureus* ATCC 25923, *B. cereus* DL5, *P. aeruginosa* ATCC 27853 and *E. coli* ATCC 25922). These standard curves were then used to determine the single MIC value reported in **Table 25**. The curve for the only potentially bio-active compound, 1,3-dihydroxy-1,1,3,3-tetraisopropyldisiloxane **268**, is shown schematically in **Graph 19**.

The 1,3-dihydroxy-1,1,3,3-tetraisopropyldisiloxane **268** showed reductions in the percentage of metabolically active cells present at concentrations above 16 mg/L; however, the only bacterial strain that could have a MIC determined for this silanol was *B. cereus*, which only dropped below the pre-defined value of 10 % metabolically active cells at a concentration of 64 mg/L. We speculate that this reduction in cell growth may be caused by a toxic effect that

occurs due to the very high concentration of silanol in the solution and as such do not consider it a positive hit for antibacterial activity.



Graph 19 Standard curve for 1,3-dihydroxy-1,1,3,3-tetraisopropyldisiloxane **268**

6.2.1.3 Conclusions

From the data reported above, one can conclude that in general the protection of uridine **12** and 5-methyluridine **233** with silicon-containing protecting groups did not increase the antibacterial activity for the group as suggested, based on the results obtained for 5'-*O*-(*tert*-butyldiphenylsilyl)uridine **107**. The exception however, occurred when the two silicon atom containing 1,1,3,3-tetraisopropyldisiloxane protecting group was used, albeit with a very low potency.

We found that converting the base in 1-[(6*aR*,8*R*,9*R*,9*aS*)-9-hydroxy-2,2,4,4-tetraisopropyl-tetrahydro-6*H*-furo[3,2-*f*][1,3,5,2,4]trioxadisilocin-8-yl]pyrimidine-2,4(1*H*,3*H*)dione **234** to

the 5-methyl derivative **254** caused a corresponding loss in antibacterial activity for the compound (from 16 mg/L to 32 mg/L for *S. aureus* and *B. cereus* respectively), whereas oxidising the secondary alcohol on the 2'-position of the sugar ring to give **239** caused a corresponding increase in antibacterial activity for the compound (from 16 mg/L to 8 mg/L for *S. aureus* and *B. cereus* respectively). As such, we have concluded that 1-[(6a*R*,8*R*,9a*R*)-2,2,4,4-tetraisopropyl-9-oxotetrahydro-6*H*-furo[3,2-*f*][1,3,5,2,4]trioxadisilocin-8-yl]pyrimidine-2,4(1*H*,3*H*)dione **239** was the best compound out of both the "first generation" and "second generation" of nucleoside derivatives for antibacterial activity.

6.2.2 Confocal Scanning Laser Microscopy (CSLM)

"Biological laser scanning confocal microscopy relies on fluorescence as an imaging mode, this is primarily due to the high degree of sensitivity afforded by the technique and coupled with the ability to specifically target both structural components and dynamic processes in chemically fixed as well as living cells and tissues."

J. Lippincott-Schwartz

Cell Biology and Metabolism Branch, National Institutes of Health

Bethesda, Maryland, USA

Fluorescent dyes are useful in monitoring cell integrity (live versus dead and apoptosis), endocytosis, exocytosis, membrane fluidity, protein trafficking, signal transduction and enzymatic activity. In this study, our aim was to exploit the use of fluorescent dyes to monitor our bacterial cell integrity in order to validate the results obtained for the percentage of metabolically active cells using the TTC assay. The protocols used are described in detail in the sections which follow.

6.2.2.1 Materials and Methods

The two Gram-positive bacterial strains, *S. aureus* ATCC 25923 and *B. cereus* DL5, were used for the confocal scanning laser microscopy study as these were the bacterial strains that had shown the most promising results for bacterial growth inhibition during our TTC assays (to determine the percentage of metabolically active cells present after treatment with our synthetic compounds).

The full description for the methodology used in this study is provided in **Appendix E, Section E.1**, as the description of the culture conditions, preparation of bacterial suspensions, staining techniques and sample analysis using the invert laser scan microscope (LSM 410, Carl Zeiss Jena, Germany) are quite extensive. This is separated from the body of the text to allow for general ease of reading.

6.2.2.2 Results and Discussion

The untreated control *S. aureus* ATCC 25923 cells appeared as small groups of cells creating microcolonies that were quite spread out over the microscope slide in our CSLM images. As expected, all the cells in the untreated control system stained green (viable) after our standard overnight culture conditions. This result confirmed that the method we employed for the isolation, rinsing and staining of the bacterial cells did not have any detrimental effect on the results observed using the LIVE/DEAD® BacLight™ Bacterial Viability Kit. Essentially, our 100 % growth control showed, as expected, that all the cells were alive, as illustrated in **Figure 58**.

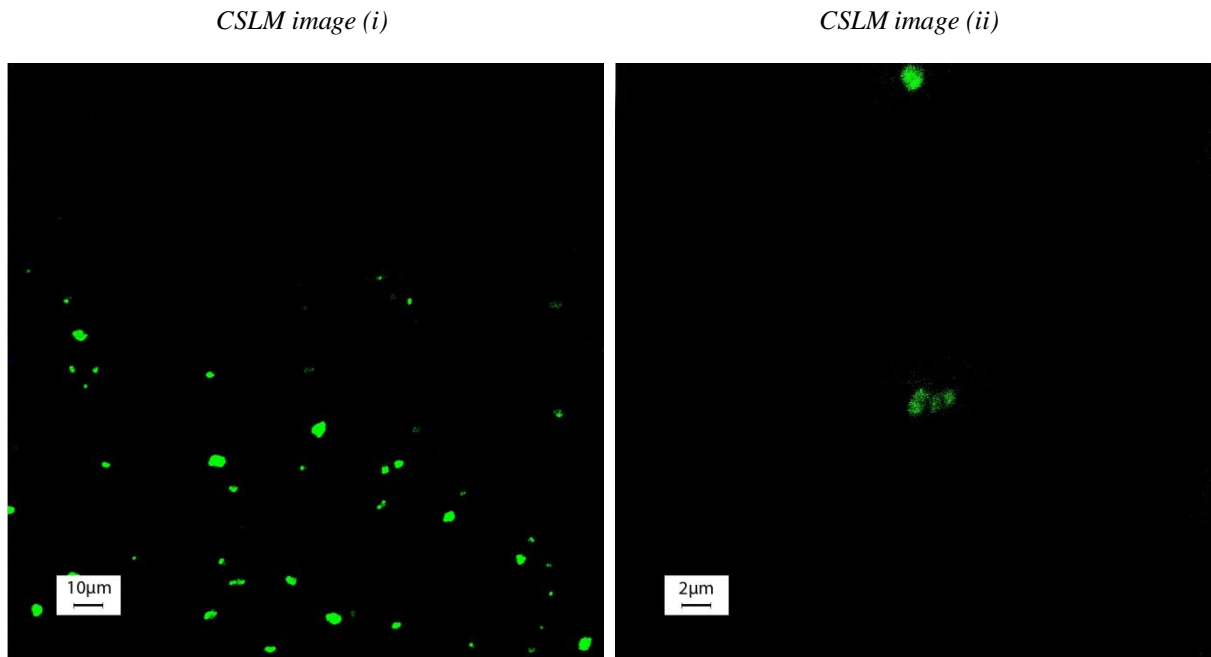


Figure 58 Confocal scanning laser image of untreated *S. aureus* ATCC 25923, with (ii) untreated *S. aureus* ATCC 25923 shown using a $5 \times$ digital zoom to illustrate the microcolonies present (*Note: 50 % laser intensity, 488 nm and 563 nm excitation wavelengths and $63 \times$ oil objective used*)

The study included the antibiotic ciprofloxacin **153** as a growth inhibition control (a 0 % growth control), which was tested at a concentration of 8 mg/L, as this was mid-range for growth inhibition on the standard curve prepared using the TTC assay (described in detail in **Chapter 3, Section 3.2.1.2** and illustrated as **Graph 1**). From the CSLM images we found, as expected, that under the standard overnight treatment conditions with the known antibiotic ciprofloxacin **153**, all of the visible *S. aureus* ATCC 25923 cells stained red (indicating cell death). This result is clearly shown in the image represented **Figure 59**.

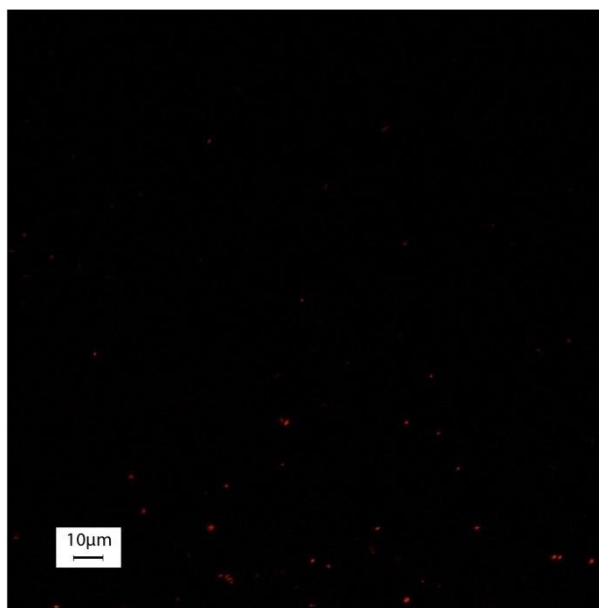


Figure 59 Confocal scanning laser image of *S. aureus* ATCC 25923 treated with ciprofloxacin **153** (concentration = 8 mg/L) for 18 hours (Note: 50 % laser intensity, 488 nm and 563 nm excitation wavelengths and 63 × oil objective used)

The uridine derivative that gave the best overall antibacterial activity with the previously reported TTC assay was 1-[(6a*R*,8*R*,9a*R*)-2,2,4,4-tetraisopropyl-9-oxotetrahydro-6*H*-furo[3,2-*f*][1,3,5,2,4]trioxadisilocin-8-yl]pyrimidine-2,4(1*H*,3*H*)dione **239**. This synthetic compound was studied using CSLM at two concentrations, 4 mg/L and 32 mg/L.

The concentrations were chosen based on the standard curve prepared for the compound **239** using the TTC assay. The concentration of 4 mg/L was chosen as it was found to lie half-way up the standard curve (at approximately 50 % inhibition of cell growth) and the concentration of 32 mg/L was as it was observed in the middle of the range of concentrations that showed complete inhibition of bacterial cell growth (it would thus give an idea as to the actual "kill ratio" for the synthetic compound). The results obtained after overnight treatment of *S. aureus* ATCC 25923 with at two concentrations of compound **239** are illustrated in **Figure 60**.

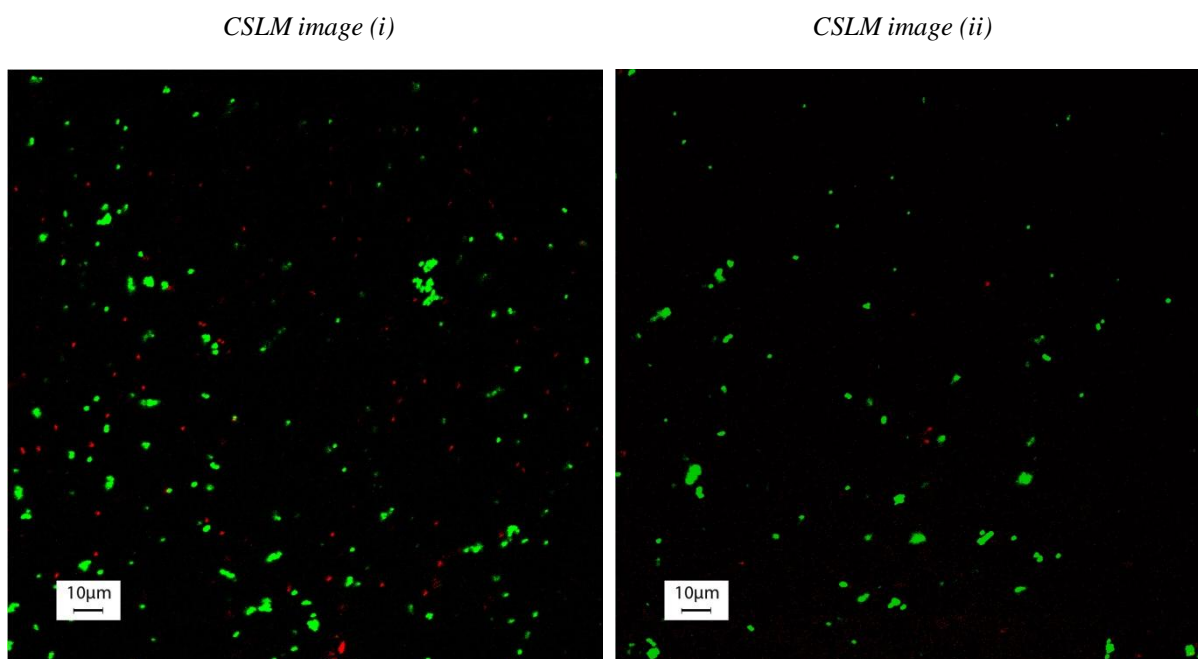


Figure 60 Confocal scanning laser images of *S. aureus* ATCC 25923 treated with 1-[(6a*R*,8*R*,9a*R*)-2,2,4,4-tetraisopropyl-9-oxotetrahydro-6*H*-furo[3,2-*f*][1,3,5,2,4]trioxadisilolcin-8-yl]pyrimidine-2,4(1*H*,3*H*)dione **239** for 18 hours: (i) concentration = 4 mg/L and (ii) concentration = 32 mg/L (Note: 50 % laser intensity, 488 nm and 563 nm excitation wavelengths and 63 × oil objective used)

The CSLM study for compound **239** at a concentration of 4 mg/L showed an average of 87 % metabolically active cells (green) vs. 13 % dead cells (red), calculated by visually counting the red/green cells in five images and then calculating an approximate percentage value for the number of metabolically active cells remaining after treatment. The results from the CSLM study corresponded well with the data previously obtained using the TTC assay, since for compound **239** at a concentration of 4 mg/L, the TTC assay indicated that 90.5 % of the cells were still metabolically active (approximately 10 % of the cells had died). Similarly, the CSLM study for compound **239** at a concentration of 32 mg/L showed an average of 97 % metabolically active cells (green) vs. 3 % dead cells (red), calculated as described above, corresponding well to the TTC assay which indicated that an average 1.8 % of the cells were still metabolically active (suggesting > 95 % of the cells had died).

In CSLM images, *B. cereus* DL5 appeared as individual cells spread out over the microscope slide with no microcolonies observed. All cells in the untreated control system stained green (viable) after the overnight culture conditions. This was as expected and confirmed that our method for the isolation, washing and staining of the bacterial cells was in no way affecting the results obtained using the BacLight Live/Dead Kit (as the 100 % growth control showed all cells alive by CSLM). This result is clearly illustrated in **Figure 61**.

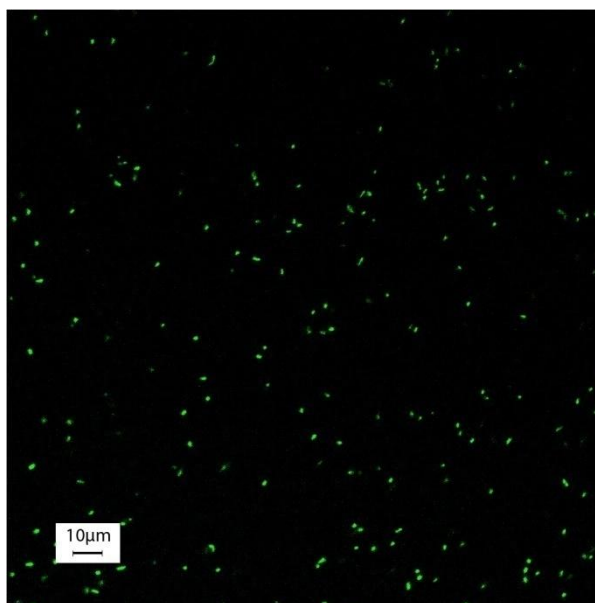


Figure 61 Confocal scanning laser image of untreated *B. cereus* DL5 (Note: 50 % laser intensity, 488 nm and 563 nm excitation wavelengths and 63 × oil objective used)

We included the antibiotic ciprofloxacin **153** as our growth inhibition control for this study and found, as expected, that under overnight treatment conditions with the known antibiotic (at a concentration of 8 mg/L) all of the visible *B. cereus* DL5 cells stained red (indicating cell death). This result is clearly shown in the CSLM image **Figure 62**.

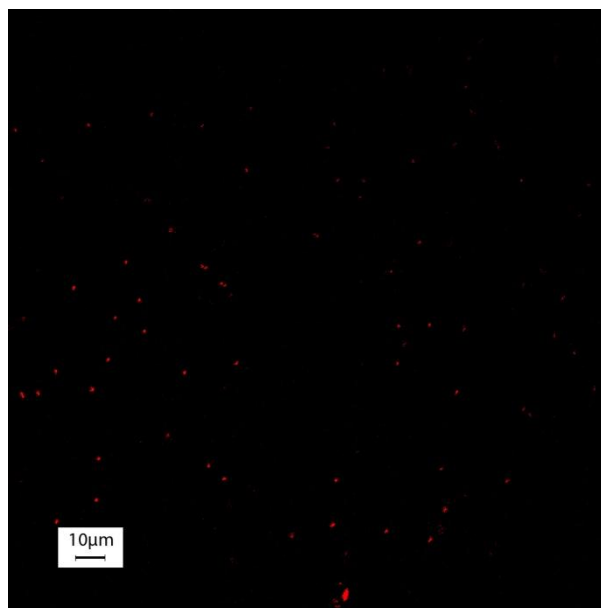


Figure 62 Confocal scanning laser image of *B. cereus* DL5 treated with ciprofloxacin **153** (concentration = 8 mg/L) for 18 hours (*Note: 50 % laser intensity, 488 nm and 563 nm excitation wavelengths and 63 × oil objective used*)

The uridine based compound that gave the best overall antibacterial activity using the TTC assay described previously, 1-[(6*aR*,8*R*,9*aR*)-2,2,4,4-tetraisopropyl-9-oxotetrahydro-6*H*-furo[3,2-*f*][1,3,5,2,4]trioxadisilocin-8-yl]pyrimidine-2,4(1*H*,3*H*)dione **239**, was studied using this CSLM procedure. The results obtained after overnight treatment of *B. cereus* DL5 at two concentrations of compound **239** (4 mg/L and 32 mg/L) are illustrated in **Figure 63**.

The concentration of 4 mg/L was chosen as it was found to occur midway on the standard curve (in the range of 50 % inhibition of cell growth) prepared for the compound **239** using the TTC assay. The compound concentration of 32 mg/L was also chosen based on the standard curve, it was observed in the middle of the range of concentrations that showed complete inhibition of bacterial cell growth and so would give an idea as to the actual "kill ratio" for the synthetic compound.

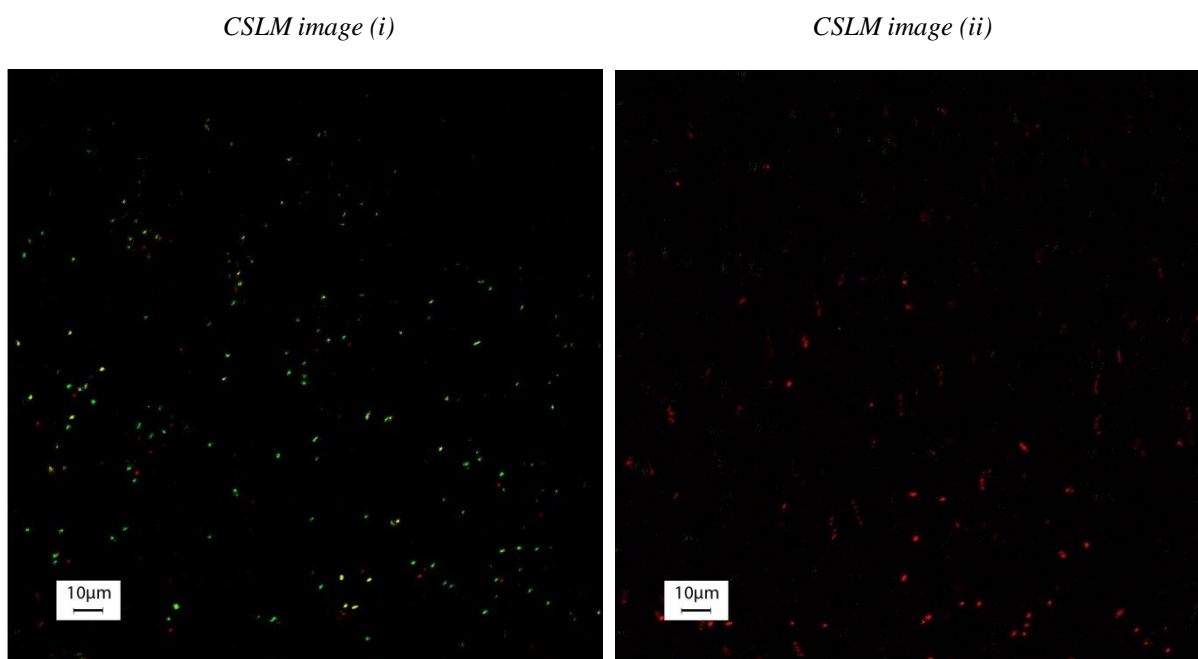


Figure 63 Confocal scanning laser images of *B. cereus* DL5 treated with 1-[(6a*R*,8*R*,9a*R*)-2,2,4,4-tetraisopropyl-9-oxotetrahydro-6*H*-furo[3,2-*f*][1,3,5,2,4]trioxadisilocin-8-yl]pyrimidine-2,4(1*H*,3*H*)dione **239** for 18 hours: (i) concentration = 4 mg/L and (ii) concentration = 32 mg/L (Note: 50 % laser intensity, 488 nm and 563 nm excitation wavelengths and 63 × oil objective used)

The results from the CSLM study for compound **239**, calculated by visually counting the red/green cells in five images and then calculating an approximate percentage value for the number of metabolically active cells remaining after treatment, showed that:

- (i) for compound **239** at a concentration of 4 mg/L, an average of 55 % of the cells are metabolically active (green) vs. 45 % dead cells (red)
- (ii) for compound **239** at a concentration of 32 mg/L, an average of 6 % of the cells are metabolically active (green) vs. 94 % dead cells (red)

These results corresponded well with the data previously obtained using the TTC assay, which showed that:

- (i) for compound **239** at a concentration of 4 mg/L, approximately 61.4 % of the cells were still metabolically active (approximately 40 % of the cells had died)
- (ii) for compound **239** at a concentration of 32 mg/L, approximately 3.6 % of the cells were still metabolically active (suggesting > 95 % of the cells had died).

6.2.2.3 Conclusions

From the CSLM study performed we validated that the results obtained from the previously performed TTC assay for the determination of the percentage of metabolically active cells present after treatment with antibiotics and synthetic compounds were accurate representations of what was occurring in our overnight bacterial cultures.

Interestingly, the CSLM images for both *S. aureus* ATCC 25923 and *B. cereus* DL5 treated with compound **239** at various concentrations showed no visible cells stained yellow, thus indicating cell injury. This suggests that the synthetic compound **239** is bacteriocidal and is inactivating the cells, not simply inhibiting their growth.

Furthermore, the BacLight kit specifically works on membrane integrity and considering that we did not observe any yellow stained cells, this could suggest that the compound **239** affects the cell membrane itself (possibly by disruption). This evidence would support our earlier proposal that the compound **239** is membrane active.

6.2.3 Scanning Electron Microscopy (SEM)

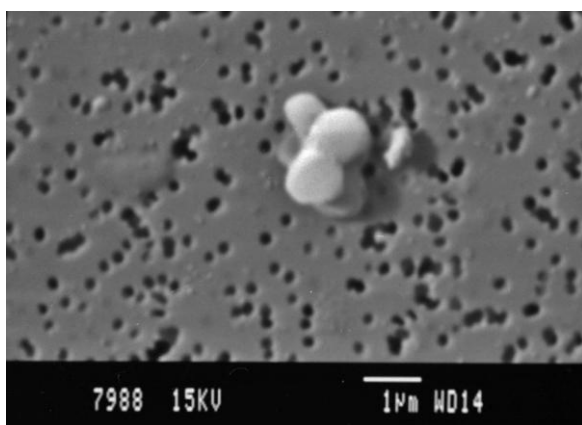
6.2.3.1 Materials and Methods

The two Gram-positive bacterial strains, *S. aureus* ATCC 25923 and *B. cereus* DL5, were selected for the scanning electron microscopy study as these were the bacterial strains that had shown the most promising results for bacterial growth inhibition during our TTC assays (to determine the percentage of metabolically active cells present after treatment with our synthetic compounds).

The full description for the methodology used in this study is provided in **Appendix E, Section E.2**, as the description of the culture conditions, dehydration procedure, critical point drying, mounting and sample analysis using the scanning electron microscope (JSM-840, JEOL Ltd, Tokyo, Japan) are quite extensive. This is separated from the body of the text to allow for general ease of reading.

6.2.3.2 Results and Discussion

Micrograph a



Micrograph b



Figure 64 Scanning electron micrographs of the untreated control 18 hour bacterial cultures (diluted to 10^6 cfu/mL in nutrient broth) for: (a) *S. aureus* ATCC 25923 (magnification = 14 000 ×, probe current = 1×10^{-9} , keV = 15) and (b) *B. cereus* DL5 (magnification = 8 000 ×, probe current = 3×10^{-10} , keV = 10)

The untreated control *S. aureus* ATCC 25923 cells appeared as small clusters or microcolonies which were composed of smooth spheres approximately 1.0-1.4 μm in diameter (shown below in **Figure 64**, *micrograph a*), while scanning electron micrographs of the control untreated *B. cereus* DL5 showed individual rods of approximately 2.5-3.0 μm in length with smooth surfaces spread out over the filter paper (**Figure 64**, *micrograph b*).

The relatively smooth surfaces of the bacterial cells, present for both the untreated *S. aureus* and *B. cereus* indicate that no cell damage has occurred in our systems, even though it had been previously noted that the stringent sample preparation procedures for SEM may result in artifact formation.¹²⁵

In comparison, the overnight bacterial cultures that were subsequently treated with an 8 mg/L solution of the known antibiotic, ciprofloxacin **153**, showed severe cell damage. *S. aureus* ATCC 25923 (**Figure 65**, *micrograph a*) showed interesting distortions to the spherical nature of the cell (*ie*: cell shape), while the rods for *B. cereus* DL5 (**Figure 65**, *micrograph b*) showed significant surface indentations and in some cases, complete rupturing of the cells.

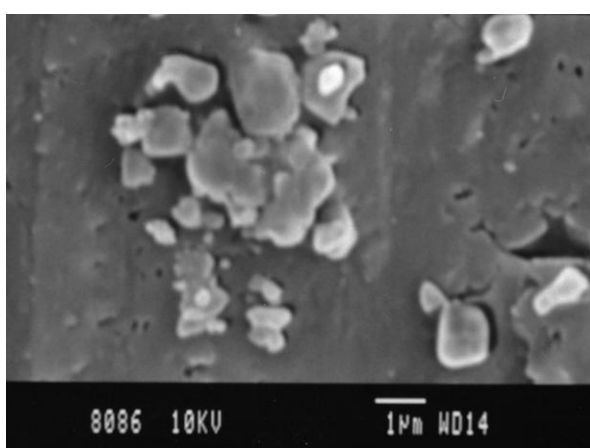
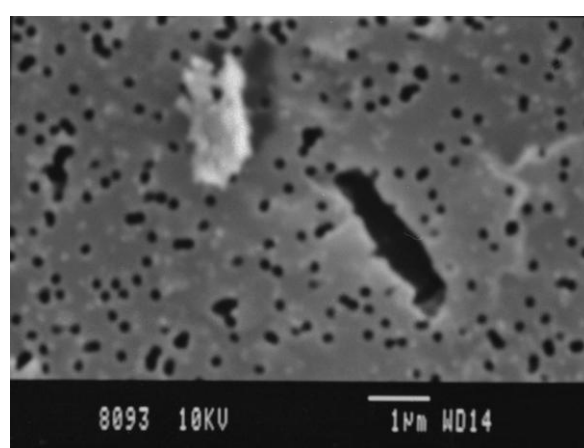
Micrograph a*Micrograph b*

Figure 65 Scanning electron micrographs of the bacterial cultures which had been treated with the known antibiotic ciprofloxacin **153** at a concentration of 8 mg/L for 22 hours: (a) *S. aureus* ATCC 25923 (magnification = 12 000 \times , probe current = 3×10^{-10} , keV = 10) and (b) *B. cereus* DL5 (magnification = 15 000 \times , probe current = 3×10^{-10} , keV = 10)

The next set in the study compared bacterial cells treated with uridine **12** (a negative control for the inhibition of cell growth as it did not affect the percentage of metabolically active cells present after treatment as determined by the TTC assay) against cells treated with two concentrations, both in the active and non-active range, of 5'-*O*-(*tert*-butyldiphenylsilyl)uridine **107**. Results are shown in **Figure 66** on the following page.

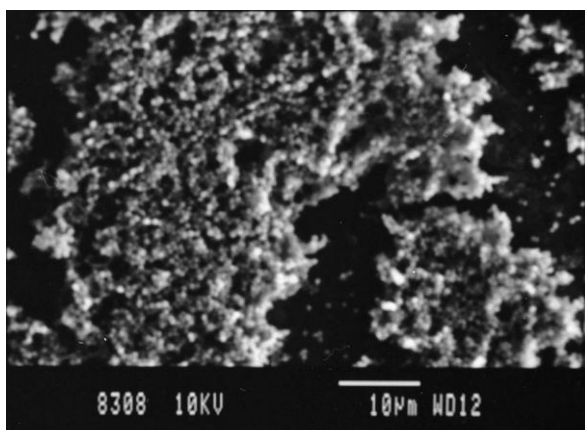
As expected, *S. aureus* (**Figure 66, micrograph a**) and *B. cereus* (**Figure 66, micrograph b**) cells treated with uridine **12** at a concentration of 0.5 mg/L (selected as it was mid-range on the standard curve from the TTC assay) showed prolific bacterial growth. In general, all cells for both bacterial strains used, showed no surface indentations or distortions to the cell shape, indicating that the unmodified nucleoside had no effect on the bacterial strains tested.

Two concentrations of 5'-*O*-(*tert*-butyldiphenylsilyl)uridine **107** were selected for the study based on the standard curve obtained using the results from the TTC assay. They were: (i) 0.25 mg/L which was found midway in the range of no inhibition of growth, and (ii) 64 mg/L which was found midway in the range of observed inhibition of cellular growth. As observed for the bacteria treated with unmodified uridine **12**, the cells treated with low concentrations of compound **107** [*S. aureus* (**Figure 66, micrograph c**) and *B. cereus* (**Figure 66, micrograph d**)] showed no surface indentations or observable distortions to the cell shape, indicating that at low concentrations outside of the active range for compound **107**, there was no specific effect on the cellular coatings for the bacterial strains tested. Note that for *B. cereus* (**Figure 66, micrograph d**) the rods were surrounded by what appeared to be extracellular polymeric substances (EPS).

We found that when *S. aureus* and *B. cereus* were treated with high concentrations of compound **107** (midway into the active range for the compound), inhibition of growth was clearly observed. At the same time, we noted that for *S. aureus* (**Figure 66, micrograph e**) the cell surface remained smooth, but distortions occurred in the spherical shape of the cells. For *B. cereus* (**Figure 66, micrograph f**), we observed that the cells had aggregated together, appeared to have rough surfaces and had ruptured in a few of the examples.

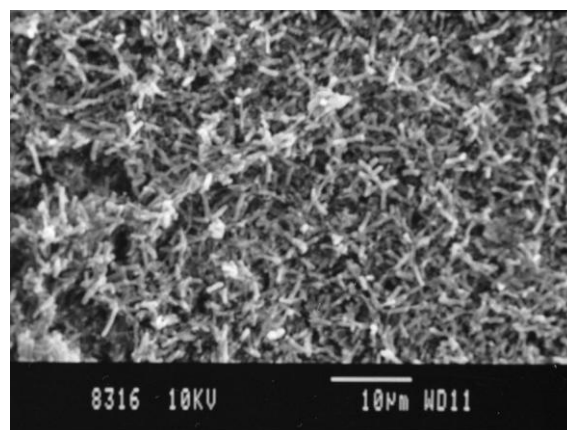
Micrograph a - S. aureus ATCC 25923

Uridine 12 (concentration = 0.5 mg/L)



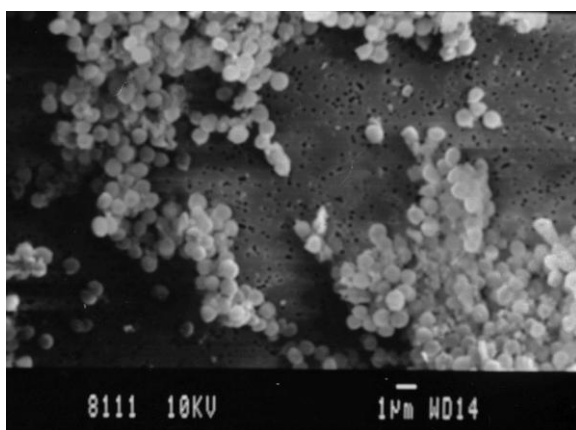
Micrograph b - B. cereus DL5

Uridine 12 (concentration = 0.5 mg/L)



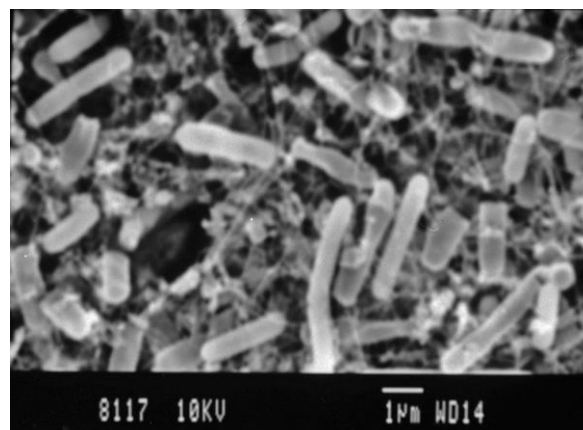
Micrograph c - S. aureus ATCC 25923

Compound 107 (concentration = 0.25 mg/L)



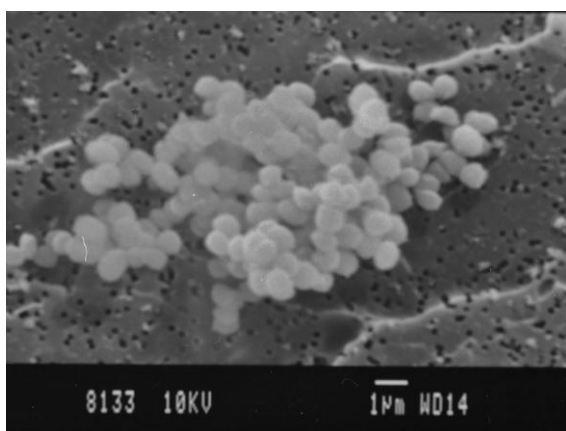
Micrograph d - B. cereus DL5

Compound 107 (concentration = 0.25 mg/L)



Micrograph e - S. aureus ATCC 25923

Compound 107 (concentration = 64 mg/L)



Micrograph f - B. cereus DL5

Compound 107 (concentration = 64 mg/L)



Figure 66 Scanning electron micrographs of the bacterial cultures which had been treated with the synthetic compounds for 22 hours: (a) magnification = 2 000 ×, probe current = 6×10^{-9} , keV = 10, (b) magnification = 2 000 ×, probe current = 6×10^{-10} , keV = 10, (c)

magnification = 5 000 ×, probe current = 3×10^{-10} , keV = 10 and (d) magnification = 10 000 ×, probe current = 3×10^{-10} , keV = 10, (e) magnification = 8 000 ×, probe current = 3×10^{-10} , keV = 10 and (f) magnification = 5 000 ×, probe current = 6×10^{-10} , keV = 10

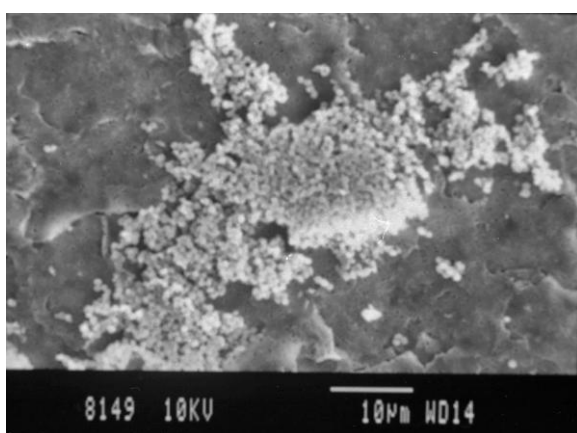
From the TTC assay (described in *Section 6.2.1.2*), we found that converting the base in 1-[(6a*R*,8*R*,9*R*,9a*S*)-9-hydroxy-2,2,4,4-tetraisopropyltetrahydro-6*H*-furo[3,2-*f*][1,3,5,2,4]-trioxadisilocin-8-yl]pyrimidine-2,4(1*H*,3*H*)dione **234** to the 5-methyl derivative **254** caused a corresponding loss in antibacterial activity for the compound (from 16 mg/L to 32 mg/L for *S. aureus* and *B. cereus* respectively), whereas oxidising the secondary alcohol on the 2'-position of the sugar ring to give compound **239**, caused a corresponding increase in antibacterial activity for the compound (from 16 mg/L to 8 mg/L for *S. aureus* and *B. cereus* respectively). As such, we previously concluded that 1-[(6a*R*,8*R*,9a*R*)-2,2,4,4-tetraisopropyl-9-oxotetrahydro-6*H*-furo[3,2-*f*][1,3,5,2,4]trioxadisilocin-8-yl]pyrimidine-2,4(1*H*,3*H*)dione **239** was the best compound for antibacterial activity coming out of both the "first generation" and "second generation" of nucleoside derivatives.

We further wished to investigate these findings by conducting a structure activity relationship (SAR) study on these compounds (**234**, **254** and **239**) using SEM in order to determine if there was some fundamental structural change in the bacteria which would suggest the active pathways. For the SAR comparison, the overnight bacterial cultures were subsequently treated with solutions of each of the test compounds **234**, **254** and **239** at two concentrations of each (one in the active range of the compound and one in the non-active range of the compound – as shown on the standard curve obtained using the results from the TTC assay). The results obtained for *S. aureus* ATCC 25923 are depicted in **Figure 67** and the results obtained for *B. cereus* DL5 are shown in **Figure 68**.

Two concentrations of 1-[(6a*R*,8*R*,9*R*,9a*S*)-9-hydroxy-2,2,4,4-tetraisopropyltetrahydro-6*H*-furo[3,2-*f*][1,3,5,2,4]trioxadisilocin-8-yl]pyrimidine-2,4(1*H*,3*H*)dione **234** were selected for the study, based on the standard curve obtained using the results from the TTC assay. They were: (i) 0.25 mg/L which was found midway in the range of no inhibition of growth, and (ii) 32 mg/L which was found midway in the range of observed inhibition of cellular growth.

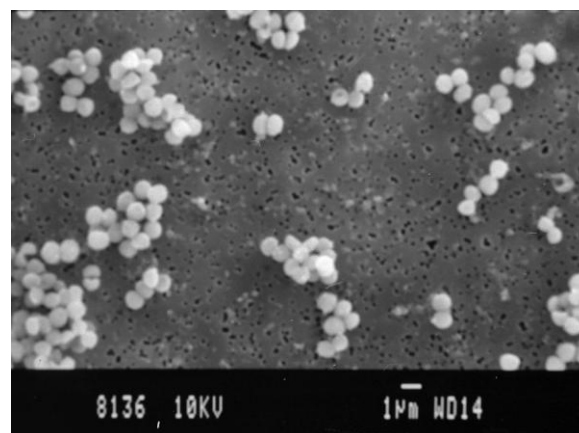
Micrograph a - S. aureus ATCC 25923

Compound 234 (concentration = 0.25 mg/L)



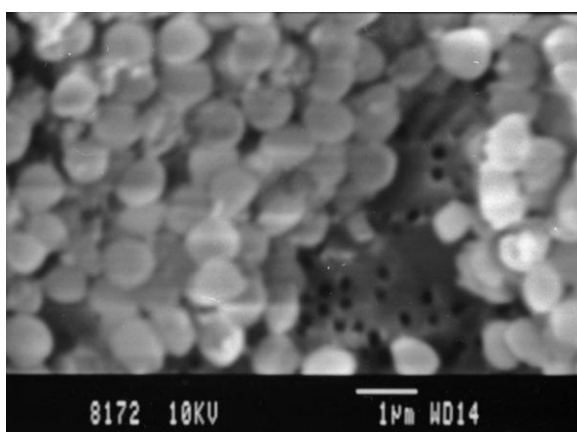
Micrograph b - S. aureus ATCC 25923

Compound 234 (concentration = 32 mg/L)



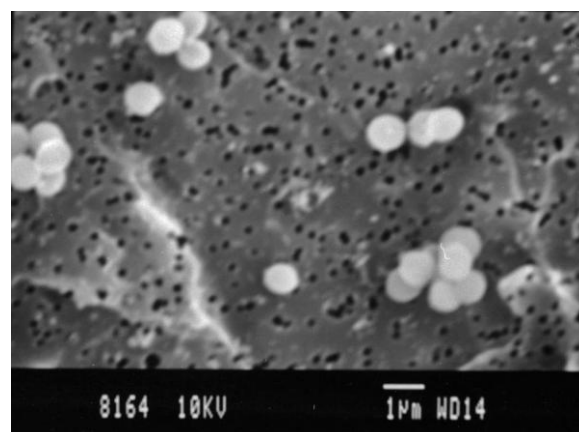
Micrograph c - S. aureus ATCC 25923

Compound 254 (concentration = 0.25 mg/L)



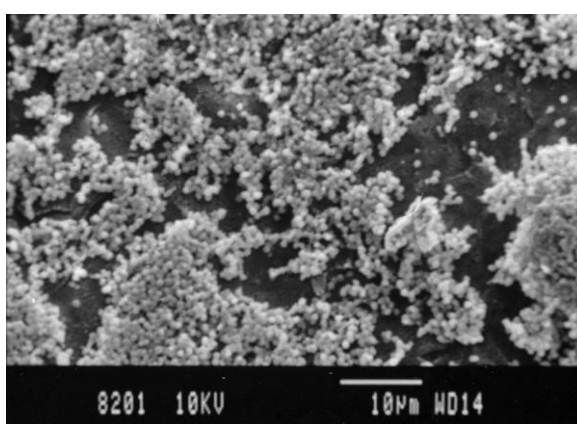
Micrograph d - S. aureus ATCC 25923

Compound 254 (concentration = 64 mg/L)



Micrograph e - S. aureus ATCC 25923

Compound 239 (concentration = 0.12 mg/L)



Micrograph f - S. aureus ATCC 25923

Compound 239 (concentration = 32 mg/L)

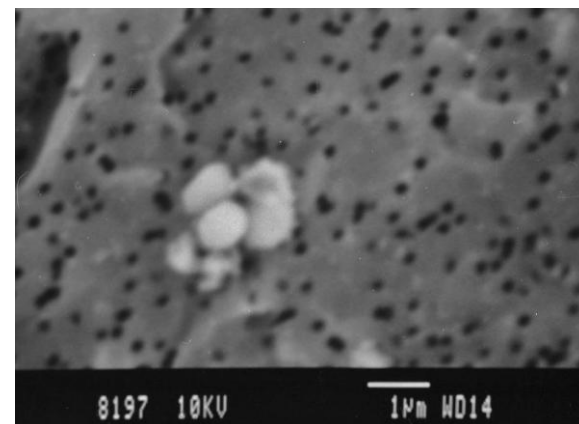


Figure 67 SAR study with scanning electron micrographs of the *S. aureus* ATCC 25923 cultures (treated with the synthetic compounds **234**, **254** and **239** for 22 hours): (a) magnification = 2 000 ×, probe current = 6×10^{-10} , keV = 10, (b) magnification = 5 000 ×,

probe current = 3×10^{-10} , keV = 10, (c) magnification = 15 000 \times , probe current = 3×10^{-10} , keV = 10 and (d) magnification = 10 000 \times , probe current = 3×10^{-10} , keV = 10, (e) magnification = 2 000 \times , probe current = 3×10^{-10} , keV = 10 and (f) magnification = 15 000 \times , probe current = 3×10^{-10} , keV = 10

As observed for the bacteria treated with unmodified uridine **12** (**Figure 66**, *micrograph a* above), the cells for *S. aureus* (**Figure 67**, *micrograph a*) showed no surface indentations or observable distortions to the cell shape, indicating that treatment at low concentrations outside the active range for the compound, 1-[(6*aR*,8*R*,9*R*,9*aS*)-9-hydroxy-2,2,4,4-tetraisopropyltetrahydro-6*H*-furo[3,2-*f*][1,3,5,2,4]trioxadisilocin-8-yl]pyrimidine-2,4(1*H*,3*H*)dione **234**, had no specific effect on the macroscopic cellular structures for the bacterial strains tested. Whereas, we found that when *S. aureus* (**Figure 67**, *micrograph b*) was treated with a high concentration of compound **234** (midway into the active range for the compound), we observed that the cells had apparently aggregated together (more so than was initially observed in the corresponding controls), and although the cell surface remained smooth, distortions occurred in the spherical shape of the cells.

In a similar manner, two concentrations of 1-[(6*aR*,8*R*,9*S*,9*aR*)-tetrahydro-9-hydroxy-2,2,4,4-tetraisopropyl-6*H*-furo[3,2-*f*][1,3,5,2,4]trioxadisilocin-8-yl](5-methylpyrimidine)-2,4-(1*H*,3*H*)-dione **254** were selected for the study based on the standard curve obtained using the results from the TTC assay. They were: (i) 0.25 mg/L which was found midway in the range of no inhibition of growth, and (ii) 64 mg/L which was found midway in the range of observed inhibition of cellular growth.

Again, the cells for *S. aureus* (**Figure 67**, *micrograph c*) showed no surface indentations or major distortions to the cell shape, indicating that at low concentrations outside the active range for the compound, 1-[(6*aR*,8*R*,9*S*,9*aR*)-tetrahydro-9-hydroxy-2,2,4,4-tetraisopropyl-6*H*-furo[3,2-*f*][1,3,5,2,4]trioxadisilocin-8-yl](5-methylpyrimidine)-2,4-(1*H*,3*H*)-dione **254**, had no specific effect on the cellular surfaces for the bacterial strains tested. We did however observe that when the *S. aureus* (**Figure 67**, *micrograph d*) was treated with a high concentration of compound **254** (midway into the active range for the compound), inhibition

of growth was clearly observed (based on the TTC assay) and we again noted that, in some instances, the cells had apparently aggregated together.

Finally, two concentrations of the active compound, 1-[(6*aR*,8*R*,9*aR*)-2,2,4,4-tetraisopropyl-9-oxotetrahydro-6*H*-furo[3,2-*f*][1,3,5,2,4]trioxadisilocin-8-yl]pyrimidine-2,4(1*H*,3*H*)dione **239**, were selected for the study based on the standard curve obtained previously. They were: (i) 0.12 mg/L which was found midway in the range of no inhibition of growth, and (ii) 32 mg/L which was found midway in the range of observed inhibition of cellular growth.

Interestingly, the differences observed when comparing the concentrations for compound **239** were much more marked. As observed for the bacteria treated with unmodified uridine **12** (**Figure 66**, *micrograph a* above), the cells for *S. aureus* (**Figure 67**, *micrograph e*) showed no surface indentations or any observable distortions to the cell shape, indicating that at low concentrations outside the active range for the compound, 1-[(6*aR*,8*R*,9*aR*)-2,2,4,4-tetraisopropyl-9-oxotetrahydro-6*H*-furo[3,2-*f*][1,3,5,2,4]trioxadisilocin-8-yl]pyrimidine-2,4-(1*H*,3*H*)dione **239**, had no specific effect on the cellular coatings for the bacterial strains tested.

As expected, we found that when the *S. aureus* (**Figure 67**, *micrograph f*) was treated with a high concentration of compound **239** (midway into the active range for the compound), inhibition of growth was clearly observed. Interestingly, compound **239** was the only *S. aureus* example where we observed that the cells had aggregated together and where the cell surface appeared to be rough (when compared to the corresponding control) with rupturing in a few examples. The significant bacterial cell wall damage observed may suggest that for the active compound **239** a possible difference in the mechanism of action may be occurring for the *S. aureus* bacterial cells. The qualitative evidence, i.e. obvious cellular damage/rupturing and cellular aggregation; suggests that compound **239** targets the wall – possibly interacting with the wall peptidoglycan molecules and causing cross-linkages between cells. But this could not be confirmed by our qualitative observations, as the filtering technique used to prepare the samples could also have contributed to the aggregation of cells which was observed.

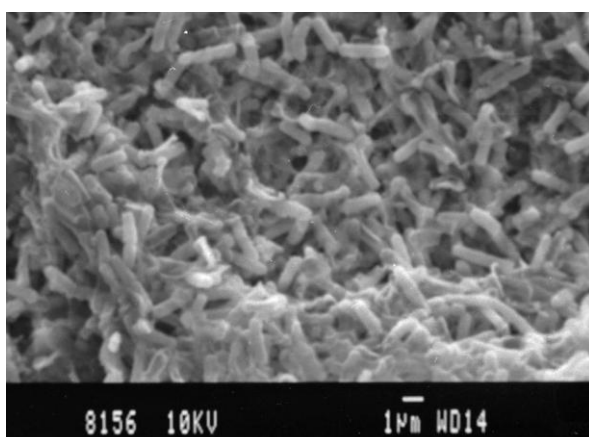
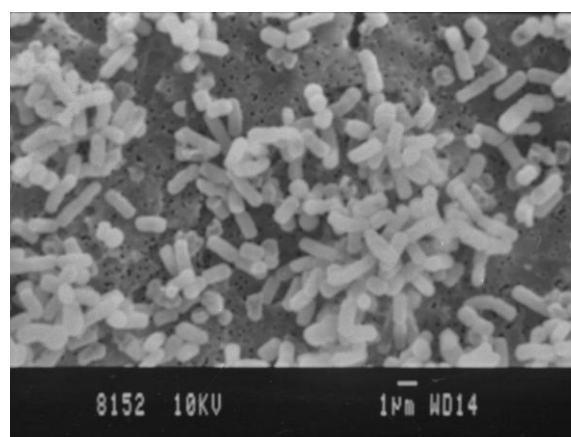
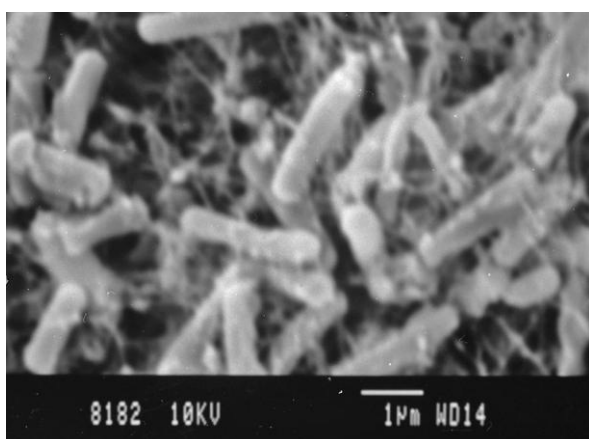
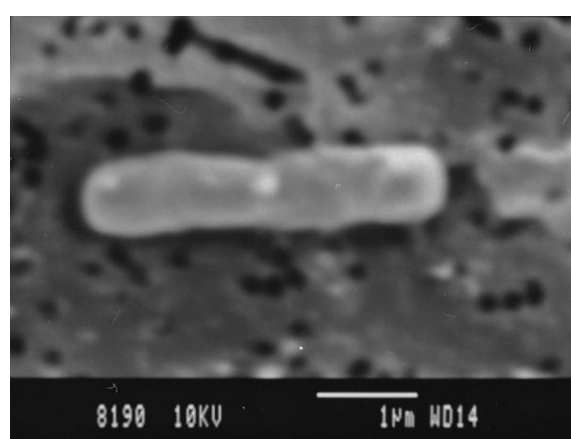
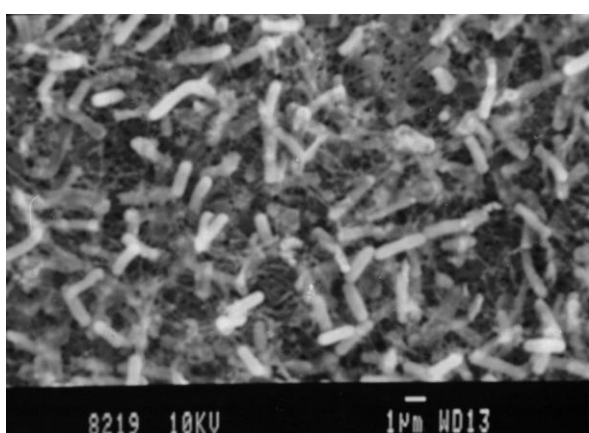
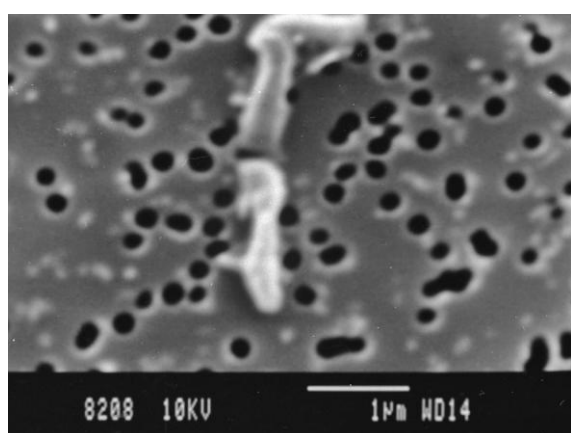
*Micrograph a – B. cereus DL5**Compound 234 (concentration = 0.25 mg/L)**Micrograph b – B. cereus DL5**Compound 234 (concentration = 32 mg/L)**Micrograph c – B. cereus DL5**Compound 254 (concentration = 0.25 mg/L)**Micrograph d – B. cereus DL5**Compound 254 (concentration = 0.64 mg/L)**Micrograph e – B. cereus DL5**Compound 239 (concentration = 0.12 mg/L)**Micrograph f – B. cereus DL5**Compound 239 (concentration = 32 mg/L)*

Figure 68 SAR study with scanning electron micrographs of the *B. cereus* DL5 cultures (treated with the synthetic compounds **234**, **254** and **239** for 22 hours): (a) magnification = 5 000 ×, probe current = 3×10^{-10} , keV = 10, (b) magnification = 5 000 ×, probe current = $3 \times$

10^{-10} , keV = 10, (c) magnification = 15 000 ×, probe current = 3×10^{-10} , keV = 10 and (d) magnification = 25 000 ×, probe current = 3×10^{-10} , keV = 10, (e) magnification = 5 000 ×, probe current = 6×10^{-10} , keV = 10 and (f) magnification = 25 000 ×, probe current = 3×10^{-10} , keV = 10

Two concentrations of 1-[(6*aR*,8*R*,9*R*,9*aS*)-9-hydroxy-2,2,4,4-tetraisopropyltetrahydro-6*H*-furo[3,2-*f*][1,3,5,2,4]trioxadisilocin-8-yl]pyrimidine-2,4(1*H*,3*H*)dione **234** were selected for the study based on the standard curve obtained using the results from the TTC assay. They were: (i) 0.25 mg/L which was found midway in the range of no inhibition of growth, and (ii) 32 mg/L which was found midway in the range of observed inhibition of cellular growth.

As observed for the bacteria treated with unmodified uridine **12** (**Figure 66**, *micrograph b* above), the cells for *B. cereus* (**Figure 68**, *micrograph a*) showed no surface indentations or observable distortions to the cell shape, indicating that at low concentrations outside the active range for the compound, 1-[(6*aR*,8*R*,9*R*,9*aS*)-9-hydroxy-2,2,4,4-tetraisopropyltetrahydro-6*H*-furo[3,2-*f*][1,3,5,2,4]trioxadisilocin-8-yl]pyrimidine-2,4(1*H*,3*H*)dione **234**, had no specific effect on the cellular coatings for the *B. cereus* bacteria tested. Whereas, we found that when the *B. cereus* (**Figure 68**, *micrograph b*) was treated with a high concentration of compound **234** (midway into the active range for the compound), inhibition of growth was clearly observed. At the same time, we observed that although the cell surface remained smooth, shortening of the rods had occurred (from an approximate average length of 6.30 μm in **Figure 68**, *micrograph a*, down to an average length of 4.32 μm in **Figure 68**, *micrograph b* – based on the manual mean random measurement of ten individual rods in each micrograph). This shortening of the rod-length usually implies that the compound has an effect on the cell wall, similar to the action of penicillin-based antibiotics which affect cell wall synthesis.^{123b} The rod-shortening is also an indication of bacterial stress, for example, when bacterial cells are starvation-stressed, it is generally noted that they will shrink in size.

In a similar manner, two concentrations of 1-[(6*aR*,8*R*,9*S*,9*aR*)-tetrahydro-9-hydroxy-2,2,4,4-tetraisopropyl-6*H*-furo[3,2-*f*][1,3,5,2,4]trioxadisilocin-8-yl](5-methylpyrimidine)-2,4-(1*H*,3*H*)-dione **254** were selected for the study based on the standard curve obtained using the

results from the TTC assay. They were: (i) 0.25 mg/L which was found midway in the range of no inhibition of growth, and (ii) 64 mg/L which was found midway in the range of observed inhibition of cellular growth.

Again, the cells for *B. cereus* (**Figure 68**, *micrograph c*) showed no surface indentations or major distortions to the cell shape; the rods were also surrounded by web-like strands, which is suggestive of extracellular polymeric substances (EPS), based on observations of SEM micrographs in other studies.^{123c} This indicated that at low concentrations outside the active range for the 1-[(6*R*,8*R*,9*S*,9*aR*)-tetrahydro-9-hydroxy-2,2,4,4-tetraisopropyl-6*H*-furo[3,2-*f*][1,3,5,2,4]trioxadisilocin-8-yl](5-methylpyrimidine)-2,4-(1*H*,3*H*)-dione **254**, the compound had no specific effect on the cellular coatings for the bacterial strains tested.

We did however observe that when *B. cereus* (**Figure 68**, *micrograph d*) was treated with a high concentration of compound **254** (midway into the active range for the compound), a significant inhibition of bacterial growth occurred. We also noted that, in most instances, the rods showed major surface indentations.

Finally, two concentrations of the active compound, 1-[(6*R*,8*R*,9*aR*)-2,2,4,4-tetraisopropyl-9-oxotetrahydro-6*H*-furo[3,2-*f*][1,3,5,2,4]trioxadisilocin-8-yl]pyrimidine-2,4-(1*H*,3*H*)dione **239**, were selected for the study based on the standard curve obtained previously. They were: (i) 0.12 mg/L which was found midway in the range of no inhibition of growth, and (ii) 32 mg/L which was found midway in the range of observed inhibition of cellular growth.

Interestingly, the differences observed when comparing the concentrations for compound **239** were more severe. As observed for the bacteria treated with unmodified uridine **12** (**Figure 66**, *micrograph b* above), the cells for *B. cereus* (**Figure 68**, *micrograph e*) showed no surface indentations or any observable distortions to the cell shape, indicating that at low concentrations outside the active range for the compound, 1-[(6*R*,8*R*,9*aR*)-2,2,4,4-tetraisopropyl-9-oxotetrahydro-6*H*-furo[3,2-*f*][1,3,5,2,4]trioxadisilocin-8-yl]pyrimidine-2,4-(1*H*,3*H*)dione **239**, had no specific effect on the cell wall for the bacterial strains tested.

As expected, we found that when the *B. cereus* (**Figure 68**, *micrograph f*) was treated with a high concentration of compound **239** (midway into the active range for the compound), inhibition of growth was clearly observable. Interestingly, compound **239** was the only *B. cereus* example where we also observed not only major indentations on the cell surface, but also appeared surface rupturing in a few of the examples. The significant bacterial cell wall damage may suggest that for the highly active compound **239** the mode of action against the *B. cereus* bacterial cells correlates directly to cell wall activity. This is supported by the qualitative evidence described above, including the shortening of the cells and the obvious cell surface damage by caused by distortion.

6.2.3.3 Conclusions

We showed that Gram-positive bacterial cells treated with uridine **12** at a concentration of 0.5 mg/L showed no inhibition of bacterial growth. In general, all cells for both bacterial strains used, showed no surface indentations or distortions to the cell shape, indicating that the unmodified nucleoside had no effect on the bacterial strains tested. In comparison, we were able to demonstrate that *S. aureus* ATCC 25923 cells treated with high concentrations of 5'-*O*-(*tert*-butyldiphenylsilyl)uridine **107** showed smooth cell surfaces, but distortions occurred in the spherical shape of the cells. In the case of *B. cereus* DL5, we observed that the cells had aggregated together, appeared to have rough surfaces and had ruptured in a few of the examples.

From the data reported above (*Section 6.2.1.2*), we showed that converting the base in 1-[(6*aR*,8*R*,9*R*,9*aS*)-9-hydroxy-2,2,4,4-tetraisopropyltetrahydro-6*H*-furo[3,2-*f*][1,3,5,2,4]trioxadisilocin-8-yl]pyrimidine-2,4(1*H*,3*H*)dione **234** to the 5-methyl derivative **254** caused a corresponding loss in antibacterial activity for the compound (from 16 mg/L to 32 mg/L for *S. aureus* and *B. cereus* respectively), whereas oxidising the secondary alcohol on the 2'-position of the sugar ring to give **239** caused a corresponding increase in antibacterial activity for the compound (from 16 mg/L to 8 mg/L for *S. aureus* and *B. cereus* respectively). As such, we indicated that 1-[(6*aR*,8*R*,9*aR*)-2,2,4,4-tetraisopropyl-9-oxotetrahydro-6*H*-furo[3,2-*f*][1,3,5,2,4]trioxadisilocin-8-yl]pyrimidine-2,4(1*H*,3*H*)dione **239** was the compound with the best

antibacterial activity out all of the "first generation" and "second generation" of nucleoside derivatives.

These results were supported by our SEM studies, in which we were able to show that all of the compounds **234**, **254** and **239** showed a major reduction in bacterial growth at high concentrations. In addition, we were able to visualize how compound **239** was the only example, where significant bacterial cell wall damage (major indentations on the cell surface, as well as surface rupturing) was observed for both *S. aureus* ATCC 25923 and *B. cereus* DL5.

Chapter 7:
Results and Discussion for Full Cancer Screens

CONTRIBUTIONS TO THIS CHAPTER

The cell proliferation studies were performed by Ms V. Mathieu, Ms. D. Lamoral-Theys, Mr. T. Gras and Ms. L. MorenoYBanuls, while under the supervision of Prof. R. Kiss. The laboratory work was carried out at the Laboratory of Toxicology, which forms part of the Institute of Pharmacy at ULB, the Free University of Brussels. However, the SAR analyses were performed by Ms. J.-L. Panayides, while under the supervision of Prof W.A.L. van Otterlo. The work was undertaken in the School of Chemistry which forms part of the Molecular Sciences Institute at the University of the Witwatersrand.

7.1 CHAPTER OVERVIEW

In order to determine if the synthetic nucleoside derivatives prepared (synthesis described in **Chapter 2** and **Chapter 5**) possessed general activity for the inhibition of cancerous cell proliferation, they were ten assayed against melanoma, glioma, prostate and breast cancer cell lines. A total of 43 first and second generation synthetic compounds and seven control compounds were screened against five human cancer cell lines and one mouse cancer cell line during the study.

7.2 INHIBITION OF CELL PROLIFERATION STUDY

7.2.1 Materials and Methods

7.2.1.1 Cell Lines and Culture Conditions

For this study, six established adherent cell lines of varying origin were used. The initial screen was performed against two human glioma lines (U373 and Hs683) and the compounds

showing activity were further subjected to analysis against another three human lines (PC-3, MCF-7 and SKMEL-28) and one murine line (B16F10).

Human cancer lines were obtained from the American Type Culture Collection (ATCC, Manassas, VA), the European Collection of Cell Culture (ECACC, Salisbury, UK), and the Deutsche Sammlung von Mikroorganismen and Zellkulturen (DSMZ, Braunschweig, Germany).

Culture media, supplements and trypsin-EDTA solution were obtained from Gibco-BRL/Invitrogen (Merelbeke, Belgium). Fetal bovine serum was inactivated before use by heating for 1 hour at 56 °C. Cells were cultured at 37 °C in Falcon tissue culture dishes (Nunc Invitrogen, Merelbeke, Belgium) in an incubator containing a 5 % CO₂ humidified atmosphere. All culture media were supplemented with fetal bovine serum (percentages below), 200 IU/mL penicillin, 200 IU/mL streptomycin and 0.1 mg/mL gentamicin.

U373 human glioma cell line

The U373 MG cell line is a human carcinoma line isolated from the brain epithelium; it was derived from a malignant tumour by the “explants technique”.¹²⁴ As a result of implementing STR analysis (DNA profiling) as part of the American Type Culture Collection’s (ATCC) routine authentication procedures, the ATCC discovered that some human cell lines were not as originally reported by the depositor.¹²⁵ The cell line U373, obtained from the original lab in Uppsala has differing genetic properties from the ATCC line (HTB-17) – as such, ATCC has stopped distribution of this cell line indefinitely.¹²⁵ The cell line used in this study and referred to as U373, was obtained from the ECACC (code 89081403) and is not involved in the controversy surrounding its origin. The cell line U373 was cultured in MEM medium (DMEM-F12 – Gibco-BRL/Invitrogen: 31330-03) supplemented with 5 % heat inactivated fetal bovine serum.

Hs683 human glioma cell line

Hs683 cells were isolated from explant cultures of a glioma taken from the left temporal lobe of a 76 year old male Caucasian. Microvilli but no desmosomes were observed on the monolayer fibroblast of the brain tissue.¹²⁶ This adherent cell line was obtained from the ATCC (code HTB-138) and was cultured in RPMI medium (RPMI 1640 – Gibco-BRL/Invitrogen: 52400-025) supplemented with 10% heat inactivated fetal bovine serum.¹²⁷

PC-3 human prostate cancer cell line

The adherent PC-3 human adenocarcinoma line is typical of the class of “classical” cell lines of prostatic cancer, with the PC-3 cell having high metastatic potential when compared to other lines of the same class.^{128,129} The PC-3 line was initiated from an advanced androgen independent bone metastasis of a grade IV prostatic adenocarcinoma from a 62 year old male Caucasian.¹³⁰ The cells exhibit low acid phosphatase and testosterone-5-alpha reductase activities, as well as expressing PSA (the prostate specific antigen).¹³¹ The line used in this study was obtained from the DSMZ (code ACC465) and cultured in RPMI medium (RPMI 1640 – Gibco-BRL/Invitrogen: 52400-025) supplemented with 10 % heat inactivated fetal bovine serum.

MCF-7 human breast cancer cell line

MCF-7 is the acronym for the Michigan Cancer Foundation – 7, referring to the institute in Detroit where the cell line was established in 1973 by Soule and co-workers.¹³² MCF-7 is an adherent breast adenocarcinoma line isolated from a 69 year old Caucasian woman. The primary tumour was an invasive breast ductal carcinoma and the cells were obtained by pleural effusion.¹³³ This cell line is interesting in that it retained several characteristics of differentiated mammary epithelium, including the ability to process estradiol via cytoplasmic estrogen receptors and the capability of forming domes. In addition, the cells express the WNT7B oncogene.¹³³ The MCF-7 line used in this study was obtained from the DSMZ (code ACC115) and cultured in RPMI medium (RPMI 1640 – Gibco-BRL/Invitrogen: 52400-025) supplemented with 10 % heat inactivated fetal bovine serum.

SKMEL-28 human melanoma cell line

SKMEL-28 is an adherent cell line which was isolated from a malignant melanoma on the skin of a 51 year old male patient and deposited with the ATCC by Takahashi.¹³⁴ It has polygonal morphology and grows as a monolayer (monoclonal continuous culture).¹³⁵ The SKMEL-28 cells used in this study were obtained from the ATCC (code: HTB-72) and were cultured in RPMI medium (RPMI 1640 – Gibco-BRL/Invitrogen: 52400-025) supplemented with 10% heat inactivated fetal bovine serum.

B16F10 mouse melanoma cell line

B16F10 is an adherent mixture of spindle-shaped and epithelial-like cells obtained from the skin of *Mus musculus* (mouse).¹³⁶ The B16F10 cells used in this study were obtained from the ATCC (code: CRL-6475) and were cultured in RPMI medium (RPMI 1640 – Gibco-BRL/Invitrogen: 52400-025) supplemented with 10% heat inactivated fetal bovine serum.

7.2.1.2 Synthetic Compounds Used in the Study

Twenty-two of the range of the “First Generation Compounds” synthesized in **Chapter 2**, twenty-one of the range of the “Second Generation Compounds” synthesized in **Chapter 5** and seven synthetic controls were used in this study. The selection was made to encompass derivatives of all five of the different nucleosides and β -(-)-ribose. Compounds and controls used in this study have been grouped according to their structural similarities and re-drawn below for ease of reading.

Illustrated in **Figure 69** are the general purine (adenosine **8**, guanosine **9** and inosine **116**) and pyrimidine (cytidine **11**) based nucleoside derivatives (excluding uridine). Whereas, **Figure 70**, shows the uridine **12** and 5-methyluridine **233** derivatives used for our structure-activity analysis.

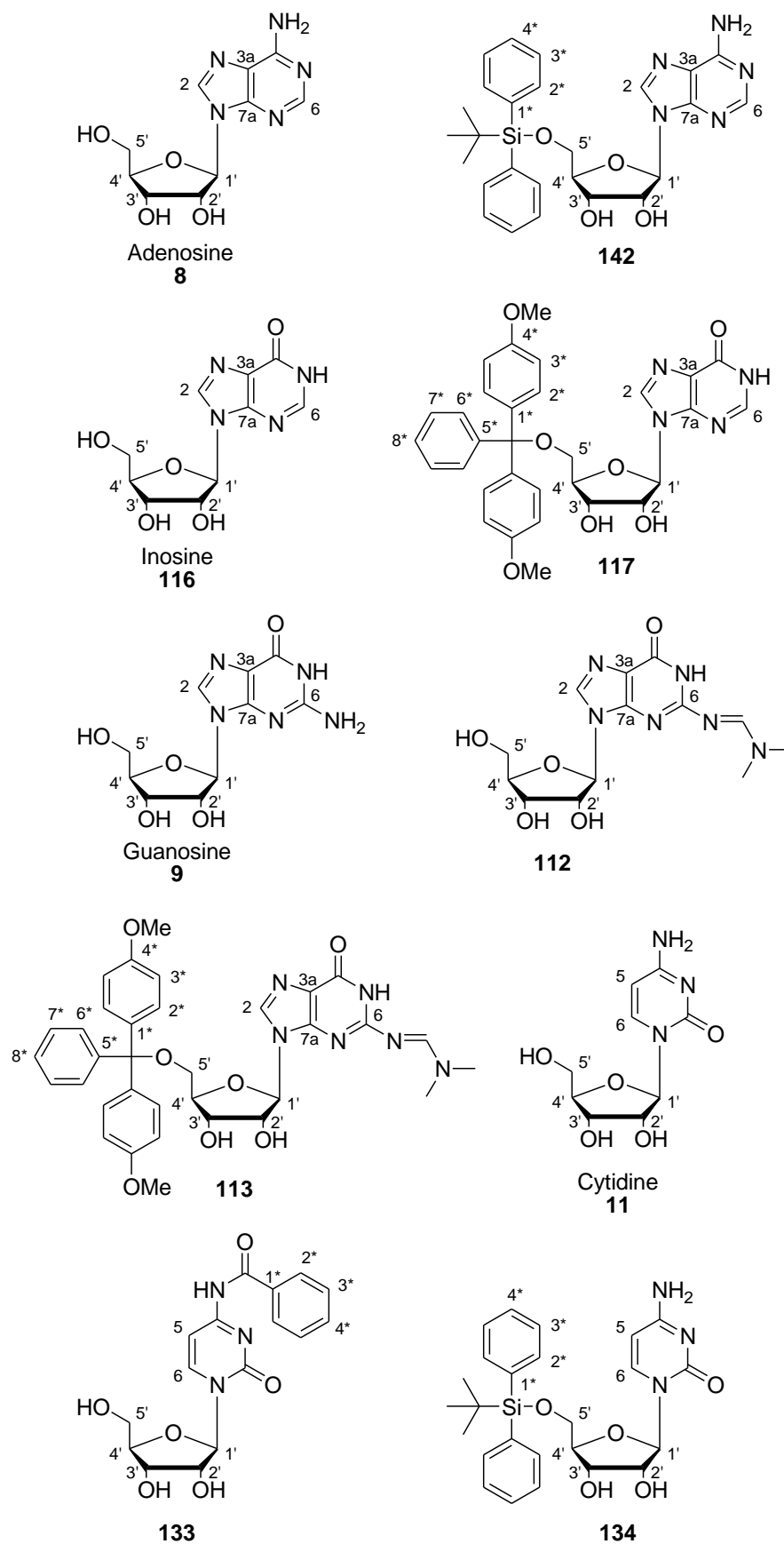


Figure 69 Structures of the general purine and pyrimidine based nucleoside derivatives

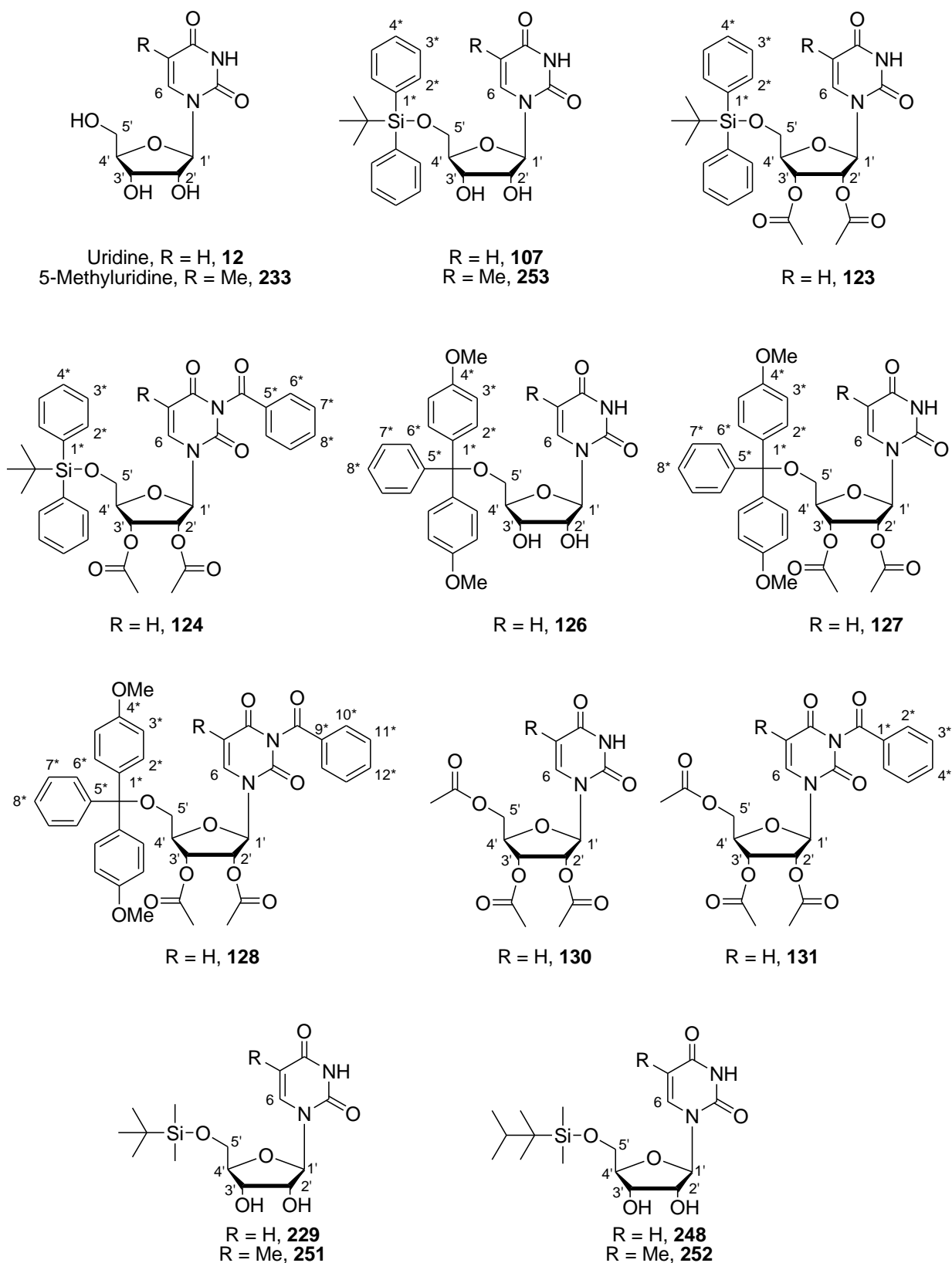


Figure 70a Structures of the uridine **12** and 5-methyluridine **233** derivatives

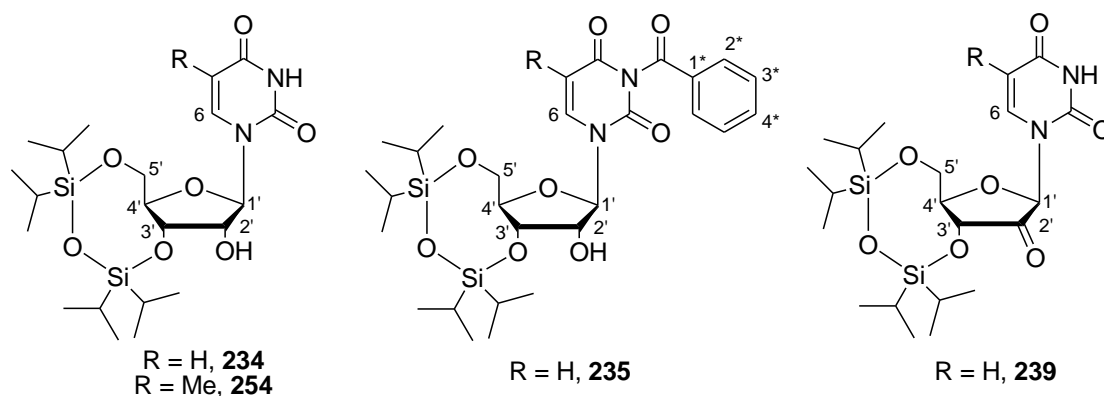


Figure 70b Structures of the uridine **12** and 5-methyluridine **233** derivatives

Illustrated in **Figure 71**, are the simple derivatives of □-(-)-ribose **100**, while highlighted in **Figure 72** are all of our synthetic silanols and the 4,4'-dimethoxytrityl control **147**.

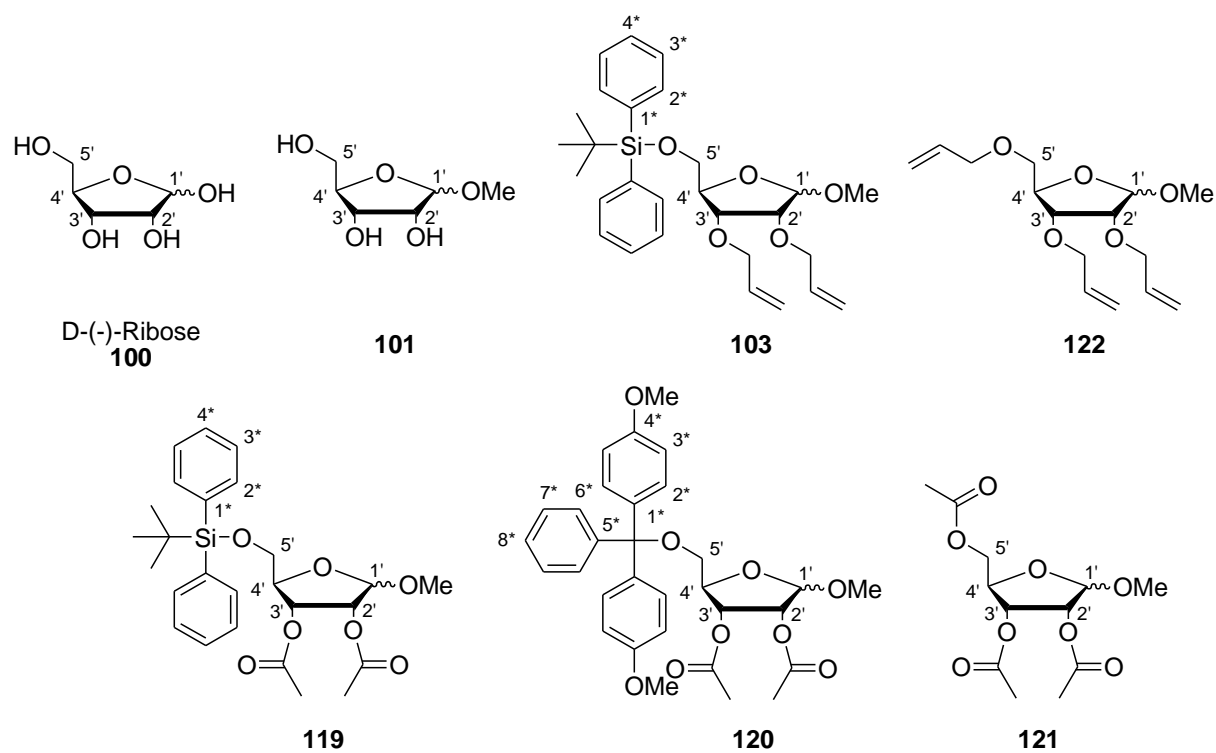


Figure 71 Structures of the □-(-)-ribose **100** derivatives

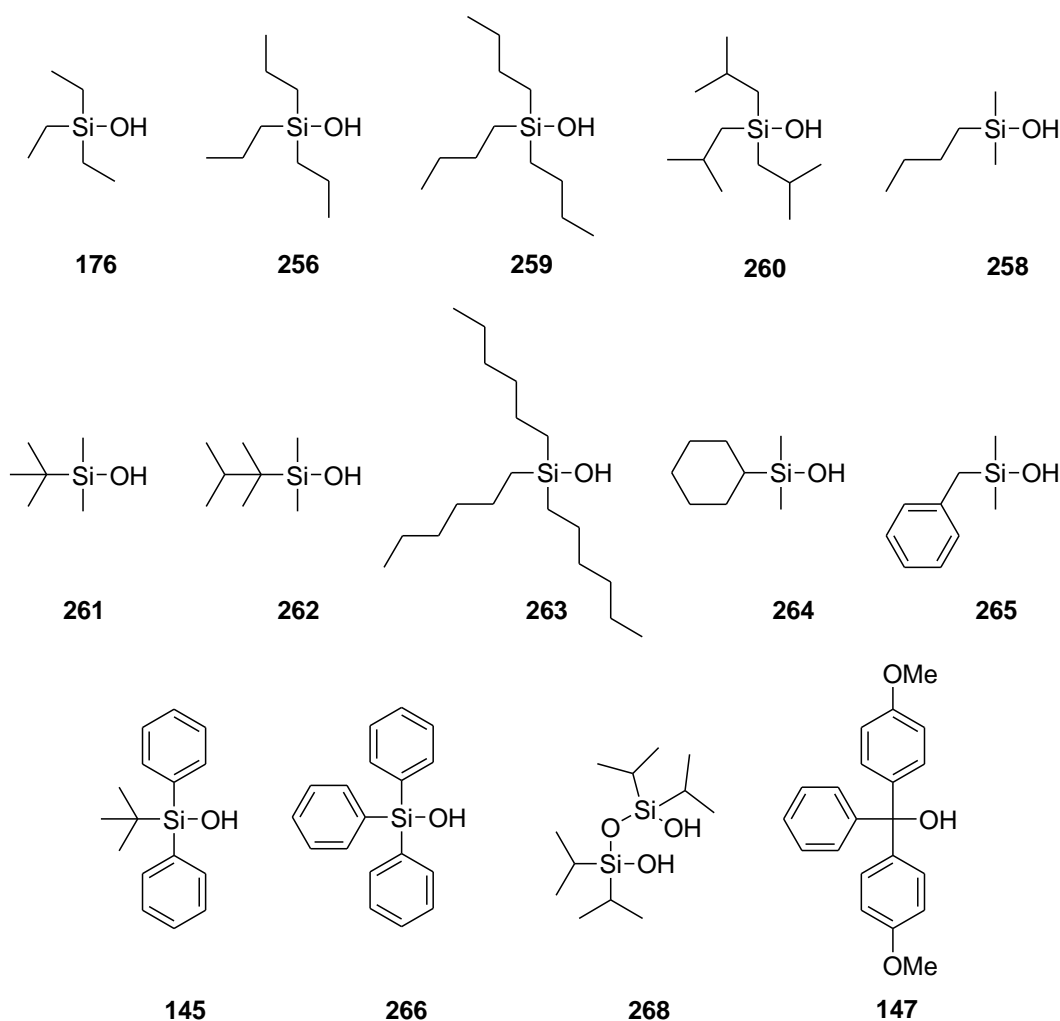


Figure 72 Structures of the synthetic silanols and the 4,4'-dimethoxytrityl control **147**

Narciclasine **269** is a plant growth regulator that has been previously demonstrated by Kiss and co-workers, to be proapoptotic to cancer cells at high concentrations ($\geq 1 \mu\text{M}$).¹³⁷ In addition, it was shown that narciclasine **269** displays potent anti-tumour effects in apoptosis-resistant as well as apoptosis-sensitive cancer cells by impairing the organization of the actin cytoskeleton in cancer cells at concentrations that are not cytotoxic (IC_{50} values of 30-90 nM).¹³⁸ In a previous publication,¹³⁸ the group observed that narciclasine **269** displayed potent antiproliferative activity, independent of the tumour type and independent of whether the cells were of human (IC_{50} range of 5-99 nM) or rodent origin (IC_{50} range of 28-35 nM). As such, narciclasine **269** was selected as our positive control for the study, which involved the

determination of inhibition of cell proliferation in both human and murine cancerous cell lines. **Figure 73** below shows the chemical structure of narciclasine **269**.

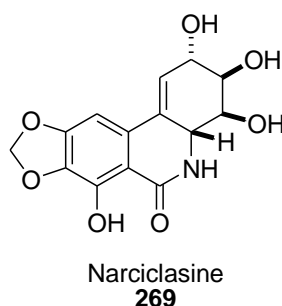


Figure 73 Structure of narciclasine **269**

Narciclasine **269** was thus isolated by the Kiss group using their standard protocol, from fresh bulbs of *Narcissus pseudonarcissus* Carlton. The experimental procedure is given in detail in the 2007 *Neoplasia* publication by Kiss and co-workers.¹³⁹

7.2.1.3 Evaluation of Compound Efficacy using the MTT Assay

Overall cell growth was assessed using the 3-(4,5-dimethylthiazol-2-yl)-2,5-diphenyl-tetrazolium bromide (MTT) colorimetric assay. Stock solutions were prepared of the synthetic compounds in DMSO at 10^{-2} M or 10^{-3} M that were then stored at -20 °C until required. The MTT colorimetric assay was used to determine the cytotoxic activity of the synthetic compounds and controls on the different cell lines, after a 72 hour exposure period to the compounds. All determinations were carried out in sextuplicate.

The controls used in the assay consisted of:

- (i) medium alone without cells giving the 0 % growth control
- (ii) cells and medium with no test compound added, giving the 100 % growth control
- (ii) cells and medium with narciclasine **269** added.

The MTT assay used here is the same as that described for the inhibition of cell proliferation study in **Chapter 3**, *Section 3.2.3.1* above, and similar to the TTC assay (used to determine anti-bacterial activity) and the XTT assay (used to determine anti-HIV activity). They are all based on the same principle, that tetrazolium structures are bio-reduced to formazan structures in metabolically active cells. As such, only a very broad description of the methodology will be discussed here – however, you may refer to previous publications by the Kiss group for more detailed discussions, as required.¹³⁹⁻¹⁴²

To perform the assay, cells were allowed to grow in 96-well micro-wells with a flat bottom with an amount of 100 μL of cell suspension per well with 5000 to 8000 cells/well depending on the cell type used.¹⁴³ Each cell line was seeded in its appropriate culture medium. After a 24 hour period of incubation at 37 °C, the culture medium was replaced by 100 μL of fresh medium in which the tested compound was previously dissolved, at the following molar concentrations: 10^{-8} M, $5 \cdot 10^{-8}$ M, 10^{-7} M, $5 \cdot 10^{-7}$ M, 10^{-6} M, $5 \cdot 10^{-6}$ M, 10^{-5} M, $5 \cdot 10^{-5}$ M and 10^{-4} M. Each experiment was performed in sextuplicate (six times).¹⁴³

After 72 hours of incubation at 37 °C, with (experimental conditions) or without (control conditions) the control compound to be tested, the medium was replaced by 100 μL MTT dissolved in RPMI (1640 without phenol red) at a concentration of 0.5 or 1 mg/mL. The micro-wells were subsequently incubated for three and a half hours at 37 °C and then centrifuged at 1300 rpm for 10 minutes. MTT was removed and formazan crystals formed were dissolved in 100 μL DMSO. The micro-wells were then shaken for 5 minutes and read on a spectrophotometer at wavelength of 570 nm (maximal formazan absorbance).¹⁴³

For each experimental condition, the mean optical density was calculated, allowing the determination of the percentage of remaining living cells in comparison to the control. The tables in the text show the IC₅₀ (representing the range of concentration of the compound tested that resulted in a 50 % inhibition of overall tumour cell growth) for each compound in each line investigated.

7.2.1.4 Data Analysis

The results for the MTT assay are expressed as the concentration of the synthetic compound that inhibits 50 % of the *in vitro* global growth of a cell line (IC₅₀), after three days incubation. Survival analyses were carried out by means of Kaplan-Meier curves and Gehan's generalized Wilcoxon test. All the statistical analyses were realized using Statistica (Statsoft, Tulsa, Oklahoma, USA).¹⁴⁴

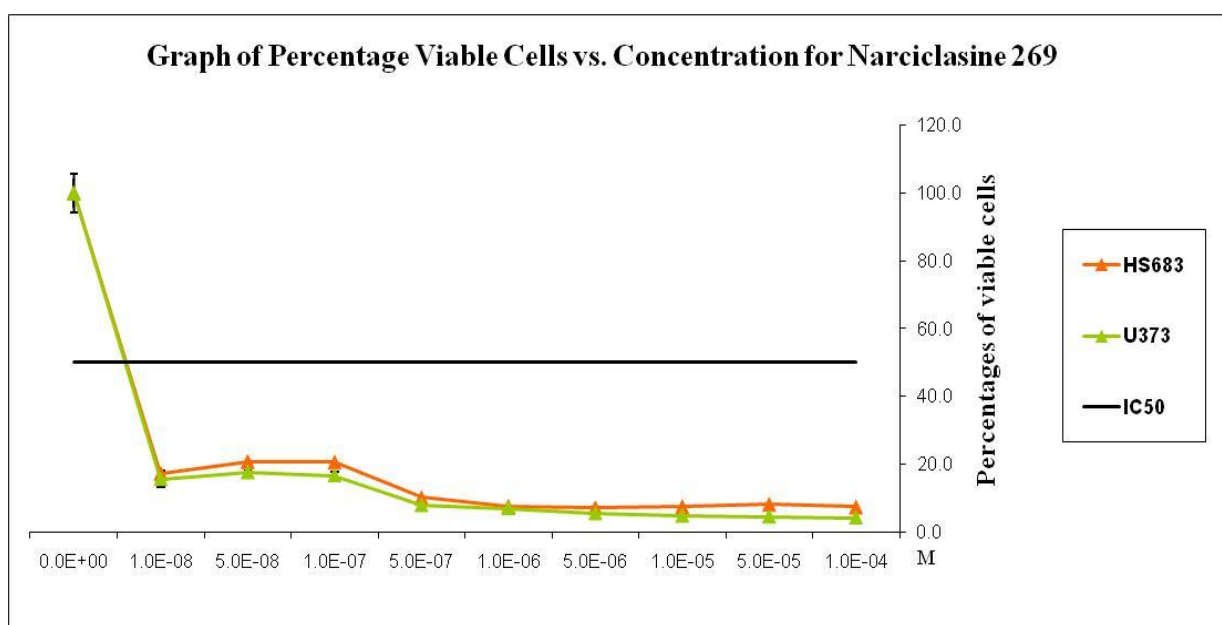
7.2.2 Results and Discussion

In our original anti-proliferation studies (discussed in detail in **Part 1, Chapter 3**) we reported percentage cell viabilities for various suspension (HL-60, Jurkat and K562) and adherent (Caco-2 and HT-29) cell lines, when treated with a single concentration, 100 µM, of the synthetic compounds for 24 hours.

In this study, we only looked at solid/adherent cell lines and not at suspension lines, as the results previously reported (*Section 3.2.3.2*) suggested that our compounds, in general, had a lesser effect against the suspension cell lines. Additionally, for this study we wanted to obtain a broader sense of our compound activity and as such did not only perform a “snapshot test” at one concentration (100 µM), but instead looked across a range of concentrations in order to accurately determine IC₅₀ values for the synthetic compounds.

As described in *Section 7.2.1.2* above, a combination of fifty of the first and second generation compounds and controls were screened for possible anti-cancer activity against five human and one murine cell line. The IC_{50} values for the synthetic compounds were determined according to the procedure described by Kiss and co-workers.¹³⁹⁻¹⁴⁴

Using the dilution series a standard dilution curve was prepared for the compound narciclasine **269**, in each of the six established adherent cell lines of varying origin used in the assay (graphs prepared separately, but not shown due to space constraints).



Graph 20 Standard Curve for narciclasine **269** with the initial HS683 and U373 cell lines

For all synthetic and control compounds, the initial screen was performed against two human glioma lines (U373 and Hs683) and the compounds showing activity were subsequently screened against another three human lines (PC-3, MCF-7 and SKMEL-28) and one murine line (B16F10). The curve shown schematically in **Graph 20** is the standard dilution curve for narciclasine **269** for the initial screen against the two glioma lines (U373 and Hs683).

The group was then able to use the standard curve shown in **Graph 20** to determine the IC₅₀ values for the control narciclasine **269**. The full set of results obtained for the control narciclasine **269** and incubated with the six cell lines are reported in detail in **Table 26**.

Table 26 *In vitro* compound-induced anti-growth effects on various cancer cell lines expressed as IC₅₀ values – *Narciclasine*

Compound	IC ₅₀ after 3 days of culture with the compounds						
	U373	Hs683	PC-3	MCF-7	SKMEL-28	B16F10	m ± SEM
269 (nM)	29	40	28	45	37	35	35 ± 6
269 (μM)	0.029	0.040	0.028	0.045	0.037	0.035	0.035 ± 0.006

As expected, narciclasine **269** showed inhibition of proliferation for all six of the cell lines screened. For these cell lines the activity range for narciclasine **269** was found to be in the nanomolar range; however, the results were converted to micromolar in order to allow for comparisons with the data obtained for our synthetic compounds.

As narciclasine **269** is not a commercially available drug, the group wished to compare our results to a number of known compounds, marketed for their anti-cancer properties. For this study we wished to compare the results obtained to compounds with varying modes of action: (i) compound which stops the synthesis of pre-DNA molecular binding blocks - 5-*fluorouracil* **270**, (ii) compound which effects the synthesis of the mitotic spindles – *paclitaxel (Taxol)* **271** and (iii) compound that acts as an intercalating agent – *cisplatin* **272**.¹⁴⁵

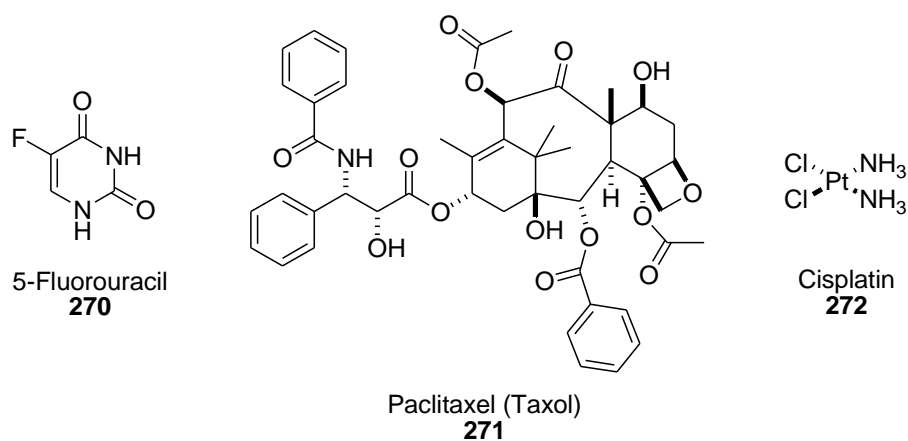


Figure 74 Structures of commercially available compounds used as comparators¹⁴⁵

The summary of literature data (IC_{50} values) currently available for the selected cell lines are given in **Table 27** below for reference purposes.

Table 27 Summary of literature data – IC_{50} values for commercial cancer drugs and the corresponding cell lines

Compound	IC_{50} values for various cell lines (μM)					
	U373	Hs683	PC-3	MCF-7	SKMEL-28	B16F10
270			0.81 ± 0.07^{146}	0.3 ± 0.1^{147}		$0.46 \pm 0.14 \mu g/mL^{148}$
271			0.0321^{149} or 0.0280^{150} or 0.0366 ± 0.0015^{146}	0.003 ± 0.002^{147} or 0.0024^{150}	0.042 ± 0.002^{151}	0.002 ± 0.001^{151}
272	5^{152}	0.4^{152}		9^{152}	$> 10^{151}$	10.01 ± 0.03^{151}

Note: For cisplatin **272**, an IC_{50} value $> 10 \mu M$ is usually indicative of an inactive compound¹⁵²

α -(-)-Ribose **100**, was included as a negative control for the assay of the α -(-)-ribose derivatives. As expected, no inhibition of cell proliferation was observed ($IC_{50} > 100 \mu M$). Not surprisingly, the same lack of inhibition of cellular growth was also observed for 1'-*O*-methoxy- α -(-)-ribose **101**. The results for the assay are given in detail in **Table 28**.

Table 28 *In vitro* compound-induced anti-growth effects on various cancer cell lines expressed as IC_{50} values – Derivatives of α -(-)-ribose

Compound	IC_{50} (μM) after 3 days of culture with the compounds						
	U373	Hs683	PC-3	MCF-7	SKMEL-28	B16F10	m \pm SEM
100	> 100	> 100	> 100	> 100	> 100	> 100	> 100
101	> 100	> 100	nd	nd	nd	nd	nd
103	42 \pm 2	46 \pm 3	35 \pm 1	26 \pm 1	36 \pm 1	37 \pm 2	34 \pm 3
119	82 \pm 1	70 \pm 1	34 \pm 2	34 \pm 1	50 \pm 2	47 \pm 4	53 \pm 8
120	57 \pm 2	69 \pm 3	34 \pm 1	30 \pm 1	59 \pm 2	36 \pm 1	48 \pm 7
121	> 100	> 100	nd	nd	nd	nd	nd
122	> 100	> 100	nd	nd	nd	nd	nd

Note: nd = not determined

We observed that 2',3'-*O*-diallyl-5'-*O*-(*tert*-butyldiphenylsilyl)-1'-*O*-methoxy- α -(-)-ribose **103**, 2',3'-*O*-diacetyl-5'-*O*-(*tert*-butyldiphenylsilyl)-1'-*O*-methoxy- α -(-)-ribose **119** and 2',3'-*O*-diacetyl-5'-*O*-(4,4'-dimethoxytrityl)-1'-*O*-methoxy- α -(-)-ribose **120** (structures shown in **Figure 71**), showed very limited activity against the cancerous cells, giving IC_{50} values for the various cell lines ranging between 26-82 μM (relative to 0.02-0.05 μM for narciclasine **269**). At the same time, we observed that compounds 2',3',5'-*O*-triacetyl-1'-*O*-methoxy- α -(-)-ribose **121** and 2',3',5'-*O*-triallyl-1'-*O*-methoxy- α -(-)-ribose **122** (**Figure 71**) were completely ineffective at limiting cellular growth in the selected concentration range. This suggests that a bulky and greasy group is required on the 5'-hydroxyl group of the sugar ring – as compounds containing such a group (**103**, **119** and **120**) were more effective at inhibiting proliferation than those with smaller, less greasy groups in the same position (**121** and **122**).

Although largely ineffective with regard to anti-cancer activity, almost direct comparisons were noted between compounds **119** and **120** (relative to compound **103**) – which may indicate that the bulky protecting group is not specific for activity, but what is important is rather the size of the group and its “fattiness”.

The results of the general “First Generation” compounds of both purine and pyrimidine classes are grouped together in **Table 29** for ease of reference. The results for the first generation of uridine derivatives have been grouped together with the other “Second Generation” uridine **12** and 5-methyluridine **253** derivatives in **Table 30**.

Table 29 *In vitro* compound-induced anti-growth effects on various cancer cell lines expressed as IC₅₀ values – General purine and pyrimidine nucleoside-based derivatives

Compound	IC ₅₀ (μM) after 3 days of culture with the compounds						
	U373	Hs683	PC-3	MCF-7	SKMEL-28	B16F10	m ± SEM
8	> 100	> 100	> 100	> 100	> 100	81 ± 4	> 81
142	44 ± 1	46 ± 3	27 ± 1	26 ± 1	33 ± 1	29 ± 1	24 ± 4
116	> 100	> 100	> 100	> 100	> 100	89 ± 4	> 89
117	44 ± 1	63 ± 3	66 ± 5	67 ± 2	65 ± 2	34 ± 2	56 ± 6
9	> 100	> 100	> 100	> 100	> 100	86 ± 2	> 86
112	> 100	> 100	nd	nd	nd	nd	nd
113	77 ± 2	> 100	nd	nd	nd	nd	nd
11	> 100	> 100	> 100	> 100	> 100	93 ± 3	> 93
133	> 100	> 100	nd	nd	nd	nd	nd
134	28 ± 1	40 ± 2	22 ± 1	14 ± 1	26 ± 1	20 ± 2	25 ± 4

Note: nd = not determined

As shown in **Table 29**, a number of unaltered nucleosides were included in the screen as our negative controls. As expected adenosine **8**, inosine **116**, guanosine **9** and cytidine **11** showed no inhibition of cell proliferation whatsoever (with $IC_{50} > 100 \mu\text{M}$) for the human cell lines. Interestingly however, all of the control compounds showed some activity at very high concentrations, 81-93 μM , towards the murine cell line (B16F10).

The adenosine **8** derivative, 5'-*O*-(*tert*-butyldiphenylsilyl)adenosine **142** (**Figure 69**) showed some interesting results, with IC_{50} values of $44 \pm 1 \mu\text{M}$ and $46 \pm 3 \mu\text{M}$ for human glioma lines U373 and Hs683 respectively. Based on the activities being lower than 100 μM , the compound **142** was further assayed against the remaining four cell lines: PC-3 ($27 \pm 1 \mu\text{M}$), MCF-7 ($26 \pm 1 \mu\text{M}$), SKMEL-28 ($33 \pm 1 \mu\text{M}$) and B16F10 ($29 \pm 1 \mu\text{M}$). The mean IC_{50} results for the six cell lines ($24 \pm 4 \mu\text{M}$) are approximately eight times higher than the average values reported for 5-fluorouracil **270**, paclitaxel (Taxol) **271** and cisplatin **272**. We considered this to be a very exciting result as continuing compound development might result in an eight-fold improvement of our derivative, which would place us in the corresponding range as the current marketed drugs.

The inosine **116** derivative, 5'-*O*-(4,4'-dimethoxytrityl)inosine **117** (**Figure 69**) gave IC_{50} values of $44 \pm 1 \mu\text{M}$ and $63 \pm 3 \mu\text{M}$ for human glioma lines U373 and Hs683 respectively. As such, the compound **116** was further assayed against the remaining four cell lines. IC_{50} values of $66 \pm 5 \mu\text{M}$ (PC-3 cells), $67 \pm 2 \mu\text{M}$ (MCF-7 cells), $65 \pm 2 \mu\text{M}$ (SKMEL-28 cells) and $34 \pm 2 \mu\text{M}$ (B16F10 cells) were obtained for compound **116**. Unfortunately, none of the IC_{50} values obtained for the remaining human cell lines were significantly lower than those obtained for the glioma lines and as the original IC_{50} values were quite high, they are classified as inactive for this study. Interestingly, the IC_{50} value obtained for the murine line was on average around half the concentration required for activity in the five human cell lines.

Two derivatives of guanosine **9** were screened in this assay: 6-*N*-(*N,N*-dimethylmethylimine)guanosine **112** and 5'-*O*-(4,4'-dimethoxytrityl)-6-*N*-(*N,N*-dimethylmethylimine)-guanosine **113** (**Figure 69**). For both of these compounds, when screened against the glioma

lines U373 and Hs683, the IC_{50} values determined were around the 100 μ M mark. As such, they were classified as inactive and were not subjected to any additional screens.

The cytidine **11** derivative, 4-*N*-benzoylcytidine **133** (**Figure 69**) gave IC_{50} values greater than the 100 μ M mark, when screened against the glioma lines U373 and Hs683 and, as such, they were classified as inactive for this assay and were not subjected to any additional screens. 5'-*O*-(*Tert*-butyldiphenylsilyl)cytidine **134** (**Figure 69**) however, exhibited a number of very interesting results. The compound **134** gave IC_{50} values of 28 ± 1 μ M and 40 ± 2 μ M for human glioma lines U373 and Hs683 respectively. As such, the compound **134** was further assayed against the remaining four cell lines. IC_{50} values of 22 ± 1 μ M (PC-3 cells), 14 ± 1 μ M (MCF-7 cells), 26 ± 1 μ M (SKMEL-28 cells) and 20 ± 2 μ M (B16F10 cells) were obtained for compound **134**. The mean IC_{50} results for the six cell lines (25 ± 4 μ M) are approximately eight times higher than the average values reported for 5-fluorouracil **270**, paclitaxel (Taxol) **271** and cisplatin **272**.

The results obtained from the cell proliferation study for the “First Generation” of uridine **12** derivatives have been grouped together with the “Second Generation” uridine **12** and 5-methyluridine **253** derivatives in **Table 30**.

A number of unaltered nucleosides were included in the screen as our negative controls, namely, uridine **12** and 5-methyluridine **233**. As expected neither of the unaltered nucleosides showed any inhibition of cell proliferation (with $IC_{50} > 100$ μ M) for the human cell lines (as shown in **Table 30** below). Interestingly, we again noted (as above in **Table 29**) that both of the control compounds showed some activity towards the murine cell line (B16F10) at very high concentrations of approximately 88-92 μ M.

Table 30 *In vitro* compound-induced anti-growth effects on various cancer cell lines expressed as IC₅₀ values – *Derivatives of Uridine and 5-Methyluridine*

Compound	IC ₅₀ (μM) after 3 days of culture with the compounds						
	U373	Hs683	PC-3	MCF-7	SKMEL-28	B16F10	m ± SEM
12	> 100	> 100	> 100	> 100	> 100	92 ± 4	> 92
107	36 ± 1	35 ± 1	25 ± 1	19 ± 1	24 ± 1	26 ± 2	28 ± 3
123	32 ± 1	29 ± 1	20 ± 1	11 ± 1	26 ± 1	30 ± 1	25 ± 3
124	26 ± 1	35 ± 2	28 ± 1	31 ± 1	25 ± 1	8 ± 1	53 ± 8
126	43 ± 3	39 ± 2	28 ± 1	27 ± 1	31 ± 2	43 ± 1	35 ± 3
127	40 ± 3	28 ± 5	18 ± 2	10 ± 1	31 ± 1	24 ± 2	25 ± 4
128	39 ± 1	45 ± 2	28 ± 1	33 ± 1	43 ± 1	41 ± 2	38 ± 3
130	> 100	> 100	nd	nd	nd	nd	nd
131	> 100	> 100	nd	nd	nd	nd	nd
229	71 ± 2	84 ± 3	> 100	> 100	> 100	> 100	nd
234	81 ± 4	83 ± 2	28 ± 1	32 ± 1	30 ± 1	27 ± 2	47 ± 11
235	29 ± 2	29 ± 2	25 ± 1	27 ± 1	28 ± 1	30 ± 1	28 ± 1
239	71 ± 2	70 ± 4	26 ± 1	25 ± 1	30 ± 1	46 ± 5	45 ± 9
248	> 100	> 100	nd	nd	nd	nd	nd
233	> 100	> 100	> 100	> 100	> 100	86 ± 6	> 86
251	> 100	77 ± 1	nd	nd	nd	nd	nd
252	68 ± 1	64 ± 2	33 ± 1	31 ± 1	30 ± 1	33 ± 2	32 ± 2
253	25 ± 1	27 ± 1	24 ± 1	28 ± 1	28 ± 1	38 ± 1	30 ± 3
254	87 ± 2	91 ± 3	72 ± 2	> 100	> 100	26 ± 2	nd

Note: nd = not determined

Table 30 shows, that 5'-*O*-(*tert*-butyldiphenylsilyl)uridine **107** (**Figure 70a**) has a mean IC₅₀ value of 28 ± 3 μM for the average of the six cell lines. When protecting the two secondary alcohols on the sugar ring, we found that the mean IC₅₀ value of 25 ± 3 μM for 2',3'-*O*-diacetyl-5'-*O*-(*tert*-butyldiphenylsilyl)uridine **123** (**Figure 70a**) was not significantly different to that obtained for the unprotected compound **107**. This allowed us to conclude that having the two secondary alcohols as unprotected alcohols was not essential for activity. However,

we found that when the amine on the base was protected with a benzoyl group, as in compound 3-*N*-benzoyl-2',3'-*O*-diacetyl-5'-*O*-(*tert*-butyldiphenylsilyl)uridine **124** (**Figure 70a**), the mean IC₅₀ value of $53 \pm 8 \mu\text{M}$ obtained for the average of the six cell lines had nearly doubled when compared to **107** and **123**. This indicated that the free amine on the base of uridine is essential for cell proliferation activity.

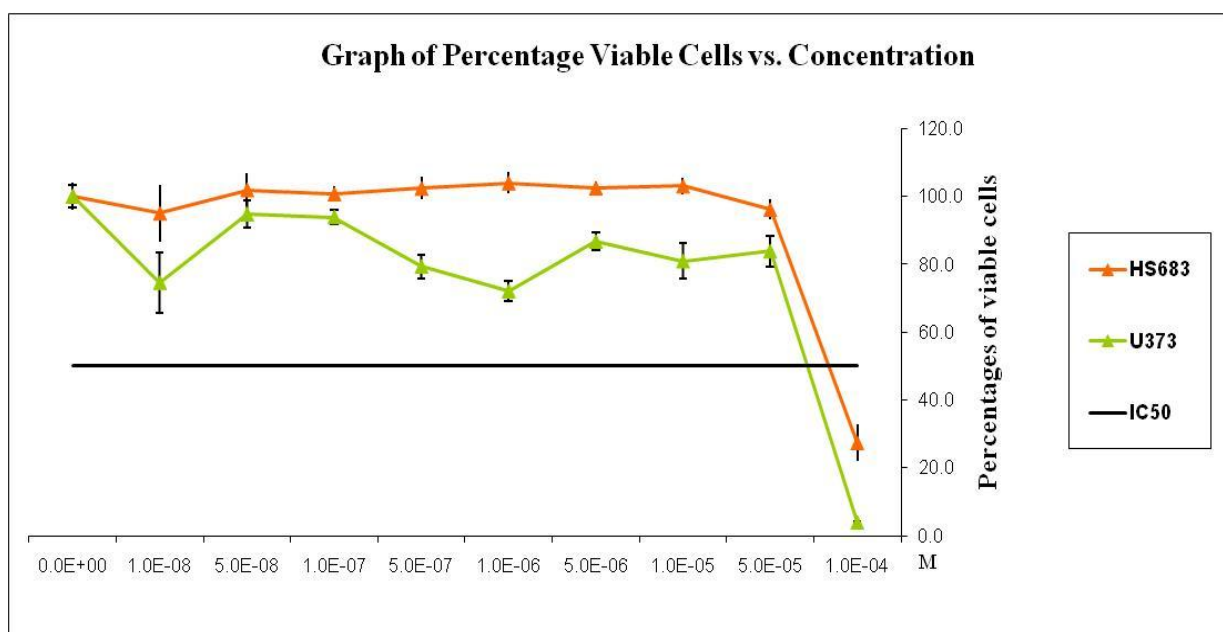
It was hoped to be able to substantiate these findings by a comparative study with the corresponding series of compounds, where the *tert*-butyldiphenylsilyl protecting group on the 5'-oxygen was exchanged for a 4,4'-dimethoxytrityl protecting group. Unfortunately, the results did not mirror those exactly for the *tert*-butyldiphenylsilyl protecting group series. It was found the mean IC₅₀ value for the average of the six cell lines to be $35 \pm 3 \mu\text{M}$ for 5'-*O*-(4,4'-dimethoxytrityl)uridine **126**, $25 \pm 4 \mu\text{M}$ for 2',3'-*O*-diacetyl-5'-*O*-(4,4'-dimethoxytrityl)uridine **127** and $38 \pm 3 \mu\text{M}$ for 3-*N*-benzoyl-2',3'-*O*-diacetyl-5'-*O*-(4,4'-dimethoxytrityl)uridine **128** (structures given in **Figure 70a**). Although the mean IC₅₀ values are in a similar concentration range, we did not observe the same doubling of the IC₅₀ value when the free amine on the base of uridine was protected.

As a further comparison, 2',3',5'-*O*-triacetyluridine **130** and 3-*N*-benzoyl-2',3',5'-*O*-triacetyluridine **131** were assayed. In both cases, the compounds gave IC₅₀ values greater than the 100 μM mark when screened against the glioma lines U373 and Hs683. As such, they were classified as inactive for this assay and were not subjected to any additional screens. This result suggested to us that we need a bulky protecting group in the 5'-hydroxyl position in order to obtain any inhibition of cell proliferation.

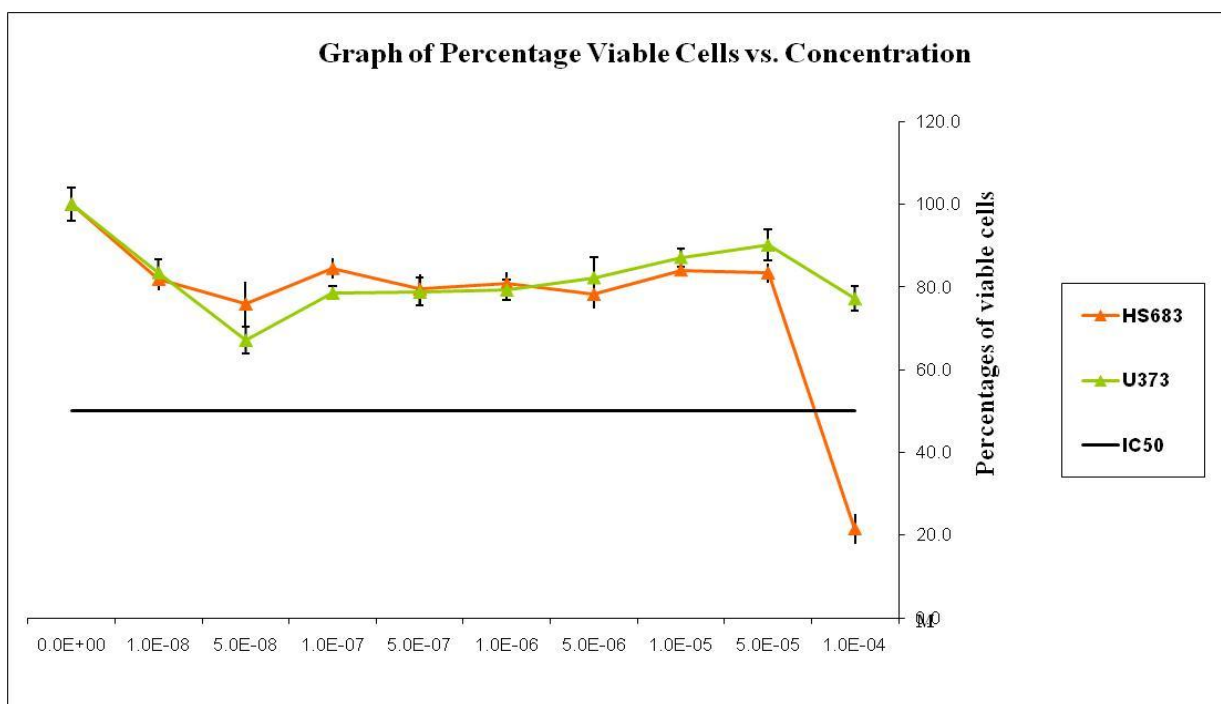
For the next part of our Structure-Activity study, the aim was to investigate if the presence of a methyl group on the 5-position of the base in uridine would have any effect on the activity. As fulfilment for this, a comparison of three sets of direct derivatives with and without the 5-methyl group on the base was undertaken. The first example involved 5'-*O*-(*tert*-butyldimethylsilyl)uridine **229** and 5'-*O*-(*tert*-butyldimethylsilyl)-5-methyluridine **251** (**Figure 70a**).

Compound **229** gave IC_{50} values of $71 \pm 2 \mu\text{M}$ and $84 \pm 3 \mu\text{M}$ for human glioma lines U373 and Hs683 respectively. As such, the compound **229** was further assayed against the remaining four cell lines. Unfortunately, the IC_{50} values obtained for all four of the cell lines were determined to fall above the $100 \mu\text{M}$ mark and the compound **229** was subsequently classified as inactive. Compound **251** did not fare much better, when screened against the glioma lines U373 and Hs683, the IC_{50} values determined were above the $100 \mu\text{M}$ mark. As such, they were classified as inactive and were not subjected to any additional screens – broadly suggesting that the 5-methyl group was not directly linked to compound activity.

As an example of what a negative result, i.e.: no observable inhibition of cell proliferation, the two standard dilution curves obtained for 5'-*O*-(*tert*-butyldimethylsilyl)uridine **229** and 5'-*O*-(*tert*-butyldimethylsilyl)-5-methyluridine **251** are included below as **Graphs 21** and **22** respectively. The results are given for only the initial activity screen in the two glioma lines U373 and Hs683.



Graph 21 Standard Curve for 5'-*O*-(*tert*-butyldimethylsilyl)uridine **229** with the initial HS683 and U373 cell lines



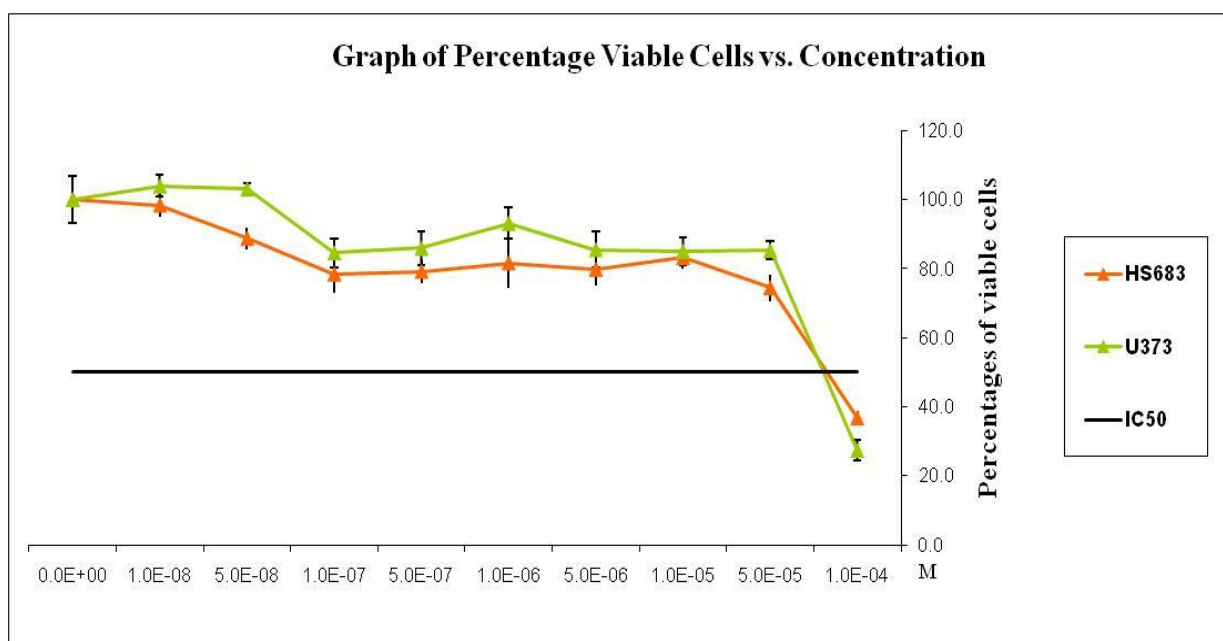
Graph 22 Standard Curve for 5'-*O*-(*tert*-butyldiphenylsilyl)-5-methyluridine **253** with the initial HS683 and U373 cell lines

The second comparative example for direct derivatives with and without the 5-methyl group on the base involved 5'-*O*-(dimethylhexylsilyl)uridine **248** and 5'-*O*-(dimethylhexylsilyl)-5-methyluridine **252**. In this instance, it was observed that compound **248** gave IC_{50} values greater than the 100 μ M mark when screened against the glioma lines U373 and Hs683. As such, it was classified as inactive for this assay and was not subjected to any additional screens.

In comparison, compound **252** (**Figure 70a**) gave IC_{50} values of $68 \pm 1 \mu$ M and $64 \pm 2 \mu$ M for human glioma lines U373 and Hs683 respectively. As such, the compound **252** was further assayed against the remaining four cell lines. IC_{50} values of $33 \pm 1 \mu$ M (PC-3 cells), $31 \pm 1 \mu$ M (MCF-7 cells), $30 \pm 1 \mu$ M (SKMEL-28 cells) and $33 \pm 2 \mu$ M (B16F10 cells) were obtained for compound **252**. The mean IC_{50} results for the six cell lines ($32 \pm 2 \mu$ M) are approximately ten times higher than the average values reported for 5-fluorouracil **270**, paclitaxel (Taxol) **271** and cisplatin **272**.

The third and final comparative example for direct derivatives with and without the 5-methyl group on the base involved the previously discussed 5'-*O*-(*tert*-butyldiphenylsilyl)uridine **107** and 5'-*O*-(*tert*-butyldiphenylsilyl)-5-methyluridine **253** (Figure 70a). The mean IC₅₀ value for the average of the six cell lines was 28 ± 3 μM for compound **107** and 30 ± 3 μM for compound **253**. As there was no significant difference between the mean IC₅₀ values for the two compounds, we concluded that the presence of the 5-methyl group on the base of the uridine derivatives did not have a marked effect on the inhibition of cell proliferation.

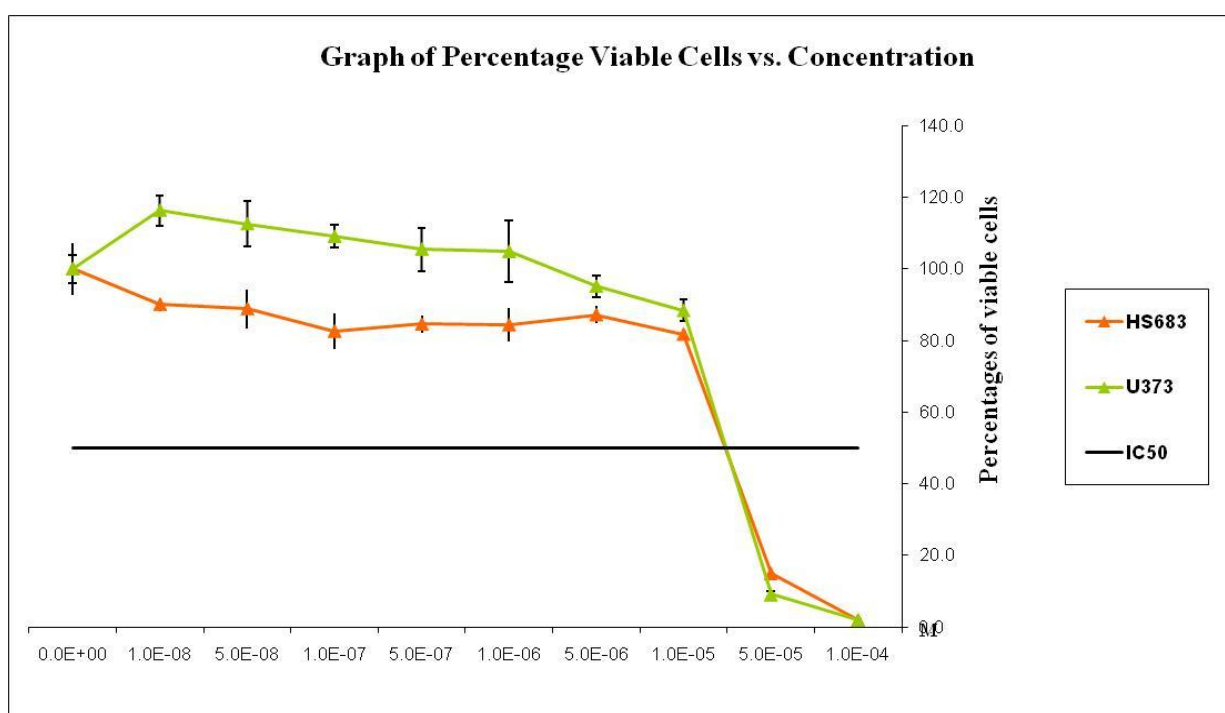
The last group of compounds investigated in our SAR study were those containing the 1,3-dihydroxy-1,1,3,3-tetraisopropylsiloxane protecting group. The simplest of these was 1-[(6*aR*,8*R*,9*R*,9*aS*)-9-hydroxy-2,2,4,4-tetraisopropyltetrahydro-6*H*-furo[3,2-*f*][1,3,5,2,4]trioxadisilocin-8-yl]pyrimidine-2,4(1*H*,3*H*)-dione **234** (Figure 70b). For compound **234** a mean IC₅₀ values for the six cell lines of 47 ± 11 μM was observed (shown schematically in Graph 23 for the two glioma cell lines).



Graph 23 Standard Curve for 1-[(6*aR*,8*R*,9*R*,9*aS*)-9-hydroxy-2,2,4,4-tetraisopropyltetrahydro-6*H*-furo[3,2-*f*][1,3,5,2,4]trioxadisilocin-8-yl]pyrimidine-2,4(1*H*,3*H*)-dione **234** with the initial HS683 and U373 cell lines

Whereas in compound 1-[(6a*R*,8*R*,9a*R*)-2,2,4,4-tetraisopropyl-9-oxotetrahydro-6*H*-furo[3,2-*f*][1,3,5,2,4]trioxadisilocin-8-yl]pyrimidine-2,4-(1*H*,3*H*)-dione **239** (**Figure 70b**), which has the 2'-hydroxyl group oxidized to a ketone, we observed a mean IC₅₀ values for the six cell lines of 45 ± 9 μM. These two results were not significantly different and allowed us to conclude that the free 2'-hydroxyl of the sugar ring on its own, is not responsible for any activity against the cancerous cell lines tested.

In the derivative with a benzoyl group attached to the amine on the base, 3-benzoyl-1-[(6a*R*,8*R*,9*R*,9a*S*)-9-hydroxy-2,2,4,4-tetraisopropyltetrahydro-6*H*-furo[3,2-*f*][1,3,5,2,4]trioxadisilocin-8-yl]pyrimidine-2,4(1*H*,3*H*)-dione **235** (**Figure 70b**), a mean IC₅₀ values for the six cell lines of 28 ± 1 μM was observed. This represents a one-third lower active concentration than for the corresponding compound **234** which does not contain the benzoyl group (shown schematically in **Graph 24** for the two glioma cell lines).



Graph 24 Standard Curve for 3-benzoyl-1-[(6a*R*,8*R*,9*R*,9a*S*)-9-hydroxy-2,2,4,4-tetraisopropyltetrahydro-6*H*-furo[3,2-*f*][1,3,5,2,4]trioxadisilocin-8-yl]pyrimidine-2,4(1*H*,3*H*)-dione **235** with the initial HS683 and U373 cell lines

It was noted that for 1-[(6a*R*,8*R*,9*S*,9a*R*)-tetrahydro-9-hydroxy-2,2,4,4-tetraisopropyl-6*H*-furo[3,2-*f*][1,3,5,2,4]trioxadisilocin-8-yl](5-methylpyrimidine)-2,4(1*H*,3*H*)-dione **254** (Figure 70b) IC₅₀ values of 87 ± 2 μM (U373 cells), 91 ± 3 μM (Hs683 cells), 72 ± 2 μM (PC-3 cells), > 100 μM (MCF-7 cells), > 100 μM (SKMEL-28 cells) and 26 ± 2 μM (B16F10 cells) were observed. Interestingly, it was observed that compound **254** showed good activity towards the murine cell line (B16F10) at a concentration of 26 μM, which was approximately one-third of that required in the human cell lines screened.

The final class of compounds screened for their inhibition of cell proliferation is the silanols. The results for this study are given in Table 31, along with those obtained for the structurally similar protecting group derivative, 4,4'-dimethoxytrityl alcohol **147**.

Table 31 *In vitro* compound-induced anti-growth effects on various cancer cell lines expressed as IC₅₀ values – *Protecting group derivatives*

Compound	IC ₅₀ (μM) after 3 days of culture with the compounds						
	U373	Hs683	PC-3	MCF-7	SKMEL-28	B16F10	m ± SEM
145	70 ± 1	70 ± 5	65 ± 2	53 ± 1	69 ± 1	79 ± 1	66 ± 5
147	43 ± 1	61 ± 6	43 ± 1	29 ± 1	53 ± 1	44 ± 1	42 ± 5
176	79 ± 1	85 ± 2	> 100	72 ± 2	94 ± 2	59 ± 4	> 78
256	> 100	> 100	nd	nd	nd	nd	nd
258	> 100	> 100	> 100	> 100	> 100	88 ± 4	> 88
259	> 100	> 100	nd	nd	nd	nd	nd
260	> 100	> 100	nd	nd	nd	nd	nd
261	> 100	> 100	nd	nd	nd	nd	nd
262	> 100	> 100	nd	nd	nd	nd	nd
263	81 ± 1	> 100	nd	nd	nd	nd	nd
264	> 100	> 100	nd	nd	nd	nd	nd
265	> 100	> 100	nd	nd	nd	nd	nd
266	63 ± 2	46 ± 2	44 ± 2	33 ± 1	60 ± 1	42 ± 1	45 ± 6
268	62 ± 3	58 ± 2	46 ± 1	37 ± 2	62 ± 1	58 ± 2	51 ± 6

Note: nd = not determined

Owing to the interesting result obtained in **Part 1**, where it was shown that *tert*-butyldiphenylsilanol **145** was active against the two adherent lines tested (HT-29 and Caco-2), we decided to further investigate this result by assaying a range of different molecular weight silanols. The compounds *tert*-butyldiphenylsilanol **145** and 4,4'-dimethoxytrityl alcohol **147** (**Figure 72**) were also included in the assay to serve as our controls.

Of the series of fourteen protecting group derivatives tested, only three additional compounds showed sufficient activity in our two glioma lines (H373 and Hs683) to warrant further investigation in the additional four cell lines (PC-3, MCF-7, SKMEL-28 and B16F10). The remaining compounds tripropylsilanol **256**, butyldimethylsilanol **258**, tributylsilanol **259**, triisobutylsilanol **260**, *tert*-butyldimethylsilanol **261**, dimethylhexylsilanol **262**, trihexylsilanol **263**, cyclohexyldimethylsilanol **264** and benzyldimethylsilanol **265** (structures given in **Figure 72**) were classified as inactive for this assay.

The first of the three “active” compounds was triethylsilanol **176** (**Figure 72**), which gave IC₅₀ values of 79 ± 1 μM and 85 ± 2 μM for human glioma lines U373 and Hs683 respectively. Additionally, compound **176** gave IC₅₀ values of > 100 μM (PC-3 cells), 72 ± 2 μM (MCF-7 cells), 94 ± 2 μM (SKMEL-28 cells) and 59 ± 4 μM (B16F10 cells). This resulted in a mean IC₅₀ value for the six cell lines of > 78 μM, which was not a significant improvement on those obtained for *tert*-butyldiphenylsilanol **145** (66 ± 5 μM) and 4,4'-dimethoxytrityl alcohol **147** (42 ± 5 μM). As such, the compound was not considered as an improvement and was not investigated further.

The second of the three “active” compounds was triphenylsilanol **266** (**Figure 72**), which gave IC₅₀ values of 63 ± 2 μM and 46 ± 2 μM for human glioma lines U373 and Hs683 respectively. Additionally, compound **266** gave IC₅₀ values of 44 ± 2 μM for the PC-3 cells, 33 ± 1 μM for the MCF-7 cells, 60 ± 1 μM for the SKMEL-28 cells and 42 ± 1 μM for the B16F10 cells. This resulted in a mean IC₅₀ value for the six cell lines of 45 ± 1 μM, which was similar to the reported mean IC₅₀ value of 42 ± 5 μM for 4,4'-dimethoxytrityl alcohol **147** and approximately 20 μM lower than the IC₅₀ value of 66 ± 5 μM for *tert*-butyldiphenylsilanol **145**. The mean IC₅₀ value for compound **266** equates to being

approximately fourteen times higher than the average values reported for 5-fluorouracil **270**, paclitaxel (Taxol) **271** and cisplatin **272** (Figure 74).

The last of the three “active” compounds was 1,3-dihydroxy-1,1,3,3-tetraisopropyldisiloxane **268** (Figure 72). It gave IC₅₀ values of: 62 ± 3 μM for U373 cells, 58 ± 2 μM for Hs683 cells, 46 ± 1 μM for PC-3 cells, 37 ± 2 μM for MCF-7 cells, 62 ± 1 μM for SKMEL-28 cells and 58 ± 2 μM for B16F10 murine cells. This resulted in a mean IC₅₀ value for the six cell lines of 51 ± 6 μM, which lies in the middle of the reported mean IC₅₀ values for *tert*-butyldiphenylsilanol **145** (66 ± 5 μM) and for 4,4'-dimethoxytrityl alcohol **147** (42 ± 5 μM). The mean IC₅₀ value for compound **268** ultimately equates to being approximately sixteen times higher than the average values reported for 5-fluorouracil **270**, paclitaxel (Taxol) **271** and cisplatin **272**.

7.2.3 Conclusions

From the inhibition of cell proliferation assay performed on the combined group of fifty first and second generation derivatives and their corresponding controls, we found that the six most active compounds had mean IC₅₀ values of approximately 24-28 μM. The results obtained are summarized below:

- 5'-*O*-(*tert*-butyldiphenylsilyl)adenosine **142** (24 ± 4 μM)
- 5'-*O*-(*tert*-butyldiphenylsilyl)cytidine **134** (25 ± 4 μM)
- 5'-*O*-(*tert*-butyldiphenylsilyl)uridine **107** (28 ± 3 μM)
- 2',3'-*O*-diacetyl-5'-*O*-(*tert*-butyldiphenylsilyl)uridine **123** (25 ± 3 μM)
- 2',3'-*O*-diacetyl-5'-*O*-(4,4'-dimethoxytrityl)uridine **127** (25 ± 4 μM)
- 3-benzoyl-1-[(6*aR*,8*R*,9*R*,9*aS*)-9-hydroxy-2,2,4,4-tetraisopropyltetrahydro-6*H*-furo[3,2-*f*][1,3,5,2,4]trioxo-disilocin-8-yl]pyrimidine-2,4(1*H*,3*H*)-dione **235** (28 ± 1 μM)

As future work specifically aligned with this chapter, the Kiss group will aim to perform cellular imaging on the interesting compounds identified above. This will be performed over a 72 h period at the IC_{50} value, during which time they will make films to observe and grossly decipher the mechanism of action of the molecules (by looking at cell proliferation, cell death, cell morphology, vacuoles, etc.). This falls beyond the scope of this thesis and as such will not be included here. However, any interesting results obtained from the study will be included in follow-up publications in the broader scientific literature.

As a general conclusion, the six compounds identified from this study act as “hit-compounds”, hidden treasures that could be analyzed in future work from a medicinal chemistry point of view; using tools such as Lipinski’s guidelines, cLogP calculations and solubility scores to map a route forward for further development of this line of compounds by subsequent graduate students.

Summary:
Work Completed in Part 2

© PART 2 SUMMARY – SYNTHESIS

As described in our aims for part 2, a decision was taken to synthesise a "second generation" of compounds that contained various silicon protecting groups, to determine if the results obtained in **Part 1**, suggested a general trend of biological activity or if they were specific to the *tert*-butyldiphenylsilyl group.

From the data reported for the anti-bacterial and the cell proliferation studies in **Part 1**, we concluded that the nucleoside showing the most promising results was uridine **12** and as such it would be the nucleoside of choice for the "second generation compounds" to be synthesised. Our mini structure-activity study on the uridine derivatives found that the best position for performing modifications to the nucleoside was at the 5'-OH position on the sugar ring and this would thus become the initial focus for the synthesis of the "second generation compounds".

The proposed "second generation compounds" included a series of uridine **12** and 5-methyluridine **233** derivatives which were protected on the primary alcohol with a range of different sized silicon-containing protecting groups. We hoped that this would allow us to find the optimally sized silicon-containing protecting group that would impart good biological activity.

Using our general approach for the synthesis of 5'-*O*-silicon protected uridine derivatives (**Figure 75**), we were able to synthesize a further five uridine derivatives and another five 5-methyluridine derivatives.

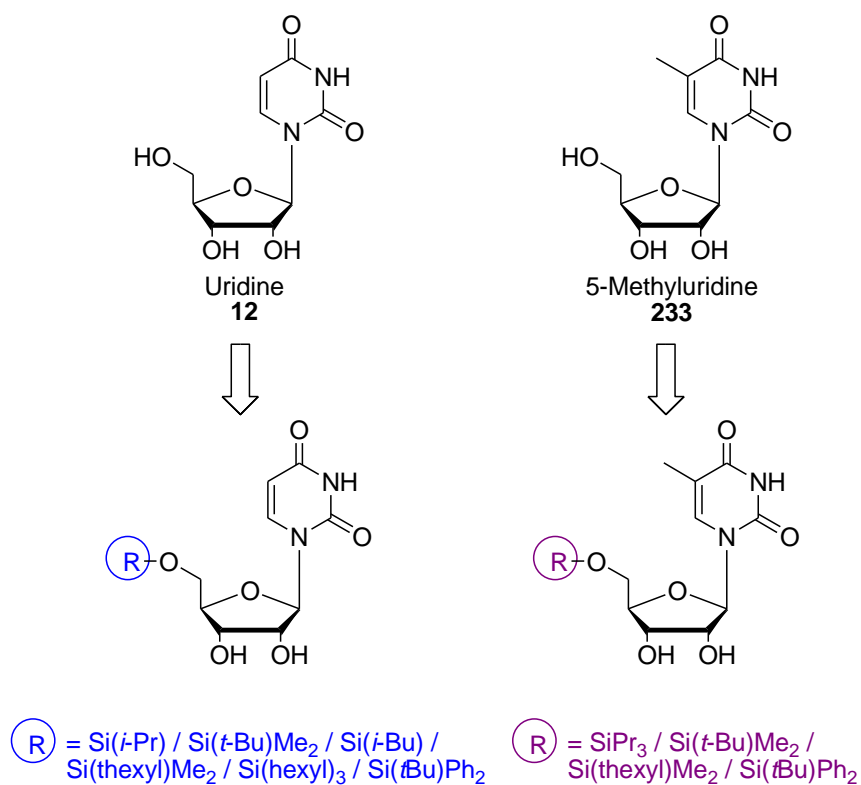


Figure 75 Proposed second generation silicon-protected uridine **12** and 5-methyluridine **233** derivatives

We also made use of an approach used to synthesize a range of tethered 1,1,3,3-tetraisopropylidisiloxane protected uridine derivatives. From this group of compounds we obtained five molecules that were modified in various positions on the sugar ring as well as at the amide position on the base (**Figure 76**).

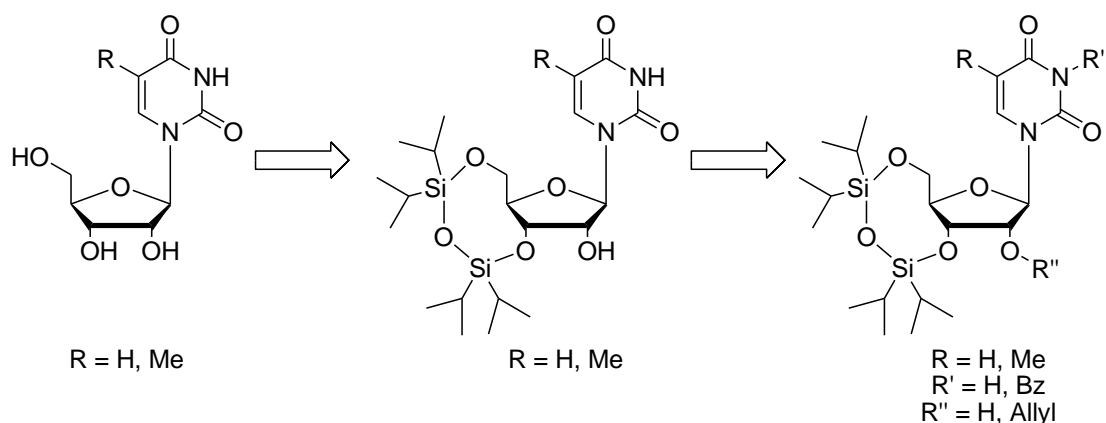


Figure 76 Proposed second generation silicon-protected uridine **12** and 5-methyluridine **233** derivatives

At the same time, we made use of a general procedure for the conversion of silyl chlorides to silanols, and used the procedure to synthesize a series of fourteen silanols, ranging from low to high molecular weight, and spanning a wide range of chemical space (**Figure 77**).

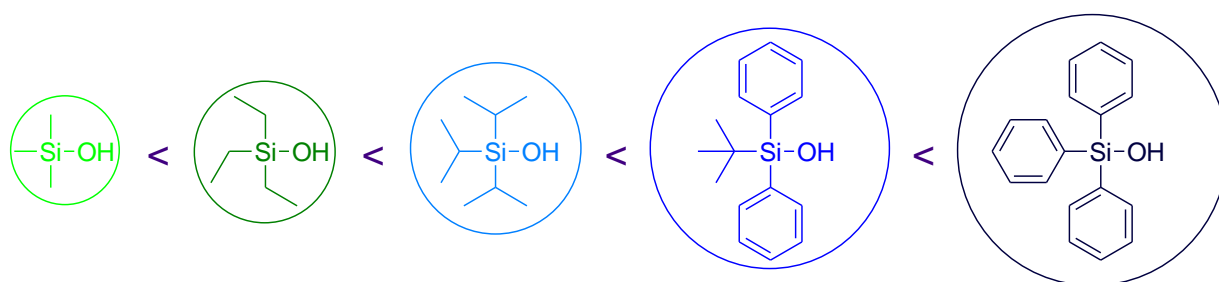


Figure 77 Proposed silanols to be included in the second generation of compounds

To summarise, for our "second generation compounds" we were able:

- (iv) to synthesise a range of silicon-protected uridine derivatives
- (v) to synthesise a range of silicon-protected derivatives of 5-methyluridine and
- (vi) to synthesise a range of corresponding silanols.

© PART 1 SUMMARY – BACTERIOLOGY AND MICROSCOPY

From the data reported above (*Section 6.2.1.2*), we were able to conclude that in general the protection of uridine **12** and 5-methyluridine **233** with silicon-containing protecting groups did not increase the anti-bacterial activity for the parent nucleoside, as suggested based on the results obtained for 5'-*O*-(*tert*-butyldiphenylsilyl)uridine **107** in **Part 1**. However, one highly active exception was found, when the two silicon atom-containing 1,1,3,3-tetra-isopropylidisiloxane protecting group was used.

From our TTC assay, we were able to show that converting the base in 1-[(6*aR*,8*R*,9*R*,9*aS*)-9-hydroxy-2,2,4,4-tetraisopropyltetrahydro-6*H*-furo[3,2-*f*][1,3,5,2,4]trioxadisilocin-8-yl]-pyrimidine-2,4(1*H*,-3*H*)dione **234** to the 5-methyl derivative **254** caused a corresponding loss in anti-bacterial activity for the compound (from 16 mg/L to 32 mg/L for *S. aureus* and *B. cereus* respectively), whereas oxidising the secondary alcohol on the 2'-position of the sugar ring to give compound **239** caused a corresponding increase in anti-bacterial activity for the molecule (from 16 mg/L to 8 mg/L for *S. aureus* and *B. cereus* respectively). As such, we concluded that 1-[(6*aR*,8*R*,9*aR*)-2,2,4,4-tetraisopropyl-9-oxotetrahydro-6*H*-furo[3,2-*f*][1,3,5,2,4]trioxadisilocin-8-yl]pyrimidine-2,4(1*H*,3*H*)dione **239** was the compound with the best anti-bacterial activity out all of the "first generation" and "second generation" of nucleoside derivatives.

These results obtained in the TTC assay, were also supported by our SEM studies. For our first SEM study, we showed that Gram-positive bacterial cells treated with uridine **12** at a concentration of 0.5 mg/L showed no inhibition of bacterial growth. In general, all cells for both bacterial strains used, showed no surface indentations or distortions to the cell shape, indicating that the unmodified nucleoside had no effect on the bacterial strains tested. In comparison, we were able to demonstrate that *S. aureus* ATCC 25923 cells treated with high concentrations of 5'-*O*-(*tert*-butyldiphenylsilyl)uridine **107** showed smooth cell surfaces, but distortions occurred in the spherical shape of the cells. For *B. cereus* DL5, we observed that the cells had aggregated together, appeared to have rough surfaces and had ruptured in a few of the examples.

In our second SEM study, we were able to show that all of the compounds **234**, **254** and **239** showed a major reduction in bacterial growth at high concentrations. In addition, we were able to visualize how compound **239** was the only example, where significant bacterial cell wall damage (major indentations on the cell surface, as well as surface rupturing) was observed for both *S. aureus* ATCC 25923 and *B. cereus* DL5.

From the CSLM study performed we validated the results obtained from the previously performed TTC assay for the determination of the percentage of metabolically active cells present after treatment with antibiotics and synthetic compounds were accurate representations of what was occurring in our overnight bacterial cultures. And, interestingly, we found that the CSLM images for both *S. aureus* ATCC 25923 and *B. cereus* DL5 treated with compound **239**, at various concentrations, showed no visible cells stained yellow indicating cell injury. This suggests that the synthetic compound **239** is bacteriocidal and is killing the cells, and not simply inhibiting their growth.

© PART 1 SUMMARY – FULL CANCER SCREEN

From the inhibition of cell proliferation assay performed on the fifty first and second generation derivatives and their corresponding controls, we found that the six most active compounds had mean IC₅₀ values of approximately 24-28 μM. The results obtained are summarized below:

- 5'-*O*-(*tert*-butyldiphenylsilyl)adenosine **142** (24 ± 4 μM)
- 5'-*O*-(*tert*-butyldiphenylsilyl)cytidine **134** (25 ± 4 μM)
- 5'-*O*-(*tert*-butyldiphenylsilyl)uridine **107** (28 ± 3 μM)
- 2',3'-*O*-diacetyl-5'-*O*-(*tert*-butyldiphenylsilyl)uridine **123** (25 ± 3 μM)
- 2',3'-*O*-diacetyl-5'-*O*-(4,4'-dimethoxytrityl)uridine **127** (25 ± 4 μM)
- 3-benzoyl-1-[(6*aR*,8*R*,9*R*,9*aS*)-9-hydroxy-2,2,4,4-tetraisopropyltetrahydro-6*H*-furo[3,2-*f*][1,3,5,2,4]trioxa-disilocin-8-yl]pyrimidine-2,4(1*H*,3*H*)-dione **235** (28 ± 1 μM)

***PART 3 - OVERALL CONCLUSIONS AND
FUTURE WORK***

Chapter 8:
Conclusions and Future Work

8.1 GENERAL CONCLUSIONS

As described in our aims for part 1, we thought it pertinent to investigate the possibility of forming fused bicyclic systems onto the 2' and 3' positions of the sugar ring of our nucleosides utilizing the RCM methodology that we were already familiar with. Using our planned strategy towards fused bicyclic ring systems, we were able to synthesize the various dienes (including 2',3'-*O*-diallyl-5'-*O*-(*tert*-butyldiphenylsilyl)-1'-*O*-methoxy- β -(-)-ribose **103** and 2',3'-*O*-diallyl-5'-*O*-(4,4'-dimethoxytrityl)-6-*N*-(*N,N*-dimethylmethylimine)-guanosine **114**, as shown in **Figure 78**), but were unable to obtain the bicyclic ring systems via our proposed RCM route. Due to the time constraints of the project, we decided not to continue along this synthetic route and instead shifted our focus to the synthesis of a range of compounds that would be used to conduct a structure-activity study.

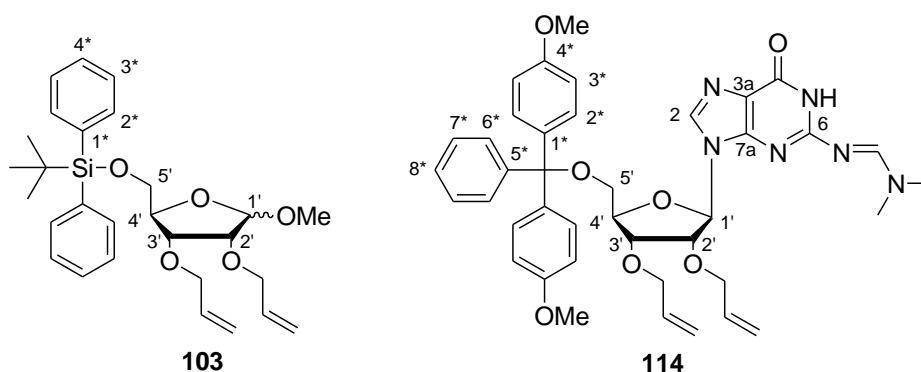


Figure 78 Dienes prepared as precursors for ring-closing metathesis

We wished to investigate the structure activity relationships (SAR) involved when the various OH and NH positions on the nucleosides and β -(-)-ribose derivatives were protected sequentially with different protecting groups. The idea was that from this data we would be able to determine on which positions in the molecules it was essential to have free OH/NH binding sites in order to maintain the activity of the compounds. For these derivatives, we prepared a series of compounds that had different functional groups present on the primary hydroxyls and secondary hydroxyls on the sugar ring, as well as different groups present on

the primary amines and/or amide groups of the bases. This synthesis was performed to obtain a range of sugar derivatives [α -(-)-ribose **100**] and nucleoside derivatives (adenosine **8**, cytidine **11**, guanosine **9**, inosine **116** and uridine **12**). Included in this group were the corresponding protecting group derivatives, *tert*-butyldiphenylsilyl alcohol **145** and 4,4'-dimethoxytrityl alcohol **147** (shown in **Figure 79**).

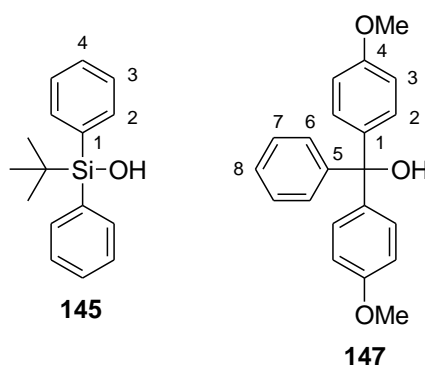


Figure 79 Protecting group derivatives

Having the range of synthetic compounds in hand, for both the approach towards the fused bicyclic ring systems and those for the structure-activity study, we then moved on to the biological testing. For the biological testing, we assayed our range of synthetic compounds for inhibitory activity against four bacterial strains, four cancer cell lines and HIV.

The nucleoside and corresponding α -(-)-ribose derivatives were evaluated for their antibacterial activity against two Gram-positive (*Staphylococcus aureus* ATCC 25923 and *Bacillus cereus* DL5) and two Gram-negative bacteria (*Pseudomonas aeruginosa* ATCC 27853 and *Escherichia coli* ATCC 25922). The results from the TTC assay for antibacterial activity showed that 5'-*O*-(*tert*-butyldiphenylsilyl)uridine **107**, 5'-*O*-(*tert*-butyldiphenylsilyl)-1'-*O*-methoxy- α -(-)-ribose **102** and *tert*-butyldiphenylsilyl alcohol **145** exhibited modest activity towards only the Gram-positive bacteria when compared to the ciprofloxacin **153** control (**Figure 80**). From the data reported for the antibacterial assay, we concluded that the nucleoside showing the most promising results was uridine and as such it would be the

nucleoside of choice for our subsequent antibacterial activity studies. Our mini SAR study on the uridine derivatives found that the best position for performing modifications to our nucleosides was at the 5'-OH position on the sugar ring and a loss of either or both of the secondary alcohols (2'-OH and 3'-OH) and/or the primary amide on the base leads to a reduction in activity of the compounds. Lastly, the comparison of α -(-)-ribose derivatives to the uridine derivatives suggested that the bases on the nucleoside derivatives were probably necessary for molecular recognition to aid transportation within the cells.

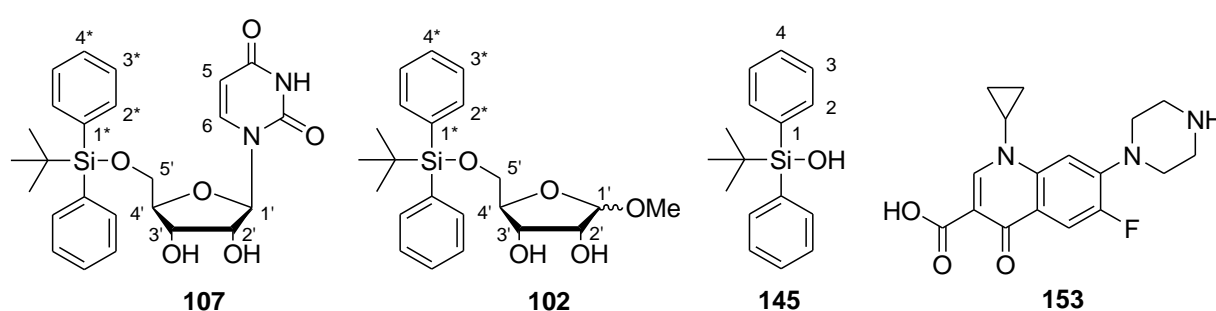


Figure 80 Selected compounds screened using the TTC assay for antibacterial activity

We found that none of the range of synthetic nucleoside and protecting group derivatives assayed showed any antiviral activity towards HIV_{III}B. However, we did observe that a large number of the compounds were toxic towards the uninfected MT-4 cells (human T-cell leukemia cell line) at millimolar levels. This was quite unexpected and we believed that it suggested that our synthetic compounds may be toxic towards specifically cancerous cells. This possibility was subsequently investigated in our cell proliferation studies, where most of the synthetic compounds were screened for their "anticancer" properties against two adherent (HT-29 and Caco-2) and three suspension (HL-60, Jurkat and K-562) cell lines. The results of this study showed that 5'-*O*-(*tert*-butyldiphenylsilyl)uridine **107**, 5'-*O*-(4,4'-dimethoxytrityl)uridine **126** and 5'-*O*-(*tert*-butyldiphenylsilyl)cytidine **134** (**Figure 81**) were active against both the suspension and the adherent cell lines. Whereas, *tert*-butyldiphenylsilylanol **145** was active against only the adherent lines and 4,4'-dimethoxytrityl alcohol **147** was active against only the suspension cell lines (illustrated in **Figure 81**).

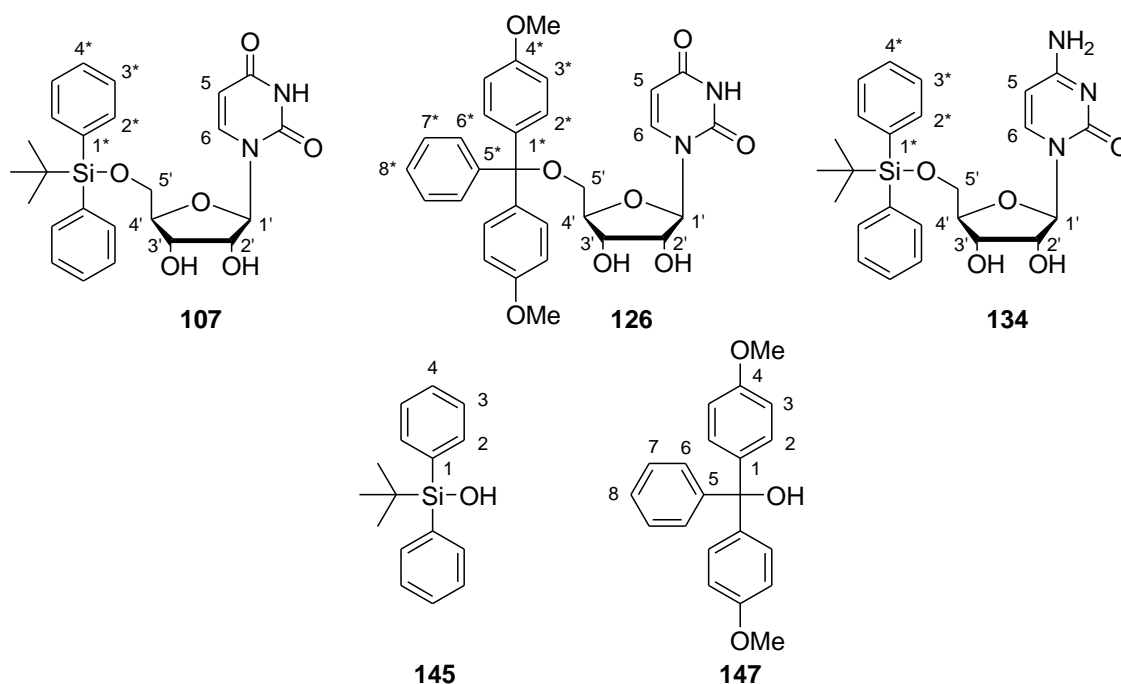


Figure 81 Selected compounds screened in the inhibition of cell proliferation assay

In general, all of the active compounds show a degree of selective cytotoxicity against the cancer cell lines tested, with minimal cytotoxicity directed against the white blood cells. The synthetic compounds, described above, also proved to be effective in inducing apoptosis, modulating the expression of caspase 3 and caspase 8, as well as causing the release of cytochrome *c* from the mitochondria into the cytosol. The cytotoxic effects of these derivatives therefore suggest potential for further development in cancer therapy.

For all of the biological testing, we have found that α -(-)-ribose derivatives, in general did not show any significant biological activity, whereas (*tert*-butyldiphenylsilyl)-protected nucleoside derivatives and the corresponding *tert*-butyldiphenylsilyl alcohol control seem to be intrinsically bio-active. As such, we extrapolated that a second generation of synthetic compounds derived from the nucleoside uridine and containing silyl-protecting groups would be the best way to develop promising lead compounds.

We then moved on to the preparation and testing of our second generation of compounds; a decision was taken to synthesise a "second generation" of compounds that contained various silicon protecting groups, to determine if the results obtained in **Part 1**, suggested a general trend of biological activity or if they were specific to the *tert*-butyldiphenylsilyl group. The proposed "second generation compounds" included a series of uridine **12** and 5-methyluridine **233** derivatives which were protected on the primary alcohol with a range of different sized silicon-containing protecting groups. We hoped that this would allow us to find the optimally sized silicon-containing protecting group that would impart good biological activity.

Using our general approach for the synthesis of 5'-*O*-silicon protected uridine derivatives, we were able to synthesize a further five uridine derivatives and another five 5-methyluridine derivatives. Similarly, we made use of a modified approach to synthesize a range of tethered 1,1,3,3-tetraisopropylidisiloxane-protected uridine derivatives. From this group of compounds we obtained five molecules that were modified in various positions on the sugar ring, as well as at the amide position on the base. At the same time, we utilized a general procedure for the conversion of silyl chlorides to silanols, and used this procedure to synthesize a series of fourteen silanols, ranging from low to high molecular weight and spanning a wide range of chemical space.

From the data reported above (*Section 6.2.1.2*), we were able to conclude that in general the protection of uridine **12** (**Figure 82**) and 5-methyluridine **233** (**Figure 82**) with silicon-containing protecting groups did not increase the antibacterial activity for the parent nucleoside, as suggested based on the results obtained for 5'-*O*-(*tert*-butyldiphenylsilyl)uridine **107** (**Figure 82**) in **Part 1**. However, one highly active exception was found, when the two silicon atom containing 1,1,3,3-tetraisopropylidisiloxane protecting group was used.

From our antibacterial TTC assay, we were able to show that converting the base in 1-[(6*aR*,8*R*,9*R*,9*aS*)-9-hydroxy-2,2,4,4-tetraisopropyltetrahydro-6*H*-furo[3,2-*f*][1,3,5,2,4]trioxadisilocin-8-yl]-pyrimidine-2,4(1*H*,-3*H*)dione **234** (**Figure 82**) to the 5-methyl derivative **254** (**Figure 82**) caused a corresponding loss in anti-bacterial activity for the compound (from 16

mg/L to 32 mg/L for *S. aureus* and *B. cereus* respectively), whereas oxidising the secondary alcohol on the 2'-position of the sugar ring to give compound **239** (Figure 82), caused a corresponding increase in anti-bacterial activity for the molecule (from 16 mg/L to 8 mg/L for *S. aureus* and *B. cereus* respectively). As such, we concluded that 1-[(6*aR*,8*R*,9*aR*)-2,2,4,4-tetraisopropyl-9-oxotetrahydro-6*H*-furo[3,2-*f*][1,3,5,-2,4]trioxadisilocin-8-yl]pyrimidine-2,4(1*H*,3*H*)dione **239** was the compound with the best antibacterial activity out all of the "first generation" and "second generation" of nucleoside derivatives.

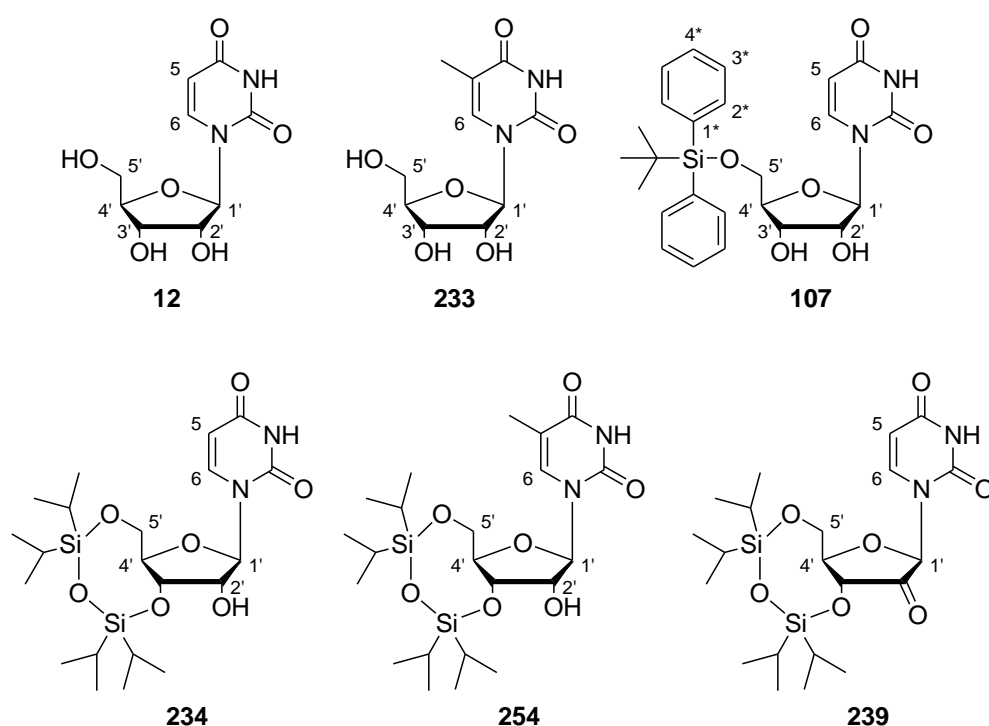


Figure 82 Active compounds identified when screened using the TTC assay for antibacterial activity and then taken into SEM and CSLM studies

These results obtained in the TTC assay, were also supported by our SEM studies. For our first SEM study, we showed that Gram-positive bacterial cells treated with uridine **12** (Figure 82) at a concentration of 0.5 mg/L showed no inhibition of bacterial growth. In general, all cells for both bacterial strains used, showed no surface indentations or distortions to the cell shape, indicating that the unmodified nucleoside had no effect on the bacterial strains tested.

In comparison, we were able to demonstrate that *S. aureus* ATCC 25923 cells treated with high concentrations of 5'-*O*-(*tert*-butyldiphenylsilyl)uridine **107** (**Figure 82**) showed smooth cell surfaces, but distortions occurred in the spherical shape of the cells. For *B. cereus* DL5, we observed that the cells had aggregated together, appeared to have rough surfaces and had ruptured in a few of the examples.

In our second SEM study, we were able to show that all of the compounds **234**, **254** and **239** (**Figure 82**) showed a major reduction in bacterial growth at high concentrations. In addition, we were able to visualize how compound **239** was the only example, where significant bacterial cell wall damage (major indentations on the cell surface, as well as surface rupturing) was observed for both *S. aureus* ATCC 25923 and *B. cereus* DL5.

From the CSLM study performed we validated the results obtained from the previously performed antibacterial TTC assay for the determination of the percentage of metabolically active cells present after treatment with antibiotics and synthetic compounds were accurate representations of what was occurring in our overnight bacterial cultures. Interestingly, we found that the CSLM images for both *S. aureus* ATCC 25923 and *B. cereus* DL5 treated with compound **239** (**Figure 82**) at various concentrations showed no visible cells stained yellow indicating cell injury. This suggests that the synthetic compound **239** is bacteriocidal and is killing the cells, not simply inhibiting their growth.

From the inhibition of cell proliferation assay, performed on the fifty first and second generation derivatives and their corresponding controls, we found that the six most active compounds had mean IC₅₀ values of approximately 24-28 μ M. The results obtained are summarized below:

- 5'-*O*-(*tert*-butyldiphenylsilyl)adenosine **142** ($24 \pm 4 \mu$ M)
- 5'-*O*-(*tert*-butyldiphenylsilyl)cytidine **134** ($25 \pm 4 \mu$ M)
- 5'-*O*-(*tert*-butyldiphenylsilyl)uridine **107** ($28 \pm 3 \mu$ M)
- 2',3'-*O*-diacetyl-5'-*O*-(*tert*-butyldiphenylsilyl)uridine **123** ($25 \pm 3 \mu$ M)
- 2',3'-*O*-diacetyl-5'-*O*-(4,4'-dimethoxytrityl)uridine **127** ($25 \pm 4 \mu$ M)

- 3-benzoyl-1-[(6*aR*,8*R*,9*R*,9*aS*)-9-hydroxy-2,2,4,4-tetraisopropyltetrahydro-6*H*-furo[3,2-*f*][1,3,5,2,4]trioxo-disilocin-8-yl]pyrimidine-2,4(1*H*,3*H*)-dione **235** ($28 \pm 1 \mu\text{M}$)

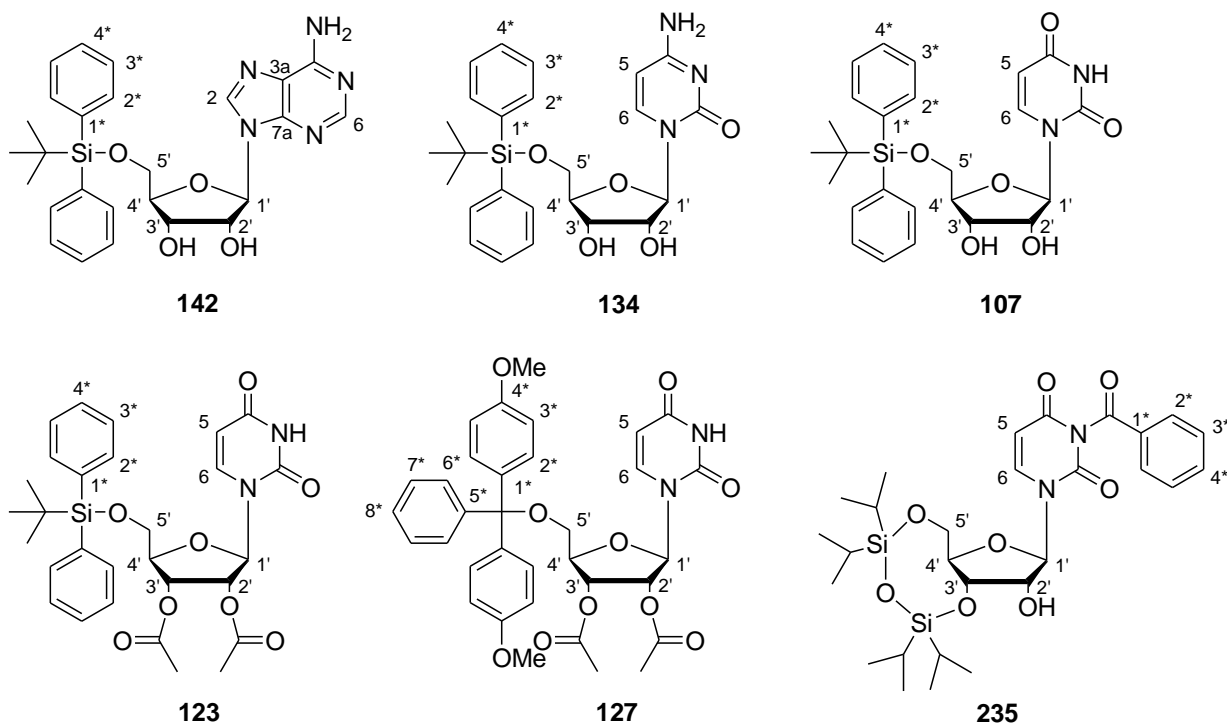


Figure 83 Active compounds identified in full inhibition of cell proliferation study

8.2 FUTURE WORK

8.2.1 Current State of the Work

On various instances during the preparation of our “second generation” compounds, we isolated compounds in which the silyl protecting groups had added to the uridine sugar ring in more than one place. As these side-products were not planned for and due to the time constraints of the project, they were not tested for any biological activity. As such, they were not included in the body of work discussed in this thesis. However, we feel that in light of the

interesting antibacterial and anticancer results obtained for compounds containing two-silicon atoms in the protecting group (such as **234**, **235** and **239**), this group of compounds may be of enough interest to re-investigate them fully in the future. To this end, a select few examples where we were able to easily isolate the multiple protecting group containing by-products have been shown graphically in **Figure 84**.

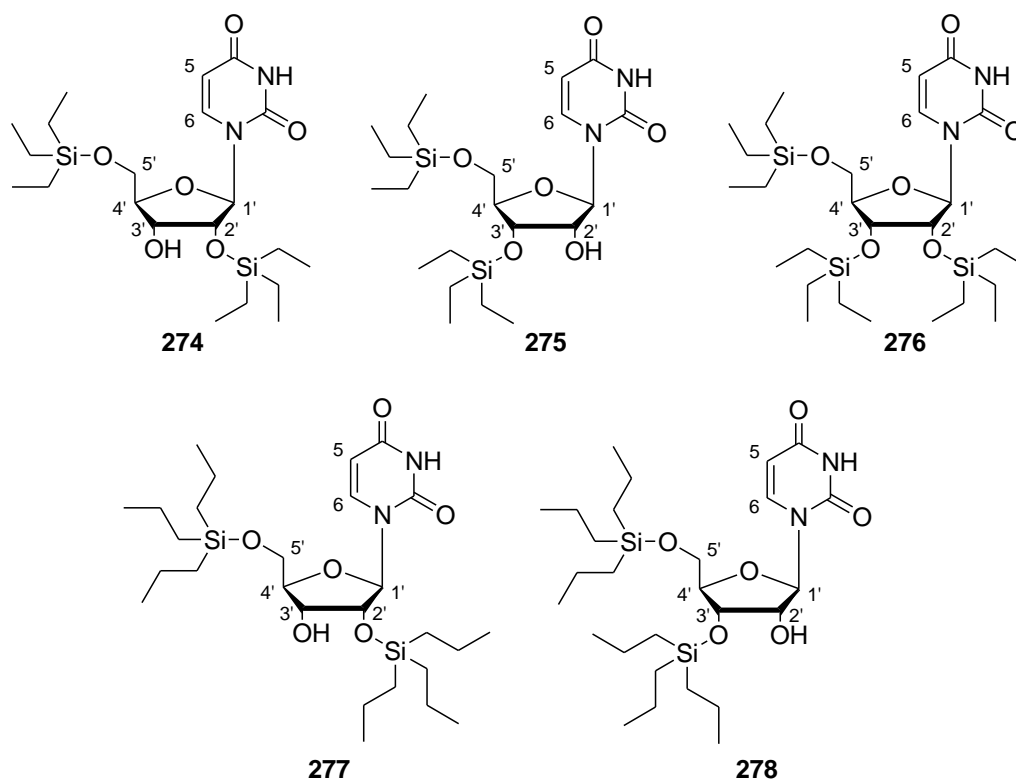


Figure 84 Selected examples of by-products containing multiple protecting group additions

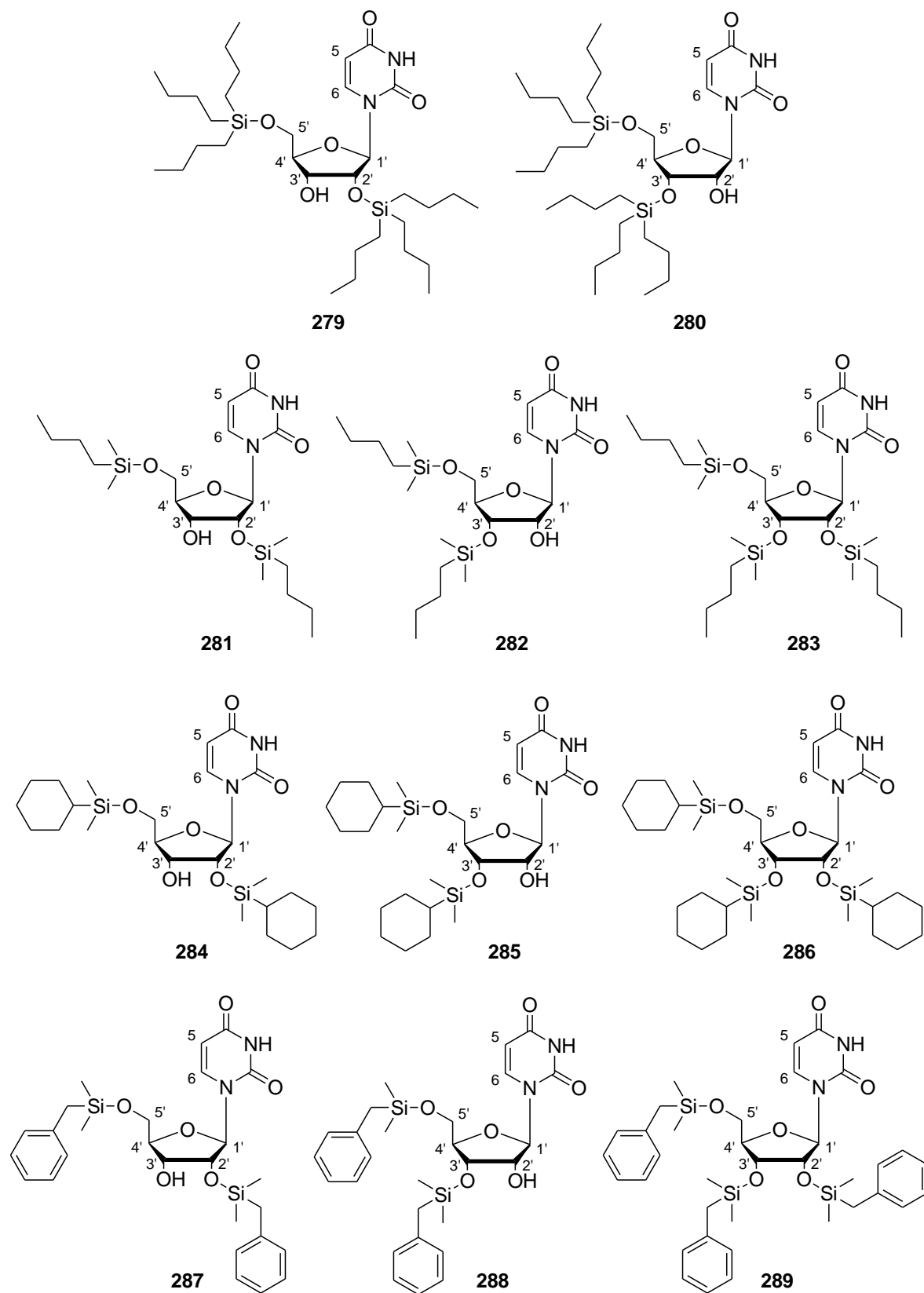


Figure 84 continued Selected examples of by-products containing multiple protecting group additions

Only one worked example will be included for general reference purposes. The example chosen is the preparation of compounds **274**, **275** and **276**, derived from the simplest of the silicon-containing protecting groups, *triethylsilyl chloride*. The full experimental procedure and the spectroscopic data are discussed in detail in **Appendix F**.

8.2.2 The Way Forward: Part 1 – Multiple Protecting Group Additions

Based on the promising results observed in our biological assays when testing compounds containing two silicon atoms (*Section 8.1*) and when considering the ease of formation of the multiple protecting group-containing by-products discussed above (*Section 8.2.1*), we feel it would be important to continue this project by selectively preparing a series of compounds with multiple protecting groups of varying steric bulk and lipophilicity (**Figure 85**).

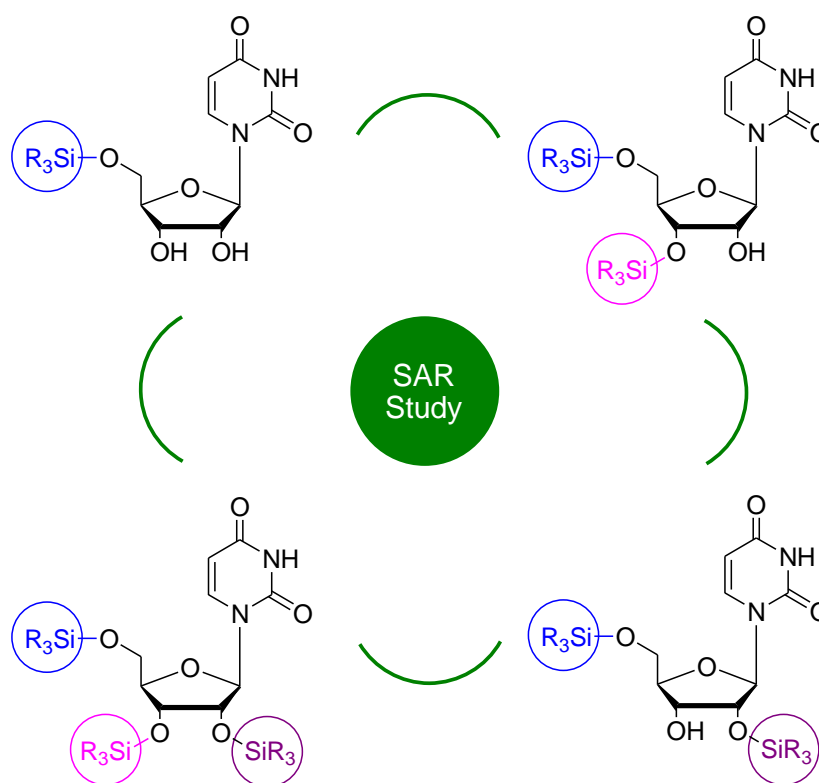


Figure 85 Possible uridine derivatives to be used in future SAR studies for biological activity

By doing this we would be able to correlate chemical structures to activity in order to determine the following relationships:

- Differentiate activity on the basis of one vs. two vs. three individual protecting groups, each containing a single silicon atom, in order to ascertain if increasing the number of silicon atoms directly increases the biological activity of the compounds
- Differentiate activity on the basis of the steric size of the protecting groups attached and the lipophilicity of those groups, to determine which silicon-protecting group “molecular size” is optimal for activity
- Identify which position/s are ideal for activity, for example: the 2'-*O*-/5'-*O*-protected combination vs. the 3'-*O*-/5'-*O*-protected combination
- Correlate activity for molecules with two silicon-protecting groups (3'-*O*-triisopropylsilyl and 5'-*O*-triisopropylsilyl) against the data previously obtained for our second generation compounds containing the two silicon-tethered protecting group (2,2,4,4-tetraisopropylidisiloxane)

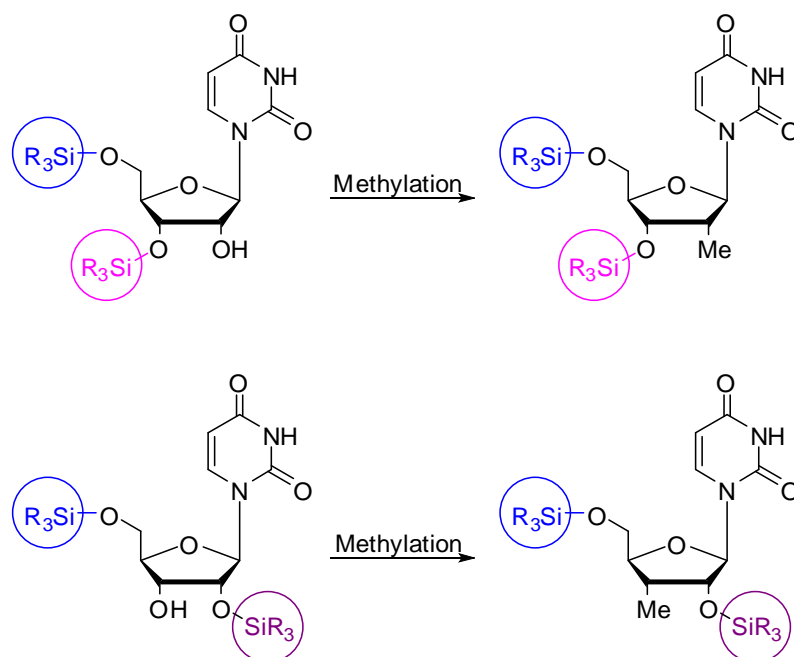
Once we have the results in hand from our standard biological assays (for antibacterial and anticancer activity) – we hope to be able to identify any conclusive link between the structures and their activity. This would allow us to ring-fence the most promising “lead-compounds” to develop in future generations.

8.2.3 The Way Forward: Part 2 – Modifications to the Sugar Ring Hydroxyl Groups

Moving forward with the best hits from the structure activity screen described in detail above (Section 8.2.2), we would proceed with the “lead-compounds” and modify the un-silylated hydroxyls of the sugar ring in order to obtain compounds that better fit Lipinski’s guidelines*, have more favorable solubility indexes and offer good cLog P values.

***Lipinski’s Guidelines State:** In general, an orally active drug has no more than one violation of the following criteria: (i) not more than five H-bond donors, (ii) not more than ten H-bond acceptors, (iii) a molecular weight under 500 daltons and (iv) an octanol-water partition coefficient log P less than five.¹⁵³⁻¹⁵⁵

This could be done in a number of ways, the first step would be to prepare simplified derivatives of the lead-compounds where the free hydroxyl group is “blocked” – an example of how this could be achieved is given in **Scheme 27**.



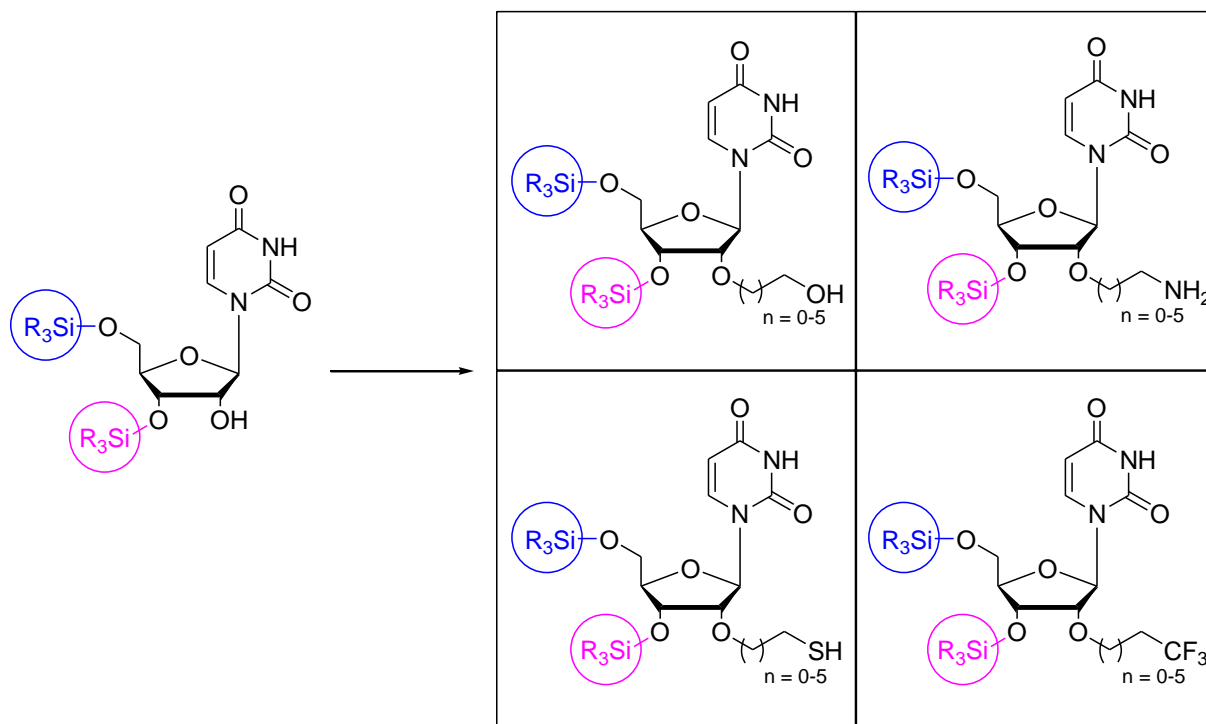
Scheme 27 General example of simple methylation reaction on the free hydroxyl group

After biological screening of these compounds, two possible outcomes are foreseeable:

- (i) if it is observed that the activity of the compounds is not negatively affected by “blocking” the free hydroxyl group, then this position can be used as a handle on which to add solubilising groups to the molecule[♦]
- (ii) if however, it is observed that the activity of the compounds is lost by “blocking” the free hydroxyl group, we could further investigate the addition of various groups containing either H-bond donors or acceptors (to try to mimic the relationship of the

[♦] The types of solubilising groups to be added are entirely dependent on the active compounds themselves – the cLogP values would directly influence the type of group that would be required to move the cLogP value into the accepted Lipinski range. For example, we would need to look at the active compound to determine if a “fatty” group is appropriate or not.

free hydroxyl group in the interactions with the active sites) as well as to favorably match Lipinski's guidelines (**Scheme 28**).



Scheme 28 Addition of H-bond donors/acceptors to the molecules where “blocking” the hydroxyl causes an inhibition of biological activity

Chapter 9:
References

9.1 REFERENCES RELATING TO CHAPTER 1

- (1) King, M.W., *Medical Biochemistry Page - IU School of Medicine*, **2006**, web-reference, see: <http://www.miking.iupui.edu> (date accessed: 21-07-2009)
- (1b) Nakata, H., Yoshioka, K., Kamiya, T., Tsuga, H., Oyanagi, K., *J. Mol. Neurosci.*, **2005**, 26, 233
- (2) *Aldrich Chemistry - Handbook of Fine Chemicals, South African Edition*, **2009-2010**, pages 60, 869, 1501, 2564 and 2736
- (3a) Voet, D., Voet, J.G., Pratt, C.W., *Fundamentals of Biochemistry*, **1999**, John Wiley and Sons, Inc., USA, 43-45
- (3b) Voet, D., Voet, J.G., Pratt, C.W., *Fundamentals of Biochemistry*, **1999**, John Wiley and Sons, Inc., USA, 48-53
- (4) Rachakonda, S., Cartee, L., *Curr. Med. Chem.*, **2004**, 11, 775
- (5) Ed: Kurstak, E., *Applied Virology*, **1984**, Academic Press, Florida, USA, Chapter 7, 87-102
- (6) de Clercq, E., *J. Clin. Virol.*, **2004**, 30, 115
- (7) Mwau, M., McMichael, A.J., *J. Gene Med.*, **2003**, 5, 3
- (8) Milroy, D., Featherstone, J., *Nat. Rev. Drug Disc.*, **2002**, 1, 11
- (9) American Cancer Society. In *American Cancer Society Statistics for 2007*, see: http://www.cancer.org/docroot/PRO/content/PRO_1_1_Cancer_Statistics_Presentation_2007.asp
- (10) Palchadhuri, R., Nesterenko, V., Hergenrother, J., *J. Am. Chem. Soc.*, **2008**, 130, 10274
- (11) Vorbrüggen, H., Ruh-Pohlenz, C., *Handbook of Nucleoside Synthesis*, **2001**, John Wiley and Sons, Inc., USA and Canada, ix-xii
- (12) Schitter, G., Wrodnigg, T.M., *Exp. Opin. Drug Disc.*, **2009**, 4, 315
- (13) Drone, J., Egorov, M., Hatton, W., Bertrand, M.-J., Len, C., Lebreton, J., *Synlett*, **2006**, 1339
- (14) Sharma, P.K., Petersen, M., Nielsen, P., *J. Org. Chem.*, **2005**, 70, 4918
- (15) Steffansen, S.I., Christensen, M.S., Børsting, P., Nielsen, P., *Nucleos. Nucleot. Nucl.*, **2005**, 24, 1015
- (16) Serra, C., Farràs, J., Vilarrasa, J., *Tetrahedron Lett.*, **1999**, 40, 9111
- (17) Raunkjær, M., Haselmann, K.F., Wengel, J., *J. Carbohydr. Chem.*, **2005**, 24, 475
- (18) Gagneron, J., Gosselin, G., Mathé, C., *J. Org. Chem.*, **2005**, 70, 6891

- (19) Yu, C.-S., Wang, R.-T., Chiang, L.-W., Lee, M.-H., *Tetrahedron Lett.*, **2007**, 48, 2979
- (20) Albæk, N., Petersen, M., Nielsen, P., *J. Org. Chem.*, **2006**, 71, 7731
- (21) Mieczkowski, A., Roy, V., Agrofoglio, L.A., *Chem. Rev.*, **2010**, 110, 1828
- (22) Sørensen, A.M., Nielsen, P., *Org. Lett.*, **2000**, 2, 4217
- (23) Børsting, P., Nielsen, P., *Chem. Commun.*, **2002**, 2140
- (24) Kirchhoff, C., Nielsen, P., *Tetrahedron Lett.*, **2003**, 44, 6475
- (25) Børsting, P., Freitag, M., Nielsen, P., *Tetrahedron*, **2004**, 60, 10955
- (26) Nielsen, P., Børsting, P., *Nucleos. Nucleot. Nucl.*, **2005**, 24, 349
- (26b) Steffansen, S.I., Christensen, M.S., Børsting, P., Nielsen, P., *Nucleos. Nucleot. Nucl.*, **2005**, 24, 1015
- (26c) Drone, J., Egorov, M., Hatton, W., Bertrand, M.-J., Len, C., Lebreton, J., *Synlett*, **2006**, 9, 1339
- (27) Børsting, P., Christensen, M., Steffansen, S.I., Nielsen, P., *Tetrahedron*, **2006**, 62, 1139
- (28) Sharma, P.K., Mikkelsen, B.H., Christensen, M.S., Nielsen, K.E., Kirchhoff, C., Pedersen, S.L., Sørensen, A.M., Østergaard, K., Petersen, M., Nielsen, P., *Org. Biomol. Chem.*, **2006**, 4, 2433
- (29) van Otterlo, W.A.L., Coyanis, E.M., Panayides, J.-L., de Koning, C.B., Fernandes, M.A., *Synlett*, **2005**, 501
- (30) Pathak, R., Panayides, J.-L., Jetic, T.D., de Koning, C.B., van Otterlo, W.A.L., *S. Afr. J. Chem.*, **2007**, 60, 1
- (31) Panayides, J.-L., Pathak, R., de Koning, C.B., van Otterlo, W.A.L., *Eur. J. Org. Chem.*, **2007**, 4953
- (32) Coyanis, E.M., Panayides, J.-L., Fernandes, M.A., de Koning, C.B., van Otterlo, W.A.L., *J. Organomet. Chem.*, **2006**, 691, 5222
- (33) Panayides, J.-L., Pathak, R., Panagiotopoulos, H., Davids, H., Fernandes, M.A., de Koning, C.B., van Otterlo, W.A.L., *Tetrahedron*, **2007**, 63, 4737
- (34) Trost, B.M., Fleming, I., Paquette, L.A., Eds, Grubbs, R.H., Pine, S.H., in *Comprehensive Organic Synthesis*, **1991**, Pergamon Press, New York, Vol 5, Chapter 9.3
- (35) Grubbs, R.H., Chang, S., *Tetrahedron*, **1998**, 54, 4413
- (36) Nguyen, S.T., Johnson, L.K., Grubbs, R.H., Ziller, J.W., *J. Am. Chem. Soc.*, **1992**, 114, 3974
- (37) Fürstner, A., *Angew. Chem. Int. Ed. Engl.*, **2000**, 39, 3012

9.2 REFERENCES RELATING TO CHAPTER 2

- (38) Földesi, A., Nilson, F.P.R., Glenmarec, C., Gioeli, C., Chattopadhyaya, J., *Tetrahedron*, **1992**, 48, 9033
- (39) Montembault, M., Bourgougnon, N., Lebreton, J., *Tetrahedron Lett.*, **2002**, 43, 8091
- (40) Wu, J.-C., Xi, Z., Gioeli, C., Chattopadhyaya, J., *Tetrahedron*, **1991**, 47, 2237
- (41) Prakash, T.P., Kawasaki, A.M., Fraser, A.S., Vasquez, G., Manoharan, M., *J. Org. Chem.*, **2002**, 67, 357
- (42) Sproat, B.S., Bejjar, B., Grøtli, M., Ryder, U., Morand, K.L., Lamond, A.I., *J. Chem. Soc. Perkin Trans. I*, **1994**, 419
- (42b) During the course of the thesis work, compound **108** was successfully synthesised by: Tanaka, S., Hirakawa, T., Oishi, K., Hayakawa, Y., Kitamura, M., *Tetrahedron Lett.*, **2007**, 48, 7320
- (43) Jin, S., Miduturu, C.V., McKinney, D.C., Silverman, S.K., *J. Org. Chem.*, **2005**, 70, 4284
- (44) Sekine, M., *J. Org. Chem.*, **1989**, 54, 2321
- (45) Khalafi-Nezhad, A., Mokhtari, B., *Tetrahedron Lett.*, **2004**, 45, 6737
- (46) Kamimura, T., Masegi, T., Sekine, M., Hata, T., *Tetrahedron Lett.*, **1984**, 25, 38, 4241
- (47) Kamimura, T., Masegi, T., Urakami, K., Honda, S., Sekine, M., Hata, T., *Chem. Lett.*, **1983**, 1051
- (48) González, A.G., Brouard, I., León, F., Padrón, J.I., Bermejo, J., *Tetrahedron Lett.*, **2001**, 42, 3187
- (49) Townsend, L.B., Tipson, R.S. (Eds), *Nucleic Acid Chemistry – Improved and New Synthetic Procedures, Methods and Techniques*, **1978**, John Wiley and Sons, New York, Volume One, 46
- (50) Mullen, D.G., Barany, G., *J. Org. Chem.*, **1988**, 53, 5240
- (51) Bleasdale, C., Ellwood, S.B., Golding, B.T., *J. Chem. Soc., Perkin Trans. I*, **1990**, 803

9.3 REFERENCES RELATING TO CHAPTER 3

- (52) *American Type Culture Collection*, web-reference, see:
<http://www.atcc.org/SearchCatalogs/linkin/?id=25923> (date accessed: 28-08-2007)
- (53) Lindsay, D., Brözel, V.S., Mostert, J.F., von Holy, A., *Int. J. Food Microbiol.*, **2000**, 54, 49
- (54) Lindsay, D., Mosupye, F.M., Brözel, V.S., von Holy, A., *Lett. Appl. Microbiol.*, **2000**, 30, 364
- (55) Lindsay, D., Brözel, V.S., Mostert, J.F., von Holy, A., *J. Appl. Microbiol.*, **2002**, 92, 352

- (56) *American Type Culture Collection*, web-reference, see:
<http://www.atcc.org/SearchCatalogs/linkin/?id=27853> (date accessed: 28-08-2007)
- (57) *American Type Culture Collection*, web-reference, see:
<http://www.atcc.org/SearchCatalogs/linkin/?id=25922> (date accessed: 28-08-2007)
- (58) Andrews, J.M., *J. Antimicrob. Chemother.*, **2001**, 48, Suppl. S1, 5
- (59) Report of the Working Party on Antibiotic Sensitivity Testing of the British Society for Antimicrobial Chemotherapy (A Guide to Sensitivity Testing): *J. Antimicrob. Chemother.*, **1991**, 27, Suppl. D, 1
- (60) L.H. Damelin, "An Investigation of the Mechanisms Required for Heavy Metal-Induced Hormesis", *Thesis Submitted to the University of the Witwatersrand*, **2002**
- (61) Pannecouque, C., Daelemans, D., De Clerq, E., *Nature Protocols*, **2008**, 3, 427
- (62) Scudiero, D.A., Shoemaker, R.H., Paull, K.D., Monks, A., Tieney, S., Hafziget, T.H., Currens, J.J., Sheriff, D., Boyd, M.R., *Cancer Res.*, **1988**, 48, 4827
- (63) Weislow, O.S., Kiser, R., Fine, D.L., Bader, J., Shoemaker, R.H., Boyd, M.R., *J. Natl. Cancer Inst.*, **1989**, 81, 577
- (64) Cos, P., Hermans, N., De Bruyne, T., Apers, S., Sindambiwe, J.B., Witvrouw, M., De Clerq, E., Vanden Berghe, D., Pieters, L., Vlietinck, A.J., *Phytomedicine*, **2002**, 9, 62
- (65) Balzarini, J., Van Aerschot, A., Pauwels, R., Baba, M., Schols, D., Herdewijn, P., De Clerq, E., *Mol. Pharmacol.*, **1989**, 35, 571
- (66) Molla, A., Mo, H., Vasavanonda, S., Han, L., Lin, C.T., Hsu, A., Kempf, D.J., *Antimicrob. Agents Chemother.*, **2002**, 46, 2249
- (67) Gallagher, R., Collins, S., Trujillo, J., McCredie, K., Ahearn, M., Tsai, S., Metzgar, R., Aulakh, G., Ting, R., Ruscetti, F., Gallo, R., *Blood*, **1979**, 54, 713
- (68) *Wikipedia*, web-reference, see: <http://en.wikipedia.org/wiki/HL60> (date accessed: 19-10-2009)
- (69) Schneider, U., Schwenk, H., Bornkamm, G., *Int. J. Cancer*, **1977**, 19, 621
- (70) *Wikipedia*, web-reference, see: http://en.wikipedia.org/wiki/Jurkat_cells (date accessed: 09-07-2010)
- (71) *Wikipedia*, web-reference, see: http://en.wikipedia.org/wiki/K562_cells (date accessed: 19-10-2009), additional information sourced from: Lozzio, C.B., Lozzio, B.B., *Blood*, **1975**, 45, 321
- (72) Lozzio, B.B., Lozzio, C.B., *Leukemia Research*, **1979**, 3, 363
- (73) *Wikipedia*, web-reference, see: <http://en.wikipedia.org/wiki/Caco-2> (date accessed: 19-10-2009), additional information sourced from: (a) Fogh, J., Trempe, G., *Human Cells In Vitro (Fogh, J., Ed.)*,

- 1975**, Plenum, USA, 115-141; (b) Pinto, M., Robine-Leon, S., Appay, M.D., *Biol. Cell.*, **1983**, 47, 323 and (c) Hidalgo, I.J., Raub, T.J., Borchardt, R.T., *Gastroenterology*, **1989**, 96, 736
- (74) Shah, P., Jogani, V., Bagchi, T., Misra, A., *Biotechnol. Prog.*, **2006**, 22, 186
- (75) Artursson, P., Palm, K., Luthman, K., *Adv. Drug Delivery Rev.*, **2001**, 46, 27
- (76) Zhivotovsky, B., Orrenius, S., *Semin. Cancer Biol.*, **2003**, 13, 125
- (77) N. Dahan-Farkis, *Dissertation to be submitted to the University of the Witwatersrand*, **in preparation**
- (78) H. Panagiotopoulos, *Dissertation to be submitted to the University of the Witwatersrand*, **in preparation**

9.4 REFERENCES RELATING TO CHAPTER 4

- (79) Michl, J., *Chem. Rev. Editorial Forward*, **1995**, 95, 5
- (80) O'Lenick, A.J., *Silicone Spectator*, **1999**, web-reference, see: www.siliconespectator.com (date accessed: 18-12-2011)
- (81) Thomas, S.E., *Oxford Chemistry Primers, Organic Synthesis – The Roles of Boron and Silicon*, **1995**, Oxford University Press, USA, 47-49
- (82) Lickiss, P.D., Stubbs, K.M., *J. Organomet. Chem.*, **1991**, 421, 171
- (83) Showell, G.A., Mills, J.S., *Drug Discovery Today*, **2003**, 8, 551
- (84) Burnis, G.W., Murcko, M.A., *J. Med. Chem.*, **1996**, 39, 2887
- (85) Burnis, G.W., Murcko, M.A., *J. Med. Chem.*, **1999**, 42, 5095
- (86) Tacke, R., Wannagat, U., *Top. Curr. Chem.*, **1979**, 84, 1
- (87) Steele, P., *Expert Opin. Ther. Pat.*, **2002**, 12, 3
- (88) Mills, J.S., Showell, G.A., *Exp. Opin. Investig. Drugs*, **2004**, 13, 1149
- (89) Reichstat, M.M., *J. Mol. Struct.*, **1991**, 244, 283
- (90) Holte, H.D., Busch, T., *Dtsch. Apoth. Ztg.*, **1986**, 38, 2007
- (91) Woo, D.V., Christian, J.E., *Can. J. Pharm. Sci.*, **1979**, 14, 12
- (92) Clark, D.E., *Drug Discov. Today*, **2003**, 8, 927

- (93) Pooni, P.K., Showell, G.A., *Mini-Reviews in Medicinal Chemistry*, **2006**, 6, 1169
- (94) Stasch, J.-P., Ruß, H., Schacht, U., Neuser, D., Gerlach, M., Leven, M., Kuhn, W., Jutzi, P., Przuntek, H., *Arzneim.-Forsch. Drug Res.*, **1988**, 38, 1075
- (95) Tacke, R., Heinrich, T., Bertermann, R., Burschka, C., Hamacher, A., Kassack, M.U., *Organometallics*, **2004**, 23, 4468
- (96) Kagechika, H., Shudo, K., *J. Med. Chem.*, **2005**, 48, 5875
- (97) Daiss, J.O., Burschka, C., Mills, J.S., Montana, J.G., Showell, G.A., Fleming, I., Gaudon, C., Ivanova, D., Gronemeyer, H., Tacke, R., *Organometallics*, **2005**, 24, 3192
- (98) Garson, L.R., Kirchner, L.K., *J. Pharm. Sci.*, **1971**, 60, 1113
- (99) Farkas, S., Kocsis, P., Bielik, N., Gémesi, L., Trafikânt, G., *Fundam. Clin. Pharmacol.*, **1999**, 13, PS144
- (100) Brufani, M., Filocamo, L., Lappa, S., Maggi, A., *Drug Future*, **1997**, 22, 397
- (101) Palazzolo, R.J., McHard, J.A., Hobbs, E.J., Fancher, O.E., Calandra, J.C., *Toxicol. Appl. Pharmacol.*, **1972**, 21, 15
- (102) Alfthan, O., Andersson, L., Esposti, P.L., *Scand. J. Uron. Nephrol.*, **1983**, 17, 37
- (103) Collste, L., Berlin, T., von Garrelts, B., Granberg, I., Lewander, R., *Eur. Urol.*, **1981**, 7, 85
- (104) Anderson, C.Y., Freye, K., Tubesing, K.A., *Photochem. Photobiol.*, **2004**, 67, 332
- (105) Kurie, J., Hong, W.K., Khuri, F., *Proc. Am. Soc. Clin. Oncol.*, **2000**, 19, 749
- (106) Schilsky, R., Hausheer, F., Bertucci, D., Berghorn, E., Kindler, H., Ratain, M., *Proc. Am. Soc. Clin. Oncol.*, **2000**, 19, 758
- (106b) Camarasa, M.-J., San-Félix, A., Valázquez, S., Pérez-Pérez, M.-J., Gago, F., Balzarini, J., *Curr. Top. Med. Chem.*, **2004**, 4, 945
- (107) Kim, Y.-M., Farrah, S., Baney, R.H., *Electronic Journal of Biotechnology*, **2006**, 9, 176
- (108) Kim, Y.-M., Farrah, S., Baney, R.H., *Electronic Journal of Biotechnology*, **2007**, 10, 252
- (109) Kim, Y.-M., Baney, R.H., Brennan, A.B., *United States Patent*, **2008**, US 7,347,970 B2
- (110) Zablotskaya, A., Segal, I., Popelis, Y., Lukevics, E., Baluja, S., Shestakova, I., Domracheva., *Appl. Organomet. Chem.*, **2006**, 20, 721
- (111) Donadel, O.J., Martín, T., Martín, V., Villar, J., Padrón, J.M., *Bioorg. Med. Chem. Lett.*, **2005**, 15, 3536
- (112) Padrón, J.M., Donadel, O.J., León, L.G., Martín, T., Martín, V.S., *Lett. Drug Des. Discov.*, **2006**, 3, 29

- (113) Josien, H., Bom, D., Curran, D.P., *Bioorg. Med. Chem. Lett.*, **1997**, 7, 3189
- (114) Bikzhanova, G.A., Touloukhonova, I.S., Gately, S., West, R., *Silicon Chemistry*, **2005**, 3, 209
- (115) McCormick, K.J., Panje, W.R., *Cancer Immunol. Immunother.*, **1986**, 21, 226
- (116) Maca, R.D., Panje, W.R., *Cancer*, **1982**, 50, 483
- (117) Panje, W.R., *Arch. Otolaryngol.*, **1981**, 107, 658
- (118) Ulrich, C.M., Bigler, J., Potter, J.D., *Nat. Rev. Cancer*, **2006**, 6, 130
- (119) Lukevits, E., Segal, I., Birgele, I., Zablotskaya, A., *Chem. Heterocycl. Compd.*, **1998**, 34, 1076
- (120) Black, C.A., Ucci, Vorpapel, J.S., Mauck M.C., Fenlon, E.E., *Bioorg. Med. Chem. Lett.*, **2002**, 12, 3521

9.5 REFERENCES RELATING TO CHAPTER 5

- (121) Matsuda, A., Tanenuki, K., Tanaka, M., Sasaki, T., Ueda, T., *J. Med. Chem.*, **1991**, 34, 812
- (121b) During the course of the thesis work, compounds **240** and **241** were successfully synthesised by: Ueda, Tohru, *Nucleos. Nucleot. Nucl.*, **1989**, 8, 743 and Iino, Tomoharu, *Tetrahedron*, **1994**, 50, 10397
- (122) Sekine, M., *J. Org. Chem.*, **1989**, 54, 2321

9.6 REFERENCES RELATING TO CHAPTER 6

- (123a) Gilmour, A., Fraser, T.W., *Biofouling*, **1991**, 5, 133
- (123b) Neu, H.C., Gootz, T.D., *Medical Microbiology, 4th Edition. (Baron, S., Ed.)*, **1996**, University of Texas Medical Branch, USA, Chapter 11 – Antimicrobial Chemotherapy
- (123c) Lindsay, D., von Holy, A., *J. Food Prot.*, **1999**, 62, 368

9.7 REFERENCES RELATING TO CHAPTER 7

- (124) *Sigma-Aldrich Company*, web-reference, see:
www.sigmaaldrich.com/catalog/ProductDetail.do?D7=0&N5=SEARCH_CONCAT_PNO|SIGMA&N25=0&QS=ON&F=SPEC (date accessed: 21-11-2011)

- (125) *American Type Culture Collection*, web-reference, see:
www.atcc.org/CulturesandProducts/CellBiology/MisidentifiedCellLines/tabid/683/Default.aspx (date accessed: 21-11-2011)
- (126) *Cell Lines Service*, web-reference, see:
www.cell-lines-service.de/content/e143/e148/e1248/index_ger.html (date accessed: 21-11-2011)
- (127) *American Type Culture Collection*, web-reference, see:
www.atcc.org/ATCCAdvancedCatalogSearch/ProductDetails/tabid/452/Default.aspx?ATCCNum=-HTB-138&Template=cellBiology (date accessed: 21-11-2011)
- (128) Alimirah, F., Chen, J., Basrawala, Z., Xin, H., Choubey, D., *FEBS Lett.*, **2006**, 580, 9, 2294
- (129) Pulukiri, S.M., Gondi, C.S., Lakka, S.S., Julta, A., Estes, N., Gujrati, M., Rao, J.S., *J. Biol. Chem.*, **2005**, 280, 36529
- (130) *American Type Culture Collection*, web-reference, see:
www.atcc.org/ATCCAdvancedCatalogSearch/ProductDetails/tabid/452/Default.aspx?ATCCNum=CR-L-1435&Template=cellBiology (date accessed: 22-11-2011)
- (131) *Wikipedia*, web-reference, see: en.wikipedia.org/wiki/PC3 (date accessed: 22-11-2011)
- (132) *Wikipedia*, web-reference, see: en.wikipedia.org/wiki/MCF-7 (date accessed: 22-11-2011), additional information sourced from: Soule, H.D., Vazquez, J., Long, A., Albert, S., Brennan, M., *J. Natl. Cancer Inst.*, **1973**, 51, 1409
- (133) *American Type Culture Collection*, web-reference, see:
www.atcc.org/ATCCAdvancedCatalogSearch/ProductDetails/tabid/452/Default.aspx?ATCCNum=HT-B-22&Template=cellBiology (date accessed: 22-11-2011)
- (134) *American Type Culture Collection*, web-reference, see:
www.atcc.org/ATCCAdvancedCatalogSearch/ProductDetails/tabid/452/Default.aspx?ATCCNum=HT-B-72&Template=cellBiology (date accessed: 23-11-2011)
- (135) *Cell Lines Service*, web-reference, see: www.cell-lines-service.de/content/e143/e1779/e1618/index_ger.html (date accessed: 23-11-2011)
- (136) *American Type Culture Collection*, web-reference, see:
www.atcc.org/ATCCAdvancedCatalogSearch/ProductDetails/tabid/452/Default.aspx?ATCCNum=CR-L-6475&Template=cellBiology (date accessed: 23-11-2011)
- (137) Ingrassia, L., Lefranc, F., Dewelle, J., Pottier, L., Mathieu, V., Spiegl-Kreinecker, S., Sauvage, S., El Yazidi, M., Dehoux, M., Berger, W., Van Quaquebeke, E., Kiss, R., *J. Med. Chem.*, **2009**, 52, 1100
- (138) Ingrassia, L., Lefranc, F., Mathieu, V., Darro, F., Kiss, R., *Transl. Oncol.*, **2008**, 1, 1

- (139) Dumont, P., Ingrassia, L., Rouzeau, S., Ribaucour, F., Thomas, S., Roland, I., Darro, F., Lefranc, F., Kiss, R., *Neoplasia*, **2007**, 9, 766
- (140) Joseph, B., Darro, F., Behard, A., Lesur, B., Collignon, F., Decaestecker, C., Frydman, A., Guillaumet, G., Kiss, R., *J. Med. Chem.*, **2002**, 45, 2543
- (141) Ingrassia, L., Nshimyumukiza, P., Dewelle, J., Lefranc, F., Wlodarczak, L., Thomas, S., Dielie, G., Chiron, C., Zedde, C., Tisnès, P., van Soest, R., Braeckman, J.C., Darro, F., Kiss, R., *J. Med. Chem.*, **2006**, 49, 1800
- (142) Hayot, C., Debeir, Van Ham, P., Van Damme, M., Kiss, R., *Toxicol. Appl. Pharmacol.*, **2006**, 211, 30
- (143) United States Patent Application Publication: Kiss, R., Dubois, J., Neve, J., Lamoral-Theys, D., Dufrasne, F., Pottier, L., *US 2011/0280940 A1*, Nov 17, **2011**
- (144) Mathieu, V., Pirker, C., Martin de Lassalle, E., Vernier, M., Mijatovic, T., DeNeve, N., Gaussin, J.-F., Dehoux, M., Lefranc, F., Berger, W., Kiss, R., *J. Cell. Mol. Med.*, **2009**, 13(9B), 3960
- (145) Ophardt, C.E., **2003**, *Virtual Chembook, Elmhurst College*, web-reference, see: www.elmhurst.edu/~chm/vchembook/655cancer.html (date accessed: 08-12-2011)
- (146) Yang, C.-C., Hsu, C.-P., Yang, S.-D., *Clin. Cancer Res.*, **2000**, 6, 1024
- (147) Putey, A., Popowycz, F., Do, Q.-T., Bernard, P., Talapatra, S.K., Kozielski, F., Galmarini, C.M., Joseph, B., *J. Med. Chem.*, **2009**, 52, 5916
- (148) Liu, X., Chan, S.Y., Ho, P.C.-L., *Cancer Chemother. Pharmacol.*, **2008**, 63, 167
- (149) Danesi, R., Figg, W.D., Reed, E., Myers, C.E., *Mol. Pharmacol.*, **1995**, 47, 1106
- (150) Chou, T.-C., O'Connor, O.A., Tong, W.P., Guan, Y., Zhang, Z.-G., Stachel, S.J., Lee, C., Danishefsky, S.J., *PNAS*, **2001**, 98, 8113
- (151) Mathieu, V., Le Mercier, M., De Neve, N., Sauvage, S., Gras, T., Roland, I., Lefranc, F., Kiss, R., *J. Invest. Dermatol.*, **2007**, 127, 2399
- (152) Özalp-Yaman, Ş., de Hoog, P., Amadei, G., Pitié, M., Gamez, P., Dewelle, J., Mijatovic, T., Meunier, B., Kiss, R., Reedijk, J., *Chem. Eur. J.*, **2008**, 14, 3418

9.8 REFERENCES RELATING TO CHAPTER 8

- (153) Lipinski, C.A., Lombardo, F., Dominy, B.W., Feeney, P.J., *Adv. Drug Deliv. Rev.*, **1997**, 23, 3
- (154) Lipinski, C.A., *Drug Discov. Today Tech.*, **2004**, 1, 337
- (155) Overington, J.P., Al-Lazikani, B., Hopkins, A.L., *Nat. Rev. Drug Discov.*, **2006**, 5, 993

9.9 REFERENCES RELATING TO APPENDIX A

- (A1) Vorbrüggen, H., Ruh-Pohlenz, C., *Handbook of Nucleoside Synthesis*; John Wiley and Sons; USA, **2001**, 100-101

9.10 REFERENCES RELATING TO APPENDIX B

- (B1) Cravatta, G., Giovenzana, G.B., Sisti, M., Palmisano, G., *Tetrahedron*, **1998**, 54, 1639
- (B2) M. Schlosser (Ed.), *Organometallics in Synthesis: A Manual*, **1994**, John Wiley and Sons, England, Chapter 5: Palladium in Organic Synthesis, Louis S. Hegedus, 448

9.11 REFERENCES RELATING TO APPENDIX C

- (C1) Pidcock, L.J.V., *J. Appl. Bacteriol.*, **1990**, 68, 307

9.12 REFERENCES RELATING TO APPENDIX D

- (D1) Krasovskiy, A., Knochel, P., *Synthesis*, **2006**, 5, 890

9.13 REFERENCES RELATING TO APPENDIX E

- (E1) Molecular Probes, Invitrogen Detection Technologies, *Product Information – LIVE/DEAD BacLight Bacterial Viability Kits L7007, L7012 and L13152*, **2004**, MP07007, 1

9.14 REFERENCES RELATING TO APPENDIX F

No additional references.

APPENDICES
RELATING TO PART 1

Appendix A:
General Synthetic Experimental Procedures

A.1 Purification of Solvents

All solvents used for reactions and preparative chromatography were distilled prior to use. Solvents used in reactions were pre-dried in their reagent bottles and then distilled over the appropriate drying mediums under a nitrogen atmosphere:

- tetrahydrofuran and diethyl ether were distilled from sodium metal wire and benzophenone
- benzene and toluene were distilled from sodium metal lumps
- acetonitrile, dichloromethane, *N,N*-dimethylformamide (stored over 4 Å molecular sieves after distillation), methanol and triethylamine were distilled from calcium hydride
- acetic anhydride was distilled from 4 Å molecular sieves
- pyridine was distilled from potassium hydroxide.

Chloroform was dried by passing it through basic alumina (Merck aluminium oxide, basic, activity grade I).

The Grubbs II catalyst **90** was stored in a Schlenk tube under an argon atmosphere. The procedure for storing the catalyst was to place the Schlenk tube under vacuum and then under argon four to five times to ensure that the system was free from air and it was then stored in the dark.

A.2 Experimental Techniques and Equipment Used

All reactions were performed under an inert atmosphere (either nitrogen or argon) using a standard manifold line and connected to a vacuum pump. The nitrogen and argon were dehydrated by bubbling the gas through sulfuric acid, and then neutralizing by passage through sodium hydroxide pellets. The vessels were flame-dried while under vacuum and were then allowed to cool to room temperature under the inert atmosphere.

Concentration or evaporation *in vacuo* refers to the removal of solvent under reduced pressure (approximately 20 mmHg, 40-50 °C) on a rotary evaporator and final drying on an oil pump (approximately 1-2 mmHg) at room temperature. Items dried under “high vacuum” were also dried using an oil pump (approximately 1-2 mmHg).

Yields are calculated from the immediate synthetic precursor, unless otherwise specified.

The microwave reactor referred to is the CEM Discovery and operating conditions employed for the reactions are outlined in the experimental procedures. The Carousel reactor employed for certain reaction sequences was manufactured by Radleys Discovery Technologies and is sold as the Carousel Reaction Station.

A.3 Chromatographic Separations

Macherey-Nagel Silica gel 60 (particle size 0.063-0.200 mm) was used as the adsorbent for conventional preparative chromatography, with a silica to compound ratio of 30:1. The silica was packed into a suitable size column; the product was loaded onto the silica surface and covered in acid washed sea sand. The elution process was performed using the indicated solvent mixtures and was usually performed under standard air pump pressure conditions.

Pre-prepared silica (basified silica) used for column chromatography, where specified in the text, was prepared as follows:

- the silica required for the column was pre-prepared by shaking with a 10 % NEt_3 : hexane (v/v) solution, used in the ratio of 1 cm^3 solution : 1 g silica, for 15 min at rt. Thereafter, the silica was dried by removing the solvent *in vacuo*.

The R_f values quoted are those obtained from thin layer chromatography on aluminium-backed Macherey-Nagel ALUGRAM Sil G/UV₂₅₄ plates pre-coated with 0.25 mm silica gel 60 or Aldrich TLC plates, silica gel on aluminum. Spray reagents were used on thin layer chromatography plates for the detection of compounds that were not highly UV active. General reagents used include acidic vanillin, basic potassium permanganate, acidic ceric ammonium sulfate, acidic anisaldehyde and iodine that had been adsorbed onto silica gel. Acidic DNPH was used for the detection of ketones and aldehydes specifically.

A.4 Spectroscopic and Physical Data

All melting points were obtained on a Reichert hot-stage microscope and are uncorrected. Because of the many possible hydrogen bonds between nucleoside molecules in the crystalline state, repeated recrystallisation from different solvents or solvent mixtures can give rise to different crystal forms (polymorphism), which have different melting points.^{A1} As such, melting points were not determined for any compounds obtained as foams and only those compounds that gave truly crystalline material were determined.

Optical rotations on the chiral compounds were obtained on a JASCO Model DIP-370 digital polarimeter using a sodium lamp at a wavelength of 589 nm. The compounds were prepared as a solution in a 1 cm³ volumetric flask using an appropriate solvent. The samples were run in a 10 mm cell, using an integration time of 60 sec and calculating the mean value by taking ten readings at 30 sec intervals.

Infrared spectra were obtained either on a Bruker Vector 22 spectrometer, or on a Varian 800FT-IR spectrometer (Scimitar Series). Both solid and liquid samples were run as a thin film under high pressure with no additional solvents added. The absorptions are reported on the wavenumber (cm⁻¹) scale in the 600-3500 cm⁻¹ range. The signals are reported: value (assignment).

Hydrogen nuclear magnetic resonance (^1H NMR) spectra were recorded on Bruker Advance-300 and Bruker DRX 400 spectrometers at 300.13 and 400.13 MHz respectively using standard pulse sequences. The probe temperature for all experiments was $300 \pm 1\text{K}$. All spectra were recorded in deuterated chloroform (CDCl_3) in 5 mm NMR spectroscopy tubes unless otherwise specified. Chemical shifts are reported in parts per million (ppm) relative to tetramethylsilane as the internal standard. The ^1H NMR spectroscopy chemical shifts are reported: value (number of hydrogens, description of signal, coupling constants in hertz (Hz) where applicable, assignment). Abbreviations used: s = singlet, d = doublet, t = triplet, q = quartet, p = pentet, sept = septet, m = multiplet and b = broad.

Decoupled carbon nuclear magnetic resonance (^{13}C NMR) spectra were recorded on Bruker Advance-300 and Bruker DRX 400 spectrometers at 75 and 100 MHz respectively. Chemical shifts are reported on the δ scale relative to the central signal of deuterated chloroform taken as δ 77.00 or relative to the signal for deuterated DMSO taken as δ 39.50. The ^{13}C NMR spectroscopy chemical shifts are reported: value (assignment).

The ^1H and ^{13}C NMR spectroscopic assignments with the same superscript are interchangeable. DEPT-135, HSQC and COSY spectra were routinely used for the complete assignment of NMR signals. D_2O washes were routinely performed on samples after general NMR spectroscopic analysis in order to quantitatively assign the -OH and -NH signals.

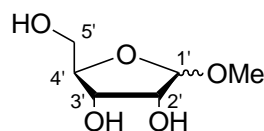
High-resolution mass spectra were recorded on a VG7-SEQ Double Focusing Mass Spectrometer at 70 eV and 200 μA . The polarity was positive, ionization employed was EI, with a resolution of 3000, a mass range of 3000 amu (8 kV) and a scan rate of 5 secs / decade. Data are quoted: m/z value (relative abundance).

A.5 Nomenclature and Numbering of Compounds

The compounds prepared during the course of this project are named in the following experimental sections according to systematic nomenclature wherever possible. However, the numbering system used to illustrate the diagrams of these compounds is one adopted for convenience and is not meant to reflect the systematic numbering of these compounds.

Appendix B:
Experimental Procedures – Relating to Chapter 2

B.1 Preparation of 1'-O-methoxy- α -(-)-ribose [101]

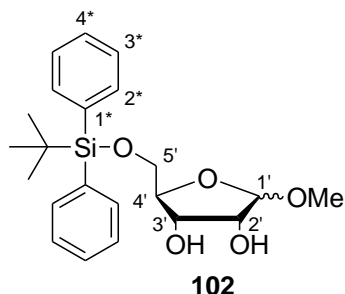


101

A solution was prepared of α -(-)-ribose **100** (33.3 mmol, 5.00 g) and distilled MeOH (75 cm³). The solution was then cooled to 0 °C in an ice-water bath, before the addition of the acid solution. The acid solution was prepared from distilled MeOH (2.5 cm³) and concentrated H₂SO₄ (0.35 cm³). The acid solution was added portionwise to the ribose solution and the mixture was stirred for 5 min. The flask was then stoppered under an argon atmosphere and placed in the fridge (4 °C) for 72 h. After this time, the solution was neutralized by passage through a column of Amberlyst A-21 resin (185 g of resin was placed in a 4 cm wide column and was rinsed with 500 cm³ MeOH prior to use). The column was eluted with MeOH (1000 cm³) and the solvent was then removed *in vacuo*. The desired compound **101** [α : β ratio found to be 2:8] was obtained as a very viscous pale yellow oil (5.47 g, 100 %). ¹H and ¹³C NMR spectra were also run in D₂O and the peaks were found to correlate well to those obtained by Chattopadhyaya and co-workers.⁴⁰

R_f = 0.36 (10 % MeOH : CH₂Cl₂); [α]_D²³ -15.464° (c = 1.94 in MeOH); $\nu_{\max}/\text{cm}^{-1}$ (thin film) 1216 (C-O), 2362 (CO₂ contaminant from air), 2851 (-OCH₃), 3021 (-O-H chelate, H-bonded), 3674 (-O-H free); δ_{H} (300 MHz, *d*₆-DMSO) 3.22 [2.1 H, s, OCH₃ (β)], 3.28 [0.5 H, s, OCH₃ (α)], 3.33-3.38 [1.7 H, m, H-5' (β)], 3.45-3.55 [0.8 H, m, H-5' (α)], 3.66-3.70 [1 H, m, H-2' (α and β)], 3.70-3.77 [1 H, m, H-4', (α and β)], 3.78-3.85 [1 H, m, H-3' (α and β)], 4.05-4.25 (0.2 H, br m, OH), 4.62 [0.9 H, s, H-1' (β)], 4.72 [0.4 H, d, J = 4.25 Hz, H-1' (α)], 4.75-4.80 (0.6 H, br s, OH), 4.93-4.99 (0.6 H, br s, OH); δ_{C} (50 MHz, *d*₆-DMSO) 54.26 [OCH₃ (β)], 54.54 [OCH₃ (α)], 61.76 [C-5' (α)], 63.20 [C-5' (β)], 69.33 [C-3' (α)], 70.98 [C-3' (β)], 71.35 [C-2' (α)], 74.25 [C-2' (β)], 83.62 [C-4' (β)], 85.02 [C-4' (α)], 102.82 [C-1' (α)], 108.09 [C-1' (β)]; **MS** m/z (M + 23⁺, 100 %) 150.18 (6), 182.13 (14), 188.17 (7), 269.08 (7), 319.21 (26), 351.05 (24), 663.44 (8), **HRMS** (+cESI) calculated for C₆H₁₂O₅: 164.06847, found: value not determined as compound was previously reported in the literature.⁴⁰

B.2 Preparation of 5'-O-(*tert*-butyldiphenylsilyl)-1'-O-methoxy- α -(-)-ribose [102]

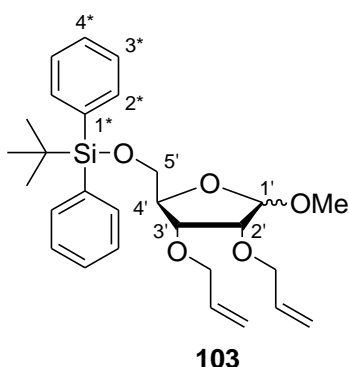


The Schlenk tube was filled with 5 % trimethylsilyl chloride : hexane and was stored at rt overnight. The glassware was then oven dried, placed under high vacuum and allowed to cool to rt under an argon atmosphere. The methoxy ribose derivative **101** (15.8 mmol, 2.59 g) and DMAP (0.1 eq, 1.58 mmol, 0.193 g) were stirred with distilled pyridine (26 cm³) until a solution had formed. To this solution was then added the *tert*-butyldiphenylsilyl chloride (1.1 eq, 17.4 mmol, 4.52 cm³) and the reaction mixture was stirred at rt under an argon atmosphere overnight (20 h). After this time, tlc indicated the formation of a new spot, so the reaction was quenched with EtOH (25 cm³). The solvent was then removed *in vacuo* to yield the desired product **102** [α : β ratio found to be 2:9] as a yellow semi-solid foam (6.36 g) that was always complexed with pyridine, as such the compound was used “crude” in the subsequent allylation and acetylation reactions and yields were determined over two steps.

$R_f = 0.19$ (10 % EtOH : CH₂Cl₂); $[\alpha]_D^{23} 5.5000^\circ$ (c = 2.00 in EtOH); $\nu_{\max}/\text{cm}^{-1}$ (**thin film**) 709 and 738 (5 adjacent aromatic H), 818 and 1071 (Si-O), 1112 (C-O), 1361 and 1390 [C(CH₃)₃], 1427 (Si-C), 1488, 1590 and 1649 (aromatic ring), 2856 (-OCH₃), 2960 (C-H stretching), 3092 (aromatic H), 3277 (-O-H); δ_H (**300 MHz, *d*₆-DMSO**) 0.96-1.26 [9 H, m, C(CH₃)₃], 3.18 [2.2 H, s, OCH₃ (β)], 3.31 [0.6 H, s, OCH₃ (α)], 3.48-3.64 [1 H, m, H-2' (α and β)], 3.72-3.90 [2 H, m, H-5' (α and β)], 3.97-4.03 [2 H, m, H-3' and H-4' (α and β)], 4.68-4.81 [1 H, m, H-1' (α and β)], 7.35-7.39 (2 H, m, H-4*), 7.40-7.48 (4 H, m, H-3*), 7.62-7.71 (4 H, m, H-2*), 8.01 (2 H, dd, $J = 6.52$ and 7.68 Hz, pyridine complex contaminant), 8.50-8.55 (1 H, m, pyridine complex contaminant), 8.89-8.92 (2 H, m, pyridine complex contaminant), OH peaks were not observed; δ_C (**50 MHz, *d*₆-DMSO**) 18.75 [C(CH₃)₃], 26.54 [C(CH₃)₃], 54.29 [OCH₃ (β)], 54.56 [OCH₃ (α)], 63.00 [C-5' (α)], 64.04 [C-5' (β)], 69.24 [C-3' (α)], 70.26 [C-3' (β)], 71.31 [C-2' (α)], 74.25 [C-2' (β)], 83.15 [C-4' (β)], 84.66 [C-4' (α)], 102.91 [C-1' (α)], 108.10 [C-1' (β)], 126.87 and 127.73 (C-3*), 129.15 and 129.77 (C-4*), 133.05 (C-2*), 134.46 (C-1*), 135.06 (pyridine complex contaminant), 142.67 (pyridine complex contaminant), 145.01 (pyridine complex contaminant); **MS *m/z*** (M + 23⁺, 100 %)

123.18 (20), 411.29 (11), 426.30 (28), 427.32 (8), 543.35 (10), 663.43 (9), 664.44 (6), **HRMS** (+**cESI**) calculated for $C_{22}H_{30}O_5SiNa^+$: 425.17457, found: $[M + 23]^+$ 425.17547.

B.3 Preparation of 2',3'-*O*-diallyl-5'-*O*-(*tert*-butyldiphenylsilyl)-1'-*O*-methoxy- α -(-)-ribose [103]



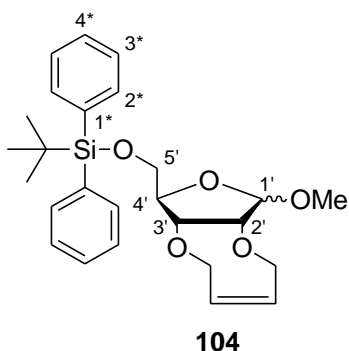
The protected ribose derivative **102** (2.80 mmol, 1.13 g) was stirred with distilled DMF (28 cm³) until a solution had formed. This was then cooled to 0 °C in an ice-water bath before the addition of the sodium hydride (used as a 60 % suspension in oil, 2.2 eq, 6.16 mmol, 0.253 g). The mixture was then stirred for 15 min, until effervescence had ceased and the allyl bromide (2.2 eq, 6.2 mmol, 0.53 cm³) was then added. The reaction mixture was then allowed to stir at rt under an argon atmosphere overnight (20 h). After this time tlc indicated the formation of a new spot, so the solvent was removed by evaporation. The crude residue was then diluted with a saturated solution of NH₄Cl (100 cm³) and extracted with EtOAc (3 × 100 cm³). The combined organics were then dried over anhydrous Na₂SO₄, filtered and the solvent was removed *in vacuo* to yield a orange oil. The crude compound was further purified by bulb-to-bulb distillation and the desired compound **103** [α : β ratio found to be 2:8] was obtained as a bright yellow oil (0.918 g, 68 % over two steps).

R_f = 0.23 (10 % EtOH : CH₂Cl₂); $[\alpha]_D^{19}$ -9.6774° (c = 0.62 in EtOAc); ν_{max}/cm^{-1} (thin film) 687 (5 adjacent aromatic H), 702 (CH₂ rocking), 740 (5 adjacent aromatic H), 862 and 1223 (Si-C), 1390 (C-H deformations), 1427 (C-O), 1461 (C-H deformations), 2856 (O-CH₃), 2929 (C-H stretch for CH₂), 3015 (aromatic H), 3072 (C-H stretch for C=CH₂); δ_H (300 MHz, CDCl₃) 1.04 [9 H, s, C(CH₃)₃], 3.36 [2.3 H, s, OCH₃ (β)], 3.45 [0.3 H, s, OCH₃ (α)], 3.51-3.62 (2 H, m, OCH₂[#]), 3.81-3.84 (1 H, m, H-2'^{##}), 3.97-4.01 (1 H, m, H-3'), 4.03-4.17 (2 H, m, OCH₂[#]), 4.20-4.24 (3 H, m, H-5' and H-4'^{##}), 4.90 (1 H, br s, H-1'), 5.08-5.42 (4 H, m, CH=CH₂), 5.85-5.96 (2 H, m, CH=CH₂), 7.34-7.43 (6 H, m, H-3* and H-4*), 7.66-7.71 (4 H, dd, J = 1.56 and 7.36 Hz, H-2*); δ_C (50 MHz, CDCl₃) 19.45 [C(CH₃)₃], 26.99 [C(CH₃)₃],

55.25 [OCH₃ (β)], 55.57 [OCH₃ (α)], 64.84 (C-5'), 71.68 (OCH₂ #), 72.41 (OCH₂ #), 78.58 (C-3'), 79.62 (C-2' ##), 80.81 (C-4' ##), 102.60 [C-1' (α)], 106.63 [C-1' (β)], 114.09 (CH=CH₂), 117.32 (CH=CH₂), 127.85 (C-3*), 129.80 (C-4*), 133.91 and 134.66 (CH=CH₂), 135.70 (C-2*), 136.94 (C-1*); **MS** *m/z* (M + 23⁺, 100 %) 253.20 (5), 267.23 (28), 307.26 (21), 465.32 (30), 506.38 (35), 507.39 (11), 663.44 (9), **HRMS** (+cESI) calculated for C₂₈H₃₈O₅SiNa⁺: 505.23807, found: [M + 23]⁺ 505.23807.

Note: Assignments denoted with # and ## are interchangeable.

B.4 Attempted synthesis of [(Z,6aS,7R,9R,9aS)-2,5,6a,7,9,9a-hexahydro-7-methoxyfuro[3,4-b][1,4]dioxocin-9-yl]methoxy}(tert-butyl)diphenylsilane [104]



Method 1:

A solution was prepared of the diene **103** (0.430 mmol, 0.207 g) in distilled CH₂Cl₂ (20 cm³) and was subsequently degassed using argon for 15 min. Then the 5 mol % of the Grubbs II catalyst **90** (0.05 eq, 0.0215 mmol, 0.0181 g) was added and the reaction mixture was stirred at rt under an argon atmosphere overnight (22 h). After this time, the

solvent was removed *in vacuo* to yield a dark brown-black oil. Crude NMR spectroscopy confirmed the presence of only unreacted starting material **103**.

Method 2:

A solution was prepared of the diene **103** (0.221 mmol, 0.107 g) and distilled CH₂Cl₂ (10 cm³). The solution was then degassed using argon for 15 min before the addition of the Grubbs II catalyst **90** (0.05 eq, 0.0111 mmol, 0.0096 g). The reaction mixture was then allowed to stir at rt under an argon atmosphere overnight (23 h). After this time, tlc only indicated the presence of unreacted starting material, so a further 5 mol % Grubbs II catalyst **104** (0.05 eq, 0.0111 mmol, 0.0096 g) was added. The reaction mixture was then refluxed overnight (22 h). After this time the solvent was removed *in vacuo* and the crude material was

purified by column chromatography (pre-prepared/basified silica and 5 % EtOAc : hexane). None of the desired **104** compound was obtained after chromatography.

Method 3:

A solution was prepared of the diene **103** (0.621 mmol, 0.300 g) in distilled toluene (30 cm³) and was then degassed using argon for 15 min. The solution was subsequently heated to 60 °C, before the addition of Grubbs II catalyst **90** (0.05 eq, 0.0310 mmol, 0.0268 g). The reaction mixture was then allowed to stir at 60 °C, under an argon atmosphere overnight (23 h). After this time, tlc indicated the presence of some unreacted starting material, so a further portion of Grubbs II catalyst **90** (0.05 eq, 0.0310 mmol, 0.0262 g) was added and the reaction mixture was stirred at 60 °C for a further 5 h. After this time, tlc indicated no further change, so the solvent was removed *in vacuo* to yield a dark brown-black oil. The crude mixture was then purified by column chromatography on the pre-prepared/basified silica, using 5 % EtOAc : hexane as the eluant. None of the desired compound **104** was isolated.

Method 4:

A solution was prepared of the diene **103** (0.219 mmol, 0.106 g) in distilled toluene (10 cm³) and was then degassed using argon for 15 min. The solution was subsequently heated to 80 °C, before the addition of Grubbs II catalyst **90** (0.05 eq, 0.0109 mmol, 0.0097 g). The reaction mixture was then allowed to stir at 80 °C, under an argon atmosphere overnight (21 h). After this time, tlc indicated the presence of some unreacted starting material, so a further portion of Grubbs II catalyst **90** (0.05 eq, 0.0109 mmol, 0.0099 g) was added and the reaction mixture was heated to reflux for a further 4 h. After this time, tlc indicated no further change, so the solvent was removed *in vacuo* to yield a dark brown-black oil. The crude mixture was then purified by column chromatography on the pre-prepared/basified silica, using 5 % EtOAc : hexane as the eluant. None of the desired compound **104** was isolated after the column chromatography.

Method 5:

The diene **103** (0.221 mmol, 0.107 g) was dissolved in distilled toluene (1 cm³) and was placed in the microwave reaction tube. To this solution was then added Grubbs II catalyst **90** (0.08 eq, 0.0177 mmol, 0.0191 g). Microwave setup used:

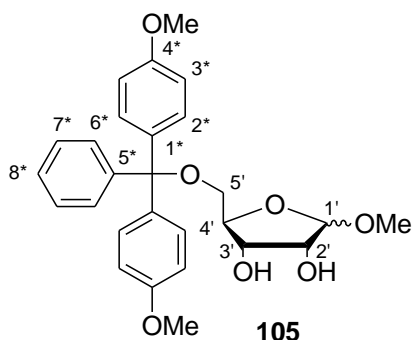
- solvent: toluene
- mode: standard
- power: 50 W
- temperature: 50 °C
- pressure: 150 psi maximum
- run time: 5 min
- hold time: 5 + 5 min
- stirring: yes
- cooling: no

After the two initial 5 min runs, no change was observable by tlc. Thus, a further 8 mol % Grubbs II catalyst **90** (0.08 eq, 0.0177 mmol, 0.0159 g) was added and the reaction was run in the microwave for a further 10 min. After this time, the solvent was removed *in vacuo* and the crude mixture was purified by column chromatography using the pre-prepared/basified silica and 2-5 % EtOAc : hexane for elution. The method seemed to be too harsh for our compounds as all by-products isolated lacked the TBDPS protecting group.

Method 6:

A solution was prepared of the diene **103** (0.214 mmol, 0.103 g) in distilled CH₂Cl₂ (10 cm³). The solution was degassed using argon for 10 min before the addition of the Grubbs I catalyst (0.1 eq, 0.0214 mmol, 0.0173 g). The reaction mixture was then allowed to stir at rt under an argon atmosphere overnight (23 h) and the solvent was then removed *in vacuo*. Crude NMR spectroscopy showed that all of our starting material had decomposed so no further purification was undertaken.

B.5 Preparation of 5'-O-(4,4'-dimethoxytrityl)-1'-O-methoxy- α -(-)-ribose [105]



The methoxy ribose derivative **101** (13.6 mmol, 2.24 g) and DMAP (0.1 eq, 1.36 mmol, 0.169 g) were stirred with distilled pyridine (22 cm³) until a solution had formed. The solution was then cooled to 0 °C in an ice-water bath before the addition of the 4,4'-dimethoxytrityl chloride (1 eq, 13.6 mmol, 4.66 g). The reaction mixture was then stirred at rt under an argon atmosphere

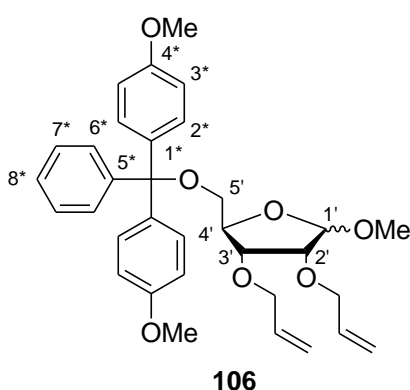
overnight (20 h). After this time, tlc indicated the formation of a new spot, so the reaction was quenched by the addition of EtOH (22 cm³) and the solvent was removed *in vacuo*. The desired compound **105** [α : β ratio could not be determined as all peaks overlapped] was obtained as a viscous yellow oil (6.36 g) that was always complexed with pyridine, as such the compound was used “crude” in the subsequent allylation and acetylation reactions and yields were determined over two steps.

R_f = 0.23 (10 % EtOH : CH₂Cl₂); $[\alpha]_D^{23}$ -3.9801° (c = 2.01 in EtOH); $\nu_{\max}/\text{cm}^{-1}$ (thin film) 670 (CH₂ rocking), 773 (5 adjacent aromatic H), 831 (2 adjacent aromatic H), 1036 (C-O stretch C-OH), 1299 (-O-H bend), 1458 (alkanes), 2830 (-O-CH₃), 3020 (Ar H), 3613 (O-H); δ_H (300 MHz, *d*₆-DMSO) 2.92-3.43 (5 H, m, H-5' and OCH₃), 3.73-3.77 (7 H, m, H-3' and 2 × Ar-OCH₃), 3.80-3.95 (3 H, m, H-2', H-4' and OH), 4.63 and 4.71 (1 H, two s, H-1'), 4.73-5.25 (1 H, br s, OH), 6.86 (4 H, dd, J = 8.85 and 13.08 Hz, H-3*), 7.08 (2 H, d, J = 8.78 Hz, H-2* #), 7.15-7.46 (7 H, m, H-2* #, H-6*, H-7* and H-8*), 8.02-8.06 (1.4 H, m, pyridine complex contaminant), 8.57 (0.7 H, t, J = 7.81 Hz, pyridine complex contaminant), 8.92 (1.4 H, d, J = 5.13 Hz, pyridine complex contaminant); δ_C (50 MHz, *d*₆-DMSO) 54.20 (OCH₃), 54.99 (2 × Ar-OCH₃), 63.16 (C-5'), 70.96 (C-3'), 74.23 (C-2'), 79.89 (C-4'), 83.58 [C(Ar)₃], 108.05 (C-1*), 112.71 (C-3*), 126.40 (C-8*), 127.02 (C-6*), 127.38 (pyridine complex contaminant), 127.62 (C-7*), 128.89 (C-2*), 140.21 (C-1*), 142.31 (pyridine complex contaminant), 145.51 (pyridine complex contaminant), 148.33 (C-5*), 157.79 (C-4*); **MS** m/z (M⁺, peak not observed) 123.20 (40), 173.15 (16), 187.15 (36), 303.24 (87), 304.25 (22), 343.23 (15), 357.25 (19), 425.29 (8), 467.24 (7), 531.20 (6), 663.44 (100), 664.45 (51),

665.42 (19), 666.46 (5), **HRMS** (+cESI) calculated for $C_{27}H_{30}O_7Na^+$: 489.18837, found: $[M + 23]^+$ 489.18781.

Note: Assignments denoted with # are exchangeable.

B.6 Attempted synthesis of 2',3'-*O*-diallyl-5'-*O*-(4,4'-dimethoxytrityl)-1'-*O*-methoxy- α -(-)-ribose [106]



Method 1:

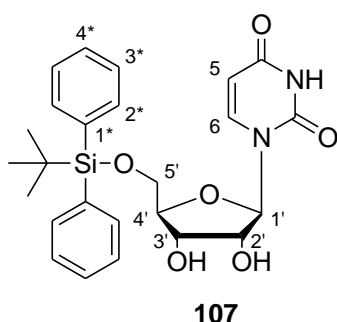
The protected ribose **105** (2.04 mmol, 0.953 g) was stirred with distilled DMF (21 cm³) until a solution had formed. This solution was then cooled to 0 °C in an ice-water bath before the addition of the sodium hydride (used as a 60 % suspension in oil, 2.2 eq, 4.49 mmol, 0.187 g) and it was subsequently stirred for 15 min until effervescence had stopped. Then the allyl bromide (2.2 eq, 4.5 mmol, 0.39 cm³) was added and the reaction mixture was stirred at rt under an argon atmosphere overnight (20 h). After this time, tlc indicated the formation of a new spot, so the solvent was removed by evaporation. The crude residue was then diluted with a saturated solution of NH₄Cl (100 cm³) and was extracted with EtOAc (3 × 100cm³). The combined organics were then dried over anhydrous Na₂SO₄, filtered and the solvent was removed *in vacuo*. The crude compound was further purified by bulb-to-bulb distillation, where two different oils were obtained - neither contained the desired product **106**.

Method 2:

The protected ribose **105** (0.656 mmol, 0.306 g) and allyl ethyl carbonate **148** (3.2 eq, 2.10 mmol, 0.280 g) were dissolved in anhydrous THF (4 cm³). A solution of bis(dibenzylideneacetone) palladium(0) **149** (0.03 eq, 0.0197 mmol, 0.0113 g) and bis(diphenylphosphino)butane (0.2 eq, 0.131 mmol, 0.0591 g) in anhydrous THF (1 cm³) was added dropwise to the starting material solution. The reaction mixture was then refluxed for 1 h, after which time the reaction mixture was concentrated under reduced pressure to give a

dark orange oil. The crude oil obtained was then purified by column chromatography using 5-30 % EtOAc : hexane for elution. None of the desired compound **106** was obtained after column chromatography.

B.7 Preparation of 5'-O-(*tert*-butyldiphenylsilyl)uridine [107]

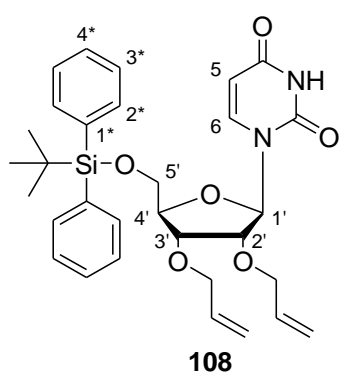


The flask used to perform the reaction was filled with a 5 % trimethylsilyl chloride : hexane (*v/v*) solution and was allowed to stand at rt overnight. After this time, the glassware was oven-dried, placed under high vacuum and allowed to cool to rt under an argon atmosphere. Then the uridine **12** (8.39 mmol, 2.05 g) and DMAP (0.1 eq, 0.839 mmol, 0.103 g) were stirred with distilled pyridine (10 cm³) until a solution had formed. To this solution was then added *tert*-butyldiphenylsilyl chloride (1.1 eq, 9.23 mmol, 2.40 cm³). The reaction mixture was then allowed to stir at rt under an argon atmosphere overnight (22 h). After this time a colour change was observed from a clear pale yellow solution to form a murky, cream coloured solution. The reaction mixture was diluted with CH₂Cl₂ (80 cm³). The organic layer was then extracted with saturated NaHCO₃ (2 × 80 cm³) and brine (80 cm³). The combined organics were then dried over anhydrous Na₂SO₄, filtered and evaporated. The crude foam was then purified by column chromatography using the pre-prepared/basified silica, with 10 % EtOH : CH₂Cl₂ being used as the eluant. The desired compound **107** was obtained as a white foam (4.04 g, 100 %,) and we found that our ¹³C NMR spectroscopic data correlated well to that reported by Sproat *et. al.*⁴²

$R_f = 0.81$ (20 % EtOH : CH₂Cl₂); $[\alpha]_D^{19} 22.400^\circ$ (c = 2.50 in MeOH); $\nu_{\max}/\text{cm}^{-1}$ (**thin film**) 700 (5 adjacent aromatic H), 740 (CH₂ rocking), 764 (5 adjacent aromatic H), 786 (RHC=CHR *cis*), 876 (Si-C), 1084 (C-O stretch from C-OH), 1231 (Si-C), 1271 (O-H bending), 1362 [-C(CH₃)₃], 1381 (CH₃ deformations), 1390 [-C(CH₃)₃], 1427 (C-H deformations), 1468 (secondary -N-H), 1608 (C=C conjugated with C=O), 1676 (-CONH-), 1709 (C=O), 1740 (-O-H, H-bonded), 2856 (-O-CH₃), 2930 (C-H stretching), 2957 (Ar H); δ_H (300 MHz, CDCl₃) 1.08 [9 H, s, C(CH₃)₃], 3.38 (1 H, br d, $J = 5.75$ Hz, OH), 3.89 (1 H, d,

$J = 10.73$ Hz, H-5'), 4.08-4.25 (2 H, m, H-4' and H-5'), 4.30-4.32 (1 H, m, H-2'), 4.35-4.37 (1 H, m, H-3'), 5.37 (1 H, d, $J = 8.08$ Hz, H-5), 5.47 (1 H, br s, OH), 5.93 (1 H, d, $J = 2.11$ Hz, H-1'), 7.37-7.44 (6 H, m, H-3* and H-4*), 7.65 (4 H, dd, $J = 6.09$ and 6.09 Hz, H-2*), 7.97 (1 H, d, $J = 8.10$ Hz, H-6), 10.38 (1 H, br s, NH); δ_c (50 MHz, $CDCl_3$) 19.54 [$C(CH_3)_3$], 27.20 ($C(CH_3)_3$), 62.76 (C-5'), 69.35 (C-2'), 75.70 (C-3'), 84.83 (C-4'), 90.50 (C-1'), 102.53 (C-5), 128.21 (C-3*), 130.29 (C-4*), 132.26 (C-1*), 135.65 (C-2*), 140.38 (C-6), 151.44 (C-2), 164.06 (C-4); **MS** m/z (M^+ , 34 %) 438.24 (3), 481.27 (100), 483.28 (10), 484.31 (2), 563.21 (5), 639.39 (2), **HRMS** (+cESI) calculated for $C_{25}H_{31}N_2O_6Si^+$: 483.19459, found: $[M + 1]^+$ 483.19407.

B.8 Attempted synthesis of 2',3'-*O*-diallyl-5'-*O*-(*tert*-butyldiphenylsilyl)uridine [108]



Method 1:

The protected uridine **107** (1.52 mmol, 0.735 g) was dissolved in DMF (15 cm³). To this solution was then added sodium hydride (used as a 60 % suspension in oil, 5 eq, 7.62 mmol, 0.308 g) and the mixture was stirred at rt for 15 min. Then allyl bromide (5 eq, 7.6 mmol, 0.66 cm³) was added and the reaction mixture was stirred at rt under an argon atmosphere overnight (20 h). After this time the solvent was removed by evaporation and the residue obtained was diluted with a saturated solution of NH_4Cl (50 cm³) and then extracted with EtOAc (3 × 50 cm³). The combined organics were then dried over anhydrous $MgSO_4$, filtered and the solvent was removed *in vacuo*. The crude mixture was then purified by column chromatography using 10-30 % EtOAc : hexane for elution. A mixture of *N*- and *O*-allylated products were obtained (**110** and **111**), with none of the desired compound **108** isolated.

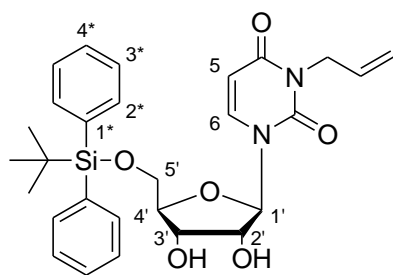
Method 2:

A solution was prepared of the 1,4-bis(diphenylphosphino)butane (0.05 eq, 0.0106 mmol, 0.0046 g) and the bis(dibenzylideneacetone) palladium(0) **149** (0.01 eq, 0.00213 mmol, 0.0016 g) in distilled THF (2 cm³), with stirring a colour change was observed from a purple

to a yellow solution. To this solution was added dropwise a solution of the protected uridine **107** (0.213 mmol, 0.103 g) and the allyl ethyl carbonate **148** (2 eq, 0.425 mmol, 0.0554 g) in THF (5 cm³). The reaction mixture was then stirred at rt under an argon atmosphere overnight (20 h). After this time, tlc indicated the presence of a lot of unreacted starting material, so a further portion of the 1,4-bis(diphenylphosphino)butane (0.05 eq, 0.0106 mmol, 0.0047 g) and the bis(dibenzylideneacetone) palladium(0) **149** (0.01 eq, 0.00213 mmol, 0.0017 g) was added. After stirring for 2-3 min, another portion of the allyl ethyl carbonate **148** (2 eq, 0.425 mmol, 0.0582 g) was then added. The reaction mixture was then stirred for a further 5 h. After this time, there was no further change by tlc, so MeOH (5 cm³) was added to quench the reaction mixture. The solvent was then removed *in vacuo* to yield a bright yellow-lime green oil. The crude oil was then purified by column chromatography using 30-40 % EtOAc : hexane for elution. None of the desired compound **108** was obtained; instead we isolated unreacted starting material **107** and the *N*-allylated byproduct **109**.

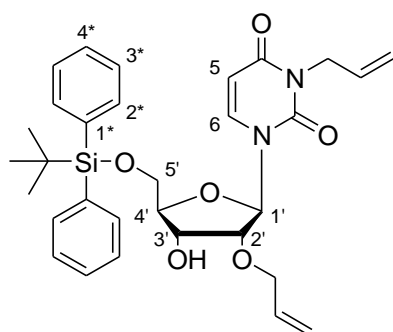
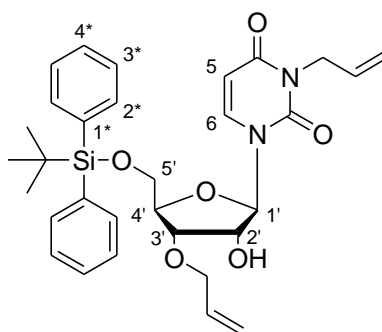
Method 3:

A solution was prepared of the 1,4-bis(diphenylphosphino)butane (0.1 eq, 0.0428 mmol, 0.0186 g) and bis(dibenzylideneacetone) palladium(0) **149** (0.05 eq, 0.0214 mmol, 0.0122 g) in distilled THF (0.5 cm³), the solution changed colour from dark purple to bright yellow with stirring. To this solution was then added dropwise a solution of the protected uridine **107** (0.428 mmol, 0.207 g) and allyl ethyl carbonate **148** (5 eq, 2.14 mmol, 0.286 g) in distilled THF (2.5 cm³). The reaction mixture immediately changed colour from yellow to dark olive green and was then stirred at rt under an argon atmosphere overnight (19 h). After this time tlc showed the formation of a number of spots, so the reaction mixture was quenched by the addition of MeOH (10 cm³). The solvent was then removed *in vacuo* to give a viscous yellow-green oil. The crude oil was purified by column chromatography using 20-50 % EtOAc : hexane for elution. None of the desired compound **108** was obtained after chromatography, isolated instead were the *N*- and *O*-allylated by products **109**, **110** and **111**.

3-N-Allyl-5'-O-(tert-butyldiphenylsilyl)uridine [109]**109**

Clear oil: $R_f = 0.40$ (50 % EtOAc : hexane); δ_H (**300 MHz, CDCl₃**) 1.02-1.08 [9 H, m, C(CH₃)₃], 1.64 (1 H, br s, OH), 2.93 (1 H, br s, OH), 3.85 and 3.99 (2 H, two d, $J = 12.10$ Hz, H-5'), 4.16-4.55 (5 H, m, H-2', H-3', H-4' and N-CH₂), 5.18-5.29 (2 H, m, CH=CH₂), 5.60 (1 H, d, $J = 8.15$ Hz, H-5), 5.80-5.95 (2 H, m, H-1' and CH=CH₂), 7.39-7.45 (6 H, m, H-3* and H-4*), 7.51-7.69 (4 H, m, H-2*), 7.78 (1 H, d, $J = 8.15$ Hz, H-6); δ_C (**50 MHz, CDCl₃**) 19.24 [C(CH₃)₃], 26.97 [C(CH₃)₃], 43.04 (N-CH₂), 63.19 (C-5'), 70.87 (C-2' #), 73.03 (C-3' #), 86.03 (C-4'), 92.00 (C-1'), 101.75 (C-5), 118.18 (CH=CH₂), 128.04 (C-3*), 130.20 (C-4*), 131.33 (C-1*), 132.54 (CH=CH₂), 135.21 (C-2*), 137.43 (C-6), 151.85 (C-2), 162.08 (C-4).

Note: Assignments denoted with # are interchangeable.

3-N-Allyl-2'-O-allyl-5'-O-(tert-butyldiphenylsilyl)uridine [110] and 3-N-allyl-3'-O-allyl-5'-O-(tert-butyldiphenylsilyl)uridine [111]**110****111**

ISOMER ONE, Pale yellow oil: $R_f = 0.72$ (50 % EtOAc : hexane); δ_H (**300 MHz, CDCl₃**) 1.10 [9 H, s, C(CH₃)₃], 2.93 (1 H, d, $J = 6.12$ Hz, OH), 3.68-4.24 (7 H, m, H-2', H-3', H-4', H-5' and N-

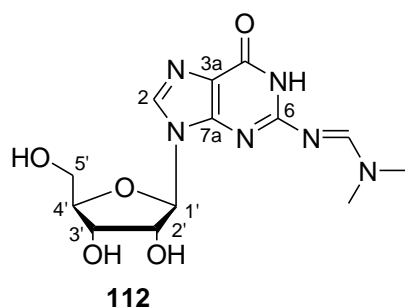
CH₂), 4.53-4.57 (2 H, m, O-CH₂), 5.10-5.30 [4 H, m, CH=CH₂ (N) and CH=CH₂ (O)], 5.51 (1 H, d, $J = 8.12$ Hz, H-5), 5.73-5.91 [2 H, m, CH=CH₂ (N) and CH=CH₂ (O)], 5.99-6.02 (1 H, m, H-1'), 7.38-7.44 (6 H, m, H-3* and H-4*), 7.62-7.70 (5 H, m, H-2* and H-6); δ_C (**50 MHz, CDCl₃**) 19.75 [C(CH₃)₃], 27.37 [C(CH₃)₃], 43.50 (N-CH₂), 63.41 (C-5'), 71.72 (O-CH₂), 74.60 (C-3'), 76.66 (C-2'), 82.83 (C-4'), 90.48 (C-1'), 102.41 (C-5), 118.52 [CH=CH₂ (O)], 119.07 [CH=CH₂ (N)], 128.41 (C-3*), 130.55 (C-4*), 131.90 [CH=CH₂ (O)], 132.58 (C-

1*), 133.82 [CH=CH₂ (*N*)], 135.90 (C-2*), 138.06 (C-6), 151.30 (C-2), 162.62 (C-4); **MS** *m/z* (M⁺, 2 %) 41.03 (56), 91.06 (34), 135.06 (33), 162.99 (75), 199.04 (58), 255.04 (22), 333.10 (21), 353.11 (48), 447.14 (10), 505.18 (100), **HRMS (EI pos)** calculated for C₃₁H₃₈N₂O₆Si: 562.24991, found: [M]⁺ 562.26234.

ISOMER TWO, Bright yellow oil: *R_f* = 0.86 (50 % EtOAc : hexane); **δ_H (300 MHz, CDCl₃)** 1.07-1.10 [9 H, m, C(CH₃)₃], 2.61 (1 H, d, *J* = 8.92 Hz, OH), 3.89-3.97 (2 H, m, N-CH₂), 4.08-4.53 (7 H, m, H-2', H-3', H-4', H-5' and O-CH₂), 5.12-5.48 [5 H, m, CH=CH₂ (*N*), CH=CH₂ (*O*) and H-5], 5.85-5.88 [2 H, m, CH=CH₂ (*N*) and CH=CH₂ (*O*)], 6.01 (1 H, s, H-1'), 7.29-7.42 (6 H, m, H-3* and H-4*), 7.51-7.75 (4 H, m, H-2*), 7.99 (1 H, d, *J* = 8.14 Hz, H-6); **δ_C (50 MHz, CDCl₃)** 19.33 [C(CH₃)₃], 27.02 [C(CH₃)₃], 43.08 (N-CH₂), 62.14 (C-5'), 67.96 (C-2'), 71.61 (O-CH₂), 81.90 (C-4'), 84.39 (C-3'), 88.12 (C-1'), 101.80 (C-5), 118.05 [CH=CH₂ (*O*)], 118.88 [CH=CH₂ (*N*)], 128.21 (C-3*), 129.81 (C-4*), 131.76 and 132.14 [CH=CH₂ (*N*) and CH=CH₂ (*O*)], 133.56 (C-1*), 135.01 (C-2*), 137.78 (C-6), 150.70 (C-2), 162.45 (C-4); **MS** *m/z* (M⁺, 2 %) 41.02 (56), 91.05 (23), 162.99 (62), 199.04 (95), 235.01 (100), 255.03 (11), 333.04 (22), 353.08 (40), 447.13 (13), 505.18 (100), 545.21 (18), **HRMS (EI pos)** calculated for C₃₁H₃₈N₂O₆Si: 562.24991, found: [M]⁺ 562.24544.

Note: Assignments denoted with # are interchangeable.

B.9 Preparation of 6-*N,N*-dimethylmethylimine)guanosine [112]

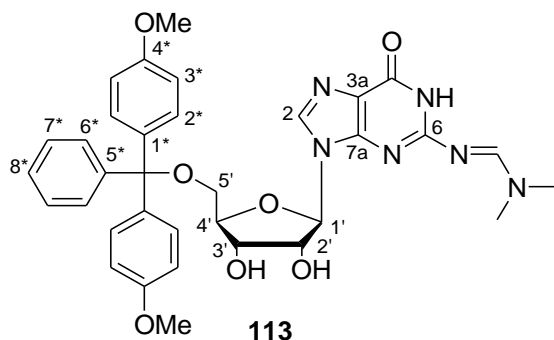


The guanosine **9** (17.7 mmol, 5.02 g) was heated to 120 °C under an argon atmosphere, using an oil bath, for 19 h. After this time, tiny water droplets were observed on the neck of the flask, so the system was placed under high vacuum and was allowed to cool to rt. The dry guanosine was then stirred with distilled DMF (25 cm³) until a suspension had formed. To this suspension was added the *N,N*-dimethylformamide dimethyl acetal (2 eq, 35.4 mmol, 4.71 cm³). The reaction mixture was allowed to stir at rt under an argon atmosphere overnight (27 h). The solvent was then removed *in vacuo* and the crude mixture was obtained as a cream semi-solid. The crude mixture was subsequently stirred with MeOH (125 cm³) until a solution had formed, it was

then allowed to stand at rt for crystallization to begin and was finally cooled in an ice-water bath to allow for complete crystallization. The white precipitate was collected by filtration and dried under high vacuum (using a drying pistol, over P₂O₅) for 3 days. The pure compound **112** was obtained as a white powder (4.74 g, 79 %).

$R_f = 0.15$ (10 % MeOH : CHCl₃); $[\alpha]_D^{23} -35.644^\circ$ (c = 2.02 in DMSO); $\nu_{\max}/\text{cm}^{-1}$ (thin film) 771 (CH₂ rocking), 1216 (C-O stretch), 1422 (C-H deformations), 1539 (-CONH-), 1651 (C=N), 1700 (-CONH-), 3021 (C-H stretching), 3613 (O-H stretching); δ_H (300 MHz, *d*₆-DMSO) 3.03 (3 H, s, N-CH₃), 3.15 (3 H, s, N-CH₃), 3.51-3.62 (2 H, m, H-5'), 3.88-3.90 (1 H, m, H-4'), 4.11-4.13 (1 H, m, H-3'), 4.47-4.51 (1 H, m, H-2'), 5.02 (1 H, t, *J* = 5.34 Hz, OH-5'), 5.17 (1 H, br s, OH-3'), 5.40 (1 H, br s, OH-2'), 5.80 (1 H, d, *J* = 6.08 Hz, H-1'), 8.04 (1 H, s, N=CH-N), 8.53 (1 H, s, H-2), 11.31 (1 H, br s, NH); δ_C (50 MHz, *d*₆-DMSO) 34.64 (N-CH₃), 40.64 (N-CH₃), 61.51 (C-5'), 70.48 (C-3'), 73.78 (C-2'), 85.43 (C-4'), 86.76 (C-1'), 119.78 (C-3a), 136.96 (N=C-N), 149.99 (C-7a), 157.27 and 157.58 (C-4 and C-6), 157.94 (C-2); **MS** *m/z* (M + 23⁺, 100 %) 269.10 (5), 339.21 (17), 362.26 (17), 467.23 (10), 505.36 (11), 536.16 (9), 537.19 (5), 633.27 (5), 663.44 (39), 664.45 (22), 665.44 (8), **HRMS** (+cESI) calculated for C₁₃H₁₉N₆O₅⁺: 339.14114, found: [M + 1]⁺ 339.14123.

B.10 Preparation of 5'-O-(4,4'-dimethoxytrityl)-6-N-(*N,N*-dimethylmethanimine)-guanosine [113]



The protected guanosine derivative **112** (3.21 mmol, 1.09 g) and DMAP (0.1 eq, 0.321 mmol, 0.0398 g) were stirred with distilled pyridine (10 cm³) until a suspension had formed. This suspension was then cooled to 0 °C in an ice-water bath before the addition of the 4,4'-dimethoxytrityl chloride (1 eq, 3.21

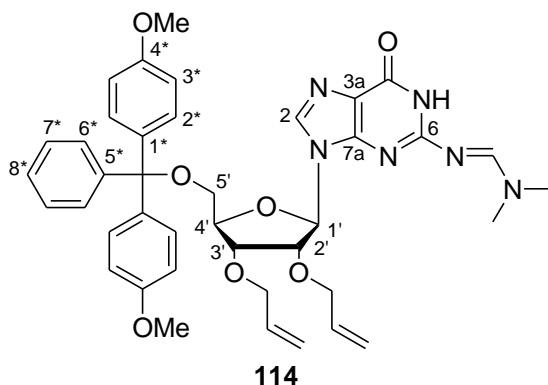
mmol, 1.09 g). The reaction mixture was then warmed to rt and stirred under an argon atmosphere overnight (25 h). After this time, tlc indicated the formation of a new spot, so the reaction mixture was diluted with CHCl₃ (100 cm³). The organic layer was extracted with a

saturated NaHCO₃ solution (100 cm³) and the aqueous layer was back-extracted with CHCl₃ (2 × 100 cm³). All of the organic layers were then combined and extracted with brine (100 cm³). The combined organics were dried over anhydrous Na₂SO₄, filtered and evaporated. The residue obtained was then dissolved in a 10 CHCl₃ : 3 EtOH (60 cm³ : 18 cm³) mixture. The solution obtained was then added dropwise to vigorously stirring Et₂O (100 cm³) and the mixture was triturated for 30 min. After this time the white precipitate was collected by filtration and dried under high vacuum (overnight: using a drying pistol, over P₂O₅). The desired product **113** was obtained as a white powder (1.43 g, 69 %).

$R_f = 0.40$ (10 % EtOH : CH₂Cl₂); $[\alpha]_D^{24} -6.7633^\circ$ (c = 2.07 in DMSO); $\nu_{\max}/\text{cm}^{-1}$ (**thin film**) 699 (5 adjacent aromatic H), 728 (CH₂ rocking), 760 (5 adjacent aromatic H), 826 (2 adjacent aromatic H), 1112 (C-O stretching from C-OH), 1356 (O-H bending), 1463 (C-H deformations), 1508 (C=N cyclic), 1563 (-CONH-), 1627 (-C=N-), 1661 (-CONH-), 2929 (C-H stretching), 3090 (Ar H); δ_{H} (**300 MHz, *d*₆-DMSO**) 3.02 (3 H, s, N-CH₃), 3.09 (3 H, s, N-CH₃), 3.17-3.19 (2 H, m, H-5'), 3.72 (6 H, s, 2 × OCH₃), 4.01 (1 H, d, $J = 3.28$ Hz, H-4'), 4.21-4.24 (1 H, m, H-3'), 4.53 (1 H, t, $J = 4.56$ Hz, H-2'), 5.26 (1 H, br s, OH-3'), 5.58 (1 H, br s, OH-2'), 5.87 (1 H, d, $J = 4.48$ Hz, H-1'), 6.83 (4 H, dd, $J = 4.02$ and 8.66 Hz, H-3*), 7.20-7.26 (7 H, m, H-2*, H-6* and H-8*), 7.28-7.31 (2 H, m, H-7*), 7.94 (1 H, s, N=CH-N), 8.50 (1 H, s, H-2), 11.39 (1 H, br s, NH); δ_{C} (**50 MHz, *d*₆-DMSO**) 34.73 (N-CH₃), 40.72 (N-CH₃), 55.06 (2 × OCH₃), 64.03 (C-5'), 70.38 (C-3'), 73.59 (C-2'), 82.98 (C-4'), 85.53 (C(Ph)₃), 87.13 (C-1'), 113.19 (C-3*), 119.79 (C-3a), 126.74 (C-8*), 127.72 (C-2*[#]), 127.87 (C-6*[#]), 129.73 (C-7*[#]), 135.54 (C-1*^{###}), 135.58 (C-5*^{###}), 136.72 (N=CH-N), 144.90 (C-4*), 150.07 (C-7a), 157.32 and 157.73 (C-4 and C-6), 158.09 (C-2); **MS *m/z*** (M + 23⁺, 50 %) 303.24 (100), 304.27 (23), 641.30 (45), 664.40 (22), 665.39 (5), **HRMS (+cESI)** calculated for C₃₄H₃₇N₆O₇⁺: 641.27182, found: [M + 1]⁺ 641.27182.

Note: assignments denoted with [#] and ^{###} are exchangeable.

B.11 Preparation of 2',3'-O-diallyl-5'-O-(4,4'-dimethoxytrityl)-6-N-(N,N-dimethylmethylimine)guanosine [114]



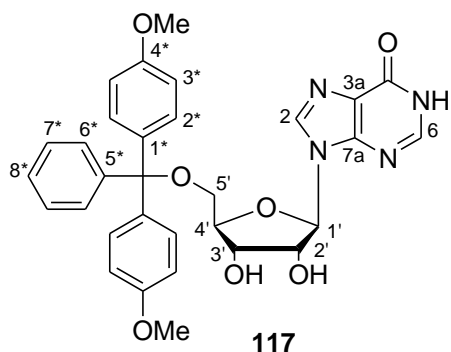
The protected guanosine derivative **113** (0.472 mmol, 0.303 g) and allyl ethyl carbonate **148** (3.2 eq, 1.51 mmol, 0.203 g) were dissolved in anhydrous THF (4 cm³). A solution of bis(dibenzylideneacetone) palladium(0) **149** (0.03 eq, 0.0142 mmol, 0.0086 g) and 1,4-bis(diphenylphosphino)butane (0.2 eq, 0.0945 mmol, 0.0414 g) in anhydrous THF (1 cm³) was added dropwise

to the guanosine derivative solution. The reaction mixture was heated to reflux and was stirred for 75 min. The solvent was then removed *in vacuo* and a yellow foam was obtained. The crude foam was purified by column chromatography with 5-50 % EtOAc : hexane, EtOAc, CH₂Cl₂ and MeOH solutions being used for elution. The desired compound **114** was obtained after chromatography as a yellow foam (0.289 g, 85 %).

$R_f = 0.05$ (50 % EtOAc : hexane); δ_H (300 MHz, CDCl₃) 3.10 (6 H, s, 2 × NCH₃), 3.40 (2 H, dd, $J = 3.34$ and 9.21 Hz, H-5'), 3.78 (6 H, s, 2 × OCH₃), 4.11-4.20 (3 H, m, H-2', H-3' and H-4'), 4.44 (2 H, d, $J = 2.33$ Hz, OCH₂), 4.96 (2 H, d, $J = 5.73$ Hz, OCH₂), 5.08-5.23 (4 H, m, 2 × CH=CH₂), 5.79-5.97 (2 H, m, 2 × CH=CH₂), 6.06-6.09 (1 H, m, H-1'), 6.79-6.82 (4 H, m, H-3*), 7.20-7.43 (9 H, m, H-2*, H-6*, H-7* and H-8*), 7.74 (1 H, s, N=CH-N), 8.52 (1 H, s, H-2); δ_C (50 MHz, CDCl₃) 35.38 (NCH₃), 41.29 (NCH₃), 55.44 (2 × OCH₃), 63.71 (C-5'), 70.60 (C-3'), 72.05 (C-2'), 81.27 (C-4'), 83.89 (C(Ph)₃), 85.45 (C-1'), 86.78 and 87.94 (2 × OCH₂), 113.38 (C-3*), 116.92 (CH=CH₂), 119.12 (CH=CH₂), 120.27 (C-3a), 127.16 (C-8*), 128.26 (C-7*), 128.81 (C-6*), 130.23 (C-2*), 130.96 (CH=CH₂), 131.00 (CH=CH₂), 133.46 (C-1*[#]), 133.65 (C-5*[#]), 135.77 (N=CH-N), 144.65 (C-4), 148.19 (C-7a), 157.12 (C-4^{##}), 157.65 (C-6^{##}), 158.77 (C-2); *LRMS* and *HRMS* data were not determined.

Note: assignments denoted with [#] and ^{##} are exchangeable.

B.13 Preparation of 5'-O-(4,4'-dimethoxytrityl)inosine [117]

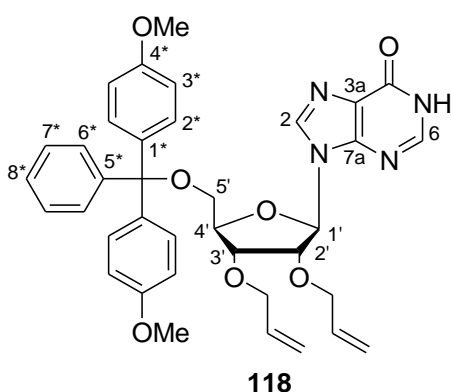


The inosine **116** (7.47 mmol, 2.00 g) and DMAP (0.1 eq, 0.747 mmol, 0.0923 g) were stirred with distilled pyridine (20 cm³) until a suspension had formed. This was then cooled to 0 °C in an ice-water bath before the addition of the 4,4'-dimethoxytrityl chloride (1 eq, 7.47 mmol, 2.53 g). The reaction mixture was then allowed to stir at rt, under an argon atmosphere overnight (21 h). After this time, tlc indicated the formation of a new spot, so a solution of saturated NaHCO₃ (200 cm³) was added to the reaction mixture and stirred for a few minutes. The aqueous reaction mixture was subsequently extracted with chloroform (3 × 200 cm³) and the combined organics were further extracted with brine (200 cm³). The combined organics were then dried over anhydrous Na₂SO₄, filtered and evaporated. The residue obtained was dissolved in a EtOH : CHCl₃ solution (6 cm³ : 30 cm³) and then added dropwise to vigorously stirred Et₂O (200 cm³). A white precipitate was immediately observed and after cooling in an ice-water bath, was collected by filtration. The white powder was then dried under high vacuum and was identified to be pure product **117** (3.31 g, 78 %).

$R_f = 0.36$ (10 % EtOH : CH₂Cl₂); $[\alpha]_D^{24} -6.6667^\circ$ ($c = 1.05$ in DMSO); $\nu_{\max}/\text{cm}^{-1}$ (**thin film**) 702 (5 adjacent aromatic H), 726 (CH₂ rocking), 755 (5 adjacent aromatic H), 827 (2 adjacent aromatic H), 1082 (C-O stretch from C-OH), 1301 (O-H bending), 1377 (CH₃ symmetrical deformation), 1464 (C-H deformations), 1509 (Ar H), 1547 (-CONH-), 1584 and 1608 (Ar H), 1676 (-C=N-), 1690 (-CONH-), 2836 (O-CH₃), 2908 (C-H stretch from CH₂ and CH₃), 3033 (Ar H), 3056 (-CONH-); δ_H (**300 MHz, *d*₆-DMSO**) 3.18-3.22 (2 H, m, H-5'), 3.69 (6 H, s, 2 × OCH₃), 4.07 (1 H, d, $J = 4.50$ Hz, H-4'), 4.23-4.27 (1 H, m, H-3'), 4.59-4.61 (1 H, m, H-2'), 5.25 (1 H, br s, OH-3'), 5.61 (1 H, br s, OH-2'), 5.92 (1 H, d, $J = 4.44$ Hz, H-1'), 6.83 (4 H, dd, $J = 4.27$ and 8.62 Hz, H-3*), 7.12-7.24 (7 H, m, H-2*, H-6* and H-8*), 7.35-7.39 (2 H, m, H-7*), 8.01 (1 H, s, H-2), 8.21 (1 H, s, H-6), 12.39 (1 H, br s, NH); δ_C (**50 MHz, *d*₆-DMSO**) 55.04 (2 × OCH₃), 63.78 (C-5'), 70.31 (C-3'), 73.41 (C-2'), 83.23 (C-4'), 85.53 (C(Ph)₃), 88.02 (C-1'), 113.16 (C-3*), 124.62 (C-3a), 126.70 (C-8*), 127.81 and 127.83 (C-6* and C-7*), 129.73 (C-2*), 135.55 (C-2), 138.87 (C-6), 144.86 (C-1*), 145.80 (C-5*),

148.21 (C-7a), 156.62 (C-4), 158.08 (C-4*); **MS** m/z ($M + 23^+$, 39 %) 303.24 (100), 304.27 (23), 505.38 (20), 536.17 (6), 571.12 (30), 594.33 (12), 663.45 (8), **HRMS** (+cESI) calculated for $C_{31}H_{31}N_4O_7^+$: 571.21873, found: $[M + 1]^+$ 571.21823 and calculated for $C_{31}H_{30}N_4O_7Na^+$: 593.20067, found: $[M + 23]^+$ 593.19995.

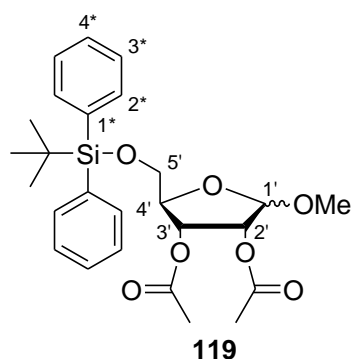
B.14 Attempted synthesis of 2',3'-O-diallyl-5'-O-(4,4'-dimethoxytrityl)inosine [118]



The protected inosine **117** (0.878 mmol, 0.501 g) was stirred with distilled DMF (9 cm³) until a solution had formed. This solution was then cooled to 0 °C in an ice-water bath, before the addition of the sodium hydride (used as a 60 % suspension in oil, 2.2 eq, 1.93 mmol, 0.0796 g). This was allowed to stir at 0 °C for 15 min, during which time the solution changed colour to a dark blue-purple. Then the allyl bromide (2.2 eq, 1.9 mmol, 0.17 cm³) was added and the solution slowly changed colour to orange. The reaction mixture was then allowed to stir at rt under an argon atmosphere overnight (21 h). After this time, tlc indicated the formation of a new spot, so the reaction mixture was diluted with EtOH and the solvent was removed *in vacuo*. The crude residue was then diluted with a solution of saturated NH₄Cl (50 cm³) and was extracted with EtOAc (3 × 50 cm³). The combined organics were then dried over anhydrous Na₂SO₄, filtered and the solvent was removed *in vacuo*. Crude NMR spectroscopy showed no peaks present for the desired product **118**, instead it seemed as though the starting material had decomposed under the harsh conditions employed.

B.15 Preparation of 2',3'-O-diacetyl-5'-O-(*tert*-butyldiphenylsilyl)-1'-O-methoxy- β -(-)-ribose [119]

The protected ribose **102** (2.70 mmol, 1.09 g) was stirred with distilled pyridine (2 eq, 5.4 mmol, 0.45 cm³) until a solution had formed. The solution was then cooled to 0 °C in an ice-

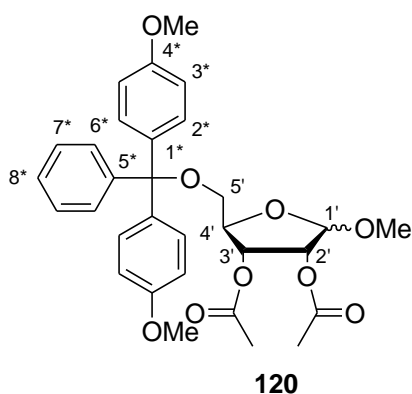


water bath. To the cooled solution was then added dropwise a mixture of distilled acetic anhydride (3 eq, 8.1 mmol, 0.76 cm³) and distilled pyridine (3 eq, 8.1 mmol, 0.65 cm³). After the addition, the reaction mixture was warmed to rt and was stirred under an argon atmosphere overnight (19 h). The reaction mixture was then diluted with EtOAc (100 cm³) while gently stirring and the solution went murky white in colour. The reaction mixture was extracted with brine (3 × 100 cm³) and the aqueous layers were combined and extracted with CH₂Cl₂ (3 × 100 cm³). The organic layers were combined and extracted with a saturated NH₄Cl solution that had been basified to pH 10 using NH₃ (150 cm³). The combined organics were then dried over anhydrous MgSO₄, filtered and the solvent was removed *in vacuo*. The compound **119** [α : β ratio found to be 1:3] was obtained as a viscous orange oil (0.930 g, 71 % over two steps).

$\nu_{\max}/\text{cm}^{-1}$ (thin film) 687 and 741 (5 adjacent aromatic H), 855 and 1243 (Si-C), 1365 and 1391 [C(CH₃)₃], 1428 and 1446 (alkanes), 1472 (CH₂ and CH₃ deformations), 1747 (C=O), 2857 (O-CH₃), 2891 (C-H stretch), 2999 (C-O), 3072 (aromatic H); δ_{H} (300 MHz, CDCl₃) 1.04-1.07 [9 H, m, C(CH₃)₃], 2.00-2.06 (3 H, m, COCH₃), 2.09-2.14 (3 H, m, COCH₃), 3.34 [2.1 H, s, OCH₃ (β)], 3.38 [0.7 H, s, OCH₃ (α)], 3.72-3.81 (1 H, m, H-5'), 4.09-4.13 (0.5 H, m, H-5'), 4.15-4.35 (1 H, m, H-4'), 4.36-4.39 (0.5 H, m, H-5'), 4.90-4.92 and 5.13-5.15 (1 H, m, H-1'), 5.22-5.28 (1 H, m, H-3' [#]), 5.30-5.33 and 5.44-5.49 (1 H, m, H-2' [#]), 7.34-7.43 (6 H, m, H-3* and H-4*), 7.67-7.74 (4 H, m, H-2*); δ_{C} (50 MHz, CDCl₃) 19.40 [C(CH₃)₃], 20.88 (COCH₃), 22.57 (COCH₃), 25.87 [C(CH₃)₃], 55.48 [OCH₃ (β)], 55.73 [OCH₃ (α)], 63.87 [C-5' (α)], 64.63 [C-5' (β)], 71.55 [C-2' (α)[#]], 72.14 [C-2' (β)[#]], 74.84 [C-3' (α and β)[#]], 78.23 [C-4' (α)], 81.27 [C-4' (β)], 101.86 [C-1' (α)], 106.35 [C-1' (β)], 127.92 (C-3*), 129.85 (C-4*), 133.31 (C-1*), 135.01 and 135.70 (C-2*), 135.91 (C-1*), 169.91 (C=O), 170.89 (C=O); **MS** m/z (M⁺, peak not observed) 275.13 (6), 307.93 (24), 455.00 (32), 503.93 (100), 699.87 (10), 798.60 (5), 994.40 (11), **HRMS** (+cESI) calculated for C₂₆H₃₄O₇SiNa⁺: 509.19660, found: [M + 23]⁺ 509.19582.

Note: Assignments denoted with [#] are interchangeable.

B.16 Preparation of 2',3'-*O*-diacetyl-5'-*O*-(4,4'-dimethoxytrityl)-1'-*O*-methoxy- α -(-)-ribose [120]



The protected ribose derivative **105** (2.23 mmol, 1.04 g) was stirred with distilled pyridine (2 eq, 4.5 mmol, 0.36 cm³) until a solution had formed and the solution was then cooled to 0 °C in an ice-water bath. To this cooled solution was then added dropwise a mixture of distilled acetic anhydride (3 eq, 6.7 mmol, 0.63 cm³) and distilled pyridine (3 eq, 6.7 mmol, 0.54 cm³). The reaction mixture was then allowed to warm to rt and was stirred

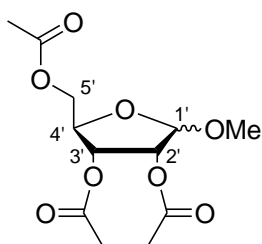
under an argon atmosphere overnight (19 h). The reaction was diluted by the addition of EtOAc (100 cm³) and the solution went murky white. The diluted reaction mixture was then extracted with brine (3 × 100 cm³) and the combined aqueous layers were extracted with CH₂Cl₂ (3 × 100 cm³). All of the organics were combined and extracted with a saturated NH₄Cl solution that had been basified to pH 10 with NH₃ (150 cm³). The combined organics were then dried over anhydrous MgSO₄, filtered and the solvent was removed *in vacuo*. The desired compound **120** [α : β ratio found to be 1:3] was obtained as a viscous orange oil (0.941 g, 77 % calculated over 2 steps).

$\nu_{\max}/\text{cm}^{-1}$ (**thin film**) 702 (5 adjacent aromatic H), 727 (CH₂ rocking), 755 (5 adjacent aromatic H), 829 (2 adjacent aromatic H), 1113 (C-O stretching for C-OH), 1297 (O-H bending), 1443 (C-H deformations), 1465 (alkane), 2837 (C-H stretch), 2908 (O-CH₃), 2934 (C-H stretch for CH₂), 2956 (-O-H), 3035 (Ar H); δ_{H} (**300 MHz, CDCl₃**) 2.01-2.14 (6 H, m, 2 × COCH₃), 3.38 [0.8 H, s, OCH₃ (β)], 3.45 [2.3 H, s, OCH₃ (α)], 3.79 (6 H, s, 2 × Ar-OCH₃), 4.10 (1 H, dd, $J = 5.45$ and 11.41 Hz, H-5'), 4.22-4.28 (1 H, m, H-4'), 4.31-4.38 (1 H, m, H-5'), 4.90-4.93 (1H, 2 × s, H-1'), 5.06-5.23 (1 H, m, H-2'), 5.31-5.35 (1 H, m, H-3'), 6.81-8.84 (4 H, m, H-3*), 7.16-7.28 (4 H, m, H-2*), 7.43-7.45 (5 H, m, H-6*, H-7* and H-8*); δ_{C} (**50 MHz, CDCl₃**) 20.80 (COCH₃), 20.99 (COCH₃), 55.24 (OCH₃ ^{##}), 55.45 (Ar-OCH₃ ^{##}), 55.64 (Ar-OCH₃ ^{##}), 64.64 (C-5'), 71.74 (C-3'), 74.85 (C-2'), 78.76 (C-4'), 81.62 [C(Ar)₃], 106.45 (C-1'), 113.29 (C-3*), 127.27 (C-8* [#]), 128.00 (C-6* [#]), 129.34 (C-2*), 130.26 (C-7* [#]), 139.70 (C-1*), 147.56 (C-5*), 158.83 (C-4*), 169.89 (C=O), 170.88 (C=O);

MS m/z ($M + 23^+$, 21 %) 245.13 (14), 289.13 (55), 303.13 (100), 1129.20 (26), **HRMS** (+**cESI**) calculated for $C_{31}H_{34}O_9Na^+$: 573.20950, found: $[M + 23]^+$ 573.20916.

Note: Assignments denoted with # and ## are interchangeable.

B.17 Preparation of 2',3',5'-*O*-triacetyl-1'-*O*-methoxy- α -(-)-ribose [121]



121

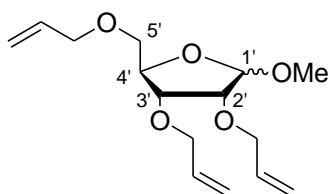
The methoxy ribose derivative **101** (6.11 mmol, 1.00 g) was stirred with distilled pyridine (3 eq, 18.3 mmol, 1.48 cm³) until a solution had formed and the solution was then cooled to 0 °C in an ice-water bath. To this cooled solution was then added dropwise a mixture of distilled acetic anhydride (4.5 eq, 27.5 mmol, 2.60 cm³) and distilled pyridine (4.5 eq, 27.5 mmol, 2.22 cm³). After the dropwise addition, the reaction mixture was allowed to warm to rt and was then stirred under an argon atmosphere overnight (22 h). The reaction was quenched by the addition of EtOAc (100 cm³) with stirring. Then the mixture was extracted with brine (3 × 100 cm³) and the combined aqueous layers were extracted with CH₂Cl₂ (3 × 100 cm³). All the organic fractions were combined and extracted with a solution of NH₄Cl that had been basified to pH 10 using NH₃ (150 cm³). The combined organics were then dried over anhydrous MgSO₄, filtered and the solvent was removed *in vacuo*. The target compound **121** [α : β ratio found to be 1:3] was obtained as a yellow oil (1.67 g, 94 %).

$\nu_{\max}/\text{cm}^{-1}$ (**thin film**) 728 (CH₂ rocking), 1194 and 1248 (C-O stretching), 1383 (alkanes), 1440 (C-H deformations), 1452 (alkanes), 1680 (C=O), 1738 (-CO-O-), 2839 (-O-CH₃), 2916 (C-H stretching), 2940 (C-H stretching from CH₂), 2998 (-CO-CH₃); δ_{H} (**300 MHz, CDCl₃**) 2.02-2.14 (9 H, m, 3 × COCH₃), 3.38 [2.3 H, s, OCH₃ (β)], 3.45 [0.8 H, s, OCH₃ (α)], 4.11 (0.8 H, dd, $J = 4.86$ and 6.58 Hz, H-5' #), 4.19-4.26 (0.3 H, m, H-5' #), 4.28-4.31 (1 H, m, H-4'), 4.33-4.39 (1.1 H, m, H-5' #), 4.91 [0.8 H, m, H-1' (β)], 4.96-5.00 [0.3 H, m, H-2' (α)], 5.13-5.14 [0.3H, m, H-1' (α)], 5.16-5.20 [0.3 H, m, H-3' (α)], 5.21-5.23 [0.8 H, m, H-2' (β)], 5.31-5.35 [0.8 H, m, H-3' (β)]; δ_{C} (**50 MHz, CDCl₃**) 20.67, 20.71, 20.75, 20.94 and 20.95 [3 × COCH₃ (α and β)], 55.42 [OCH₃ (β)], 55.79 [OCH₃ (α)], 63.63 [C-5' (α)], 64.57 [C-5' (β)], 69.96 [C-3' (α)], 70.75 [C-2' (α)], 71.67 [C-3' (β)], 74.78 [C-2' (β)], 78.68 [C-4' (β)], 79.64

[C-4' (α)], 101.71 [C-1' (α)], 106.38 [C-1' (β)], 169.83, 169.87 and 170.09 [$3 \times$ C=O (α)^{##}], 170.64, 170.76 and 170.83 [$3 \times$ C=O (β)^{##}]; **MS** *m/z* no LRMS spectrum was run, **HRMS** (+**cESI**) calculated for C₁₂H₁₈O₈Na⁺: 313.08939, found: [M + 23]⁺ 313.08943.

Note: Assignments denoted with [#] represent splitting of the same signal and those with ^{##} are interchangeable.

B.18 Preparation of 2',3',5'-*O*-triallyl-1'-*O*-methoxy- α -(-)-ribose [122]



122

The ribose derivative **101** (6.76 mmol, 1.11 g) was stirred with distilled DMF (40 cm³) until a solution had formed. The solution was then cooled to 0 °C in an ice-water bath before the addition of the sodium hydride (used as a 60 % suspension in oil, 3.3 eq, 22.3 mmol, 0.894 g). The mixture was stirred for a

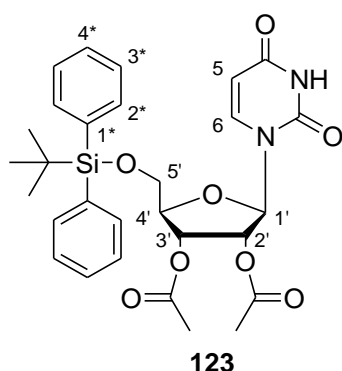
few minutes until effervescence had ceased, before the allyl bromide (3.3 eq, 22.3 mmol, 1.93 cm³) was added. The reaction mixture was then stirred at rt under an argon atmosphere overnight (23 h). After this time, tlc indicated complete consumption of the starting material, so the reaction mixture was diluted with EtOH and all the solvent was removed by evaporation. The crude residue obtained was then diluted with a saturated NH₄Cl solution (150 cm³) and extracted with EtOAc (3 \times 150 cm³). The combined organics were dried over anhydrous Na₂SO₄, filtered and the solvent was removed *in vacuo*. The expected compound **122** [α : β ratio found to be 1:3] was obtained pure as a yellow oil (1.92 g, 100 %).

R_f = 0.85 (10 % EtOH : CH₂Cl₂); **v_{max}/cm⁻¹ (thin film)** 725 (CH₂ rocking), 869, 920 and 991 (RCH=CH₂), 1159 (C-O), 1371 (alkanes), 1382 (C-OCH₃), 1452 (C-H deformations), 1647 (C=C), 2834 (O-CH₃), 2859 (C-H stretch for CH₂), 3080 (C=CH₂); **δ _H (300 MHz, CDCl₃)** 3.36 [2.3 H, s, OCH₃ (β)], 3.45 [0.8 H, s, OCH₃ (α)], 3.48-3.60 (2 H, m, H-5'), 3.81-3.83 (1 H, m, H-2'), 3.86-3.98 (1 H, m, H-3'), 4.01-4.17 (6 H, m, 3 \times OCH₂), 4.20-4.24 (1 H, m, H-4'), 4.89 [0.8 H, s, H-1' (β)], 4.94-4.96 [0.3 H, m, H-1' (α)], 5.14-5.23 (3 H, m, 3 \times CH=CH₂, proton *trans* to R group), 5.24-5.36 (3 H, m, 3 \times CH=CH₂, proton *cis* to R group), 5.84-5.98 (3 H, m, 3 \times CH=CH₂); **δ _C (50 MHz, CDCl₃)** 55.26 [OCH₃ (β)], 55.57 [OCH₃ (α)], 70.51 [C-5' (α)], 71.19 [C-5' (β)], 71.65 [OCH₂ at C-2' (β)[#]], 71.70 [OCH₂ at C-3' (β)[#]], 72.01 [OCH₂

at C-2' (α)^{##}, 72.07 [OCH₂ at C-3' (α)^{##}], 72.41 [OCH₂ at C-5' (β)[#]], 72.64 [OCH₂ at C-5' (α)^{##}], 75.66 [C-3' (α)], 78.42 [C-2' (α)], 78.56 [C-3' (β)], 79.95 [C-2' (β)], 80.57 [C-4' (β)], 82.26 [C-4' (α)], 102.58 [C-1' (α)], 106.61 [C-1' (β)], 116.99, 117.63 and 117.73 [$3 \times$ CH=CH₂ (β)], 117.28, 117.35 and 117.86 [$3 \times$ CH=CH₂ (α)], 134.61, 134.65, 134.86, 134.96 and 135.28 [$3 \times$ CH=CH₂ (α and β)]; **MS** m/z ($M + 23^+$, 21 %) 253.18 (5), 267.24 (13), 460.09 (5), 465.32 (30), 505.35 (100), 506.35 (34), 507.37 (11), 537.35 (7), 663.44 (8), 664.44 (5), **HRMS** (+cESI) calculated for C₁₅H₂₄O₅Na⁺: 307.15159, found: [$M + 23$]⁺ 307.15160.

Note: Assignments denoted with # and ## are interchangeable.

B.19 Preparation of 2',3'-O-diacetyl-5'-O-(*tert*-butyldiphenylsilyl)uridine [123]

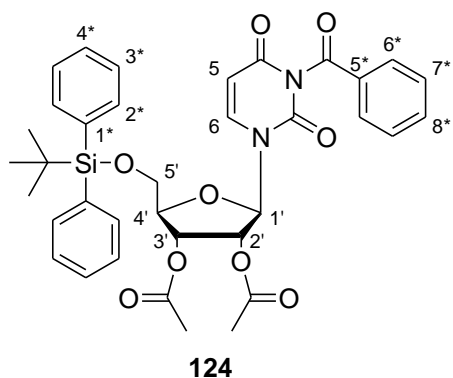


The silylated uridine **107** (8.69 mmol, 4.19 g) was stirred with distilled pyridine (2 eq, 17.4 mmol, 1.41 cm³) until a solution had formed and was then cooled to 0 °C in an ice-water bath. To this cooled solution was then added dropwise a mixture of distilled acetic anhydride (3 eq, 26.1 mmol, 2.50 cm³) and distilled pyridine (3 eq, 26.1 mmol, 2.11 cm³). The reaction mixture was then warmed to rt and was stirred under an argon atmosphere overnight (20 h). After this time, tlc indicated product formation, so EtOAc (400 cm³) was added to the reaction mixture and it was stirred for a few min. The organic layer was extracted with brine (3×400 cm³) and the combined aqueous layers were back-extracted with CH₂Cl₂ (3×400 cm³). All of the organic layers were then combined and extracted with saturated NH₄Cl that had been basified to pH ~10 using NH₃ (600 cm³). The combined organics were dried over anhydrous MgSO₄, filtered and the solvent was removed *in vacuo*. This gave the desired compound **123** as a cream foam (4.39 g, 89 %).

$R_f = 0.42$ (50 % EtOAc : hexane); $[\alpha]_D^{19} 30.000^\circ$ ($c = 0.50$ in DMF); $\nu_{\max}/\text{cm}^{-1}$ (**thin film**) 684 (RHC=CHR *cis*), 706 (5 adjacent aromatic H), 727 (CH₂ rocking), 743 (5 adjacent aromatic H), 849 (Si-C), 1113 and 1233 (C=O), 1256 (Si-C), 1327 and 1378 (C(CH₃)₃), 1453

(C-H deformation), 1588 (secondary amide), 1635 (C=C conjugated with C=O), 1697 (secondary amide), 2859 (C-H stretching), 3279 (-CONH-); δ_{H} (300 MHz, CDCl_3) 1.07-1.13 [9 H, m, $\text{C}(\text{CH}_3)_3$], 2.11-2.14 (6 H, m, $2 \times \text{COCH}_3$), 3.85 and 4.02 (2 H, two d, $J = 11.76$ Hz, H-5'), 4.18 (1 H, s, H-4'), 5.40-5.47 (2 H, m, H-2' and H-5), 5.51-5.53 (1 H, m, H-3'), 6.30 (1 H, d, $J = 6.51$ Hz, H-1'), 7.35-7.43 (6 H, m, H-3* and H-4*), 7.64-7.74 (5 H, m, H-2* and H-6), 9.39 (1 H, br s, NH); δ_{C} (50 MHz, CDCl_3) 19.50 [$\text{C}(\text{CH}_3)_3$], 20.63 and 20.85 ($2 \times \text{COCH}_3$), 27.15 [$\text{C}(\text{CH}_3)_3$], 63.73 (C-5'), 71.21 (C-3'), 73.31 (C-2'), 83.39 (C-4'), 85.40 (C-1'), 103.42 (C-5), 128.14 (C-3*), 130.38 (C-4*), 132.76 (C-1*), 135.85 (C-2*), 139.57 (C-6), 150.80 (C-2), 163.15 (C-4), 169.77 and 170.00 ($2 \times \text{COCH}_3$); **MS** m/z ($\text{M} + 23^+$, 100 %) 467.20 (9), 505.30 (26), 506.32 (8), 547.33 (6), 590.34 (38), 591.35 (12), 647.18 (7), 663.45 (20), 664.45 (11), 670.85 (5), **HRMS** (+cESI) calculated for $\text{C}_{29}\text{H}_{34}\text{N}_2\text{O}_8\text{SiNa}^+$: 589.19766, found: $[\text{M} + 1]^+$ 567.21532 and $[\text{M} + 23]^+$ 589.19699.

B.20 Preparation of 3-*N*-benzoyl-2',3'-*O*-diacetyl-5'-*O*-(*tert*-butyldiphenylsilyl)uridine [124]

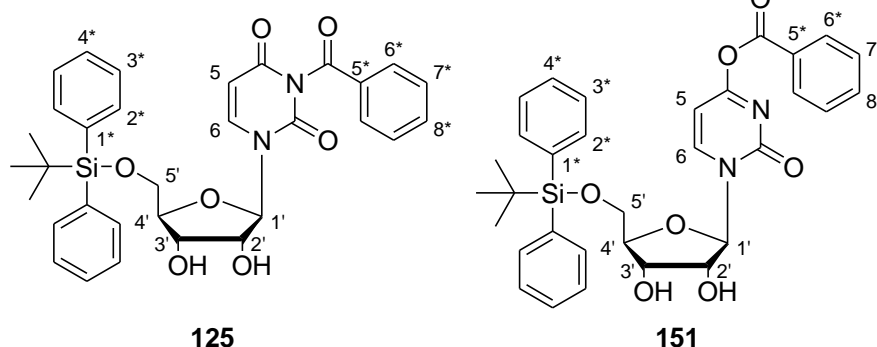


The protected uridine **123** (1.88 mmol, 1.07 g) was stirred with distilled pyridine (20 cm^3) until a pale yellow solution had formed. Then the *N,N*-diisopropylethylamine (5 eq, 9.41 mmol, 1.64 cm^3) was added and the solution was stirred at rt for 5 min. To this solution was added the distilled benzoyl chloride (5 eq, 9.41 mmol, 1.10 cm^3) and a white gas was immediately observed. The reaction mixture was then allowed to stir at rt under an argon atmosphere for 2 h. After this time the reaction mixture had gone a dark burgandy colour and the tlc indicated no further change. The reaction mixture was diluted with CH_2Cl_2 (100 cm^3) and then extracted with distilled water ($3 \times 100 \text{ cm}^3$). The combined aqueous layers were then extracted with CH_2Cl_2 (100 cm^3), subsequently dried over anhydrous Na_2SO_4 , filtered and the solvent was removed *in vacuo*. The crude dark red-brown oil was purified by column chromatography and the solvents used for elution were 10-50 % EtOAc : hexane. After purification, the desired compound **124** was obtained as a yellow foam (0.896 g, 71 %).

$R_f = 0.71$ (50 % EtOAc : hexane); $[\alpha]_D^{22} 18.367^\circ$ ($c = 0.98$ in CH_2Cl_2); $\nu_{\text{max}}/\text{cm}^{-1}$ (**thin film**) 682 (RHC=CHR cis), 701 and 742 (5 adjacent aromatic H), 858 (Si-C), 1113 and 1208 (C=O), 1235 (Si-C), 1309 and 1377 [$\text{C}(\text{CH}_3)_3$], 1446 (C-H deformations), 1585 (C=C conjugated with C=O), 1632 and 1670 (tertiary amide), 1678 (C=C conjugated with C=O), 2932 (-CONR₂); δ_{H} (**300 MHz, CDCl₃**) 1.15 [9 H, s, $\text{C}(\text{CH}_3)_3$], 2.05 (3 H, s, COCH_3), 2.10 (3 H, s, COCH_3), 3.87 and 4.05 (2 H, two d, $J = 11.85$ Hz, H-5'), 4.20 (1 H, d, $J = 2.06$ Hz, H-4'), 5.48-5.55 (3 H, m, H-2', H-3' and H-5), 6.24 (1 H, d, $J = 5.98$ Hz, H-1'), 7.41-7.48 (8 H, m, H-3*, H-4* and H-7*), 7.63-7.67 (5 H, m, H-2* and H-8*), 7.86 (1 H, d, $J = 8.26$ Hz, H-6), 7.95 (2 H, d, $J = 7.34$ Hz, H-6*); δ_{C} (**50 MHz, CDCl₃**) 19.52 [$\text{C}(\text{CH}_3)_3$], 20.61 and 20.81 ($2 \times \text{COCH}_3$), 27.20 [$\text{C}(\text{CH}_3)_3$], 63.71 (C-5'), 71.21 (C-3'), 73.54 (C-2'), 83.56 (C-4'), 85.90 (C-1'), 103.23 (C-5), 128.35 (C-3*), 129.32 (C-6*), 130.33 (C-7*), 131.54 (C-4* #), 132.68 (C-1* ##), 135.31 (C-5* ##), 135.54 (C-8* #), 135.87 (C-2*), 139.33 (C-6), 149.67 (C-2), 161.94 (C-4), 168.62 (N-C=O), 169.97 (O-C=O); **MS** m/z (M^+ , 23 %) 687.6 (67), 688.7 (31), 693.0 (21), 1357.2 (100), 1358.4 (59), 1362.4 (32), 1363.4 (26), 1364.5 (16), **HRMS** (+**cESI**) calculated for $\text{C}_{36}\text{H}_{39}\text{N}_2\text{O}_9\text{Si}^+$: 671.24193, found: $[\text{M} + 1]^+$ 671.24173 and calculated for $\text{C}_{36}\text{H}_{38}\text{N}_2\text{O}_9\text{SiNa}^+$: 693.22388, found: $[\text{M} + 23]^+$ 693.22317.

Note: Assignments denoted with # and ## are interchangeable.

B.21 Attempted synthesis of 3-N-benzoyl-5'-O-(tert-butyl-diphenylsilyl)uridine [125]

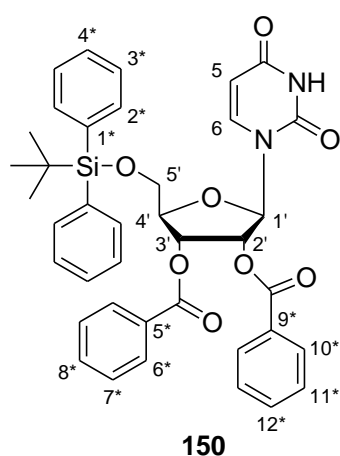


The protected uridine **107** (0.5 mmol, 0.241 g), sodium carbonate (8 eq, 4 mmol, 0.425 g) and tetrabutylammonium bromide (0.04 eq,

0.02 mmol, 0.0076 g) were dissolved in a two-phase solution of CH_2Cl_2 : H_2O (10 cm^3 : 20 cm^3). Then the benzoyl chloride (1.3 eq, 0.65 mmol, 0.076 cm^3) was added to the mixture with vigorous stirring. The reaction mixture was then stirred at rt for 30 min, after which time two spots were observed by tlc. The reaction mixture was then transferred to a separating

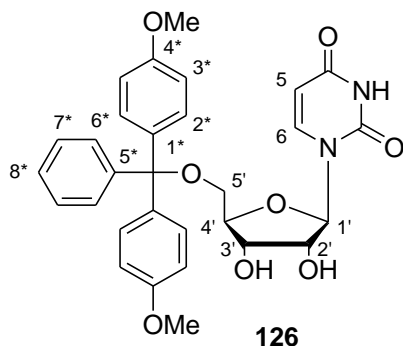
funnel, the organic phase was collected and the aqueous phase was extracted with CH_2Cl_2 ($3 \times 20 \text{ cm}^3$). The combined organics were then allowed to stand in the solvent at rt overnight (18 h) to allow conversion of the enol derivative to the keto derivative. After this time, tlc analysis still showed the presence of the two spots, so the organics were dried over anhydrous Na_2SO_4 , filtered and evaporated. The resulting residue was then dissolved in 1,2-dichloroethane (5 cm^3) and allowed to stand at rt overnight (19 h), tlc indicated no further change, so the solution was heated to $60 \text{ }^\circ\text{C}$ for 15 min and the solvent was then removed *in vacuo*. The residue obtained was then purified by column chromatography using 5-40 % EtOAc : hexane for elution. The desired compound **125** was not isolated from the reaction mixture, we obtained compound **150** as a white foam (0.183 g) instead.

2',3'-O-dibenzoyl-5'-O-(tert-butyl-diphenylsilyl)uridine [150]



White foam: $R_f = 0.63$ (50 % EtOAc : hexane); δ_{H} (**300 MHz, CDCl_3**) 1.17-1.19 [9 H, m, $\text{C}(\text{CH}_3)_3$], 4.02-4.10 (2 H, m, H-5'), 4.42 (1 H, d, $J = 2.04 \text{ Hz}$, H-4'), 5.44 (1 H, d, $J = 8.13 \text{ Hz}$, H-5), 5.71-5.75 (1 H, m, H-2' #), 5.90 (1 H, dd, $J = 2.50$ and 5.59 Hz , H-3' #), 6.58 (1 H, d, $J = 6.90 \text{ Hz}$, H-1'), 7.34-7.54 (12 H, m, H-3*, H-4*, H-7*, H-8*, H-11* and H-12*), 7.67-7.81 (5 H, m, H-2* and H-6), 7.95-7.96 (4 H, m, H-6* and H-10*), 8.09 (1 H, br s, NH); δ_{C} (**50 MHz, CDCl_3**) 19.61 (C-3'), 84.06 (C-4'), 85.82 (C-1'), 103.48 (C-5), 128.32 and 128.36 (C-3*), 128.69 and 128.75 (C-6* and C-10*), 129.08 (C-4*), 129.99 and 130.16 (C-7* and C-11*), 130.17 (C-8* and C-12*), 130.51 and 130.52 (C-8* and C-12*), 131.90 (C-9*), 132.95 (C-5*), 133.86 (C-1*), 135.57 and 135.89 (C-2*), 139.76 (C-6), 150.57 (C-2), 162.97 (C-4), 165.31 (O-C=O), 165.66 (O-C=O); **MS** m/z (M^+ , 56 %) 151.80 (10), 303.27 (27), 504.00 (12), 579.13 (23), 707.93 (81), 1397.87 (100), 1744.13 (22), **HRMS** (+pESI) calculated for $\text{C}_{39}\text{H}_{38}\text{N}_2\text{O}_8\text{Si}$: 690.23974, HRMS was not run on the sample.

B.22 Preparation of 5'-O-(4,4'-dimethoxytrityl)uridine [126]

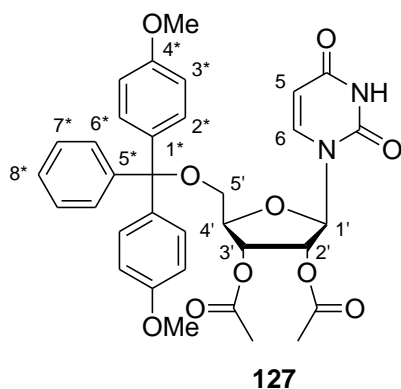


The uridine **12** (2.08 mmol, 0.507 g) was dissolved in pyridine (10 cm³). To this solution was then added 4,4'-dimethoxytrityl chloride (1.2 eq, 2.49 mmol, 0.846 g) and DMAP (0.1 eq, 0.025 mmol, 0.0033 g). The reaction mixture was then stirred at 60 °C under an argon atmosphere overnight (22 h). After this time tlc indicated no further change, so the solvent was removed *in vacuo*.

The crude compound was purified by column chromatography using the pre-prepared/basified silica, with 0-10 % MeOH : CH₂Cl₂ used as the elution solutions. The desired fractions were combined to yield a cream foam that was dissolved in MeOH (4.5 cm³). This solution was then added dropwise to a vigorously stirring flask of Et₂O (35 cm³) and a white precipitate was observed. The mixture was then cooled to 0°C in an ice-water bath to allow for complete crystallization. The white solid was filtered off through a sintered funnel and the mother liquor was evaporated and dried *in vacuo*. The mother liquor yielded the pure product **126** as a cream foam (0.947 g, 83 %).

$R_f = 0.16$ (5 % MeOH : CH₂Cl₂); $[\alpha]_D^{19} 0.4950^\circ$ (c = 2.02 in DMF); $\nu_{\max}/\text{cm}^{-1}$ (thin film) 584 (RHC=CHR *cis*), 669 (5 adjacent aromatic H), 779 (CH₂ rocking), 928 (2 adjacent aromatic H), 1215 (C-OH stretch), 1464 (CH₂ deformations), 1510 (aromatic ring), 1689 (N-CO- secondary amide), 2962 (-OCH₃), 3020 (-NCO-), 3674 (H-bonded OH), 3748 (free OH); δ_H (300 MHz, CDCl₃) 3.45-3.49 (2 H, m, H-5'), 3.78 (6 H, s, 2 × OCH₃), 4.18-4.20 (1 H, m, H-3'), 4.32-4.34 (1 H, m, H-4'), 4.44 (1 H, t, $J = 5.24$ Hz, H-2'), 5.34 (1 H, d, $J = 8.13$ Hz, H-5), 5.95 (1 H, d, $J = 3.43$ Hz, H-1'), 6.83 (4 H, d, $J = 8.70$ Hz, H-3*), 7.22-7.39 (9 H, m, H-2*, H-6*, H-7* and H-8*), 7.90 (1 H, d, $J = 8.13$ Hz, H-6), NH peak not observed; **MS** m/z (M + 23⁺, 26 %) 303.23 (100), 304.26 (22), 467.22 (5), 570.28 (8), 663.44 (6), **HRMS** (+cESI) calculated for C₃₀H₃₁N₂O₈⁺: 547.20749, found: [M + 1]⁺ 547.20717 and calculated for C₃₀H₃₀N₂O₈Na⁺: 569.18944, found: [M + 23]⁺ 569.18944.

B.23 Preparation of 2',3'-*O*-diacetyl-5'-*O*-(4,4'-dimethoxytrityl)uridine [127]



The protected uridine **126** (3.65 mmol, 2.00 g) was stirred with distilled pyridine (5 eq, 18.3 mmol, 1.50 cm³) until a solution had formed. This solution was then cooled to 0°C in an ice-water bath. To this solution was added dropwise a mixture of distilled acetic anhydride (3 eq, 11.0 mmol, 1.05 cm³) and distilled pyridine (3 eq, 11 mmol, 0.90 cm³). The reaction mixture was then warmed to rt and allowed to stir under an argon atmosphere

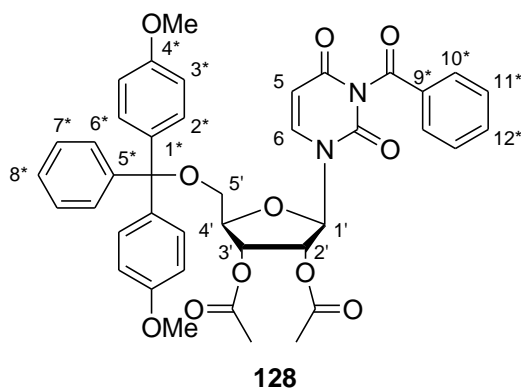
overnight (24 h). After this time, tlc indicated product formation, so the reaction mixture was diluted with EtOAc (200 cm³) and stirred for a few minutes. Then the organic layer was extracted with brine (3 × 200 cm³). The combined aqueous layers were then extracted with CH₂Cl₂ (3 × 200 cm³). All of the organic layers were combined and extracted with saturated NH₄Cl that had been basified to pH ~10 with NH₃ (300 cm³). The combined organics were dried over anhydrous MgSO₄, filtered and the solvent removed *in vacuo*. The desired product **127** was obtained as a pale orange foam that did not require further purification (2.06 g, 90 %).

$R_f = 0.24$ (50 % EtOAc : hexane); $[\alpha]_D^{22} 33.645^\circ$ ($c = 1.07$ in CH₂Cl₂); $\nu_{\max}/\text{cm}^{-1}$ (**thin film**) 703 (RHC=CHR *cis*), 727 (CH₂ rocking), 755 (5 adjacent aromatic H), 829 (2 adjacent aromatic H), 1375 and 1444 (C-H deformations), 1509 (-CONH-), 1607 (C=O), 1632 (C=C conjugated with C=O), 1693 (-CONH-), 2837 (O-CH₃), 2875 and 2935 (C-H stretching from CH₂ and CH₃), 3003 (-CO-CH₃), 3060 (Ar H), 3101 (-CONH-); δ_H (**300 MHz, CDCl₃**) 2.13 and 2.14 (6 H, two s, 2 × COCH₃), 3.50-3.53 (2 H, m, H-5'), 3.82 (6 H, s, 2 × Ar-OCH₃), 4.25-4.27 (1 H, m, H-4'), 5.36 (1 H, d, $J = 8.08$ Hz, H-5), 5.58-5.60 (1 H, m, H-3'), 5.62-5.65 (1 H, m, H-2'), 6.28 (1 H, d, $J = 6.32$ Hz, H-1'), 6.88 (4 H, d, $J = 8.09$ Hz, H-3*), 7.29-7.40 (9 H, m, H-2*, H-6*, H-7* and H-8*), 7.73 (1 H, d, $J = 8.14$ Hz, H-6), 9.34 (1 H, br s, NH); δ_C (**50 MHz, CDCl₃**) 20.65 and 20.85 (2 × COCH₃), 55.44 (2 × Ar-OCH₃), 62.91 (C-5'), 71.54 (C-3'), 73.02 (C-2'), 82.24 (C-4'), 85.54 (C-1'), 87.77 [C(Ar)₃], 103.27 (C-5), 113.55 (C-3*), 127.48 (C-8*), 128.30 (C-6* #), 128.39 (C-7* #), 130.37 (C-2*), 134.98 (C-1*), 139.93 (C-6), 144.01 (C-5*), 150.80 (C-2), 158.97 (C-4*), 163.14 (C-4), 169.81 and 170.01 (2 × C=O);

MS m/z ($M + 23^+$, 100 %) 269.07 (6), 303.23 (64), 304.26 (15), 467.24 (10), 536.16 (5), 569.26 (37), 570.32 (13), 654.28 (38), 663.44 (12), 665.47 (5), **HRMS** (+cESI) calculated for $C_{34}H_{35}N_2O_{10}^+$: 631.22862, found: $[M + 1]^+$ 631.22851 and calculated for $C_{34}H_{34}N_2O_{10}Na^+$: 653.21057, found: $[M + 23]^+$ 653.21020.

Note: assignments denoted with # are interchangeable.

B.24 Preparation of 3-*N*-benzoyl-2',3'-*O*-diacetyl-5'-*O*-(4,4'-dimethoxytrityl)uridine [128]



The protected uridine **127** (0.629 mmol, 0.397 g) was stirred with distilled pyridine (8 cm³) until a pale yellow solution had formed. Then the *N,N*-diisopropylethylamine (5 eq, 3.1 mmol, 0.55 cm³) was added and the solution was stirred at rt for five min. To this solution was then added the distilled benzoyl chloride (5 eq, 3.1 mmol, 0.37 cm³). A white gas was

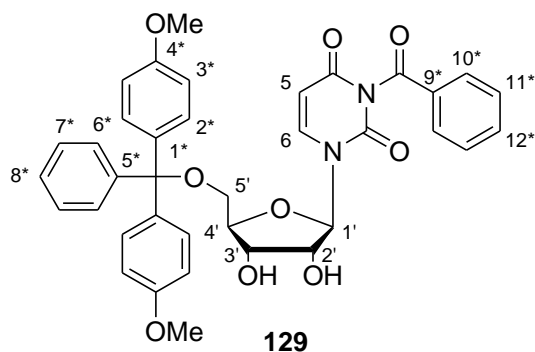
immediately liberated and the solution began to visibly darken. The reaction mixture was then allowed to stir at rt under an argon atmosphere for 2 h. After this time, tlc indicated no further change. The reaction mixture was diluted with CH₂Cl₂ (40 cm³) and extracted with distilled water (3 × 40 cm³). The combined aqueous layers were then extracted with CH₂Cl₂ (40 cm³). The combined organic layers were dried over anhydrous Na₂SO₄, filtered and evaporated. The crude mixture was obtained as a dark red-brown oil that was subsequently purified by column chromatography. Eluants used for the column were 10-50 % EtOAc : hexane. The desired compound **128** was obtained as a yellow foam (0.272 g, 59 %).

R_f = 0.53 (50 % EtOAc : hexane); $[\alpha]_D^{22}$ 18.000° (c = 1.00 in CH₂Cl₂); ν_{max}/cm^{-1} (thin film) 699 (RHC=CHR *cis*), 727 (CH₂ rocking), 758 (5 adjacent aromatic H), 829 (2 adjacent aromatic H), 1376 and 1344 (C-H deformations), 1606 (C=O), 1633 (C=C conjugated with C=O), 1671 (tertiary amide), 2838 (O-CH₃), 2908 (C-H stretching from CH₂ and CH₃), 2934 (-CONR₂), 2955 (-CO-CH₃); δ_H (300 MHz, CDCl₃) 2.07 and 2.10 (6 H, two s, 2 × COCH₃),

3.51-3.53 (2 H, m, H-5'), 3.81 (6 H, s, 2 × Ar-OCH₃), 4.25 (1 H, d, $J = 2.60$ Hz, H-4'), 5.45 (1 H, d, $J = 8.24$ Hz, H-5), 5.58-5.60 (1 H, m, H-3'), 5.62-5.67 (1 H, m, H-2'), 6.21 (1 H, d, $J = 6.22$ Hz, H-1'), 6.87 (4 H, d, $J = 8.76$ Hz, H-3*), 7.27-7.68 (12 H, m, H-2*, H-6*, H-7*, H-8*, H-11* and H-12*), 7.84 (1 H, d, $J = 8.23$ Hz, H-6), 7.96 (2 H, d, $J = 8.80$ Hz, H-10*); δ_C (50 MHz, CDCl₃) 20.65 and 20.82 (2 × COCH₃), 55.49 (2 × Ar-OCH₃), 62.84 (C-5'), 71.50 (C-3'), 73.40 (C-2'), 82.43 (C-4'), 86.05 (C-1'), 87.88 [C(Ar)₃], 103.09 (C-5), 113.63 (C-3*), 127.56 (C-8*), 128.30 (C-6*[#]), 128.37 (C-7*[#]), 129.33 (C-10*), 130.37 (C-11*), 130.78 (C-2*), 131.56 (C-12*), 134.96 (C-1*), 135.32 (C-9*), 139.71 (C-6), 144.02 (C-5*), 149.70 (C-2), 159.04 (C-4*), 161.99 (C-4), 168.68 (N-C=O), 169.96 and 169.99 (2 × CO-CH₃); **MS** m/z (M⁺, no peak found) 320.8 (7), 432.6 (11), 449.7 (25), 450.7 (5), 881.4 (100), 882.6 (28), 886.5 (11), **HRMS** (+cESI) calculated for C₄₁H₃₈N₂O₁₁Na⁺: 757.23678, found: [M + 23]⁺ 757.23653.

Note: assignments denoted with [#] are interchangeable.

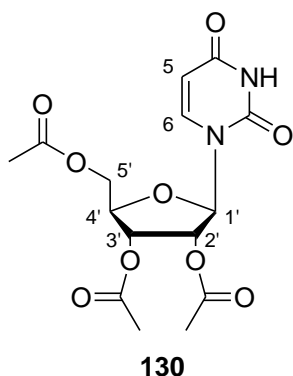
B.25 Attempted synthesis of 3-*N*-benzoyl-5'-*O*-(4,4'-dimethoxytrityl)uridine [129]



The protected uridine **126** (0.219 mmol, 0.120 g), sodium carbonate (8.3 eq, 1.82 mmol, 0.194 g) and tetra-butylammonium bromide (0.037 eq, 0.0081 mmol, 0.0035 g) were dissolved in a biphasic solution of CH₂Cl₂ : H₂O (4.5 cm³ : 9 cm³). Then the benzoyl chloride (1.3 eq, 0.3 mmol, 0.03 cm³) was added to the mixture with

vigorous stirring. The reaction mixture was then stirred at rt for 30 min, after which time multiple spots were observed by tlc. The reaction mixture was then transferred to a separating funnel by the addition of CH₂Cl₂ (5 cm³). The organic phase was collected and the aqueous phase was extracted with CH₂Cl₂ (3 × 20 cm³). The combined organics were then dried over anhydrous Na₂SO₄, filtered and evaporated. The crude mixture was obtained as a pale yellow-orange oil that darkened to a dark orange red overnight. The crude residue was then purified by column chromatography, with 5-50 % EtOAc : hexane used for elution and none of the desired compound **129** was isolated.

B.26 Preparation of 2',3',5'-*O*-triacetyluridine [130]

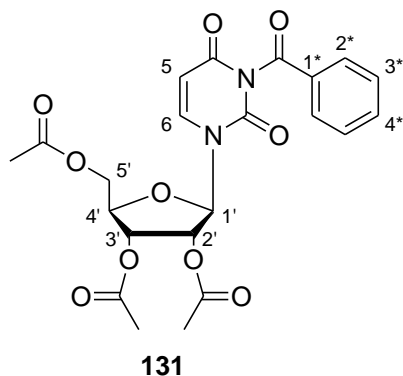


Uridine **12** (4.46 mmol, 1.09 g) was dissolved in distilled pyridine (3 eq, 13.4 mmol, 1.08 cm³) and the solution was stirred at rt under an argon atmosphere for a few minutes. To this solution was then added dropwise a solution of distilled pyridine (4.5 eq, 20.1 mmol, 1.60 cm³) and distilled acetic anhydride (4.5 eq, 20.1 mmol, 1.90 cm³). After the addition, the reaction mixture was allowed to stir at rt under an argon atmosphere overnight (22 h).

After this time, tlc indicated product formation, so EtOAc (100 cm³) was added to the reaction mixture and it was allowed to stir for a few min. Then the organic layer was extracted with brine (3 × 100 cm³) and the combined aqueous layers were extracted with CH₂Cl₂ (3 × 100 cm³). All the organic layers were combined and extracted with a saturated NH₄Cl solution that had been basified to pH ~10 with NH₃ (150 cm³). The combined organics were then dried over MgSO₄, filtered and evaporated. The crude compound was purified by column chromatography, using EtOAc as the eluant. The desired compound **130** was obtained as a white foam after purification (1.54 g, 93 %).

$R_f = 0.59$ (100 % EtOAc); $[\alpha]_D^{23} 8.3333^\circ$ (c = 2.04 in EtOAc); $\nu_{\max}/\text{cm}^{-1}$ (**thin film**) 669 (RHC=CHR *cis*), 775 (CH₂ rocking), 1216 (-CO-CH₃), 1379 (-CH₃ symmetrical deformation), 1457 (C-H deformations), 1540 (-CONH-), 1698 (C=C conjugated with C=O), 1750 (C=O), 3391 (-CONH-); δ_H (**300 MHz, CDCl₃**) 2.11, 2.13 and 2.15 (9 H, 3 × s, 3 × CH₃), 4.32-4.39 (3 H, m, H-3' and H-5'), 5.34-5.36 (2 H, m, H-2' and H-4'), 5.80 (1 H, d, $J = 8.12$ Hz, H-5), 6.05 (1 H, d, $J = 4.72$ Hz, H-1'), 7.41 (1 H, d, $J = 8.16$ Hz, H-6), 9.61 (1 H, br s, NH); δ_C (**50 MHz, CDCl₃**) 20.56, 20.65 and 20.79 (3 × CH₃), 63.32 (C-5'), 70.36 (C-4'), 72.89 (C-2'), 80.08 (C-3'), 87.68 (C-1'), 103.59 (C-5), 139.55 (C-6), 150.50 (C-2), 163.19 (C-4), 169.84 (2 × C=O, on C-2' and C-3'), 170.36 (C=O on C-5'); **MS** m/z (M + 23⁺, 100 %) 139.13 (12), 217.15 (13), 259.13 (78), 351.19 (14), 387.98 (22), 394.23 (16), **HRMS** (+**cESI**) calculated for C₁₅H₁₉N₂O₉⁺: 371.10851, found: [M + 1]⁺ 371.10849 and calculated for C₁₅H₁₈N₂O₉Na⁺: 393.09045, found: [M + 23]⁺ 393.09029.

B.27 Preparation of 3-*N*-benzoyl-2',3',5'-*O*-triacetyluridine [131]

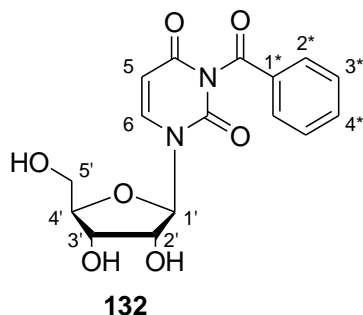


A solution was prepared of the protected uridine **130** (10.7 mmol, 3.95 g) and distilled pyridine (80 cm³). To this solution was then added *N,N*-diisopropylethylamine (5 eq, 53.3 mmol, 9.30 cm³) and the solution was stirred for 10 min. To the stirred solution was then added distilled benzoyl chloride (5 eq, 53.3 mmol, 6.20 cm³). The reaction mixture was stirred at rt under an argon atmosphere for 2 h, during which time the solution

changed colour to a very dark red. After this time, the reaction mixture was diluted with CH₂Cl₂ (390 cm³) and extracted with distilled water (3 × 390 cm³). The combined aqueous layers were then extracted with CH₂Cl₂ (390 cm³). All the organic layers were combined, dried over anhydrous Na₂SO₄, filtered and evaporated. The crude compound was obtained as a dark brown semi-solid and was further purified by column chromatography using the pre-prepared/basified silica. The solvent used for eluting the column was 50 % EtOAc : hexane. The desired compound **131** was obtained as a bright yellow foam (4.71 g, 93 %).

$R_f = 0.21$ (50 % EtOAc : hexane); $[\alpha]_D^{23} 0.9901^\circ$ ($c = 2.02$ in EtOAc); $\nu_{\max}/\text{cm}^{-1}$ (thin film) 670 (RHC=CHR *cis*), 775 (5 adjacent aromatic H), 1375 (-CH₃ symmetrical deformation), 1452 (C-H deformations), 1540 (tertiary amide), 1678 (C=C conjugated with C=O), 1752 (tertiary amide), 3022 (Ar H); δ_H (300 MHz, CDCl₃) 2.05, 2.11 and 2.13 (9 H, 3 × s, 3 × CH₃), 4.37 (3 H, m, H-3' and H-5'), 5.36-5.40 (2 H, m, H-2' and H-4'), 5.90 (1 H, d, $J = 8.22$ Hz, H-5), 6.02 (1 H, d, $J = 4.94$ Hz, H-1'), 7.48-7.53 (3 H, m, H-3* and H-6), 7.64-7.66 (1 H, m, H-4*), 7.95 (2 H, d, $J = 7.84$ Hz, H-2*); δ_C (50 MHz, CDCl₃) 20.56, 20.64 and 20.92 (3 × CH₃), 63.16 (C-5'), 70.40 (C-4'), 73.11 (C-2'), 80.38 (C-3'), 88.10 (C-1'), 103.44 (C-5), 129.35 (C-3*), 130.75 (C-2*), 131.47 (C-1*), 135.37 (C-4*), 139.21 (C-6), 149.41 (C-2), 161.75 (C-4), 168.37 (N-C=O), 169.76, 169.98 and 170.28 (3 × COCH₃); **MS** m/z ($M + 23^+$, 100 %) 259.13 (11), 475.15 (10), 492.01 (24), 498.24 (25), 499.25 (5), **HRMS** (+cESI) calculated for C₂₂H₂₃N₂O₁₀⁺: 475.13472, found: $[M + 1]^+$ 475.13429 and calculated for C₂₂H₂₂N₂O₁₀Na⁺: 497.11667, found: $[M + 23]^+$ 497.11584.

B.28 Attempted synthesis of 3-*N*-benzoyluridine [132]



Method 1:

The protected uridine **131** (0.410 mmol, 0.195 g) was dissolved in distilled MeOH (5 cm³) and to this solution was then added the potassium carbonate (4.5 eq, 1.85 mmol, 0.259 g). The reaction mixture was then stirred at rt for 2 h.

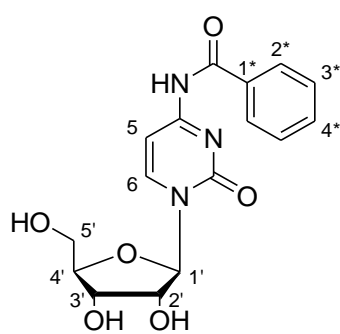
After this time, tlc indicated consumption of the starting material, so the inorganic salts were filtered off through celite and rinsed with MeOH. The solvent was removed *in vacuo* to yield a cream solid. The crude material was recrystallised from hot MeOH and the cream crystals were collected by filtration and dried under high vacuum. NMR spectroscopy showed that none of the desired compound **132** had formed.

Method 2:

The protected uridine **131** (0.234 mmol, 0.111 g) was stirred with a distilled CH₂Cl₂ : MeOH (9 cm³ : 1 cm³) mixture until a solution had formed. Then the *p*-TsOH.H₂O (3 eq, 0.700 mmol, 0.137 g) was added and the reaction mixture was allowed to stir at rt under an argon atmosphere for 24 h. After this time the reaction mixture was diluted with CH₂Cl₂ (10 cm³) and the organic phase was extracted with saturated NaHCO₃ (10 cm³). The organics were then dried over anhydrous Na₂SO₄, filtered and the solvent was removed *in vacuo*. The crude residue was obtained as a yellow foam and was subjected to NMR spectroscopy. It was found that none of the desired compound **132** had formed.

B.29 Preparation of 4-*N*-benzoylcytidine [133]

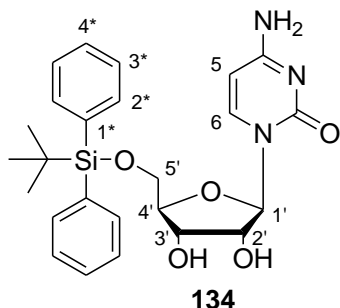
The cytidine **11** (8.25 mmol, 2.01 g) was stirred with absolute EtOH (200 cm³) and then heated to reflux. To the refluxing solution was then added benzoic anhydride (1 eq, 8.25 mmol, 1.87 g) and the reaction mixture was stirred at reflux for 1 h. After this time, the second amount of benzoic anhydride (1 eq, 8.25 mmol, 1.87 g) was added and the reaction

**133**

mixture was stirred at reflux for a further hour. Following this time, the third amount of benzoic anhydride (1 eq, 8.25 mmol, 1.87 g) was added and the reaction mixture was stirred at reflux for a further hour. Subsequently, the fourth and final amount of benzoic anhydride (1 eq, 8.25 mmol, 1.87 g) was added and the reaction mixture was stirred at reflux for another hour. After this time, the reaction mixture was allowed to cool to rt and the solvent was removed *in vacuo* to yield a white solid. The crude compound was triturated with Et₂O (200 cm³) for approximately 1 h. The solid precipitate was then filtered off through a sintered funnel and it was then rinsed with Et₂O (3 × 100 cm³). The precipitate was dried under high vacuum and the desired compound **133** was obtained as a fluffy white powder (2.79 g, 97 %).

$R_f = 0.31$ (10 % EtOH : CH₂Cl₂); $[\alpha]_D^{23} 36.585^\circ$ (c = 2.05 in DMSO); $\nu_{\max}/\text{cm}^{-1}$ (**thin film**) 670 (5 adjacent aromatic H), 690 (RHC=CHR *cis*), 707 (CH₂ rocking), 741 (5 adjacent aromatic H), 1114 (C-O stretching from C-OH), 1205 (C-O), 1394 (O-H bending), 1457 (C-H deformations), 1504 (Ar H), 1578 (-CONH-), 1601 (Ar H), 1615 (C=C conjugated with C=O), 1672 (-CONH-), 3159 (Ar H), 3422 (-CONH-); δ_H (**300 MHz, *d*₆-DMSO**) 3.62-3.74 (2 H, m, H-5'), 3.92-3.94 (1 H, m, H-4'), 3.97-4.02 (2 H, m, H-2' and H-3'), 5.09 (1 H, d, $J = 5.39$ Hz, OH-3'), 5.22 (1 H, t, $J = 4.92$ Hz, OH-5'), 5.54 (1 H, d, $J = 4.68$ Hz, OH-2'), 5.82 (1 H, d, $J = 2.42$ Hz, H-1'), 7.34 (1 H, d, $J = 5.95$, Hz, H-5), 7.46-7.50 (2 H, m, H-3*), 7.53-7.62 (1 H, m, H-4*), 8.00 (2 H, d, $J = 7.46$ Hz, H-2*), 8.50 (1 H, d, $J = 7.23$ Hz, H-6), 11.24 (1 H, br s, NH); δ_C (**50 MHz, *d*₆-DMSO**) 59.98 (C-5'), 68.72 (C-3'), 74.64 (C-2'), 84.30 (C-4'), 90.31 (C-1'), 96.11 (C-5), 128.55 (C-2* and C-3*), 132.85 (C-4*), 133.21 (C-1*), 145.43 (C-6), 154.75 (C-2), 163.12 (C-4), 167.44 (N-C=O); **MS *m/z*** (M⁺, 18 %) 255.25 (5), 303.20 (32), 346.19 (100), 459.40 (10), 561.40 (7), 639.38 (18), 640.39 (8), **HRMS (+cESI)** calculated for C₁₆H₁₈N₃O₆⁺: 348.11901, found: [M + 1]⁺ 348.11509.

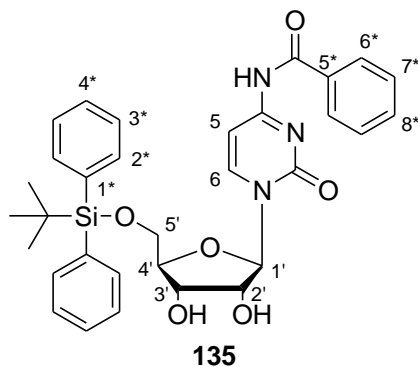
B.30 Preparation of 5'-O-(*tert*-butyldiphenylsilyl)cytidine [134]



A Schlenk tube was filled with a 5 % trimethylsilyl chloride : hexane solution and was stored at rt overnight. The glassware was then oven dried, placed under high vacuum and allowed to cool to rt under an argon atmosphere. The cytidine **11** (8.51 mmol, 2.07 g) and DMAP (0.1 eq, 0.851 mmol, 0.106 g) were stirred with distilled pyridine (10 cm³) until a cream suspension had formed. To this suspension was then added the *tert*-butyldiphenylsilyl chloride (1.1 eq, 9.37 mmol, 2.45 cm³). The reaction mixture was then allowed to stir at rt under an argon atmosphere overnight (23 h). After this time, the reaction mixture was diluted with CH₂Cl₂ (80 cm³) and then extracted with a saturated NaHCO₃ solution (2 × 80 cm³) and brine (80 cm³). The organic layer was dried over anhydrous Na₂SO₄, filtered and the solvent was removed *in vacuo*. The crude compound was purified by column chromatography using the pre-prepared and basified silica and 10-20 % EtOH : CH₂Cl₂ as the eluant. The desired product **134** was obtained as a white foam (4.08 g, 100 %).

$R_f = 0.23$ (10 % EtOH : CH₂Cl₂); $[\alpha]_D^{19} 24.138^\circ$ (c = 2.03 in DMF); $\nu_{\max}/\text{cm}^{-1}$ (**thin film**) 670 (RHC=CHR *cis*), 765 (CH₂ rock), 1109 (Si-O), 1216 (C-OH stretch), 1423 (CH₂ deformations or O-H bend), 1523 (NH₂), 1650 (N-CO-N), 3021 (Ar H), 3651 (H-bonded OH), 3575 (free OH); δ_H (**300 MHz, *d*₆-DMSO**) 1.02 [9 H, s, C(CH₃)₃], 3.74-3.79 (1 H, m, H-5'), 3.90-3.95 (3 H, m, H-2', H-4' and H-5'), 4.08-4.11 (1 H, m, H-3'), 5.07 (1 H, d, $J = 6.02$ Hz, OH-3'), 5.43 (1 H, d, $J = 5.05$ Hz, OH-2'), 5.53 (1 H, d, $J = 7.41$ Hz, H-5), 5.83 (1 H, d, $J = 3.35$ Hz, H-1'), 7.15 (2 H, br s, NH₂), 7.39-7.49 (6 H, m, H-3* and H-4*), 7.63-7.65 (4 H, m, H-2*), 7.66 (1 H, d, $J = 7.40$ Hz, H-6); δ_C (**50 MHz, *d*₆-DMSO**) 18.79 [C(CH₃)₃], 26.65 [C(CH₃)₃], 63.19 (C-5'), 68.88 (C-3'), 74.22 (C-2'), 82.91 (C-4'), 89.31 (C-1'), 93.74 (C-5), 127.96 (C-3*), 129.96 (C-4*), 132.27 (C-1*), 134.96 (C-2*), 140.59 (C-6), 155.12 (C-2), 165.46 (C-4); **MS** m/z (M⁺, 34 %) 255.23 (5), 327.24 (5), 480.28 (100), 482.32 (10), 561.37 (6), 639.37 (14), 640.43 (7), **HRMS** (+cESI) calculated for C₂₅H₃₂N₃O₅Si⁺: 482.21057, found: [M + 1]⁺ 482.20978.

B.31 Attempted synthesis of 4-*N*-benzoyl-5'-*O*-(*tert*-butyldiphenylsilyl)cytidine [135]



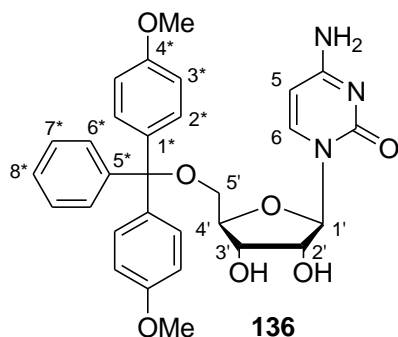
Method 1:

The Schlenk tube was filled with a 5 % trimethylsilyl chloride : hexane solution and was stored at rt overnight. The glassware was then oven dried, placed under high vacuum and allowed to cool to rt under an argon atmosphere. The benzoyl-protected cytidine **133** (5.32 mmol, 1.85 g) and DMAP (0.1 eq, 0.532 mmol, 0.0666 g) were stirred with distilled pyridine (18.5 cm³) until a suspension had formed. To this suspension was added the *tert*-butyldiphenylsilyl chloride (1.1 eq, 5.85 mmol, 1.52 cm³). The reaction mixture was then stirred at rt under an argon atmosphere overnight (22 h). After this time, tlc indicated the formation of a new spot, so the reaction was quenched by the addition of EtOH (20 cm³) and the solvent was removed *in vacuo*. The crude mixture was purified by column chromatography using the pre-prepared/basified silica and 10 % EtOH : CH₂Cl₂ for elution. None of the desired compound **135** was isolated after purification.

Method 2:

The silylated cytidine compound **134** (0.631 mmol, 0.304 g) was dissolved in absolute EtOH (15 cm³) and was heated to reflux, before the first addition of benzoic anhydride (1 eq, 0.631 mmol, 0.145 g). The reaction mixture was stirred at reflux for 1 h before the second addition of benzoic anhydride (1 eq, 0.631 mmol, 0.142 g). This was repeated for a further two additions of benzoic anhydride (addition 3: 1 eq, 0.631 mmol, 0.146 g and addition 4: 1 eq, 0.631 mmol, 0.147 g), which were added at hourly intervals. After the final addition, the reaction mixture was stirred at reflux for another hour and was then allowed to cool to rt. After this time the solvent was removed *in vacuo* to give a cream residue, that was then triturated with Et₂O (30 cm³) for 15 min. After this time the precipitate was filtered off, rinsed with further portions of Et₂O and then allowed to dry in a desiccator overnight. A white powder was obtained from the reaction which contained the unreacted starting material **134**. None of the desired compound **135** was isolated from the reaction.

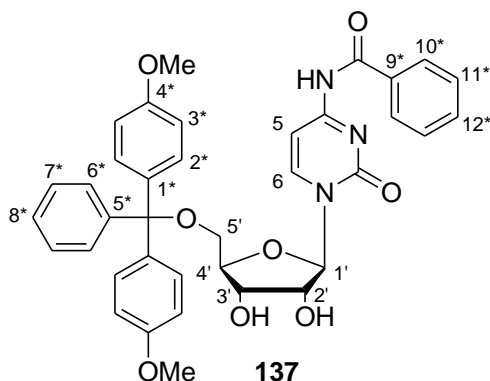
B.32 Attempted synthesis of 5'-O-(4,4'-dimethoxytrityl)cytidine [136]



The cytidine **11** (12.4 mmol, 3.02 g) and DMAP (0.1 eq, 1.24 mmol, 0.158 g) were stirred with distilled pyridine (30 cm³) until a solution had formed. To the solution was then added 4,4'-dimethoxytrityl chloride (1.2 eq, 14.9 mmol, 5.06 g). The reaction mixture was then allowed to stir at rt under an argon atmosphere overnight (23 h).

After this time, the reaction mixture was transferred to a round-bottomed flask using EtOH and the solvent was removed *in vacuo*. The crude compound was then purified by column chromatography with the pre-prepared/basified silica and 5-20 % EtOH : CH₂Cl₂ as the eluant. The desired fractions were combined to yield a pale yellow foam, which contained a mixture of the desired product and a triethylamine salt (confirmed by NMR spectroscopy). The pale yellow foam mixture obtained from the column was dissolved in MeOH (25 cm³) with gentle heating. This solution was then added dropwise to vigorously stirring Et₂O (250 cm³) and a white precipitate was observed. This was then cooled in an ice-water bath to allow for complete crystallization and the solid precipitate was filtered off through a sintered funnel. NMR spectroscopy confirmed that the white crystalline material obtained by this method was the triethylamine salt. The solvent was removed from the mother liquor *in vacuo* and a pale yellow foam was obtained. NMR spectroscopy again confirmed the presence of the desired product, but it was still contaminated with the triethylamine salt. The recrystallization procedure was repeated as described above, unfortunately the desired compound was again obtained contaminated with the triethylamine salt. A different recrystallization procedure was then attempted, where the contaminated foam was dissolved in MeOH (25 cm³) with gentle heating. This solution was then added drop wise to vigorously stirring H₂O (100 cm³) and a white precipitate was immediately observed. The white precipitate was collected by filtration and dried in a desiccator, NMR analysis found it to be the 4,4'-dimethoxytrityl alcohol. None of the desired compound **136** was isolated from the reaction mixture.

B.33 Attempted synthesis of 4-*N*-benzoyl-5'-*O*-(4,4'-dimethoxytrityl)cytidine [137]



Method 1:

The benzoyl cytidine **133** (0.726 mmol, 0.252 g) and DMAP (0.02 eq, 0.0145 mmol, 0.0024 g) were dissolved in pyridine (5 cm³). To this solution was then added 4,4'-dimethoxytrityl chloride (1 eq, 0.726 mmol, 0.243 g) and the reaction mixture was stirred at rt under an argon atmosphere overnight (20 h). To the reaction

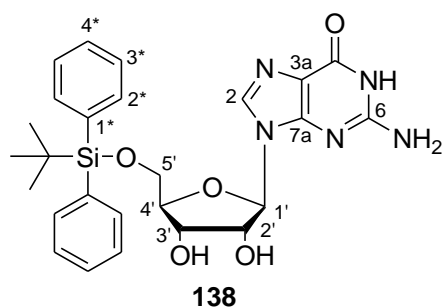
mixture was then added a saturated solution of NaHCO₃ (25 cm³) and the mixture was then extracted with CHCl₃ (3 × 25 cm³). The organic layers were then combined and extracted with brine (25 cm³). The combined organics were dried over anhydrous Na₂SO₄, filtered and the solvent removed *in vacuo*. The resulting oily residue was then dissolved in a EtOH (3 cm³) and CHCl₃ (10 cm³) mixture. The solution formed was then added dropwise to vigorously stirring Et₂O (100 cm³) and a precipitate formed. The white precipitate was then collected by filtration and NMR spectroscopy confirmed it contained only unreacted starting material **133**. At the same time, the mother liquor was evaporated and yielded a very viscous clear oil, which solidified to give a cream foam under high vacuum. The crude foam was then purified by column chromatography on the pre-prepared/basified silica using 5 % EtOH : CH₂Cl₂ for elution. Isolated from the column were both the starting material and trace amounts of 4,4'-dimethoxytrityl alcohol. None of the desired compound **137** was isolated from the column and we believe that if it had formed it subsequently decomposed under the chromatography conditions.

Method 2:

The benzoyl cytidine **133** (3.87 mmol, 1.35 g) and DMAP (0.1 eq, 0.387 mmol, 0.0496 g) were stirred with distilled pyridine (13 cm³) until a suspension had formed. The suspension was then cooled to 0 °C in an ice-water bath before the addition of the 4,4'-dimethoxytrityl chloride (1.2 eq, 4.65 mmol, 1.57 g). The reaction mixture was then allowed to stir at rt under an argon atmosphere overnight (21 h). After this time it was noted that all of the solid had

solubilised to give a clear orange solution and that tlc indicated the formation of new spots. The reaction was thus quenched by the addition of EtOH (13 cm³) and the solvent was removed *in vacuo* to yield an orange foam. The crude foam was then dissolved in hot MeOH (25 cm³) and allowed to cool to rt, during which time a white precipitate was observed. The mixture was then cooled to 0 °C to allow for complete crystallization to occur and the precipitate was collected by filtration. At the same time the mother liquor was evaporated and the viscous orange oil obtained was dried under high vacuum. NMR spectra obtained for both the white precipitate and the orange oil did not show the presence of any sugar ring protons for the two compounds. Thus, none of the desired compound **137**, was isolated from the reaction.

B.34 Attempted synthesis of 5'-O-(*tert*-butyldiphenylsilyl)guanosine [**138**]



Method 1:

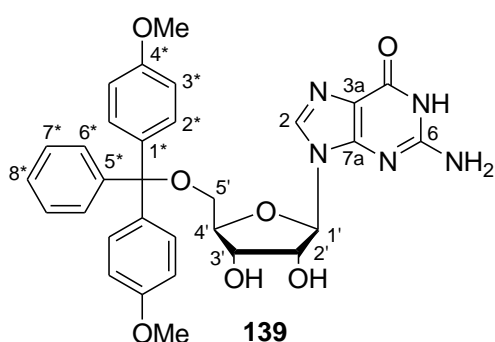
Guanosine **9** (1.79 mmol, 0.507 g) and DMAP (0.01 eq, 0.0232 mmol, 0.0038 g) were dissolved in anhydrous pyridine (2.5 cm³) and the solution was stirred for 15 min at rt before the addition of the *tert*-butyldiphenylsilyl chloride (1.1 eq, 2.0 mmol, 0.51 cm³). The reaction mixture was then stirred at rt under an argon atmosphere overnight (24 h). After this time, tlc indicated no further change, so the solution was concentrated to a white semi-solid residue under reduced pressure. This crude residue was then dissolved in CH₂Cl₂ (50 cm³) and was extracted with a saturated NaHCO₃ solution (2 × 40 cm³) and brine (40 cm³). The organic layer was dried over anhydrous Na₂SO₄, filtered and the solvent was removed *in vacuo*. A clear oil was obtained from the organic phase that was identified to be the silanol **145** by NMR spectroscopy. None of the desired compound **138** was isolated from the reaction mixture.

Method 2:

Guanosine **9** (1.80 mmol, 0.509 g) was dissolved in distilled DMF (20 cm³) and to the solution was added imidazole (2 eq, 3.60 mmol, 0.259 g). The solution was stirred for 15 min before the addition of the *tert*-butyldiphenylsilyl chloride (1 eq, 1.8 mmol, 0.47 cm³). The reaction mixture was then stirred for 48 h at rt and no change was observed by tlc. The reaction mixture was thus heated to 50 °C for a further 72 h. After this time, tlc indicated no further change, so the reaction mixture was quenched by the addition of EtOH (2 cm³) and the solvent was removed *in vacuo*. The crude mixture was obtained as a white semi-solid - numerous attempts at recrystallization failed and each time unidentifiable by-products were isolated.

Method 3:

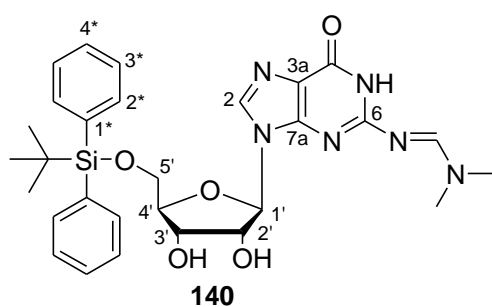
A Schlenk tube was filled with a 5 % trimethylsilyl chloride : hexane (*v/v*) solution and it was stored at rt overnight. All the glassware was then oven dried, placed under high vacuum and allowed to cool to rt under an argon atmosphere. Guanosine **9** (1.81 mmol, 0.513 g) and DMAP (0.01 eq, 0.023 mmol, 0.0028 g) were stirred with distilled pyridine (2.5 cm³) until a suspension had formed. To the suspension was then added the *tert*-butyldiphenylsilyl chloride (1.1 eq, 2.0 mmol, 0.52 cm³) and the reaction mixture was stirred at rt under an argon atmosphere overnight (21 h). After this time tlc showed no further change, so the reaction was quenched with the addition of EtOH (5 cm³). The solvent was removed *in vacuo* and the crude mixture was obtained as a white solid. NMR analysis found none of the desired peaks for the silyl protecting group and showed that starting material **9** had been isolated.

B.35 Attempted synthesis of 5'-O-(4,4'-dimethoxytrityl)guanosine [139]

Guanosine **9** (1.80 mmol, 0.509 g) was dissolved in distilled pyridine (10 cm³) and the solution was heated to 60 °C. To the solution was then added the 4,4'-dimethoxytrityl chloride (1.2 eq, 2.16 mmol, 0.756 g) and DMAP (0.01 eq, 0.022 mmol,

0.0029 g). The reaction mixture was then stirred at 60 °C under an argon atmosphere overnight (20 h). After this time, tlc indicated the formation of a new spot, so the reaction mixture was allowed to cool to rt and the solvent was removed *in vacuo*. The crude mixture was purified by column chromatography using 10-50 % EtOH : CH₂Cl₂ as the eluant. Unfortunately, the only compounds isolated from the column were 4,4'-dimethoxytrityl chloride degradation products and unreacted guanosine, it appeared as though the desired compound **139** had decomposed during purification.

B.36 Attempted synthesis of 5'-O-(*tert*-butyldiphenylsilyl)-6-N-(*N,N*-dimethylmethanimine)guanosine [**140**]



Method 1:

The Schlenk tube was filled with a 5 % trimethylsilyl chloride : hexane solution (*v/v*) and was stored at rt overnight. After this time, the glassware was oven dried, placed under high vacuum and allowed to cool to rt under an argon atmosphere. Then the protected guanosine **112** (2.82 mmol, 0.954 g) and DMAP (0.1 eq, 0.282 mmol, 0.0354 g) were stirred with distilled pyridine (10 cm³) until a suspension had formed. To this suspension was then added the *tert*-butyldiphenylsilyl chloride (1.1 eq, 3.1 mmol, 0.81 cm³). The reaction mixture was then allowed to stir at rt under an argon atmosphere overnight (25 h). After this time, tlc indicated the formation of a new spot, so the reaction was quenched by the addition of EtOH (10 cm³) and the solvent was removed *in vacuo*. The crude mixture was purified by column chromatography using the pre-prepared/basified silica and 10 % EtOH : CH₂Cl₂ for elution. None of the desired compound **140** was obtained after column chromatography, instead only degradation products were isolated which lead us to believe that the desired compound **140** was decomposing during chromatography.

Method 2:

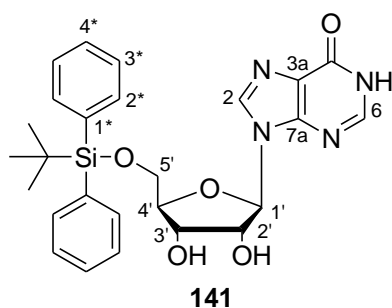
The Schlenk tube was filled with a 5 % trimethylsilyl chloride : hexane solution (*v/v*) and was stored at rt overnight. After this time, the glassware was oven dried, placed under high vacuum and allowed to cool to rt under an argon atmosphere. The protected guanosine **112** (6.73 mmol, 2.28 g) and DMAP (0.1 eq, 0.673 mmol, 0.0823 g) were stirred with distilled pyridine (22 cm³) until a suspension had formed. To this suspension was then added the *tert*-butyldiphenylsilyl chloride (1.1 eq, 7.40 mmol, 1.92 cm³) and the reaction mixture was allowed to stir at rt under an argon atmosphere overnight (20 h). After this time, tlc indicated no further change, so the reaction was quenched by the addition of EtOH (22 cm³) and the solvent was removed *in vacuo*. The residue obtained was dissolved in MeOH (50 cm³) with gentle heating and this was added dropwise to vigorously stirring H₂O (100 cm³). A precipitate was immediately observed, it was collected by filtration and was then dried in a desiccator overnight. NMR spectroscopy showed that the *N,N*-dimethylmethyimine group was missing from the by-product isolated and none of the desired compound **140** was obtained.

Method 3:

The Schlenk tube was filled with a 5 % trimethylsilyl chloride : hexane solution (*v/v*) and was stored at rt overnight. After this time, the glassware was oven dried, placed under high vacuum and allowed to cool to rt under an argon atmosphere. The guanosine **9** (1.76 mmol, 0.500 g) was dissolved in pre-distilled and dried DMF (25 cm³). To this solution was then added imidazole (2 eq, 3.53 mmol, 0.243 g) and the solution was stirred at rt for 15 min. After this time, the *tert*-butyldiphenylsilyl chloride (1 eq, 1.8 mmol, 0.46 cm³) was added to the solution and the reaction mixture was stirred at rt under an argon atmosphere overnight (20 h). Following this time, the reaction mixture was quenched by the addition of EtOH (5 cm³) and the solvent was removed *in vacuo*. The crude residue obtained was then dissolved in freshly distilled MeOH (25 cm³) and transferred to an oven dried Schlenk tube. After stirring for a few minutes the *N,N*-dimethylformamide dimethyl acetal (3.5 cm³) was added (note: in previous attempts at this reaction, 2 eq of the reagent were added, but no product was isolated). The reaction mixture was then stirred at rt under an argon atmosphere for 90 h. After this time, the solution was diluted with CH₂Cl₂ (50 cm³) and then washed with 0.5 M NaHCO₃ (2 × 50 cm³). The organic fraction was dried over anhydrous Na₂SO₄, filtered and

the solvent was removed *in vacuo*. The residue obtained was triturated with Et₂O (20 cm³) for 30 min and the white precipitate was collected by filtration. The mother liquor was evaporated and a clear oil was obtained. NMR spectroscopy confirmed that the clear oil obtained was the silanol **145** and that the white precipitate was unreacted starting material **9**.

B.37 Attempted synthesis of 5'-O-(*tert*-butyldiphenylsilyl)inosine [**141**]



Method 1:

The Schlenk tube was filled with a 5 % trimethylsilyl chloride : hexane solution (*v/v*) and was stored at rt overnight. The glassware was then oven dried, placed under high vacuum and allowed to cool to rt under an argon atmosphere. The inosine **116** (4.03 mmol, 1.08 g) and DMAP (0.1 eq, 0.403 mmol, 0.0498 g) were stirred with distilled pyridine (5 cm³) until a suspension had formed. To this suspension was then added the *tert*-butyldiphenylsilyl chloride (1.1 eq, 4.43 mmol, 1.15 cm³) and the reaction mixture was stirred at rt under an argon atmosphere overnight (22 h). After this time, tlc indicated the presence of a new spot, so the reaction was quenched by the addition of EtOH (10 cm³) and the solvent was removed *in vacuo*. The crude residue was purified by column chromatography using the pre-prepared/basified silica and 5-15 % EtOH : CH₂Cl₂ for elution. Only inosine **116** was isolated from the column - we have assumed that if the desired product **141** is formed during the reaction, it then decomposes on the column.

Method 2:

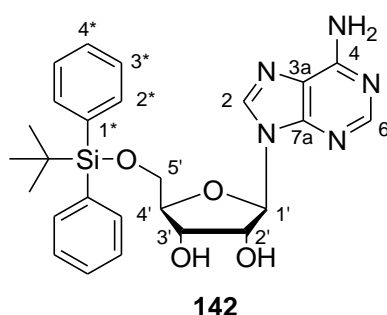
The reaction described in method 1 above was repeated (scale: 3.82 mmol, 1.02 g), but instead of purification by column chromatography, we attempted to purify the crude residue by an acid-base extraction procedure. The crude residue was dissolved in CH₂Cl₂ (100 cm³) and this was extracted with 0.5 M HCl (100 cm³), followed by distilled water (3 × 100 cm³). The organic layer was then extracted with 0.5 M NaOH (100 cm³) and distilled water (3 × 100

cm³). The organic layer was then dried over anhydrous Na₂SO₄, filtered and the solvent was removed *in vacuo*. As before, only decomposition products were isolated using this method.

Method 3:

The Schlenk was filled with a 5 % trimethylsilyl chloride : hexane solution (*v/v*) and was stored at rt overnight. The glassware was then oven dried, placed under high vacuum and allowed to cool to rt under an argon atmosphere. Then the inosine **116** (11.3 mmol, 3.02 g) and DMAP (0.1 eq, 1.13 mmol, 0.140 g) were stirred with distilled pyridine (15 cm³) until a suspension had formed. To this suspension was added the *tert*-butyldiphenylsilyl chloride (1.1 eq, 12.4 mmol, 3.22 cm³) and the reaction mixture was stirred at rt under an argon atmosphere overnight (20 h). After this time, tlc showed no further change, so the reaction was quenched by the addition of EtOH (30 cm³) and the solvent was removed *in vacuo*. NMR spectroscopy on the crude residue showed that none of the desired product **141** had formed during the reaction. Other attempts at the reaction had employed various methods of recrystallization of the crude residue - none of these attempts yielded the desired product **141**.

B.38 Preparation of 5'-*O*-(*tert*-butyldiphenylsilyl)adenosine [142]



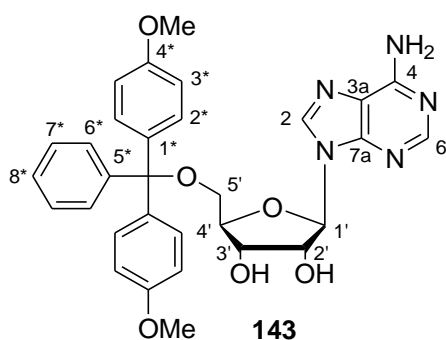
A Schlenk tube was filled with a 5 % trimethylsilyl chloride : hexane (*v/v*) solution and was stored at rt overnight in order to silylate the glassware prior to use. The Schlenk was then oven dried, placed under high vacuum and allowed to cool to rt under an argon atmosphere. The adenosine **8** (1.90 mmol, 0.509 g) and DMAP (0.01 eq, 0.025 mmol, 0.0049 g) were stirred with distilled pyridine (2.5 cm³) until a solution had formed. To this solution was then added the *tert*-butyldiphenylsilyl chloride (1.1 eq, 2.1 mmol, 0.55 cm³) and the reaction mixture was stirred at rt under an argon atmosphere overnight (19 h). After this time, tlc showed no further change so the reaction mixture was transferred to a separating funnel using CH₂Cl₂ (20 cm³). The organic layer was extracted with a saturated NaHCO₃ solution (2 × 20 cm³), which was then followed by extraction with brine (20 cm³). The organic layer was dried over anhydrous

Na₂SO₄, filtered and the solvent was removed *in vacuo* to yield the crude product as a white foam. The crude sample was purified by column chromatography, using the pre-prepared/basified silica and 10 % EtOH : CH₂Cl₂ as the eluant. The desired compound **142** was obtained pure as a white foam (0.703 g, 73 %).

$R_f = 0.44$ (10 % EtOH : CH₂Cl₂); $[\alpha]_D^{19} -4.2857^\circ$ ($c = 2.10$ in DMF); $\nu_{\max}/\text{cm}^{-1}$ (thin film) 626 (Si-O), 670 and 780 (5 adjacent aromatic H), 1109 (C-O stretch), 1216 (O-H bend), 1423 (CH₂), 1522 (Ar H), 1651 (NH₂), 3021 (Ar H), 3651 (NH₂), 3675 (free OH); δ_H (300 MHz, **1** : **1** CDCl₃ : *d*₆-DMSO) 0.99 [9 H, s, C(CH₃)₃], 3.78 and 3.93 (2 H, two dd, $J = 3.91$ and 11.30 Hz, H-5'), 4.03-4.07 (1 H, m, H-4'), 4.34-4.36 (1 H, m, H-3'), 4.59-4.61 (1 H, m, H-2'), 5.07 (1 H, d, $J = 5.40$ Hz, OH-3'), 5.45 (1 H, d, $J = 5.63$ Hz, OH-2'), 5.95 (1 H, d, $J = 4.88$ Hz, H-1'), 7.30-7.38 (6 H, m, H-3* and H-4*), 7.59 (4 H, dd, $J = 1.44$ and 7.85 Hz, H-2*), 8.08 (1 H, s, H-2[#]), 8.11 (1 H, s, H-6[#]); δ_C (50 MHz, **1** : **1** CDCl₃ : *d*₆-DMSO) 18.68 [C(CH₃)₃], 26.44 [C(CH₃)₃], 63.52 (C-5'), 69.72 (C-3'), 73.48 (C-2'), 84.11 (C-4'), 87.48 (C-1'), 119.12 (C-3a), 127.41 (C-3*), 129.39 (C-4*), 132.40 (C-1*), 134.82 (C-2*), 138.51 (C-2), 149.19 (C-7a), 152.32 (C-6), 155.83 (C-4); **MS** m/z ($M + 1^+$, 100 %) 136.00 (55), 237.93 (2), **HRMS** (+cESI) calculated for C₂₆H₃₂N₅O₄Si⁺: 506.22181, found: $[M + 1]^+$ 506.22098.

Note: assignments denoted with [#] are interchangeable

B.39 Attempted synthesis of 5'-O-(4,4'-dimethoxytrityl)adenosine [143]

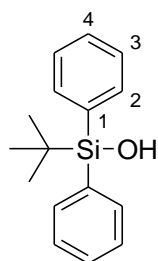


The adenosine **8** (3.81 mmol, 1.02 g) and DMAP (0.1 eq, 0.381 mmol, 0.0469 g) were stirred with distilled pyridine (10 cm³) until a solution had formed. The solution was heated to 60 °C before the addition of the 4,4'-dimethoxytrityl chloride (1.2 eq, 4.57 mmol, 1.55 g). The reaction mixture was then allowed to stir at 60 °C under an argon atmosphere overnight (20 h). After

this time, the reaction mixture was transferred to a round-bottomed flask using EtOH (10 cm³) and the solvent was removed *in vacuo*. The crude compound was then purified by column chromatography with the pre-prepared/basified silica and 10 % EtOH : CH₂Cl₂ as the eluant.

The desired fractions were combined to yield a cream foam, that contained a mixture of the desired product and a triethylamine salt. We attempted further purification to remove the triethylamine contaminant by crystallization of the contaminant (as the desired compound did not appear to be crystalline). The cream foam mixture obtained from the column was dissolved in MeOH (6 cm³) with gentle heating. This solution was then added dropwise to vigorously stirring Et₂O (60 cm³) and a white precipitate was observed. This was then cooled in an ice-water bath to allow for complete crystallization and the solid precipitate was filtered off through a sintered funnel. NMR spectroscopy confirmed that the white crystalline material obtained by this method was the triethylamine salt. The solvent was removed from the mother liquor *in vacuo* and a cream foam was obtained. NMR spectroscopy again confirmed the presence of the desired product, but it was still contaminated with the triethylamine salt. The recrystallization procedure was repeated, unfortunately the desired compound **143** was always obtained contaminated with the triethylamine salt.

B.40 Preparation of *tert*-butyldiphenylsilanol [**145**]



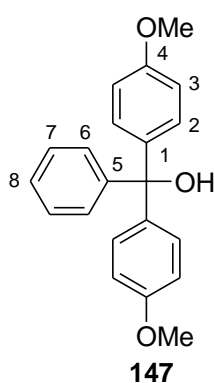
145

A solution was prepared of *tert*-butyldiphenylsilyl chloride **144** (7.33 mmol, 2.01 g) in Et₂O (6 cm³). To this solution was then added portionwise a solution of KOH (1.1 eq, 8.06 mmol, 0.497 g) in a mixture of H₂O : MeOH (1 cm³ : 4 cm³). The reaction mixture warmed up on addition and a white precipitate was immediately observed. The reaction mixture was then allowed to stir at rt overnight (24 h). After this time, the reaction mixture was transferred to a separating funnel and the Et₂O layer was removed. The aqueous layer was then extracted with further portions of Et₂O (3 × 10 cm³). All the organic fractions were combined, dried over anhydrous MgSO₄, filtered and the solvent was removed *in vacuo*. The desired compound **145** was obtained pure as a colourless opaque oil (1.72 g, 92 %). The experimental procedure was modified from, and data obtained correlated well to that reported Mullen and Barany.⁵⁰

$\nu_{\text{max}}/\text{cm}^{-1}$ (**thin film**) 700 and 764 (5 adjacent aromatic H), 821 (Si-C), 938 and 1029 (Si-O), 1084 (C-O stretch from C-OH), 1261 (Si-C), 1331 (O-H bending), 1391 (CH₃ symmetrical

deformations), 1589 (aromatic ring), 2857 (C-H stretch from CH₃), 3015 (Ar H), 3071 (-OH); δ_{H} (300 MHz, CDCl₃) 1.06 [9 H, s, C(CH₃)₃], 3.53 (1 H, br s, OH), 7.37-7.41 (6 H, m, H-3* and H-4*), 7.67-7.72 (4 H, m, H-2*); δ_{C} (50 MHz, CDCl₃) 19.22 [C(CH₃)₃], 26.77 [C(CH₃)₃], 127.92 (C-3*), 129.85 (C-4*), 135.02 (C-2*), 135.73 (C-1*); MS *m/z* (M + 23⁺, 55 %) 269.12 (39), 462.01 (67), 485.21 (30), 536.14 (54), 559.24 (49), 560.30 (27), 633.26 (48), 663.45 (100), 664.45 (50), HRMS (+cESI) calculated for C₁₆H₂₀OSi: 256.12834, HRMS not determined.

B.41 Preparation of 4,4'-dimethoxytrityl alcohol [147]

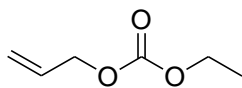


To the 4,4'-dimethoxytrityl chloride **146** (5.00 mmol, 1.70 g) was added a solution of THF : 0.5 M aqueous NaOH (10 cm³ THF : 10 cm³ NaOH) and the reaction mixture was then allowed to stir at rt for 30 min. After this time, the reaction mixture was extracted with CH₂Cl₂ (40 cm³). The organic layer was then dried over anhydrous Na₂SO₄, filtered and the solvent was removed *in vacuo*. The crude oil was purified by column chromatography using 10 % MeOH : CH₂Cl₂ for elution. The desired compound **147** was obtained as a yellow-orange semi-solid after column

chromatography (1.40 g, 87 %). Spectroscopic data obtained for the compound was found to correlate well to that reported by Bleasdale *et.al.*⁵¹ for the similar procedure.

R_f = 0.86 (10 % MeOH : CH₂Cl₂); $\nu_{\text{max}}/\text{cm}^{-1}$ (thin film) 702 and 753 (5 adjacent aromatic H), 849 (2 adjacent aromatic H), 1115 (C-O stretch from C-OH), 1360 (O-H bending), 1507, 1581 and 1608 (aromatic ring), 2838 (-OCH₃), 3070 (Ar H), 3504 (O-H stretching); δ_{H} (300 MHz, CDCl₃) 2.76 (1 H, br s, OH), 3.79 (6 H, s, 2 × OCH₃), 6.82 (4 H, d, J = 8.74 Hz, H-3*), 7.16 (4 H, d, J = 8.75 Hz, H-2*), 7.25-7.29 (5 H, m, H-6*, H-7* and H-8*); δ_{C} (50 MHz, CDCl₃) 55.44 (2 × OCH₃), 81.62 [C(Ar)₃], 113.35 (C-3*), 127.27 (C-8*), 127.96 (C-6*[#]), 128.04 (C-7*[#]), 129.33 (C-2*), 139.65 (C-1*), 147.52 (C-5*), 158.80 (C-4*); MS *m/z* (M + 23⁺, 7 %) 303.23 (100), 304.26 (22), HRMS (+cESI) calculated for C₂₁H₂₀O₃: 320.14124, HRMS not determined.

Note: assignments denoted with [#] are interchangeable.

B.42 Preparation of allyl ethyl carbonate [148]**148**Method 1:

The allyl alcohol (73.5 mmol, 5.00 cm³) was dissolved in distilled CH₂Cl₂ (50 cm³) and the solution was cooled to 0 °C in an ice-water bath. Then NEt₃ (1 eq, 73.5 mmol, 10.3 cm³) was added and the solution was stirred for 5 min. After this time, ethyl chloroformate (1 eq, 73.5 mmol, 7.0 cm³) was added dropwise and the reaction mixture was stirred at 0 °C for 15 min. Then Et₂O (100 cm³) was added and the reaction mixture was stirred for a further 30 min. During this time a very thick white precipitate formed (assumed to be the by-product, a triethylamine hydrochloride salt) and the solid was then filtered off through a celite plug. The solid precipitate was washed with a further portion of cold Et₂O (50 cm³) and the mother liquor solvent was removed by evaporation. The crude mixture was then purified by distillation at atmospheric pressure under an argon atmosphere. The pure product **148** was obtained as a clear oil after distillation (2.79 g, 29 %).

Method 2:

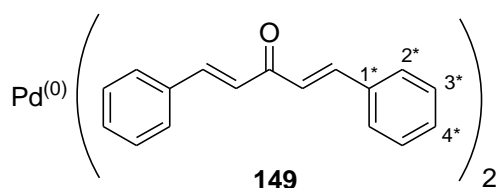
The allyl alcohol (200 mmol, 13.6 cm³) was dissolved in distilled pyridine (50 cm³). The solution was then cooled to 0 °C before the dropwise addition of ethyl chloroformate (1.1 eq, 220 mmol, 21 cm³). A white gas was immediately liberated from the reaction mixture and by the end of the addition a white precipitate was observed as well. After the addition the reaction mixture was warmed to rt and stirred overnight (20 h). The reaction mixture was then poured into a beaker containing crushed ice (100 cm³) and 2 M HCl (100 cm³). Further portions of the 2 M HCl (400 cm³ in total) were added until the pH was at 6. The mixture was then stirred until all the ice had melted and it was then extracted with CH₂Cl₂ (3 × 200 cm³). The combined organics were then extracted with distilled H₂O (200 cm³). The combined organics were dried over anhydrous Na₂SO₄, filtered and evaporated. The crude mixture was purified by distillation at atmospheric pressure, under an argon atmosphere. The pure product **148** was obtained as a clear oil which boiled at 139 °C (2.38 g, 9 %), mixed fractions were also obtained but were not re-distilled.

$R_f = 0.75$ (30 % EtOAc : hexane); $\nu_{\max}/\text{cm}^{-1}$ (thin film) 740 (CH_2 rocking), 933 ($\text{RCH}=\text{CH}_2$), 1216 (C-O), 1378 (O-CO-O), 1455 (C-H deformations from CH_2 and CH_3), 1651 (C=C), 3021 (C-H stretching or $\text{C}=\text{CH}_2$); δ_{H} (300 MHz, CDCl_3) 1.32 (3 H, t, $J = 7.14$ Hz, OCH_2CH_3), 4.21 (2 H, q, $J = 7.12$ and 7.13 Hz, OCH_2CH_3), 4.62 (2 H, dt, $J = 1.32$ and 5.76 Hz, $\text{OCH}_2\text{CH}=\text{CH}_2$), 5.31 (2 H, dddd, $J = 1.30, 2.65, 10.42$ and 13.97 Hz, $\text{CH}=\text{CH}_2$), 5.93 (1 H, ddd, $J = 7.56, 8.55$ and 10.43 Hz, $\text{CH}=\text{CH}_2$); δ_{C} (50 MHz, CDCl_3) 14.43 (CH_3), 64.20 (OCH_2CH_3), 68.43 ($\text{OCH}_2\text{CH}=\text{CH}_2$), 118.93 ($\text{CH}=\text{CH}_2$), 131.85 ($\text{CH}=\text{CH}_2$), 155.16 (C=O); MS m/z (M^+ , 0.85%) 41.03 (23), 72.08 (10), 100.11 (100), 115.07 (5), 127.04 (6), 173.08 (13), 199.04 (8), 287.11 (5), HRMS (+cESI) calculated for $\text{C}_6\text{H}_{10}\text{O}_3$: 130.06299, found: $[\text{M}]^+$ 130.11864.

Data obtained correlated well to that reported by Cravatta *et.al.*^{B1}

B.43 Preparation of bis(dibenzylideneacetone) palladium(0) [149]

The dibenzylidene acetone stock (20.07 g) was purified by column chromatography using 10-20 % EtOAc : hexane for elution. After chromatography and drying under high vacuum, the pure product was obtained as bright yellow crystals (9.24 g).



Based on the procedure described by Schlosser,^{B2} a solution of dibenzylidene acetone (3.3 eq, 19.6 mmol, 4.60 g) and sodium acetate (8 eq, 47.6 mmol, 3.90 g) was prepared in hot MeOH (150 cm^3). To this solution was then added palladium chloride (5.93 mmol, 1.05 g) and the reaction mixture was stirred at 40 °C, under an argon atmosphere for 4 h. After this time, the solution was allowed to cool to rt and then crystallisation was completed in an ice-water bath. The dark purple crystals were collected by filtration and subsequently washed with distilled water (150 cm^3), which was followed by distilled acetone (150 cm^3). The dark purple crystals were then dried under high vacuum and were found to be the pure compound **4.111** (3.06 g, 90 %).

m.p. 148-149 °C; $\nu_{\text{max}}/\text{cm}^{-1}$ (**thin film**) 669 and 768 (5 adjacent aromatic H), 1071 (RHC=CHR *trans*), 1216 (C-O stretch), 1541 (C=O), 1652 (C=C conjugated with C=O or C=C conjugated with aromatic ring), 3020 (Ar H); δ_{H} (**300 MHz, CDCl₃**) 7.09 (2 H, d, $J = 15.96$ Hz, CO-CH=CH-Ar), 7.40-7.42 (6 H, m, H-3* and H-4*), 7.61-7.64 (4 H, m, H-2*), 7.74 (2 H, d, $J = 15.96$ Hz, CO-CH=CH-Ar); δ_{C} (**50 MHz, CDCl₃**) 125.65 (CO-CH=CH-Ar), 128.61 (C-2*), 129.02 (C-3*), 130.71 (C-4*), 135.03 (C-1*), 143.53 (CO-CH=CH-Ar), 189.13 (C=O).

Appendix C:
Experimental Procedures – Relating to Chapter 3

C.1 Growth and Purification of Bacteria from Freezer Stocks

The freezer stocks for *S. aureus* strain ATCC 25923, *B. cereus* strain DL5 and *P. aeruginosa* strain ATCC 27853 were defrosted by warming in hands and then standing at room temperature until they had completely thawed. The Eppendorff tubes were then gently inverted to mix the contents. We then aliquoted the entire 1000 μL into the pre-prepared conical flask containing 100 cm^3 nutrient broth (prepared according to manufacturer's instructions and autoclaved at 1 atm /121 $^{\circ}\text{C}$ for 20 min). The cultures were then incubated at 37 $^{\circ}\text{C}$ with shaking (100 rpm) overnight.

After this time, the overnight broth cultures were used to prepare three streak plates. This is a standard microbiological method used to guarantee culture purity. The *S. aureus* and *B. cereus* were grown on standard nutrient agar plates (solution prepared according to manufacturer's instructions, autoclaved at 1 atm /121 $^{\circ}\text{C}$ for 20 min, poured and then incubated at 37 $^{\circ}\text{C}$ overnight to check for contamination), whereas the *P. aeruginosa* was grown on nutrient agar plates which had a CFC selective supplement added (the nutrient agar solution was prepared according to manufacturer's instructions, then the cefalotin sodium supplement was added, the mixture was autoclaved at 1 atm /121 $^{\circ}\text{C}$ for 20 min, poured and the plates then incubated at 37 $^{\circ}\text{C}$ overnight to check for contamination).

The streak plates were incubated at 37 $^{\circ}\text{C}$ overnight and checked for colony growth and possible contamination. Once we were satisfied that the plates were not contaminated, a single colony was removed from the plates and used to inoculate 100 cm^3 nutrient broth (prepared as described previously). The cultures were incubated at 37 $^{\circ}\text{C}$ with shaking (100 rpm) overnight. Following incubation, the overnight broth cultures were used to prepare another three streak plates on nutrient agar for each of the bacteria used (solution prepared according to manufacturer's instructions, autoclaved at 1 atm /121 $^{\circ}\text{C}$ for 20 min, poured and then incubated at 37 $^{\circ}\text{C}$ overnight to check for contamination), as well as new freezer stocks (described in **Section C.3**).

The plates were incubated at 37 °C overnight and checked for contamination. If satisfactory, the plates were then sealed with Parafilm, placed inside polyethylene bags and stored at 4 °C until required. The plates were subcultured every 21 days when in active use and were prepared fresh from new freezer stocks when long periods of time elapsed between the assays being performed.



Figure C.1 Examples of the types of streak plates obtained after overnight incubation, showing *S. aureus* strain ATCC 25923 (left) and *E. coli* strain 25922 (right)

C.2 Growth and Purification of Bacteria from Freeze-Dried Swabs (as delivered by ATCC)

The freeze-dried “stick” containing *E. coli* strain ATCC 25922 was opened aseptically and rehydrated with 1000 µL of pre-prepared nutrient broth. This mixture was then transferred to a conical flask containing 100 cm³ nutrient broth (prepared according to manufacturer's instructions and autoclaved at 1 atm /121 °C for 20 min). The culture was incubated at 37 °C with shaking (100 rpm) overnight.

After this time, the overnight broth cultures were used to prepare three streak plates for *E. coli*, on either TBX agar plates (Oxoid, contains: tryptone, bile salts, agar and X-glu) or

selective RAPID' *E. coli* 2 agar plates (both sets of plates were prepared according to the manufacturer's instructions, autoclaved at 1 atm /121 °C for 20 min, poured and then incubated at 37 °C overnight to check for contamination). The streak plates were then incubated at 37 °C overnight and checked for growth and possible contamination. Once we were satisfied that the plates were not contaminated, a single colony (blue/purple) was removed from the plates and used to inoculate 100 cm³ nutrient broth (prepared as described previously). The culture was incubated at 37 °C with shaking (100 rpm) overnight.

Following incubation, the overnight broth culture was used to prepare another three streak plates for *E. coli* on nutrient agar (solution prepared according to manufacturer's instructions, autoclaved at 1 atm /121 °C for 20 min, poured and then incubated at 37 °C overnight to check for contamination) as well as new freezer stocks (described in **Section C.3**). The plates were incubated at 37 °C overnight and then checked for contamination. The plates were sealed with Parafilm, placed inside polyethylene bags and stored at 4 °C until required. The plates were subcultured every 21 days when in active use and were prepared fresh from new freezer stocks when long periods of time elapsed between assays being performed.

C.3 Preparation of Freezer Stocks

We began by adding 150 µL of pre-warmed glycerol into 1000 µL Eppendorff tubes and these were then autoclaved at 1 atm /121 °C for 20 min. The overnight broth cultures prepared in **Sections C.1** and **C.2** above were used to aliquot 850 µL of the culture into the autoclaved glycerol under aseptic techniques. The Eppendorff tubes were gently inverted and shaken to mix the contents and were then sealed with Parafilm. This procedure was repeated to prepare six Eppendorff tubes for each of the four bacteria used (*S. aureus* ATCC 25923, *B. cereus* DL5, *P. aeruginosa* ATCC 27853 and *E. coli* ATCC 25922). The freezer stocks were then stored at -20 °C until required.

C.4 Droplet Plate Technique

Method based on procedure described by Lindsay and von Holy.^{123c} A 0.85 % NaCl_(aq) solution was prepared and then 9 cm³ portions were transferred to test tubes. These were capped and autoclaved at 1 atm /121 °C for 20 min. One colony for each of the four bacteria used in the study (*S. aureus* ATCC 25923, *B. cereus* DL5, *P. aeruginosa* ATCC 27853 and *E. coli* ATCC 25922) was used to inoculate conical flasks containing 100 cm³ of nutrient broth (prepared according to the manufacturer's instructions). This was performed in duplicate and the cultures were then incubated at 37 °C with shaking (150 rpm) for exactly 18 hours.

After this time, 1000 µL of each overnight broth culture was transferred to a test tube containing 9 cm³ of 0.85 % NaCl_(aq) solution. The contents of the tube were mixed thoroughly and this tube was then used for a series of serial dilutions, the procedure is outlined in **Figure C.2**.

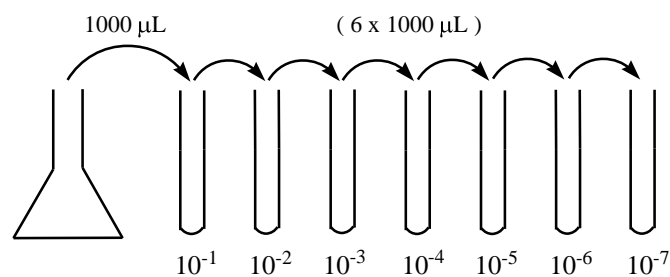


Figure C.2 Serial dilution series for the droplet plate technique

Following this, 50 µL was taken from each test tube from dilutions 10⁻² to 10⁻⁷ and were added carefully to each of the six segments of the nutrient agar plate (prepared according to the manufacturer's instructions). Once all of the drops were added, the plate was gently swirled to spread out the culture. This was performed in duplicate for each of the four bacterial strains. The approach used is shown schematically in **Figure C.3**.

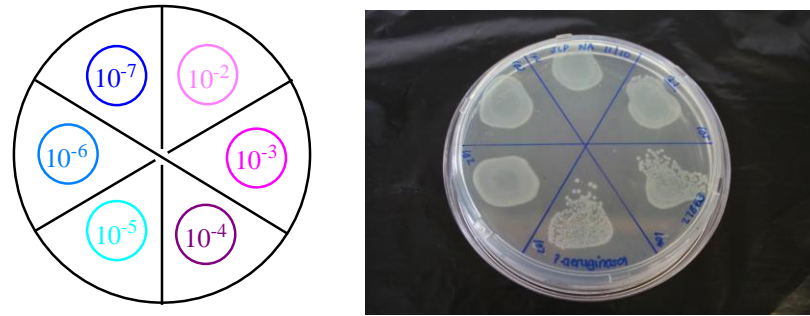


Figure C.3 Layout used for the drop plate and example of drop plate obtained for *P. aeruginosa* ATCC 27853 after overnight growth on a nutrient agar plate

The plates were then incubated at 37 °C overnight. After this time, the plates were removed from the incubator for colony counting. Unfortunately, for all four of the bacteria, at these dilutions there were either too many colonies to count or a lawn had formed.

As such, the method described above was repeated at higher dilutions. As outlined in **Figure C.4**, the serial dilutions were repeated from 10^{-1} to 10^{-10} for the overnight cultures of the four bacteria (*S. aureus* ATCC 25923, *B. cereus* DL5, *P. aeruginosa* ATCC 27853 and *E. coli* ATCC 25922).

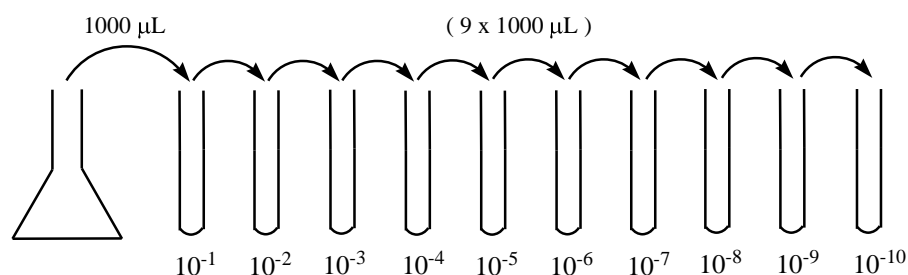


Figure C.4 Serial dilution series for the droplet plate technique

As before, 50 μL was taken from each test tube from dilutions 10^{-5} to 10^{-10} and were added carefully to each of the six segments of the nutrient agar plate (prepared according to the manufacturer's instructions). Once all of the drops were added, the plate was gently swirled to spread out the culture. This was performed in duplicate for each of the four bacterial strains. The approach used is shown schematically in **Figure C.5**.

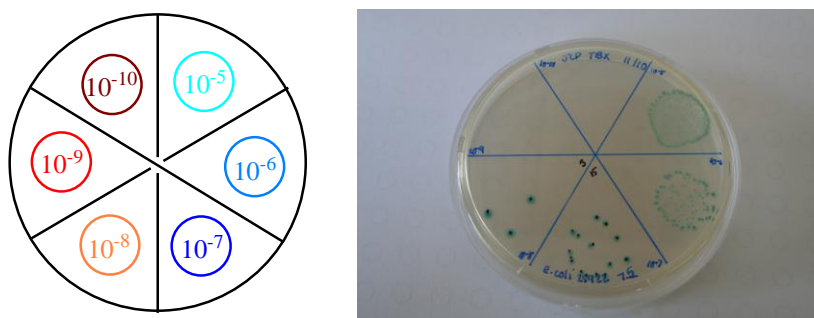


Figure C.5 Layout used for the drop plate and example of drop plate obtained for *E. coli* ATCC 25922 (blue/green colonies) after overnight growth on a TBX plate

The plates were then incubated at 37 $^{\circ}\text{C}$ overnight. After this time, the plates were removed from the incubator for colony counting. This time, the dilutions were in the correct range and we were able to count the number of colonies that had formed on the plates. These values were then used to determine the average viable count for the four bacterial strains.

For *S. aureus* strain ATCC 25923 the plates were prepared in duplicate. We counted 46 colonies in the 10^{-6} dilution range and 5 colonies in the 10^{-7} dilution range on the first plate. On the second plate we counted 25 colonies in the 10^{-6} dilution and 3 colonies in the 10^{-7} dilution. This gave us four replicates for the data set.

The plate preparation was repeated on a separate day in order to have more accurate and reproducible results. The plates for *S. aureus* strain ATCC 25923 were again prepared in duplicate. This time, we counted 40 colonies in the 10^{-6} dilution and 5 colonies in the 10^{-7}

dilution on the first plate, and 28 colonies in the 10^{-6} dilution and 3 colonies in the 10^{-7} dilution on the second plate. This repetition gave four replicates for the data set.

The data from the two days were combined in order to obtain an average for the eight replicates present in the complete data set. The calculation for cfu/mL and log cfu/mL is shown below.

$$\begin{aligned} \text{cfu/mL} &= \{ [(46 + 50 + 25 + 30 + 40 + 50 + 28 + 30) / 8] \times 10^6 \} \times 20 \\ &= 747\,500\,000 \end{aligned}$$

and

$$\begin{aligned} \log \text{ cfu/mL} &= \log 747\,500\,000 \\ &= 8.87 \end{aligned}$$

The same procedure was used for the determination of cfu/mL and log cfu/mL for the other bacterial strains. From our calculations, we obtained:

- *B. cereus* DL5
 - cfu/mL = 1 432 500 000
 - log cfu/mL = 9.16

- *P. aeruginosa* ATCC 27853
 - cfu/mL = 1 536 666 667
 - log cfu/mL = 9.19

- *E. coli* ATCC 25922
 - cfu/mL = 3 375 000 000
 - log cfu/mL = 9.53

C.5 Determination of Antibacterial Activity through the use of the Triphenyl Tetrazolium Chloride (TTC) Assay

C.5.1 Preparation of Antibiotic/Compound Stock Solutions

Ciprofloxacin is a commercially marketed broad-spectrum antibiotic and was chosen as our positive control for the TTC assay. We purchased our ciprofloxacin from Sigma-Aldrich, under license of Fluka (code: 17850). Information obtained from the supplier indicated a potency of 85 % (ie: 850 $\mu\text{g}/\text{mg}$) for the sample.

The mass required to make a 10 000 mg/L stock solution was calculated from the equation:

$$(1000 / P) \times V \times C = W$$

where: P = potency ($\mu\text{g}/\text{mg}$)

V = volume (mL)

C = final concentration in multiples of 1000 (mg/L)

W = mass of antibiotic (mg)

From the calculation, we determined that 117.65 mg of ciprofloxacin was required to prepare the 10 000 mg/L stock solution. For all of the synthetic compounds we used 100 mg of material (either solid foam, powder or oil) that was determined on a balance, no densities were used, for the preparation of the 10 000 mg/L stock solutions.

The accurately weighed material was dissolved in molecular grade DMSO (99.99 % purity), this solution was added to a test tube containing 9 cm³ autoclaved de-ionised water and mixed by vortex (occasionally, gentle heating was required to maintain the solution). The 10 000 mg/L stock solution was then used in serial dilutions to prepare the 1 000 mg/L, 100 mg/L, 10 mg/L and 1 mg/L stock solutions. The procedure is outlined in **Figure C.6**.

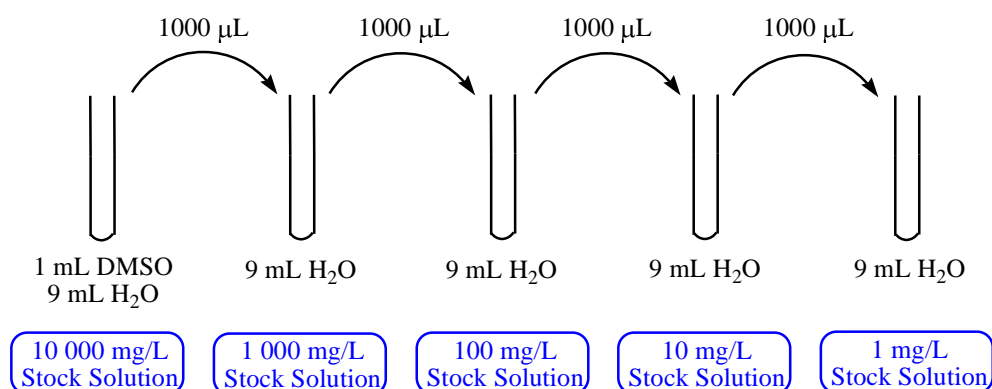


Figure C.6 Serial dilution series - preparation of the antibiotic/ compound stock solutions

The stock solutions were prepared fresh, and used immediately for the preparation of the antibiotic and compound dilutions as described in detail in **Section C.5.2**.

C.5.2 Preparation of Antibiotic/Compound Dilution Series

The antibiotic and synthetic compound dilution series were prepared from the stock solutions using nutrient broth (prepared according to the manufacturer's specifications and autoclaved at 1 atm /121 °C for 20 min) as the solvent. The test tubes were prepared prior to use, with each one containing 10 mL nutrient broth.

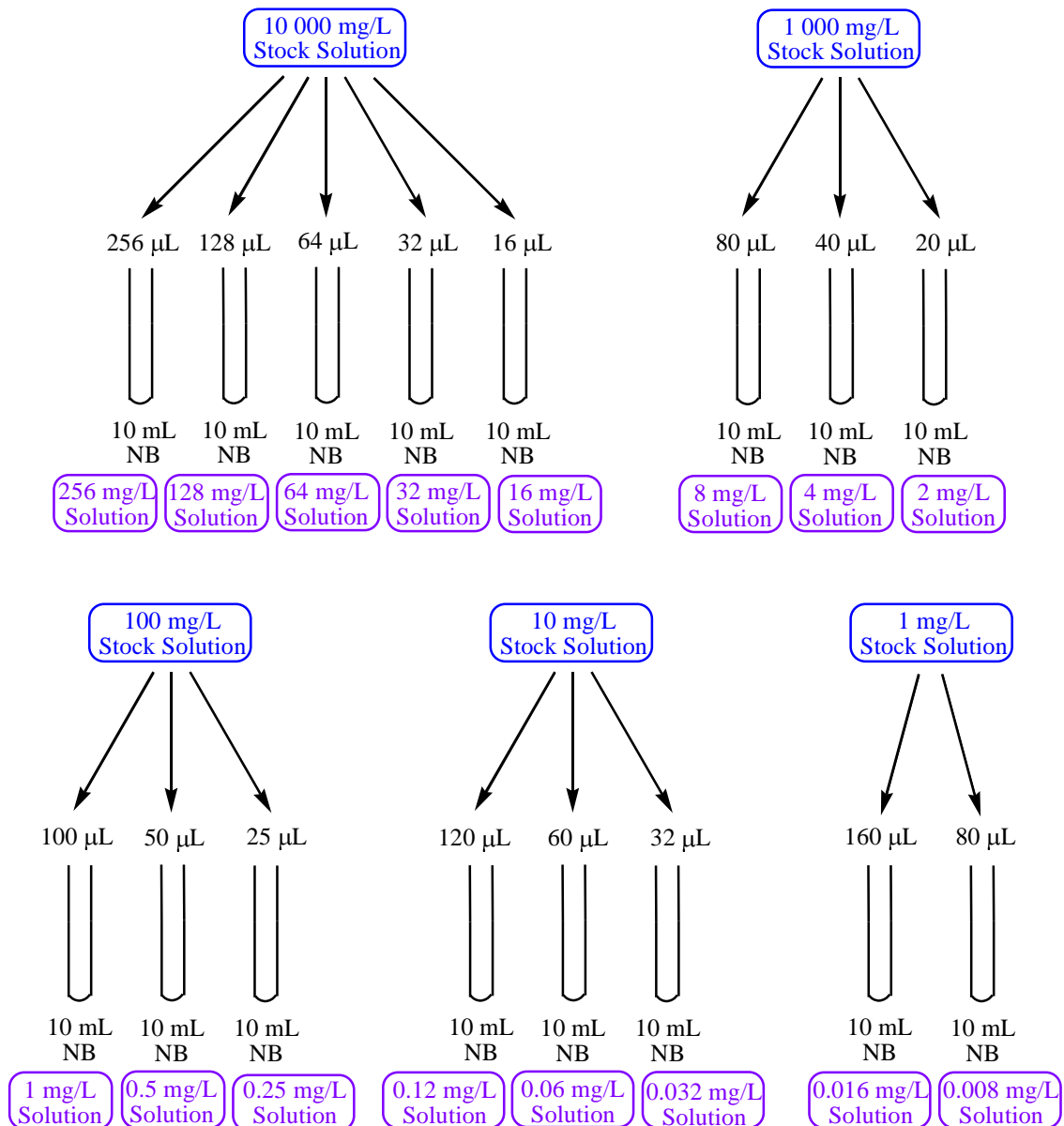


Figure C.7 Preparation of antibiotic/compound dilution range

The dilution series used ranges from 256 mg/L to 0.008 mg/L. The procedure used was based on that used by J.M. Andrews⁵⁸ is shown in detail in **Figure C.7**.

The solutions were in general prepared 1-3 days prior to use in the TTC assay and as such the test tubes were sealed with Parafilm before being stored at 4 °C. They were allowed to warm

to room temperature and were mixed prior to use (on the rare occasion that a precipitate formed that would not re-solubilise at room temperature, the precipitate was solubilised with gentle heating).

In order to ensure that there had been no decomposition of the compounds in the process of cooling and warming, each time a set of synthetic compound dilutions were prepared, a corresponding set of ciprofloxacin stock solutions were also prepared. These were then used as a control for the determination of antibiotic activity. This was done using a nutrient agar plate, adding 100 μL of the inoculum prepared in Section F.5.3 below and then preparing a spread plate. The surface of the plate was then allowed to dry and 20 μL of the ciprofloxacin control dilution was added as a drop to the centre of the plate. The test plates were then incubated at 37 $^{\circ}\text{C}$ overnight. Examples of the plates obtained are outlined below in **Figure C.8**.

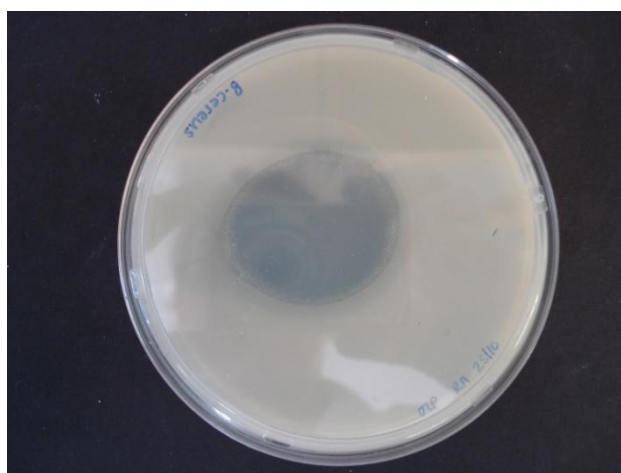


Figure C.8 The ciprofloxacin control dilution is active so one sees a bacterial lawn, with a circle of inhibition where the antibiotic was added. This is based on the standard microbiological procedure of the spot-on-lawn assay described by Piddock.^{C1}

C.5.3 Preparation of Inoculum

One colony was removed from each of the streak plates that were previously prepared on nutrient agar plates and stored at 4 °C, as described in **Section C.1** and **Section C.2**. This colony was then used to inoculate 100 cm³ nutrient broth (prepared according to the manufacturer's specifications and autoclaved at 1 atm /121 °C for 20 min). This process was repeated for each of the bacterial strains used in the study, namely the *S. aureus* strain ATCC 25923, *B. cereus* strain DL5, *P. aeruginosa* strain ATCC 27853 and *E. coli* strain ATCC 25922. All of the flasks were then incubated at 37 °C with shaking (150 rpm) for exactly 18 hours.

A final inoculum of 10⁵ cfu/mL (5 log cfu/mL) was required for the assay, as described by J.M. Andrews.⁵⁸ Thus, the 18 hour bacterial cultures were diluted to 10⁶ cfu/mL based on the average viable count determined using the droplet plate technique described in **Section C.4**. With a further dilution on the 96-wells plates. The dilution procedure is outlined in **Figure C.9**.

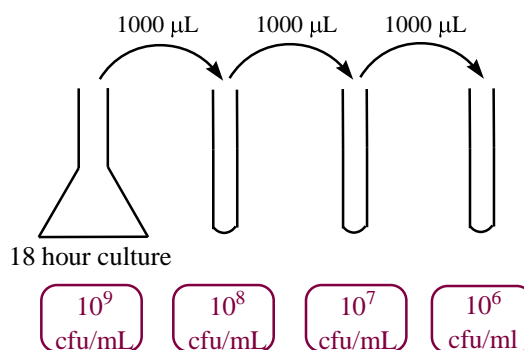


Figure C.9 Dilution series for 18 hour bacterial cultures

C.5.4 TTC Assay

The antibiotic/compound dilution series prepared in **Section C.5.2** above was added in 100 μL portions to each well of the 96-well plates (NUNC, 96-well flat-bottomed polystyrene plates with lids, certified sterile). Immediately after preparation, the solutions containing 10^6 cfu/mL cells for each of the four bacteria, *S. aureus*, *B. cereus*, *P. aeruginosa* and *E. coli*, were added in 100 μL portions to each well of the 96-well plates.

Included on each of the plates were a series of controls: (i) the 0 % growth control (200 μL of nutrient broth), (ii) the 100 % growth control (100 μL of nutrient broth and 100 μL of the desired bacterial strain at 10^6 cfu/mL), (iii) the DMSO controls (100 μL of the DMSO control and 100 μL of the desired bacterial strain at 10^6 cfu/mL) and (iv) the sterility control (200 μL of autoclaved de-ionised water).

The layout of the 96-well plates used for all compounds tested with the TTC assay is illustrated in **Figure C.10** and **Figure C.11**. We were able to test one compound/antibiotic against all four bacterial strains and obtain four replicates for each compound concentration/bacterial strain combination by working across four 96-well plates.

RUN 1 (PLATE 1) / RUN 2 (PLATE 1)

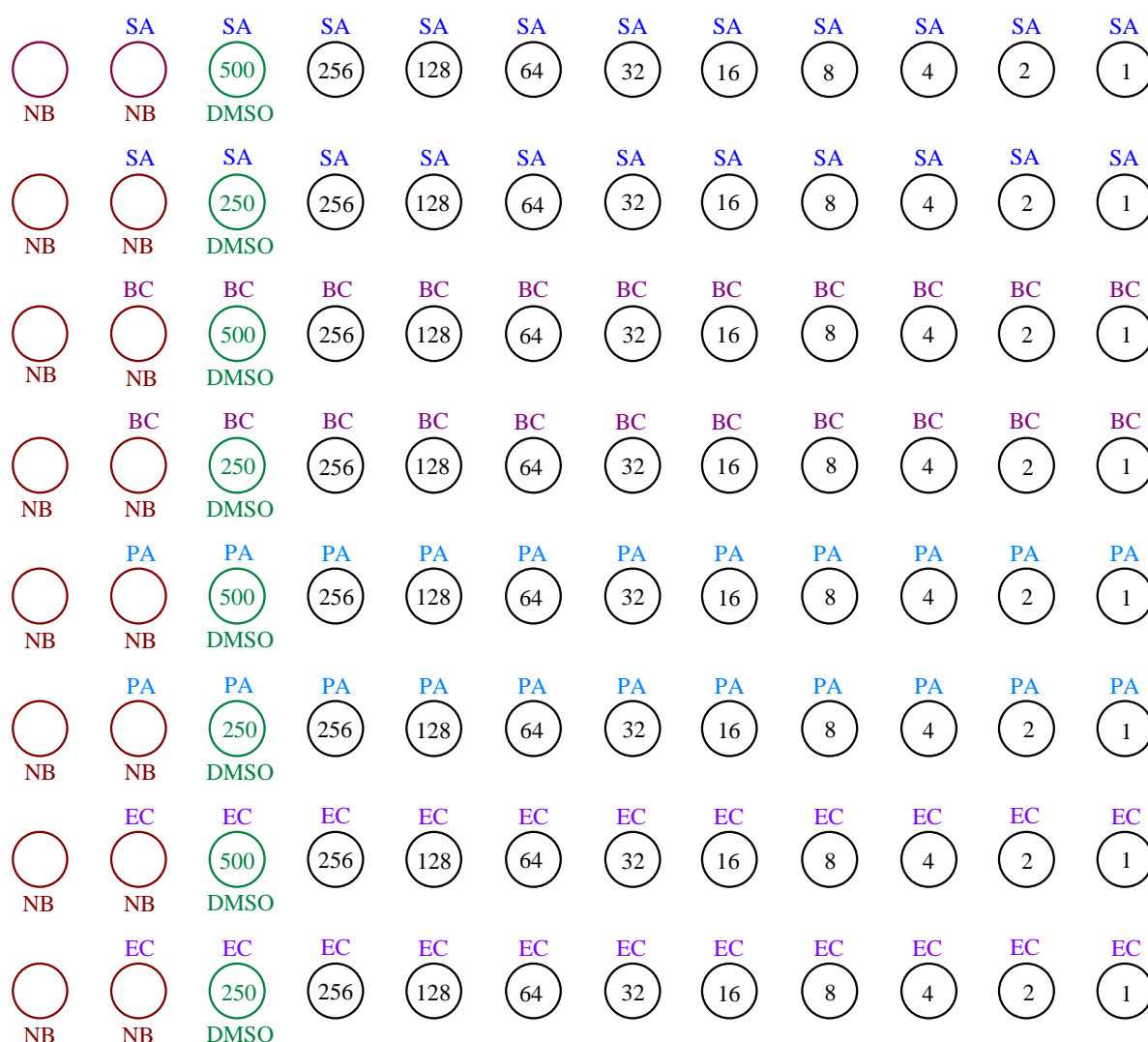


Figure C.10 Layout of 96-well plates for TTC assay

(Code: NB = nutrient broth, SA = *S. aureus* strain ATCC 25923, BC = *B. cereus* strain DL5, PA = *P. aeruginosa* strain ATCC 27853, EC = *E. coli* strain ATCC 25922 and the numbers represented in the wells indicate the antibiotic/compound dilution concentration in mg/L added to the plate)

RUN 1 (PLATE 2) / RUN 2 (PLATE 2)

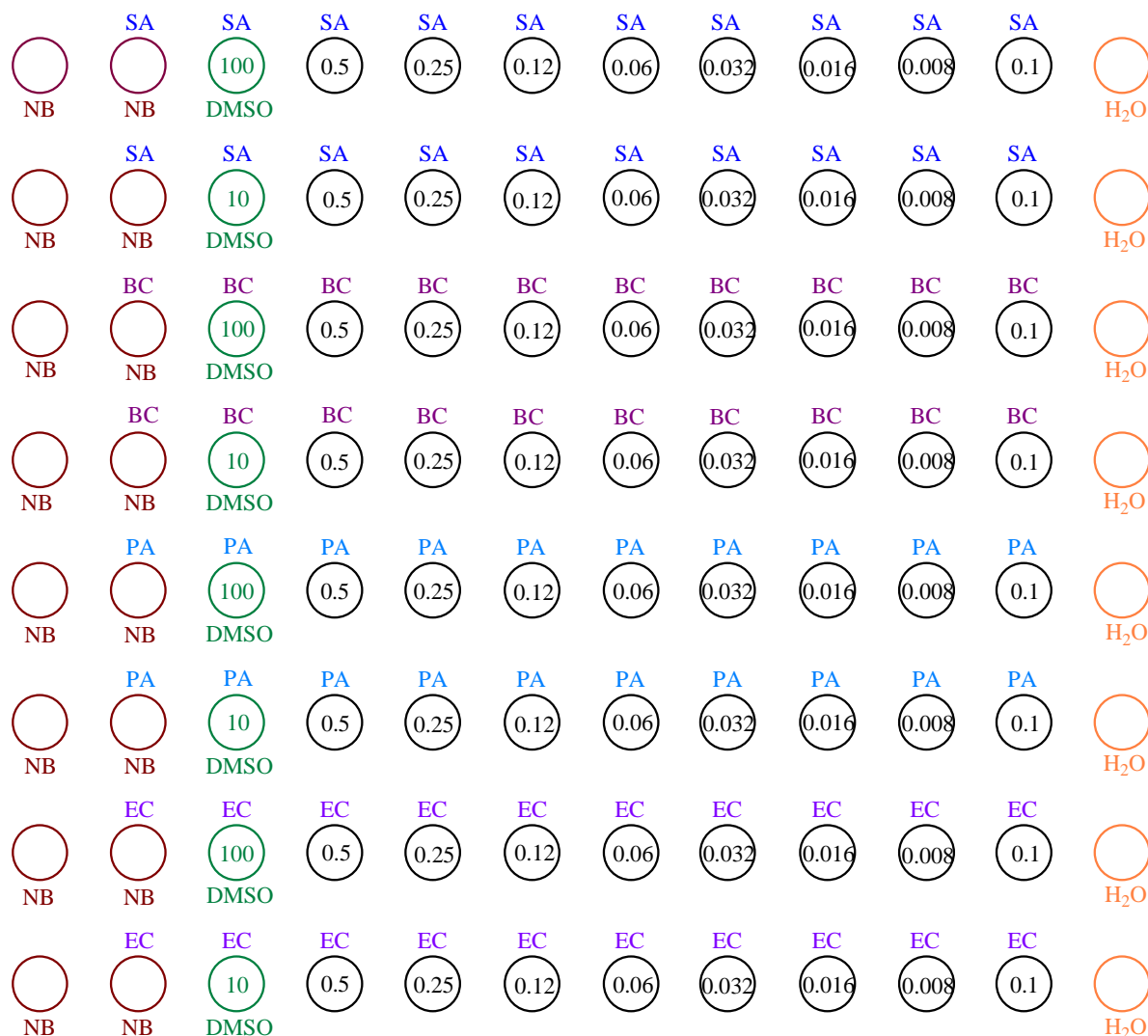


Figure C.11 Layout of 96-well plates for TTC assay

(Code: NB = nutrient broth, SA = *S. aureus* strain ATCC 25923, BC = *B. cereus* strain DL5, PA = *P. aeruginosa* strain ATCC 27853, EC = *E. coli* strain ATCC 25922 and the numbers represented in the wells indicate the antibiotic/compound dilution concentration in mg/L added to the plate)

Once the bacterial strains had been added to the 96-well plates, they were incubated at 37 °C for 22 hours. Following this time period, the plates were removed from the incubator. To each well of the plates was then added 10 µL of a freshly prepared solution of 5 mg/mL 2,3,5-triphenyltetrazolium chloride in phosphate buffered saline (PBS autoclaved prior to use in the solution). The plates were then incubated for a further 4 hours at 37 °C.

After this time, solubilisation of the formazan precipitate was conducted by the addition of the following reagents to each well of the 96-well plates:

- 10 µL of 3N HCl_(aq)
- 10 µL of 10 % NP-40_(aq)
- 25 µL of modified Weaver Reagent (66 % paraffin oil : 33 % CCl₄ : 1 % NP-40 (v/v))

The plates were then incubated at 4 °C for a further 20 hours. After incubation, the plates were analyzed on an Elisa plate reader (Titertek Multiskan[®] PLUS), at both 450 nm and 590 nm. From our pilot study, we found that the data obtained at wavelength 450 nm was in the correct absorption spectrum and gave considerably less variance than data obtained at 590 nm. Therefore, the data obtained at 450 nm was used for all subsequent assays performed.

Note: Digital photographs were taken for each of the plates after they had been scanned on the Elisa plate reader. This supplemental information is available on the attached DVD, under *Supporting Information for Biological Testing (Part 1)*.

C.6 Antiviral Assays

The percentage protection was determined using the recorded absorbance values obtained from reading the plates on the Tecan Sunrise ELISA plate reader. The equations outlining how the percentage protection was determined are based on those published by Cos and co-workers⁶⁴ and are described in detail below.

C.6.1 Formula for Percentage of Uninfected Treated Cells

$$\% \text{ of Uninfected Treated Cells} = (Y / A) \times 100$$

where: A = the optical density reading for uninfected and untreated cells (100 %)

Y = the optical density readings at varying concentrations

C.6.2 Formula for the Percentage Protection

$$\% \text{ Protection} = [(X - B) / (A - B)] \times 100$$

where: A = the optical density reading for the control untreated and uninfected cells (mock-infected)

B = the optical density reading for the control untreated and HIV-infected cells

X = the optical density measured with a given concentration of the test compound in HIV-infected cells

C.6.3 Effective Concentration

EC₅₀ (50 % effective concentration) is defined as the concentration of the test compound that achieves a fifty percent protection in infected cultures according to the formula for percentage protection.

An equation based on linear extrapolation was used to determine the EC₅₀ from the values obtained in the experiment:

$$EC_{50} = V - \left\{ \left[\frac{(W - 50\%)}{(W - U)} \right] \times (V - T) \right\}$$

where: V = the concentration of the test compound that corresponds to the closest percentage *above* 50 %

T = the concentration of the test compound that corresponds to the closest percentage *below* 50 %

W = the closest percentage *above* 50 %

U = the closest percentage *below* 50 %

C.6.4 Cytotoxic Concentration

CC₅₀ (50 % cytotoxic concentration) is defined as the concentration of the test compound that reduces the absorbance of the uninfected (mock-infected) control by fifty percent.

In a similar manner to EC₅₀, the CC₅₀ will be calculated as:

$$CC_{50} = V + \left\{ \left[\frac{(W - 50\%)}{(W - U)} \right] \times (T - V) \right\}$$

where: V = the concentration of the test compound that corresponds to the closest percentage *below* 50 %

T = the concentration of the test compound that corresponds to the closest percentage *above* 50 %

W = the closest percentage *above* 50 %

U = the closest percentage *below* 50 %

C.6.5 Selectivity Index

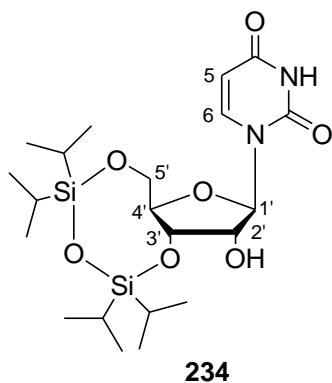
The SI (selectivity index) is defined as the ratio:

$$CC_{50} / EC_{50}$$

***APPENDICES
RELATING TO PART 2***

Appendix D:
Experimental Procedures – Relating to Chapter 5

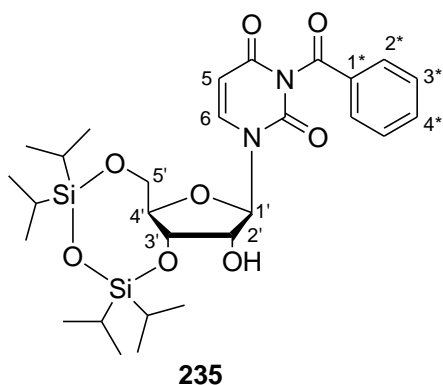
D.1 Preparation of 1-[(6*aR*,8*R*,9*R*,9*aS*)-9-hydroxy-2,2,4,4-tetraisopropyltetrahydro-6*H*-furo[3,2-*f*][1,3,5,2,4]trioxadisilocin-8-yl]pyrimidine-2,4(1*H*,3*H*)-dione [234]



A solution was prepared of uridine **12** (6.87 mmol, 1.68 g) in distilled pyridine (20.5 cm³). The solution was then cooled to 0 °C in an ice-water bath before the addition of the 1,3-dichloro-1,1,3,3-tetraisopropylidisiloxane (1.05 eq, 7.2 mmol, 2.3 cm³). The reaction mixture was then stirred at rt overnight (21 h). After this time, the reaction was quenched by the addition of distilled water (21 cm³). The mixture was then transferred to a round-bottomed flask using a small amount of EtOAc and all of the solvents were removed by evaporation (60 °C). The residue obtained was then partitioned between EtOAc (70 cm³) and distilled water (2 × 25 cm³). The organic layer was dried over anhydrous Na₂SO₄, filtered and evaporated to yield a white foam. The crude foam was then purified by column chromatography, using 10-50 % EtOAc : hexane for elution. The desired compound **234** was obtained as a white foam (2.80 g, 85 %). ¹H and ¹³C NMR spectra obtained correlated well to those reported by Matsuda and co-workers.¹²¹

$R_f = 0.13$ (30 % EtOAc : hexane); $[\alpha]_D^{20} 15.596^\circ$ ($c = 1.09$ in CH₂Cl₂); $\nu_{\max}/\text{cm}^{-1}$ (**thin film**) 693 (RCH=CHR *cis*), 1091 (C-OH, C-O stretching), 1247 (Si-CH), 1334 (-O-H, O-H bending), 1385 [-C(CH₃)₂, -CH₃ symmetrical deformation], 1461 (-CH₃, C-H deformation), 1623 (C=C conjugated with C=O), 1674 (-CONH-), 2894 (C-H, C-H stretching), 2926 (-CH₃, C-H stretching), 2965 (-O-H), 3097 (-CONH- in solution), 3410 (-CONH- in solution); δ_H (**300 MHz, CDCl₃**) 1.02-1.10 [28 H, m, 4 × CH(CH₃)₂ and 4 × CH(CH₃)₂], 3.62 (1 H, br s, OH-2'), 4.00 (1 H, dd, $J = 2.5$ and 13.2 Hz, H-5'), 4.14-4.25 (3 H, m, H-2', H-4' and H-5'), 4.32 (1 H, dd, $J = 4.7$ and 8.8 Hz, H-3'), 5.69-5.73 (1 H, m, H-5), 5.75 (1 H, s, H-1'), 7.77 (1 H, d, $J = 8.1$ Hz, H-6), 9.64 (1 H, br s, NH); δ_C (**50 MHz, CDCl₃**) 12.42, 12.88, 12.93 and 13.33 (4 × SiCH), 16.76, 16.88, 16.92, 16.99, 17.20, 17.25, 17.34 and 17.43 (8 × CH₃), 60.09 (C-5'), 68.66 (C-3'), 75.10 (C-2'), 81.83 (C-4'), 90.91 (C-1'), 101.95 (C-5), 139.87 (C-6), 150.21 (C-2), 163.53 (C-4); **MS** m/z (M⁺, 100 %) 487.8 (29), 972.5 (41), 995.6 (22), 1475.4 (16), 1477.3 (10), 1718.6 (12), **HRMS** (+cESI) calculated for C₂₁H₃₉N₂O₇Si₂⁺: 487.22903, found: [M + H]⁺ 487.22848.

D.2 Preparation of 3-benzoyl-1-[(6a*R*,8*R*,9*R*,9a*S*)-9-hydroxy-2,2,4,4-tetraisopropyl-tetrahydro-6*H*-furo[3,2-*f*][1,3,5,2,4]trioxadisilocin-8-yl]pyrimidine-2,4(1*H*,3*H*)-dione [235]

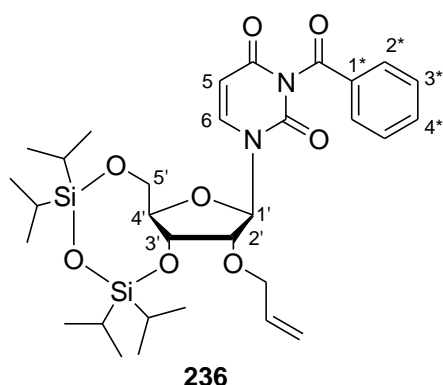


The 1-[(6a*R*,8*R*,9*R*,9a*S*)-9-hydroxy-2,2,4,4-tetraisopropyltetrahydro-6*H*-furo[3,2-*f*][1,3,5,2,4]trioxadisilocin-8-yl]pyrimidine-2,4(1*H*,3*H*)-dione **234** (12.5 mmol, 6.02 g), Na₂CO₃ (96 mmol, 10.1 g) and tetrabutylammonium bromide (0.48 mmol, 0.156 g) were dissolved in a two-phase solution of CH₂Cl₂ (240 cm³) and distilled water (480 cm³). Then the benzoyl chloride (1.3 eq, 16.2 mmol, 1.88 cm³) was added and the reaction mixture was vigorously stirred at rt for 2 h. The reaction mixture was then transferred to a separating funnel using excess CH₂Cl₂. The organic phase was collected and the aqueous phase was further extracted with CH₂Cl₂ (3 × 480 cm³). The combined organic layers were then dried over anhydrous Na₂SO₄, filtered and evaporated. The residue obtained was then dissolved in 1,2-dichloroethane (120 cm³) with gentle heating and the solution was allowed to stand at rt for 66 h. This step was performed to allow the O-/N-rearrangement to occur. After this time, the solvent was removed *in vacuo* to yield a very viscous pale-yellow oil. The crude mixture was then purified by column chromatography, with 5-50 % EtOAc : hexane used for elution. The desired compound **235** was obtained pure as a white foam (7.26 g, 99 %) after chromatography. ¹H and ¹³C NMR spectra obtained correlated well to those reported previously by Sekine.¹²²

$R_f = 0.33$ (30 % EtOAc : hexane); $[\alpha]_D^{20} 27.451^\circ$ (c = 1.02 in CH₂Cl₂); $\nu_{\max}/\text{cm}^{-1}$ (thin film) 680 (5 adjacent aromatic H), 694 (RHC=CHR *cis*), 762 (5 adjacent aromatic H), 1079 (C-OH, C-O stretching), 1236 (Si-CH), 1337 (-O-H, O-H bending), 1375 (-C(CH₃)₂, -CH₃ symmetrical deformation), 1466 (-CH₃, C-H deformation), 1628 (C=C conjugated with C=O), 1658 (-CONH-), 2867 (-C-H, C-H stretching), 2926 (-CH₃, C-H stretching), 2946 (-O-H); δ_H (300 MHz, CDCl₃) 1.03-1.10 [28 H, m, 4 × CH(CH₃)₂ and 4 × CH(CH₃)₂], 2.04 (1 H, br s, OH-2'), 4.01 (1 H, dd, $J = 2.6$ and 13.3 Hz, H-5'), 4.11-4.21 (3 H, m, H-2', H-4' and H-5'), 4.37 (1 H, dd, $J = 4.8$ and 8.6 Hz, H-3'), 5.76 (1 H, s, H-1'), 5.80 (1 H, d, $J = 8.2$ Hz, H-5),

7.50 (2 H, t, $J = 7.7$ Hz, H-3*), 7.66 (1 H, t, $J = 7.4$ Hz, H-4*), 7.81 (1 H, d, $J = 8.2$ Hz, H-6), 7.93 (2 H, d, $J = 7.2$ Hz, H-2*); δ_C (50 MHz, CDCl_3) 12.46, 12.87, 13.34 and 14.14 ($4 \times \text{SiCH}$), 16.77, 16.87, 16.91, 16.98, 17.20, 17.22, 17.30 and 17.39 ($8 \times \text{CH}_3$), 60.20 (C-5'), 68.94 (C-3'), 75.16 (C-2'), 82.07 (C-4'), 90.79 (C-1'), 101.77 (C-5), 129.11 (C-3*), 130.43 (C-2*), 131.38 (C-1*), 135.10 (C-4*), 139.57 (C-6), 148.87 (C-2), 162.08 (C-4), 168.53 (Ph-C=O); **MS** m/z (M^+ , 55 %) 478.96 (16), 607.70 (30), 1197.47 (100), 1792.17 (32), **HRMS** (+**cESI**) calculated for $\text{C}_{28}\text{H}_{43}\text{N}_2\text{O}_8\text{Si}_2^+$: 591.25525, found: $[\text{M} + \text{H}]^+$ 591.25494.

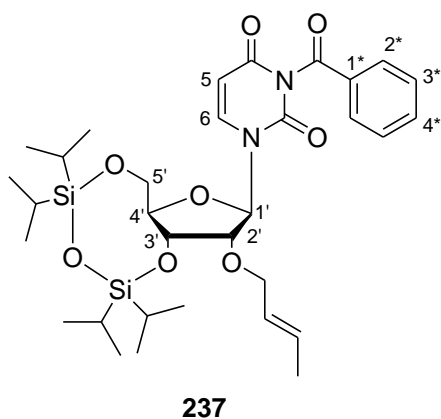
D.3 Preparation of 3-benzoyl-1-[(6*aR*,8*R*,9*R*,9*aR*)-9-allyl-9-hydroxy-2,2,4,4-tetra-isopropyltetrahydro-6*H*-furo[3,2-*f*][1,3,5,2,4]trioxadisilocin-8-yl]pyrimidine-2,4(1*H*,3*H*)-dione [236]



The 1-[(6*aR*,8*R*,9*R*,9*aS*)-9-hydroxy-2,2,4,4-tetra-isopropyltetrahydro-6*H*-furo[3,2-*f*][1,3,5,2,4]trioxadisilocin-8-yl]pyrimidine-2,4(1*H*,3*H*)-dione **235** (0.174 mmol, 0.103 g) was dissolved in freshly distilled THF (1 cm^3) and to this solution was then added sodium hydride (obtained as a 60% suspension in oil, 2.5 eq, 0.436 mmol, 0.0193 g) in distilled THF (1 cm^3). The solution was allowed to stir at rt for ~10 min, during which time the effervescence stopped and the solution went yellow in colour. Allyl bromide (2.5 eq, 0.4 mmol, 0.04 cm^3) was then added and the reaction mixture was allowed to stir under an argon atmosphere at rt overnight (23 h). After this time, the solvent was removed by evaporation and the residue obtained was dissolved in CH_2Cl_2 (20 cm^3). The solution obtained was then extracted with saturated NH_4Cl (10 cm^3) and distilled water (10 cm^3). The organic fraction was then dried over anhydrous Na_2SO_4 , filtered and the solvent was removed *in vacuo*. The crude mixture was subjected to column chromatography, with 5-50 % EtOAc : hexane solutions used for elution. The desired compound **236** was obtained after chromatography as a clear oil (0.0232 g, 21 %).

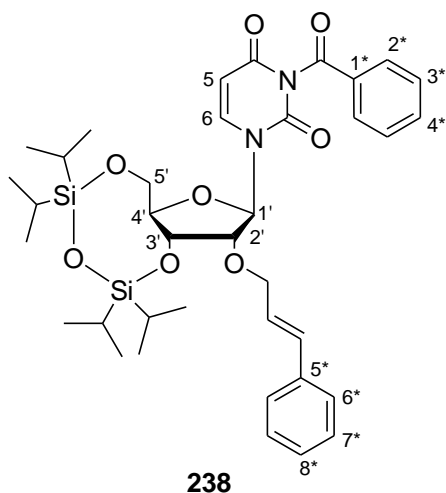
$R_f = 0.82$ (50 % EtOAc : hexane); δ_H (300 MHz, $CDCl_3$) 1.03-1.09 [28 H, m, $4 \times CH(CH_3)_2$ and $4 \times CH(CH_3)_2$], 4.01-4.35 (3 H, m, H-4' and H-5'), 4.39 (2 H, dd, $J = 1.2$ and 5.3 Hz, $CH_2CH=CH_2$), 4.52 (1 H, dd, $J = 5.0$ and 9.1 Hz, H-3'), 5.21 (1 H, dd, $J = 1.4$ and 10.5 Hz, $CH=CH_2$), 5.39 (1 H, dd, $J = 1.7$ and 17.2 Hz, $CH=CH_2$), 5.64-5.66 (1 H, m, H-2'), 5.73-5.76 (1 H, m, H-5), 5.76 and 5.97 (1 H, $2 \times$ s, H-1'), 5.81-5.95 (1 H, m, $CH=CH_2$), 7.46 (2 H, t, $J = 7.6$ Hz, H-3*), 7.59 (1 H, d, $J = 7.4$ Hz, H-4*), 7.74 (1 H, d, $J = 8.2$ Hz, H-6), 8.05-8.10 (2 H, m, H-2*); δ_C (50 MHz, $CDCl_3$) 12.86, 12.91, 13.12 and 13.41 ($4 \times$ SiCH), 16.96, 17.06, 17.24, 17.27, 17.32, 17.37, 17.44 and 17.50 ($8 \times$ CH_3), 59.75 (C-5'), 67.99 (C-3'), 71.22 ($CH_2CH=CH_2$), 75.85 (C-2'), 82.42 (C-4'), 88.83 (C-1'), 102.24 (C-5), 117.41 ($CH=CH_2$), 128.35 (C-3*), 129.54 (C-1*), 129.78 (C-2*), 133.23 (C-4*), 134.27 ($CH=CH_2$), 139.58 (C-6), 149.62 (C-2), 163.12 (C-4), 164.82 (Ph-C=O).

D.4 Attempted synthesis of 3-benzoyl-1-[(6*aR*,8*R*,9*R*,9*aR*)-9-crotyl-9-hydroxy-2,2,4,4-tetraisopropyltetrahydro-6*H*-furo[3,2-*f*][1,3,5,2,4]trioxadisilicon-8-yl]pyrimidine-2,4(1*H*,3*H*)-dione [237]



Previously prepared compound **235** (0.181 mmol, 0.107 g) was dissolved in freshly distilled THF (1 cm^3). To this solution was then added sodium hydride (obtained as a 60 % suspension in oil, 2.5 eq, 0.452 mmol, 0.0240 g) in THF (1 cm^3) and the mixture was stirred at rt for ~15 min to allow the effervescence to stop. After this time, the crotyl bromide (2.5 eq, 0.5 mmol, 0.05 cm^3) was added and the reaction mixture was stirred at rt under an argon atmosphere overnight (23 h). The solvent was then removed by evaporation and the residue obtained was dissolved in CH_2Cl_2 (20 cm^3), before extraction with saturated NH_4Cl (10 cm^3) and distilled water (10 cm^3). The organic layer was dried over anhydrous Na_2SO_4 , filtered and evaporated. The crude residue was purified by column chromatography (solvents used for elution were: 5-50 % EtOAc : hexane). None of the desired compound **237** was obtained, with a number of unidentifiable by-products instead being isolated.

D.5 Attempted synthesis of 3-benzoyl-1-[(6a*R*,8*R*,9*R*,9a*R*)-9-cinnamyl-9-hydroxy-2,2,4,4-tetraisopropyltetrahydro-6*H*-furo[3,2-*f*][1,3,5,2,4]trioxadisilocin-8-yl]-pyrimidine-2,4(1*H*,3*H*)-dione [238]

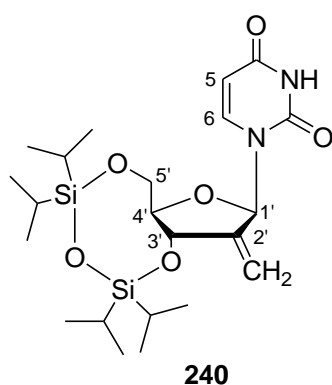


Compound **235** (0.175 mmol, 0.103 g) was dissolved in freshly distilled THF (1 cm³) and to this solution was then added sodium hydride (obtained as a 60 % suspension in oil, 2.5 eq, 0.438 mmol, 0.0192 g) in distilled THF (1 cm³). The solution was allowed to stir at rt for ~10 min, during which time the solution stopped effervescing. Cinnamyl bromide/3-bromo-1-phenyl-1-propene (2.5 eq, 0.438 mmol, 0.0835 g) was then added and the reaction mixture was allowed to stir at rt under an argon atmosphere overnight (23 h).

After this time, the solvent was removed by evaporation and the residue obtained was dissolved in CH₂Cl₂ (20 cm³). The solution obtained was then extracted with saturated NH₄Cl (10 cm³) and distilled water (10 cm³). The organics were then dried over anhydrous Na₂SO₄, filtered and the solvent was removed *in vacuo*. The crude mixture was subjected to column chromatography, with 5-50 % EtOAc : hexane solutions used for elution. Unfortunately, a number of possible decomposition fractions were obtained, with none of the desired compound **238** isolated.

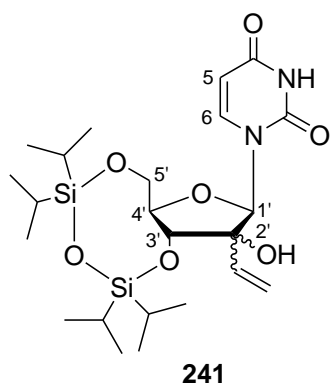
D.6 Preparation of 1-[(6a*R*,8*R*,9a*R*)-2,2,4,4-tetraisopropyl-9-oxotetrahydro-6*H*-furo[3,2-*f*][1,3,5,2,4]trioxadisilocin-8-yl]pyrimidine-2,4(1*H*,3*H*)-dione [239]

The oxidation complex was pre-formed by preparing 3 eq of the complex relative to the starting material **234**. Initially, the chromium (VI) trioxide (3 eq, 6.76 mmol, 0.688 g) was dissolved in freshly distilled CH₂Cl₂ (24 cm³). To this solution was added the distilled pyridine (6 eq, 16 mmol, 1.1 cm³) and the distilled acetic anhydride (3 eq, 6.8 mmol, 0.64 cm³). The mixture was stirred for a few minutes to allow for complete formation of the oxidation complex. A solution was then prepared of **234** (2.25 mmol, 1.09 g) in distilled



The methyl triphenylphosphonium bromide (7 eq, 1.47 mmol, 0.523 g) and distilled THF (5 cm³) were stirred until a suspension formed. This was then cooled to 0 °C in an ice-water bath before the addition of the *n*-butyllithium (concentration determined by titration³ prior to use: 0.9 M in THF, 7 eq, 1.47 mmol, 1.63 cm³). The reaction mixture immediately changed colour from a white suspension to a dark orange solution and was then stirred for a further 10 min to allow all of the precipitate to dissolve. To the solution was then added the 1-[(6*aR*,8*R*,9*aR*)-2,2,4,4-tetraisopropyl-9-oxotetrahydro-6*H*-furo[3,2-*f*][1,3,5,2,4]trioxadisilocin-8-yl]pyrimidine-2,4(1*H*,3*H*)-dione **239** (0.209 mmol, 0.101 g) batch-wise and the foam was rinsed into the flask with an additional portion of THF (1 cm³). The reaction mixture was then allowed to stir at rt under an argon atmosphere for 3 hours. After this time, tlc showed consumption of the starting material, so the reaction mixture was extracted with saturated NH₄Cl (3 × 10 cm³). The organic fraction was then dried over anhydrous Na₂SO₄, filtered and evaporated. The viscous orange oil obtained was then purified by column chromatography, using 10-15 % EtOAc : hexane for elution. Unfortunately, none of the desired compound **240** was obtained after chromatography.

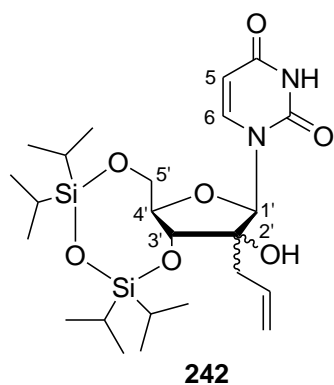
D.8 Attempted synthesis of 1-[(6*aR*,8*R*,9*aS*)-tetrahydro-9-hydroxy-2,2,4,4-tetraisopropyl-9-vinyl-6*H*-furo[3,2-*f*][1,3,5,2,4]trioxadisilocin-8-yl]pyrimidine-2,4(1*H*,3*H*)-dione [241]



A solution was prepared of 1-[(6*aR*,8*R*,9*aR*)-2,2,4,4-tetraisopropyl-9-oxotetrahydro-6*H*-furo[3,2-*f*][1,3,5,2,4]trioxadisilocin-8-yl]pyrimidine-2,4(1*H*,3*H*)-dione **239** (0.216 mmol, 0.104 g) in freshly distilled THF (10 cm³) and was cooled to -60 °C, in an acetone bath, using a cryostat. To this solution was then added the vinyl magnesium bromide (1.0 M in THF, 5 eq, 1.1 mmol, 0.15 cm³). The reaction mixture was allowed to stir at -60 °C under an argon atmosphere overnight (20 h). After

this time, the reaction mixture was allowed to warm to rt and was then diluted with distilled water (10 cm³). The solution was then neutralised (pH ~ 7) using 0.5 M HCl_(aq) and the THF was removed by evaporation. The residue obtained was extracted with EtOAc (3 × 40 cm³) and the combined organic fractions were dried over anhydrous MgSO₄, filtered and evaporated. The crude foam obtained was purified by column chromatography (20-30 % EtOAc : hexane as eluants). None of the desired compound **241** was isolated after chromatography, with only unreacted starting material **239** obtained after purification.

D.9 Preparation of 1-[(6*R*,8*R*,9*aS*)-9-allyl-tetrahydro-9-hydroxy-2,2,4,4-tetraisopropyl-6*H*-furo[3,2-*f*][1,3,5,2,4]trioxadisilocin-8-yl]pyrimidine-2,4(1*H*,3*H*)-dione [242]



The 1-[(6*R*,8*R*,9*aR*)-2,2,4,4-tetraisopropyl-9-oxotetrahydro-6*H*-furo[3,2-*f*][1,3,5,2,4]trioxadisilocin-8-yl]pyrimidine-2,4-(1*H*,3*H*)-dione **239** (0.216 mmol, 0.104 g) was stirred with freshly distilled THF (10 cm³) until a solution had formed. This solution was then cooled to -60 °C (acetone bath, cryostat) before the addition of the allyl magnesium bromide (1.0 M in Et₂O, 5 eq, 1.1 mmol, 0.18 cm³). The reaction mixture was then allowed to stir at -60 °C under an argon atmosphere overnight (18 h). After this time, tlc indicated no further change, so the reaction mixture was allowed to warm to rt. To the warmed reaction mixture was then added distilled water (10 cm³) and the solution was made to pH ~7 by the dropwise addition of 0.5 M HCl_(aq). The THF was then removed by evaporation and the resulting aqueous residue was extracted with EtOAc (3 × 40 cm³). The combined organics were dried over anhydrous Na₂SO₄, filtered and the solvent was removed *in vacuo*. The crude mixture was obtained as a pale yellow semi-solid and it was subsequently purified by column chromatography. Solvents used for elution were 20-30 % EtOAc : hexane. The desired compound **242** was isolated as a clear oil (0.0299 g, 38 % based on recovery of starting material) along with some of the unreacted starting material **239** (0.0276 g).

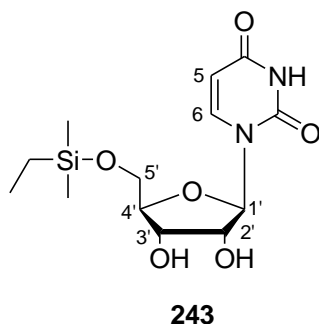
$R_f = 0.57$ (50 % EtOAc : hexane); δ_H (300 MHz, $CDCl_3$) 1.04-1.13 [28 H, m, $4 \times CH(CH_3)_2$ and $4 \times CH(CH_3)_2$], 2.48 (1 H, br s, OH-2'), 2.70-2.72 (2 H, m, $CH_2CH=CH_2$), 3.78-4.25 (4 H, m, H-3', H-4' and H-5'), 5.33-5.37 (2 H, m, $CH=CH_2$), 5.90 (1 H, s, H-1'), 6.05-6.09 (1 H, m, $CH=CH_2$). 7.83 (1 H, d, $J = 8.1$ Hz, H-6), 9.17 (1 H, br s, NH); δ_C (50 MHz, $CDCl_3$) 11.53, 12.05, 12.40 and 13.20 ($4 \times SiCH$), 15.81, 15.85, 15.89, 16.02, 16.10, 16.24, 16.40 and 16.53 ($8 \times CH_3$), 36.80 ($CH_2CH=CH_2$), 59.26 (C-5'), 72.00 (C-3'), 77.89 (C-2' #), 78.65 (C-4' #), 86.54 (C-1'), 100.49 (C-5), 121.10 ($CH=CH_2$), 130.19 ($CH=CH_2$), 139.56 (C-6), 150.03 (C-2), 161.91 (C-4); MS m/z ($M + 1^+$, 100 %) 151.87 (16), 307.93 (55), 455.00 (16), 485.13 (56), 544.07 (5), 1042.93 (67), HRMS (+cESI) calculated for $C_{24}H_{43}N_2O_7Si_2^+$: 527.26033, found: $[M + H]^+$ 527.26033.

Note: assignments denoted with # are exchangeable.

D.10 General procedure for the synthesis of 5'-O-silyl protected uridine derivatives

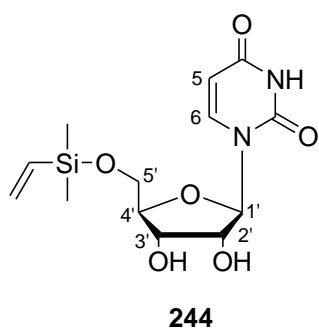
The glassware used in the reaction was filled with a 5 % trimethylsilyl chloride : hexane solution and was allowed to stand at rt overnight. After this time, the glassware was oven-dried, placed under high vacuum and allowed to cool to rt under an argon atmosphere. The uridine **12** (usual scale: approximately 1.00 g) and DMAP (0.1 eq) were stirred with distilled pyridine (5 cm^3 : 1.00 g starting material) until a solution had formed. To this solution was then added the silyl chloride (1.1 eq). The reaction mixture was then allowed to stir at rt under an argon atmosphere overnight (18-22 h). After this time, the reaction was quenched by the addition of distilled water (5 cm^3 : 1.00 g starting material) and the mixture was allowed to stir for a few minutes. The reaction mixture was then transferred to a round bottomed flask with excess EtOAc and all of the solvents (including the water) were removed by evaporation (rotary evaporator set to $60 \text{ }^\circ\text{C}$). The residue obtained was then partitioned between EtOAc (10 cm^3 : 1.00 g starting material) and distilled water ($3 \times 10 \text{ cm}^3$: 1.00 g starting material). The organic fraction was dried over anhydrous Na_2SO_4 , filtered and the solvent was removed *in vacuo*. Crude NMR spectra were obtained to determine if further purification was required.

D.10.1 Attempted synthesis of 5'-O-(dimethylethylsilyl)uridine [243]



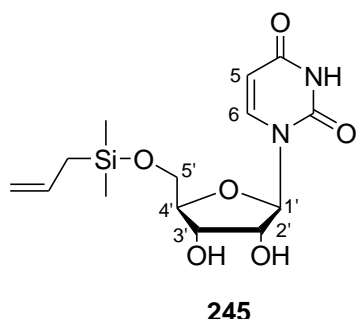
The synthesis was attempted on a 1.02 g scale with the protecting group chlorodimethylethyl silane, according to the general procedure described in **Section D.10** above. A white residue was obtained (0.0062 g) from the organic fraction. Due to the low mass of material obtained from the organic fraction, the aqueous layer was subsequently dried *in vacuo* and yellow oil was isolated (1.60 g). No further purification of the compound was attempted as the crude NMR spectra indicated that none of the desired compound **243** was present in either fraction.

D.10.2 Attempted synthesis of 5'-O-(dimethylvinylsilyl)uridine [244]



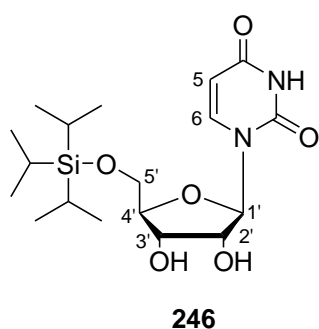
The synthesis was attempted on a 1.01 g scale and was performed according to the general procedure described above in **Section D.10** using dimethylvinylchlorosilane for the protecting group. The only modification was that the base imidazole (2 eq) was added, in place of the DMAP catalyst. The NMR spectra of the crude residue indicated the presence of pyridine. Thus, the residue was further purified by partitioning between CH_2Cl_2 (25 cm^3) and distilled water ($4 \times 25 \text{ cm}^3$), then the organic fraction was dried over anhydrous Na_2SO_4 , filtered and the solvent was removed *in vacuo*. At the same time the aqueous fraction was also dried *in vacuo*. Unfortunately, none of the desired compound **244** was present in the organic fraction and only unreacted uridine **12** was isolated from the aqueous fraction.

D.10.3 Attempted synthesis of 5'-O-(allyldimethylsilyl)uridine [245]



The synthesis was attempted on a 1.00 g scale and was performed according to the general procedure described above in **Section D.10** using allyldimethylsilyl chloride for the protecting group. The only modification was that the base imidazole (2 eq) was added, in place of the DMAP catalyst. The NMR spectra of the crude residue indicated the presence of pyridine. Thus, the residue was further purified by partitioning between CH_2Cl_2 (25 cm^3) and distilled water ($4 \times 25 \text{ cm}^3$), then the organic fraction was dried over anhydrous Na_2SO_4 , filtered and the solvent was removed *in vacuo*. At the same time the aqueous fraction was also dried *in vacuo* and the crude compound was obtained as a viscous yellow oil (1.46 g). Unfortunately, none of the desired compound **245** was present and only unreacted uridine **12** was isolated from the aqueous fraction.

D.10.4 Preparation of 5'-O-(triisopropylsilyl)uridine [246]

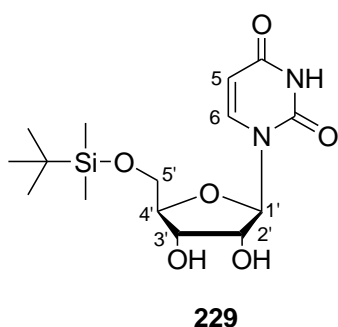


The reaction was performed on a 1.02 g scale using triisopropylsilyl chloride as the protecting group. The procedure that was used is described in **Section D.10** above and the crude compound was obtained as a clear glass (1.28 g). Crude NMR indicated a mixture of products, so the compound was further purified by column chromatography. Solvents used for elution were 30-50 % EtOAc : hexane, followed by 100 % EtOAc. The desired compound **246** was obtained pure as a cream semi-solid (0.753 g, 45 %) after chromatography. At the same time, we isolated some triisopropylsilanol **257** (0.2103 g) from the column, which had formed from the excess unreacted silyl chloride. The synthesis of triisopropylsilanol **257** is described in detail in **Section D.16.4** below.

$R_f = 0.15$ (50 % EtOAc : hexane); δ_H (300 MHz, $CDCl_3$) 1.04-1.14 [21 H, m, $3 \times CH(CH_3)_2$ and $3 \times CH(CH_3)_2$], 3.25 (1 H, d, $J = 6.3$ Hz, OH-2' [#]), 3.95 (1 H, d, $J = 10.2$ Hz, H-5'), 4.11-4.15 (2 H, m, H-4' and H-5'), 4.25-4.32 (2 H, m, H-2' and H-3'), 5.37 (1 H, br s, OH-3' [#]), 5.68 (1 H, d, $J = 8.1$ Hz, H-5), 5.89 (1 H, d, $J = 2.3$ Hz, H-1'), 8.11 (1 H, d, $J = 8.1$ Hz, H-6), 10.15 (1 H, br s, NH); δ_C (50 MHz, $CDCl_3$) 11.90 [$CH(CH_3)_2$], 17.94 [$CH(CH_3)_2$], 60.43 (C-5'), 69.04 (C-3'), 75.76 (C-2'), 79.60 (C-4'), 90.75 (C-1'), 101.97 (C-5), 139.30 (C-6), 151.11 (C-2), 163.79 (C-4); **MS** m/z (M^+ , 100 %) 167.89 (12), 478.83 (11), 586.94 (15), 800.88 (66), 822.85 (24), 1219.04 (44), 1418.27 (31), 1618.53 (35), 1818.35 (20), **HRMS** (+cESI) calculated for $C_{18}H_{33}N_2O_6Si^+$: 401.21024, found: $[M + H]^+$ 401.20968.

Note: assignments denoted with [#] are exchangeable.

D.10.5 Preparation of 5'-O-(tert-butyldimethylsilyl)uridine [229]



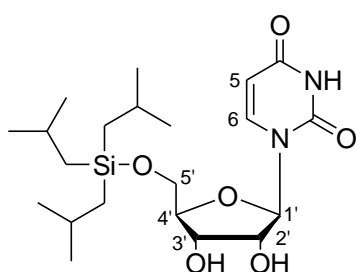
The reaction was performed on 2.00 g scale, with *tert*-butyldiphenylsilyl chloride as the protecting group, according to the protocol described in **Section D.10** above. Crude NMR spectra indicated the formation of pure product and no further purification was undertaken. The desired compound **229** was obtained as a white foam (2.58 g, 88 %).

$R_f = 0.70$ (50 % EtOAc : hexane); ν_{max}/cm^{-1} (thin film) 690 (RHC=CHR *cis*), 715 (CH_2 rocking), 829 (Si- CH_3), 1130 (-C-OH, C-O stretching), 1252 (Si- CH_3), 1330 (-O-H, O-H bending), 1362 and 1391 [-C(CH_3)₃, - CH_3 symmetrical deformation], 1462 and 1468 (- CH_2 and - CH_3 , C-H deformations), 1622 (C=C conjugated with C=O), 1690 (-CONH-), 2928 (- CH_3 , C-H stretching), 2954 (- CH_2 , C-H stretching); δ_H (300 MHz, $CDCl_3$) 0.12 [6 H, s, $Si(CH_3)_2$], 0.92 [9 H, s, $C(CH_3)_3$], 3.66 (1 H, br s, OH-2' [#]), 3.85 and 4.03 (2 H, two d, $J = 11.3$, H-5'), 4.14 (1 H, d, $J = 5.3$ Hz, H-4'), 4.23-4.26 (2 H, m, H-2' and H-3'), 5.52 (1 H, br s, OH-3' [#]), 5.65 (1 H, d, $J = 8.1$ Hz, H-5), 5.91 (1 H, d, $J = 2.1$ Hz, H-1'), 8.08 (1 H, d, $J = 8.1$ Hz, H-6), 10.53 (1 H, br s, NH); δ_C (50 MHz, $CDCl_3$) -5.55 [$Si(CH_3)_2$], 18.40 [$C(CH_3)_2$], 25.90 [$C(CH_3)_2$], 61.78 (C-5'), 69.21 (C-3'), 75.60 (C-2'), 84.84 (C-4'), 90.23 (C-1'), 102.02

(C-5), 140.47 (C-6), 151.29 (C-2), 163.98 (C-4); **MS** m/z (M^+ , 100 %) 213.07 (7), 228.87 (15), 399.60 (7), 783.20 (8), 1173.13 (8), **HRMS** (+cESI) calculated for $C_{15}H_{27}N_2O_6Si^+$: 359.16329, found: $[M + H]^+$ 359.16336.

Note: assignments denoted with # are exchangeable.

D.10.6 Preparation of 5'-O-(triisobutylsilyl)uridine [247]



247

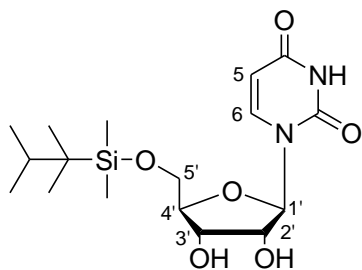
The reaction was performed on a 1.03 g scale using chlorotriisobutylsilane as the protecting group. The procedure that was used is described in **Section D.10** above and the crude compound was obtained as a white semi-solid (1.81 g). Crude NMR indicated a mixture of products, so the compound was further purified by column chromatography. Solvents used for elution were 30-50 % EtOAc : hexane. The

desired compound **247** was obtained pure as a white semi-solid (0.498 g, 27 %) after chromatography.

R_f = 0.18 (50 % EtOAc : hexane); δ_H (300 MHz, $CDCl_3$) 0.67 (6 H, dd, J = 1.6 and 6.9 Hz, $3 \times SiCH_2$), 0.96 [18 H, d, J = 6.6 Hz, $3 \times CH(CH_3)_2$], 1.83 [3 H, sept, J = 6.6 Hz, $3 \times CH(CH_3)_2$], 3.46 (1 H, d, J = 5.6 Hz, OH-2' #), 3.82-4.04 (2 H, m, H-5'), 4.13 (1 H, d, J = 5.3 Hz, H-4'), 4.22-4.23 (2 H, m, H-2' and H-3'), 5.55 (1 H, br s, OH-3' #), 5.70 (1 H, d, J = 8.1 Hz, H-5), 5.90 (1 H, d, J = 1.0 Hz, H-1'), 8.10 (1 H, d, J = 8.1 Hz, H-6), 10.49 (1 H, br s, NH); δ_C (50 MHz, $CDCl_3$) 24.20 [$3 \times CH(CH_3)_2$], 24.99 ($3 \times SiCH_2$), 26.36 and 26.43 [$3 \times CH(CH_3)_2$], 60.87 (C-5'), 69.01 (C-3'), 75.47 (C-2'), 84.68 (C-4'), 90.41 (C-1'), 101.912 (C-5), 140.53 (C-6), 151.17 (C-2), 164.03 (C-4); **MS** m/z ($M + 1^+$, 92 %) 156.87 (100), 275.07 (12), 520.80 (16), 641.13 (45), 884.87 (45), 1344.53 (21), 1565.80 (16), 1786.60 (17), **HRMS** (+cESI) calculated for $C_{21}H_{39}N_2O_6Si^+$: 443.25719, found: $[M + H]^+$ 443.25685.

Note: assignments denoted with # are exchangeable.

D.10.7 Preparation of 5'-O-(dimethylhexylsilyl)uridine [248]



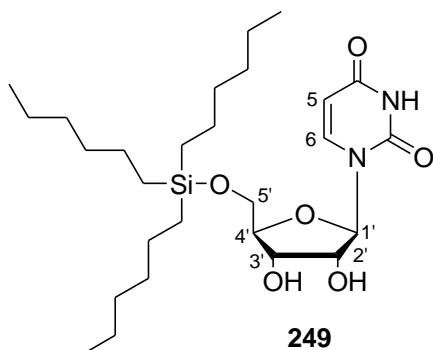
248

The reaction was performed on a 1.01 g scale using dimethylhexylsilyl chloride as the protecting group. The procedure that was used is described in **Section D.10** above and the crude compound was obtained as a white foam. Crude NMR spectra indicated the formation of pure product and no further purification was undertaken. The desired compound **248** was obtained as a white foam (1.59 g, 99 %).

$R_f = 0.58$ (50 % EtOAc : hexane); $[\alpha]_D^{23} -11.000^\circ$ ($c = 1.00$ in CH_2Cl_2); $\nu_{\text{max}}/\text{cm}^{-1}$ (**thin film**) 688 (RHC=CHR *cis*), 714 ($-\text{CH}_2$ rocking), 834 (Si- CH_3), 1111 ($-\text{C}-\text{OH}$, C-O stretch), 1250 (Si- CH_3), 1364 ($-\text{O}-\text{H}$, O-H bending), 1378 and 1393 [$-\text{C}(\text{CH}_3)_2$], 1430 and 1468 ($-\text{CH}_2$ and $-\text{CH}_3$, C-H deformations), 1624 (C=C conjugated with C=O), 1697 ($-\text{CONH}-$), 2927 ($-\text{CH}_3$, C-H stretching), 2958 ($-\text{CH}_2$, C-H stretching); δ_{H} (**300 MHz, CDCl_3**) 0.02 [6 H, s, $\text{Si}(\text{CH}_3)_2$], 0.75 [12 H, dd, $J = 4.4$ and 7.0 Hz, $\text{CH}(\text{CH}_3)_2$ and $\text{C}(\text{CH}_3)_2$], 1.50 [1 H, sept, $J = 6.6$ Hz, $\text{CH}(\text{CH}_3)_2$], 2.04 (1 H, br s, OH-2' [#]), 3.49 (1 H, br s, OH-3' [#]), 3.71 and 3.88 (2 H, two d, $J = 11.4$ Hz, H-5'), 4.10 (1 H, d, $J = 5.4$ Hz, H-4'), 4.11-4.14 (2 H, m, H-2' and H-3'), 5.53 (1 H, d, $J = 8.1$ Hz, H-5), 5.77 (1 H, d, $J = 2.6$ Hz, H-1'), 7.90 (1 H, d, $J = 8.1$ Hz, H-6), 10.39 (1 H, br s, NH); δ_{C} (**50 MHz, CDCl_3**) -3.49 [$\text{Si}(\text{CH}_3)_2$], 18.44 [$\text{C}(\text{CH}_3)_2$], 20.20 [$\text{CH}(\text{CH}_3)_2$], 25.41 [$\text{C}(\text{CH}_3)_2$], 34.06 [$\text{CH}(\text{CH}_3)_2$], 61.68 (C-5'), 69.29 (C-3'), 75.56 (C-2'), 84.87 (C-4'), 90.15 (C-1'), 102.04 (C-5), 140.42 (C-6), 151.30 (C-2), 163.97 (C-4); **MS m/z** (M^+ , 100 %) 279.05 (39), 772.58 (17), 794.61 (10), 1176.09 (38), 1368.73 (27), 1562.26 (100), 1754.63 (15), 1948.74 (30), **HRMS (+cESI)** calculated for $\text{C}_{17}\text{H}_{31}\text{N}_2\text{O}_6\text{Si}^+$: 387.19459, found: $[\text{M} + \text{H}]^+$ 387.19505.

Note: assignments denoted with [#] are exchangeable.

D.10.8 Preparation of 5'-O-(trihexylsilyl)uridine [249]

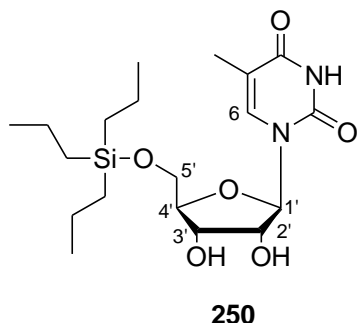


The reaction was performed on a 1.03 g scale using chlorotrihexylsilane as the protecting group. The procedure that was used is described in **Section D.10** above and the crude compound was obtained as a clear oil (2.12 g). Crude NMR indicated a mixture of products, so the compound was further purified by column chromatography. Solvents used for elution

were 30-50 % EtOAc : hexane. The desired compound **249** was obtained pure as a clear semi-solid (0.695 g, 31 %) after chromatography.

$R_f = 0.33$ (50 % EtOAc : hexane); δ_H (300 MHz, $CDCl_3$) 0.60-0.65 (6 H, m, $3 \times SiCH_2$), 0.88 (9 H, t, $J = 6.7$ Hz, $3 \times CH_3$), 1.27-1.30 (24 H, m, $3 \times SiCH_2CH_2$, $3 \times SiCH_2CH_2CH_2$, $3 \times CH_2CH_2CH_3$ and $3 \times CH_2CH_3$), 3.26 (1 H, d, $J = 6.4$ Hz, OH-2'), 3.82 and 3.98 (1 H, two d, $J = 10.5$ Hz, H-5'), 4.14-4.16 (1 H, m, H-4'), 4.21-4.23 (2 H, m, H-2' and H-3'), 5.41 (1 H, d, $J = 3.6$ Hz, OH-3'), 5.69 (1 H, d, $J = 8.1$ Hz, H-5), 5.90 (1 H, d, $J = 1.5$ Hz, H-1'), 8.14 (1 H, d, $J = 8.1$ Hz, H-6), 10.25 (1 H, br s, NH); δ_C (50 MHz, $CDCl_3$) 13.32 ($3 \times SiCH_2$), 14.09 ($3 \times CH_3$), 22.56 ($3 \times SiCH_2CH_2$), 23.04 ($3 \times CH_2CH_3$), 31.46 ($3 \times CH_2CH_2CH_3$), 33.23 ($3 \times SiCH_2CH_2CH_2$), 61.14 (C-5'), 69.34 (C-3'), 75.85 (C-2'), 85.20 (C-4'), 90.90 (C-1'), 101.79 (C-5), 140.49 (C-6), 151.15 (C-2), 163.86 (C-4); **MS** m/z ($M + H^+$, 100 %) 443.07 (18), 641.13 (16), 809.40 (51), 1052.93 (53), 1334.07 (11), 1596.53 (20), 1860.20 (14), **HRMS** (+cESI) calculated for $C_{27}H_{51}N_2O_6Si^+$: 527.35109, found: $[M + H]^+$ 527.35042.

D.11 Preparation of 5'-O-(tripropylsilyl)-5-methyluridine [250]

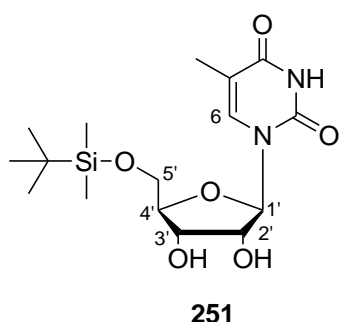


The glassware used in the reaction was filled with a 5 % trimethylsilyl chloride : hexane solution and was allowed to stand at rt overnight. After this time, the glassware was oven-dried, placed under high vacuum and allowed to cool to rt under an argon atmosphere. The 5-methyluridine **233** (4.11 mmol, 1.06 g) and DMAP (0.1 eq, 0.411 mmol, 0.0530 g) were stirred with distilled pyridine (5 cm³) until a solution had formed. To this solution was then added the chlorotripropylsilane (1.1 eq, 4.5 mmol, 0.99 cm³). The reaction mixture was then allowed to stir at rt under an argon atmosphere overnight (21 h). After this time, the reaction was quenched by the addition of distilled water (5 cm³) and the mixture was allowed to stir for a few minutes. The reaction mixture was then transferred to a round bottomed flask with excess EtOAc and all of the solvents (including the water) were removed by evaporation (rotary evaporator set to 60 °C). The residue obtained was then partitioned between EtOAc (10 cm³) and distilled water (3 × 10 cm³). The organic fraction was then dried over anhydrous Na₂SO₄, filtered and the solvent was removed *in vacuo*. The crude compound was obtained as a white semi-solid (1.38 g) and the crude NMR spectra indicated a mixture of products. Thus, the mixture was purified by column chromatography, using 30-50 % EtOAc : hexane for elution. The desired compound **250** was obtained pure as a white semi-solid (0.326 g, 19 %).

$R_f = 0.10$ (50 % EtOAc : hexane); δ_H (300 MHz, CDCl₃) 0.61-0.67 (6 H, m, 3 × SiCH₂), 0.94-0.99 (9 H, m, 3 × CH₂CH₃), 1.33-1.42 (6 H, m, 3 × CH₂CH₃), 1.91 (3 H, s, CH₃), 3.40 (1 H, br s, OH-2' #), 3.77-3.98 (2 H, m, H-5'), 4.17-4.23 (3 H, m, H-2', H-3' and H-4'), 5.29 (1H, br s, OH-3' #), 5.93 (1 H, d, $J = 3.5$ Hz, H-1'), 7.67 (1 H, s, H-6), 10.21 (1 H, br s, NH); δ_C (50 MHz, CDCl₃) 12.48 (3 × SiCH₂), 16.18 (CH₃), 16.73 (3 × CH₂CH₃), 18.34 (3 × CH₂CH₃), 62.00 (C-5'), 70.50 (C-3'), 75.34 (C-2'), 85.51 (C-4'), 90.08 (C-1'), 110.59 (C-5), 135.82 (C-6), 151.44 (C-2), 164.29 (C-4); MS m/z (M⁺, 51 %) 828.79 (100), 850.88 (24), 1260.64 (35), 1467.11 (15), 1674.63 (18), HRMS (+cESI) calculated for C₁₉H₃₅N₂O₆Si⁺: 415.22589, found: [M + H]⁺ 415.22569.

Note: assignments denoted with # are interchangeable.

D.12 Preparation of 5'-O-(*tert*-butyldimethylsilyl)-5-methyluridine [251]

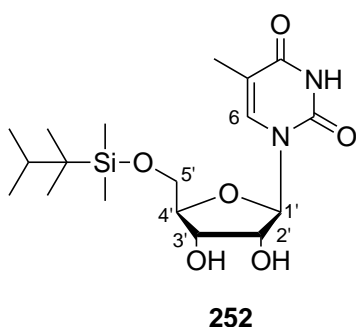


The glassware and attachments were filled with a 5 % trimethylsilyl chloride : hexane solution and were allowed to stand at rt overnight. After this time, the glassware was oven-dried, placed under high vacuum and allowed to cool to rt under an argon atmosphere. The 5-methyluridine **233** (4.02 mmol, 1.04 g) and DMAP (0.1 eq, 0.402 mmol, 0.0514 g) were stirred with distilled pyridine (5 cm³) until a solution had formed. To this solution was then added the *tert*-butyldimethylsilyl chloride (1.1 eq, 4.43 mmol, 0.673 g). The reaction mixture was then allowed to stir at rt under an argon atmosphere overnight (20 h). After this time, the reaction mixture was quenched by the addition of distilled water (5 cm³). After a few minutes of stirring, all of the solvents in the reaction mixture (including the water) were removed by evaporation. The residue obtained was partitioned between EtOAc (20 cm³) and distilled water (3 × 10 cm³). The organic fraction was dried over anhydrous Na₂SO₄, filtered and the solvent was removed *in vacuo*. The desired compound **251** was obtained pure as a white powder (1.39 g, 93 %) and as such, no further purification was required.

$R_f = 0.73$ (50 % EtOAc : hexane); $\nu_{\max}/\text{cm}^{-1}$ (**thin film**) 709 (CH₂ rocking), 812 (R₂C=CHR), 831 (Si-CH₃), 1120 (-C-OH, C-O stretching), 1258 (Si-CH₃), 1311 (-O-H, O-H bending), 1362 and 1388 [-C(CH₃)₃, CH₃ symmetrical deformations], 1432 and 1470 (-CH₂ and -CH₃, C-H deformations), 1645 (C=C conjugated with C=O), 1688 (-CONH-), 2928 (-CH₃, C-H stretching), 2955 (-CH₂, C-H stretching), 3067 (O-H stretching); δ_{H} (**300 MHz, CDCl₃ : MeOD, 1 : 1 ratio**) 0.15 and 0.16 [6 H, two s, Si(CH₃)₂], 0.96 [9 H, s, C(CH₃)₃], 1.91 (3 H, s, CH₃), 3.86 and 3.95 (2 H, two dd, $J = 2.1$ and 11.6 Hz, H-5'), 4.07-4.15 (3 H, m, H-2', H-3' and H-4'), 5.96 (1 H, d, $J = 5.0$ Hz, H-1'), 7.57 (1 H, s, H-6), both NH and OH peaks were not observed in the spectrum; **MS** m/z (M⁺, 75 %) 744.70 (49), 766.60 (14), 947.79 (10), 1134.41

(62), 1320.31 (60), 1506.34 (100), 1692.12 (74), 1877.92 (88), **HRMS** (+cESI) calculated for $C_{16}H_{29}N_2O_6Si^+$: 373.17894, found: $[M + H]^+$ 373.17903.

D.13 Preparation of 5'-O-(dimethylhexylsilyl)-5-methyluridine [252]

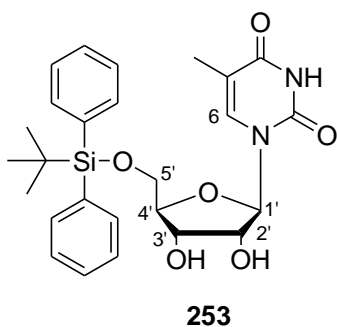


The glassware used in the reaction was filled with a 5 % trimethylsilyl chloride : hexane solution and was allowed to stand at rt overnight. After this time, the glassware was oven-dried, placed under high vacuum and allowed to cool to rt under an argon atmosphere. The 5-methyluridine **233** (3.93 mmol, 1.02 g) and DMAP (0.1 eq, 0.393 mmol, 0.0522 g) were stirred with distilled pyridine (5 cm³) until a clear solution had formed. To this solution was then added the dimethylhexylsilyl chloride (1.1 eq, 4.3 mmol, 0.85 cm³). The reaction mixture was then allowed to stir at rt under an argon atmosphere overnight (21 h). After this time, the reaction was quenched by the addition of distilled water (5 cm³) and the mixture was allowed to stir for a few minutes. The reaction mixture was then transferred to a round bottomed flask with excess EtOAc and all of the solvents (including the water) were removed by evaporation (rotary evaporator set to 60 °C). The residue obtained was then partitioned between EtOAc (10 cm³) and distilled water (3 × 10 cm³). The organic fraction was then dried over anhydrous Na₂SO₄, filtered and the solvent was removed *in vacuo*. The crude compound **252** was obtained pure as a white solid (1.31 g, 80 %) and as such, no further purification was required.

R_f = 0.72 (50 % EtOAc : hexane); δ_H (300 MHz, d_6 -DMSO : CDCl₃, 1 : 1 ratio) 1.00 [6 H, s, Si(CH₃)₂], 1.75 [12 H, dd, J = 1.9 and 7.3 Hz, CH(CH₃)₃ and C(CH₃)₂], 1.49 [1 H, sept, J = 6.7 Hz, CH(CH₃)₂], 4.20 (3 H, s, CH₃), 4.62 and 4.67 (2 H, two dd, J = 2.6 and 11.5 Hz, H-5'), 4.77-4.79 (1 H, m, H-4'), 4.84-4.85 (2 H, m, H-2' and H-3'), 5.83 (1 H, d, J = 3.7 Hz, OH-2' [#]), 6.14 (1 H, d, J = 5.2 Hz, OH-3' [#]), 6.73 (1 H, d, J = 5.2 Hz, H-1'), 8.22 (1 H, s, H-6), 12.13 (1 H, br s, NH); **MS** m/z (M + H⁺, 100 %) 256.93 (8), 445.07 (11), 845.07 (20), 867.33 (26), 1067.67 (9), 1290.40 (9), **HRMS** (+cESI) calculated for $C_{18}H_{33}N_2O_6Si^+$: 401.21024, found: $[M + H]^+$ 401.20987.

Note: assignments denoted with # are exchangeable.

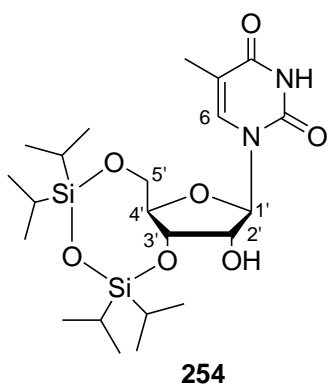
D.14 Preparation of 5'-O-(*tert*-butyldiphenylsilyl)-5-methyluridine [253]



The glassware used in the reaction was filled with a 5 % trimethylsilyl chloride : hexane solution and was allowed to stand at rt overnight. After this time, the glassware was oven-dried, placed under high vacuum and allowed to cool to rt under an argon atmosphere. The 5-methyluridine **233** (4.26 mmol, 1.10 g) and DMAP (0.1 eq, 0.426 mmol, 0.0529 g) were stirred with distilled pyridine (5 cm³) until a solution had formed. To this solution was then added the *tert*-butyldiphenylsilyl chloride (1.1 eq, 4.69 mmol, 1.22 cm³). The reaction mixture was then allowed to stir at rt under an argon atmosphere overnight (20 h). After this time, the reaction mixture was diluted with CH₂Cl₂ (40 cm³) and extracted with a saturated NaHCO₃ solution (2 × 40 cm³) followed by brine (40 cm³). The combined organics were then dried over anhydrous Na₂SO₄, filtered and the solvent removed *in vacuo*. NMR spectra of the crude mixture showed that the desired product **253** had formed, but that it was contaminated with pyridine. Thus, the mixture was purified by the azeotropic distillation of pyridine using toluene as the co-solvent. The desired compound **253** was obtained pure as a white foam (2.11 g, 100 %).

$R_f = 0.68$ (50 % EtOAc : hexane); δ_H (300 MHz, CDCl₃ : MeOD, 1 : 1 ratio) 1.12 [9 H, s, Si(CH₃)₃], 1.49 (3 H, s, CH₃), 3.90 (1 H, dd, $J = 2.3$ and 11.6 Hz, H-5'), 4.03-4.11 (2 H, m, H-4' and H-5'), 4.24-4.33 (2 H, m, H-2' and H-3'), 6.02 (1 H, d, $J = 5.7$ Hz, H-1'), 7.40-7.43 (6 H, m, H-3* and H-4*), 7.68-7.71 (4 H, m, H-2*), 7.82 (1 H, s, H-6), 8.53 (1 H, br d, $J = 5.8$ Hz, NH); MS m/z (M + H⁺, 31 %) 227.00 (18), 287.07 (30), 305.07 (48), 419.07 (100), 541.13 (55), 586.93 (10), 1037.07 (77), 1117.13 (10), 1308.13 (22), 1578.33 (26), 1837.67 (19), HRMS (+cESI) calculated for C₂₆H₃₃N₂O₆Si⁺: 497.21024, found: [M + H]⁺ 497.20971.

D.15 Preparation of 1-[(6*aR*,8*R*,9*S*,9*aR*)-tetrahydro-9-hydroxy-2,2,4,4-tetraisopropyl-6*H*-furo[3,2-*f*][1,3,5,2,4]trioxadisilocin-8-yl](5-methylpyrimidine)-2,4(1*H*,3*H*)-dione [254]



The glassware used in the reaction was filled with a 5 % trimethylsilyl chloride : hexane solution and was allowed to stand at rt overnight. After this time, the glassware was oven-dried, placed under high vacuum and allowed to cool to rt under an argon atmosphere. A solution was prepared of 5-methyluridine **233** (3.94 mmol, 1.02 g) in distilled pyridine (12 cm³). The solution was then cooled to 0 °C in an ice-water bath before the addition of the 1,3-dichloro-1,1,3,3-tetraisopropylidisiloxane (1.05 eq, 4.14 mmol, 1.33 cm³). The reaction mixture was then stirred at rt overnight (20 h). After this time, the reaction was quenched by the addition of distilled water (12 cm³). The mixture was then transferred to a round-bottomed flask using a small amount of EtOAc and all of the solvents were removed by evaporation (60 °C). The residue obtained was then partitioned between EtOAc (40 cm³) and distilled water (3 × 15 cm³). The organic layer was dried over anhydrous Na₂SO₄, filtered and evaporated to yield a white foam. The crude foam was then purified by column chromatography, using 10-50 % EtOAc : hexane for elution. The desired compound **254** was obtained as a white foam (0.781 g, 40 %).

$R_f = 0.53$ (50 % EtOAc : hexane); $[\alpha]_D^{21} -2.8846^\circ$ (c = 1.04 in CH₂Cl₂); $\nu_{\max}/\text{cm}^{-1}$ (thin film) 791 (R₂C=CHR), 1061 (C-OH, C-O stretching), 1247 (Si-CH), 1333 (O-H bending), 1385 [-C(CH₃)₂, -CH₃ symmetrical deformation], 1464 (-CH₃, C-H deformation), 1640 (C=C conjugated with C=O), 1666 (-CONH-), 2893 (-C-H, C-H stretching), 2926 (-CH₃, C-H stretching), 2964 (-O-H), 3068 (-CONH- in solution); δ_H (300 MHz, CDCl₃) 1.04-1.10 [28 H, m, 4 × CH(CH₃)₂ and 4 × CH(CH₃)₂], 1.91 (3 H, s, CH₃), 3.68 (1 H, d, *J* = 1.4 Hz, OH-2'), 3.98-4.12 (2 H, m, H-5'), 4.14-4.23 (2 H, m, H-2' and H-4'), 4.33-4.37 (1 H, m, H-3'), 5.72 (1 H, s, H-1'), 7.46 (1 H, s, H-6), 9.47 (1 H, br s, NH); δ_C (50 MHz, CDCl₃) 12.45, 12.57, 12.68 and 12.93 (4 × SiCH), 16.81, 16.94, 16.96, 17.04, 17.22, 17.23, 17.33 and 17.41 [4 × CH(CH₃)₂], 60.24 (C-5'), 68.92 (C-3'), 74.97 (C-2'), 81.83 (C-4'), 91.07 (C-1'), 110.55 (C-5),

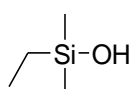
135.61 (C-6), 150.17 (C-2), 163.97 (C-4); **MS** m/z (M^+ , 78 %) 306.94 (7), 1000.67 (100), 1518.10 (26), 1768.58 (12), **HRMS** (+cESI) calculated for $C_{22}H_{41}N_2O_7Si_2^+$: 501.24468, found: $[M + H]^+$ 501.24409.

D.16 General procedure for the preparation of silanols

A solution was prepared of the silyl chloride (usual scale: 750 mg, 1 eq) in Et_2O (3 cm^3 : 750 mg starting material). To this solution was then added portion wise a solution of KOH (1.1 eq) in a mixture of distilled water (2 cm^3 : 750 mg starting material) and MeOH (0.5 cm^3 : 750 mg starting material). The solution warmed up after the addition and a white precipitate was immediately observed. The reaction mixture was then allowed to stir at rt overnight (18 h). After this time, the organic fraction was collected from the reaction mixture and the aqueous fraction was extracted with Et_2O ($3 \times 10\text{ cm}^3$: 750 mg starting material). The combined organics were then dried over anhydrous $MgSO_4$, filtered and the solvent was removed *in vacuo*. NMR spectra were obtained for the crude mixtures to determine if further purification was required.

Note: due to the low molecular masses and high volatility of the silanols prepared, LRMS and HRMS were not determined.

D.16.1 Preparation of dimethylethylsilanol [255]

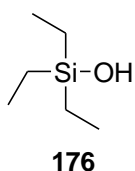


255

The reaction was performed on 750 mg scale, using chlorodimethylethylsilane as the starting material, as described in **Section D.16**. No further purification was required and the pure compound **255** was obtained as a clear oil (0.0122 g, 2 %).

R_f = sample was not observable by tlc (50 % EtOAc : hexane); $\nu_{\max}/\text{cm}^{-1}$ (thin film) 830 (Si-CH₂), 1220 (Si-CH₂), 1370 (-CH₃ symmetrical deformations), 2880 and 2921 (-CH₂ and -CH₃, C-H stretching), 2965 (-O-H), 3510 (O-H stretching); δ_{H} (300 MHz, CDCl₃) 0.06 [6 H, s, Si(CH₃)₂], 0.47 (2 H, q, $J = 7.9$ Hz, SiCH₂), 0.93 (3 H, t, $J = 7.9$ Hz, CH₂CH₃), OH peak not observed in spectrum; δ_{C} (50 MHz, CDCl₃) -0.65 (2 x CH₃Si), 6.80 (CH₃CH₂), 9.62 (CH₂).

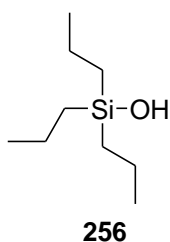
D.16.2 Preparation of triethylsilanol [176]



The reaction was performed on 750 mg scale, using chlorotriethylsilane as the starting material, as described in **Section D.16**. No further purification was required and the pure compound **176** was obtained as a clear oil (0.565 g, 86 %).

R_f = sample was not observable by tlc (50 % EtOAc : hexane); $\nu_{\max}/\text{cm}^{-1}$ (thin film) 726 (-CH₂ rocking), 812 (Si-CH₂), 894 and 1002 (Si-O), 1236 (Si-CH₂), 1378 (-CH₃ symmetrical deformation), 1413 (O-H bending), 1458 (-CH₂ and -CH₃, C-H deformations) 2876 and 2911 (-CH₂ and -CH₃, C-H stretching), 2955 (-O-H), 3574 (O-H stretching); δ_{H} (300 MHz, CDCl₃) 0.52 (6 H, q, $J = 7.9$ Hz, 3 x SiCH₂), 0.93 (9 H, t, $J = 7.9$ Hz, 3 x CH₂CH₃), OH peak not observed in spectrum; δ_{C} (50 MHz, CDCl₃) 6.40 (3 x CH₂CH₃), 6.80 (3 x SiCH₂).

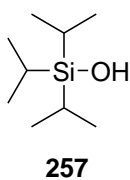
D.16.3 Preparation of tripropylsilanol [256]



The reaction was performed on 750 mg scale, using chlorotripropylsilane as the starting material, as described in **Section D.16**. No further purification was required and the pure compound **256** was obtained as a clear oil (0.722 g, 100 %).

$R_f = 0.90$ (100 % EtOAc); $\nu_{\max}/\text{cm}^{-1}$ (thin film) 709 (-CH₂ rocking), 800 (Si-CH₂), 895 and 1002 (Si-O), 1218 (Si-CH₂), 1375 (-CH₃ symmetrical deformations), 1408 (-O-H bending), 1460 (-CH₂ and -CH₃, C-H deformations), 2868 and 2926 (-CH₂ and -CH₃, C-H stretching), 2954 (-O-H), 3574 (O-H stretching); δ_{H} (300 MHz, CDCl₃) 0.47-0.62 (6 H, m, 3 × SiCH₂), 0.96 (9 H, q, $J = 7.3$ Hz, 3 × CH₃), 1.29-1.41 (6 H, m, 3 × CH₂CH₃), OH peak not observed in spectrum; δ_{C} (50 MHz, CDCl₃) 16.7 (3 × Si-CH₂), 18.0 (3 × CH₃), 18.3 (3 × CH₂CH₃).

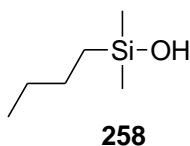
D.16.4 Preparation of triisopropylsilanol [257]



The reaction was performed on 750 mg scale, using triisopropylsilyl chloride as the starting material, as described in **Section D.16**. No further purification was required and the pure compound **257** was obtained as a clear oil (0.686 g, 98 %).

$R_f = 0.90$ (100 % EtOAc); δ_{H} (300 MHz, CDCl₃) 1.04-1.06 [18 H, m, CH(CH₃)₂], 1.08 (1 H, br s, OH), 1.48-1.50 [3 H, m, CH(CH₃)₂]; δ_{C} (50 MHz, CDCl₃) 13.5 (3 × CH), 18.5 (6 × CH₃).

D.16.5 Preparation of butyldimethylsilanol [258]

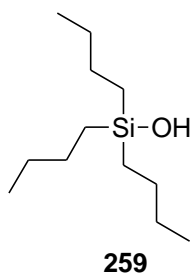


The reaction was performed on 750 mg scale, using butyldimethylsilyl chloride as the starting material, as described in **Section D.16**. No further purification was required and the pure compound **258** was obtained as a clear oil (0.436 g, 66 %).

$R_f = 0.91$ (100 % EtOAc); $\nu_{\max}/\text{cm}^{-1}$ (thin film) 703 (-CH₂ rocking), 820 (Si-CH₂), 890 and 1016 (Si-O), 1230 (Si-CH₃), 1378 (-CH₃ symmetrical deformation), 1412 (O-H bending), 1465 (-CH₂ and -CH₃, C-H deformations), 2850 and 2919 (-CH₂ and -CH₃, C-H stretching),

2959 (-OH), 3575 (O-H stretching); δ_{H} (300 MHz, CDCl_3) 0.03 [6 H, s, $\text{Si}(\text{CH}_3)_2$], 1.48-1.53 (2 H, m, SiCH_2), 0.88 (3 H, t, $J = 6.8$ Hz, CH_2CH_3), 1.25-1.36 (4 H, m, CH_2CH_3 and SiCH_2CH_2), OH peak not observed in spectrum; δ_{C} (50 MHz, CDCl_3) 0.36 [$\text{Si}(\text{CH}_3)_2$], 13.83 (CH_2CH_3), 18.11 (SiCH_2), 25.52 (SiCH_2CH_2), 26.39 (CH_2CH_3).

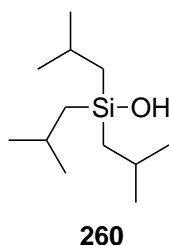
D.16.6 Preparation of tributylsilanol [259]



The reaction was performed on 750 mg scale, using chlorotributylsilane as the starting material, as described in Section D.16. No further purification was required and the pure compound **259** was obtained as a clear oil (0.677 g, 98 %).

$R_f = 0.94$ (50 % EtOAc : hexane); $\nu_{\text{max}}/\text{cm}^{-1}$ (thin film) 731 ($-\text{CH}_2$ rocking), 823 ($\text{Si}-\text{CH}_2$), 886 and 1081 ($\text{Si}-\text{O}$), 1231 ($\text{Si}-\text{CH}_2$), 1377 ($-\text{CH}_3$ symmetrical deformation), 1409 (O-H bending), 1464 ($-\text{CH}_2$ and $-\text{CH}_3$, C-H deformations), 2855 and 2919 ($-\text{CH}_2$ and $-\text{CH}_3$, C-H stretching), 2956 ($-\text{O}-\text{H}$), 3346 (O-H stretching); δ_{H} (300 MHz, CDCl_3) 0.47-0.62 (6 H, m, $3 \times \text{SiCH}_2$), 0.87-0.92 (9 H, m, $3 \times \text{CH}_3$), 1.30-1.35 (12 H, m, $3 \times \text{SiCH}_2\text{CH}_2$ and $3 \times \text{CH}_2\text{CH}_3$), 1.48 (1 H, br s, OH); δ_{C} (50 MHz, CDCl_3) 13.9 ($3 \times \text{SiCH}_2$), 14.7 ($3 \times \text{CH}_2\text{CH}_3$), 25.4 ($3 \times \text{SiCH}_2\text{CH}_2$), 26.5 ($3 \times \text{CH}_2\text{CH}_3$).

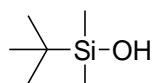
D.16.7 Preparation of triisobutylsilanol [260]



The reaction was performed on 750 mg scale, using chlorotriisobutylsilane as the starting material, as described in Section D.16. No further purification was required and the pure compound **260** was obtained as a clear oil (0.679 g, 98 %).

$R_f = 0.94$ (50 % EtOAc : hexane); $\nu_{\max}/\text{cm}^{-1}$ (thin film) 751 (-CH₂ rocking), 831 (Si-CH₂), 872 and 1039 (Si-O), 1219 (Si-CH₂), 1364 (-CH₃ symmetrical deformation), 1401 (O-H bending), 1465 (-CH₂ and -CH₃, C-H deformations), 2867 and 2925 (-CH₂ and -CH₃, C-H stretching), 2952 (-O-H); δ_{H} (300 MHz, CDCl₃) 0.61 (6 H, d, $J = 7.0$ Hz, 3 × SiCH₂), 0.96 [18 H, d, $J = 6.5$ Hz, 3 × CH(CH₃)₂], 1.33 (1 H, br s, OH), 1.82-1.87 [3 H, m, 3 × CH(CH₃)₂]; δ_{C} (50 MHz, CDCl₃) 24.6 (3 × CH), 26.7 (3 × SiCH₂), 27.4 (6 × CH₃).

D.16.8 Preparation of *tert*-butyldimethylsilanol [261]

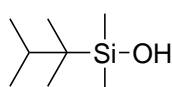


261

The reaction was performed on 770 mg scale, using *tert*-butyldimethylsilyl chloride as the starting material, as described in **Section D.16**. No further purification was required and the pure compound **261** was obtained as a colourless oil with some needles, but would not solidify completely even after standing (0.448 g, 72 %).

R_f = sample was not observable by tlc (50 % EtOAc : hexane); $\nu_{\max}/\text{cm}^{-1}$ (thin film) 772 (-CH₂ rocking), 831 (Si-CH₂), 864 and 1039 (Si-O), 1217 (Si-CH₂), 1361 (-CH₃ symmetrical deformation), 1407 (O-H bending), 1462 (-CH₂ and -CH₃, C-H deformations), 2884 and 2928 (-CH₂ and -CH₃, C-H stretching), 2952 (-O-H), 3244 (O-H stretching); δ_{H} (300 MHz, CDCl₃) 0.08 [6 H, s, Si(CH₃)₂], 0.90 [9 H, s, C(CH₃)₃], 1.91 (1 H, br s, OH); δ_{C} (50 MHz, CDCl₃) -3.61 [Si(CH₃)₂], 17.97 [C(CH₃)₃], 25.63 [C(CH₃)₃].

D.16.9 Preparation of dimethylhexylsilanol [262]

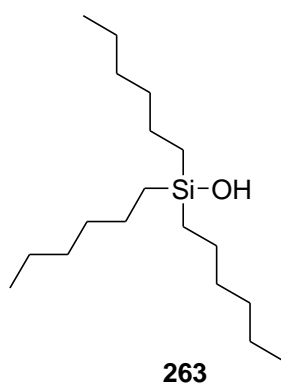


262

The reaction was performed on 750 mg scale, using dimethylhexylsilyl chloride as the starting material, as described in **Section D.16**. No further purification was required and the pure compound **262** was obtained as a clear oil (0.640 g, 95 %).

R_f = sample was not observable by tlc (50 % EtOAc : hexane); $\nu_{\max}/\text{cm}^{-1}$ (thin film) 827 (Si-CH), 875 and 1048 (Si-O), 1252 (Si-CH₃), 1364 (-CH₃ symmetrical deformation), 1409 (O-H bending), 1465 (-CH₃, C-H deformations), 2867 and 2929 (-CH₃, C-H stretching), 2976 (-OH), 3298 (O-H stretching); δ_{H} (300 MHz, CDCl₃) 0.13 [6 H, s, Si(CH₃)₂], 0.86 [6 H, s, C(CH₃)₂], 0.89 [6 H, d, $J = 6.9$ Hz, CH(CH₃)₂], 1.60 (1 H, br s, OH), 1.63-1.66 [1 H, m, CH(CH₃)₂]; δ_{C} (50 MHz, CDCl₃) -1.11 [Si(CH₃)₂], 18.56 [C(CH₃)₂], 20.30 [CH(CH₃)₂], 24.87 [C(CH₃)₂], 34.13 [CH(CH₃)₂].

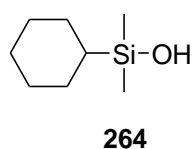
D.16.10 Preparation of trihexylsilanol [263]



The reaction was performed on 750 mg scale, using chlorotrihexylsilane as the starting material, as described in Section D.16. No further purification was required and the pure compound **263** was obtained as a clear oil (0.716 g, 100 %).

$R_f = 0.85$ (50 % EtOAc : hexane); $\nu_{\max}/\text{cm}^{-1}$ (thin film) 748 (-CH₂ rocking), 822 (Si-CH₂), 890 and 1074 (Si-O), 1228 (Si-CH₂), 1378 (-CH₃ symmetrical deformation), 1409 (O-H bending), 1467 (-CH₂ and -CH₃, C-H deformations), 2852 and 2919 (-CH₂ and -CH₃, C-H stretching), 2957 (-O-H); δ_{H} (300 MHz, CDCl₃) 0.55-0.61 (6 H, m, 3 × SiCH₂), 0.88 (9 H, t, $J = 6.7$ Hz, 3 × CH₃), 1.28-1.40 (24 H, m, 3 × SiCH₂CH₂, 3 × SiCH₂CH₂CH₂, 3 × CH₂CH₂CH₃ and 3 × CH₂CH₃), 3.44 (1 H, br s, OH); δ_{C} (50 MHz, CDCl₃) 15.1 (3 × SiCH₂), 16.5 (3 × CH₃), 23.9 (3 × SiCH₂CH₂), 24.7 (3 × CH₂CH₃), 33.0 (3 × CH₂CH₂CH₃), 34.6 (3 × SiCH₂CH₂CH₂).

D.16.11 Preparation of cyclohexyldimethylsilanol [264]

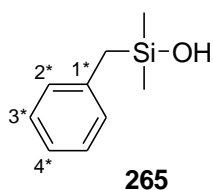


The reaction was performed on 750 mg scale, using chlorocyclohexyldimethylsilane as the starting material, as described in

Section D.16. No further purification was required and the pure compound **264** was obtained as a clear oil (0.620 g, 92 %).

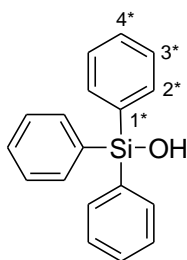
R_f = sample was not observable by tlc (50 % EtOAc : hexane); $\nu_{\max}/\text{cm}^{-1}$ (**thin film**) 739 (-CH₂ rocking), 834 (Si-CH), 889 and 1062 (Si-O), 1250 (Si-CH₃), 1379 (-CH₃ symmetrical deformation), 1408 (O-H bending), 2846 and 2918 (-CH₂ and -CH₃, C-H stretching), 2957 (O-H); δ_{H} (**300 MHz, CDCl₃**) 1.60-1.73 (5 H, m, 5 × CH₂), 1.02-1.11 (5 H, m, 5 × CH₂), 0.54-0.57 (1 H, m, Si-CH), 0.08 (6 H, s, 2 × Si-CH₃); δ_{C} (**50 MHz, CDCl₃**) -2.2 (2 × SiCH₃), 26.8 (Si-CH), 27.1 (ring CH₂), 27.5 (ring CH₂), 27.9 (ring CH₂).

D.16.12 Preparation of benzyldimethylsilanol [265]



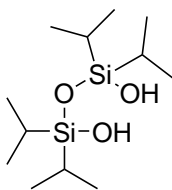
The reaction was performed on 750 mg scale, using benzylchlorodimethylsilane as the starting material, as described in **Section D.16**. No further purification was required and the pure compound **265** was obtained as a clear oil (0.608 g, 90 %).

R_f = 0.95 (50 % EtOAc : hexane); $\nu_{\max}/\text{cm}^{-1}$ (**thin film**) 696 (-CH₂ rocking), 760 (5 adjacent aromatic H), 836 (Si-CH₂), 904 and 1070 (Si-O), 1317 (Si-CH₃), 1405 (O-H bending), 1452 (-CH₂, C-H deformations), 1493 (aromatic H), 1601 (aromatic H), 2890 (-CH₂, C-H stretching), 3025 (aromatic H), 3082 (O-H stretching); δ_{H} (**300 MHz, CDCl₃**) 0.20 [6 H, s, Si(CH₃)₂], 2.27 (2 H, s, SiCH₂), 7.20 (2 H, d, J = 7.1 Hz, H-2*), 7.28 (1 H, t, J = 7.3 Hz, H-4*), 7.42 (2 H, dd, J = 6.2 and 13.5 Hz, H-3*); δ_{C} (**50 MHz, CDCl₃**) 0.1 (2 × Si-CH₃), 29.6 (Si-CH₂), 125.7 (C-4*), 129.8 (C-3*), 130.0 (C-2*), 145.5 (C-1*).

D.16.13 Preparation of triphenylsilanol [266]**266**

The reaction was performed on 750 mg scale, using triphenylsilyl chloride as the starting material, as described in **Section D.16**. No further purification was required and the pure compound **266** was obtained as white solid (0.649 g, 93 %).

R_f = 0.90 (50 % EtOAc : hexane); *m.p.* 153-156 °C; $\nu_{\max}/\text{cm}^{-1}$ (**thin film**) 774 (5 adjacent aromatic H), 917 and 1093 (Si-O), 1427 (O-H bending), 1485 and 1567 (aromatic H), 2912 (-OH), 3020 (aromatic H), 3088 (O-H stretching); δ_{H} (**300 MHz, CDCl₃**) 2.72 (1 H, br s, OH), 7.25-7.49 (9 H, m, 3 × H-3* and 3 × H-4*), 7.60-7.63 (6 H, m, 3 × H-2*); δ_{C} (**50 MHz, CDCl₃**) 127.8 (C-3*), 130.2 (C-4*), 135.0 (C-2*), 135.1 (C-1*).

D.16.14 Preparation of 1,3-dihydroxy-1,1,3,3-tetraisopropyldisiloxane [268]**268**

The reaction was performed on 770 mg scale, using 1,3-dichloro-1,1,3,3-tetraisopropyldisiloxane as the starting material, as described in **Section D.16**. No further purification was required and the pure compound **268** was obtained as white solid (0.662 g, 100 %).

R_f = sample not observable by tlc (50 % EtOAc : hexane); $\nu_{\max}/\text{cm}^{-1}$ (**thin film**) 837 (Si-CH), 883 and 1057 (Si-O), 1249 (Si-CH), 1366 (-CH₃ symmetrical deformation), 1384 (O-H bending), 1462 (-CH₃, C-H deformations), 2866 and 2926 (-CH₃, C-H stretching), 2952 (-OH), 3349 (O-H stretching); δ_{H} (**300 MHz, CDCl₃**) 0.83-0.92 [4 H, m, 4 × CH(CH₃)₂], 0.95-1.05 [24 H, m, 4 × CH(CH₃)₂], 2.71 (2 H, br s, 2 × OH).

Appendix E:
Experimental Procedures – Relating to Chapter 6

E.1 General Procedure for Confocal Scanning Laser Microscopy (CSLM)

E.1.1 Sample Preparation

General Culture Conditions

For the untreated control cultures of *S. aureus* strain ATCC 25923 and *B. cereus* strain DL5, a single colony was taken from the previously prepared stock plates that had been sealed with Parafilm, placed inside polyethylene bags and stored at 4 °C until required (note: plates were subcultured every 21 days when in active use and were prepared fresh from new freezer stocks when long periods of time elapsed between assays). This single colony was used to inoculate 100 cm³ of fresh nutrient broth (prepared according to the manufacturer's instructions, autoclaved at 1 atm/121 °C for 20 min, poured and then incubated overnight to check for contamination). These conicals were then incubated at 37°C with shaking (150 rpm) for exactly 18 hours, before being used immediately for the preparation of the bacterial suspensions, described below.

For the treated bacterial cultures, a single colony was taken from the stock plates that had been stored at 4 °C, and was used to inoculate 100 cm³ of nutrient broth as described above. These conicals were then incubated at 37 °C with shaking (150 rpm) for exactly 18 hours. After this time, the 18 hour bacterial cultures were diluted to 10⁶ cfu/mL based on the average viable count determined using the droplet plate technique described in **Section C.4, Appendix C**. Then 15 cm³ of the 10⁶ culture was placed aseptically into a McConkey bottle containing 15 cm³ of the desired compound dilution (compounds dissolved in DMSO, diluted with water and then stocks were used for serial dilutions in nutrient broth, procedure described in detail in **Section C.5, Appendix C**). These bottles were then incubated at 37°C for a further 18 hours, before being used immediately for the preparation of the bacterial suspensions, described in detail below

🌀 *General Procedure for the Preparation of Bacterial Suspensions*

After this time, 25 cm³ of each of the overnight cultures was placed in a 50 cm³ disposable plastic centrifuge tube (Corning, NY) and was sealed. The culture was then concentrated by centrifugation at 5000 rpm for 20 minutes - essentially a 15 minute run with time added to speed up and slow down the rotor. The supernatant was then removed and the pellet was resuspended in 2000 µL of a freshly prepared 0.85 % NaCl_(aq) solution. 1000 µL of this solution was then added to a second centrifuge tube containing 19 cm³ of the 0.85 % NaCl_(aq) solution. The mixture was then incubated at room temperature for 1 hour, with mixing by hand every 15 minute interval.

The mixture was then concentrated by centrifugation at 5000 rpm for 20 minutes. The supernatant was decanted off and the pellet was resuspended in 1000 µL of 0.85 % NaCl_(aq) solution. This was then added to a third centrifuge tube containing 19 cm³ of the 0.85 % NaCl_(aq) solution and was gently mixed. The mixture was immediately concentrated by centrifugation at 5000 rpm for 20 minutes. The supernatant was again decanted off and the pellet was resuspended in 1000 µL of 0.85 % NaCl_(aq) solution. This was then added to a fourth centrifuge tube, containing 9 cm³ of the 0.85 % NaCl_(aq) solution.

The optical density was then determined for both samples:

- (i) 1000 µL of 0.85 % NaCl_(aq) solution was placed in a disposable cuvette (BLANK)
- (ii) 1000 µL of each bacterial solution (from the fourth centrifuge tube) was placed in a disposable cuvette (SAMPLE)
- (iii) optical density was measured at 670 nm (values obtained ranged from 0.82 - 1.15)

General Procedure for Staining of Bacteria in Suspension

Both components of the BacLight Kit (LIVE/DEAD BacLight Bacterial Viability Kit L7012, Molecular Probes, Leiden, the Netherlands, imported by Invitrogen SA) were allowed to warm to room temperature and were then centrifuged using the mini-spin for 10 seconds (to allow the contents of the vials to settle to the bottom). Then 10 μL of the SYTO9 dye and 10 μL of the propidium iodide dye were placed in a autoclaved Eppendorf tube, and were mixed together by centrifugation on the mini-spin for 10 seconds to give the two-component dye mixture.

Then 1000 μL of the bacterial suspension (from the fourth centrifuge tube, prepared as described above) was placed in an autoclaved Eppendorf tube and to this was then added 3 μL of the two-component dye mixture. The contents of the tube were then mixed by inversion and were incubated at room temperature in the dark for 15 minutes.

5 μL of the stained bacterial suspension was then placed on a microscope slide and was covered gently with a coverslip. Slides were prepared in triplicate for each of the bacterial strains tested. The slides were placed carefully in a box covered with tin foil to keep them in the dark. The prepared slides were then viewed on a confocal scanning laser microscope. The protocol described above is based on the standard method for the BacLight Kit as supplied by the manufacturers.^{E1}

E.1.2 Sample Analysis

The prepared slides were viewed on an invert laser scan microscope (LSM 410, Carl Zeiss Jena, Germany) using 50 % laser intensity, with 488 nm and 563 nm as the excitation wavelengths and using a 63 \times oil objective.

E.2 General Procedure for Scanning Electron Microscopy (SEM)

E.2.1 Sample Preparation

Ⓢ General Culture Conditions - Untreated Controls

For the untreated control cultures of *S. aureus* strain ATCC 25923, *B. cereus* strain DL5, *P. aeruginosa* strain ATCC 27853 and *E. coli* strain ATCC 25922, a single colony was taken from the previously prepared stock plates that had been sealed with Parafilm, placed inside polyethylene bags and stored at 4 °C until required (note: plates were subcultured every 21 days when in active use and were prepared fresh from new freezer stocks when long periods of time elapsed between assays). This single colony was used to inoculate 100 cm³ of fresh nutrient broth (prepared according to the manufacturer's instructions, autoclaved at 1 atm/121 °C for 20 min, poured and then incubated overnight to check for contamination). These conicals were then incubated at 37°C with shaking (150 rpm) for exactly 18 hours, before being used immediately for the preparation of the bacterial suspensions, as described below.

After this time, the 18 hour bacterial cultures were diluted to 10⁶ cfu/mL based on the average viable count determined using the droplet plate technique described in **Section C.4, Appendix C**. Then 1000 µL of the 10⁶ bacterial culture was placed aseptically into a McConkey bottle and this solution was then fixed with 1000 µL of a 3 % glutaraldehyde_(aq) solution (prepared immediately prior to use, glutaraldehyde purchased from BDH), by allowing to stand at room temperature for exactly 24 hours.

Ⓢ General Culture Conditions - Treatment with Synthetic Compounds and Antibiotic

For the treated bacterial cultures, a single colony was taken from the stock plates that had been stored at 4 °C, and was used to inoculate 100 cm³ of nutrient broth as described above.

These conicals were then incubated at 37 °C with shaking (150 rpm) for exactly 18 hours. The 18 hour bacterial cultures were then diluted to 10⁶ cfu/mL based on the average viable count determined using the droplet plate technique described in **Section C.4, Appendix C**. Then 1000 µL of the 10⁶ bacterial culture was placed aseptically into a McConkey bottle containing 1000 µL of the desired compound dilution. The mixture was then incubated at 37 °C for exactly 22 hours.

After this time, the cell suspension/compound dilution mixture (2000 µL in total) was fixed with 2000 µL of a 3 % glutaraldehyde_(aq) solution, by allowing to stand at room temperature for exactly 24 hours.

Ⓢ *General Dehydration Procedure*

In all cases, the fixed solution of either the bacterial cell suspension or the mixture of the bacterial cells plus compound dilution, were used for the dehydration procedure. Firstly, 2000 µL of the suspension was gently sucked up into a 10 mL syringe. To this syringe was then attached a sterilized filter holder (PALL Life Sciences 13 mm Plastic Filter Holder) containing Millipore filter paper (Isopore Membrane Filters 0.2 µm GTTP). Once the suspension had been filtered through the Millipore filter paper, a sterile pair of tweezers were used to transfer the filter paper to the dehydration solutions.

For the dehydration procedure, an ethanol dilution series was prepared using absolute ethanol (99 %) in de-ionised water. The ethanol dilution series used was as follows:

- (i) 10 % ethanol in de-ionised water (v/v)
- (ii) 20 % ethanol in de-ionised water (v/v)
- (iii) 30 % ethanol in de-ionised water (v/v)
- (iv) 40 % ethanol in de-ionised water (v/v)

- (v) 50 % ethanol in de-ionised water (v/v)
- (vi) 60 % ethanol in de-ionised water (v/v)
- (vii) 70 % ethanol in de-ionised water (v/v)
- (viii) 80 % ethanol in de-ionised water (v/v)
- (ix) 90 % ethanol in de-ionised water (v/v)
- (x) 95 % ethanol in de-ionised water (v/v)
- (xi) 100 % ethanol in de-ionised water (v/v)

Initially, 5 mL of each of the ethanol solutions were placed in clean screw-cap bottles and these were then used. The procedure works by placing the filter paper sequentially in each of the ethanol solutions for 10 minute intervals that are accurately timed (in order from lowest concentration of ethanol to highest). The filter paper was then stored in the 100 % ethanol container and was immediately submitted for critical point drying.

Critical Point Drying and Sample Mounting

Performed by members of the Microscopy Unit at Wits. Dried filter paper specimens were then cut in half using scissors and mounted directly onto double sided graphite tape, which was attached on one side to the metal holder. The two halves of the filter paper were mounted with one facing "up" and one facing "down" to ensure that the bacterial surface was visible on one of the half-moons (as illustrated in **Figure E.1**). The edges of the filter paper were then carefully sealed using graphite paste and allowed to dry open to the atmosphere, before being coated in a gold/palladium mixture by the members of the Microscopy Unit at Wits. Once the coating was completed, samples could be stored at room temperature in a desiccator until analysed.

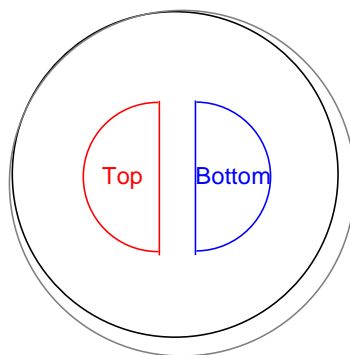


Figure E.1 Layout used when mounting filter paper for SEM

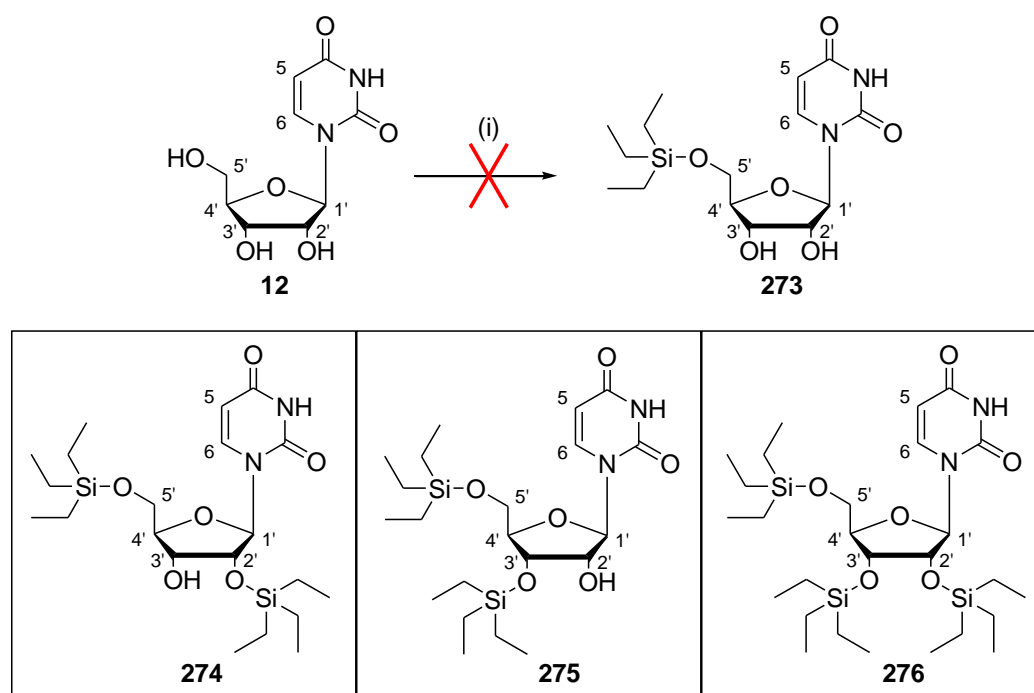
E.2.2 Sample Analysis

Our samples were mounted onto the brass holder using graphite paste that was dried under a warm lamp. These were then viewed on a scanning electron microscope (JSM-840, JEOL Ltd, Tokyo, Japan) and photographed using a standard 35 mm Nikon camera (black and white film, Ilford Pan F PLUS), with myself as the operator. Magnification, probe current and keV were manually adjusted when viewing the samples and as such are reported with the photographs themselves. The negatives were developed by a member of the Microscopy Unit and were then scanned using a EPSON Perfection 4870 Photo Scanner (thanks go to the Organometallic Research Group in the School of Chemistry at Wits for the use of their equipment) to obtain the data in the positive phase in the standard electronic format reported herein.

Appendix F:
Experimental Procedures – Relating to Chapter 8

F.1 General Experimental Procedure for Multiple Protecting Group Additions

Only one worked example will be included in this appendix for general reference purposes. The example chosen is that system containing the simplest of all the silicon-containing protecting groups used, *triethylsilyl chloride*.



Scheme F.1 Attempted synthesis of 5'-O-(triethylsilyl)uridine **273**: (i) 1.1 eq triethylsilyl chloride, 0.1 eq DMAP, pyridine, rt, 18 h, 0 %

When attempting the synthesis of compound 5'-O-(triethylsilyl)uridine **273** using the general procedure for the synthesis of 5'-O-silyl protected uridine derivatives (described in **Appendix D**, Section D.10) we obtained none of the desired product **273**, but instead isolated a number of by-products showing multiple protecting group additions (compounds **274**, **275** and **276**). The results of the reaction are shown in detail in **Scheme F.1**.

The full assignments for the ^1H NMR spectrum (**Table F.1**) and the ^{13}C NMR spectrum (**Table F.2**) are tabulated below for ease of reference.

Table F.1 ^1H NMR Assignments for compounds **274**, **275** and **276**

<i>Position on Molecule</i>	<i>Compound A</i> (Either 274 or 275)	<i>Compound B</i> (Either 274 or 275)	<i>Compound C</i> (Identified as 276)
H-1'	5.96 ppm, d	5.98 ppm, d	5.86 ppm, d
H-2'	4.08-4.23 ppm, m	4.27-4.31 ppm, m	4.05-4.14 ppm, m
H-3'	4.08-4.23 ppm, m	4.27-4.31 ppm, m	4.05-4.14 ppm, m
OH-2' or OH-3'	2.68 ppm, br d	2.96, br d	N/A
H-4'	4.08-4.23 ppm, m	4.27-4.31 ppm, m	4.05-4.14 ppm, m
H-5'	3.90 ppm, dd	3.84 ppm, dd	3.74 ppm, dd
H-5	5.69 ppm, d	5.70 ppm, d	5.68 ppm, d
H-6	8.08 ppm, d	7.88 ppm, d	8.10 ppm, d
NH	9.15 ppm, br s	8.96 ppm, br s	8.85 ppm, br s
2'-O-Si(CH ₂ CH ₃) ₃	0.61-0.70 ppm, m	0.64-0.70 ppm, m	0.65-0.70 ppm, m
2'-O-Si(CH ₂ CH ₃) ₃	0.93-0.99 ppm, m	0.96-1.01 ppm, m	0.93-1.02 ppm, m
3'-O-Si(CH ₂ CH ₃) ₃	0.61-0.70 ppm, m	0.64-0.70 ppm, m	0.65-0.70 ppm, m
3'-O-Si(CH ₂ CH ₃) ₃	0.93-0.99 ppm, m	0.96-1.01 ppm, m	0.93-1.02 ppm, m
5'-O-Si(CH ₂ CH ₃) ₃	0.61-0.70 ppm, m	0.64-0.70 ppm, m	0.65-0.70 ppm, m
5'-O-Si(CH ₂ CH ₃) ₃	0.93-0.99 ppm, m	0.96-1.01 ppm, m	0.93-1.02 ppm, m

Table F.2 ^{13}C NMR Assignments for compounds **274**, **275** and **276**

<i>Position on Molecule</i>	<i>Compound A</i> (Either 274 or 275)	<i>Compound B</i> (Either 274 or 275)	<i>Compound C</i> (Identified as 276)
C-1'	88.61 ppm	88.99 ppm	88.98 ppm
C-2'	70.20 ppm*	70.99 ppm ^{\$}	70.62 ppm [#]
C-3'	76.18 ppm*	75.50 ppm ^{\$}	76.33 ppm [#]
C-4'	84.62 ppm	85.07 ppm	84.14 ppm
C-5'	61.77 ppm	61.80 ppm	61.06 ppm
C-2	150.30 ppm	150.53 ppm	150.19 ppm
C-4	163.30 ppm	163.18 ppm	163.33 ppm
C-5	102.02 ppm	102.30 ppm	101.52 ppm
C-6	140.23 ppm	140.13 ppm	140.41 ppm
2'-O-Si(CH ₂ CH ₃) ₃	6.65 ppm**	N/A ^{\$\$}	6.67 ppm ^{##}
2'-O-Si(CH ₂ CH ₃) ₃	4.42 ppm***	N/A ^{\$\$\$}	4.71 ppm ^{###}
3'-O-Si(CH ₂ CH ₃) ₃	N/A**	6.72 ppm ^{\$\$}	6.79 ppm ^{##}
3'-O-Si(CH ₂ CH ₃) ₃	N/A***	4.69 ppm ^{\$\$\$}	4.81 ppm ^{###}
5'-O-Si(CH ₂ CH ₃) ₃	6.48 ppm**	6.66 ppm ^{\$\$}	5.77 ppm
5'-O-Si(CH ₂ CH ₃) ₃	4.09 ppm***	4.17 ppm ^{\$\$\$}	4.09 ppm

Note: Values with the same superscript markers are interchangeable

Identification of the by-products described above was conducted through the extensive use of NMR spectroscopy, specifically: ^1H , ^{13}C , COSY, HSQC, DEPT-135 and NOESY.

Unfortunately, even with the large amount of data at hand we were unable to unambiguously distinguish between compounds **274** and **275** – as the peaks for the protons on the sugar ring overlapped in the ^1H NMR spectra. Further experiments would be required to distinguish the compounds (irradiation/NOE experiments or labeling experiments using, for example deuterium), at this moment we feel that they fall outside the scope of this thesis.